PETROGRAPHY, MINERAL CHEMISTRY, GEOCHEMISTRY
AND SULPHUR ISOTOPE STUDIES OF THE ABHAINN
SRATHAIN COPPER MINERALISATION, MEALL MÓR,
SOUTH KNAPDALE, SCOTLAND

by

Hiyam A. Mohammed B.Sc.

A Thesis submitted to the
University of Strathclyde for the Degree
of Doctor of Philosophy

November 1987

Department of Applied Geology
University of Strathclyde
Glasgow
G1 IXJ

To my two brothers
Mohammed and Abdu-Al Baki,
whom I lost while I am here
preparing this thesis

PETROGRAPHY, MINERAL CHEMISTRY, GEOCHEMISTRY AND SULPHUR ISOTOPE STUDIES OF

THE ABHAINN SRATHAIN COPPER MINERALISATION, MEALL MÓR,

SOUTH KNAPDALE, SCOTLAND

ABSTRACT

The Abhainn Srathain copper mineralisation with at least 10 million tonnes of rock containing copper was worked during the Eighteenth Century and is situated 1-2km to the south of Meall Mór, South Knapdale. The mineralisation is hosted by epidiorites, quartzites and schists of the Upper Erins Quartzite Formation in which the levels of copper reach up to 2%, 1.3% and 0.8% respectively. The main sulphide phases, pyrite and chalcopyrite, occur in disseminations, in layers and as large crystals in quartz and/or calcite cross-cutting veins.

The observed opaque mineral textures are due to recrystallisation, deformation and limited mobilisation indicating a premetamorphic origin for the mineralisation. Microscopic compositional variation of the minerals and isotopic geothermometry of analysed pyrite-chalcopyrite pairs suggest disequilibrium conditions during the regional metamorphism. Sulphides contain low minor element concentrations with a high Co:Ni ratio in pyrite (12.5:1).

The mineralisation is associated with the local development of epidote, Mn-rich garnet, chlorite, muscovite and calcite and/or quartz cross-cutting veins which all resulted from premetamorphic alteration during ore formation. During this alteration CaO, Fe_2O_3, CO_2, MnO, Cu, S and some trace elements were added, Al_2O_3 was diluted and MgO, FeO, alkalis and some trace elements were removed. The isotopic composition of bacteriogenically reduced sulphur from sulphides throughout the Knapdale Pyrite Horizon ranges between $\delta^{34}S=+4.5$ and 12.8 per mil. The consistent isotopic values of the sulphides from the Abhainn Srathain copper mineralisation with an average of. around +7 per mil regardless of location, depth, lithology and style of mineralisation suggest that the source of the hydrothermal sulphur is a mixture of inorganically reduced downward percolating Dalradian seawater sulphate and sulphur leached from interbedded basic igneous rocks.

Weak exhalative activity caused by the shallow intrusion of sill bodies into the wet unlithified sediments of the Lower and Upper Erins Quartzite accompanied the deposition of the Upper Erins Quartzite and is expressed by weak disseminated and

stratiform pyrite with traces of chalcopyrite and sphalerite (Knapdale Pyrite Horizon). Increasing intensity of this exhalation was due to the creation of a geothermal system centred at the site of the present copper mineralisation. During this stage the hot ascending water reacted with the rocks causing local alteration and precipitation of pyrite and chalcopyrite as disseminations, layers and cross-cutting veins. At the same time cold water descended into the hot intrusives and altered the rocks by dissolving silica and precipitating calcite and oxides.

ACKNOWLEDGMENTS

go to my parent and friends in Iraq for their support and understanding of being away from home for such a long time.

LIST OF CONTENTS

PARTICULARLY IN THE STUDIED AREA

Appendices

major elements.

LIST OF FIGURES

xxv

CHAPTER 1

INTRODUCTION

1.1 LOCATION

The area under study, Meall Mór, forms part of the Southwest Highlands of Scotland. It is located within South Knapdale west of Loch Fyne, mid-way between Tarbert and Lochgilphead and about 60km due west of Glasgow (Fig. 1.1). The main site of the study is the area around the old Abhainn Srathain mine (NR 8340 7375, Fig. 1.2, folded map in the back pocket) about 1-2km to the south of Meall Mór summit.

The majority of the studied samples in this research represent drillcore taken from the B.G.S. boreholes 1, 2 and 3 (Fig. 5.1). Besides, during the field work in 1981 and 1982, sixty-three hand specimens were collected from the poorly exposed outcrops together with twenty stream sediment samples and their location is marked on the folded map (Fig. 1.2). The area sampled is bounded to the north and south by latitudes $55^{\circ}58$ N and $55^{\circ}53\frac{1}{2}$ N respectively. Its eastern boundary is the Loch Fyne coast. This area is covered by Ordnance Survey 1:50,000 maps Sheet No. 62 of the Landranger Series and also by Ordnance Survey 1:10,000 maps Sheets No. NR, 87 SE, 87 NW, 87 SW and 87 NE and was described in the Memoir on Jura-Knapdale and North-Kintyre (Peach et al. 1911), and is included in Sheets No. 28 and 29 of the one-inch geological map of Scotland.

The area is largely utilised for sheep farming and deer stalking and it has been extensively planted especially in the Abhainn Srathain valley. The population of the area is small and public transport is available; the area is served by the A83 Glasgow-Campbeltown trunk road.

1
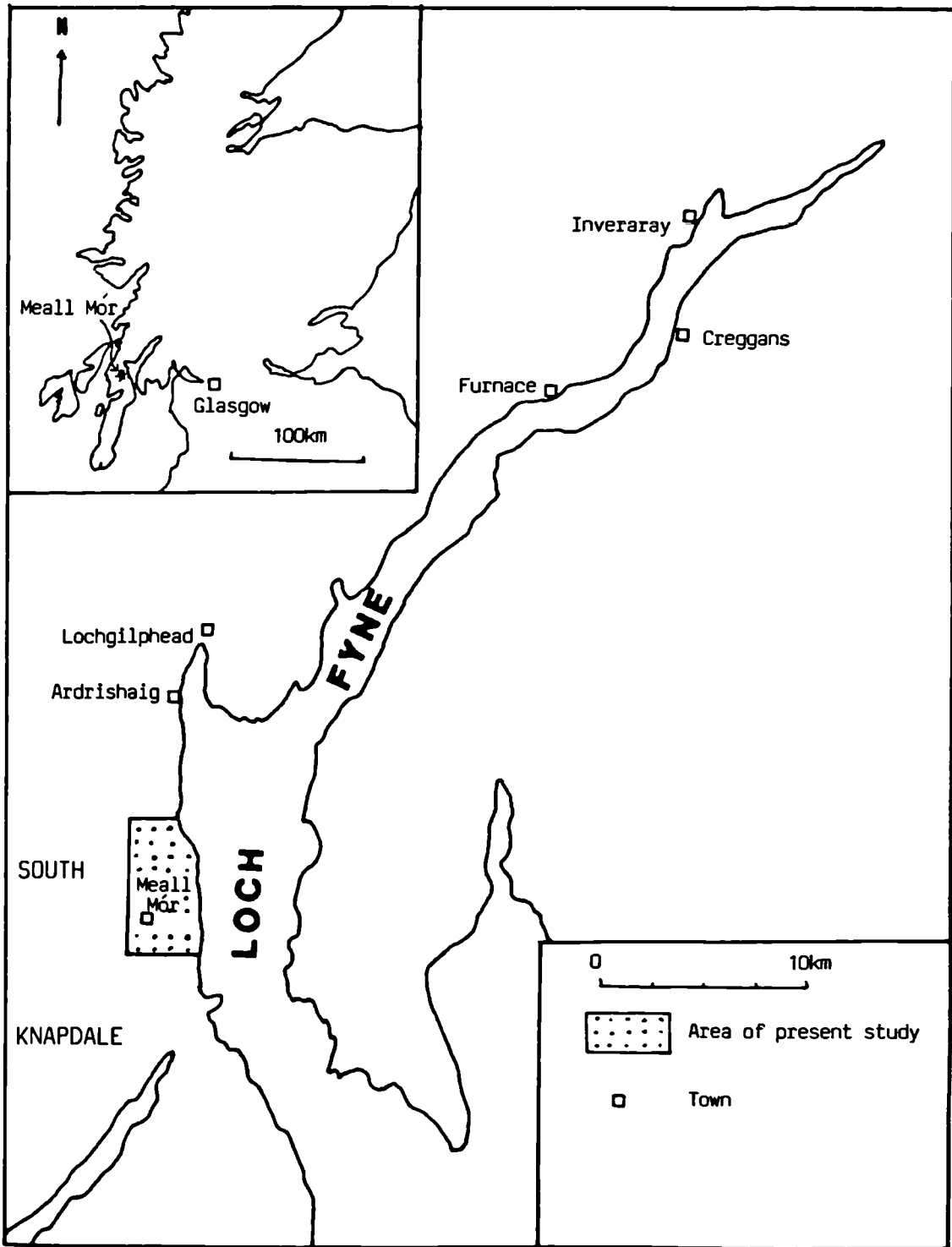
Fig. 1.1 : Map showing the location of the area studied.

1.2 REASONS FOR RESEARCH

This project is concerned with mineralogical, textural, geochemical and sulphur isotope studies and attempts to construct a model for the genesis of the Abhainn Srathain copper mineralisation, south of Meall Mór summit, hosted by the Upper Erins Quartzite of the regionally metamorphosed Middle Dalradian rocks. The research was undertaken at the Department of Applied Geology under the supervision of Dr. Allan Hall. This research forms one of many projects undertaken in this department started in 1977 concerning the Middle Dalradian mineralisations after revealing their stratiform nature.

The area was invstigated by the B.G.S. in 1976 as part of their Mineral Reconnaissance Programme. The investigation delineated the existence of a zone of weak sulphide mineralisation, the Knapdale Pyrite Horizon, and revealed the stratiform nature of the Meall Mór copper mineralisation. Also, the investigation demonstrated the existence of an epidotised zone that coincides with the copper mineralisation and remobilisation process during regional metamorphism was proposed to be responsible for the epidotisation and the formation of large sulphide porphyroblasts in cross-cutting veins.

The aim of this study is to describe the mineralisation in detail in an attempt to examine the possibility of a premetamorphic hydrothermal alteration of the host rocks during the mineralisation process in order to explain the cross-cutting nature of the Abhainn Srathain copper mineralisation at the site of epidotisation and to understand the process of ore formation.

1.3 LAYOUT OF THESIS

This thesis reports the mineralogical, geochemical and sulphur isotope investigation of the Abhainn Srathain copper mineralisation,

3

Meall Mór. The results of all these investigations are presented and discussed in Chapters 5, 6 and 7 respectively. In order to have a complete picture and to understand the genesis of the mineralisation, a brief summary of the background information is given in Chapters 2, 3 and 4. Chapter 2 reviews the early history of mining and thoughts on the genesis up to 1922 in the Loch Fyne district, which the studied mineralisaton is part of. Chapter 3 of this thesis attempts to place the mineralisation in its geological setting and is mainly based on published information on the Dalradian of Scotland. Chapter 4 describes the studied mineralisation in relation to the other stratiform mineralisation in the Dalradian and is based mainly on the Mineral Reconnaissance Reports of the B.G.S.

A detailed description of hand specimens, textural and petrographic examination of microscopic sections of materials from exposure and drillcore together with the results of microprobe analysis of selected sulphide, oxide, phosphate and silicate minerals are reported and discussed in Chapter 5. Chapter 6 describes and discusses the chemistry of the host rocks in an attempt to delineate any premetamorphic hydrothermal alteration during the mineralisation process. Chapter 7 reports the sulphur isotope values from the area and discusses the source of sulphur and equilibrium during metamorphism. And finally Chapter 8 gives a possible model for the formation of the Abhainn Srathain copper mineralisation and also summarises the possible conclusions that are drawn from this study. Detailed descriptions of the techniques used in this study constitute Appendices (A.5.1 to A.7.1).

4

CHAPTER 2
THE MINING HISTORY OF THE LOCH FYNE DISTRICT,
ARGYLLSHIRE

2.1 INTRODUCTION

Metalliferous mining is an old industry in Scotland. Ores of lead and zinc have a wide distribution and were worked for several centuries. Copper ores are less frequent, and nickel ores are found in only a few places.

Production of lead ore in Scotland dates back to pre-Roman times and probably the earliest authentic record refers to the Lead Hills district; in west Argyllshire mining of lead started in 1424 (Hunter 1884, quoted in Wilson & Flett 1921), or probably earlier, and the mines seem to have been worked for silver only up to about the Sixteenth Century when the extraction of silver seems to have become unprofitable and accordingly the mines were worked for lead alone [Cochran Patrick, quoted in Wilson and Flett (1921)].

Great activity in mining and prospecting was recorded during the period from the latter part of the Fifteenth Century to the beginning of the Seventeenth Century following the discovery of the gold-bearing gravels in the Lead Hills district (Hunter 1884). From that time to up to the end of the Napoleonic Wars the lead industry reached its height but after the signing of peace in 1815, the price of lead fell rapidly, and accordingly several of the mines were closed down between 1840 and 1880.

Zinc ore has been worked only on a small scale, and the earliest record is as early as 1865 at Black Craig mines, Kircudbrightshire.

5

Ores of copper have been worked in Scotland since remote times and quite likely back to 1500 or 1800 B.C (Graham Callander 1904). The first authentic records of copper mines date to 1597 (Cochran Patrick 1878). It reached the maximum activity just prior to the war due to the discovery of a mass of copper ore near Kilfinan, in Argyllshire.

Most of the mining activity was concentrated on vein deposits, porphyry style mineralisation and concordant mineralisation. By 1925 base-metal mining had ceased in the Highlands and in many cases these old mines have fallen in, and their sites are now covered up and grassed over making reinvestigation very difficult.

2.2 LOCH FYNE DISTRICT

This comprises the district on both sides of Loch Fyne in Argyllshire (Fig. 2.1). The Abhainn Srathain old mine of the studied area "Meall Mór" belongs to this district. This region has long been known to contain base-metal concentrations of economic proportions, and in some localities, for instance, near Loch Arail (NR 8080 7950), the country rock was known prior to the Eighteenth Century to be impregnated with sulphide ores to such an extent that the water of the loch are poisoned, and fish are said to be unable to live (Peach et al. 1911).

There are about thirty reported occurrences of mineralisation in the area, most of them are of minor character, and despite this wide mineralisation, only three of these occurrences were developed as mines: these are at Kilfinan, Coillie Bhraghad and Craignure (Hopkinson 1970). The accounts of mining activity are summarised in Table (2.1) for the worked mines, and in Table (2.2) a description of the unworked localities is given. The information represented in Tables (2.1 & 2.2) is taken from the following references: Gunn et al. (1897), Hill et al. (1905), Peach et al. (1909), Peach et al. (1911), Clough (1913) and Wilson & Flett (1921).
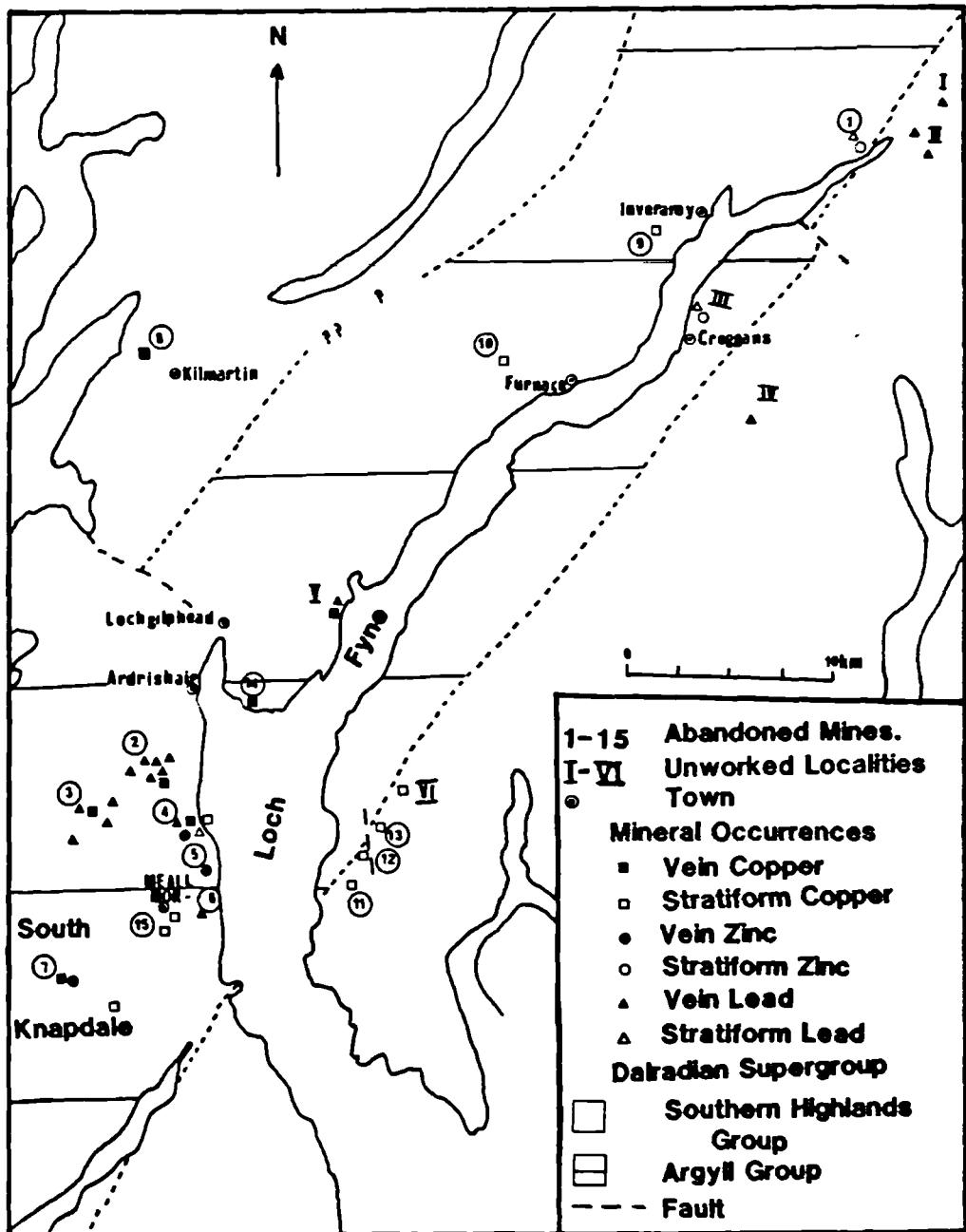
Fig. 2.1 : Distribution of the metalliferous mines and
localities in the Loch Fyne district. See
Tables 2.1 & 2.2 for the key to numbers.

No. on Fig. 2.1	Mine Locality	Dates of working	"Ore" Minerals	Element Assay	Description
1	Clachan Bheag NN 1820 1250	c. 1792	galena, sphalerite and pyrite	Pb 12 wt% Ag 2 oz/t Au traces Zn 20 wt%	The deposit is about 25cm thick, and was thought to occur as a metasomatic replacement of part of a limestone bed. The ore minerals are disseminated in siderite matrix.
		A	c. 1797	--	--	A level has been driven about 7.6m, but there is no sign of any vein material.
	B	--	galena and pyrite	--	A quartz vein 30-46cm wide.
	C	--	galena	--	The vein consists mainly of quartz and calcite.
2	D	--	pyrite and galena	--	A 2.5m quartz vein
	E	--	galena, pyrite and chalcopyrite	Pb 17 wt% Ag 2 oz/t Au 12 g/t	The vein is about 23-25cm wide, and consists of quartz with a little siderite.
	F	--	--	--	A few small trials have been made, but no ore appears to have been found.

Inverneil NR 8110 8290

Table 2.1 : Summary information on the old mines of the Loch Fyne district.

No. on Fig. 2.1	Mine Locality		Dates of working	"Ore" Minerals	Element Assay	Description
3	Loch Arail NR 8080 7950	A	---	galena and pyrite	---	Several small trials for lead ore have been made on thin quartz veins,but none is of any importance
		B	---	galena and chalco-pyrite	---	A quartz vein about 66cm wide and mainly of quartz.
		C	---	galena	---	A vein consists of quartz, about 25-51cm wide.
		D	---	galena	---	The vein is about 66cm wide and mainly of quartz.
4	Stroncullin NR 8430 7910		---	galena,sphalerite chalcopyrite and pyrite	Cu 2.2 wt% Zn 14.6 wt% Pb 21.5 wt% Ag 6 oz/t Au 7.05 oz/t	The vein consists of quartz.
5	Artilligan Burn NR 8535 7749		---	sphalerite	-----	The old mine is about 537m up the Artilligan Burn
6	Erins NR 8575 7538		---	---	---	A white quartz vein about 51-56cm wide.

Table 2.1 : Continued.

No. on Fig. 2.1	Mine Locality	Dates of Working	"Ore" Minerals	Element Assay	Description
7	Coire Mhair NR 7980 7200	---	chalcopyrite and sphalerite	--	The vein is about 2m wide and the fillings consists of dolomite and quartz.
8	Kilmartin NM 8200 9999	c. 1793	chalcopyrite	Cu 30.31 wt%, Ag 1 dt & 7g/t, Au 6 g/t	The veins are small and occur in a large epidio-rite sill. The chief vein is about 10cm wide and consists of calcite and quartz.
9	Coillie Bhraghad NN 9945 0115	1815-1867	pyrrhotite, pyrite, chalcopyrite and pentlandite	Cu 7wt%, Ni 10.01 wt%, Co 1.02 wt%	The ore were thought to be of metasomatic origin.
10	Craignure NN 9945 0115	c. 1845	pyrrhotite, pyrite, chalcopyrite and pentlandite	Cu 7.08 wt%, Ni 10-20 wt%, Co 1 wt%	Seams about 10cm thick and 60m along strike.
11	Inveryne NR 9195 7565	--	chalcopyrite	Cu 8.2 wt%	A vein about 2.8m wide.
12	Tigh-an-rathaid NR 9300 7750	--	--	--	A few small levels.
13	Murder Lode (Kilfinan) NR 9400 7900	1911-1917	chalcocite, mala-chite and bornite	Cu 8.2 wt%	51-76cm thick and 10m long pods extend for 7 km along strike.
14	Castle Town NR 8868 8490	c. 1912	pyrite, galena and chalcopyrite	Au 4 dt/t	A north-east vein about 1.5m wide consists mainly of quartz.
15	Abhainn Srathain NR 8340 7375	c. 1800	chalcopyrite, pyrite and malachite	Cu 1 wt%	12 trials within an area of 0.15 km, about 1-2 km south of Meall Mòr.

Table 2.1 : Continued.

No. on Fig 2.1	Locality Name	"Ore" Minerals	Element Assay	Description
I	Eagles Fall NN 2240 1420	galena and baryte	---	The vein consists of a few stringers of baryte and siderite, and is associated with basaltic dyke.
II	Achadunan NN 2055 1300	galena	---	Two veins, the first one consists of about 2.5cm of baryte, while the second is of siderite.
III	McPhun's Cairn NN 0890 0320	pyrite, galena and sphalerite	Ag 11 dt&18 g/t Au 1 dt&7 g/t Zn 3.5 wt% Pb 3 wt%	A band of schist 6m wide, consists of siliceous bands reaching up to 1.5m in width.
IV	Bridgend NN 1190 9790	galena	---	The vein is about 1.5m wide, and is associated with a felsite dyke.
V	Kames NR 9155 8930	pyrite,chalco-pyrite and galena	---	A quartz vein, about 6.4 km east of Lochgilphead.
VI	Doire-nan Caorach NR 9500 8020	malachite	---	Copper ores associated with limestone.

Table 2.2 : Summary information on the (unworked) mineralised localities in the Loch Fyne district.

Generally, prospecting for lead, zinc, copper and nickel in
this area seems to be prior to the Sixteenth Century though mining
activity apparently did not reach its zenith until the Eighteenth
Century. During that earliest time of prospecting it was considered
that the east side of Loch Fyne was of less economic value than the
west side until a few years before the First World War when the
Otter Company discovered copper ores north-east at Inveryne (NR 9195
7565).

The ore deposits in this region are usually associated with the
Ardrishaig Phyllites and the underlying quartzites and were thought
to be either vein type or metasomatic replacements (metallic
sulphide replacing limestone) and/or of magmatic segregations in the
case of copper ores. The veins vary from mere stringers to 2.5 or 3
metres in width and in many cases they consist of either quartz or
calcite and to a lesser extent of siderite. Many of these veins
trend north-east, but others have north-west and east-west trends.
The amount of precious metals occurring in these veins is rather
higher than the average for Scotland especially at Stronchullin (NR
8430 7910), which yields on assay, gold to the average value of 2 oz
to the ton and up to 4 oz to the ton.

2.3 ABHAINN SRATHAIN MINE

The old mines are situated on the sides of the Abhainn
Srathain, in a gorge known as Eas Cruach nan Cuillean about 3km
south-west of Erins.

Several trials have been made (Wilson and Flett 1921); the
lower one is about 114 metres up the gorge. It consists of a level
driven along a quartz-schist containing specks of copper ore. A
little overhead stoping has been done at the end of the level, and a
shaft was sunk, but it is now full of water. About 38 metres
further up another level has been driven in a north-west direction
along the strike of the quartz-schist that contains chalcopyrite.

Other small levels have been driven north-east along the schist band that bears pyrite. The "Old Copper Mine", shown on the six-inch map (Fig. 1.2), consists of a shaft, now full of water (Plate 2.1). There is another shaft about 190 metres farther along the strike.

Plate 2.1 : The Abhainn Srathaın copper mine south of Meall Mór
(NR 8340 7375).

CHAPTER 3
THE GEOLOGICAL HISTORY OF THE DALRADIAN
HOST ROCKS

3.1 INTRODUCTION

The Dalradian Supergroup is known to host the highest number of significant base metal showings amongst the main rock divisions in Scotland. The majority of these occurrences are hosted by the Middle Dalradian Easdale Subgroup, notably in the Ardrishaig Phyllite or its lateral equivalent the Erins Quartzite (Fig. 4.1). The latter formation is the host to the present studied Abhainn Srathain copper mineralisation.

In the first three sections of this chapter, a brief summary of the geological history (sedimentation, structure, metamorphism and tectonism) of the Dalradian Supergroup, based mainly on reviews of Caledonian and Dalradian geology, Harris and Pitcher 1975, Harris et al. 1975, Harris et al.1978, Harris et al. 1979, Bowes and Leake 1978, Anderton et al. 1979, Anderton 1977, 1982 and 1985, Johnson 1983 and Graham and Harte 1985, is given with emphasis placed on the Middle Dalradian Group, in order to provide a background to their geological setting that could throw a light on the characteristics and genesis of the mineralisation. The fourth section of this chapter is a summary of the geology of the studied area, Meall Mór.

3.2 THE GRAMPIAN HIGHLANDS

Scotland can be divided geologically into five regions namely: (1) the Southern Uplands, (2) the Midland Valley, (3) the Grampian Highlands, (4) the Northwest Highlands and finally, (5) the Hebridean Craton. They are separated by the Southern Uplands Fault,

the Highlands Boundary (Border) Fault, Great Glen Fault, and the Moine Thrust respectively (Fig. 3.1).

The Grampian Highlands, an area of 25,000 km^2, is dominated by the lithologically diverse Dalradian Supergroup (Cowie et al. 1972). This Supergroup is of late Precambrian to early Ordovician age and was deposited in a 250km wide basin oriented northeast-southwest on the southeast margin of the Laurentian Continent. The deposition of the Dalradian sediments was interrupted on occasion by the eruption of volcanic rocks. The whole sedimentary pile was then deformed and metamorphosed during the Grampian Orogeny which represents an early stage of the Caledonian Orogeny.

The Highlands comprise the highest land in Britain. Ben Nevis reaches (>1200m) O.D. and a considerable area in the Cairngorms exceed 1000m above sea-level (Johnstone 1966). Many of the summits of the remainder of the mountainous area reach or exceed 600m . Two contrasted types of mountain-scenery are presented in the Grampian Highlands and their evolution was reviewed in detail by Sissons (1976). In the Cairngorm area and around Glen Clova great relicts of an uplifted peneplain still remain. Towards the southwest, it passes into a more highly dissected type of crests and ridges.

During the maximum Pleistocene glaciation the Grampian Highlands were a great centre of ice dispersal with the main distribution-centre situated in the western half of the region. As a result of this glaciation, the Highland peneplain is deeply dissected forming an extremly rugged mountainous landscape with peaks and ridges separated by glacially overdeepened valleys, now housing the great lochs.

3.3 THE DALRADIAN SUPERGROUP

The British Caledonides were divided by Read (1961) and Kennedy

1958) into early and late zones, which were then named by Dewey (1969), the Orthotectonic (the Northern Belt) and the Paratectonic (Southern Belt) Zones respectively (Fig. 3.2), separated by the Midland Valley Graben. The Southern Caledonian Belt includes the Southern Uplands of Scotland, the Lake District, Isle of Man, Wales and the Northern Caledonian Belt includes Palaeozoic rocks to the southeast of the Moine Thrust and consists of two great metasedimentary assemblages, the Moine and Dalradian (Johnstone 1975 and Harris and Pitcher 1975). The Moine occupying the northern two-thirds of the belt and consists of a monotonous sequence of psammite and pelite (Johnstone et al. 1969) of probably middle to late Proterozoic age. These Moine rocks suffered earlier deformation and metamorphism about 730 Ma ago (Powell 1974, Van Breemen et al. 1974 and Phillips et al. 1975) and/or possibly about 1000 Ma ago (Brook et al. 1977 and Brewer et al. 1979). The remaining southern one-third of the belt is occupied by the Dalradian Supergroup.

The Dalradian Supergroup of Britain extends from the Banffshire Coast through the Central Highlands into the Southwest Highlands (Fig. 3.3) and the large islands of Islay and Jura. This Supergroup is about 20-25km thick (Harris et al. 1978 and Anderton et al. 1979), although its original thickness may have been in excess of 30km regarding the suggestion of thinning (20-80 %) caused by deformation as explained by Borradaile and Johnstone (1973), Borradaile (1973 , Roberts (1974) and Harris et al. (1976). The sediments are lithologically diverse, mainly metasedimentary and metaigneous rocks, which were accumulated between the late Precambrian (Upper Riphean) and Cambro-Ordovician (c. 500 m.y.) and underwent polyphase deformation and metamorphism during the Grampian Orogeny.

3.3.1 Stratigraphy and Sedimentation

In order to study such an extended outcrop, the Dalradian Supergroup was divided into four groups separated by distinctive

17
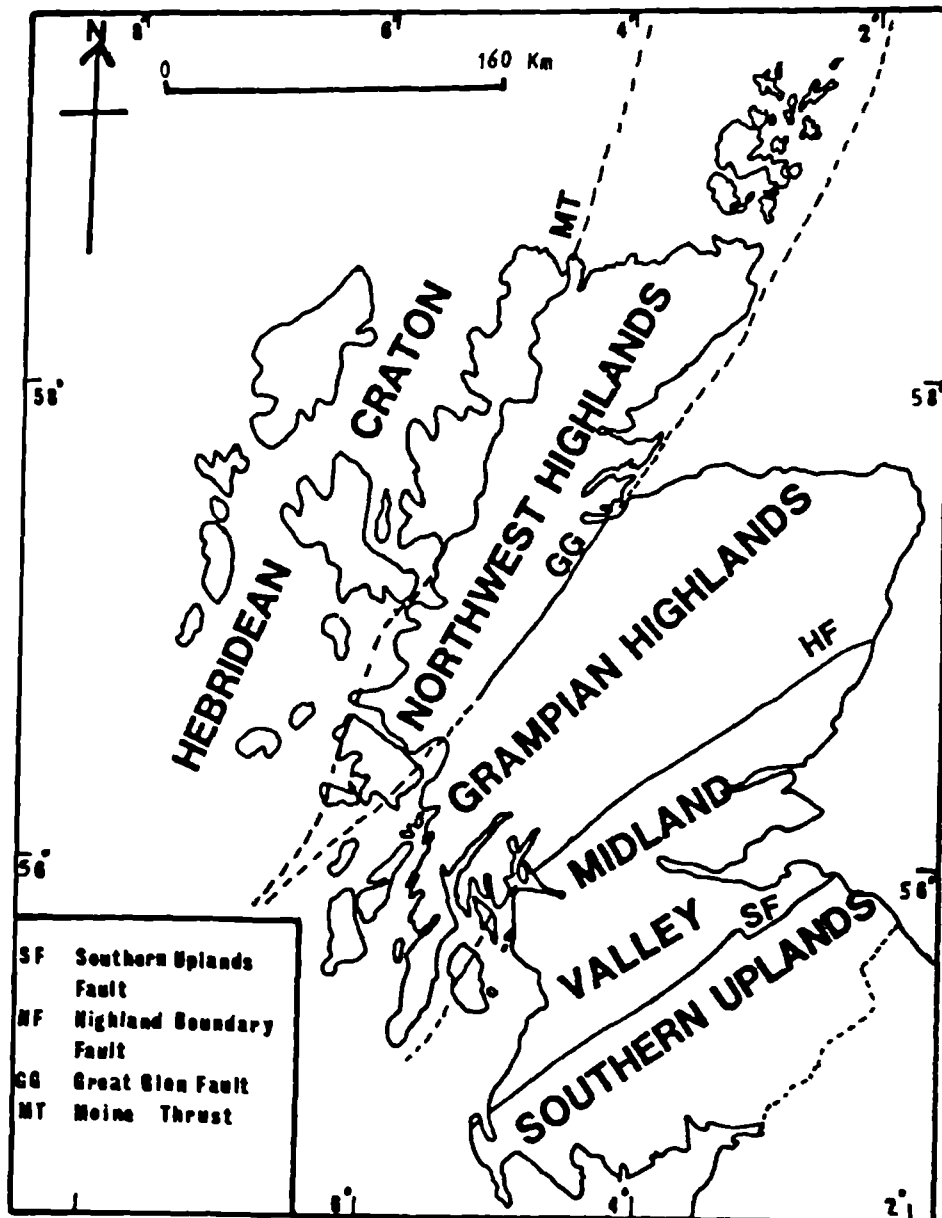
Fig. 3.1 : The geological subdivisions of Scotland taken from
Johnstone 1966 with few modifications.
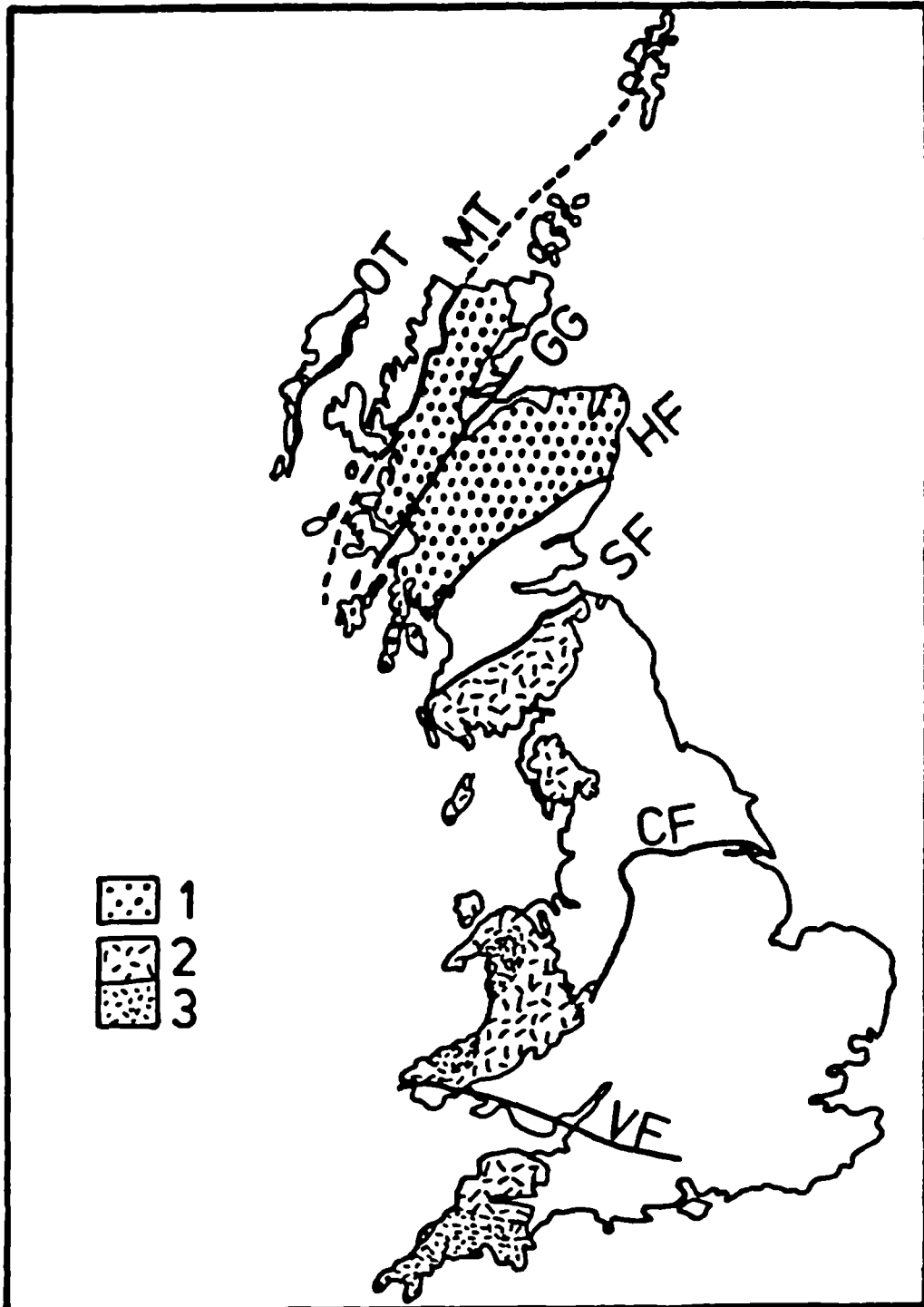
Fig 3.2 . Metamorphic rocks of the British Caledonides.
1,northern belt.2,southern belt,weakly metamor
phosed.3,southern belt,greenschist facies. OT,
Outer Hebrides Thrust. MT, Moine Thrust. GG,
Great Glen Fault. HF, Highland Boundary Fault.
SF, Southern Uplands Fault. CF, southern limit of
caledonian effects. VF,Variscan Front.
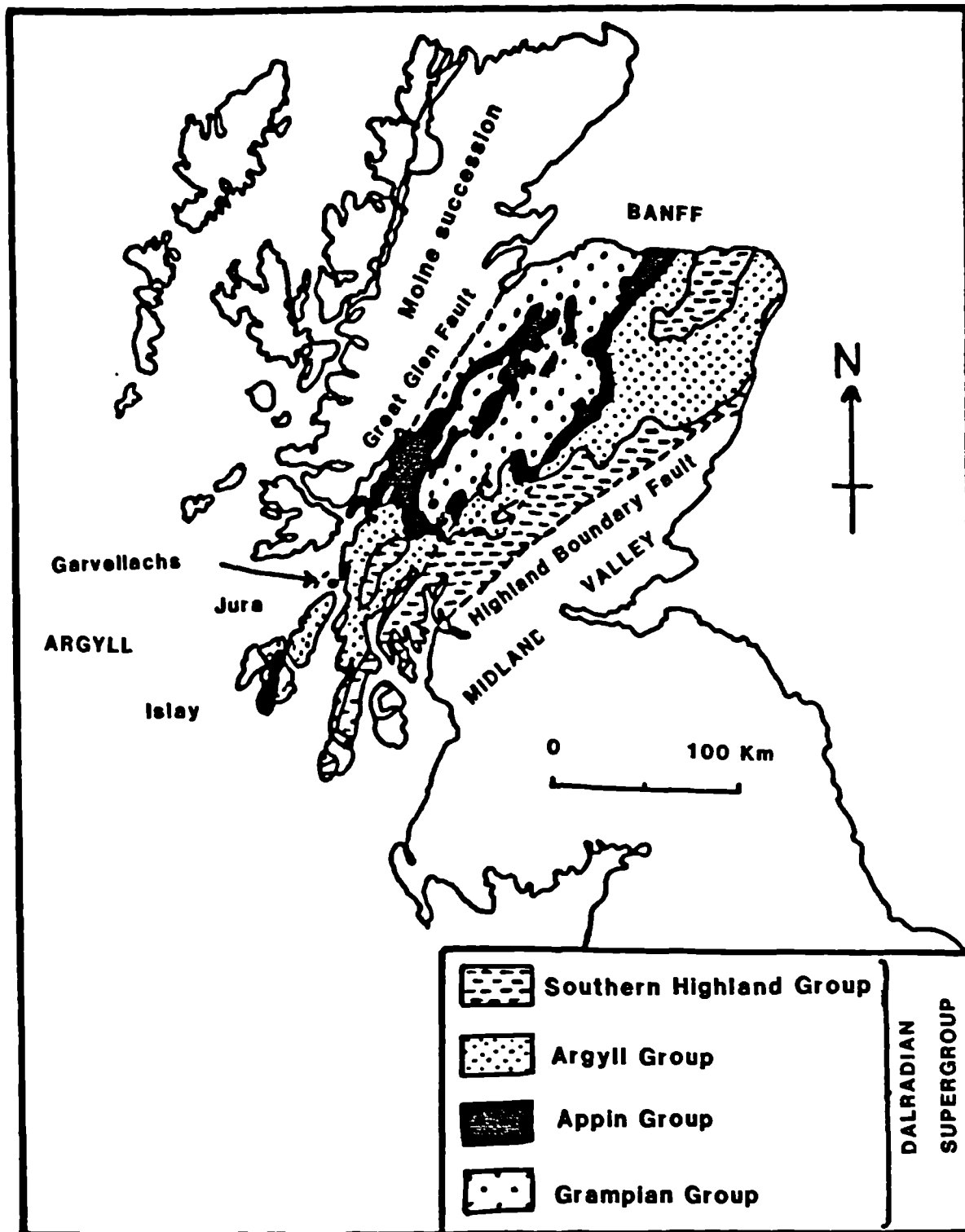
Fig 3.3 : Outcrop map of Dalradian rocks in Britain,
taken from Anderton et al 1979.

marker-horizons (Table 3.1) and every group is further subdivided into individual subgroups on the bases of particular lithological or sedimentological characteristics. Each subgroup consists of several formations, which are of local status only and this implies many correlation problems. As the Dalradian Supergroup in the central area, in Argyll and Donegal (Table 3.1), exhibits the least deformed and metamorphosed rocks, it has been used as a type area for the whole of the Dalradian (Anderton et al. 1979). Accordingly, in the following summary, the Dalradian subdivisions will include the names of the type area together with some local equivalents. The stratigraphic succession of the Scottish Dalradian is divided into four groups namely: the Grampian (oldest), Appin, Argyll and Southern Highland Groups, each of which will be summarised in more detail in the following sections.

(1) The Grampian Group

Although the base of the Dalradian is not visible in Scotland, it may overlie Moine rocks in Ireland and hence the date of initiation of Dalradian sedimentation can only be guessed. It is unlikely to be younger than 700 Ma (Dunning 1972) and may be as old as 800 Ma (Brook et al. 1977). The Grampian Group (Harris et al. 1978) represents the lowest group in the Dalradian and was formerly named (Harris and Pitcher 1975) the Central Highlands Granulites and included within the Moine. This was questioned by Thomas (1980) and Haselock et al. (1982). Also Anderton (1985) pointed out that geochemical differences between Grampian and Appin Groups, together with the discussions given by Piasecki (1980) and Lambert et al. (1982) are sufficient to regard the Grampian Group as a separate stratigraphic unit within the Dalradian.

The sediments were originally silts and muds interbedded with poorly sorted, immature, locally pebbly quartz and feldspathic sands, with cross stratification, ripple marks, grading and erosional features indicating derivation from the south and
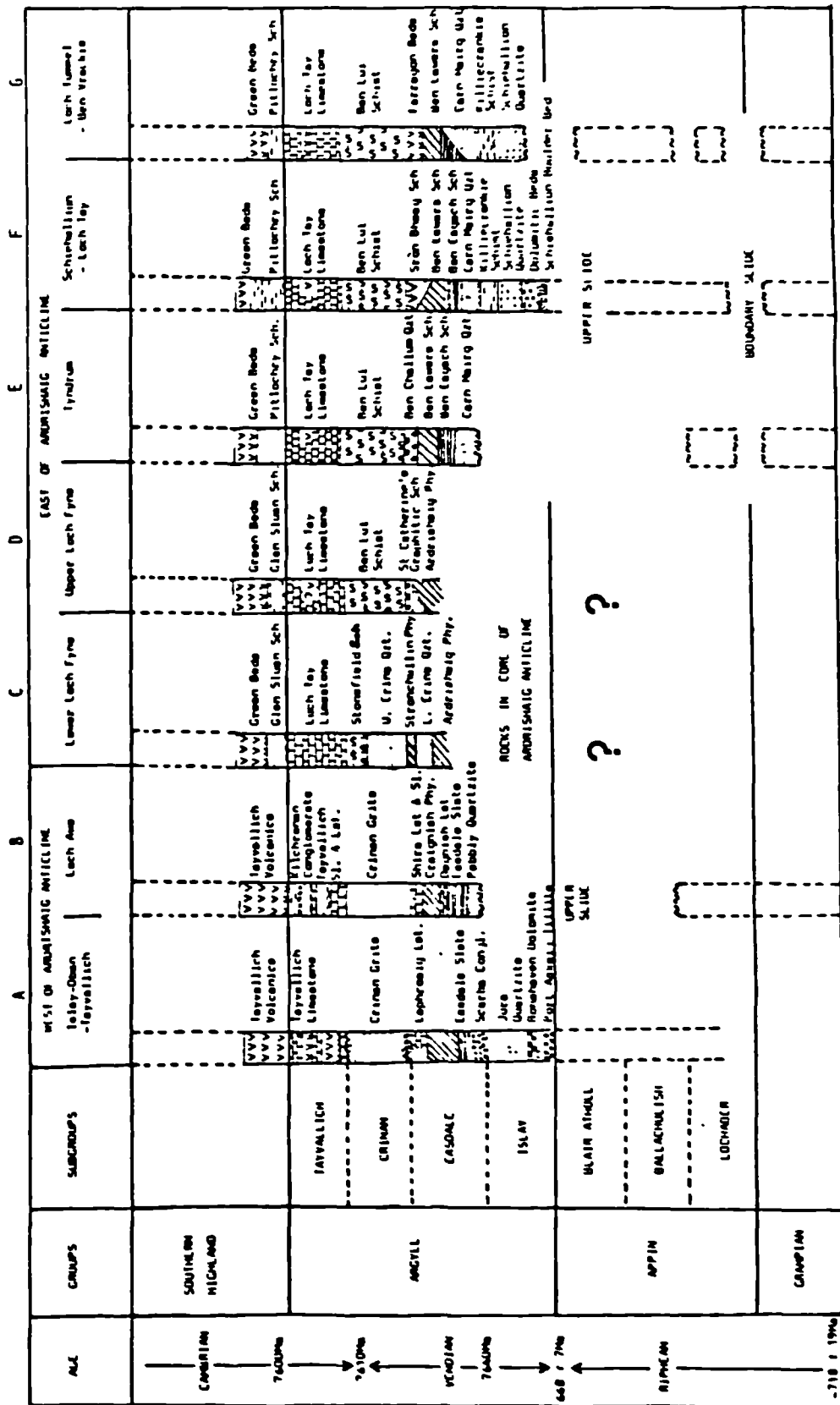
Table 3.1: The stratigraphic subdivision of the Dalradian Supergroup in the Southwest and Central Grampian Highlands — succession present, but only formations in the Argyll and lower part of the Southern Highland Groups are shown. ⌐ = tectonic slide, vvv = metabasite, interpreted as extrusive volcanics. Column A refers to the West Coast, the area of lowest metamorphic grade. This table is taken from Willan 1983.

deposition from northerly-flowing currents in tidal flat or deltaic environments Hickman 1975 and Thomas 1980).

(ii) The Appin Group

The boundary between the Grampian and Appin Groups in the Appin area is shown to be significantly diachronous (Hickman 1975). This group is consists of mud and limestones (now metamorphosed to quartzite and slates or schists). Stromatolites are found in the uppermost limestone, the Lismore Limestone. Many formations can be traced for considerable distances, although lateral facies changes are recognised (Litherland 1970 and Smith and Harris 1976). However, the presence of shallow-water sedimentary structures and the palaeocurrent data, are consistent with a shallow shelf origin (Anderton et al. 1979). In slates of the Ballachulish Subgroup, pseudomorphs after gypsum are evidence of local high seawater salinity in the enclosed Dalradian Basin (Hall 1982).

(iii) The Argyll Group

Islay Subgroup

The base of the Argyll Group is marked by the Port Askaig Tillite(Kilburn et al. 1965, Spencer 1969 and Howarth 1971). It can be traced for nearly the whole length (~660km) of the Dalradian outcrop from Conemara to Banff, but it is not found in Shetland. It can be correlated with the Varangian or Eocambrian Tillite found throughout the Caledonian Belt and dated in Finmark at 670 Myr (dated by Pringle 1972). In the Garrvellachs-Easdale area, the Port Askaig Tillite (c. 750m thick, Spencer 1971) contains up to forty-seven beds of tillite separated by siltstones, dolomites, conglomerates and cross- bedded marine sandstones and quartzites. They were deposited from floating and grounded ice sheets derived from a metamorphic and granitic terrain to the southeast (Spencer 1975 and Anderton 1980b). Eyles and Eyles (1983) suggested a

glaciomarine, rather than a grounded ice-sheet origin for part of the Port Askaig Tillite.

Following the Port Askaig Tillite, Dalradian deposition started to follow some new trends. Very thick formations are found and major lateral facies changes become important. Deep-water facies are first found and a tectonic control on sedimentation becomes evident (Anderton 1974 and 1979).

The Islay Subgroup, with its oldest unit the Bonahaven Dolomite is composed of dolomitic shales, siltstones and sandstones (Spencer 1971) normally 30-80m thick, but 300m in Islay (Spencer and Spencer 1972) where it was deposited in a semi-restricted coastal zone of lagoons and tidal flats (Fairchild 1980 a&b). Within these dolomitic rocks are abundant stromatolitic algal deposits (Hackman and Knill 1962 and Spencer and Spencer 1972) and the depositional environment was interpreted as shallow sub-tidal to supra-tidal in a hot dry climate. In the Loch Creran area the Port Askaig Tillite is absent and the base of the Islay Subgroup is marked by the earliest recorded turbidites and chlorite-albite-epidote schist (the Green Beds) in the Dalradian (Section 3.3.2). These were interpreted as sediments with volcanic conglomerate, possibly basic tuffs (Litherland 1980), and together with the turbidites are evidence of a dramatic onset of instability resulting in the formation of the first deep water, second order, basins in the Dalradian. Overlying the Bonahaven Dolomite, is the Jura Quartzite, which shows considerable lateral variation, both in thickness and facies. In Jura this quartzite reaches 5km, but it thins rapidly northeast (Knill 1963). It was deposited on a tidal shelf subsiding along a hingeline in the Scarba area (Anderton 1974 & 1976).

In the Schiehallion-Pitlochry district, the Islay Subgroup is represented by part of the Perthshire Quartzite Series; the Schiehallion Quartzite and the Killiecrankie Schist (Heterogenous Schist of Bradbury et al. 1979).

A major break in depositional conditions occurred at the top of the Jura Quartzite and is reflected in significant variations in both thickness and facies in the succeeding formations, which can often be related to tectonic hingelines and can best be interpreted as the result of major syndepositional faults defining the margins of small turbidite basins. Syndepositional movement of several kilometres along these faults occurred and from mid-Argyll times onwards the movement of such faults was probably the major control over sedimentation (Anderton et al. 1979).

Easdale Subgroup

The transition from the Islay to the Easdale Subgroup marks the first basin-deepening event in the Dalradian. The base of the Easdale Subgroup is defined by the Scarba Conglomerate, mainly comprising turbidite deposits which fine northwards, from the Islay-Jura area towards Kerrera (Baldwin and Johnson 1977). To the east of Islay-Oban-Tayvallich overlying the Easdale Slate is the Carn Mairg Quartzite (Table 3.1). It consists of coarse, often graded pebbly quartzites. The rapid, probably fault-controlled, subsidence during Carn Mairg Quartzite times, and a possible marine transgression towards the northwest, resulted in a sediment starved basin in which up to 500m of carbonaceous mud accumulated with dark limestone forming the Ben Eagach Schist. The presence of graded pebbly quartzites and thin sands with minor hornblende schist within the Ben Eagach Schist indicate continuing instability and a relatively deep water environment. The Ben Eagach Schist hosts the Aberfeldy Ba, Zn, Pb deposits.

In the Islay-Oban-Tayvallich and Loch Awe area, the deep basins seemed to be filled up, as shown by the succeeding sediment, the Craignish Phyllite, which includes shallow marine and tidal flat facies with gypsum pseudomorphs (Anderton 1975). To the east of the Ardrishaig Anticline, in the Loch Fyne area, is the Ardrishaig Phyllite correlated with the Craignish Phyllite (Roberts 1966) to

the west and with the Ben Lawers Schist to the east. The Ben Lawers Schist and the Ardrishaig Phyllite were deposited in a relatively deep second order basin, separated from the Craignish Phyllite by the Loch Fyne carbonate ridge. The Ben Lawers Schist hosts the Perthshire Pyrite Horizon, whereas the minor Coillie Bhraghad, Craignure and McPhun's Cairn mineralisations are found within the Ardrishaig Phyllite.

In Loch Tummel-Ben Vrackie area the succeeding formation is the Farragon Beds a 400m succession of hornblende-schist, green beds, quartz- mica schist and quartzite. This represents the first metabasite horizon in the Dalradian. At the same horizon is the Sron Bheag Schist which again consists of hornblende schist and green beds mixed with calcareous quartzite and schist. In the Tyndrum area is the Ben Challum Quartzite (Smith et al. 1981) hosting the Auchtertyre and Ben Challum sulphidic horizons. In the Loch Fyne area, the lateral equivalent of the Ben Challum Quartzite, is the St. Catherine's Graphitic Schist, correlated on lithostratigraphic grounds with the Stronchullin Phyllite (Clough et al. 1911 and Roberts 1966) of Knapdale and in turn correlating the Lower Erins Quartzite to the Ardrishaig Phyllite (Smith et al. 1978).

Crinan Subgroup

This subgroup is composed mainly of turbidites with great thickness and facies variations, which again involve deepening of the basin as a result of syndepositional faulting. This led to the deposition of turbidites with northeast flowing palaeocurrents (Knill 1963) together with rare tuffaceous sediments, carbonate and mud containing pseudomophs of reworked gypsum (Barraclough 1981).

The Crinan Grits are correlated with the Upper Erins Quartzite (Peach 1930 and Roberts 1966 and 1977) which forms a thick sequence of rather fine-grained quartzites in Knapdale and North Kintyre and

can be traced along strike towards the head of Loch Fyne, where it wedges out to give way to the Ben Lui Schist. Associated with the Ben Lui Schist are abundant metabasaltic layers which are probably high level intrusions (Wilson and Leake 1972). Within the Crinan Grits is the Garbh Achadh Cu-mineralisation and the Upper Erins Quartzite, which hosts the Knapdale Pyrite Horizon and the Meall Mór copper mineralisation.

Tayvallich Subgroup

Increasing instability in the deposition of the Argyll Group became more evident by the first volcanic outburst (Gower 1973) that led to the deposition of tuffs interbedded with shallow water limestone, the Tayvallich Limestone, whose base could define the boundary between Cambrian and Precambrian (Downie et al. 1971) and is taken as a marker horizon between the Argyll and Southern Highland Groups (Rast 1963 and Knill 1963). The Loch Tay Limestone is a lateral equivalent of the Tayvallich Limestone (Bailey 1938 and Roberts 1966) and hosts the Kilfinan, Clachan Bheag and Tom na Gobhair mineralisations.

At the southern end of the Tayvallich Penisula and on the adjacent small islands, the Tayvallich Volcanics, form part of the Tayvallich Subgroup and not the basal unit of the Southern Highland Group.

(iv) The Southern Highland Group

Increasing extension and instability noted in the Argyll Group, reached its climax by the eruption (dated 600 Ma, Anderton 1980a) of the Tayvallich Volcanics and the opening of the Dalradian Ocean (Anderton 1980a & 1982) which was first christened by (Harland and Gayer 1972) as the Iapetus Ocean. The Tayvallich Volcanics are a 2km thick sequence of basaltic lavas and tuffs with minor interbeds of marine limestones, grits and slates. They show excellent pillow

structures (Borradaile 1973), and in places the lava seems to have been intruded into a wet sediment beneath the sea floor. Above this is the green beds of lava, sporadic tuffs and resedimented volcanic material. Of similar mineralogy and chemistry are a large number of sill and dyke bodies within the Argyll Group which were considered probably contemporaneous with these lavas (Graham 1976). However, Anderton (1985), interpreted the sill pile in the Islay-Loch Awe area as being intruded progressively from bottom to top during Easdale and Crinan Grits Subgroups times, each sill being injected at a shallow depth into soft sediment, a process similar to that now forming the quasi-oceanic crust at the head of the Gulf of California (Fig. 3.7).

The Loch Avich Grits is about 1.1km thick and composed of chloritic grits, green slates and subordinate black slates. It overlies the Tayvallich Lava but chemically has higher MgO/Fe_2O_3 ratio (Fe_2O_3 represent total iron).

The youngest rocks affected by the Grampian Orogeny, i.e. the top of the Dalradian and Cambro-Ordovician Sequences, are of lower Ordovician (Arenig or Llanvirn) age. The Dalradian is unconformably overlain by lower Old Red Sandstone in Scotland.

3.3.2 Dalradian Metabasites

Pretectonic igneous activity within the Dalradian Supergroup of Scotland finds its most voluminous expression in the "epidiorites" of the Argyll and Southern Highland Groups. Their distribution (Fig. 3.4) shows that they are best developed in the Southwest Highlands and to a lesser extent in the Loch Tay-Portsoy area. Dalradian metabasites of the Southwest Highlands constitute an abundant, about 5km thick, broadly contemporaneous, and comagmatic suite of doleritic and gabbroic sills and overlying submarine lavas (Borradaile 1972, Wilson and Leake 1972 and Graham 1974) all of probable Lower Cambrian age (Downie et al. 1971 and Borradaile

28
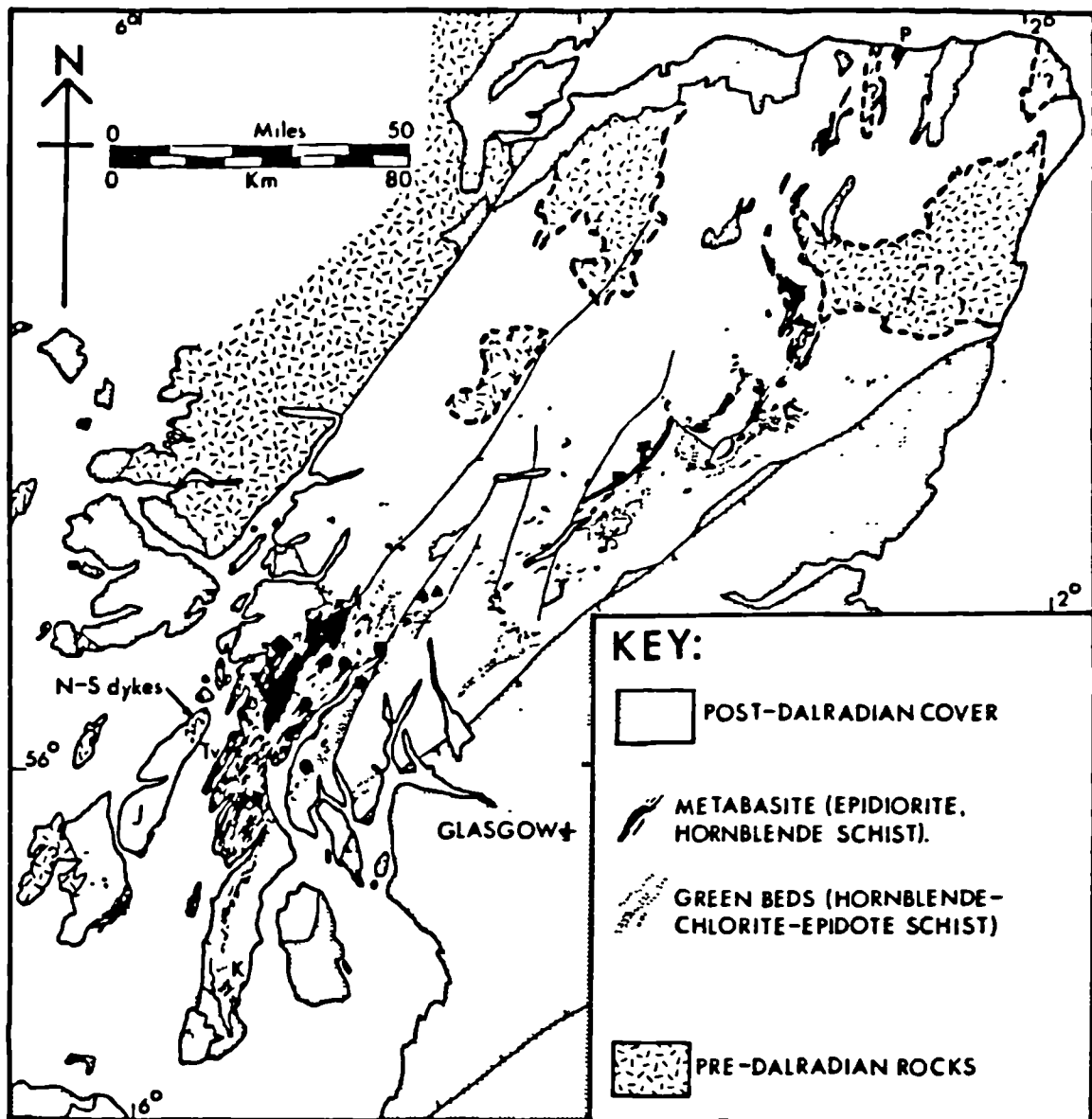
Fig 3.4 : Distribution of deformed and metamorphosed basic rocks

in the Grampian Highlands.TV Tayvallich, P Portsoy,

K Kintyre, J Jura. From Willan 1983.

1972). They have undergone polyphase deformation and metamorphism (Wiseman 1934 and Graham 1974) during the Caledonian Orogeny. On the bases of field and textural relationships they can be classified into eruptive lavas and pyroclasts (Tayvallich Volcanics and Loch Avich Lavas of the Southern Highland Group) and intrusive bodies mainly within the Argyll Group.

(i) Extrusive metabasites

A series of eruptive rocks, now metamorphosed to chlorite grade, are exposed in the core of the Loch Awe Syncline and also along the Sound of Jura, south of Carsaig. They show very well developed pillow structures (Peach et al. 1911, MacGregor and Roberts 1963, Wood 1964, Mercy 1965 and Borradaile 1973). The first eruption in the Dalradian Supergroup is marked by the 2km thick Tayvallich Volcanics which are chemically tholeiitic lavas with minor spilites (Wilson and Leake 1972 and Graham 1974) now metamorphosed to calcite, quartz, albite, chlorite and epidote assemblages. Later outbreaks include the Loch Avich Lavas (Borradaile 1973), consisting of more than 500m of tholeiitic basaltic lava similar to the underlying Tayvallich Volcanics but comparably more felsic. Of lateral equivalence to this eruptive suite is the " Green Beds " (Roberts 1966) which are considered by Phillips (1930), Roberts (1966) and Van de Kamp (1970) to constitute intermediate metabasic and pelitic material. However their lack of igneous textures and their gradational contacts with the surrounding metasediments suggest an origin either as basic tuffs, or eroded volcanic material mixed with sedimentary detritus.

(ii) Intrusive metabasites

The remaining two kilometres of metabasites are found as sheets intruded into the sedimentary sequence below the Tayvallich Volcanics mainly in the Easdale, Crinan Grits and Tayvallich Subgroups. The Upper Erins Quartzite, the host to the present

studied copper mineralisation, contains several tabular amphibolite bodies belonging to this group. These will be described later in Sections (3.4.1, 5.3.8, 5.3.9 and 6.7). The distribution of these intrusive sheets shows that they are very well developed in the vicinity of the Loch Awe Syncline axis. The intruded bodies are about 140m thick and are composed of tholeiitic basalt and doleritic sills and a few dykes, chemically similar to the main overlying Tayvallich Lavas. The intrusion of these bodies as sills rather than dykes could indicate intrusion into a thick pile of wet, unlithified sediment (Graham 1976) and some of these intrusions, particularly the north-south oriented dykes of Jura, could represent feeders to the Tayvallich Lavas.

3.3.3 Metamorphism

The Dalradian Supergroup underwent polyphase deformation and metamorphism during the Grampian Orogeny (Johnson 1963, Rast 1963, Rast and Crimes 1969 and Lambert and McKerrow 1976) which was one of three orogenic episodes (named by Wright 1969 : Celtic, Grampian and Cymrian). Each is localised in time and place and together they constitute the Caledonian Orogeny. Regional metamorphism of the Dalradian rocks has been the subject of several studies starting with Barrow (1893 and 1912), who studied the progressive regional metamorphism in the pelitic rocks of the Dalradian in the Southeast Highlands, and was able to produce a metamorphic isograd map based on occurrence of certain index minerals.

Following the work of Barrow, Tilley (1925) and Elles and Tilley (1930) continued the isograd map for the Central and Southwest Highlands; while Elles (1931) continued that of the west Banff-nappe area. Phillips (1930) and Wiseman (1934) reported a progressive regional metamorphism study of the Dalradian "Green Beds" and "Epidiorites" respectively. In the Northeast Highlands, Read (1923 and 1925) reported an area of unusual mineral assemblages and he evolved a zonal scheme for what he termed the "Buchan" type

metamorphism.

In summary, two contrasted and classified styles of regional metamorphism the "Barrovian" and the "Buchan", are developed in the Dalradian rocks of the Scottish Highlands. Barrovian metamorphism is characterised by an extensive chlorite zone in the lowest grade areas, and by the occurrence of almandine, kyanite and sillimanite at successively higher grades; it falls within the kyanite-sillimanite facies series (Miyashiro 1961) and the grade rises from low greenschist facies in the South and Southwest Highlands to upper amphibolite facies in the Central Highlands. Buchan metamorphism, also of greenschist to upper amphibolite facies, falls within the low-pressure intermediate facies series of Miyashiro (1961) and can be distinguished by the occurrence of andalusite and corderite in higher grade and by biotite in the lower grade rocks. The boundary between the Buchan and Barrovian provinces is the kyanite andalusite inversion (Chinner 1966, Porteous 1973, Chinner and Haseltine 1979 and Chinner 1980).

Figure (3.5) represents a metamorphic isograd map for the Dalradian rocks in the Grampian Highlands (after Winchester 1974) and the nature and attitude of these isograds are described in detail by Anderton (1977), while Fettes (1979 & 1983) gave a review on the metamorphism of the British Caledonides.

Systematic variations in pressure and temperature are present across the Dalradian rocks, between the Barrovian and Buchan type on one hand, and within the Barrovian rocks on the other hand. Porteous (1973), Fettes et al. (1976) and Graham (1976) showed an increase in pressure within the Barrovian zone towards the southeast. Oxygen isotope work (Kerrick, Beckinsdale and Durham in Atherton (1977)) on Dalradian rocks gives temperatures ranging between 305-588°C. Dalradian rocks in the northwest falling within the lower part of the garnet isograd were metamorphosed at temperature of 535°C and pressure of 5 kb (Richardson and Powell

N

0   50 Km

andalusite zone in
Buchan area only

sillimanite

kyanite

almandine

biotite

chlorite
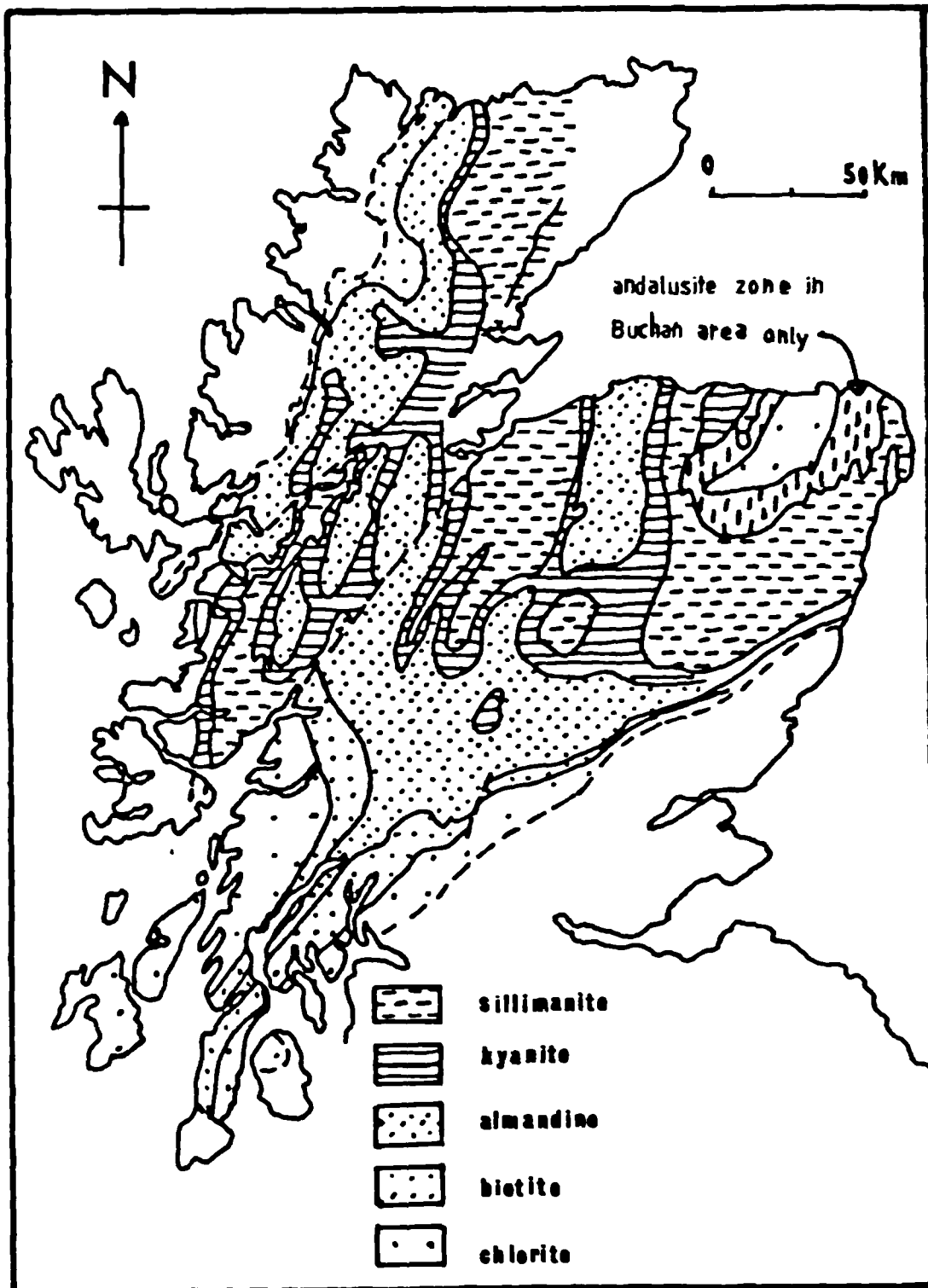
Fig. 3.5 : Metamorphic isograd map (after Winchester 1974).

1976). More recently, Wells and Richardson (1979) propose a temperature of 550-620°C and a pressure of 9-12 kb responsible for the peak of metamorphism in the Central Highlands and Graham (1983 & 1985) propose a temperature of 410-530°C and a pressure of 8-10 kb in the Knapdale region of the Southwest Highlands.

The age of metamorphism can be fixed both relative to the deformation history of the rocks and by radiometric and stratigraphic age dates. However the stratigraphical constraints on the age of the Dalradian metamorphism are poor (Fettes 1983). The youngest sediment affected by the main metamorphism is probably lower to middle Cambrian providing a maximum age of 530-540 Ma. A minimum age of 410-420 Ma is found by the post-kinematic granites and by the nonmetamorphic cover of Lower Devonian Old Red Sandstone. Radiometric data on the age of the Dalradian metamorphism and deformation are available (e.g. Pankhurst and Pidgeon 1976, Bradbury et al. 1976, Harper 1967, Pankhurst 1970 and Lambert and McKerrow 1976), and on the basis of the above data, Fettes (1979), has concluded that the metamorphic climax event had occurred about 490-500 Ma (Lower Ordovician).

3.3.4 Structure

Deformation and uplift of the Dalradian rocks during the Grampian Orogeny had transferred the area into large, NE-SW trending, often tight and isoclinal folds, now presented by the Central and Southwest Highlands (Fig. 3.6). Several phases of deformation can be recognised and their nature is dependent on the structural levels and lithology (Harris et al. 1976) and they can be simply classified into primary and secondary phases.

Several workers studied the structure of the Dalradian rocks in different areas and accordingly various models have been proposed (Roberts 1974, Roberts and Treagus 1977 and 1979, Bradbury et al. 1979, Johnson et al. 1979, Shackleton 1979, Thomas 1979 and
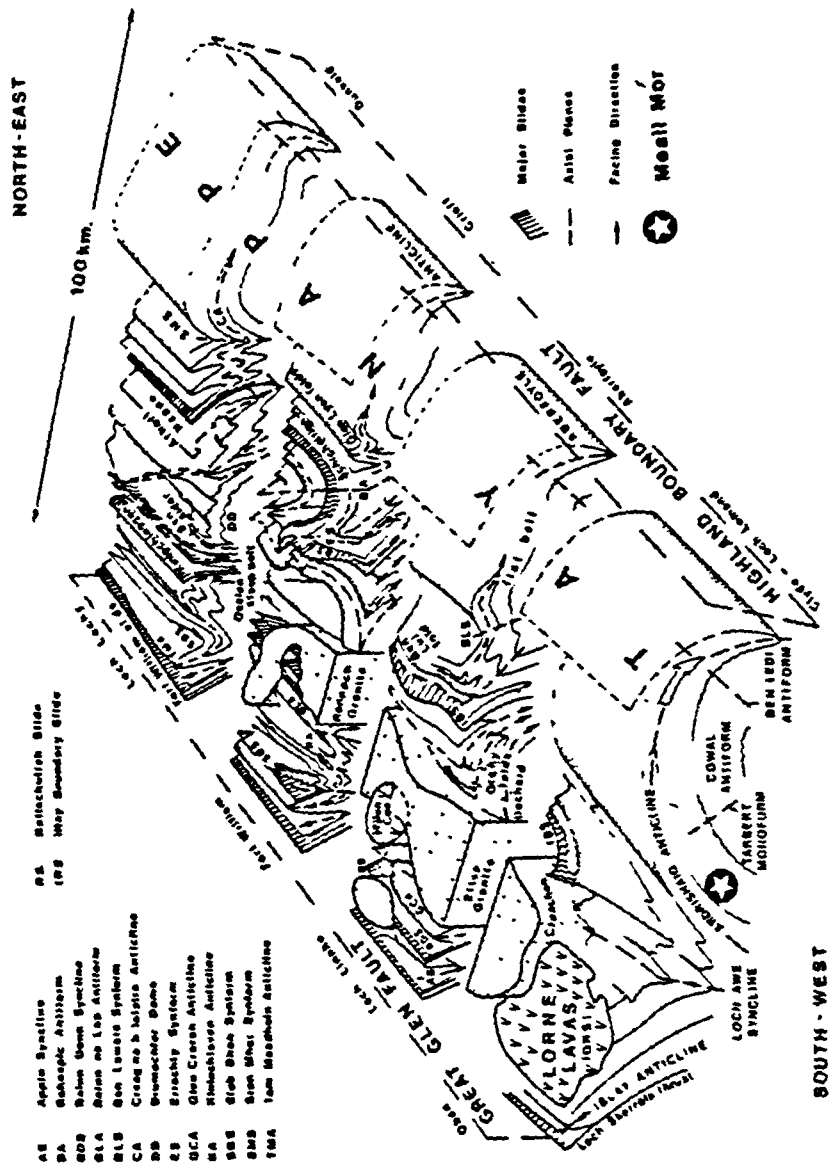
Fig 3.6 : Structural block diagram of major structures in the Southwest and Central Grampian Highlands.
Faults between Great Glen and the Highland border have been removed (from Thomas 1979).

Litherland 1982).

In summary, the regional structure is dominated by an anticlinal nappe (the Tay Nappe) whose upper limb has been removed by erosion and whose lower limb is inverted. The upwards, SE facing root of the Tay Nappe can be traced as the Ardrishaig Anticline through the Loch-Awe-Loch-Fyne district of Argyllshire (Roberts 1974). Its downward facing closure (Aberfoyle Anticline) can be traced along the adjacent Highland Border to the southeast (Shackleton 1958).

Deformational history of the Southwest Highlands can be divided into two parts; primary and secondary (Roberts and Treagus 1964, 1977 and 1979). The primary deformation is associated with the formation of early folds such as the Islay Anticline, the Loch-Awe Syncline and the Ardrishaig-Aberfoyle Anticline, forming an involuted mushroom structure (Rast 1963). The secondary deformation is responsible for the refolding of the primary structures and the formation of secondary ones such as the Tarbert and Ben Ledi Monoforms (Fig. 3.6).

3.3.5 Tectonism

Despite the general agreement that plate tectonics should be applicable to the Caledonian belt, considerable differences in opinion exist regarding the details and accordingly many plate tectonic models have been constructed (e.g. Dewey 1969, 1971 and 1982, Dewey and Pankhurst 1970, Garson and Plant 1973, Phillips et al. 1976, Lambert and McKerrow 1976, Wright 1976, Moseley 1977, Harris et al. 1978, Mitchell 1978, Yardley et al. 1982, Watson 1984 and Dewey and Shackleton 1984). The simplest model, in Anderton's 1982 view, that provides a reasonable basis for the Dalradian evolution, is that of Phillips et al. (1976).

The tectonic evolution of the Dalradian in the British Isles during the late Precambrian to Lower Ordovician can be formulated as follows:

(1) The Dalradian Supergroup was deposited in a basin undergoing subsidence by lithosphere stretching (McKenzie 1978, Le Pichon and Sibuet 1981 and Dewey 1982).

(2) During the Late Riphean, the Grampian and Appin Groups, were deposited on a slowly subsiding, intra-cratonic shelf.

(3) During the Vendian, an increasing rate of crustal stretching, reflected by an increase in instability accomplished by major syndepositional faulting (Harris et al. 1978 and Anderton 1979) started to affect the shelf which by mid-Vendian times or Eocambrian (c. 625 Ma onwards) had been broken into a series of blocks and basins (Argyll Group). In the Southwest Highlands, the Dalradian terrain, developed into a type of quasi-oceanic crust (Fig. 3.7) similar to that now forming at the head of the Gulf of California (Moore 1973 and Soper and Anderton 1984). The spreading centre is suppressed by the rapid influx of sediment and takes place on a limited scale by sill and dyke injection.

(4) Further increase in the crustal tension led, by the end of Precambrian or early in the Cambrian (600 myr), to rupture of the Proterozoic Supercontinent (Piper 1982) and birth of the Iapetus Ocean. This was marked by the extrusion of the tholeiitic Tayvallich Volcanics.

(5) Later subsidence, following abandonment of the incipient rifting centre, accommodated the Southern Highland Group.

(6) As a result of regional thermal subsidence on a spreading margin plus the increasing volume of the mid-ocean ridges, a marine transgression then spread towards the present Northwest Highlands

37
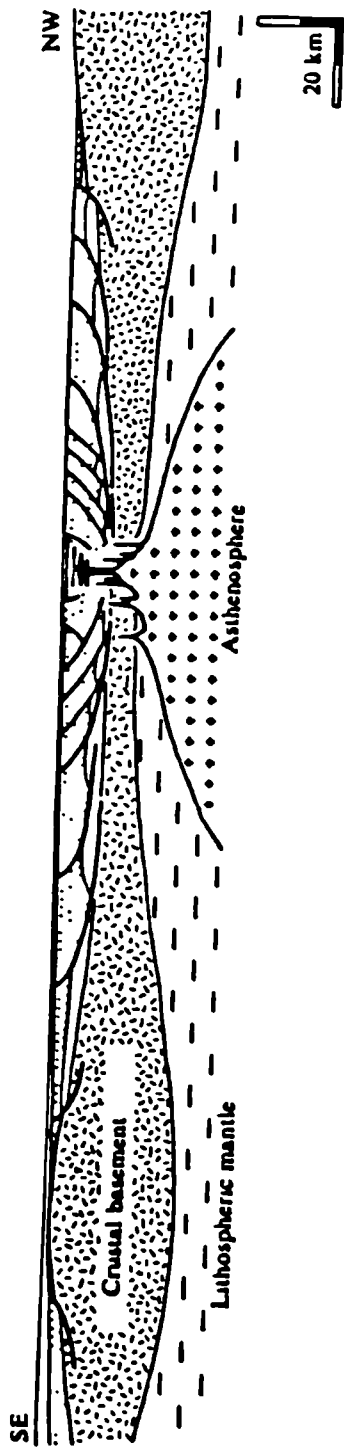
KEY

ARGYLL GROUP

APPIN GROUP

Fig. 3.7 : Sketch illustrating the crustal structure of the Dalradian terrain,in late Argyll Group times,showing listric and other normal faults.Continental crust is on the verge of rupturing with the formation of quasi-oceanic crust by sill and dyke emplacement.Crustal stretching subsequently ceased here,the complete failure of the Laurentian-Baltic plate taking place at another site of crustal attenuation to the soth-east of the area shown on this diagram(from Soper and Anderton 1984).

early in the Lower Cambrian and a blanket of carbonate sediment developed.

(7) As a result of the development of this carbonate platform, the Dalradian terrain became a sediment starved basin in which the mudstones and cherts of the Highland Border Series were deposited.

(8) In the early Ordovician, subduction started along a north steeply dipping subduction zone under northern Britain. Compression above this subduction zone caused the Grampian Orogeny. A phase of extension may have immediately preceded this, allowing the intrusion of ocean floor into the already thinned continental crust and probably the formation of back-arc ophiolitic rocks.

(9) During the Silurian to early Devonian, subduction eventually led to continental collision and final closure of the Iapetus along a line that can be drawn across the British Isles through the Solway Firth and Shannon Estuary. This collision must have been fairly gentle because it did not produce the towering mountain ranges and gigantic nappe structures typical of the Alpine-Himalayan collision Orogeny.

3.4 DETAILED GEOLOGY OF MEALL MÓR

3.4.1 Stratigraphy

Three lithostratigraphic units belonging to the Middle Dalradian Group, are exposed in Meall Mór area (Fig. 3.8) :

(1) Upper Erins Quartzite   (youngest)
(2) Stronchullin Phyllite
(3) Lower Erins Quartzite   (oldest)

The Erins Quartzite Formation is divisible into two portions by

39
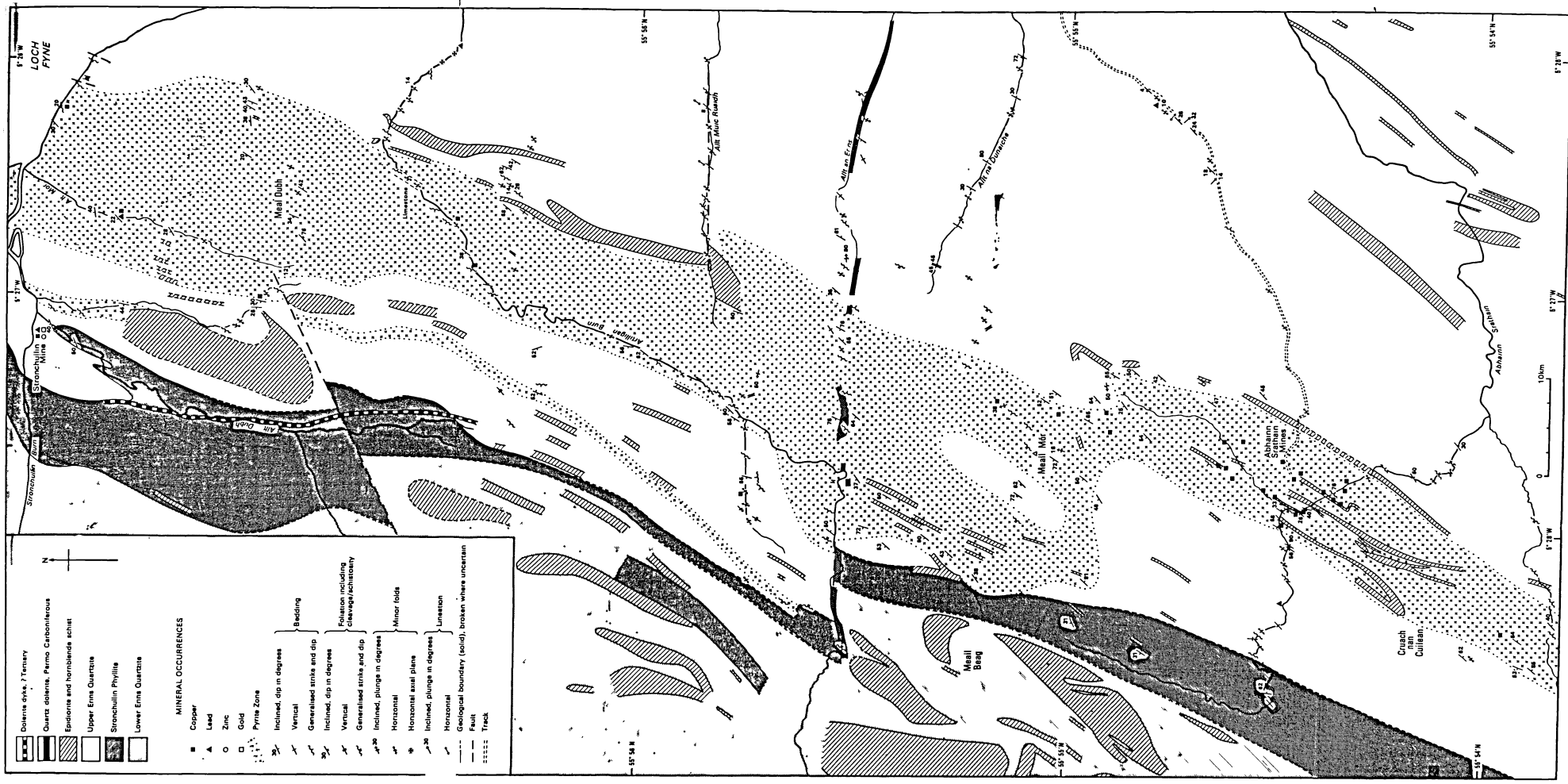
Fig. 3.8 : General geology and mineral occurrences in Meall Mòr, from Smith et al. (1978).

40

the occurrence, near the middle, of a subordinate group of phyllite, the Stronchullin Phyllite. The Lower Erins Quartzite, northwest of the Stronchullin Phyllite Band, is represented by assemblages of siliceous schist with alternating pelitic bands of subordinate mica and quartz schist. Bands and thin layers of limestone, locally quartzose are also common.

The Stronchullin Phyllite consists mostly of interbedded quartzite, quartzose schist, phyllite (occasionally calcareous) and locally developed black graphitic schist mainly in the Stronchullin and Artilligan Burns and in the stream northeast of Meall Bheag (Fig. 3.8). It is correlated with the St. Catherine's Graphitic Schist (Roberts 1966 and 1974) of the northern Loch Fyne succession.

The Upper Erins Quartzite, to the southeast of Stronchullin Phyllite, hosts the Abhainn Srathain copper mineralisation and will be outlined below in detail. The Lower and Upper Erins Quartzites are considered to represent lateral facies variation in the Ardrishaig Phyllite and Ben Lui Schist Formations (Table 3.1).

Upper Erins Quartzite

In the Meall Mór area, the Upper Erins Quartzite, consists of less than 40% true quartzite. It is mainly psammitic with quartz and siliceous schist being the most commonly encountered rock types and a complete gradation from orthoquartzite to mica-schist is present. The quartzite forms massive bands several tens of metres thick, mostly pale green or white, but a pistachio green variety occurs locally where epidote is present. Gritty bands are occasionally seen with clasts up to 4mm across of quartz.

The pelitic units range in thickness from 10cm to several metres, though interbedded psammite and pelite are more common. Identification of the Stronchullin Phyllite as a separate stratigraphic unit would appear to be heavily dependent on the

presence of graphitic schist and since the latter is only locally developed, the validity of the Stronchullin Phyllite as a stratigraphic unit is questionable.

At the southeast shoulder of Meall Mór and in the Artilligan Burn, brownish-weathered metamorphosed limestone bands were noted. Also, fragments of similar rock were noted in the spoil heaps at the site of the old copper mines. The limestone band near Meall Mór is folded and although about 2-4m in thickness, it can not be traced along strike for more than 5-6m. In the Artilligan Burn, the band is about 2m thick and can be traced for 150m along the stream bed. To the east, it passes into dolomitic schist comprising muscovite (30%), dolomite (30%), chlorite, quartz and pyrite.

Epidiorites

The term "epidiorite" was introduced into geological literature by Von Gümbel (1874), and he defined it as a rock composed of pale green fibrous hornblende with plagioclase, chlorite, ilmenite or magnetite, and occasional augite. To British petrographers the name was regarded as a field term and it signified a metamophosed igneous rock containing hornblende.

The metasedimentary rocks of South Knapdale contain a considerable volume of amphibolite bodies which are considered to be metamophosed basic igneous rock. Most of these bodies are, in fact, metamorphosed basic sills. Within the Upper Erins Quartzite of Meall Mór (Fig. 3.8), several tabular epidiorite bodies ranging in thickness from 0.5 to 250m are present. Unbroken bodies seldom exceed one kilometre in length, but disrupted remnants of one continuous unit can be traced for many kilometres along strike. These rocks consist of fine to medium grained actinolite and albite with minor biotite, chlorite, garnet and epidote and accessory magnetite, ilmenite, pyrite and chalcopyrite. These epidiorite bodies also show a variable amount of alteration to epidotite and

detail mineralogical descriptions of the epidiorite and the metasediments are given in Sections (5.3.1-5.3.9).

3.4.2 Structure and Metamorphism

The Meall Mór area lies on the inverted southeast limb of the Ardrishaig Anticline (Fig. 3.6), which forms the root zone of a major recumbent fold, the Tay Nappe (Section 3.3.4). Isoclinal minor folds which fold the schistosity in the Upper Erins Quartzite are common and these were considered as B_{1a} of Roberts (1974) and were formed at a stage in the creation of the Ardrishaig Anticline. At some localities, these isoclinal minor folds are refolded by another set (B_{2b}). These folds are thought to be responsible for the great variation in the thickness of the Knapdale Pyrite Horizon in the immediate vicinity of Meall Mór (Smith et al. 1981 and Willan 1983).

Three strike faults are present in the area (Fig. 3.8) and the major displacements all trend approximately east-west. Two faults affect the Stronchullin Phyllite and are sinistral, but no sense of movement could be detected in faults occurring in the Upper Erins Quartzite.

During the Grampian Orogeny, these rocks, like the whole of the Dalradian, underwent polyphase deformation and metamorphism, and they were transformed into metamorphic rocks belonging to the greenschist facies and falling within the garnet isograd (Fig. 3.5). Temperatures of metamorphism ranged from about 410°C to about 530°C across Knapdale to the highest-grade garnet-zone rocks near Tarbert and pressuress ranged between 8-10 kb (Graham 1983 & 1985).

CHAPTER 4
STRATIFORM MINERALISATION IN THE DALRADIAN ROCKS
OF THE GRAMPIAN HIGHLANDS

4.1 INTRODUCTION

Significant barium and/or base metal deposits occur within a restricted stratigraphic interval for about 190km in the Dalradian Supergroup of the Grampian Highlands. Most of these mineralisations are small in comparison to the Foss barium + zinc deposit of Aberfeldy (Coats et al. 1980 and Swenson et al. 1981) discovered in 1975 by the British Geological Survey. These deposits are contained within the Argyll Group (Fig. 4.1); most of these mineral showings are of vein type, notably those of the Tyndrum mine (Dunham et al. 1978) but some, such as those at Creggans, McPhun's Cairn and Meall Mór, are by description stratiform, and others for example Coillie Bhraghad and Craignure, although earlier described as metasomatic replacement (Wilson and Flett 1921), are evidently stratabound.

In the Loch Fyne area is the Clachan Bheag lead + zinc replacement mineralisation contained in the Loch Tay Limestone at the top of the Middle Dalradian succession. The Lecht iron-manganese deposit occurs in the Dalradian rocks of uncertain age of Banffshire. The latter deposit was regarded as being fault-controlled (Hinxman 1896), but its orientation led to it being considered as a secondary deposit related to stratiform sulphide (Smith et al. 1984 and 1981). However, it is now known to be related more closely to post-metamorphic breccia zones (Nicholson 1984).

Outside the Grampian Highlands but still within the Dalradian Supergroup are the Vidlin Ness deposit in Shetland (Garson and May 1976 a&b), and the Dalradian mineralisation at Ireland (Arthurs

1	Aberfeldy	NN85305640
2	Beinn Heasgarnich	NN41403863
3	Coille Bhraghad	NN08000750
4	Craignure	NN99450115
5	McPhuns Cairn	NN08900320
6	Meall Mor	NR83407360
7	Auchtertyre	NN35503025
8	Ben Challum	NN39353260
9	Garbh Achad	NN04351010
10	Kilfinan	NR93007750
11	Clachan Bheag	NN18201250

KEY

	M. Dalradian
---	Fault
■	Cu
▲	Zn
●	Pb
⊚	Town
+++	Pyr.Horizon
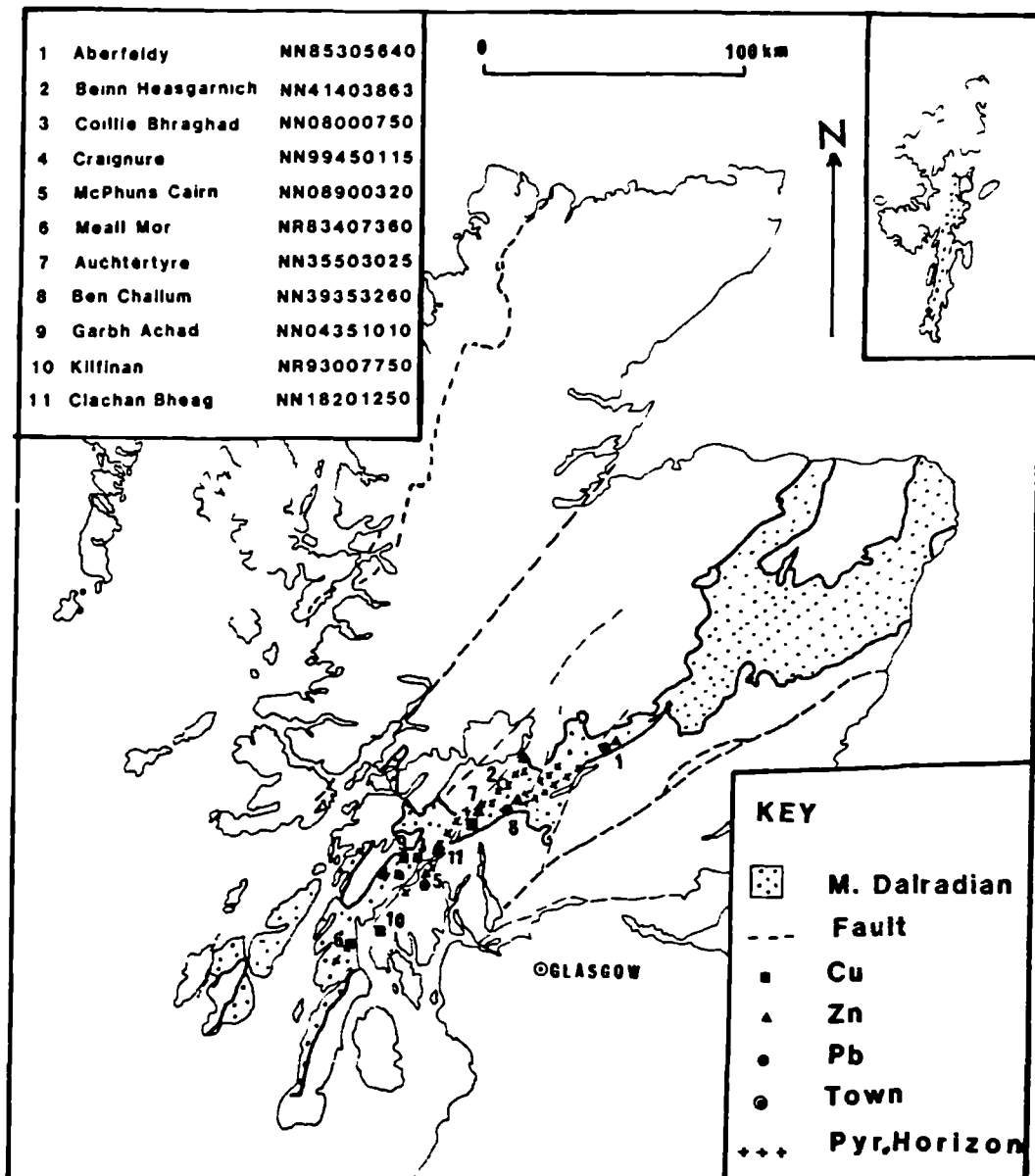
Fig. 4.1 : Location of stratiform mineralisations in the
Middle Dalradian of the Grampian Highlands.
Summarised from Johnstone and Gallagher
1980b, Willan 1983, Coats et al. 1984 and
Smith et al. 1984.

1976, 1977, and Williams and McArdle 1978). The former mineralisation occurs in rocks that immediately overlie the Moine and are, therefore, probably the oldest stratabound mineralisation recorded in the Dalradian.

The majority of these mineral showings were mined a long time ago and were recorded in the old reports of mining activities in Scotland (Wilson and Flett 1921) and were summarised partly in Chapter Two.

4.2 EXPLORATION AND REINVESTIGATION THAT POST-DATE THE MINING ACTIVITIES (i.e. after 1921)

At the beginning of the 19th Century prospecting for metals was limited in scale, and mining activity was concentrated on vein deposits (Table 2,1) which were thought to be of metasomatic-replacement or epigenetic origin. Although examples of what could be explained as stratiform were mentioned for some of the localities, e.g. the description of the weakly cupriferous pyrite mineralisation in the Ben Lawers Schist by Grant Wilson (1884) during the competition of the one-inch geological map. Sixty years later during examination of hydroelectric excavations by the geological survey in the late 1950, this zone was confirmed to be stratiform (Johnstone and Smith 1965). However its economic significance was not appreciated until 1972, after a series of exchange visits with the Geological Survey of Sweden. Its similarities with the Scandinavian stratabound ore deposit: Stekenjokk (Zachrisson 1971, Juve 1974 and 1977) and Røros (Rui and Bakke 1975) encouraged the promotion of a reconnaissance as it was considered a likely locus of base metal occurrences.

Extensive soil and stream sediment sampling west of the Loch Fyne area were carried out by the B.G.S., but no new significant mineralisation was discovered (Wright 1974). At the same time, and since 1972, the British Geological Survey has been engaged in a

programme of mineral reconnaissance in selected regions of Britain to identify areas of economic metalliferous minerals and to develop the best methods to explore for them.

The programme in the Grampian Highlands commenced with the reinvestigation of the previously known mineralisations, and each locality has been described in detail using a combination of different techniques and published in specific Mineral Reconnaissance Programme Reports by the B.G.S. Geological mapping established the existence of a discrete zone of stratiform sulphide mineralisation close to the top of the Ben Lawers Schist near Loch Tay, extending along the Middle Dalradian rocks strike for at least 50km (Fig. 4.1). Subsequent reconnaissance surveys (Smith 1977) confirmed its existence from Glenshee to Tyndrum. More recently, during the follow-up programme of stream sediment anomalies in the Scottish Highlands, over an area of 10,000km^2, the B.G.S. discovered : the barium and zinc mineralisation near Aberfeldy in 1975 (Coats et al. 1980) and barium enrichment near Loch Lyon (Coats et al. 1984); volcanogenic copper, zinc mineralisation at Vidlin, Shetland (Garson and May 1976 a&b); and finally two horizons (Auchtertyre and Ben Challum) of base metal concentrations near Tyndrum (Smith 1977 and Smith et al. 1981).

In summary, five distinct mineralised horizons within the Dalradian Supergroup have been delimited which are in ascending stratigraphic order: Vidlin copper mineralisation in Shetland; Aberfeldy-Beinn Heasgarnich mineralisation; Perthshire-Knapdale Pyrite Horizons and their minor mineralised localities; Auchtertyre zinc, copper mineralisation; and Ben Challum lead, zinc mineralisation. The last four horizons are located within the Grampian Highlands and a summary of each horizon will be given in the following sections, based on the relevant Mineral Reconnaissance Programme Report.

4.3 THE ABERFELDY-BEINN HEASGARNICH DEPOSITS

A zone of barium, zinc and lead mineralisation, near Aberfeldy, was discovered by the B.G.S. in 1975 during the reconnaissance geochemical drainage survey. The deposits contain at least ten million tonnes of baryte, 25 million tonnes of barium silicates and one million tonnes of sulphides containing up to 8.5% Zn, 3.6% Pb, and 31 ppm Ag. The maximum thickness of the ore horizon is 140m (Willan 1983) hosted by the Ben Eagach Schist Formation. It has been located in four main sectors, within a 7km strike length. The mineralised zone is situated within a belt of steeply inclined strata which lies between southeast-dipping rocks to the north of Loch Tummel and the gently inclined inverted limb of the Tay Nappe to the south of Aberfeldy. For detailed geological, geochemical and geophysical investigation of this mineralisation, refer to Coats et al. (1980 & 1981).

The mineralisation consists of layers and lenses, a few centimetres to tens of metres thick, of massive baryte and quartz-celsian rocks, together with sulphide-bearing carbonate, muscovite schist, and graphitic-mica schist. Other lithologies intersected in boreholes comprise dolomite-chlorite schists, calc-biotites and calc-hornblende-biotite-plagioclase rocks which may represent tuffs (Willan 1983). Individual baryte bands are up to 16m thick and 1.8km long. Graphitic schist, closely associated with the mineralised horizon, often contains layers up to 15cm thick of massive pyrite and thin laminae of pyrrhotite. The celsian-quartz rocks contain up to 80% celsian. The main sulphide-bearing lithology is a carbonate containing up to 9.5% MnO and 0.75% SrO. The principal sulphides comprise intimately intergrown pyrite, sphalerite (including a manganiferous variety), galena, and pyrrhotite. Chalcopyrite is a minor constituent together with magnetite, fuchsite, rutile, hyalophane, and cymrite.

Massive baryte within the Aberfeldy mineralised zone contains more than 30% BaO, compared to quartz-celsian rocks with 5-25% BaO, and the barium-enriched schists with up to 4% BaO, compared with 0.03% BaO in average black shale (Vine and Toutelot 1970). The base metals reach a maximum in carbonate rock of up to 8% Zn and 4% Pb (Smith et al. 1980) and in graphitic schist up to 1000 ppm Zn and 600 ppm Pb (Coats et al. 1981). There are weak pre-ore sedimentary enrichments of barium spanning the 400m of Ben Eagach Schist (Willan 1983).

A thin zone of barium-enriched sulphidic schist has been identified 45km southwestward along the strike, from the Aberfeldy Ba, Zn, and Pb deposits, at Beinn Heasgarnich (Fig. 4.1) near Loch Lyon (Coats et al. 1984). The zone is enriched in barium (Grout and Gallagher 1980).

4.4 THE PERTHSHIRE PYRITE HORIZON

The presence of pyrite with minor chalcopyrite in the Ben Lawers Schist, west of Loch Tay, was first recorded by Grant Wilson (1884) and was later delimited by the B.G.S. as a definite horizon, the Perthshire Pyrite Horizon. This horizon is up to 180m thick, and its top lies some 10-300m stratigraphically below the top of the Ben Lawers Schist Formation. It extends for 90km (Fig. 4.1) from Tyndrum to Glenshee (Smith 1977 and Smith et al. 1977a). Throughout much of its length the horizon lies on the lower inverted limb of the Tay Nappe, but between Glen Lyon and Tyndrum its outcrop is below the axial trace of the underlying Ben Lui Fold (Cummins and Shackleton 1955). The boundaries of the horizon are quite sharp and hosted in calc, chlorite, muscovite, and quartz schists. For detailed information of the investigation, together with geological, geophysical and geochemistry maps and data, see the relative Mineral Reconnaissance Programme No.8 (Smith et al. 1977a).

Within this horizon, pyrite generally forms no more than 5% by volume, but in some thin units it locally exceeds 20%, occurring as isolated porphyroblasts up to 1cm in size. The pyrite grains show considerable variation in shape and size, and some grains were deformed during formation of earlier schistosity and hence are pretectonic. In places, trace quantities of chalcopyrite and pyrrhotite are found filling cracks or as inclusions in pyrite grains.

Analysis of samples collected from six cross-sections along the strike of the horizon, show that the horizon contains low base metal concentrations (Table 4.1a). Copper, though the most abundant base metal, seldom exceeds 60 ppm on average. The Pyrite Horizon is similar to disseminated pyrite mineralisation in calc-schist associated with large stratiform base metal deposits in Scandinavia, for examples at Stekkenjokk (Juve 1974 and 1977) and Røros (Rui and Bakke 1975).

Southwest of Tyndrum similar pyrite mineralisation occurs in the Ardrishaig Phyllite, the equivalent to the Ben Lawers Schist, as for example at Creggans. In Knapdale the equivalent of the Ben Lawers Schist is the Erins Quartzite, containing a zone of weak pyritic enrichment, the Knapdale Pyrite Horizon (Smith et al. 1978). It contains several copper showings (Fig. 3.8), all of which lie at approximately the same level. At the intersection of the sulphide zone with the west coast of Loch Fyne, pyritic schist and quartzite, similar to those around Loch Tay are exposed. The similarity, lateral continuity and low base metal concentration of the Knapdale and Central Pyrite Horizons suggest that they might be of the same age (Smith et al. 1984) and that the total strike length of weak pyrite mineralisation within the Dalradian of the Grampian Highlands is 190km.

As was mentioned earlier, although the Perthshire Pyrite Horizon appears to have low base metal concentration, its presence

Element	Range ppm	Mean ppm	Location of Highest Levels
Cu	0-1270	79	Brerachan Water
Zn	10-130	55	Brerachan Water
Pb	10-40	18	Creggans, Glen Lochay
Ag	0-2	--	Glen Lochsie
Au	0-0.028	--	Glen Lochsie
Ni	25-65	--	Glen Lochsie

Table 4.1a : Base metal content within the Pyrite Horizon. Data is taken from Rice 1970, Smith et al. 1977a and Smith 1977.

Deposit	Grading, wt%			Metal Ratio		
	Cu	Zn	Pb	Cu	Zn	Pb
Ben Challum	0.03	1.0	0.13	3	86	11
Auchtertyre	0.07	0.3	0.001	19	81	1
Meall Mór	0.58	0.013	0.006	97	2	1
Loch Tay	0.032	-----	0.001	97	0	3
Aberfeldy	0.008	1.2	0.44	0	73	27
Vidlin	0.72	0.55	0.03	56	42	2

Table 4.1b : Estimates of grade and metal ratios in the Dalradian sulphide deposits. Data is taken from Smith et al. 1984.

is considered significant, as it indicates widespread and possibly syngenetic sulphide enrichment. Related to and within this horizon are the following mineralisations that have so far been recognised in the Dalradian Supergroup in the Grampian Highlands.

4.4.1 The McPhun's Cairn Zn and Pb Mineralisation

The McPhun's Cairn Zn and Pb mineralisation (Smith et al. 1977b) is located about 950m north-northeast of Creggan Point at the north end of Loch Fyne (Fig. 4.1) and occurs near the top of the Ardrishaig Phyllite, in host rocks that consist mainly of argillaceous, calcareous and siliceous rocks. These were folded into tight isoclinal folds and underwent greenschist facies metamorphism during the Grampian Orogeny.

There are two distinctive sulphide assemblages present. The surface mineralisation constitutes a pyrite ore with sphalerite and subordinate amounts of pyrrhotite and galena, and the down-hole mineralised intersection is essentially a pyrrhotite ore, with traces of chalcopyrite and sphalerite; galena is rare and pyrite is wholly or nearly absent.

There is a marked contrast in the base metal contents between the two assemblages, with the surface mineralisation assaying 7.5% Zn, 5.6% Pb, with traces of arsenic, copper, nickel, silver and gold, while the pyrrhotitic mineralisation contains 1.7% Zn, 1.0% Pb, and 0.4% Cu.

Reinvestigation of this mineralisation by the B.G.S. led them to consider it as of no economic potential and to suggest that there is a reasonable possibility that a large body of massive sulphide may occur in the area, especially if this mineralisation forms a lateral extension of the adjacent Creggan Point pyritous schist.

A syngenetic exhalative origin for the mineralisation at McPhun's Cairn was proposed by the B.G.S., and this was later supported by the textural, minor and trace elements studies, in particular sphalerite-geobarometry and Co:Ni and S:Se ratios carried out by Willan and Hall (1980).

4.4.2 The Garbh Achadh Cu and Ni Mineralisation

A minor stratiform sulphide mineralisation in Garbh Achadh, on the west side of Loch Fyne (Fig. 4.1), was associated with a small calc-alkaline porphyry intrusion with a sequence of quartzites, quartz-schists and occasional pelites which comprise the Crinan Grits Subgroup (Ellis et al. 1978). Interbedded within this sequence are a number of epidiorite sheets which represent metamorphosed basic sills and possibly some lava flows.

Two distinct types of sulphide mineralisation have been recognised at Garbh Achadh :

(a) a sporadic sulphide mineralisation occurring in quartzitic horizons less than one metre thick, similar in mode of occurrence to the Craignure and Coillie Bhraghad deposits. It is characterised by small pockets of massive replacement pyrrhotite with pyrite, and occasional later veins and impregnations of chalcopyrite with traces of arsenopyrite and sphalerite. In some places the sulphides become predominantly pyrite and chalcopyrite with less pyrrhotite and assays up to 13.2% Cu and 0.74% Ni, with traces of Zn, As, Cd, Ba, and Ag.

(b) a disseminated sulphide mineralisation within the porphyry intrusion and adjacent hornfelsed epidiorite, forming up to 3% by volume of the rock. It is associated with pervasive sericitisation, kaolinisation and hydrothermal alteration. It is characterised by the presence of pyrite with subordinate chalcopyrite forming up to 0.24% Cu and the occurrence of molybdenite probably of magmatic

origin.

Results of chargeability and resistivity pseudo-sections indicate that the geometry of the main conducting sources producing the major anomalies at Garbh Achadh is shallow. Consequently it is unlikely that "Porphyry Copper" style mineralisation as defined by Lowell and Guilbert (1970) exists here at depth.

4.4.3 The Coillie Bhraghad and Craignure Ni and Cu Mineralisations

The Coillie Bhraghad mineralisation is located 2.4km southwest of Inverary in the Loch Fyne area (Fig. 4.1). It is hosted by the Ardrishaig Phyllite and consists of nickeliferous pyrrhotite and chalcopyrite and assays 14% Ni, 7% Cu, 1% Co, with traces of Zn, As, and Pb (Wilson and Flett 1921).

The Craignure deposit occurs about 13km southwest of Inverary (Fig. 4.1) and consists of thin concordent layers of nickeliferous pyrrhotite, pyrite, chalcopyrite, and pentlandite in quartzitic layers within the Ardrishaig Phyllite. The ore assays 10-12% Ni, 1% Co, and traces of Zn and Cu.

Odeh (1970) had studied the Craignure mineralisation and described it as synsedimentary in origin. Also, Hopkinson (1970) recognised the synsedimentary origin of both Craignure and Coillie Bhraghad deposits and concluded that the ores appear to have been formed by a combination of sedimentary process and hot spring activity.

4.4.4 The Kilfinan Cu and Clachan Bheag Pb Mineralisations

Both mineralisations occur in association with the Loch Tay Limestone in the Loch Fyne area (Fig. 4.1). The Kilfinan copper deposit, up to 8.2% Cu, lies within a mineralised belt about 6.4km long and consists of chalcocite, malachite, covellite, pyrite, and

chalcopyrite minerals. This deposit was studied by Hopkinson (1970) who suggested that it was formed by the leaching of disseminated copper from epidiorites and Ben Lui Schist by meteoric water and redeposition in the Loch Tay Limestone.

The Clachan Bheag deposit consists of galena, sphalerite, and pyrite layers (30cm thick). The ore assays 12% Pb and 29 ppm Ag (Wilson and Flett 1921) and has been studied recently by Ringrose (1978) who described it as epigenetic and caused by solution passing up the Tyndrum-Glen Fyne Fault. He also reports pyrite, pyrrhotite and chalcopyrite occurrences at two localities in the immediate vicinity of the deposit, which may be of syngenetic origin.

4.5 THE KNAPDALE PYRITE HORIZON

In South Knapdale several sulphide showings have been reported (Wilson and Flett 1921). Most comprise iron and copper, but significant amounts of lead with some gold and silver are also present. Geological mapping confirmed that they lie within a zone of pyritic quartzite and schist which define the Knapdale Pyrite Horizon. It extends for at least 10km southwest of Loch Fyne (Fig. 3.8) and consists mainly of orthoquartzite and quartz-mica schist, weakly enriched in pyrite and chalcopyrite (Smith et al. 1978). Its cross-strike width varies from 200 to 800m and estimates of its true thickness are confused by folding (B_{2b}, Section 3.4.2), but it is considered to be less than 200m in comparison with the Perthshire Pyrite Horizon averaging 180m in thickness (Smith et al. 1977a).

In the northern part of the Meall Mór area a further zone of pyrite enrichment (Fig. 3.8) ranging in width from 39-70m was recorded 200-300m to the west, but it is not clear whether this represents a separate horizon or a tectonic repetition of the main zone.

4.5.1 Mineralogy of the Knapdale Pyrite Horizon

Mineralogically the Knapdale Pyrite Horizon resembles the Perthshire Pyrite Horizon (Section 4.4) except that the pyrite is finer grained and occurs in trails parallel to the bedding and early schistosity, rather than isolated porphyroblasts. The pyrite forms the dominant sulphide phase forming up to 23% of the quartzites and 13% of the pelites. Small quantities of chalcopyrite occur sporadically as stratiform blebs and trails throughout the horizon. An increase in the chalcopyrite content is notable between Meall Mór and the Abhainn Srathain mine workings. In the Abhainn Srathain region chalcopyrite and pyrite occur as large crystals associated with cross-cutting veins mainly of quartz and calcite, as local disseminations and stratiform. The Abhainn Srathain copper mineralisation is hosted by metasedimentary rocks and epidiorite bodies of the Upper Erins Quartzite which are highly epidotised and will be discussed later in the relative sections.

Another copper occurrence is where a tributary of the Artilligan Burn flows through a deep gorge eroded along a fault. On the north side roughly 100m from the western end of the gorge (NR 8390 7615), phyllites are coated with malachite. Similar cupriferous schists are present a few metres to the east and assays give up to 26% Cu, 150 ppm Pb, 260 ppm Zn, 25 ppm Ag, 600 ppm Co, 860 ppm Ni, 10 ppm Mo, and 43 ppm As.

4.5.2 Geochemistry of the Knapdale Pyrite Horizon

A geochemical drainage survey was carried out by the B.G.S. in 1975 and 1976 and the results of the distribution of each element will be summarised below.

Copper

Copper is of high concentrations and stream sediment samples

which are highly anomalous in copper were collected on the Abhainn Srathain, Allt an Erin (NR 8537 7546), and a tributary of Artilligan Burn.

Antimony

The presence of antimony in the panned concentrates was unexpected and no antimony mineral was known from the area before investigation began. It is strongly correlated with copper and is a sensitive indicator of the mineralisation. Two panned concentrates from the Allt Mór contain high Sb.

Zinc, cobalt, and nickel

Generally, they show low concentrations in stream sediment samples. Zinc when anomalous reflects the presence of sphalerite bearing veins, for example Artilligan Burn and Stronchullin Burn.

Lead

It is of low concentration, but anomalous values in the panned concentrates reflects galena-bearing veins. Examples are the Artilligan and Stronchullin Burns.

Barium

In panned concentrates, it has a very irregular frequency distribution and where locally anomalous it reflects the presence of baryte as a heavy mineral.

4.6 THE MEALL MÓR Cu MINERALISATION

Copper mineralisation occurs about 1-2km to the south of Meall Mór, in the Abhainn Srathain region (Fig. 4.2), within the Knapdale Pyrite Horizon in the Upper Erins Quartzite. Previously, it was

reported to occur as veins and segregations in epidiorite and quartzite rocks, probably derived from disseminated chalcopyrite in the country rocks (Peach et al. 1911) and was worked along time ago (Wilson and Flett 1921).

During 1975 and 1976, the B.G.S. established a coordinated geochemical, geophysical and geological investigation in the area and the results imply that the mineralisation is of stratiform nature. Geological mapping in areas of poor exposure around Meall Mór was greatly facilitated by using geochemical and geophysical surveys in order to delineate extensions of outcropping mineralisation.

4.6.1 Geophysical Survey

Induced polarisation (IP) is the most widely used method to delineate mineralised areas. Chargeability and resistivity measurments were taken to cover the area, using Huntec Mark III (IP) equipment for both surface and downhole surveys. Surface (IP) surveys detected an anomalous chargeability zone about 6.5km long, within the Erins Quartzite and closely associated with the mapped pyrite zone. The causing body is near the surface with a possible width of 60m. The downhole survey indicates a correlation between anomalous chargeability and the copper analysis log.

A magnetic survey was also carried out to supplement (IP) in the area but no significant correlation of magnetic and (IP) anomalies is noted, indicating that appreciable quantities of pyrrhotite are not associated with the sulphide mineralisation. The magnetic anomalies are caused by the presence of magnetite whose quantities are insufficient to affect the (IP) response significantly.
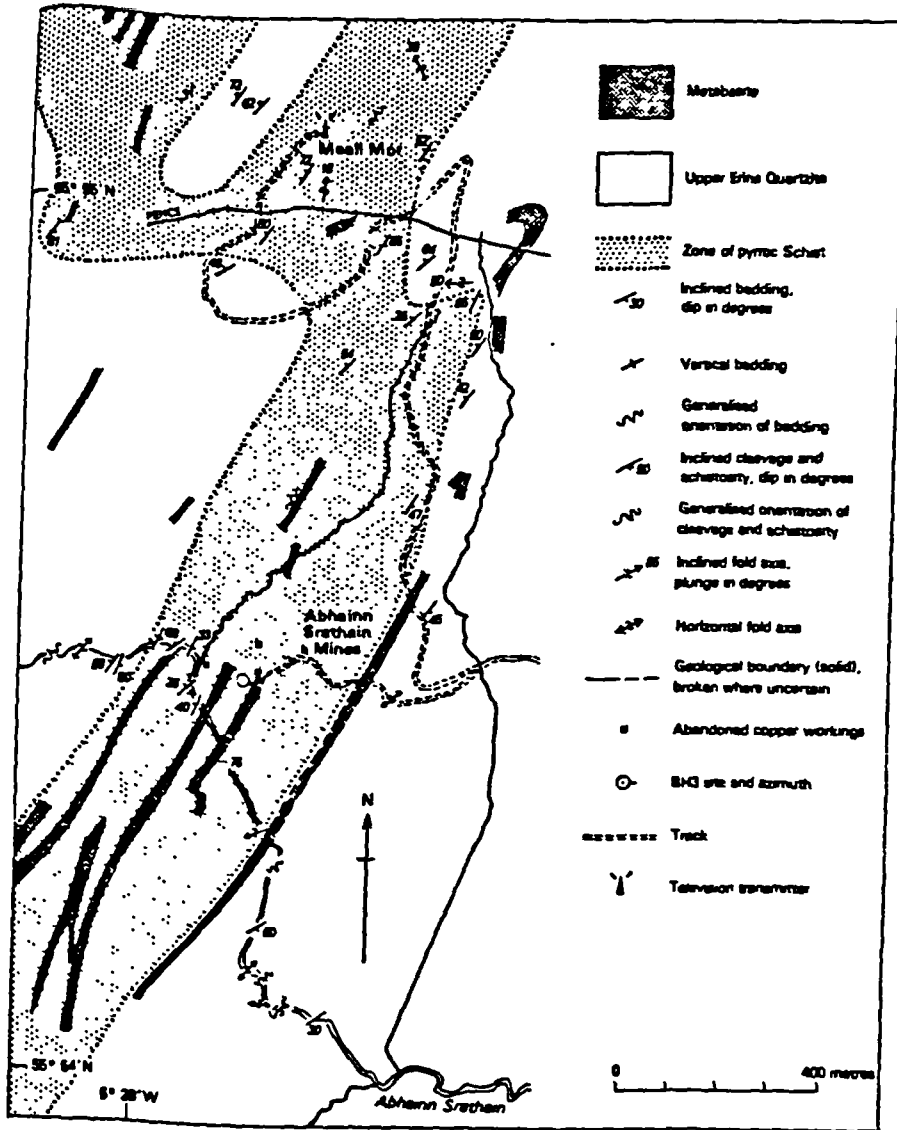
Fig 4. 2 : Geology and mineralisation of
Meall Mór area,(adopted from
Smith *et al.* 1981).

4.6.2 Soil and Rock Sampling

The detailed soil survey outlined a broad anomalous area to the south of Meall Mór and a series of narrow linear anomalies further to the east. Deeper sampling of the soil profile by mechanical auger has confirmed the metal distribution indicated by the shallower, hand auger sampling.

The soil anomalies are believed to be caused by two distinct styles of mineralisation, a broad disseminated copper source and narrow copper-rich veins. The larger disseminated copper occurrence offers the more promising target for future investigation by drilling.

4.6.3 The Abhainn Srathain Cu Mineralisation

Around the Abhainn Srathain mine workings, cross-cutting and stratiform chalcopyrite and pyrite are abundant and restricted to a zone 250m wide, which extends along strike 400m north-northeast and 1300m south-southwest of the Abhainn Srathain mine. The mineralisation is hosted by both epidiorite and metasedimentary rocks.

Around the old mine, several tabular epidiorite bodies occur up to 250m thick and extending several kilometres along strike (Section 3.2.1). These bodies were considered (Graham 1976) to be sills and contemporaneous with the Tayvallich Volcanics. However, at Meall Mór, the metabasites seem to be interbedded with the quartzite and quartz-chlorite schist and some of the quartzitic rocks contain amphibole suggesting that contemporaneous magmatism occured during sedimentation.

Mineralogical study of cores from boreholes shows that the mineralisation is associated with high development of epidote and that both the metasedimentary and epidiorite rocks contain variable

amounts of epidote. The distribution of epidote is quite patchy, with some enriched layers. In the Southwest Highlands, epidotisation of epidiorite and related volcanics is very common, but it is not always associated with copper mineralisation.

4.6.4 Mineralogy of Meall Mór Cu Mineralisation

The principal sulphide minerals are pyrite and chalcopyrite which occur as stratiform threads and trails of small grains parallel to the early schistosity and develop prefentially on micaceous partings. In the Abhainn Srathain region, chalcopyrite is very abundant and both pyrite and chalcopyrite form large crystals in two contrasting styles of mineralisation, stratiform and cross-cutting veinlets, in both the epidiorite and metasedimentary rocks. The vein-type in the epidiorites is much coarser and more irregularly developed. This is particularly apparent in the Abhainn Srathain mine epidiorite body where chalcopyrite and pyrite form irregular patches (5cm) and veinlets often associated with quartz and calcite.

Other copper-bearing minerals are also present, but in minor quantities; examples are, bornite, covellite, chalcocite, and secondary malachite. Azurite is only rarely present. Microscopic amounts of sphalerite occur forming stratiform trails in the quartzites, and a peripheral growth on pyrite in the epidiorites. Galena is the least common base metal sulphide in the area.

4.6.5 Geochemistry of Meall Mór Cu Mineralisation

Drill-cores taken from five boreholes were analysed by the B.G.S. for Cu, Pb, Zn, Co, Ni, and Ag by atomic absorption spectrophotometry. The copper analysis log shows little correlation with rock type and a good broad agreement between copper rich zones and recorded chalcopyrite. Generally, the levels of copper are below 2,000 ppm and in places show anomalous values. The highest

copper value (≥2.7% Cu) occurs in quartzite between 2.45 and 3.31m in B.G.S., BH.3. Zn, Pb, Co, Ni, and Ag levels are very low. Ni and Zn have a close correspondence with the chloritic units and possibly indicate a volcanic origin for these metasediments.

The geochemical drainage survey reveals the existence of strongly anomalous distributions of Cu and Sb in the Abhainn Srathain draining south from Meall Mór and the highest copper value is 245 ppm. Antimony has a similar pattern to copper and probably the element is present as a poorly resistant mineral, e.g. stibnite or tetrahedrite.

4.7 THE AUCHTERTYRE Zn, Cu AND BEN CHALLUM Zn, Pb HORIZONS

Two horizons of disseminated pyritic base metal mineralisation occur within the newly defined Ben Challum Quartzite Formation to the north of Auchtertyre farm. This formation was previously mapped as an irregular wedge of quartzite within the Ben Lawers Schist. Later survey (Smith et al. 1977a) confirmed that this quartzitic rock persists along a strike length over 9km and on its southern margin is directly overlain by the Ben Lui Schist. It was regarded as a separate formation referred to as the " Ben Challum Quartzite ", consisting mainly of feldspathic and micaceous quartzite interbedded with mica-schist and metabasaltic rocks. It is correlated with the Sron Bheag Schist and the Farragon Beds (Table 3.1).

The lower horizon, the Auchtertyre Horizon can be traced along strike for over 9km from Tyndrum northeastwards into the upper part of Glen Lochay. It is about 80m thick and comprises two units totalling 36m. Zn average 0.3% and in thinner units goes up to 1.7% Zn and 0.1% Cu. The mineralisation consists mainly of pyrite as disseminations and in trails parallel to the lithological layering, with which variable amounts of sphalerite and chalcopyrite are associated and best developed in the quartzites, which in places

62

have a cherty appearance. Petrographic work reveals that up to 30% of some of the quartzites consist of albite and orthoclase.

The upper horizon, the Ben Challum Horizon, is well exposed only on the mountainside of Ben Challum. It is 10-20m thick extending 2.5m along strike and consists of elongate lenses and thin layers of quartzite with trails, disseminations and lenses of sphalerite and galena forming 3% Zn and 0.1% Pb.

4.8 SUMMARY OF THE IDEAS ON ORE GENESIS

As was mentioned earlier in Chapter Two, the beginning of the 19th Century represents a period of maximum mining activity. The dominant ideas on ore genesis at that time was epigenetic replacement and cavity-fill models. These models seems to prevail until the late 1960's and, for example, Dunham (1952) regarded the Loch Fyne Cu and Ni mineralisation as associated with the acid Caledonian intrusions in the area.

Sturt (1961) studied the structure and metamorphism of the area between Loch Tummel and Aberfeldy and suggested a postmetamorphic origin for the mineralisation in the area. This was succeeded by a period where the remobilisation of disseminated sulphides in the country rocks during metamorphism was the current idea on ore genesis, for example Moorbath (1962) for Kilfinan.

Modern syngenetic ideas characterised the period from 1960 to the present day. This commenced in the late 1960's, particularly in Ireland (e.g. Russell 1968). However, the potential of the Scottish Dalradian in hosting stratiform mineralisation was not generally recognised until 1970 after exchange visits with Swedish geologists. Accordingly the B.G.S. reinvestigated the known mineralisation, and during a regional geochemical survey discovered new mineralisation. The results reveal a synsedimentary nature for most of the known and newly discovered deposits.

Studies on the Cu, Ni mineralisation at Craignure (Odeh 1970 and Hopkinson 1970) and Coillie Bhraghad (Hopkinson 1970) concluded with syngenetic ideas on ore genesis.

The B.G.S. workers assumed a syngenetic exhalative origin for McPhun's Cairn, Aberfeldy, the Pyrite Horizon, and the Ben Challum mineralisation.

At Aberfeldy, Coats et al. (1980) considered the deposit to be of synsedimentary origin and to represent deposition of barium, iron, zinc, lead, manganese, silicon, and other elements from metal-rich hydrothermal brine introduced into a black shale enviroment. Russell (1978) postulated that the Irish deposits resulted from convection of fluids derived from saline seawater in a terrain having a high geothermal gradient under rifting conditions. The hydrothermal convection cells widened and deepened with time as the crust cooled by this process. Application of this genetic model to the Dalradian mineralisation of Scotland, especially the Aberfeldy deposit (Russell et al. 1981a) explains the 400m of pre-ore phase mineralisation (Willan 1981).

Comparison of the Dalradian deposits (Russell et al. 1981a) to the sediment-hosted exhalative deposits (SEDEX) formed during early rifting in continents (Russell et al. 1981b & 1983) leads to the suggestion that the Dalradian deposits appear to belong to this class. Similarly Willan (1983) postulated a genetic model for the Aberfeldy deposits. Briefly, this model involves percolation of saline Dalradian seawater down through zones of high permeability along normal and listric faults into the hot sedimentary pile. The heated, acidified, and highly reduced brines leached Si, Ba, Zn, Pb, and other elements from the sediments and convectively returned to the sea floor precipitating the sulphide and sulphate deposit.

More recently Russell et al. (1984) questioned the presence of aluminium in the acid hydrothermal solutions and presented a more

developed model which seeks to explain the origin of the aluminium in the celsian rocks. The model states that, $Al\ (OH)_4^-$ is derived from the deep weathering of the Canadian-Greenland Shield. The resulting highly alkaline ground and river waters rich in potassium, silica, and alumina, mixed with the dense hypersaline sea-water in evaporitic tidal flats and lagoons which finally sank into the adjacent Dalradian basin, filling fault-bounded troughs such as newly developing sub-basins at Aberfeldy. Mixing of this brine with the issuing acid hydrothermal solutions containing Ba, Mn, Fe, Zn, Pb, Ag, and Si resulted in the precipitation of Ba-aluminosilicates, possibly cymrite by combination of excess barium and silica in the hydrothermal solutions with $Al\ (OH)_4^-$ in sulphate-free brine pools. The exact nature of the precursor to celsian is unknown, but relict cymrite (Forty and Stephens 1982) is evidence that this or a similar hydrous phase formed celsian by dehydration during metamorphism.

For the Perthshire Pyrite Horizon, Smith et al. (1977a) considered the horizon to contain a synsedimentary enrichment of Fe, Cu, and S and represent a weak precursor exhalative activity related to the Farrogan Beds and Sron Bheag Schist.

Smith et al. (1981 and 1984) described the Ben Challum Quartzite with the two sphaleritic horizons as representing either siliceous, metal rich exhalites or porous, coarse sandstone units which acted as channel-ways for hydrothermal fluids and were sealed at the top and bottom by more pelitic units.

4.8.1 Genesis of the Meall Mór Cu Mineralisation

Copper mineralisation at Meall Mór was first described by Peach et al. (1911) to be formed from chalcopyrite disseminated in the country rocks. Later the B.G.S. reinvestigated the area taking into consideration its stratiform nature and accordingly Smith et al. (1978) proposed that it might have originated in two stages. The first stage involved weak stratiform disseminations of pyrite and

chalcopyrite with traces of Zn, Ba, Ni, and Sb during the deposition of the host formation, the Upper Erins Quartzite, and the synsedimentary epidiorite sills. The second stage involved modifications enhanced by metamorphism : transformation of the epidiorites to assemblages of chlorite, biotite, hornblende, garnet, calcite, and sphene; development of abundant epidote in some epidiorites and adjacent sediments during the early stages of metamophism; and redistribution of metals by late metamorphic fluids and recrystallisation of pyrite and chalcopyrite as coarse grains in cross-cuttings veins of quartz and calcite.

Recently Willan (1983) studied stratiform mineralisations in the Dalradian of the Grampian Highlands and concluded that the Meall Mór mineralisation may have originated as follows :

(i) Weak exhalative activity, during the deposition of the Upper Erins Quartzite and prior to sill intrusion, had resulted in a stratiform assemblage of Mn, Fe, Cu, Zn, Ti, Pb, Ba, Sb, As, and Ag with the major sulphides, pyrite and chalcopyrite, being precipitated on combination with bacteriogenic reduced sulphur.

(ii) Shortly afterwards, whilst the sediments were in a wet and unconsolidated state, (within 300m of the surface?). The shallow intrusion of gabbroic sills into seawater-saturated rapidly accumulating sediment results in the expulsion of porewaters and the shallow convection of seawater, resulting in the spilitic alteration of the sills, and remobilisation of the stratiform zone of weak Cu enrichment that was later reprecipitated in cross-cutting veins.

CHAPTER 5
PETROGRAPHY AND MINERAL CHEMISTRY OF
MINERALISED ROCKS

5.1 INTRODUCTION

The purpose of this chapter is to summarise the mineralogical composition of the host rocks and to give a description of the textures and chemistry of both the ore and their associated transparent minerals. Samples for this study consist of forty surface samples collected at the site of the Abhainn Srathain old copper mine and from poor outcrops near the mine and throughout the Knapdale Pyrite Horizon, while the majority (n=86) are core from three diamond drill holes, provided by the B.G.S.

The first part of this chapter is an examination of the petrography of these rocks. This investigation starts with examination of the microscopic sections to identify their mineralogical composition under both reflected and transmitted light using a Vickers M73 Microscope. This is followed by description of the texture of both opaque and transparent minerals, in an attempt to understand the relationship between mineralisation and metamorphism, and mineralisation and the intrusion of the epidiorite sills. The preparation of the different microscopic sections is outlined in Appendix (A.5.1). The mineralogical composition of the rocks examined, expressed by percentages, is given as a visual estimate over the scale of the microscopic section and therefore is approximate, and is represented in Appendix (A.5.2). Photomicrographs were taken using an Amplival Pol-V polarising microscope (Carlzeis-Jena) with an Mf camera attachment and automatic timing unit.

The second part of this chapter provides information on the chemistry of the minerals using electron microprobe analysis with both energy dispersive (EDS) and wavelength dispersive (WDS) on selected sections. The remainder of the chapter discusses the textural and mineralogical characteristics of the mineralisation, the extent of effect of metamorphism on the mineralisation considering the changes in mineralogy and in fabrics produced by metamorphism as well as the mobilisation of minerals and elements.

5.2 THE KNAPDALE PYRITE HORIZON : GENERAL CHARACTERISTICS
AND PETROGRAPHY OF THE HOST ROCKS

The Knapdale Pyrite Horizon forms a distinct mapable unit, about 200m thick, extending at least 10km southwest of Loch Fyne (Fig. 3.8). It has been described in detail earlier in Section (4.5) and in this section an outline of its general characteristics will be mentioned. This Horizon is weakly pyritic with traces of chalcopyrite and is hosted by the Upper Erins Quartzite Formation. It resembles the Perthshire Pyrite Horizon but with finer pyrite grains as trails parallel to the foliation, rather than isolated porphyroblasts, forming up to 23% of the quartzites and 13% of the mica schist. Traces of chalcopyrite are present throughout the Horizon and become highly abundant in the area between Meall Mór and the Abhainn Srathain mine.

In this study twenty-four surface samples of different lithologies were collected along the horizon (see Fig. 1.2 and Appendix (A.5.2) for location) and were microscopically examined in order to report their petrographic description. The examined twenty-four microscopic sections are divided into the following rock types.

5.2.1 Quartzite

The quartzitic rocks are pale-grey to white, massive, with

ill-defined foliation marked by the discontinuous micaceous partings. In places the quartzitic rocks contain a considerable amount of mica (>10%) which enhances the compositional layering.

Examination of nine microscopic sections reveals that they consist of quartz (65-90%), muscovite (5-20%), chlorite (5-10%) and biotite (usually < 5%) and accessory albite (only sample HMM 2,<5%), calcite (<5%), epidote, sphene and zircon. Opaque minerals include pyrite (> 5% and locally up to 10%), with traces of chalcopyrite (locally up to 20%), pyrhotite, bornite and covellite. Samples (HMM 18 &19) contain secondary bornite and covellite up to 7%.

Pyrite occurs in disseminated cubes average 0.5mm across and in places up to 2.5mm across with rare silicate inclusions and in places forming alternative thin laminations which underwent folding during deformation (Plate 5.3). Chalcopyrite occurs in fine disseminations and trails , locally large porphyroblasts and in places where it is highly enriched filling fractures in the quartzitic rocks (Plate 5.4). Ilmenite occurs as very fine flakes or trails (<0.01mm) parallel with the ill-defined schistosity.

5.2.2 Feldspathic Quartzite

Some of the sampled quartzites contain about 10% or more feldspar, mainly albite as porphyroblasts averaging 0.25mm across and reaching up to 0.5mm. These rocks are composed of quartz (65-80%), albite (10-15%), muscovite (5-15%), with accessory biotite, calcite, epidote and zircon.

Opaque minerals include pyrite (2-7%) with traces of chalcopyrite, ilmenite, rutile and sphalerite. Pyrite is present as disseminated cubes (0.1 - 0.5mm across), free of inclusions and locally as large subhedral grains up to 4mm across containing inclusions. Traces of chalcopyrite occur either replacing the pyrite or as trails parallel to the foliation. The ilmenite and/or

69

rutile occur in fine anhedral grains usually parallel to the schistosity.

5.2.3 Quartz-Mica Schist

These relatively mafic rocks are finely striped, in part with highly crumpled foliation (Plate 5.1), and consist principally of light (quartz + feldspar + muscovite) and dark (biotite and chlorite) laminae. When garnetiferous, garnet forms large sieved porphyroblasts up to 0.6mm across. The quartz-sericite variety occurs as a light rock of alternating sericite and quartz $\pm$ feldspar layers, with thin partings of biotite and chlorite usually highly foliated and deformed into tight isoclinal folds with axial planes.

Compositionally they consist of quartz (15-45%), muscovite and/or sericite (30-40%), biotite (15-30%), chlorite (15%), garnet (0-20%), with accessory calcite and sphene. Opaque assemblages, include chalcopyrite (15%), pyrite (<5%), with traces of ilmenite, rutile and sphalerite.

Pyrite is found as fine elongated grains (<0.1mm across) parallel to the foliation and following minor folds, and in places is associated with traces of rutile and ilmenite. Chalcopyrite occurs either as fine disseminations or trails (< 0.01mm across) sometimes with sphalerite, quartz and chlorite inclusions, or filling the interstices between pyrite grains.

5.2.4 Epidotised Rocks

These include some quartzites and mica-schists, collected to the south of Meall Mor summit and are characterised by their epidote content. Epidote is found as fine scattered grains (<0.5mm across), in places (0.2mm) and locally large porphyroblasts up to 1mm across. It is also found as elongated grains marking a thin foliation alternating with quartzitic layers or laminae.

Plate 5.1 : Photograph of mineralised quartzite and schists of the Upper Erins Quartzite from the Knapdale Pyrite Horizon (photographed by Willan 1983). Left: quartzite with alternating thin laminae of pyrite and sphalerite. Middle: quartz-chlorite-schist with thick stratiform pyrite laminae. Right: chlorite-muscovite-quartz schist with disseminated pyrite.

Plate 5.2 : Photograph showing thin chalcopyrite laminations in epidiorite rock from the Abhainn Srathain mine. Specimen No. HMM 8, NR 836 737.

71

Compositionally they consist of quartz (50-80%), epidote (5-30%), micaceous minerals (5-10%), with accessory calcite and albite. Opaque minerals include chalcopyrite (4-10%), pyrite (<5%), with traces of ilmenite, hematite, rutile, magnetite, sphalerite and secondary bornite and covellite.

The sulphides, mainly chalcopyrite and pyrite, occur as stratiform discontinuous layers (0.2-0.6mm wide) of subhedral grains, in places associated with quartz and/or carbonate veins.

5.3 ABHAINN SRATHAIN COPPER MINERALISATION

This mineralisation is localised within the Knapdale Pyrite Horizon, about 1-2km to the south of Meall Mór (Fig. 4.3). The general characteristics of this mineralisation, as summarised earlier in detail in Section (4.6.3), are : (1) the maximum development of chalcopyrite with pyrite in stratiform, disseminated and cross-cutting form, (2) the presence of several epidiorite sills and (3) its association with the local development of metamorphic minerals such as epidote, garnet, chlorite, calcite and quartz. Epidotisation and carbonation of the epidiorites and the metasediments was reported to be restricted to a zone 250m across and 1,700m long coinciding with the Knapdale Pyrite Horizon and centered on the epidiorite sills (Fig. 5.1). The distribution of epidote is patchy and the variable development of epidote is present as epidote-rich lenses and in places alternating epidotised and non-epidotised layers or laminae.

Samples for this study are taken from outcrops, spoil heaps (n=36) and from the B.G.S. boreholes 1, 2, and 3 (n=86). Location of the samples and the boreholes sites are shown in Fig. (5.1). The structural location of the boreholes are also represented on cross-sections through the mineralised area (Fig. 5.2A). Figure (5.2B) represents the distribution of the studied samples from the B.G.S boreholes. 122 thin, polish-thin and polish sections were
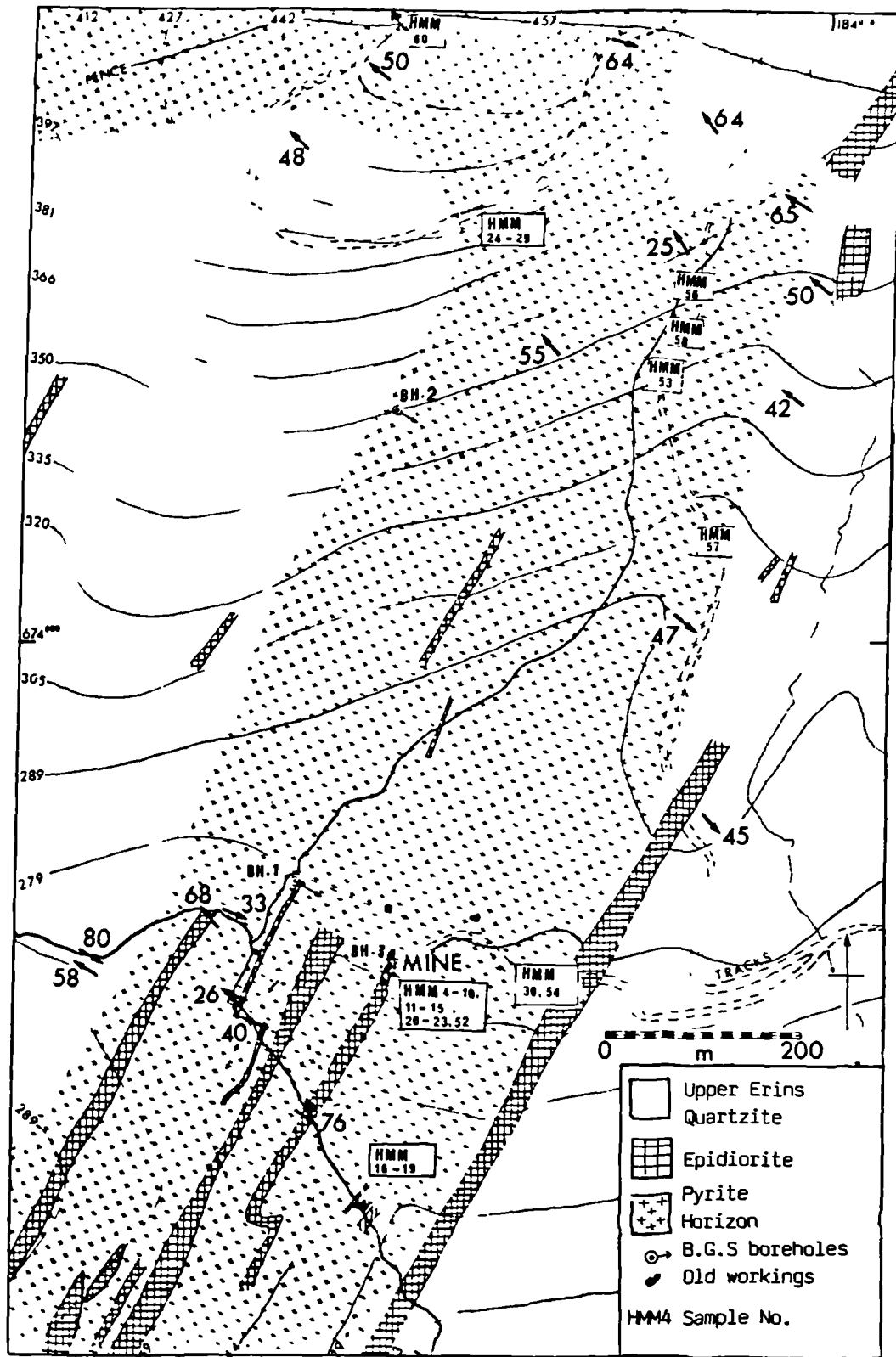
Fig. 5.1 : The location of the sectioned surface samples and the sites
of the B.G.S. boreholes (BH.1, BH.2 and BH.3).

73

examined from nine different rock types and will be described separately in the following sections.

5.3.1 Quartzites

Among the lithologies that were sampled from the mineralised area are the quartzitic rocks. They are pale-grey or white, massive and rarely foliated. In places they contain considerable amounts of mica, feldspar and epidote.

The orthoquartzites consist mainly of banded quartz with a little mica. The mica generally forms thin discontinuous partings consisting principally of muscovite, biotite and chlorite flakes. When garnetiferous, garnet occurs as fine pinkish porphyroblasts with quartz and mica inclusions. In places considerable amounts of carbonate (calcite and/or dolomite) are present subordinate to the quartz or replacing it, locally forming patches and very rarely foliations alternating with the quartz. Narrow veinlets of quartz, carbonate and sphene (less common) cross-cut the rocks.

Compositionally they consist of quartz (60-90%), with accessory mica (<10%), calcite (<15%) and traces of albite, epidote, garnet, sphene, zircon and apatite. The opaques consist mainly of pyrite (5-20%), with traces of chalcopyrite, locally (20%), sphalerite, ilmenite, rutile and very rarely magnetite.

The sulphides occur as disseminated fine grains (0.1mm across). Pyrite is found as fine disseminated cubes, free of inclusions and in places as large porphyroblasts (1mm across) engulfing transparent minerals from the matrix. The porphyroblasts are either individually scattered or aligned in defined layers usually parallel with the compositional layering of the rock. Chalcopyrite is found either as trails parallel with the micaceous partings or as subhedral grains intergrown with the pyrite or replacing it. In places chalcopyrite is found veining the

Meall Mór Southern Slope

Abhainn Srathain Mine Area

Key

▦ epidiorite

☐ Upper Erins Quartzite

▨ Pyrite Horizon
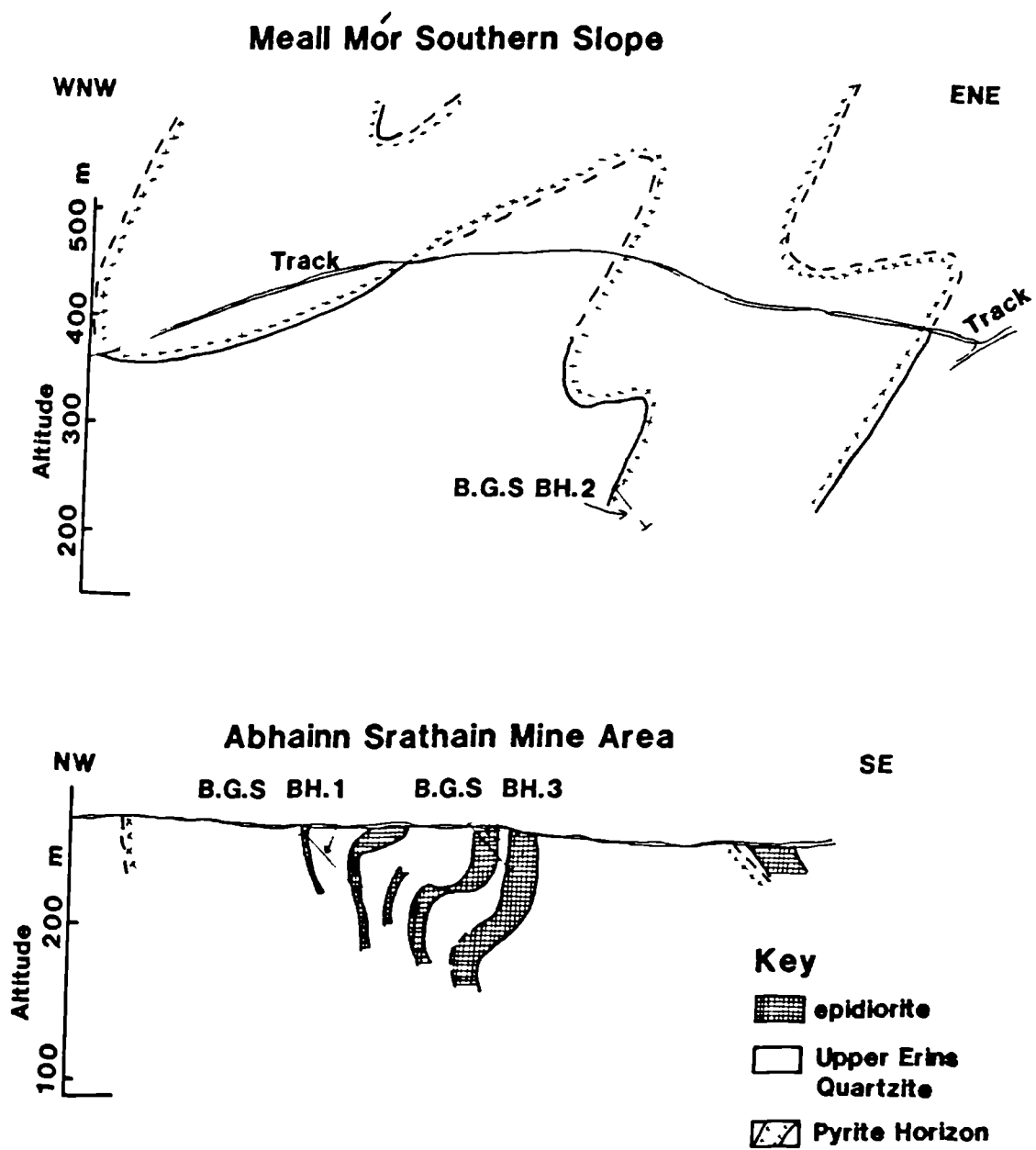
Fig. 5.2A : Structural position of the sampled B.G.S boreholes across two

vertical sections. Taken from Willan(1983)with few modifications.

Fig. 5.2B : The location of the studied cores sampled from three B.G.S boreholes The borehole
information and the copper content are taken from Smith et al. (1978).

Key

Overburden
Epidotised rock
Epidiorite
Micaceous quartzite
Chlorite-quartz-schist
Chlorite-schist
Quartz-chlorite-schist
Quartz-schist
Quartz vein
Studied samples
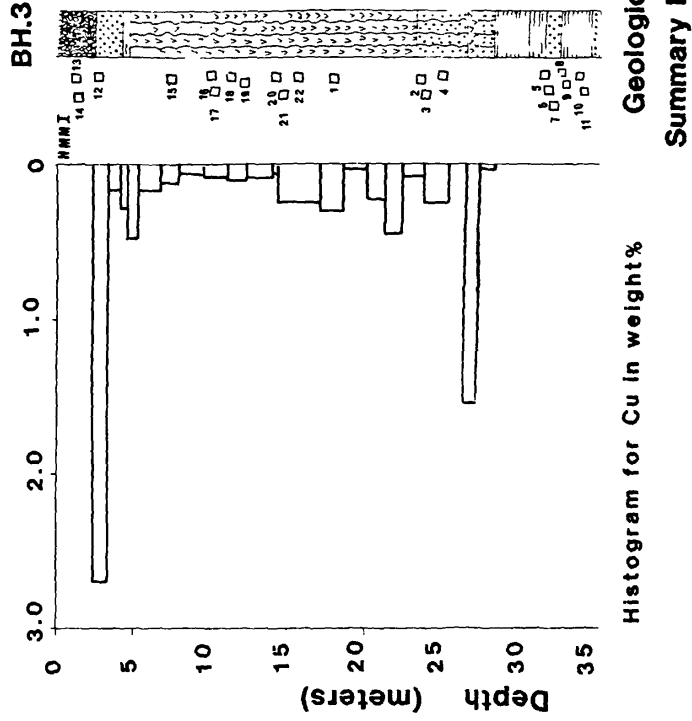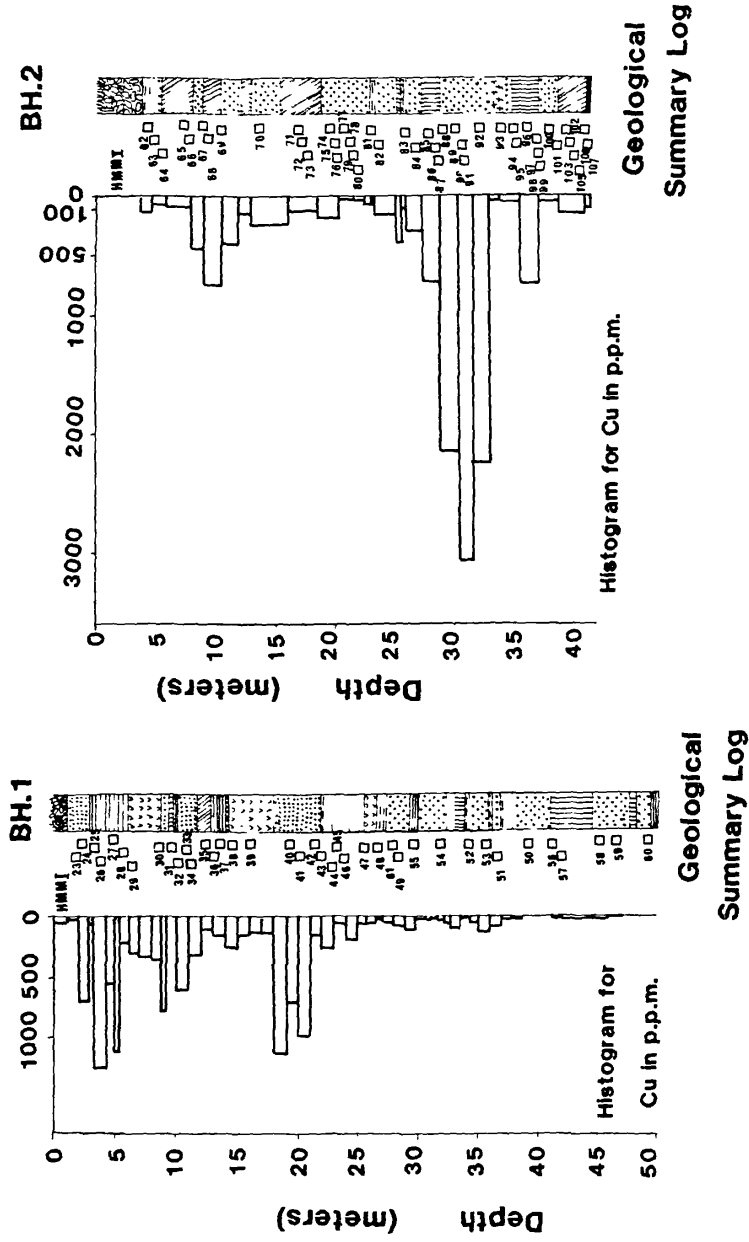
P.s. Few core samples does not correspond to the rock type in
the above sections as shown in Appendix (A.5.2) and Tables
(6.1 a&b and 6.2).

76

quartzites (Plate 5.4).

5.3.2 Micaceous Quartzite

Some of the quartzitic rocks that host the mineralisation are micaceous (10-20% mica). These rocks are similar to the previously described quartzites with higher mica content which enhances the foliation or compositional layering in the rock. They consist of closely spaced sericite/muscovite and minor chlorite partings with occasional biotite porphyroblasts. In places the foliation is wavy or crumpled. In the biotitic quartzites thicker bands of quartz and biotite (with minor chlorite and white mica) are interbedded. Carbonate is either replacing the quartz in the quartzitic layers or is associated with the sericite in the deformed parts. Garnet is rare and occurs as fine grains with quartz inclusions and is partly replaced by chlorite.

The examined microscopic sections reveal that this lithological group consists of quartz (50-80%), white mica (0-20%), biotite (0-20%), chlorite (0-10%), calcite (0-15%), with accessory albite, epidote, garnet, sphene and zircon. Among the opaque minerals are : pyrite (1-15%), chalcopyrite (0-5%), with traces of sphalerite, rutile, ilmenite, magnetite, bornite and covellite.

The sulphides are either traces (<5%) as trails parallel to the micaceous laminae, or as disseminations (>10%) of fine grains (0.5mm across), locally developed into large porphyroblasts up to 8mm across and are highly fractured and sieved with transparent mineral inclusions. Rutile is found as spongy trails parallel to the micaceous laminae, while ilmenite is found as tabular elongate crystals (0.1mm across).

5.3.3 Feldspathic Quartzite and Micaceous Schist

This lithological group includes all the examined sections that

77

Plate 5.3 : Photograph of polished hand specimen of quartzite with finely, alternating, folded laminations of sulphide. Specimen No. (HMM 56, from Meall Mór track).

Plate 5.4 : Photograph of Upper Erins Quartzitic rock with fractures filled by chalcopyrite, from Meall Mór track (HMM 29, NR 837 745).

contain (> 5%) feldspar, mostly albite. Albite occurs as comparatively large porphyroblasts up to 0.5mm across with polysynthetic and simple twinning (Plate 5.5). Sieve texture develops in the untwinned porphyroblasts which contain calcite, mica and epidote inclusions. This lithological group comprises two subgroups : (a) feldspathic quartzite and (b) feldspathic mica-schist.

(a) Feldspathic quartzite

Compositionally this subgroup consists of quartz (45-80%), albite (10-15%), white mica (0-10%), calcite (0-10%), with accessory epidote, biotite, chlorite, sphene, zircon and apatite. Opaque minerals comprise pyrite (7%), chalcopyrite (3%), with traces of ilmenite, rutile, and sphalerite.

The pyrite occurs as fine disseminated cubes (0.01-0.05mm across), occasionally as large cubes up to 0.5mm across, free of inclusions. In a few cases it occurs as very large porphyroblasts (4mm across), full of sphalerite, chalcopyrite, quartz and calcite inclusions and highly cataclased and fractured and in places in definite layers. Chalcopyrite occurs as fine disseminated trails (<0.1mm across).

(b) Feldspathic mica-schist

This lithological subgroup consists of quartz (30-65%), albite (10- 20%), white mica (0-20%), biotite (0-25%), chlorite (0-30%), calcite (0-19%), epidote (where present 5-10%), with traces of garnet, sphene, zircon and apatite. Opaque mineral assemblages are : pyrite (2-30%), ilmenite (0-7%), chalcopyrite (0-3%), rutile (0-5%), with traces of sphalerite, magnetite and bornite.

200 μm
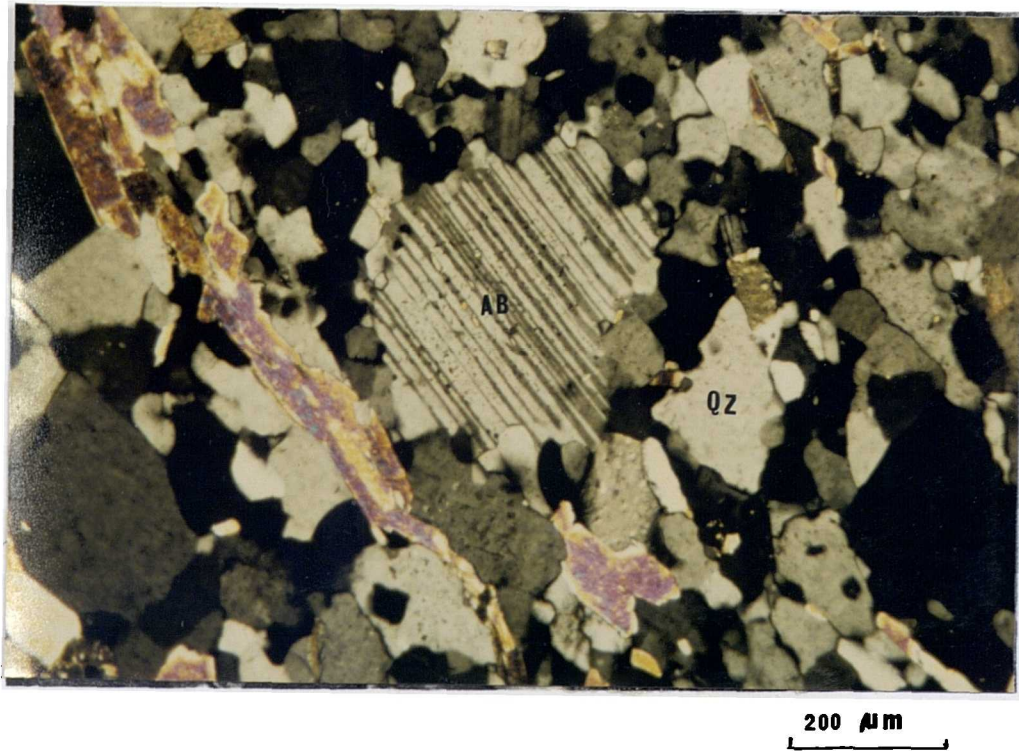
Plate 5.5 : Photomicrograph (in transmitted xed polars) of albite
(AB) porphyroblast in feldspathic quartzite. Sample No. HMMI 28,
B.G.S BH.1, 4.5m.

100 μm
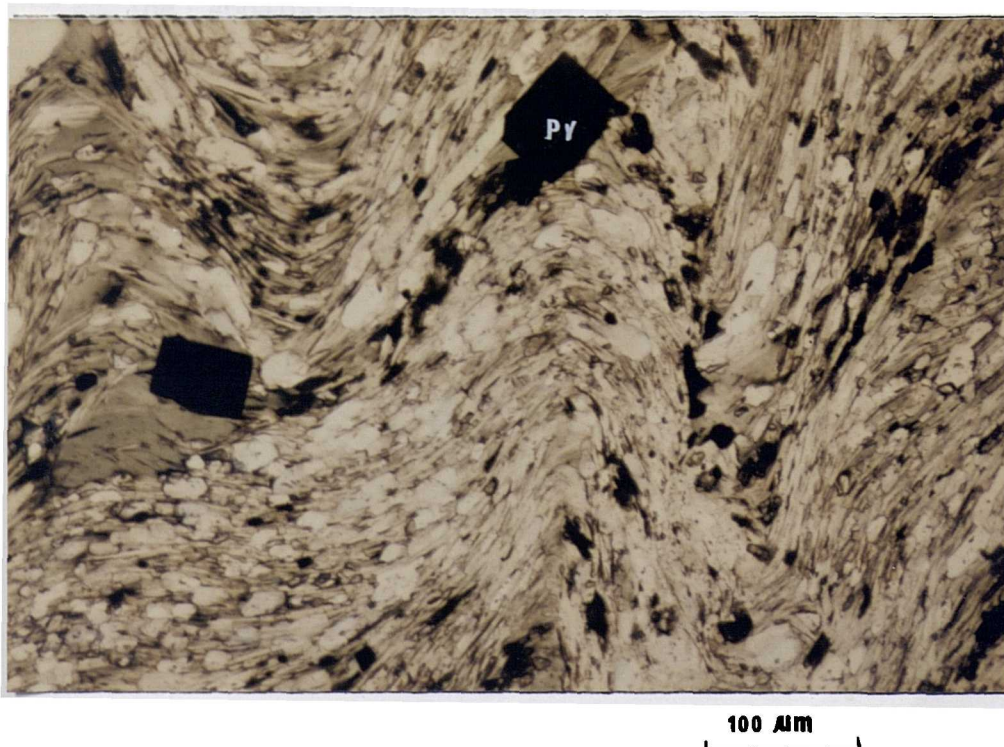
Plate 5.6 : Photomicrograph (in plane transmitted light) of a quartz-
mica-chlorite schist with folded schistosity. Note the very fine pyrite
grains along the schistosity and the large pyrite cubes (PY) at the
hinge and the apex of the folds. Specimen No. HMMI 34, B.G.S, BH.1, 9.8m.

Pyrite occurs as disseminated cubes, rarely trails and blebs, on average 0.4mm across, free of inclusions, sometimes with local large cataclastic porphyroblasts up to 1.5cm, with chalcopyrite, bornite, magnetite and transparent mineral inclusions. Pyrite may be associated or not with quartz and/or carbonate veins. Chalcopyrite where present, occurs in subhedral grains and trails (<0.1mm across) parallel to the schistosity, intergrown with the pyrite or replacing it. The sulphides show a response to deformation either by elongation parallel to the schistosity or by cataclasting and fracturing of the large porphyroblasts. Ilmenite is quite common and occurs as subhedral grains, free of inclusions, in places forming layers up to 2cm thick. Rutile occurs in spongy disseminated grains and blebs (< 0.1mm across) closely associated with the chlorite-carbonate layers.

5.3.4 Epidotised Quartzite

The Abhainn Srathain copper mineralisation is characterised by the presence of epidote. Epidotisation is not restricted to the epidiorite rocks only but epidotised quartzites and schists are also noted. The epidote is found either as scattered individual grains (0.05mm) or aggregates of grains (>0.2mm, locally up to 1mm across). Elongated epidote grains are also present marking, with the micaceous minerals, alternating layers of epidote-rich and quartz rich layers

Under the microscope, examination of these rocks reveals that they consist of quartz (50-80%), epidote (5-35%), micaceous minerals (<15%), with traces of calcite and albite. Opaques are : chalcopyrite (3-10%), pyrite (0- 4%), with traces of sphalerite, rutile, ilmenite, bornite, covellite and magnetite.

The sulphides are found as fine disseminated grains up to 0.2mm across or as large elongated subhedral grains full of inclusions forming discontinuous laminations, sometimes associated with quartz

and/or carbonate veins.

5.3.5 Epidotised Schist

This lithological group resembles the previously described epidotised quartzite but with more micaceous minerals. Epidote shows more or less the same characteristics as the previous rock type but in addition mobilised large porphyroblasts and folded epidote-rich laminations occur.

These rocks are composed of quartz (10-65%),epidote (5-35%), chlorite (3 -50%), biotite (0-25%), albite (0-20%), white mica (0-25%), calcite (0-15%), with accessory garnet, sphene and apatite. The opaque mineral assemblage consists of pyrite (3-17%), chalcopyrite (0-6%), ilmenite (0-7%), with traces of sphalerite, rutile, magnetite, bornite and covellite.

The sulphide minerals occur as disseminations (0.2mm across) either free of inclusions or containing calcite and epidote. Locally they develop large porphyroblasts up to 4mm across and, as subhedral grains form discontinuous laminae (2.5mm thick). In the deformed rocks where the original schistosity is refolded the disseminated cubes (pyrite) and anhedral grains (chalcopyrite) are oriented along the refolded schistosity and become coarser at the fold apex (Plate 5.6). Ilmenite occurs either as trails (< 0.01mm across) parallel to the shistosity or as subhedral elongated grains up to 0.2mm across.

5.3.6 Quartz-Mica Schist

This relatively mafic lithological group can be divided into three subgroups on the basis of micaceous mineral assemblages.

(a) Quartz-sericite schist

Light coloured rocks, consisting mainly of finely interbedded quartz $\pm$ feldspar layers and sericite layers, with occasional chlorite and biotite flakes forming a discontinuous foliation. In places the foliation is highly crumpled and/or refolded (Plate 5.1), with sericite being enriched in the core of the minor folds or crenulations.

(b) Quartz-sericite-chlorite schist

Finely foliated rocks of chlorite + sericite layers and quartz + calcite layers, in places highly deformed. The predominantly folded or crumpled foliation is associated with relatively thick sericite layers.

(c) Quartz-chlorite-biotite schist

Dark rock, with wavy and highly crumpled foliation of finely interbedded chlorite and biotite (occasional sheaves) rich layers with layers of quartz with traces of muscovitic flakes.

(d) Quartz-chlorite-sericite-biotite schist

Dark green rocks with very irregular and poorly developed foliation, consisting mainly of irregular layers of chloritic or sericite groundmass with large euhedral biotite porphyroblasts and sheaves, alternating with more quartzitic layers.

Mineralogically the quartz-mica schists consist of quartz (10-70%), white mica (0-50%), biotite (0-40%), chlorite (0-30%), calcite (0-15%), with traces of albite, epidote, garnet (locally 20%), amphibole, sphene (locally 10%), zircon and apatite. Opaques are mainly pyrite (0-15%), chalcopyrite (0-15%), with traces of rutile (locally 7%), ilmenite, sphalerite, magnetite, bornite and

covellite.

The sulphides occur as fine disseminated grains (< 0.5mm across), mostly free of inclusions and/or locally large porphyroblasts (2-4mm across) full of transparent mineral inclusions. Pyrite is found as cubes (<0.5mm across) disseminated in the rock and locally forming distinct rich layers. Large anhedral porphyroblasts of pyrite are also common engulfing the surrounding matrix. In rocks that have suffered deformation, the pyrite grains are arranged parallel to the refolded schistosity and are associated with sericite (e.g. HMMI8 & HMMI79). A few grains show deformation either by cataclasting or by fragmentation and elongation parallel with the foliation (e.g. HMMI84). Pyrite is sometimes replaced or intergrown with chalcopyrite and traces of sphalerite. Inclusions of chalcopyrite, transparent minerals, and less commonly bornite and magnetite in the pyrite are noted. Chalcopyrite occurs as trails usually (<0.1mm across) parallel to the schistosity, and rarely as large porphyroblasts (1mm across). Ilmenite occurs as subhedral elongated grains parallel to the general trend of the micaceous minerals. Rutile where present occurs as trails of spongy grains (<0.1mm across) parallel to the schistosity and locally enriched in the sericite-muscovite layers.

5.3.7 Calcareous Rocks

Thin layers of limestone are present as a minor constituent of the Upper Erins Quartzite Formation. One surface sample (HMM 53) was collected from outcrop of a thin limestone bed along the track leading to the Meall Mòr summit. This sample contains calcite (65%), quartz (25%), albite 5% and white mica (5%), with traces of disseminated pyrite.

Among the lithologies sampled, is a group of calcareous rocks with 20% carbonate, occurring as either brown patches replacing quartz or as laminae alternating with quartz + mica. This group

consists of quartz (20-70%), carbonate (20%), (albite 5-8%), white mica (<5%, locally up to 33%), with minor biotite and chlorite (locally 20%) and traces of zircon and sphene. Opaque minerals, include pyrite (5-20%), chalcopyrite (0-5%), rutile (0-5%), magnetite (0-5%), with traces of sphalerite, bornite, ilmenite and covellite.

Pyrite occurs as disseminations of fine grains (0.1mm across) highly fractured and cataclased, with chalcopyrite, magnetite and transparent mineral inclusions. Chalcopyrite where present is found as medium and large porphyroblasts with bornite inclusions, or as anhedral grains intergrown with pyrite or replacing it along cracks, veins and margins. Rutile is rare and occurs as blebs parallel to the schistosity. Magnetite, as very fine grains, rim the sulphides.

5.3.8 Epidiorites

Associated with the metasediments that host the Abhainn Srathain copper mineralisation are several epidiorite sill bodies. Their general description was given earlier in Section (3.4.1). Intrusion of these bodies, in this area and elsewhere in Knapdale, as sills rather than dykes was regarded (Graham 1976) as a result of their intrusion into thick, wet and unlithified sediment below an estimated half-km deep sea. However, Willan (1983) pointed out the interbedding and grading of these rocks with the metasediments at Abhainn Srathain. One borehole (AMax BH.1), intersected fourteen layers of epidiorite, each approximately one metre thick interbedded with quartzite and quartz-chlorite schist in 25m of drillcore and therefore may represent lavas or tuffs. This is also supported by the presence of stratiform sphalerite and chalcopyrite in these rocks and by the presence of amphibole in the quartzitic rocks of the Upper Erins Quartzite.

The epidiorites are dark grey or greenish-grey, medium to fine grained actinolitic rock. Microscopically some rocks are massive, while others show evidence of deformation and are therefore premetamorphic, often marked by a schistose arrangement of actinolite alternating with quartzitic layers, with occasional biotite porphyroblasts. When garnetiferous, garnet occurs as porphyroblasts either scattered in the rock or developed into definite layers mostly parallel to the compositional layering (Plate 5.7). Veinlets of quartz, carbonate, oxides, chlorite and amphibole are common in these rocks; some are parallel to , others are cross-cutting the compositional layering (Plate 5.8). These epidiorites show a variable epidote content and the rocks that consist of (>15%) epidote, will be described in the next section under the term "epidotised epidiorites".

Microscopically these rocks, consist of actinolite (20-60%), epidote (5 -15%), garnet (10-35%), carbonate (5-25%). Accessory minerals include albite, chlorite and sphene. Only sample HMM 7 contains biotite (20%) and chlorite (10%). The opaque mineral assemblages consist of mainly chalcopyrite (1-7%), pyrite (1-7%) and magnetite (1-8%), with traces of sphalerite, bornite, marcasite, hematite, chalcocite, covellite, ilmenite and rutile. Some of the epidiorites contain 15% ilmenite as stratiform grains (e.g. HMMI 31).

Generally the sulphides occur as large porphyroblasts up to 3mm across, associated with oxides forming patches in quartz and/or carbonate veins. The chalcopyrite porphyroblasts are anhedral to subhedral, with bornite, pyrite and magnetite inclusions. The large porphyroblasts show alteration near the margin to a complex intergrowth of pyrite, marcasite, hematite and magnetite (Plate 5.9). Pyrite occurs as large euhedral to subhedral grains 4mm across, containing chalcopyrite, bornite and transparent mineral inclusions. In places they are highly veined, fractured and replaced by chalcopyrite and less commonly by oxides. The oxide
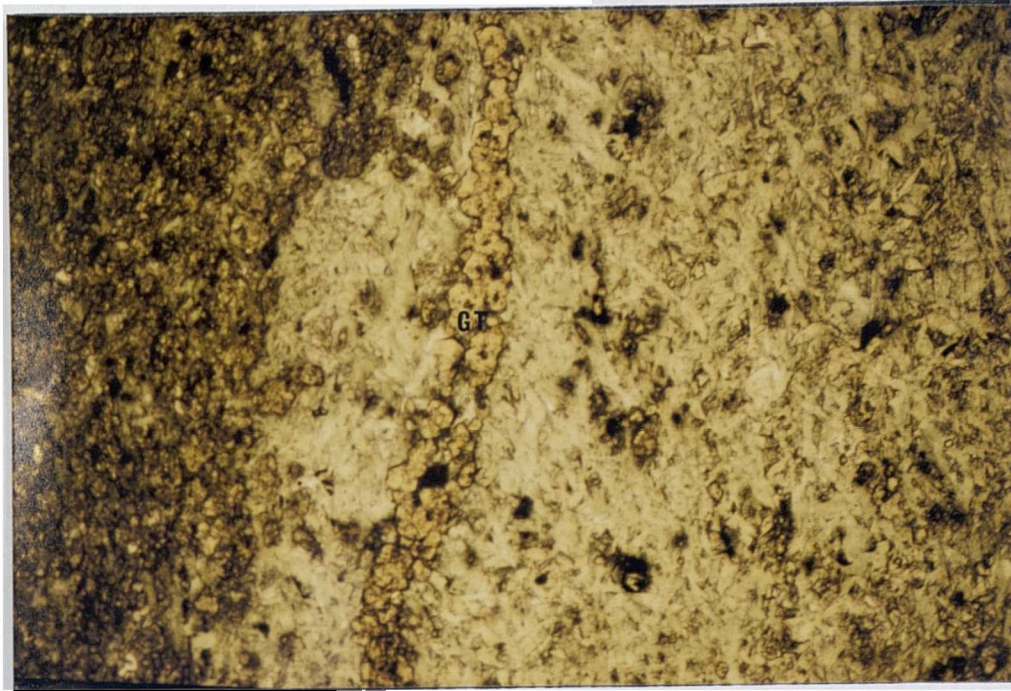
Plate 5.7 : Photomicrograph (in plane transmitted light) of epid-
otised epidiorite, note the two compositional layerings; the very
rich epidote layer(left part) and the actinolitic rich layer
(right part) with a parallel garnet (GT) vein? or lamination?. Sample
No. HMMI 15, B.G.S, BH.3, 7.6m.

400 μm

Plate 5.8 : Photomicrograph (in plane transmitted light) showing
quartz (QZ) and calcite (CC) veinlets cutting across highly epidot-
ised layer in epidotised epidiorite. Specimen No. HMMI 15, B.G.S,
BH.3, 7.6m.

minerals consist mainly of magnetite porphyroblasts forming either separate patches or in aureoles surrounding the sulphides and/or intergrown with them (Plate 5.10). The magnetite porphyroblasts are up to 1mm across, mostly free of inclusions and highly replaced by hematite around the margin and along cleavages and veinlets. Although not so common, magnetite sometimes contains chalcopyrite inclusions. A few magnetite grains with hematite rims are enclosed within the sulphide porphyroblasts.

Stratiform chalcopyrite and pyrite is also present in these rocks. The chalcopyrite grains are subhedral to anhedral, free of inclusions,forming thin laminae up to 2mm thick, locally associated with quartz and/or carbonate veins parallel to the compositional layering of the rocks, and associated with comparatively coarse porphyroblasts of garnet, epidote and actinolite.

Disseminated sulphides and oxides were also noticed in these rocks. Pyrite grains are up to 6mm across, with chalcopyrite and sphalerite inclusions and are highly veined and fractured by quartz and carbonate. The chalcopyrite grains are up to 2mm across and contain pyrite, bornite and sphalerite inclusions. In the deformed rocks, chalcopyrite and pyrite are mobilised along the folded schistosity forming relatively large grains and engulfing some transparent minerals (Plate 5.11).

5.3.9 Epidotised Epidiorites

As was mentioned earlier, many of the epidiorite samples from the site of the old copper mine show considerable and variable alteration to epidote. Epidotisation had resulted in the development of epidosite bands and lenses within the epidiorites, and true epidosite bands are up to 15cm thick. Microscopically, epidote in the epidiorites has developed in definite horizons or in lenses, forming a yellowish-green foliation ranging from 1mm to 3cm
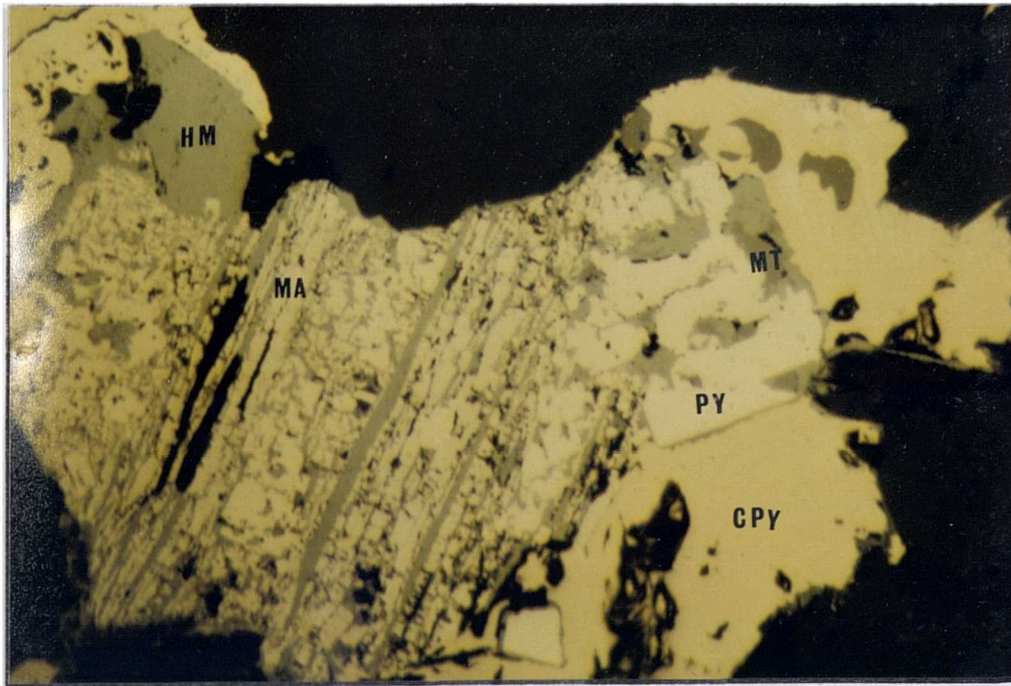
200 μm

Plate 5.9 : Photomicrograph (in plane reflected light) of chalco-
pyrite (CPY) and pyrite (PY) altered to complex intergrowth of mar-
casite (MA), magnetite (MT) and hematite (HM) near the edge in
epidotised epidiorite rock from the Abhainn Srathain mine. Specimen
No. HMM 8, (NR 836 737).
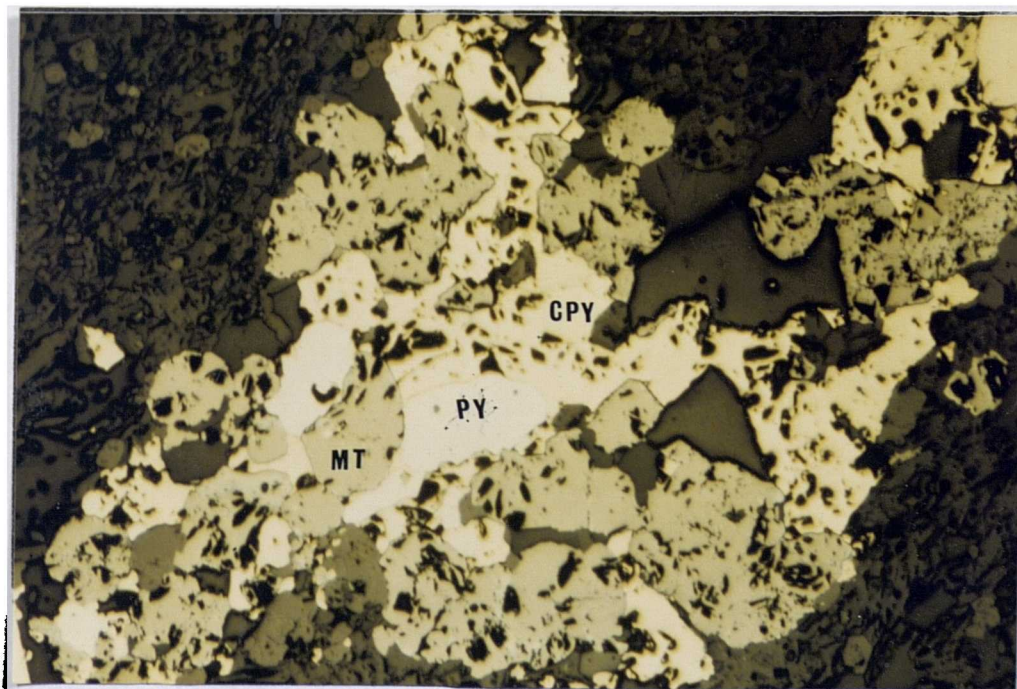
100 μm

Plate 5.10 : Photomicrograph (in plane reflected light) of magnetite
(MT) rimmed with hematite (HM), pyrite (PY) and chalcopyrite (CPY)
in epidiorite rock. Specimen No. HMM 5, from the mine area (NR 836 737).

89
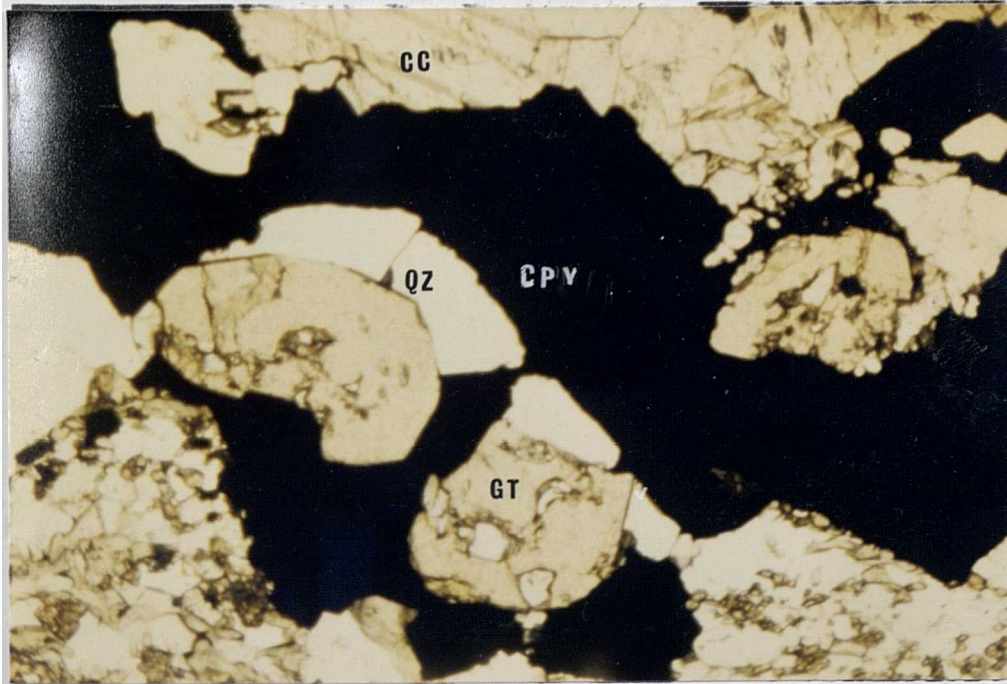
400 Ал m

Plate 5.11 : Photomicrograph (in plane transmitted light) of chalco-
pyrite growth (CPY) engulfing garnet (GT), quartz (QZ) and calcite
(CC) in epidiorite. Specimen No. HMMI 17, B.G.S, BH.3,10.3m.
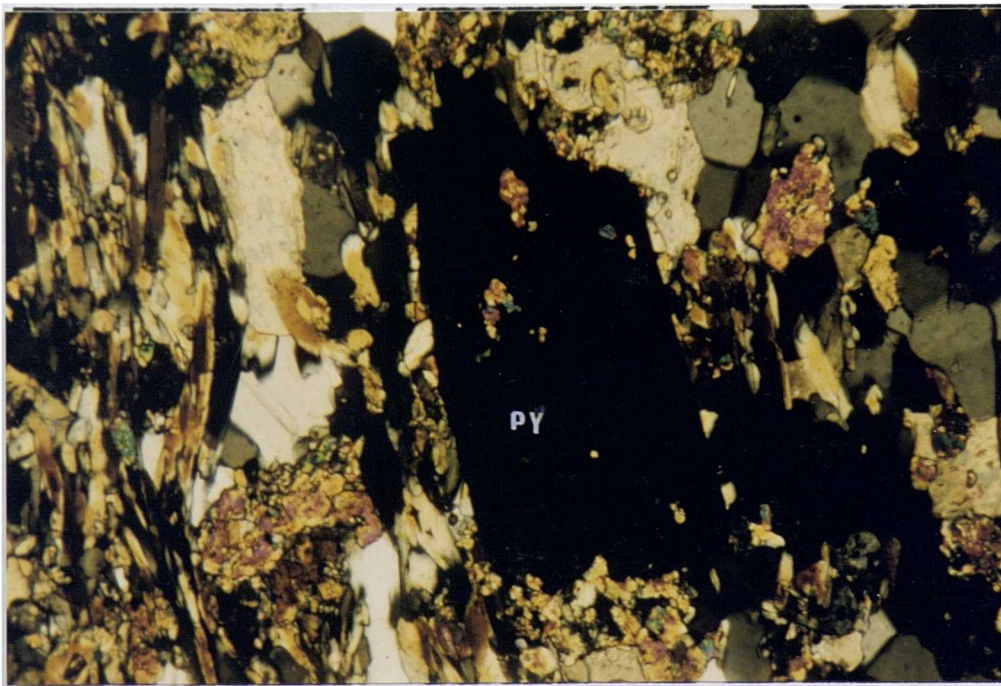
200 Ал m

Plate 5.12 : Photomicrograph (in transmitted xed polars) of pyrite
cube (PY) with epidote inclusion in epidotised epidiorite, specimen
No.HMMI 1, B.G.S., BH.3, 17.95m.

90

in thickness and alternating with dark greenish-grey actinolitic foliations. Porphyroblasts or aggregates of fine-grained epidote are also common. In some rocks, the epidotised layers are cut by veins/veinlets (Plate 5.8) of various minerals showing truncation at the boundaries between the different compositional layers and these veins/veinlets are deformed either by annealing or by segmentation, suggestive of a predeformation origin.

Compositionally, these rocks consist of epidote (20-75%), actinolite (5-45%), quartz (5-25%), carbonate (5-20%), garnet (0-15%), with accessory biotite, muscovite, chlorite and sphene (locally 10%). Opaque minerals include pyrite (2-10%), chalcopyrite (2-15%), magnetite (0-5%), with traces of sphalerite, marcasite, chalcocite, covellite , bornite and hematite.

The sulphides and the oxides occur as disseminations (0.2mm across), free of inclusions. Occasionally they develop large porphyroblasts 4cm across. Trace sphalerite is either interstitial to the sulphides or replacing them. Large sulphide porphyroblasts also show alteration near the margins.

Stratiform lamination of chalcopyrite is also common (Plate 5.2), these laminations are up to 4mm thick; in places they are deformed and folded.

5.4 TEXTURAL DESCRIPTION OF THE MINERALS

5.4.1 Amphibole

Amphibole constitutes the essential mineral of the epidiorites and most commonly occurs as actinolitic, bluish-green, highly pleochroic from pale yellowish-green to dark bluish-green, euhedral prismatic grains with conspicuous cleavage, and in a variation in sizes and shapes. In the schistose rocks, the grains range from fine flakes (< 0.1mm across) to comparatively moderate tabular

(>0.2mm across, occasionally 0.5mm) and elongated (5mm) poikiloblastic porphyroblasts with feldspar, quartz, carbonate, epidote and less commonly zircon inclusions. These large porphyroblasts are commonly associated with ores in quartz and/or carbonate veins, oriented either parallel to the compositional layering or cutting across it. In the poorly schistose rocks, actinolite occurs as stumpy equidimensional grains, with occasional euhedral tabular crystals and more rarely as patches intergrown with quartz, carbonate and feldspar. Although not so common, some of the actinolite grains show partial alteration to fan-shape chlorite.

5.4.2 Feldspar

Feldspar is present in both the epidiorites and the metasediments. In the epidiorites, feldspar occurs as fine (0.05mm) to moderate (2mm) crystals, mostly untwinned albite plagioclase, making its petrographic distinction from fine quartz very difficult and its presence may easily be overlooked. In the foliated epidiorites, elongated grains and crystals are oriented parallel to the foliation. Occasional albite porphyroblasts are also common and are up to 1mm across, with simple, polysynthetic and rarely chess board twinning, often crowded with epidote, muscovite and chlorite inclusions. Large twinned crystals, up to 2mm across, occur in quartz and carbonate veins cored with sulphides.

In the metasediments, especially the feldspathic quartzite and schist, large albite porphyroblasts(0.2mm and locally 0.5mm), (Plate 5.5), with simple and polysynthetic twinning are sieved with epidote, muscovite and quartz inclusions.

5.4.3 Epidote

Epidote is used here to refer to any member of the epidote family, including zoisite and clinozoisite. As was mentioned earlier, the copper mineralisation is characterised by the

epidotisation of both the metasediments and the epidiorites.

Epidote in the metasediments occurs in small amounts, generally as fine pale yellowish-green, anhedral grains (< 0.1mm) across. When present in relative abundance, epidote occurs in coarse columnar crystals (2mm across) and, in places elongated marking a thin foliation. In the deformed rocks, these epidote layers are refolded. Less commonly, epidote is found as clusters of grains especially in the poorly foliated rocks. Epidote is present as inclusions in the feldspar and in the sulphides (Plate 5.12).

Epidote hosted by the epidiorites occurs in a variety of sizes, forms and orientations of which the most common occurrence is in streaks, layers (< 2mm) and bands (up to 2cm) thick (Plates 5.7 & 5.8) that do show foliation in the shistose rocks. Epidote is also present in fine grains or aggregates of grains. In places, the latter form an obstacle, causing the amphibole crystals that define the schistosity to wrap around them. Also present, but less commonly, are epidote-rich nodules (2cm) across. In places, especially along veins that host the ore, epidote is mobilised into comparatively large equant or tabular crystals up to 1.5mm across. Fine veinlets of epidote are also present parallel or cutting across the foliation. Epidote also occurs as inclusions within plagioclase with various grain size.

5.4.4 Garnet

The distribution of garnets in the host rocks is somewhat, sporadic. A rock in a scale of the microscopic section may be garnetiferous in one portion and non-garnetiferous in the other. Garnet seems to be developed prefentially in size and amount in the epidiorites compared to the metsediments with a correspondingly distinct chemical variation (Section 5.5.4). It is also worth noting that the garnet has an affinity to the site of the copper mineralisation, as the majority of the identified garnetiferous

rocks are encountered in BH.3, at the site of the old copper mines and a few from the spoil heaps.

Petrographically, garnet hosted by the metasediments, preferentially in the mica schists, occurs as pale pink, fine (<0.1mm) to moderate (0.2mm), generally euhedral porphyroblasts, completely isotropic, scattered through the rocks (typically two to five grains per slide). Occasionally they develop large porphyroblasts, up to 0.6mm across, sieved with epidote, chlorite and quartz inclusions (in places, with a concentric spiral pattern). Less common are large skeletal porphyroblasts with a lot of rounded quartz inclusions. In the deformed rocks where the schistosity is marked by the alignment of the micaceous minerals, garnet forms obstructions and causes the schistosity to flow around them. Retrograde chlorite replaces garnet on the margin and along fractures. The garnet is of almandine type with a considerable spessartine and grossular content (Section 5.5.4).

Garnet hosted by the epidiorites, shows a wide range in composition (Section 5.5.4) and petrographically occurs in orange brown, comparatively large euhedral and polygonal porphyroblasts (1mm across), not completely isotropic (probably due to the high spessartine content), full of epidote, feldspar, quartz and sphene inclusions and in places free of inclusions. They are present either scattered through the rocks or in fine layers composed almost of a chain of garnet grains, mostly parallel to the rock foliation (Plate 5.7) but occasionaly cutting across it. Garnet is closely associated with the ore in veins where it occurs in comparatively large mobilised porphyroblasts (>2mm across), in places engulfed or being engulfed by the ore minerals (Plate 5.11). Sphene inclusions in the garnet are very common forming a core to the large porphyroblasts. Alteration of garnet to chlorite is very rare compared to garnet hosted by the metasediments.

94

5.4.5 Chlorite

Chlorite in the more psammitic rocks, where it is present in small amounts, occurs in fine flakes averaging 0.1mm across, making with other micaceous flakes, a discontinuous foliation. It less commonly occurs in irregular laminae of chlorite groundmass with sericite and biotite flakes (in places with coexisting sphene). Also patches of stumpy chlorite result from retograde alteration of biotite and garnet.

When present in significant amounts, especially in the pelitic rocks, chlorite tends to assume a crystal habit up to 1mm across and characteristically shows green pleochroic colour with one cleavage set. Chlorite occurs intergrown with coexisting biotite and muscovite. Thick layers of chlorite (with occasional biotite) alternate with sericite layers in the deformed rocks. In the highly chloritic rocks, chlorite occurs in thick layers of poorly crystalline grains containing muscovite and carbonate porphyroblasts (0.5mm across). Besides the patchy chloritisation of biotite and garnet, in the pelitic rocks chloritisation of biotite has developed into definite layers and the remains of the altered biotite have a brown colour with abundant sphene. In places fan-shaped chlorite crystals are associated with the ore.

In the epidiorites, chlorite is not common and is only present in a few samples (HMMI 49 & HMMI 31), either as fine flakes intergrown with actinolite or other micas or more rarely in patches in retrograde garnet, biotite and to a lesser extent actinolite.

5.4.6 Biotite

In the less pelitic rocks, fine flakes (0.1mm across) of yellowish-brown and less commonly green biotite is present intergrown with chlorite and/or muscovite flakes, with occasional euhedral crystals (1mm across).

In the more pelitic rocks, where it constitutes one of the essential minerals, biotite occurs in schistose layers of coarse intergrown crystals, with locally developed sheaves (>1mm across) radiating in all directions. Brown biotite showing alteration to chlorite occurs, either in single porphyroblasts or in layers. Biotite is also found as inclusions in the feldspar and ore minerals. Inclusions in the biotite are quartz , muscovite and less commonly feldspar.

Biotite in the epidiorites occurs as brown, small flakes of interstitial habit, often intergrown with chlorite, as local euhedral porphyroblasts, and as inclusions in the actinolite.

5.4.7 White Micas

Muscovite occurs in the psammite as small laths (<0.05mm across) and flakes intergrown with biotite and chlorite, with local larger crystals (>0.15mm across). In the pelitic rocks, especially the deformed ones, thick layers of sericite alternating with chloritic layers are present. In addition, fine flakes of muscovite and occasional large tabular idioblastic crystals are also common in the pelitic rocks. White micas form inclusions in the feldspar, and in places are replaced by the growing sulphide porphyroblasts (Plate 5.13).

In the epidiorites, white micas are very rare or completely absent.

5.4.8 Carbonate

Carbonate as calcite constitutes a minor component in the metasediments, and occurs in anhedral, untwinned grains either replacing quartz (locally as patches in the quartzitic rocks) or interstitial to it. In a few cases thin carbonate layers alternate with quartzitic layers. Less commonly, carbonate occurs partly in

200 μm
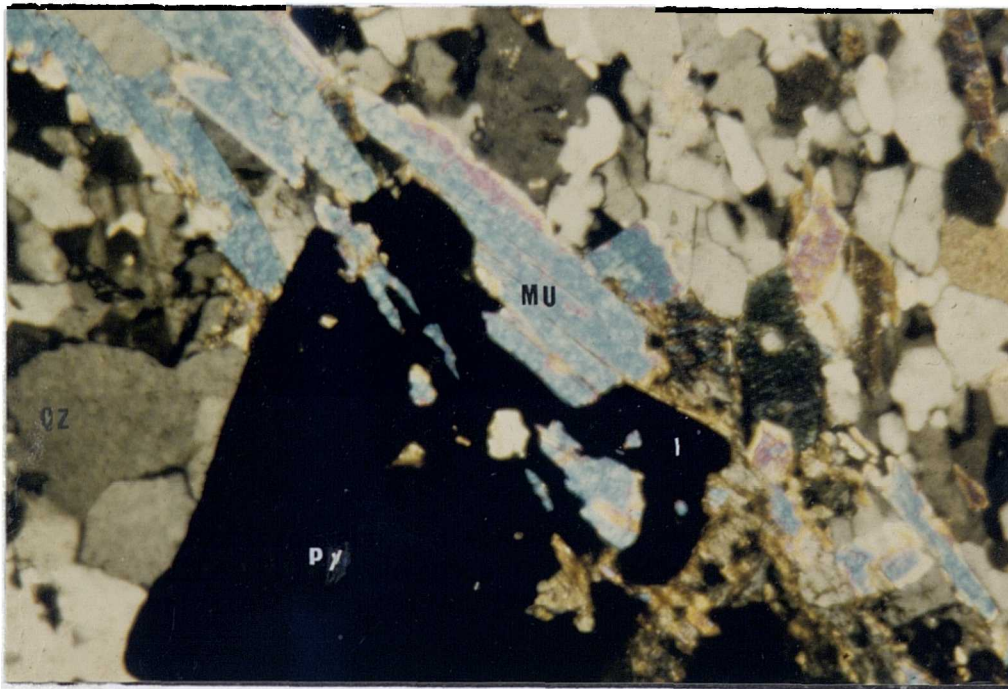
Plate 5.13 : Photomicrograph (in transmitted xed polars) of a growing
idiomorphic pyrite (PY) porphyroblast replacing muscovite crystal in
epidotised quartzite. Specimen No. HMMI 53, B.G.S, BH.1, 32.6m.

200 μm
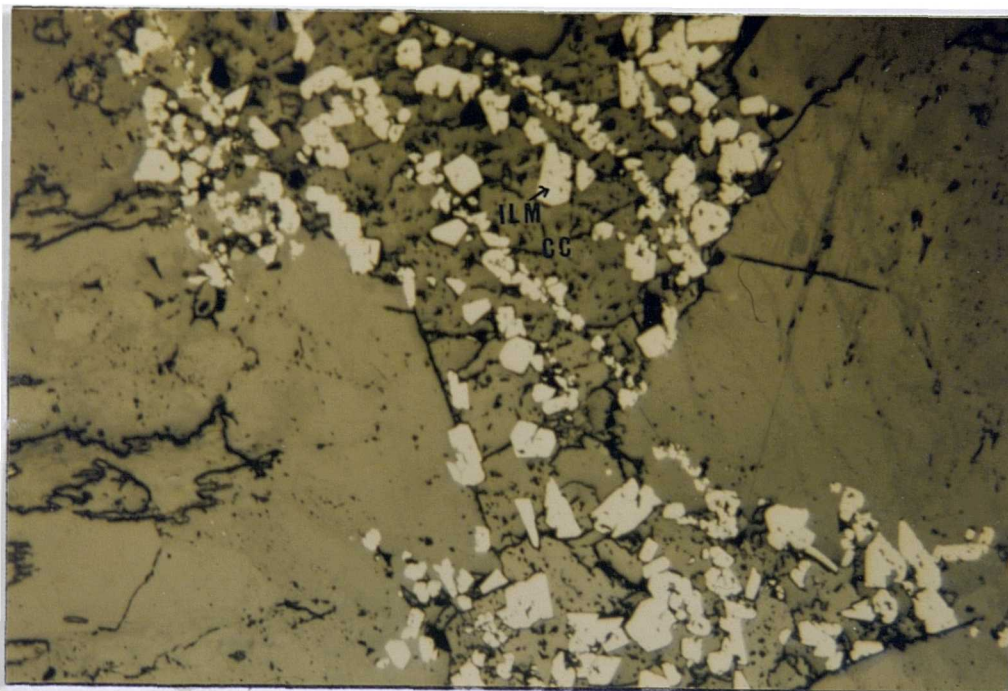
Plate 5.14 : Photomicrograph (in plane reflected light) of a fracture
filled with calcite (CC) matrix with ilmenite grains (ILM) partially
altered to sphene in feldspathic schist. Specimen No. HMMI 25, B.G.S,
BH.1, 2.0m.

brown patches, probably dolomite, associated with sericite and chlorite in the deformed rocks. It is present in relatively large amounts in veins and veinlets with or without quartz. Here it occurs in coarse, twinned crystals, in places full of epidote inclusions and hosting the ore minerals. In the relatively calcareous rocks with (>20%) carbonate, it occurs in very large lenses of calcite with dolomite. It forms an essential mineral in the metamorphosed limestones (HMM 53, with 60% carbonate).

In the epidiorites, carbonate (principally calcite) is of widespread occurrence and may assume the status of a major rock-forming mineral within some rocks. It occurs in relatively fine grains with interstitial habit and in very coarse, twinned crystals with or without quartz filling veinlets, fractures and veins that host the ore minerals.

5.4.9 Minor Non-Opaque Minerals

These minerals include sphene, zircon and apatite. Sphene is present in both the epidiorites and the metasediments as an accessory mineral, usually (< 5%), but locally enriched up to 10% (HMMI 25). It occurs in dark brown, very fine aggregates forming stringers or patches distributed in the rock. In the chloritic and sericitised rocks it forms very fine grains sieving the sericite layers. Sphene also forms a core to the large garnet porphyroblasts. It is less common in the epidote and actinolite. In places it replaces ilmenite and in some rocks, carbonate infilling fractures is full of ilmenite, crystals showing replacement to sphene (Plate 5.14).

Apatite, a less common accessory mineral, is present as rounded, sometimes elongated prismatic grains.

Zircon is also found in minor amounts with well developed egg-shaped form.

98

5.4.10 <u>Sulphides</u>

(a) <u>Pyrite</u>

In the Knapdale Pyrite Horizon, pyrite occurs as disseminations which texturally exhibit a considerable variation in both size and shape. Pyrite commonly forms single euhedral crystals ranging from 0.1-5mm across with cubic habit with or without inclusions. It also occurs as large subhedral to anhedral porphyroblasts (>2mm across) full of inclusions. In the deformed rocks elongated anhedral pyrite grains and trails are either parallel to the foliation or follow minor folds.

In the Abhainn Srathain copper mineralisation, despite the presence of chalcopyrite enrichment, pyrite is still the principal sulphide mineral and it is present in various styles.

The pyrite occurs in disseminations, both in the epidiorites and the metasediments, either as separate individual grains scattered in the rock or as scattered aggregates of grains. The disseminated grains are highly variable in both size and shape. The diameter of pyrite in polished sections averages 1mm, with maximum of 3mm and the local pyrite patches reach up to a few centimetres. Grain shape is variable; disseminated pyrite grains occur as idiomorphic crystals with common metamorphic cube form, mostly free of inclusions. The large disseminated pyrite grains or aggregates of grains occur in euhedral, subhedral and anhedral forms most commonly with opaque and gangue inclusions. In places they are highly fractured and cataclased and are replaced by chalcopyrite and rare sphalerite. In one polished section, a large pyrite porphyroblast containing a small veinlet of gold was noted (Hall 1984, pers. comm.), (Plate 5.15).

Another common style of pyrite occurrence in both the epidiorites and the metasediments is as large porphyroblasts

embedded in quartz and/or carbonate veins. These porphyroblasts are subhedral to anhedral, a few centimeters across, highly fractured and cataclased and sieved with inclusions. These large porphyroblasts are found either intergrown with the metamorphic minerals or engulfing them (Plate 5.11).

Pyrite is also found, especially in the metasediments as massive disseminated laminations or layers, and in the deformed samples, these laminations or layers are cofolded along with the host rocks (Plate 5.3).

Pyrite shows replacement by chalcopyrite along fractures and near the edges. The large porphyroblasts are altered to a complex mineral assemblage of marcasite, hematite, magnetite and others (Plate 5.9). Elongated and fragmented pyrite parallel to the rock foliation is also present.

Stratiform layers of pyrite and chalcopyrite are common, mostly parallel to the compositional layering of the rocks. These layers are continuous/discontinuous, ranging from fine laminae (0.6mm) thick to layers (>4mm) thick and in places are associated with quartz and/or carbonate veins. In one sample alternating stratiform pyrite and sphalerite was noted (Plate 5.1).

(b) Chalcopyrite

Traces of chalcopyrite are associated with the Knapdale Pyrite Horizon, either as minute trails parallel to the foliation or as anhedral fine grains intergrown with the pyrite or replacing it. Chalcopyrite inclusions in the pyrite are also common.

In the Abhainn Srathain area, chalcopyrite is abundant and has a different mode of occurrence. It occurs as alternating stratiform layers up to 4mm thick (Plate 5.2) and on the scale of a microscopic section either continuous or discontinuous. These layers are
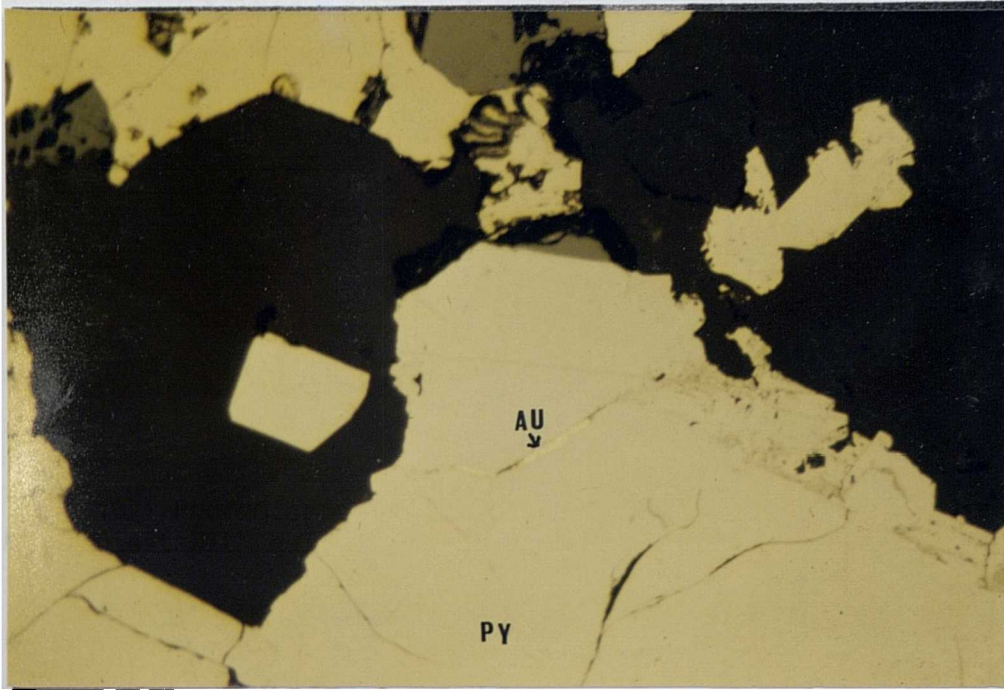
100 μm

Plate 5.15 : Photomicrograph (in plane reflected light) of pyrite (PY) porphyroblast with gold (Au) vein from Meall Mór.
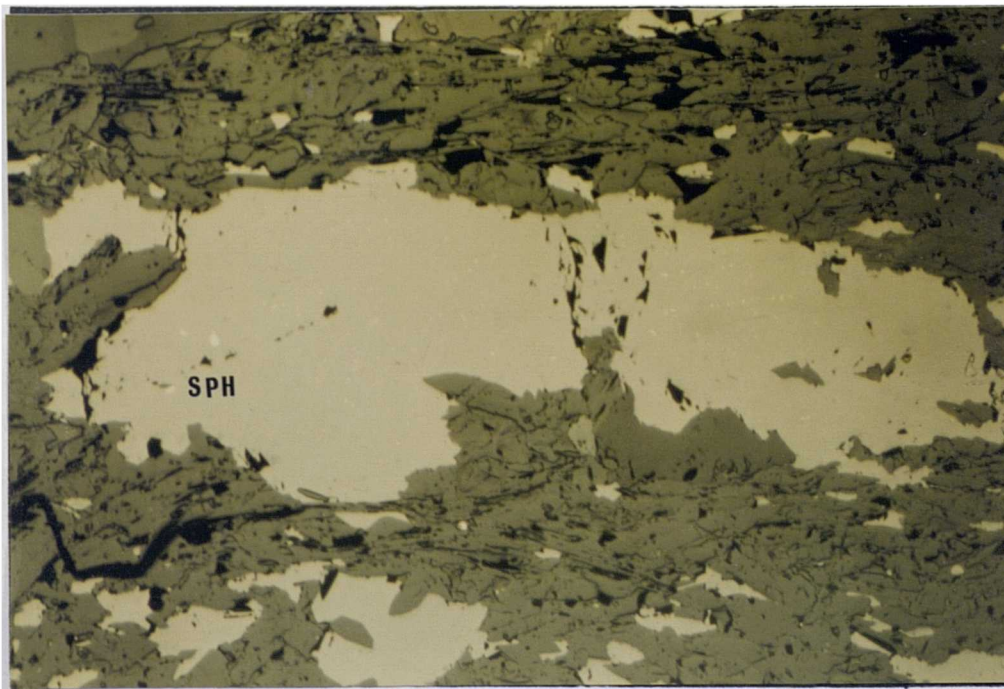
400 μm

Plate 5.16 : Photomicrograph (in plane reflected light) of sphalerite layers (SPH) with chalcopyrite inclusions in epidotised quartzite from the Abhainn Srathain mieralisation, unlocated sample.

composed of anhedral to subhedral chalcopyrite grains and in places are intergrown with pyrite.

Most commonly, it occurs as very large porphyroblasts up to 5cm across, with or without pyrite, usually embedded in quartz and/or carbonate veins. In these veins the sulphide minerals are intergrown with each other and with the magnetite (rimmed with hematite) and the silicate minerals (Plate 5.10). Like the pyrite porphyroblasts, chalcopyrite porphyroblasts are replaced near the edges by marcasite, magnetite, hematite and other minerals.

Disseminated chalcopyrite is also present and the disseminated grains, like the disseminated pyrite, have variable sizes and shapes.

In the deformed rocks, chalcopyrite exhibits mobilisation through gangue minerals and migration of the chalcopyrite is noticed on the microscopic scale.

Replacement of chalcopyrite by chalcocite, bornite and covellite along veinlets and fractures is common. Inclusions of pyrite, bornite and transparent minerals are very common. Rare magnetite inclusions were also noted. In a few slides, stratiform chalcopyrite was replaced by sphalerite (Plate 5.16).

(c) Sphalerite

Generally, sphalerite is only present in small amounts, either filling the interstices between pyrite and/or chalcopyrite or replacing them along edges, fractures and veinlets. Sphalerite is found as an inclusion in pyrite and chalcopyrite. In places sphalerite is more common and occurring either in alternating stratiform lamination with pyrite (Plate 5.1) or in stratiform layers replacing chalcopyrite (Plate 5.16). In places the sphalerite is full of chalcopyrite inclusions, chalcopyrite disease,

200 μm
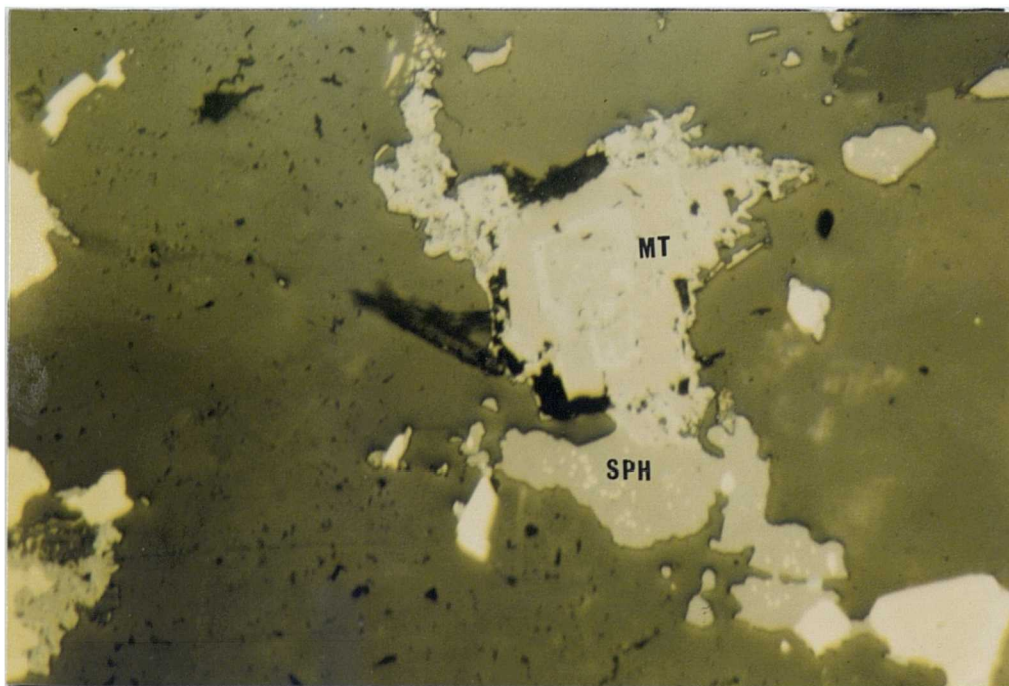
Plate 5.17 : Phototomicrograph of magnetite (MT) partially oxidised to hematite (HM) in contact with sphalerite (SPH) with chalcopyrite disease. Epidotised epidiorite, Specimen No. HMM 10, Abhainn Srathain mine (NR 836 737).
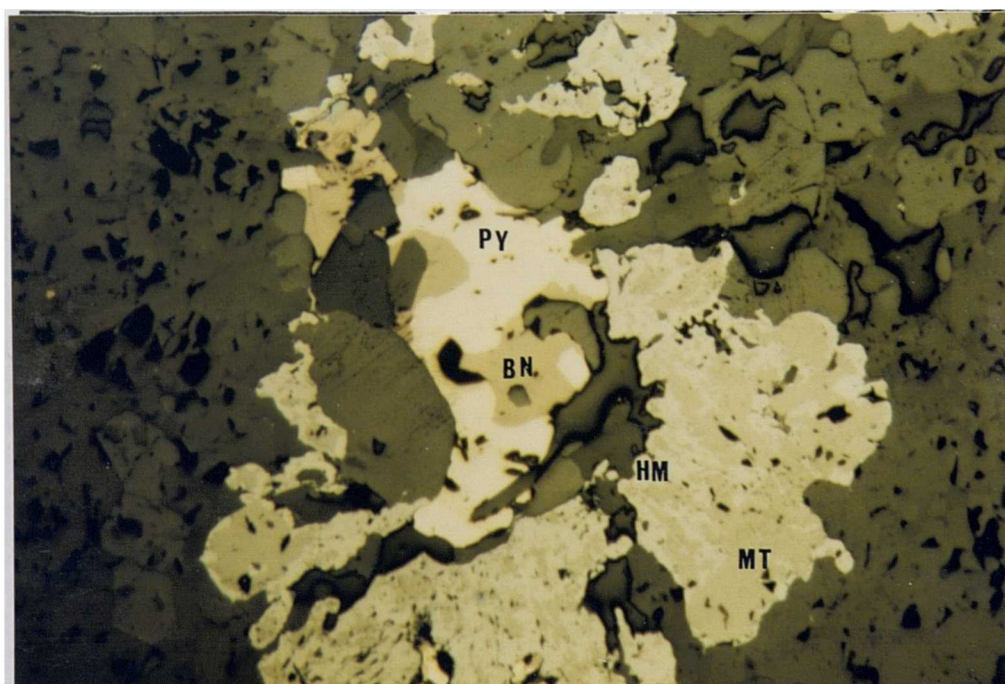
200 μm

Plate 5.18 : Photomicrograph (in plane reflected light) of chalco-pyrite (CPY) replaced by bornite (BN) and surrounded by magnetite (MT)partially oxidised to hematite in epidiorite rock. Specimen No. HMMI 16, B.G.S, BH.3, 10.2m.

103

(Plate 5.17).

(d) Pyrrhotite

Although pyrrhotite is not so common among most of the examined
sections, it is worth mentioning that it has been noticed in one
section.

(e) Marcasite

Marcasite is only present in minor quantities replacing pyrite
and chalcopyrite along margins (Plate 5.9).

(f) Other Cu-Fe sulphides

These include bornite, chalcocite and covellite. Trace bornite
is found either as inclusions in the pyrite and chalcopyrite or
replacing them (Plate 5.18). Blue iron-copper sulphides (chalcocite
and covellite) are found in cracks and along boundaries of
chalcopyrite grains. Secondary stratiform chalcocite and covellite
are found replacing the stratiform chalcopyrite.

5.4.11 Oxides

(a) Magnetite

Magnetite is more prominant in the epidiorites compared to the
metasediments, particularly in the epidotised rocks. They occur in
idiomorphic disseminations either individually distributed or
intergrown with the sulphide (Plate 5. 10). Locally they form
massive lenses or patches (Plate 5.19). The magnetite
porphyroblasts are euhedral polygonal of, variable size averging
(>2mm) across, mostly free of inclusions and in places with
chalcopyrite inclusions. They are extensively replaced by hematite
in fractures and along the margins.

(b) <u>Hematite</u>

Minor hematite is present, principally rimming magnetite and replacing it (Plate 5.19). It is also found with marcasite replacing the pyrite and chalcopyrite porphyroblasts (Plate 5.9) and as bladed laths in sulphide (Plate 5.20) and/or infilling veinlets in sulphides.

(c) <u>Rutile</u>

Rutile occurs in accessory amounts, preferentially in the metasediments either as fine granular spongy grains (<0.1mm across) or as trails parallel to the foliation. It also occurs as elongated grains up to 0.1mm across. In places rutile coexists with ilmenite and traces of magnetite.

(d) <u>Ilmenite</u>

Ilmenite occurs as subhedral to anhedral grains, usually tabular and elongated ranging in size from 0.01-2mm across. In places it shows alteration to sphene, but ilmenite forms separate grains coexisting with sphene.

5.5 <u>CHEMICAL COMPOSITION OF THE MINERALS</u>

5.5.1 <u>The Analytical Method</u>

The analyses were performed on a Cambridge Instruments Microscan Mark Five microanalyser, at the Grant Institute of Geology, University of Edinburgh, under the guidance of Dr. Peter Hill. The techniques used are both Energy Dispersive Spectrometry (EDS), and Wave Dispersive (Crystal Spectrometry; WDS).
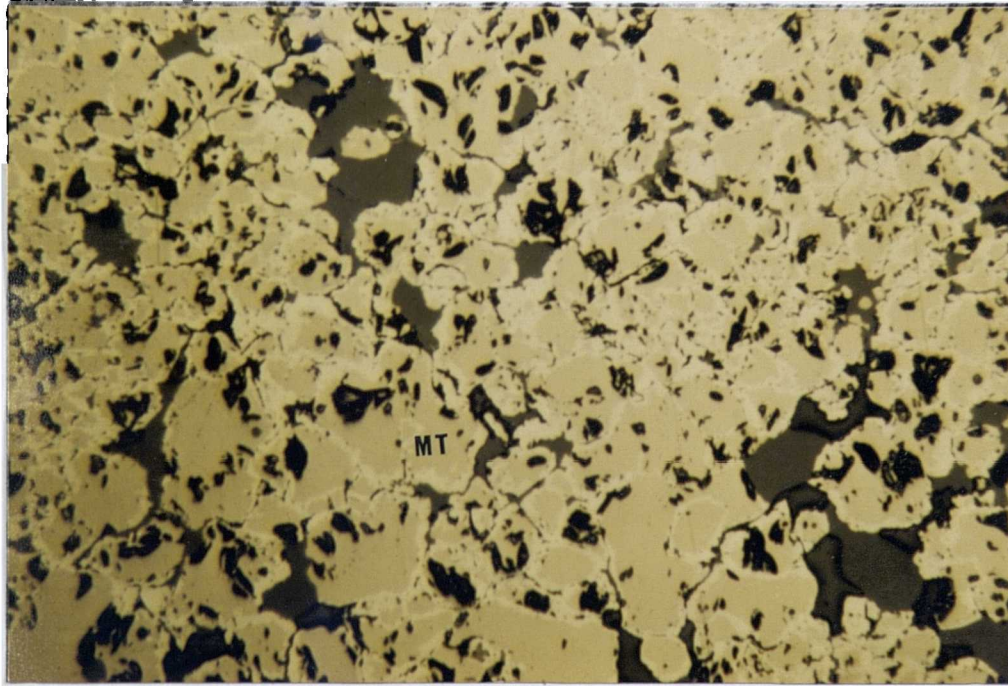
100 µm

Plate 5.19 : Photomicrograph (in plane reflected light) of massive magnetite (MT) rimmed with hematite in epidiorite from the Abhainn Srathain mine (HMM 5, NR 836 737).
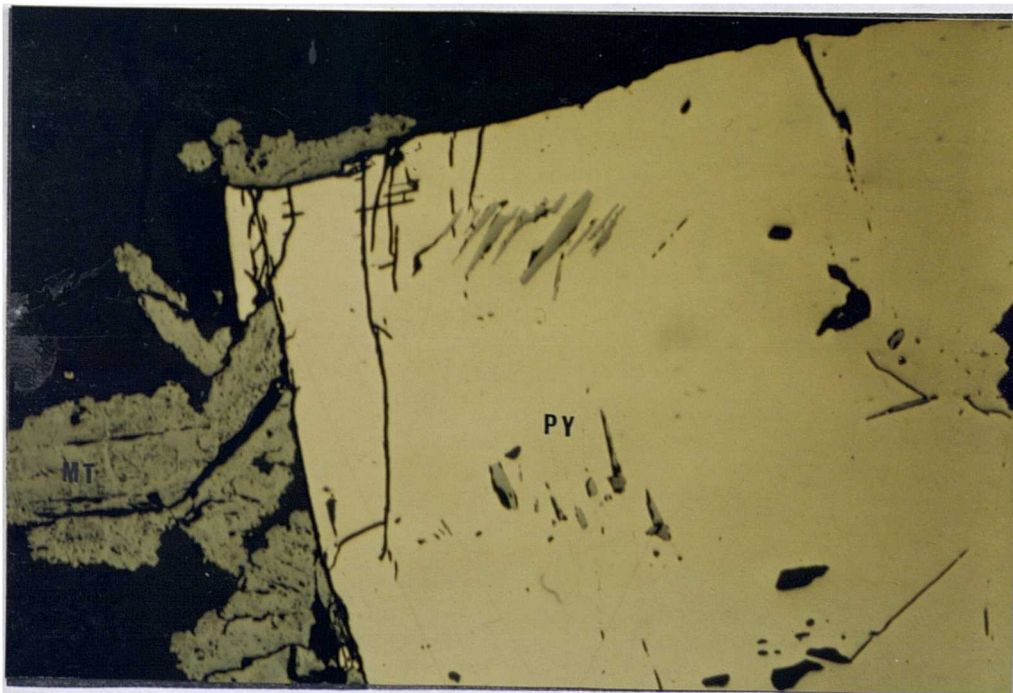
400 µm

Plate 5.20 : Photomicrograph (in plane reflected light) of pyrite euhedral (PY) and hematite (HM) in epidotised quartzite to the south of the mine (HMM 17, NR 8355 7350).

Flat, well polished, and ultrasonically clean polished blocks and thin sections (with a dimension of 48x25mm) were prepared for this analysis. Before analysis, the samples and standards were coated (under vacuum) with a thin film of carbon to enable the probe current to flow to earth. During all analyses performed using (EDS) technique, the accelerating potential was 20 Kv, the specimen current was 6 µA, the electron beam diameter was 1 µm, and the counting time 100 seconds. When using (WDS) technique, the accelerating poential was 20Kv, the probe current was 0.03 µA, collecting time was 4x10s for peaks and 2x10s for backgrounds, and the spot size was 1 µm.

Pure metals, simple oxides and silicates were used as the standards. The intensity data of the standards for all elements analysed are stored in the EDS programme. The values were monitored every few hours by measuring a Co standard, since the intensity ratios of Co to other elements are known.

Normally three grains of each mineral per slide and three spots on each single grain were analysed. Spots from both the centre and the margin were analysed to detect any zoning. As a rule, we accepted analyses varying in sum between 99.0 and 101.5 wt%.

The microprobe techniques used in the analyses have been reviewed and described in detail by Reed (1975), Statham (1975), Smith (1976), Sweatman and Long (1966), and Long (1977). In brief, the (EDS) technique involves production of an x-ray beam equivalent to elements present in the samples as a result of electron bombardment. The generated x-ray photons are detected by a solid state detector and are transferred into electrical pulses that are proportional to the incident radiation. These pulses are translated into a horizontal linear energy scale which contain 1024 channels. Thus, a correlation is built between the various x-ray energies (representing elements) and the counts (representing intensities) for a definite period of time.

The (WDS) technique involves electron bombardment by focussing a fine electron beam under high vacuum into a small area (1 μm). This results in the emission of x-rays with wavelengths and intensities characteristic of the elements present in the specimen and their concentrations. This radiation is resolved into the continuous x-ray spectrum by analysing crystals in Bragg Spectrometers and the intensity of the x-ray line characteristic of each element is measured by gas flow proportional counters, and recorded as the number of counts over a certain analytical period.

Data processing of the collected spectrum was performed by an on-line computer (EMAS, Edinburgh Computing System). This involves the calculation of the apparent concentrations of elements present from the ratio of the unknown counts to the standard counts. This was followed by compositional corrections for dead-time, escape peak and peak-overlapping, atomic number effect, secondary adsorption and secondary fluoresence to produce weight percent values. These weight percent data are calculated to atomic percent values.

5.5.2 Chemical Composition of the Minerals

Nineteen mineral phases including silicates, oxides and sulphides were analysed using the electron microprobe at the Grant Institute of Geology, Edinburgh University. For each analysis a structural formula was calculated and presented together with the result of the probe analysis in Tables (5.1-5.14) and Appendix (A. 5.3-A.5.8). In the case of hydrous minerals, since the structural water was not determined, all the formulae were calculated on an anhydrous basis.

The electron microprobe permits determination only of total iron, here expressed as FeO. Although most of the published mineral analyses by electron microprobe were presented by assuming all the iron as FeO for calculating the structural formulae of the minerals, the writer finds this inaccurate and gives deviations in the number

of cations from the theoretical values. Also, this assumption cannot be acceptable for minerals that contain a considerable value of Fe_2O_3 (e.g. garnet, amphibole, epidote, etc.). So an attempt to assign part of the FeO as Fe_2O_3 for each analysis was carried out using a computer programme (Bowes 1982, pers. comm.), and following procedures given by Vieten and Hamm (1971), Stout (1972), Papike et al. (1974), Laird and Albee (1981) and McDowell and Elders (1980), with some modifications. The value of Fe_2O_3 presented in each analysis (Tables 5.1-5.10, except for epidote), is the value that gives the best stoichiometric formula.

In calculating the structural formulae of the minerals that contain significant Fe_2O_3 , two structural formulae were calculated for each phase, one by assuming all iron as FeO (except for epidote, where the total iron was assumed as Fe_2O_3), and the other one by assigning part of the total iron as Fe_2O_3 consistent with stoichiometry as mentioned above. The writer prefers representation by the latter calculation (Tables 5.1-5.10).

The reported analyses in this chapter are average and/or individual analyses of up to four grains per phase in each slide, and three analyses in each grain. The problem of deciding whether or not a given analysis is of acceptable accuracy is judged from the total summation. The writer accepted analyses, in the case of anhydrous minerals, varying in sum between 99.0 and 101.5 wt%.

5.5.3 Amphibole

Fourteen microprobe analyses of calciferous amphibole in both epidiorites (n=13) and metasediments (n=1) are presented in Table (5.1) and in Appendix (A.5.3).

Table 5.1 : Electron microprobe analysis of amphibole. Recalculation is made by fixing part of the total iron (as FeO) into Fe_2O_3:

VAR. / ID.	HMM 5	HMM 8	HMM 9	HMM 10	HMM 12	HMM 14	HMM 15	HMM 1	HMM 3	HMM 19	HMM 31	HMM 11	HMM 16	HMM 23*
SiO_2	51.69	54.10	53.41	52.56	55.05	53.63	54.49	53.77	56.10	53.01	49.09	54.36	52.88	43.77
Al_2O_3	2.74	0.87	1.04	1.56	0.46	0.70	1.92	0.99	1.57	4.38	5.36	1.75	0.47	11.05
TiO_2	0.04	0.00	0.00	0.00	0.00	0.00	0.00	0.00	0.00	0.00	0.00	0.00	0.01	0.30
Cr_2O_3	0.04	0.00	0.00	0.00	0.00	0.00	0.00	0.00	0.00	0.00	0.00	0.12	0.00	0.00
Fe_2O_3	5.01	0.90	1.56	3.65	1.07	0.00	1.19	0.81	0.23	1.19	6.19	0.33	1.66	5.03
FeO	12.74	13.48	16.35	14.36	11.00	17.36	10.04	14.48	7.83	16.31	12.46	12.96	16.25	15.74
MnO	0.97	0.90	1.36	1.34	0.86	1.23	0.75	1.07	0.86	1.05	0.30	0.65	1.50	0.20
MgO	12.55	14.90	12.68	12.38	16.50	12.47	16.82	13.53	18.82	11.11	11.83	15.00	12.09	8.34
CaO	11.40	12.09	11.82	11.84	12.57	11.83	12.40	11.82	12.38	11.23	11.57	11.97	11.82	11.06
Na_2O	0.56	0.00	0.00	0.33	0.00	0.00	0.00	0.25	0.00	0.63	0.89	0.00	0.15	1.87
K_2O	0.03	0.00	0.00	0.00	0.00	0.00	0.00	0.05	0.00	0.21	0.22	0.00	0.03	0.41
TOTAL (wt %)	97.77	97.24	98.22	98.02	97.51	97.22	97.61	96.77	97.79	99.12	97.91	97.14	96.86	97.77

NUMBER OF IONS ON BASIS OF 23 (O)

VAR. / ID.	HMM 5	HMM 8	HMM 9	HMM 10	HMM 12	HMM 14	HMM 15	HMM 1	HMM 3	HMM 19	HMM 31	HMM 11	HMM 16	HMM 23*
Si	7.58	7.88	7.83	7.72	7.91	7.94	7.78	7.91	7.88	7.67	7.22	7.87	7.89	6.58
Al	0.42	0.12	0.17	0.28	0.08	0.06	0.22	0.09	0.12	0.33	0.78	0.13	0.08	1.42
Total	8.00	8.00	8.00	8.00	8.00	8.00	8.00	8.00	8.00	8.00	8.00	8.00	8.00	8.00
Al6	0.05	0.03	0.01	0.00	0.00	0.06	0.10	0.08	0.14	0.42	0.15	0.17	0.00	0.54
Ti	0.01	0.00	0.00	0.00	0.00	0.00	0.00	0.00	0.00	0.00	0.00	0.00	0.00	0.03
Cr^{3+}	0.01	0.00	0.00	0.00	0.00	0.00	0.00	0.00	0.00	0.00	0.00	0.00	0.00	0.00
Fe^{3+}	0.55	0.10	0.17	0.40	0.10	0.00	0.13	0.09	0.02	0.13	0.69	0.04	0.16	0.57
Fe^{2+}	1.52	1.53	1.87	1.72	1.26	2.03	1.10	1.73	0.80	1.97	1.53	1.47	1.96	1.98
Mn	0.12	0.11	0.17	0.17	0.11	0.15	0.09	0.13	0.10	0.09	0.04	0.08	0.19	0.03
Mg	2.74	3.23	2.77	2.71	3.53	2.75	3.58	2.97	3.94	2.39	2.59	3.24	2.69	1.87
Total	5.00	5.00	5.00	5.00	5.00	4.99	5.00	5.00	5.00	5.00	5.00	5.00	5.00	5.02
Ca	1.79	1.89	1.86	1.86	1.94	1.88	1.90	1.86	1.86	1.74	1.82	1.86	1.89	1.78
Na	0.16	0.00	0.00	0.09	0.00	0.00	0.00	0.07	0.00	0.18	0.25	0.00	0.04	0.54
K	0.01	0.00	0.00	0.00	0.00	0.00	0.00	0.01	0.00	0.04	0.04	0.00	0.01	0.08
Fe^{2+}	0.04	0.11	0.13	0.04	0.06	0.12	0.10	0.06	0.12	0.04	0.00	0.10	0.06	0.00
Total	2.00	2.00	1.99	1.99	2.00	2.00	2.00	2.00	1.98	2.00	2.12	1.96	2.00	2.40

* amphibole in micaceous quartzite.

110

Recalculation of the analyses

The amphibole analyses have been recalculated both on the basis of 23 oxygen atoms and on a fixed numbers of cations (Table 5.1). In Appendix (A.5.3), the analyses are calculated to stoichiometric formulae assuming all the iron as FeO, which is undoubtedly incorrect for calcic amphiboles (Robinson and Jaffe 1969), especially in the metamorphic rocks where amphibole may have as much as 50% of the total iron in the ferric state (Deer et al. 1963).

In a typical calcic amphibole of the general formulae $A_1B_2C_5T_8O_{22}$ $(OH,F,Cl)_2$, the cation sites are distributed as follows (Stout 1972).

8 tetrahedral sites (T-site) occupied by $Si+Al^4$

5 octahedral sites (C-site) occupied by $Mg+Fe+Al+Mn+(Ti)^6$

2 large octahedral sites (B-site) occupied by Ca+Na+excess (Fe+Mg+Mn)

1 (A-site) occupied by Na+K.

A persistent defeciency in the occupancy of the B-sites (<2), matched by a complementery surplus in the occupancy of the C-sites (>5), was formed when assuming all the iron as FeO (Appendix A.5.3). This is probably because some of the iron is present as Fe_2O_3 in the calcic amphiboles. However different schemes and methods have been constructed to give a rough estimate of the Fe^{3+}-content of the amphiboles (e.g. Papike et al. 1974 and Stout 1972) from microprobe data.

In this study , a recalculation of the analysed calcic amphiboles (Table 5.1), was based on a rough estimate of the Fe^{3+}-content consistent with the stoichiometry. Assuming no cation or oxygen vacancies in the structure and no higher oxidation states of

metals other than Fe^{3+}, the amount of oxygen required to bring the sum to 23 is a measure of that amount of oxygen compounded as Fe_2O_3. Cation vacancies are important only in the A-sites of the calcic amphiboles and as the analysed amphiboles are very poor in K (0-0.05, except Specimens HMMI 23 & 31), it was assumed that the A-site is empty and the analyses total 15 cations, which requires maximum oxidation (Stout 1972). This was done by assigning part of the total iron as Fe_2O_3 such that a C-site occupancy of (5) and B-site occupancy of (2) were achieved. In case of Specimens HMMI 23&31, which contain significant K, it was assumed that the A-site is not empty and hence recalculation of the analyses to 15 cations excluding Na+K was accomplished by forcing all Na to enter the A-site.

Nomenclature

In the calculation of the standard amphibole formulae, a recommended calculation procedure constructed by Leake (1978) was used. This permitted application of the proposed names of amphiboles by the same author to the analysed samples. In his scheme, he classified the amphibole first into four principal groups namely iron-maganesium-manganese, calcic, sodic-calcic, and alkali amphiboles, on the basis of the number of (Ca+Na) and Na in the B-site. Then each of these groups was treated separately and subdivided into different end-members represented in a two dimensional diagram on the basis of the number of Si atoms and the ratio Mg/ (Mg+Fe).

The analysed amphiboles fall into the calcic amphibole group in which $(Ca+Na)_B \geq 1.34$ and $Na_B < 0.67$ and generally $Ca_B > 1.34$ atom per 23 (0) formula. Using the two dimensional diagram of Leake (1978), the analysed amphiboles hosted by the epidiorites fall within the actinolitic field (Fig. 5.3), while the pelitic amphiboles fall within the field of ferro-hornblende.

Chemistry

The chemistry of the calciferous amphiboles is notoriously complex, all the major rock forming elements occurring in significant abundance and showing appreciable variation. While a variety of ionic substitutions are possible within the amphibole lattice, chemical variation within the analysed amphiboles may be desribed to a first approximation by three basic substitutions within the basic tremolite formula :

$$Fe^{2+} = Mg$$

$$NaAl^{+} = Si \qquad \text{edenite substitution}$$

$$MgSi = Al^{+}Al^{6} \qquad \text{tschemarkite substitution}$$
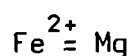
and combination of the latter substitution derives the paragasite molecule.

Chemical variation is represented diagramatically in Fig. (5.4a-d) where the inter relationships of Mg, Al^{+}, Al^{6}, Si, and alkali contents is discussed. Fig. (5.4 a&b) reflects the interdependence of Mg and Al, in which the analysed amphiboles are Mg rich and Al poor. Fig. (5.4c) shows that the high Si is accompanied by low Al^{6}, while Fig. (5.4d) shows that the Na+K content depends on the Al, especially Al^{6}. A considerable amount of MnO (0.2-1.54 MnO wt%) with a mean of 0.93 wt% and a standard deviation of 0.36 is present (Fig. 5.9). In Figs. (5.3 & 5.4d), a distinct chemical variation between amphibole hosted by epidiorites and that hosted by metasediments is apparent. The latter are more alkali and closer to paragasite than to actinolite.

Variation in the amphibole chemistry could be related to bulk rock chemistry. The wide range of amphibole Mg/Mg+Fe (Fig. 5.5) is related to the rock Mg/Mg+Fe variations.
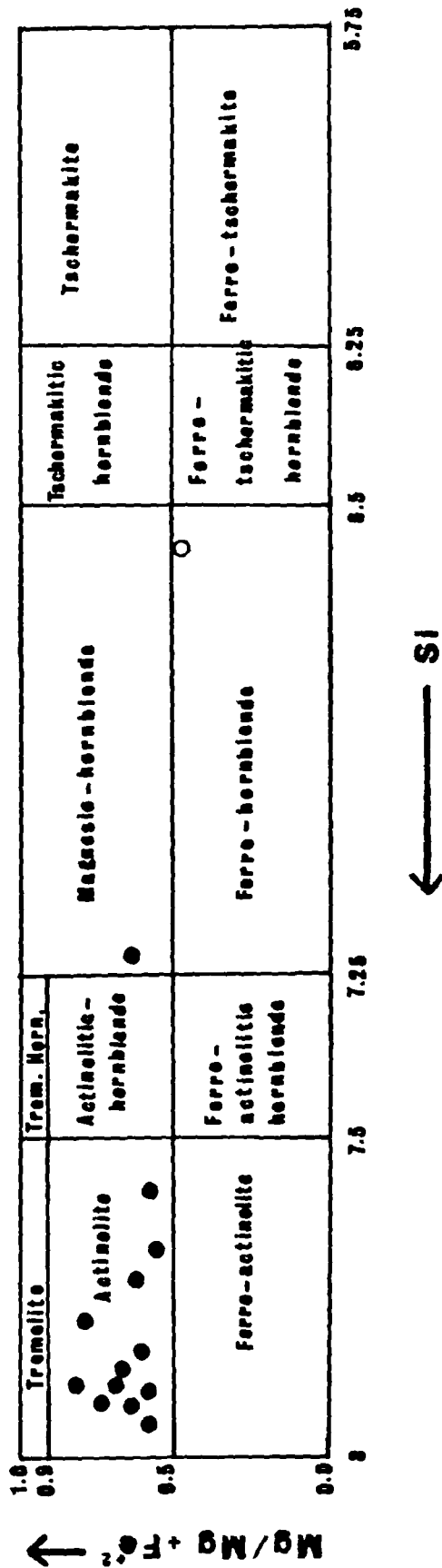
Fig. (5.3) : The analysed amphiboles according to the classification of Leake (1978).
●: represent amphiboles from epidiorites, ○: from metasediments.

114
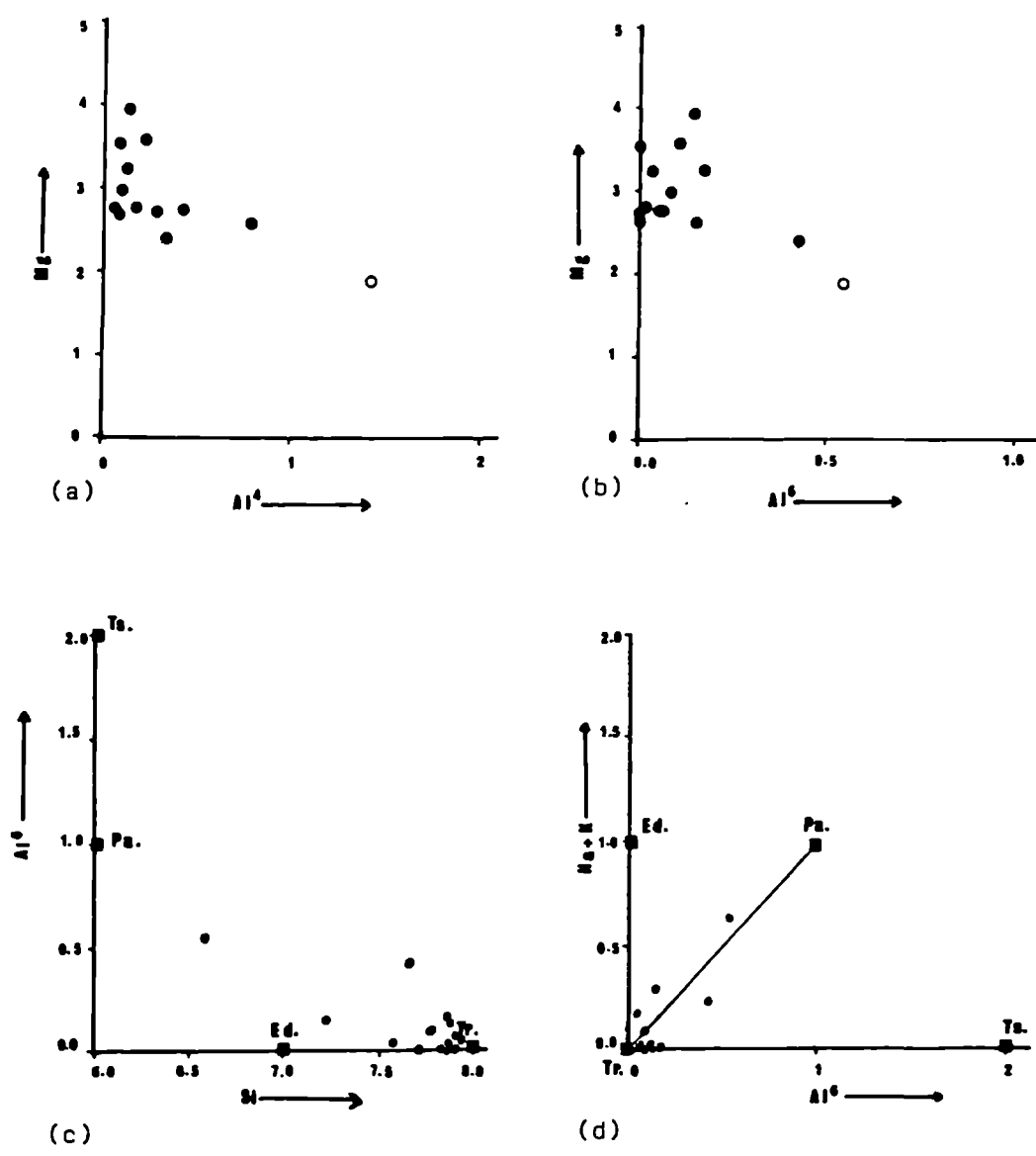
Fig. (5.4) : The relationship between; (a) Al^4 & Mg, (b) Al^6 & Mg, (c) Si & Al^6 and (d) Al^6 & Na+k in the analysed amphiboles. ●: from epidiorites, O: from metasediments.

115
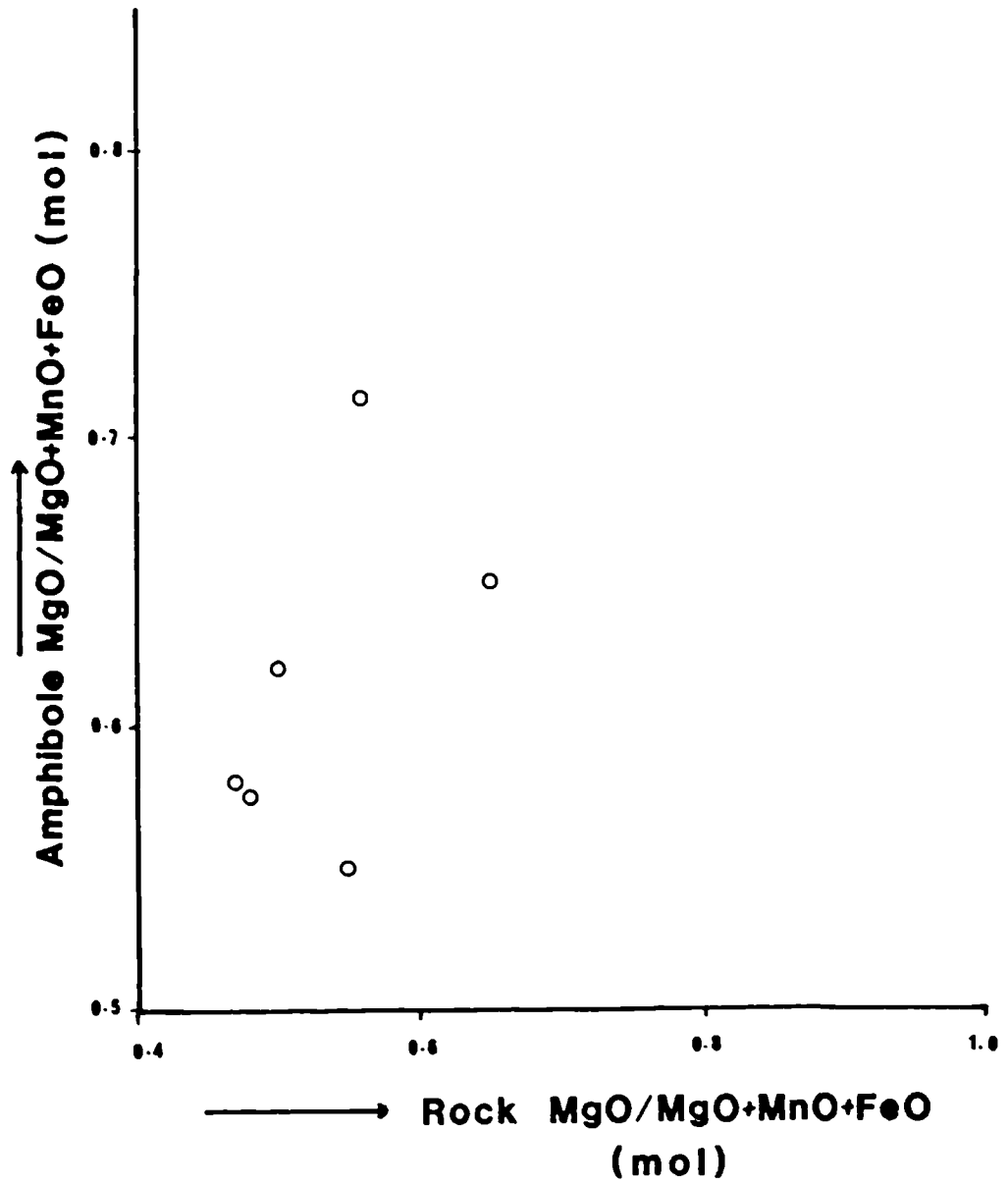
Fig. 5.5 : The relation between rock MgO/MgO+MnO+FeO and the amphibole
MgO/MgO+MnO+FeO.

116

5.5.4 Garnet

Fifteen microprobe analyses of garnets from both epidiorites (n=9) and from metasediments (n=6) are presented in Table (5.2), together with their recalculated stoichiometry. The presented end-member composition is recalculated following the procedure given by Rickwood (1968).

Recalculation of the analysis

On calculating to stoichiometric molecules by assuming all iron as FeO (Appendix A.5.4), it is found that a persistent defeciency in the occupancy of the Y-site in the garnet molecule $(X_6 Y_4 Z_6 O_{24})$ is matched by a complementry surplus in the X-site. This is because of the presence of Fe^{3+} in the garnet molecule which would enter the Y-site. This problem was overcome by assigning part of the total iron as $Fe_2 O_3$ such that a Y-site occupancy of 4, X-site of 6 and Z-site of 6 is achieved (Table 5.2).

Chemistry

Variation within single grain

Comparison of analyses of several spots in a single garnet grain reveals that they are slightly inhomogeneous especially with MnO, FeO, CaO, and MgO wt%. In most cases MnO wt% content decreases and MgO and FeO wt% content increases towards the rim of the grain. CaO wt% behaviour is not consistent, sometimes similar to MnO wt% and sometimes it shows an opposite pattern. Various compositional zoning in garnets from the Dalradian and from elsewhere, was reported and studied by many authors (e.g. Atherton 1968, Graham 1973, Sivaprakash 1981 and Tyler and Ashworth 1981).

Table 5.2 : Electron microprobe analysis of garnet. Recalculation is made by fixing part of the total iron (as FeO) into Fe_2O_3.

VAR. / ID.	HMM 4	HMM 5	HMM 8	HMM 9	HMM 11	HMM 14	HMM 1	HMM 16	HMM 19	HMM 1	HMM 44	HMM 25	HMM 29	HMM 33	HMM 46
				Epidiorites								Metasediments			
SiO_2	37.41	37.41	37.66	37.20	38.27	37.51	37.28	36.75	36.48	37.76	37.99	37.61	36.95	46.79	37.55
Al_2O_3	18.19	18.00	20.07	18.43	20.16	18.52	18.69	17.42	18.04	21.10	21.47	20.47	20.58	17.63	20.83
TiO_2	0.34	0.17	0.17	0.19	0.17	0.26	0.19	0.15	3.94	0.00	0.14	0.17	0.13	0.17	0.00
Cr_2O_3	0.00	0.00	0.00	0.09	0.00	0.06	0.01	0.00	0.00	0.00	0.00	0.01	0.02	0.00	0.00
Fe_2O_3	4.16	4.73	2.18	4.13	2.67	4.33	3.65	5.84	1.33	0.29	0.00	1.00	0.86	0.00	0.49
FeO	13.51	14.04	11.30	10.07	13.11	13.00	10.45	11.41	9.90	24.40	26.27	23.66	20.25	16.91	25.06
MnO	12.56	11.62	15.51	18.41	13.01	14.40	16.00	15.43	14.00	8.26	6.86	9.31	13.48	12.11	6.91
MgO	0.00	0.00	0.13	0.23	0.44	0.08	0.20	0.21	0.00	0.53	0.89	0.71	0.60	0.40	0.76
CaO	14.14	14.73	14.08	12.12	14.79	13.56	13.75	13.24	15.85	8.71	8.11	7.99	7.39	7.71	8.87
TOTAL(wt %)	100.31	100.70	101.10	100.87	102.62	101.72	100.22	100.45	99.54	101.05	101.73	100.93	100.26	101.73	100.47
NUMBER OF IONS ON BASIS OF 24 (O)															
Si	6.02	6.00	5.97	5.98	5.97	5.97	5.99	5.95	5.88	6.01	6.00	6.01	5.97	7.10	6.02
Al^*	0.00	0.00	0.03	0.02	0.03	0.03	0.01	0.05	0.12	0.00	0.00	0.00	0.03	0.00	0.00
Total	6.02	6.00	6.00	6.00	6.00	6.00	6.00	6.00	6.00	6.01	6.00	6.01	6.00	7.10	6.02
Al'	3.45	3.40	3.72	3.47	3.67	3.44	3.53	3.27	3.43	3.96	4.00	3.86	3.88	3.15	3.94
Ti	0.04	0.02	0.02	0.02	0.02	0.03	0.02	0.02	0.48	0.00	0.02	0.02	0.02	0.02	0.00
Cr	0.00	0.00	0.00	0.01	0.00	0.01	0.00	0.00	0.00	0.00	0.00	0.00	0.00	0.00	0.00
Fe^{3+}	0.50	0.57	0.26	0.50	0.31	0.52	0.44	0.71	0.09	0.04	0.00	0.12	0.10	0.00	0.03
Total	3.99	3.99	4.00	4.00	4.00	4.00	4.00	4.00	4.00	4.00	4.02	4.00	4.00	3.17	3.97
Fe^{2+}	1.82	1.88	1.50	1.35	1.71	1.73	1.41	1.54	1.34	3.25	3.47	3.17	2.74	2.14	3.36
Mn	1.71	1.58	2.08	2.51	1.72	1.94	2.18	2.12	1.91	1.12	0.92	1.26	1.84	1.56	0.94
Mg	0.00	0.00	0.03	0.06	0.10	0.02	0.05	0.05	0.00	0.13	0.21	0.17	0.14	0.09	0.18
Ca	2.44	2.53	2.39	2.09	2.47	2.31	2.37	2.30	2.74	1.49	1.37	1.37	1.28	1.25	1.53
Total	5.97	5.99	6.00	6.01	6.00	6.00	6.01	6.01	5.99	5.99	5.97	5.97	6.00	5.05	6.01
END-MEMBER COMPOSITION (MOL %)															
Andradite	12.70	14.40	6.50	12.60	7.90	13.00	11.10	17.90	2.32	0.00	0.00	3.00	2.60	0.00	0.78
Pyrope	0.00	0.00	0.00	0.00	1.70	0.00	0.00	0.00	0.00	2.10	3.51	2.80	2.40	1.97	3.06
Spessartine	28.90	26.50	34.90	42.20	28.80	32.50	36.60	35.60	36.31	18.80	15.29	21.10	30.90	32.91	15.78
Grossular	28.40	28.10	33.50	22.50	33.50	25.70	28.70	20.70	49.67	25.00	22.89	19.90	18.80	26.49	24.85
Almandine	30.00	31.00	25.10	22.80	28.10	28.80	23.60	25.80	11.70	54.20	58.31	53.10	45.30	38.64	55.53
Total	100.00	100.00	100.00	100.10	100.00	100.00	100.00	100.00	100.00	100.10	100.00	99.90	100.00	100.00	100.00

118

Chemical variation within garnet

The analysed garnets show a considerable variation in terms of total FeO, MnO, and CaO wt%. In Fig. (5.6) a linear variation of (FeO + MgO wt%) against (MnO + CaO wt%) is noted. Decreasing (MgO + FeO wt%) is accompanied by increasing (CaO + MnO wt%) and this can be consistently presented by the relation of Fe and Mn atoms (Fig. 5.7). However this linear relationship between (CaO + MnO wt%) and (FeO + MgO wt%) was observed by Miyashiro (1953) and Sturt (1962) between garnet from different grades of metamorphism, and they relate this variation to increasing grade of metamorphism which cannot be applied to Meall Mòr garnets as they belong to one grade (Barrovian garnet zone).

Calculation of the garnet end-member composition, shows that they are far from being of constant composition, and that spessartine, grossular, and almandine are the principal molecules in the garnets and are present in variable proportions (Table 5.2).

Figure (5.8a) represents the variation in the garnet end-members. Two groupings are distinguished, one close to the almandine end-member and representing garnets from metasediments, and the other close to the spessartine end-memeber and representing garnets from epidiorites.

Variation among different grains

The distinct optical variation between garnets hosted by epidiorites and those hosted by the metasediments (Section 5.4.4) is again documented here by their chemical variation. Garnets hosted by the metasediments are almandine rich (Fig. 5.8a), but with significant amounts of spessartine and grossular and little pyrope and andradite. The almandine content ranges from 38.64 to 58.31 % ($\bar{x}$=50.85, σ=6.75), grossular from 18.8 to 25 % ($\bar{x}$=22.99, σ=2.8), and spessartine from 15.29 to 32.91 % ($\bar{x}$=22.46, σ=6.97).
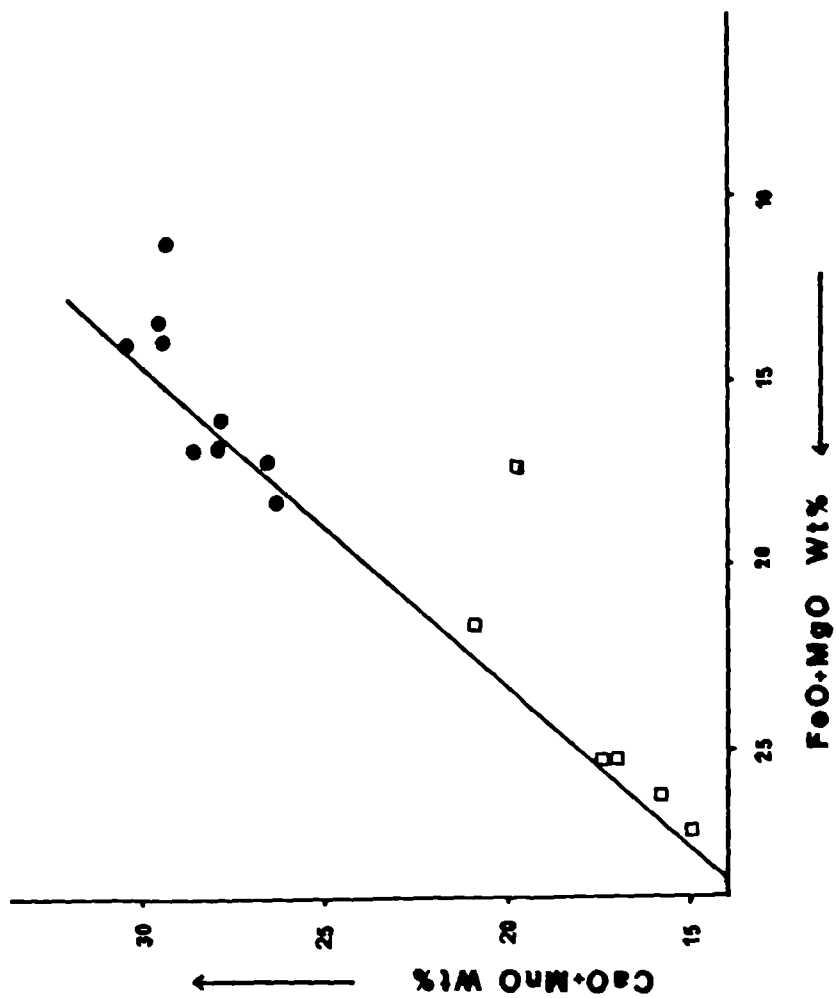
Fig. 5.6 : The relationship between CaO+MnO and FeO+MgO (as wt%) in the analysed garnets.
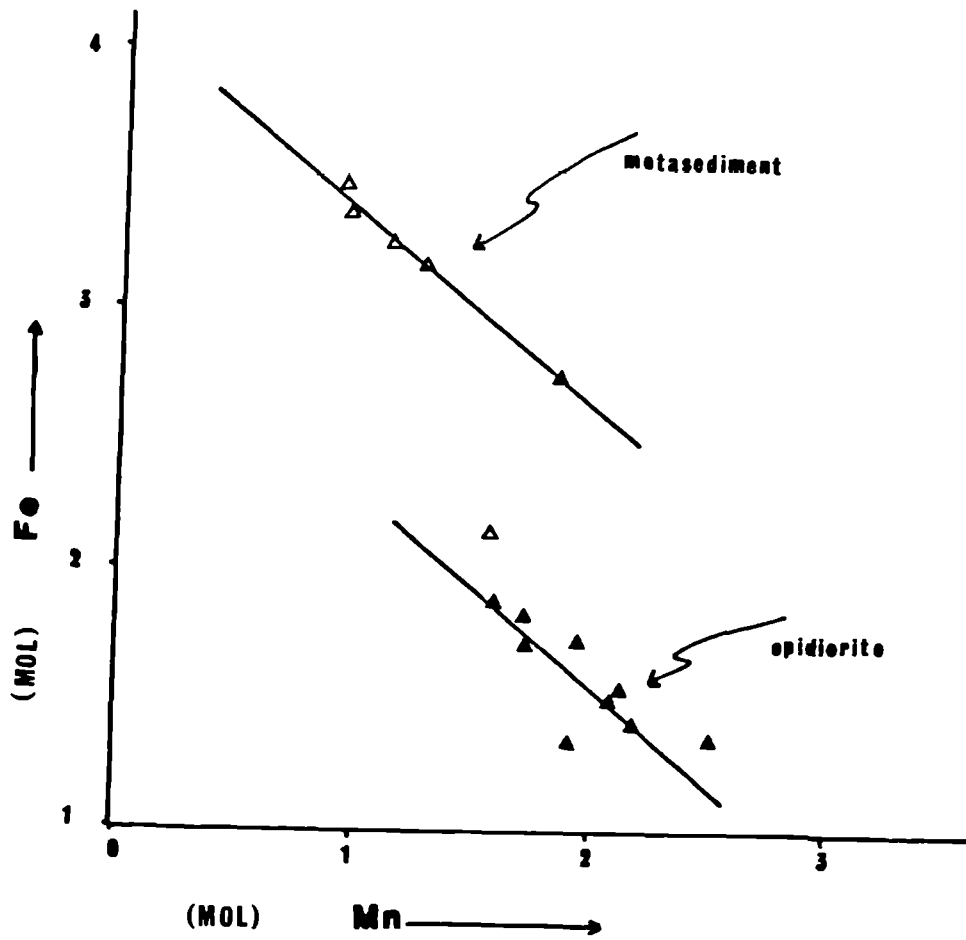
Fig. 5.7 :   The molecular relation of Mn and Fe in
the analysed garnets.
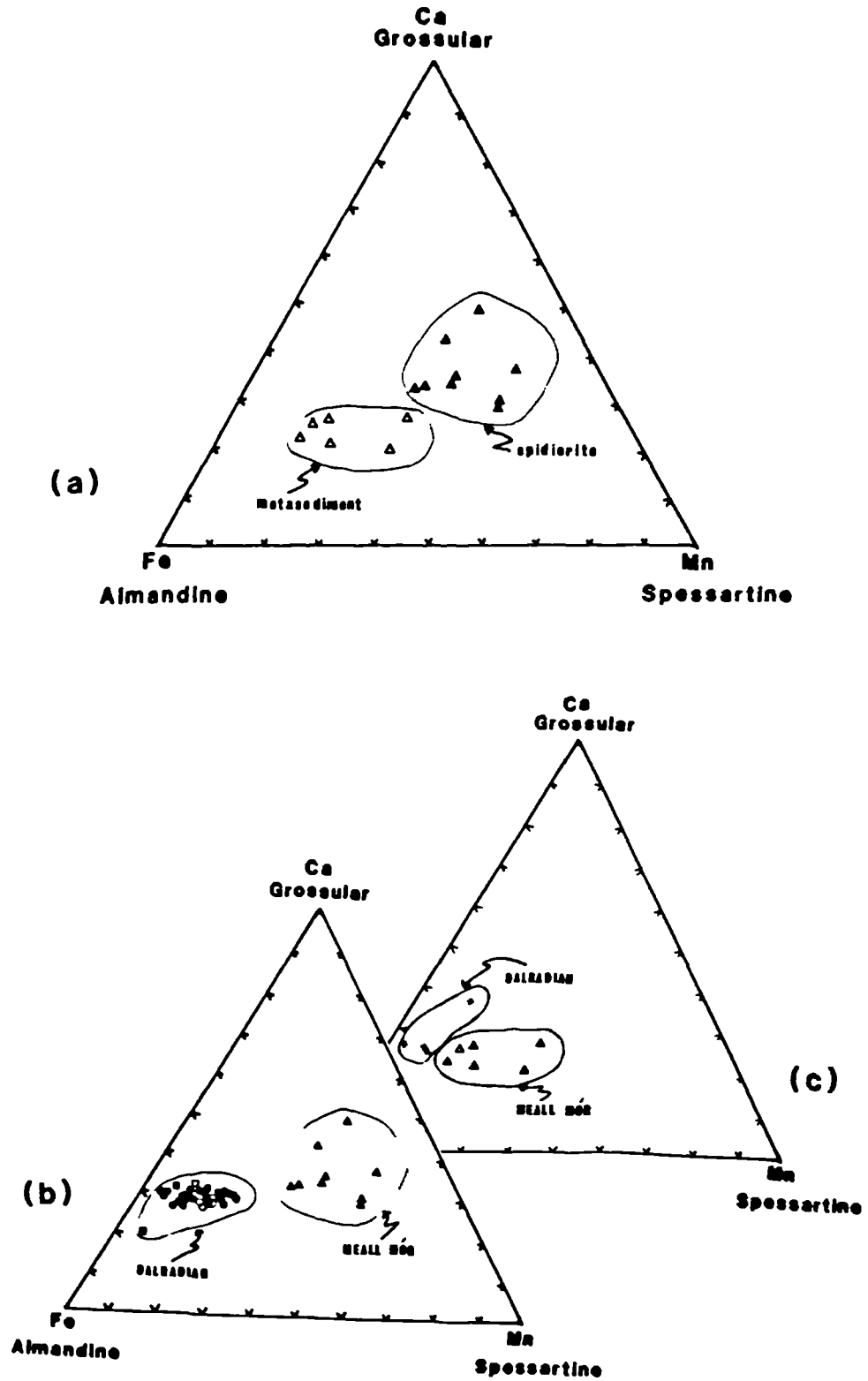
Fig. 5.8 : (a) The triangular compositional variation of the
present analysed garnets from Meall Mór. (b) Com-
parison of the Meall Mór epidiorite garnets with
other Dalradian epidiorite garnets.●: metabasite
garnets from SW-Highlands(Graham 1973); o : meta-
basite garnets from Perthshire; □: metabasite garnet
garnet,garnet zone, SW-Highlands (Wiseman 1934);
■: metabasite garnet from Ben vrackie, Perthshire
(Pantin 1956). (c) Comparison of the metasediment
garnets of Meall Mór with other analysed garnets
from pelites from Dalradian and Moines rocks
(Atherton 1965).

Garnets hosted by the metasediments are spessartine rich with significant and variable amounts of grossular and almandine, while pyrope is almost absent. The andradite content is very high compared to the garnets hosted by the metasediments, ranging from 2.32 to 17.9 % ($\bar{x}$=10.94, σ=4.39) while Spessartine ranges from 26.5 to 42.2 % ($\bar{x}$=33.59, σ=4.63), grossular from 20.7 to 49.67 % ($\bar{x}$=30.09, σ=8.03) and almandine from 11.7 to 31 % ($\bar{x}$=25.21, σ=5.47).

Manganese content of the analysed garnets

The garnets are notably manganese bearing. Fifteen analyses of garnet from the mineralised area give values of MnO wt% ranging from 6.86 to 18.41, with a mean ($\bar{x}$=12.52) and a standard deviation σ=3.31 . The manganese is prefentially concentrated in garnets compared with the other manganese-bearing minerals (Fig. 5.9). Garnet analyses from the Dalradian rocks from the garnet zone and from elsewhere by many authors are presented in Fig. (5.8 b&c). The present analysed garnets from epidiorites in Meall Mór are compared with other Dalradian epidiorite garnets (Fig. 5.8b), and it is clear that the garnets from the studied area are richer in spessartine and grossular molecules. Although the analysed garnets from the Dalradian represent garnets from different grades of metamorphism, they all plotted into one scatter close to the almandine end-member. This comparison reveals that :

(1) Meall Mór garnets from the garnet zone are richer in spessartine and grossular molecules than the metabasite garnets from the same zone in the Southwest Highlands analysed by Graham (1973).

(2) All the analysed Dalradian garnets plot close to the almandine composition irrespective of their location and grade of metamorphism, while the Meall Mór garnets form a distinct group closer to the spessartine end-member, and with higher grossular content, exhibiting a wide range of variation within themselves.
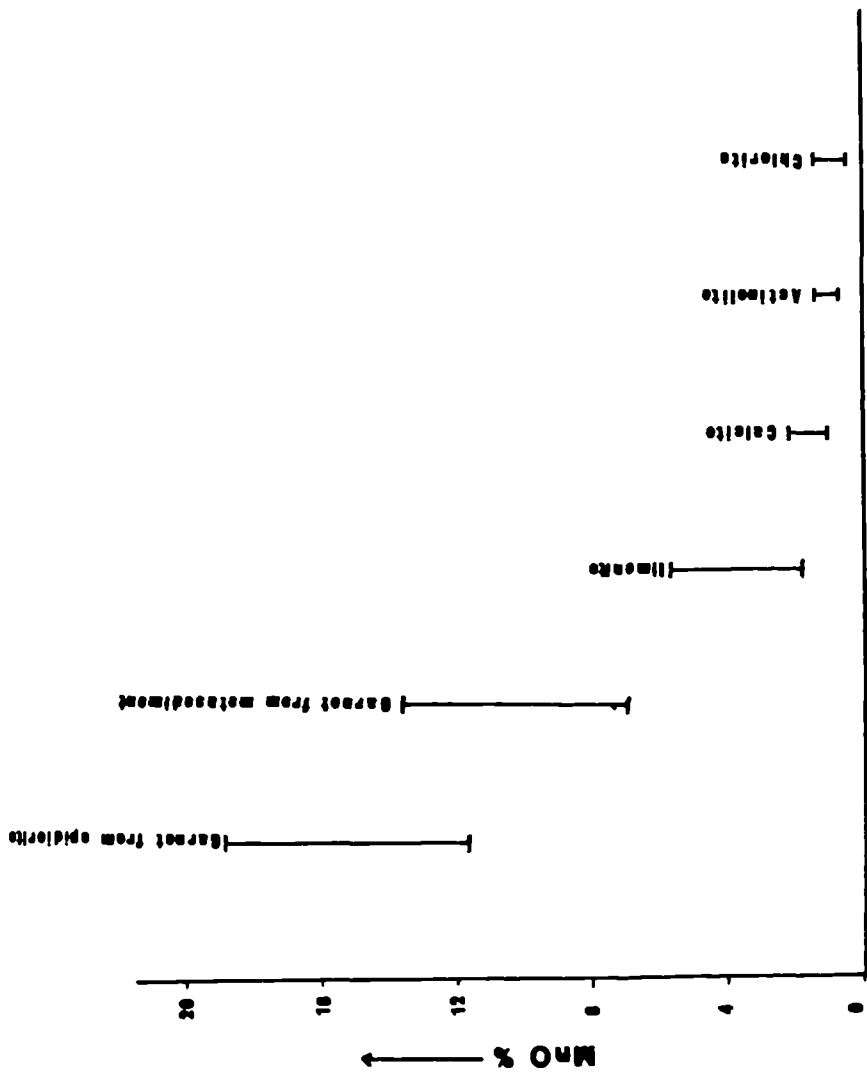
Fig. 5.9 : The distribution of MnO wt% among the Mn-bearing minerals.

The same observation is also clear in Fig. (5.8c) when comparing the analysed garnets hosted by metasediments of Meall Mór with others from the Dalradian and Moinian metasediments.

Factors controlling manganese in garnet

The dependence of the manganese-content of garnet upon temperature and pressure, chemistry of the parent rocks, and oxygen fugacity was discussed by Müller and Schneider (1971). For the present analysed garnets, as they belong to one metamorphic grade (garnet zone) temperature and pressure variations cannot be applied as a factor controlling their manganese content.

Oxygen fugacity

Sensitivity of Mn-content of garnet to oxygen fugacity was studied by (Chinner 1960, Eugster and Wones 1962, and Hsu 1968). They concluded that manganese-content of garnets increases at given temperature and/or pressure with increasing oxygen fugacity. In Fig. (5.10), although only very few analyses are presented, an increase in the manganese-content of garnet as a result of increasing rock oxidation ratio is noted but the correlation is weak.

Parent rock composition

Studies on the effect of different metamorphic conditions on the manganese content of garnets in the Dalradian by Atherton (1964 and 1965) has resulted in the conclusion that parent rock composition is the sensitive factor controlling the Mn-content of the garnets. Matkovskiy (1971) described the manganese-rich garnets from Ukrainian Carpathians as a characteristic of unusual Mn-rich rocks. In the present analysed garnets, the rock manganese-content seems to play a factor in controlling their manganese-content (Fig. 5.11).
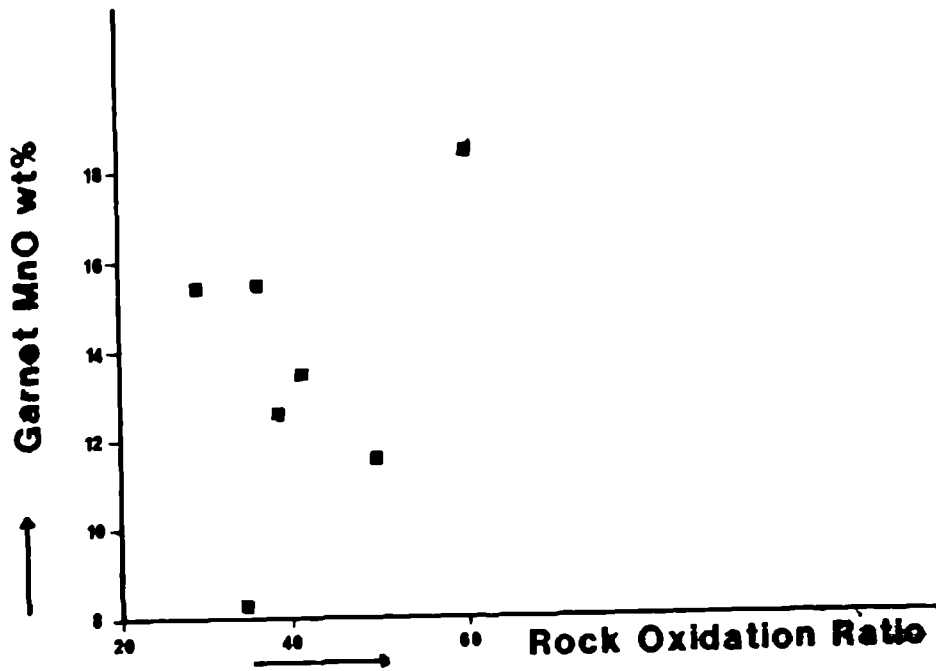
Fig. 5.10 : Weak correlation between the MnO wt% of the
garnet and the oxidation ratio of the rocks.
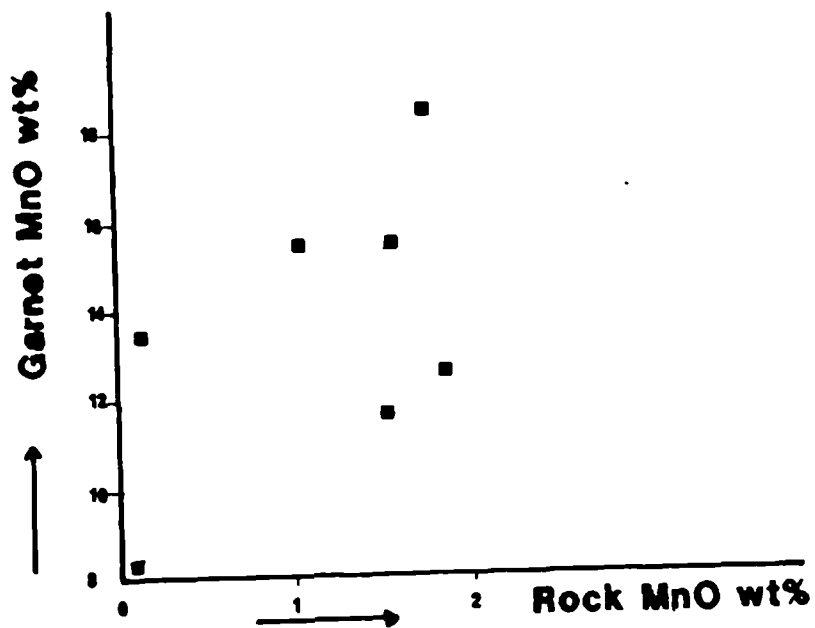
Fig. 5.11: Moderate correlation between rock MnO wt%
and garnet MnO wt%.

126

5.5.5 Epidote

Sixteen microprobe analyses of epidote from both epidiorites (n=8) and from metasediments (n=8) are presented in Table (5.3). All the analyses are recalculated to stoichiometric formulae on the basis of 13(O) and assuming all Fe as Fe_2O_3.

Chemical variation

The analysed epidotes show a slight variation in the Fe content and was represented in terms of pistachite (Ps %) content ranging between 23-32 Ps %, where the pistacite percentage is given as octahedral $Fe^{3+}/Fe^{3+} + Al^6$.

Two factors may be of important in controlling the composition of epidote; oxygen fugacity and bulk rock composition. In the present study, only a very limited number of epidote-bearing rocks were analysed, insufficient to establish the relationship between epidote and bulk rock composition. But as a preliminary interpretation, it seems that rocks rich in aluminium have abundant epidote with low iron content, while rocks poor in aluminium have less epidote with higher iron content.

5.5.6 Chlorite

Chlorite analyses of twenty samples in both metasediments (n=16) and in epidiorites (n=4) are set in Table (5.4). The analyses are recalculated to stoichiometric molecules on the basis of 28(O) atoms and on a fixed number of cations with some of the total iron as Fe_2O_3 consistent with stoichiometry. For comparison Appendix (A.5.5) represents calculation of the chlorite stoichiometric formulae assuming all the iron as FeO.

Chlorite chemistry and classification have been reviewed by Hey (1954) and Foster (1962). Two series of ionic replacements are

Table 5.3 : Electron microprobe analysis of epidote. Recalculation is made
by assuming the total iron as Fe_2O_3.

a) epidiorites

VAR. / ID.	HMM 8	HMM 11	HMM 12	HMM 14	HMMI 1	HMMI 3	HMMI 19	HMMI 31
SiO_2	37.45	36.96	37.22	37.03	37.42	37.97	37.27	37.56
Al_2O_3	21.70	22.09	21.92	21.42	21.12	21.92	23.55	24.55
TiO_2	0.00	0.00	0.00	0.00	0.04	0.00	0.23	0.00
Cr_2O_3	0.00	0.12	0.00	0.03	0.00	0.00	0.12	0.00
Fe_2O_3	15.54	14.65	15.45	15.78	15.73	15.64	13.41	12.08
FeO	0.00	0.00	0.00	0.00	0.00	0.00	0.00	0.00
MnO	0.22	0.00	0.15	0.39	0.26	0.19	0.55	0.20
MgO	0.00	0.00	0.00	0.15	0.03	0.00	0.00	0.00
CaO	23.33	23.23	23.39	22.91	22.88	23.64	22.89	22.97
Na_2O	0.00	0.00	0.00	0.00	0.02	0.00	0.00	0.00
K_2O	0.00	0.00	0.00	0.00	0.00	0.00	0.08	0.00
TOTAL wt %	98.24	97.05	98.13	97.71	97.50	99.36	98.10	97.36

NUMBER OF IONS ON BASIS OF 13 (O)

Si	3.12	3.11	3.11	3.11	3.14	3.13	3.09	3.11
Al	0.00	0.00	0.00	0.00	0.00	0.00	0.00	0.00
Total	3.12	3.11	3.11	3.11	3.14	3.13	3.09	3.11
Al	2.13	2.19	2.16	2.12	2.09	2.13	2.30	2.40
Ti	0.00	0.00	0.00	0.00	0.00	0.00	0.01	0.00
Cr	0.00	0.01	0.00	0.00	0.00	0.00	0.01	0.00
Fe^{3+}	0.98	0.93	0.97	1.00	0.99	0.97	0.84	0.75
Total	3.11	3.13	3.13	3.12	3.08	3.10	3.16	3.15
Fe^{2+}	0.00	0.00	0.00	0.00	0.00	0.00	0.00	0.00
Mn	0.02	0.00	0.01	0.03	0.02	0.01	0.04	0.01
Mg	0.00	0.00	0.00	0.02	0.00	0.00	0.00	0.00
Ca	2.08	2.09	2.09	2.06	2.06	2.09	2.03	2.04
Na	0.00	0.00	0.00	0.00	0.00	0.00	0.00	0.00
K	0.00	0.00	0.00	0.00	0.00	0.00	0.01	0.00
Total	2.10	2.09	2.10	2.11	2.08	2.18	2.08	2.05
Pistacite %	31.50	29.80	31.00	32.10	32.10	31.29	26.58	23.81

(b) metasediments

VAR. ID.	HMMI 23	HMMI 25	HMMI 35	HMMI 42	HMMI46	HMMI 47	HMMI 55	HMM 44
SiO_2	38.99	26.52	36.46	36.63	38.04	37.03	43.26	38.31
Al_2O_3	22.81	17.52	23.91	23.72	24.24	23.99	24.33	24.66
TiO_2	0.06	0.08	0.11	0.10	0.00	0.02	0.00	0.00
Cr_2O_3	0.00	0.00	0.00	0.00	0.12	0.00	0.00	0.00
Fe_2O_3	13.37	35.93	13.04	12.87	12.31	11.55	9.07	12.17
FeO	0.00	0.00	0.00	0.00	0.00	0.00	0.00	0.00
MnO	0.12	0.23	0.26	0.23	0.32	0.13	0.00	0.21
MgO	0.07	0.04	0.49	0.14	0.00	0.02	0.00	0.00
CaO	22.28	10.57	20.79	22.39	23.17	22.96	19.63	23.29
Na_2O	0.27	0.00	0.01	0.00	0.00	0.00	0.00	0.00
K_2O	0.00	0.00	0.00	0.00	0.00	0.00	0.00	0.00
TOTAL wt%)	97.97	90.89	95.07	96.08	98.20	95.70	96.29	98.64

NUMBER OF IONS ON BASIS OF 13 (O)

Si	3.21	2.53	3.09	3.09	3.13	3.12	3.50	3.13
Al	0.00	0.47	0.00	0.00	0.00	0.00	0.00	0.00
Total	3.21	3.00	3.09	3.09	3.13	3.12	3.50	3.13
Al	2.22	1.50	2.39	2.36	2.35	2.38	2.32	2.38
Ti	0.00	0.01	0.01	0.01	0.00	0.00	0.00	0.00
Cr	0.00	0.00	0.00	0.00	0.01	0.00	0.00	0.00
Fe^{3+}	0.83	2.58	0.83	0.82	0.76	0.73	0.55	0.75
Total	3.05	4.09	3.23	3.19	3.12	3.11	2.87	3.13
Fe^{2+}	0.00	0.00	0.00	0.00	0.00	0.00	0.00	0.00
Mn	0.01	0.02	0.02	0.02	0.02	0.01	0.00	0.02
Mg	0.01	0.01	0.06	0.02	0.00	0.00	0.00	0.00
Ca	1.97	1.08	1.89	2.02	2.04	2.07	1.70	2.04
Na	0.04	0.00	0.00	0.00	0.00	0.00	0.00	0.00
K	0.00	0.00	0.00	0.00	0.00	0.00	0.00	0.00
Total	2.03	1.11	1.97	2.06	2.06	2.08	1.70	2.06
Pistacite %	27.20	63.00	25.80	25.80	24.36	23.50	19.16	23.96

128

important in the chlorite chemistry:

$$SiMg \rightleftharpoons AlAl^6$$
$$Fe^{2+} \rightleftharpoons Mg$$
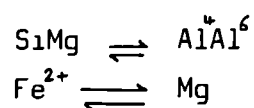
A classification scheme (Foster 1962) for chlorites based on these two series of replacements was followed and is represented in Fig. (5.12). The majority of the analysed chlorites are ripidolites, others are brunsvigite (n=2), diabantite (n=3), and clinochlore (n=1). An exception is the chlorite in Specimen HMMI 31A which has excess silica.

Chemical variation of the analysed chlorites includes variation in the major constituents; FeO, MgO, and Al_2O_3, and are represented in the compositional triangle (Fig. 5.13). The degree of Mg = Fe replacement is large, while the Al_2O_3 variation is limited. Of the minor constituents, chlorite shows variable enrichment in the MnO wt% content (Fig. 5.9) ranging from 0.0 to 1.51 wt%, with a mean ($\bar{x}$=0.48) and a standard deviation (σ=0.32).

5.5.7 Biotite

Twenty-one analyses of biotite of both metasediments and epidiorites are presented in Table (5.5). The analyses are recalculated to stoichiometric molecules on the anhydrous basis of 22 (O) atoms. All the analysed biotites (except in Spec. HMMI 97) have total number of octahedral cations between 5.15 and 5.95, rather than the theoretical number 6, and therefore no attempt was made to assign part of the total iron as Fe_2O_3. Only biotite in Spec. HMMI 97 has total number of octahedral cations (6), probably as a result of assuming all the iron as FeO and therefore recalculation is made by assigning part of the total iron as Fe_2O_3 to bring the total down to 6. The deficiency in the total number of octahedral cations, could be explained partly by analytical procedure and partly by real vacancies in the octahedral site

Table 5.4 : Electron microprobe analysis of chlorite. Recalculation is made by fixing part of the total iron (as FeO) into Fe_2O_3.

VAR. / ID.	HMM 1	HMM 44	HMM 57	HMMI 25	HMMI 26	HMMI 29	HMMI 33	HMMI 35	HMMI 42	HMMI 46
					metasediments					
SiO_2	35.53	25.21	25.22	27.00	24.91	24.18	24.57	24.67	24.42	24.30
Al_2O_3	21.31	21.15	21.59	16.35	20.78	20.74	20.91	20.80	20.02	20.13
TiO_2	0.00	0.00	0.00	0.05	0.05	0.08	0.00	0.06	0.09	0.00
Fe_2O_3	0.00	0.00	0.07	0.00	1.89	1.79	2.01	1.22	1.11	1.27
FeO	20.82	25.07	24.16	29.77	19.78	24.66	21.23	22.17	26.26	30.42
MnO	0.00	0.54	0.38	0.22	0.35	0.44	0.56	0.49	0.44	0.60
MgO	7.37	15.10	15.89	13.45	18.12	14.50	16.89	16.38	13.69	11.19
CaO	0.00	0.00	0.00	0.09	0.01	0.00	0.00	0.01	0.02	0.00
Na_2O	0.00	0.00	0.00	0.02	0.01	0.01	0.00	0.02	0.02	0.00
K_2O	0.00	0.00	0.00	0.02	0.00	0.00	0.00	0.00	0.00	0.00
TOTAL (wt%)	85.03	87.07	87.31	86.97	85.90	86.40	86.17	85.81	86.07	87.91

NUMBER OF IONS ON BASIS OF 28 (O)

	HMM 1	HMM 44	HMM 57	HMMI 25	HMMI 26	HMMI 29	HMMI 33	HMMI 35	HMMI 42	HMMI 46
Si	7.25	5.36	5.31	5.89	5.26	5.22	5.22	5.27	5.33	5.31
Al^{iv}	0.75	2.64	2.69	2.11	2.74	2.78	2.78	2.73	2.67	2.69
Total	8.00	8.00	8.00	8.00	8.00	8.00	8.00	8.00	8.00	8.00
Al^{vi}	4.40	2.66	2.68	2.10	2.43	2.49	2.46	2.52	2.47	2.49
Ti	0.00	0.00	0.00	0.01	0.01	0.01	0.00	0.01	0.01	0.00
Fe^{3+}	0.00	0.00	0.01	0.00	0.30	0.29	0.32	0.20	0.18	0.21
Fe^{2+}	3.55	4.46	4.27	5.44	3.49	4.45	3.77	3.96	4.79	5.55
Mn	0.03	0.10	0.07	0.04	0.06	0.08	0.10	0.09	0.08	0.11
Mg	2.24	4.78	4.99	4.38	5.70	4.66	5.35	5.22	4.45	3.64
Ca	0.00	0.00	0.00	0.02	0.00	0.00	0.00	0.00	0.00	0.00
Na	0.00	0.00	0.00	0.01	0.00	0.01	0.00	0.01	0.01	0.00
K	0.00	0.00	0.00	0.01	0.00	0.00	0.00	0.00	0.00	0.00
Total	10.22	12.00	12.00	12.01	11.99	11.99	12.00	12.01	11.99	12.00

130

Table 5.4 : Continued

VAR. / ID.	metasediments						HMM 11	epidiorites		
	HMMI 50	HMMI 55	HMMI 61	HMMI 67	HMMI 69	HMMI 96	HMM 11	HMMI 19	HMMI 31	HMMI 31A
SiO_2	25.26	26.20	25.58	36.71	36.15	29.11	25.63	26.78	24.05	41.94
Al_2O_3	20.35	20.28	20.59	15.98	15.50	16.41	19.82	19.07	20.16	13.12
TiO_2	0.06	0.00	0.04	0.00	0.00	0.00	0.00	0.00	0.06	0.00
Fe_2O_3	0.00	1.31	0.02	0.00	0.00	1.02	0.49	0.00	1.33	0.00
FeO	21.67	20.05	18.23	23.68	21.23	11.94	24.81	31.60	28.22	20.19
MnO	0.44	0.48	0.25	0.13	0.16	0.26	1.13	1.51	0.43	0.26
MgO	17.30	19.02	19.44	7.31	9.26	25.83	15.22	11.16	12.27	7.37
CaO	0.00	0.00	0.00	0.00	0.00	0.00	0.00	0.00	0.01	0.00
Na_2O	0.01	0.00	0.02	0.00	0.00	0.00	0.00	0.00	0.02	0.00
K_2O	0.02	0.00	0.00	0.00	0.00	0.00	0.00	0.00	0.00	0.00
TOTAL (wt %)	85.11	87.34	84.17	83.81	82.30	84.47	87.10	90.12	86.55	82.88

NUMBER OF IONS ON BASIS OF 28 (O)

	HMMI 50	HMMI 55	HMMI 61	HMMI 67	HMMI 69	HMMI 96	HMM 11	HMMI 19	HMMI 31	HMMI 31A
Si	5.45	5.42	5.41	7.76	7.70	5.95	5.47	5.70	5.28	8.69
Al^+	2.55	2.58	2.59	0.24	0.30	2.05	2.53	2.30	2.72	0.00
Total	8.00	8.00	8.00	8.00	8.00	8.00	8.00	8.00	8.00	8.69
Al^6	2.55	2.37	2.55	3.74	3.60	1.90	2.46	2.48	2.49	3.20
Ti	0.01	0.00	0.01	0.00	0.00	0.00	0.00	0.00	0.01	0.00
Fe^{3+}	0.00	0.20	0.03	0.00	0.00	0.16	0.08	0.00	0.22	0.00
Fe^{2+}	3.86	3.47	3.23	4.19	3.78	2.04	4.43	5.62	5.18	3.50
Mn	0.08	0.08	0.04	0.02	0.03	0.05	0.20	0.27	0.08	0.05
Mg	5.49	5.87	6.13	2.30	2.94	7.86	4.84	3.54	4.01	2.28
Ca	0.00	0.00	0.00	0.00	0.00	0.00	0.00	0.00	0.00	0.00
Na	0.00	0.00	0.01	0.00	0.00	0.00	0.00	0.00	0.01	0.00
K	0.00	0.00	0.00	0.00	0.00	0.00	0.00	0.00	0.00	0.00
Total	11.99	12.00	12.00	10.25	10.35	12.01	12.00	11.91	12.00	9.03
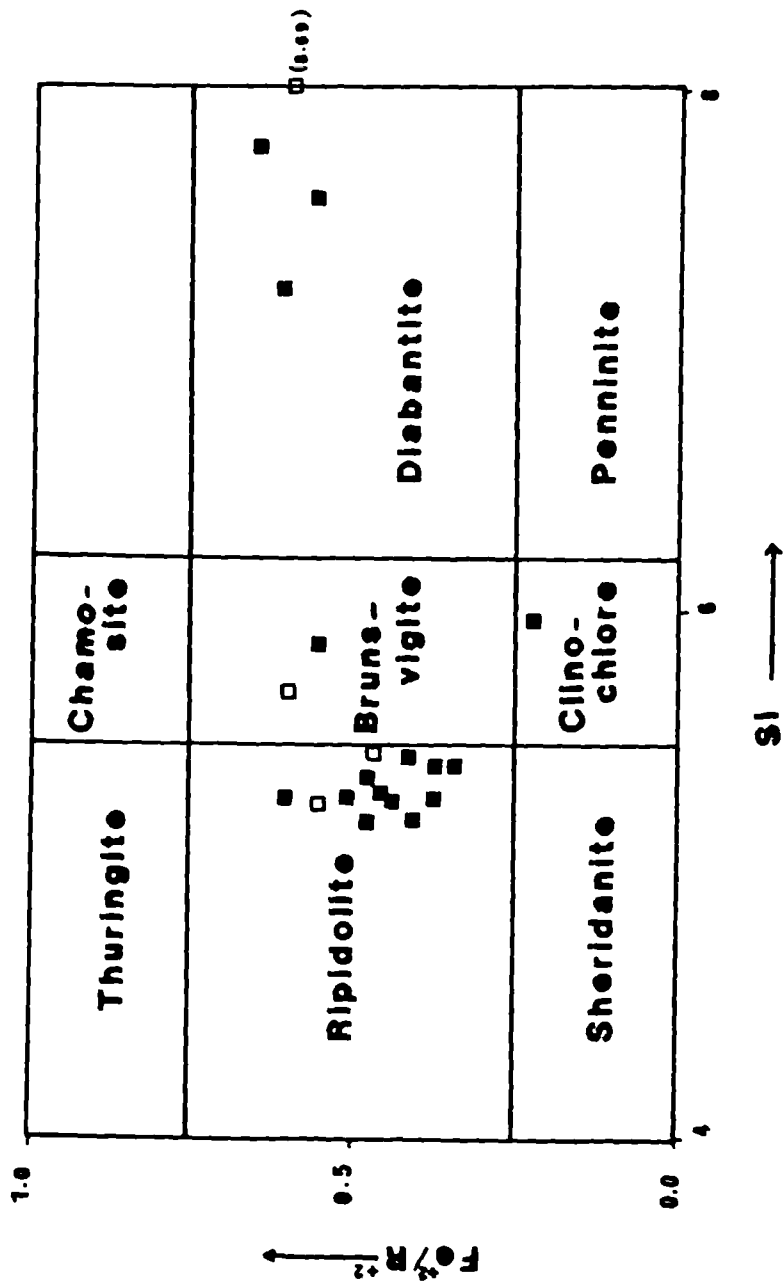
Fig. 5.12 : The analysed chlorites according to the classification of Foster (1962). ■: chlorite in metasediments; □ : chlorite in epidiorites.
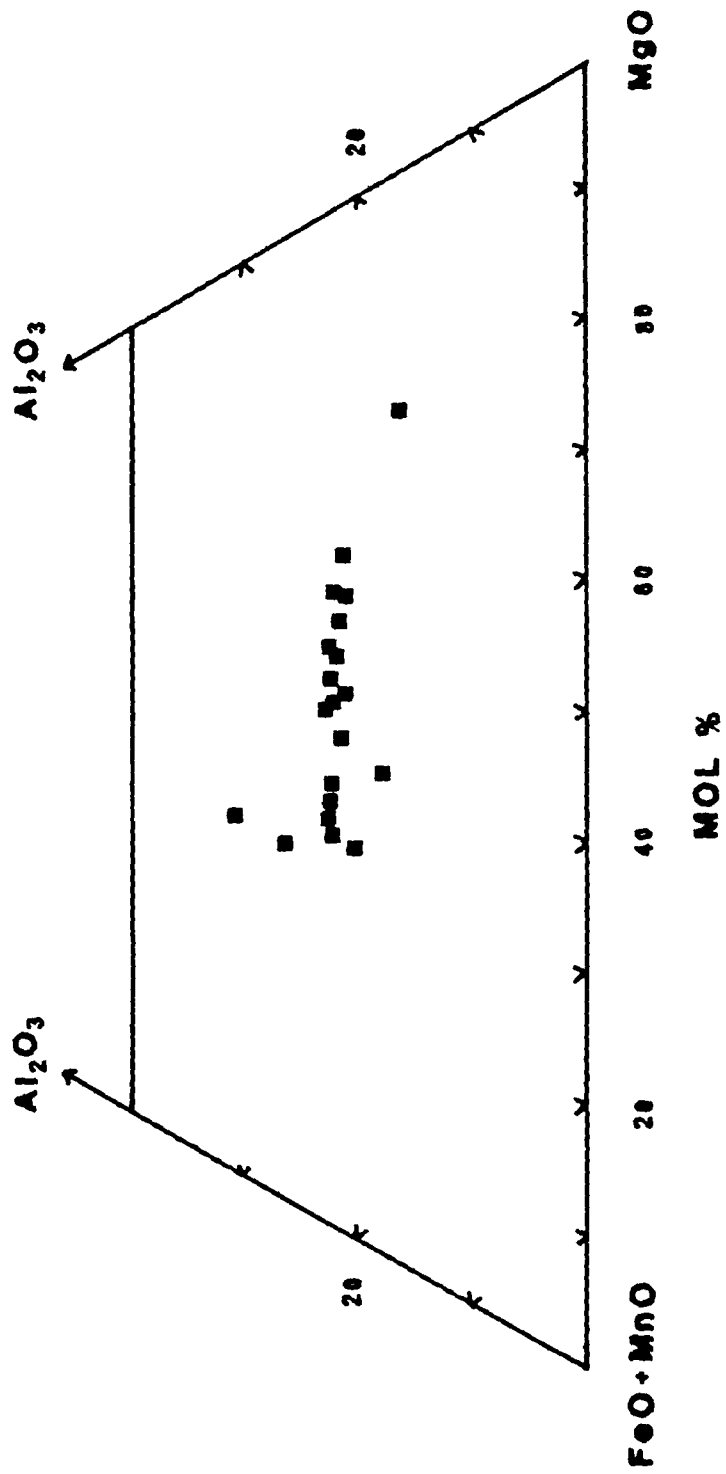
Fig. 5.13 : Al_2O_3 - FeO - MgO - MnO triangular diagram, showing the compositional field of the analysed chlorites.

(Guidotti 1984). The total atoms for alkalis appear to be less than the ideal 2 atoms for a formula based on 22 oxygens, with the majority between 1.8 and 1.95, only four analyses having values less than 1.8 and one more than 2. This defeciency in the alkali site of the mica has been reported by many authors and will be discussed later in Section (5.5.8).

Classification

Most of the compositional variation in the trioctahedral dark micas can be related to the following ionic replacements (Foster 1960) :

$$KAl^{+} \qquad Si$$
$$MgSi \qquad Al\overset{3}{Al}^{6}$$
$$Fe^{2+} \qquad Mg$$
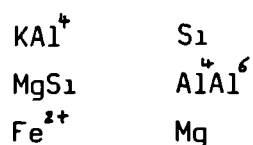
and can be described in terms of the end-members presented in Fig. (5.14). The type of mica in the phlogopite-biotite compositional field depends on its Mg : Fe ratio (Gribble and Hall 1985). thus;

Phlogopite is a mica with Mg between 100 & 70%

Biotite is a mica with Mg between 60 & 20%

and accordingly all the analysed trioctahedral micas fall within the biotite field (Fig. 5.14).

Chemical variation

The observed chemical variations within the analysed biotites (Figs. 5.14 & 5.15) seem to be restricted to the variation in the Fe:Mg ratio, ranging between 0.31 and 0.62 which in turn is controlled by the rock Mg : Fe ratio. Variation in the Al : Si ratio is not significant and is generally constant.

Table 5.5 : Electron microprobe analysis of biotite. Calculation is made by assuming the total iron as FeO, except for biotite from Specimen HMMI 97, where recalculation is made by fixing part of the total iron as Fe_2O_3.

VAR. / ID.	HMM 1	HMM 44	HMM 57	HMMI 23	HMMI 25	HMMI 26	HMMI 29	HMMI 33	HMMI 35	HMMI 42
SiO_2	35.87	38.71	36.95	35.58	34.53	37.07	35.08	36.21	35.49	34.80
Al_2O_3	16.89	20.42	16.62	14.60	16.22	15.68	16.04	15.91	16.59	14.67
TiO_2	1.92	2.00	1.91	2.07	1.82	1.68	1.91	2.03	2.03	1.72
Fe_2O_3	0.00	0.00	0.00	0.00	0.00	0.00	0.00	0.00	0.00	0.00
FeO	23.48	18.59	18.62	23.12	23.31	16.81	20.32	18.35	18.25	21.36
MnO	0.17	0.15	0.21	0.12	0.24	0.22	0.19	0.30	0.24	0.22
MgO	7.71	5.71	11.54	9.99	9.00	12.65	9.70	11.40	10.89	10.38
CaO	0.02	0.10	0.00	0.01	0.02	0.01	0.02	0.00	0.02	0.01
Na_2O	0.00	0.00	0.00	0.07	0.09	0.11	0.09	0.00	0.06	0.13
K_2O	9.24	9.19	9.15	9.05	8.51	9.54	9.38	9.27	9.69	9.26
TOTAL (wt %)	95.30	94.87	95.00	94.61	93.74	93.80	92.73	93.47	93.26	92.55
NUMBER OF IONS ON BASIS OF 22 (O)										
Si	5.57	5.81	5.61	5.58	5.46	5.68	5.55	5.61	5.53	5.56
Al^{iv}	2.43	2.19	2.39	2.42	2.54	2.32	2.45	2.39	2.47	2.44
Total	8.00	8.00	8.00	8.00	8.00	8.00	8.00	8.00	8.00	8.00
Al^{vi}	0.66	1.42	0.58	0.28	0.49	0.51	0.54	0.51	0.57	0.33
Ti	0.22	0.23	0.22	0.24	0.22	0.19	0.23	0.24	0.24	0.21
Fe^{3+}	0.00	0.00	0.00	0.00	0.00	0.00	0.00	0.00	0.00	0.00
Fe^{2+}	3.05	2.33	2.36	3.03	3.08	2.15	2.69	2.38	2.38	2.86
Mn	0.02	0.02	0.03	0.02	0.03	0.03	0.03	0.04	0.03	0.03
Mg	1.79	1.28	2.61	2.34	2.12	2.89	2.29	2.63	2.53	2.47
Total	5.74	5.28	5.80	5.91	5.94	5.77	5.78	5.80	5.75	5.90
Ca	0.00	0.02	0.00	0.00	0.00	0.00	0.00	0.00	0.00	0.00
Na	0.00	0.00	0.00	0.02	0.03	0.03	0.03	0.00	0.02	0.04
K	1.82	1.75	1.76	1.80	1.71	1.86	1.88	1.82	1.91	1.88
Total	1.82	1.77	1.76	1.82	1.74	1.89	1.91	1.82	1.93	1.92

135

Table 5.5 : Continued

VAR. /ID.	HMMI 46	HMMI 47	HMMI 50	HMMI 55	HMMI 67	HMMI 68	HMMI 69	HMMI 97	HMMI 103	HMMI 107	HMMI 31 *
SiO_2	35.71	35.85	35.66	38.28	37.46	40.01	36.05	34.60	37.20	34.20	35.42
Al_2O_3	16.09	15.44	16.01	14.49	16.31	15.99	15.28	14.95	16.32	19.87	15.63
TiO_2	2.34	0.94	2.05	0.79	1.72	3.36	2.11	0.66	1.96	0.00	1.93
Fe_2O_3	0.00	0.00	0.00	0.00	0.00	0.00	0.00	3.58	0.00	0.00	0.00
FeO	21.59	16.99	18.49	16.27	23.05	22.19	21.82	16.14	18.12	19.55	23.53
MnO	0.23	0.35	0.16	0.15	0.17	0.00	0.18	0.39	0.00	0.14	0.26
MgO	9.23	13.21	10.89	15.11	6.84	5.47	8.98	13.85	11.74	10.86	7.98
CaO	0.00	0.02	0.01	0.00	0.40	0.19	0.00	0.00	0.00	0.00	0.00
Na_2O	0.00	0.06	0.06	0.00	0.00	2.05	0.00	0.00	0.00	0.00	0.11
K_2O	9.29	9.39	9.71	9.83	9.41	8.25	9.66	8.96	9.84	9.83	9.57
TOTAL (wt %)	94.48	92.24	93.04	94.92	95.36	97.51	94.08	93.13	95.18	94.45	94.43
NUMBER OF IONS ON BASIS OF 22 (O)											
Si	5.56	5.61	5.57	5.77	5.79	5.97	5.66	5.41	5.64	5.28	5.59
Al	2.44	2.39	2.43	2.23	2.21	2.03	2.34	2.59	2.36	2.72	2.41
Total	8.00	8.00	8.00	8.00	8.00	8.00	8.00	8.00	8.00	8.00	8.00
Al	0.51	0.46	0.52	0.35	0.76	0.78	0.48	0.16	0.56	0.90	0.50
Ti	0.27	0.10	0.24	0.09	0.20	0.38	0.25	0.08	0.23	0.00	0.23
Fe^{3+}	0.00	0.00	0.00	0.00	0.00	0.00	0.00	0.42	0.00	0.00	0.00
Fe^{2+}	2.81	2.22	2.42	2.05	2.98	2.77	2.86	2.11	2.30	2.53	3.11
Mn	0.03	0.05	0.02	0.02	0.02	0.00	0.02	0.05	0.00	0.02	0.04
Mg	2.14	3.08	2.54	3.40	1.58	1.22	2.10	3.23	2.65	2.50	1.88
Total	5.76	5.92	5.74	5.91	5.54	5.15	5.71	6.05	5.74	5.95	5.76
Ca	0.00	0.00	0.00	0.00	0.07	0.03	0.00	0.00	0.00	0.00	0.00
Na	0.00	0.02	0.02	0.00	0.00	0.59	0.00	0.00	0.00	0.00	0.03
K	1.83	1.86	1.92	1.88	1.84	1.56	1.92	1.78	1.89	1.93	1.92
Total	1.83	1.88	1.94	1.88	1.91	2.18	1.92	1.78	1.89	1.93	1.95

biotite in epidiorite.
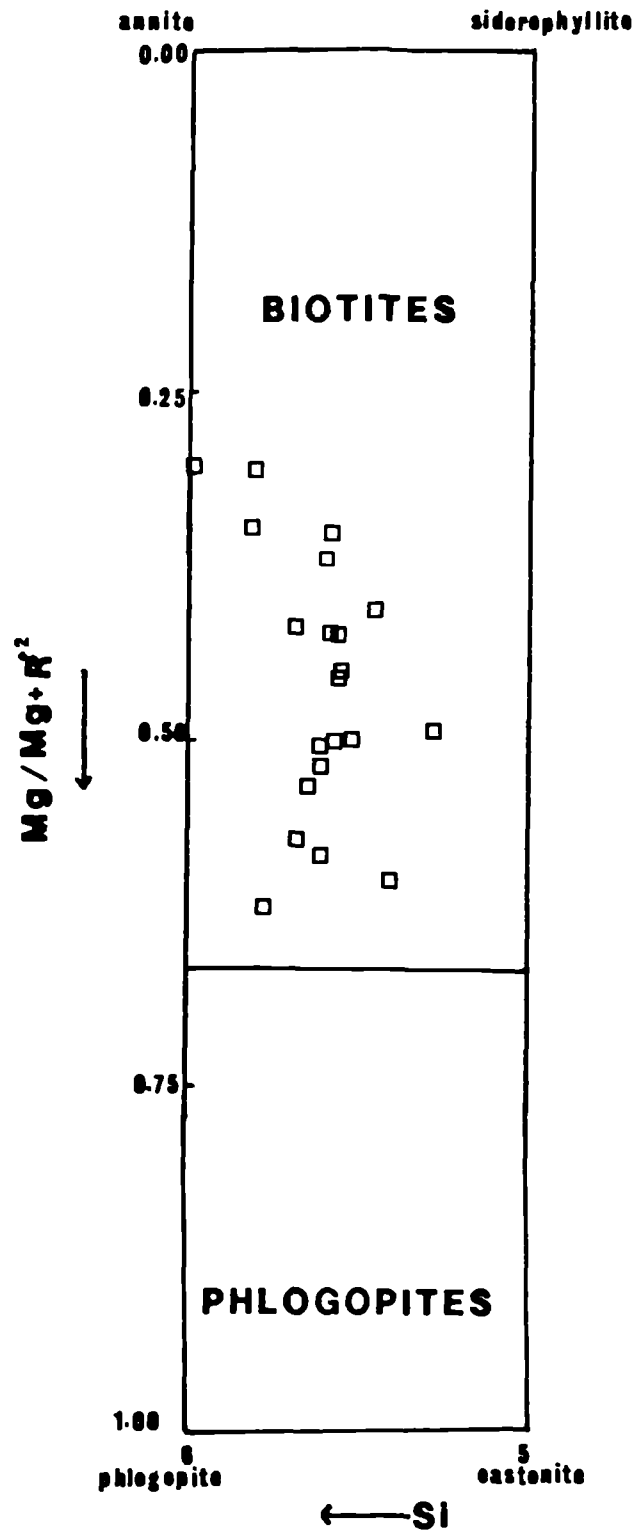
Fig. 5.14 : Plot of the analysed biotite in the biotite-phlogopite
compositional fields. The boundary is chosen to be where
Mg:Fe = 2:1 (Deer et al. 1966).

137
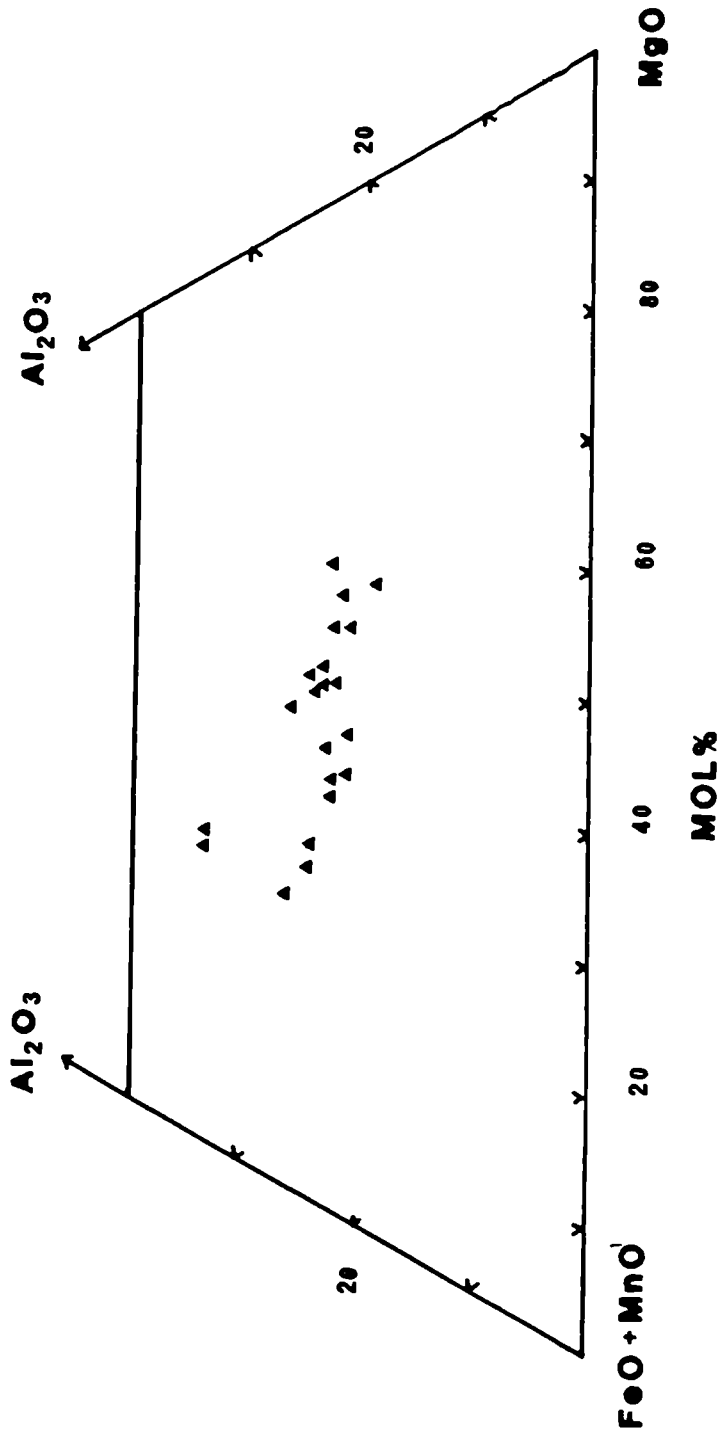
Fig. 5.15 : Compositional variation of biotite in the Al-Fe-Mg system.

5.5.8 White mica

Recalculation of the analyses

Nine white mica analyses from metasediments have been listed in Table (5.6) and in Appendix (A.5.6). All analyses have been recalculated to stoichiometric molecules on the basis of 22 (O) atoms (Appendix A.5.6) and on fixed number of cations that permit assigning part of the total iron as Fe_2O_3 (Table 5.6). In Appendix (A.5.6) by assuming all the iron as FeO, the total number of the cations in the octahedral site is slightly greater than the theoretical 4 atoms per formulae. Therefore, recalculation is made by assigning some of the total iron as Fe_2O_3 to bring the total down to around 4 (Table 5.6). However various authors (e.g. Brown 1967, McDowell and Elders 1980, and Zen 1981) have attempted to devise methods by which one could calculate in an approximate fashion the amount of Fe^2 and Fe^2 in white micas from microprobe data. Some of these schemes involve charge balance, others involve a fixed number of total cations in certain sites. Zen (1981) concluded that the oxidation states of iron from microprobe data of white micas remain unsolved.

The total number of the cations assigned to the 12-coordinated-site is less than the theoretical 2 atoms per 22(O). The majority range from 1.84 -1.91, only one is less than 1.84. This defeciency was considered by some workers to be real rather than due to analytical error (Lambert 1959 and Zen 1981).

This defeciency might be due to vacancies resulting from several substitutions in this site including :

(1) Substitution of K by H_3O^+ (Brown and Norrish 1952, and White and Burns 1963), normally up to 5% only (Miyashiro 1973). Although no one has yet demonstrated that H_3O^+ is present in metamorphic muscovite (Gudotti 1984).

Table 5.6 : Electron microprobe analysis of white mica. Recalculation is made by fixing part of the total iron (as FeO) into Fe_2O_3.

VAR. / ID.	HMM 1	HMM 57	HMMI 26	HMMI 50	HMMI 69	HMMI 78	HMMI 96	HMMI 97	HMMI 103
SiO_2	47.69	48.13	47.57	48.16	46.98	48.44	46.85	45.35	47.25
Al_2O_3	30.82	29.62	28.12	27.17	27.14	23.12	30.51	29.83	28.41
TiO_2	0.40	0.75	0.38	0.42	0.87	1.55	0.60	0.76	0.60
Fe_2O_3	1.90	2.69	3.93	3.64	5.23	3.45	2.06	3.88	2.68
FeO	1.42	1.09	0.24	0.12	1.10	2.60	0.49	0.57	1.39
MnO	0.00	0.11	0.01	0.02	0.00	0.00	0.00	0.14	0.00
MgO	1.65	2.15	2.68	2.94	2.03	2.76	2.00	1.68	2.10
CaO	0.09	0.00	0.00	0.00	0.00	0.09	0.00	0.12	0.00
Na_2O	0.59	0.53	0.50	0.30	0.00	0.00	0.67	0.34	0.36
K_2O	10.05	10.44	9.84	9.31	10.62	10.58	9.88	9.87	10.35
TOTAL (wt %)	94.61	95.51	93.27	92.07	93.97	92.56	93.06	92.54	93.14

NUMBER OF IONS ON BASIS OF 22 (O)

	HMM 1	HMM 57	HMMI 26	HMMI 50	HMMI 69	HMMI 78	HMMI 96	HMMI 97	HMMI 103
Si	6.43	6.45	6.51	6.63	6.47	6.79	6.40	6.28	6.50
Al^4	1.57	1.55	1.49	1.37	1.53	1.21	1.60	1.72	1.50
Total	8.00	8.00	8.00	8.00	8.00	8.00	8.00	8.00	8.00
Al^6	3.32	3.13	3.04	3.04	2.87	2.60	3.30	3.16	3.11
Ti	0.04	0.08	0.04	0.04	0.09	0.16	0.06	0.08	0.06
Fe^{3+}	0.19	0.27	0.46	0.38	0.54	0.36	0.21	0.41	0.28
Fe^{2+}	0.16	0.12	0.03	0.01	0.13	0.30	0.06	0.07	0.16
Mn	0.00	0.01	0.00	0.00	0.00	0.00	0.00	0.02	0.00
Mg	0.33	0.43	0.55	0.60	0.42	0.58	0.41	0.35	0.43
Total	4.04	4.04	4.06	4.07	4.05	4.00	4.04	4.09	4.04
Ca	0.01	0.00	0.00	0.00	0.00	0.01	0.00	0.02	0.00
Na	0.16	0.14	0.13	0.08	0.00	0.00	0.18	0.09	0.10
K	1.72	1.77	1.71	1.63	1.85	1.88	1.71	1.73	1.81
Total	1.89	1.91	1.84	1.71	1.85	1.89	1.89	1.84	1.91

(2) Ca substitution in this site.

(3) Ba sustitution in this site.

(4) Isomorphous series substitution between dioctahedral and trioctahedral micas.

Other authors (Hoffer 1978) considered this defeciency to be as a result of some evaporation of alkalis during probe analysis. However, Gudotti (1984) pointed to the presence of this defeciency in both probe and wet chemical analyses, and therefore he questioned the possibility of volatilisation of alkalis by the probe beam as a factor causing this defeciency.

Nomenclature and chemical variation

Chemical variations of the white micas in metamorphic rocks is most easily discussed in terms of the end-members; muscovite, paragonite, margarite, and celadonite in the muscovite celadonite series of Schaller (1950) and Foster (1956). Intermediate in composition between these two end-members are the phengite micas (Michel 1953 and Ernst 1963), which represent muscovite with $Si:Al^{4}$ ratio more than 3.

The chemical compositions of the analysed white mica suggest that they are phengites with the atomic ratio $Si:Al^{4}$ more than 3. The amount of Na_2O present, between 0.0 to 0.67 wt%, corresponds to about 0.0 to 9.5 % paragonite.

5.5.9 Feldspar

Fifteen microprobe analyses of feldspars from both epidiorites (n=3) and metasediments (n=12), together with the stoichiometric molecules based on 32(O) and their-end member composition are

presented in Table (5.7)

Chemistry

All the analysed feldspars are plagioclase close to the albite end-member. They contain small amounts of anorthite ranging between 0.0 to 4.69 mole% and orthoclase ranging between 0.00 to 0.74 mol%. Only Specimen HMMI 68 represents orthoclase with 5.77 mol% anorthite.

Minor elements are present in the analysed plagioclase in very limited amounts including, BaO (0-1.51 wt%), FeO (0-0.53 wt%, excluding HMMI 68 with 5.74 wt%), and MgO (0-1.73 wt%). These elements are considered to replace Ca, and contribute to the anorthite molecule (Deer et al. 1963).

5.5.10 Minor Non-Opaque Minerals

(a) Sphene

Five sphene analyses are given in Table (5.8), where they have been recalculated on the basis of 20(O,OH,F) per unit cell. The titanium is partly replaced by aluminium and ferrous iron. In the fifth analysis, there is a substitution of calcium by sodium.

(b) Apatite

Microprobe analyses of four apatite grains are given in Table (5.8), where they have been calculated on the basis of 25(O). The analyses showed that the sum of CaO, P_2O_5, SiO_2, and FeO was always less than 100 wt%, indicating the possible presence of Cl, F, and CO_2.

Table 5.7 : Electron microprobe analysis of feldspar.

VAR./ID.	Epidiorites									metasediments					
	HMMI 4	HMMI 11	HMMI 19	HMMI 29	HMMI 33	HMMI 35	HMMI 42	HMMI 46	HMMI 47	HMMI 68	HMMI 78	HMMI 96	HMMI 97	HMMI 103	HMMI 107
SiO_2	67.84	71.60	70.81	69.22	68.30	69.72	68.63	68.01	67.70	46.23	67.37	68.20	68.49	68.40	68.40
Al_2O_3	19.61	20.18	19.17	20.10	19.46	19.94	19.48	19.45	19.43	27.63	19.01	19.29	19.05	19.05	19.34
FeO	0.00	0.07	0.06	0.08	0.00	0.08	0.07	0.53	0.05	5.74	0.00	0.00	0.00	0.00	0.00
MgO	0.00	0.02	0.02	0.02	0.00	0.02	0.02	0.00	0.01	1.73	0.00	0.00	0.00	0.00	0.00
CaO	0.00	0.12	0.09	0.60	0.12	0.05	0.13	1.01	0.24	0.00	0.00	0.14	0.00	0.07	0.08
BaO	0.00	0.03	0.00	0.04	0.00	0.03	0.05	0.00	0.02	1.51	0.00	0.00	0.00	0.00	0.00
Na_2O	11.69	7.97	11.02	10.38	11.85	10.06	11.38	11.33	11.66	0.00	11.53	11.77	11.86	11.60	11.80
K_2O	0.00	0.06	0.06	0.06	0.00	0.08	0.07	0.08	0.07	10.36	0.08	0.11	0.00	0.08	0.00
TOTAL (wt %)	99.14	100.05	101.23	100.50	99.73	99.98	99.83	100.41	99.18	93.20	97.99	99.51	99.40	99.20	99.62
NUMBER OF IONS ON BASIS OF 32 (O)															
Si	11.95	12.26	12.16	11.98	11.97	12.08	12.00	11.89	11.94	9.49	12.01	11.98	12.03	12.04	11.99
Al	4.07	4.07	3.88	4.10	4.02	4.07	4.02	4.01	4.04	6.69	3.99	4.00	3.95	3.95	4.00
Fe	0.00	0.01	0.01	0.01	0.00	0.01	0.01	0.07	0.01	0.99	0.00	0.00	0.00	0.00	0.00
Mg	0.00	0.01	0.01	0.01	0.00	0.01	0.01	0.00	0.00	0.53	0.00	0.00	0.00	0.00	0.00
Ca	0.00	0.02	0.02	0.11	0.02	0.01	0.02	0.19	0.05	0.00	0.00	0.03	0.00	0.01	0.02
Ba	0.00	0.00	0.00	0.00	0.00	0.00	0.00	0.00	0.00	0.12	0.00	0.00	0.00	0.00	0.00
Na	3.99	2.65	3.67	3.48	4.03	3.38	3.86	3.84	3.99	0.00	3.98	4.01	4.04	3.96	4.01
K	0.00	0.01	0.01	0.01	0.00	0.02	0.01	0.02	0.02	2.71	0.02	0.03	0.00	0.02	0.00
Total	20.01	19.03	19.76	19.70	20.04	19.58	19.93	20.02	20.05	20.53	20.00	20.05	20.02	19.98	20.02
END-MEMBER COMPOSITION (MOL %)															
Albite	100.00	98.51	98.92	96.40	99.51	98.83	98.97	94.82	98.28	0.00	99.50	98.52	100.00	99.25	99.50
Anorthite	0.00	1.12	0.81	3.32	0.49	0.59	0.77	4.69	1.23	15.77	0.00	0.74	0.00	0.25	0.50
Orthoclase	0.00	0.37	0.27	0.28	0.00	0.58	0.26	0.49	0.49	84.23	0.50	0.74	0.00	0.50	0.00
Total	100.00	100.00	100.00	100.00	100.00	100.00	100.00	100.00	100.00	100.00	100.00	100.00	100.00	100.00	100.00

143

(c) Zircon

Two zircon analyses are given in Table (5.8), where they have been recalculated on the basis of 16(O) per unit cell. The analyses showed that the sum of SiO_2, ZrO_2, and FeO was less than 100 wt%, indicating the presence of other elements (not determined).

5.5.11 Oxides

(a) Rutile

Nine microprobe analyses of rutile were calculated on the basis of 2(O) and by assigning part of the total iron as Fe_2O_3, consistent with best stoichiometry, are represented together in Table (5.9). The titanium content of the rutile ranges between 95.89-99.55 wt%, except Specimen HMMI 55 with TiO_2=85.73 wt%. Trace amounts of Cr_2O_3 and MnO less than 0.1 wt% are present and higher SiO_2 and Al_2O_3, which is questionable.

(b) Ilmenite

Thirteen microprobe analyses of ilmenite with their calculated stoichiometry are presented in Table (5.10). The analyses were recalculated on the basis of 6(O) and on assuming part of the total iron as Fe_2O_3, consistent with stoichiometry. The analysed ilmenites have a variable amount of TiO_2 ranging between 50.25-68.33 wt%. Al_2O_3, Cr_2O_3, MgO, and CaO are present in trace amounts and a relatively large amount of MnO (0-5.66 wt%) is present.

(c) Magnetite

Ten microprobe analyses of magnetite with their calculated stoichiometry are presented in Table (5.11). In the recalculation of magnetite stoichiometric formulae, some workers had assumed a constant percentage of total iron as Fe_2O_3 (Buddington and Lindsley

Table 5.8 : Electron microprobe analysis of the accessory non-opaque minerals.

a) Sphene

VAR. / ID.	HMM 57	HMMI 3	HMMI 26	HMMI 47	HMMI 55
SiO_2	31.28	35.15	30.66	30.13	48.07
Al_2O_3	2.16	3.76	2.51	1.40	10.45
TiO_2	38.14	31.64	37.65	39.23	19.45
Cr_2O_3	0.00	0.00	0.01	0.00	0.00
FeO	0.40	0.39	0.32	0.30	0.32
MnO	0.00	0.00	0.00	0.02	0.00
MgO	0.00	0.00	0.02	0.02	0.00
CaO	28.51	27.22	28.76	28.52	15.07
Na_2O	0.00	0.00	0.00	0.00	6.20
TOTAL WT %)	100.50	98.15	99.93	99.63	99.88

NUMBER OF IONS ON BASIS OF 20 (O)

Si	4.05	4.56	3.99	3.95	5.78
Al	0.00	0.00	0.01	0.05	0.00
Total	4.05	4.56	4.00	4.00	5.78
Al	0.33	0.58	0.38	0.17	1.48
Ti	3.71	3.01	3.69	3.87	1.76
Cr	0.00	0.00	0.00	0.00	0.00
Fe	0.04	0.04	0.04	0.03	0.03
Total	4.08	3.71	4.11	4.07	3.27
Mn	0.00	0.00	0.00	0.00	0.00
Mg	0.00	0.00	0.00	0.00	0.00
Ca	3.95	3.79	4.01	4.01	1.94
Na	0.00	0.00	0.00	0.00	1.45
Total	3.95	3.79	4.01	4.01	3.39

(b) Apatite

VAR. / ID.	HMMI 33	HMMI 46	HMMI 68	HMMI 78
SiO_2	0.00	0.28	0.30	0.00
FeO	0.13	0.00	0.00	0.00
CaO	54.78	55.76	54.85	54.16
P_2O_5	42.42	42.39	41.78	41.53
TOTAL (wt %)	97.33	98.43	96.93	95.69

NUMBER OF IONS ON BASIS OF 25 (O)

Si	0.00	0.05	0.05	0.00
Fe	0.02	0.00	0.00	0.00
Ca	9.88	9.96	9.94	9.94
Total	9.90	10.01	9.99	9.94
P	6.04	5.98	5.98	6.02

(c) Zircon

VAR. ID.	HMMI 96	HMMI 103
SiO_2	32.75	32.39
FeO	0.00	0.15
ZrO	60.29	61.45
TOTAL (wt %)	93.05	93.99

NUMBER OF IONS ON BASIS OF 16 (O)

Si	4.22	4.15
Fe	0.00	0.02
Zr	3.79	3.84
Total	8.01	8.01

145

TABLE 5.9 : Electron microprobe analysis of rutile.

VAR. / ID.	HMM 22	HMM 29	HMMI 25	HMMI 25a	HMMI 29	HMMI 55	HMMI 61	HMMI 96	HMMI 97
SiO_2	0.76	0.37	0.13	0.48	0.08	8.33	0.10	0.48	0.55
Al_2O_3	0.19	0.20	0.03	0.00	0.04	2.37	0.05	0.20	0.48
TiO_2	99.02	98.59	96.35	96.30	99.10	85.73	99.55	99.39	95.89
Cr_2O_3	0.00	0.00	0.01	0.00	0.02	0.00	0.09	0.00	0.00
Fe_2O_3	0.49	0.00	0.00	0.19	0.00	0.11	0.00	0.03	0.13
FeO	0.32	1.24	0.91	1.36	0.63	0.59	0.66	0.50	1.28
MnO	0.00	0.00	0.00	0.00	0.01	0.00	0.01	0.00	0.00
MgO	0.00	0.00	0.00	0.00	0.00	0.00	0.00	0.00	0.00
TOTAL (wt %)	100.78	100.40	97.43	98.33	99.88	97.13	100.46	100.60	98.33

NUMBER OF IONS ON BASIS OF 2 (O)

	HMM 22	HMM 29	HMMI 25	HMMI 25a	HMMI 29	HMMI 55	HMMI 61	HMMI 96	HMMI 97
Si	0.01	0.01	0.00	0.01	0.00	0.11	0.00	0.01	0.01
Al	0.00	0.00	0.00	0.00	0.00	0.04	0.00	0.00	0.01
Ti	0.98	0.99	0.99	0.98	0.99	0.86	0.99	0.99	0.98
Cr	0.00	0.00	0.00	0.00	0.00	0.00	0.00	0.00	0.00
Fe^{3+}	0.01	0.00	0.00	0.00	0.00	0.00	0.00	0.00	0.02
Fe^{2+}	0.00	0.01	0.01	0.02	0.01	0.01	0.01	0.01	0.00
Mn	0.00	0.00	0.00	0.00	0.00	0.00	0.00	0.00	0.00
Mg	0.00	0.00	0.00	0.00	0.00	0.00	0.00	0.00	0.00
Total	1.00	1.01	1.00	1.01	1.00	1.01	1.00	1.00	1.01

Table 5.10 : Electron microprobe analysis of ilmenite.

VAR. / ID.	HMMI 16	HMM 44	HMMI 23	HMMI 25	HMMI 25a	HMMI 29	HMMI 33	HMMI 35	HMMI 42	HMMI 46	HMMI 78	HMMI 103	HMMI 31*
SiO_2	0.32	0.52	0.03	5.48	0.78	0.00	0.43	0.03	0.00	0.38	0.51	0.61	0.19
Al_2O_3	0.00	0.00	0.02	0.34	0.26	0.01	0.00	0.02	0.03	0.25	0.28	0.23	0.04
TiO_2	54.18	51.00	50.59	50.25	68.33	51.95	51.86	52.56	50.97	52.51	56.61	53.01	57.37
Cr_2O_3	0.00	0.00	0.02	0.00	0.00	0.01	0.00	0.01	0.01	0.00	0.00	0.00	0.02
Fe_2O_3	0.00	0.32	1.83	0.00	0.00	0.45	0.00	0.00	1.34	0.00	0.00	0.00	0.00
FeO	39.28	42.56	46.28	34.16	25.79	43.56	42.18	42.62	44.48	41.80	24.00	45.28	37.41
MnO	1.77	4.30	1.70	0.00	0.00	3.67	4.35	4.62	3.16	5.66	0.69	1.38	0.31
MgO	0.00	0.00	0.04	0.00	0.00	0.05	0.00	0.00	0.02	0.00	0.74	0.00	0.02
CaO	0.00	0.00	0.00	4.15	0.00	0.00	0.00	0.00	0.00	0.00	0.00	0.00	0.00
TOTAL (WT %)	95.55	98.70	100.51	94.38	95.16	99.70	98.82	99.86	100.01	100.60	82.83	100.51	95.36

NUMBER OF IONS ON BASIS OF 6 (O)

VAR. / ID.	HMMI 16	HMM 44	HMMI 23	HMMI 25	HMMI 25a	HMMI 29	HMMI 33	HMMI 35	HMMI 42	HMMI 46	HMMI 78	HMMI 103	HMMI 31*
Si	0.02	0.03	0.00	0.27	0.04	0.00	0.02	0.00	0.00	0.02	0.03	0.03	0.01
Al	0.00	0.00	0.00	0.02	0.02	0.00	0.00	0.00	0.00	0.02	0.02	0.01	0.00
Ti	2.10	1.96	1.93	1.89	2.44	1.98	1.99	2.00	1.95	1.98	2.36	1.99	2.19
Cr^{3+}	0.00	0.00	0.00	0.00	0.00	0.00	0.00	0.00	0.00	0.00	0.00	0.00	0.00
Fe	0.00	0.01	0.07	0.00	0.00	0.02	0.00	0.00	0.05	0.00	0.00	0.00	0.00
Total	2.12	2.00	2.00	2.18	2.50	2.00	2.01	2.00	2.00	2.02	2.40	2.03	2.20
Fe^{2+}	1.69	1.82	1.96	1.43	1.02	1.85	1.80	1.80	1.89	1.75	1.11	1.89	1.59
Mn	0.08	0.19	0.07	0.00	0.00	0.16	0.19	0.20	0.14	0.24	0.03	0.06	0.01
Mg	0.00	0.00	0.00	0.00	0.00	0.00	0.00	0.00	0.00	0.00	0.06	0.00	0.00
Ca	0.00	0.00	0.00	0.22	0.00	0.00	0.00	0.00	0.00	0.00	0.00	0.00	0.00
Total	1.77	2.01	2.03	1.65	1.02	2.01	1.99	2.00	2.03	1.99	1.20	1.95	1.60

* ilmenite analysis in epidiorite.

147

Table 5.11 : Electron microprobe analysis of magnetite. Recalculation is made by fixing part of the total iron (as FeO) into Fe_2O_3.

VAR. / ID.	HMM 4	HMM 5	HMM 9	HMM 11	HMMI 1	HMMI 16	HMM 17	HMM 23	HMMI 69	HMMI 107
SiO_2	0.14	0.24	0.27	0.30	0.01	0.40	0.56	0.57	0.80	1.02
Al_2O_3	0.07	0.00	0.00	0.16	0.08	0.04	0.47	0.00	0.00	0.17
TiO_2	0.11	0.00	0.04	0.00	0.05	0.02	0.00	0.00	0.00	0.00
Cr_2O_3	0.00	0.00	0.00	0.00	0.06	0.00	0.00	0.00	0.00	0.00
Fe_2O_3	68.19	68.31	67.00	69.21	68.21	66.98	58.26	66.84	67.51	64.81
ZnO	0.00	0.00	0.12	0.23	0.00	0.00	0.46	0.12	2.46	0.23
FeO	30.62	30.84	30.96	31.29	30.55	30.18	26.00	30.27	27.99	16.30
MnO	0.11	0.00	0.07	0.00	0.20	0.17	0.00	0.00	0.14	0.28
MgO	0.00	0.00	0.09	0.00	0.04	0.03	0.18	0.00	0.00	0.33
CaO	0.13	0.00	0.00	0.00	0.00	0.00	0.11	0.00	0.49	9.85
TOTAL	99.32	99.39	100.54	101.19	99.20	97.82	86.04	97.80	99.39	92.99
NUMBER OF IONS ON BASIS OF 32 (O)										
Si	0.05	0.07	0.08	0.09	0.00	0.13	0.20	0.18	0.24	0.33
Al	0.03	0.00	0.00	0.06	0.03	0.02	0.20	0.00	0.00	0.06
Ti	0.03	0.00	0.01	0.00	0.01	0.00	0.00	0.00	0.00	0.00
Cr	0.00	0.00	0.00	0.00	0.02	0.00	0.00	0.00	0.00	0.00
Fe^{3+}	15.88	15.91	15.88	15.82	15.94	15.82	15.56	15.78	15.68	15.52
Total	15.99	15.98	15.97	15.97	16.00	15.97	15.96	15.96	15.93	15.91
Zn	0.00	0.00	0.03	0.05	0.00	0.00	0.12	0.03	0.56	0.05
Fe^{2+}	7.93	7.99	7.92	7.95	7.93	7.92	7.72	7.94	7.23	4.34
Mn	0.03	0.00	0.02	0.00	0.05	0.05	0.00	0.00	0.04	0.08
Mg	0.00	0.00	0.04	0.00	0.02	0.01	0.10	0.00	0.00	0.16
Ca	0.04	0.00	0.00	0.00	0.00	0.00	0.04	0.00	0.16	3.36
Total	8.00	7.99	8.01	8.00	8.00	7.98	7.98	7.98	7.99	7.98

148

1964), while others assumed a theoretical molecular ratio of 1:1 (Mohamad 1980). However, in this study recalculation is made by assuming part of the total iron as Fe_2O_3, consistent with best stoichiometry. The magnetites contain trace amounts of Si, Al, Ti, Cr, Mn, Mg, and Ca. A notable amount of zinc ranges between 0.00-2.46 wt% and averages 0.36 wt%.

5.5.12 Sulphides

(a) Pyrite

Twenty-eight microprobe analyses of pyrite are presented in Table (5.12), together with their calculated stoichiometric formulae. Almost all the analyses show $S:(Fe+......Zn)<2$. This nonstoichiometry was observed in pyrite analyses from other deposits and was attributed to the S-vacancies in the pyrite structure as a result of low sulphur fugacity (Scott 1974).

Pyrites were analysed for their major elements Fe and S, and for trace elements such as Cu, Zn, and Pb. The minor elements determined include Co, Ni, and Se because of their use in the quantitative interpretation of environment of mineralisation. Arsenic, antimony, silver, and cadmium were also determined because they can be accomodated in the pyrite lattice (Vaughan and Craig 1978). Bismuth and tin were not determined and Se was not detected. Minor-element concentrations are generally low, many are near or below the detection limits. However, a considerable amount of cobalt is present ranging between 0-1.07 wt% and averaging about 0.25 wt%.

In metamorphosed terrain the origin of pyrite may be more reliably determined using minor elements and sulphur isotopes as a tracer. Many workers have used the ratios Co:Ni and S:Se as a means of distinguishing between sulphides of a sedimentary origin and those derived from igneous and hydrothermal processes (Hegemann

149

Table 5.12 : Electron microprobe analysis of pyrite.

VAR. / ID.	Epidiorites									Metasediments					
	HMM 5	HMM 8	HMM 10	HMM 11	HMM 12	HMM 1	HMM 3	HMM 16	HMM 19	HMM 22	HMM 23	HMM 29	HMM 57	HMM 25	HMM 26
Fe	46.69	39.10	46.57	46.75	46.74	47.25	46.96	47.28	46.36	46.42	46.44	46.23	47.02	46.82	46.55
Ni	0.00	0.16	0.00	0.00	0.29	0.02	0.00	0.00	0.15	0.00	0.00	0.00	0.00	0.00	0.00
Co	0.27	0.49	0.61	0.12	0.00	0.10	0.00	0.14	0.20	0.24	0.39	0.39	0.00	0.37	0.14
Ag	0.00	0.00	0.00	0.00	0.00	0.02	0.00	0.00	0.00	0.00	0.00	0.00	0.00	0.00	0.00
Cd	0.00	0.00	0.00	0.00	0.00	0.00	0.00	0.00	0.00	0.00	0.00	0.00	0.00	0.16	0.12
Sb	0.00	0.00	0.00	0.00	0.00	0.00	0.00	0.00	0.00	0.00	0.00	0.00	0.00	0.00	0.01
As	0.16	0.00	0.00	0.00	0.00	0.00	0.00	0.00	0.00	0.16	0.00	0.00	0.00	0.15	0.20
Cu	0.18	0.89	0.34	0.18	0.29	0.00	0.00	0.00	0.64	0.31	0.00	0.43	0.00	0.06	0.08
Zn	0.51	0.39	0.47	0.42	0.63	0.01	0.30	0.00	0.34	0.44	0.48	0.35	0.26	0.00	0.00
S	53.20	42.27	52.09	53.35	53.49	53.28	53.59	53.40	52.32	53.48	53.22	53.67	53.96	52.64	53.65
TOTAL (WT%)	101.01	83.30	100.08	100.82	101.44	100.68	100.85	100.82	100.01	101.05	100.53	101.07	101.24	100.20	100.75

NUMBER OF ATOMS ON BASIS OF 2 (S)

VAR. / ID.	HMM 5	HMM 8	HMM 10	HMM 11	HMM 12	HMM 1	HMM 3	HMM 16	HMM 19	HMM 22	HMM 23	HMM 29	HMM 57	HMM 25	HMM 26
Fe	1.008	1.062	1.027	1.006	1.003	1.018	1.006	1.017	1.018	0.997	1.002	0.989	1.001	1.021	0.996
Ni	0.000	0.004	0.000	0.000	0.006	0.000	0.000	0.000	0.003	0.000	0.000	0.000	0.000	0.000	0.000
Co	0.006	0.013	0.013	0.002	0.000	0.002	0.000	0.003	0.004	0.005	0.008	0.008	0.000	0.008	0.003
Ag	0.000	0.000	0.000	0.000	0.000	0.000	0.000	0.000	0.000	0.000	0.000	0.000	0.000	0.000	0.000
Cd	0.000	0.000	0.000	0.000	0.000	0.000	0.000	0.000	0.000	0.000	0.000	0.000	0.000	0.002	0.001
Sb	0.000	0.000	0.000	0.000	0.000	0.000	0.000	0.000	0.000	0.000	0.000	0.000	0.000	0.000	0.000
As	0.003	0.000	0.000	0.000	0.000	0.000	0.000	0.000	0.000	0.003	0.000	0.000	0.000	0.002	0.003
Cu	0.003	0.021	0.007	0.003	0.006	0.000	0.000	0.000	0.012	0.006	0.000	0.008	0.000	0.001	0.002
Zn	0.009	0.009	0.009	0.008	0.001	0.000	0.006	0.000	0.006	0.008	0.009	0.006	0.005	0.000	0.000
Total	1.029	1.109	1.055	1.020	1.026	1.021	1.012	1.020	1.044	1.018	1.019	1.012	1.005	1.034	1.005
S/(Fe+..Zn)	1.944	1.803	1.896	1.961	1.949	1.959	1.977	1.962	1.917	1.965	1.963	1.977	1.989	1.934	1.990

150

Table 5.12 : Continued

VAR. / ID.	HMMI 29	HMMI 33	HMMI 35	HMMI 46	HMMI 55	Metasediments HMMI 67	HMMI 68	HMMI 69	HMMI 78	HMMI 96	HMMI 97	HMMI 103	HMMI 107
Fe	46.90	46.83	46.89	46.35	46.50	45.93	46.83	46.83	46.68	46.78	46.88	46.61	47.22
Ni	0.00	0.00	0.00	0.00	0.00	0.00	0.00	0.00	0.00	0.00	0.00	0.00	0.00
Co	0.26	0.25	0.11	0.26	0.00	1.07	0.00	0.20	0.25	0.22	0.14	0.45	0.28
Ag	0.01	0.00	0.04	0.00	0.00	0.00	0.00	0.00	0.00	0.00	0.00	0.00	0.00
Cd	0.07	0.00	0.16	0.00	0.00	0.00	0.00	0.00	0.00	0.00	0.00	0.00	0.00
Sb	0.02	0.00	0.01	0.00	0.00	0.00	0.00	0.00	0.00	0.00	0.00	0.00	0.00
As	0.16	0.00	0.12	0.00	0.00	0.00	0.00	0.00	0.00	0.00	0.00	0.00	0.00
Cu	0.12	0.18	0.06	0.27	0.28	0.00	0.00	0.22	0.22	0.28	0.23	0.28	0.00
Zn	0.00	0.34	0.00	0.53	0.61	0.55	0.30	0.47	0.34	0.28	0.32	0.28	0.55
S	53.99	52.88	54.24	53.18	53.00	53.21	53.81	53.00	53.63	53.28	53.27	53.29	53.62
TOTAL (WT%)	101.53	100.48	101.63	100.59	100.39	100.76	100.94	100.72	101.12	100.84	100.84	100.63	101.67

NUMBER OF ATOMS ON BASIS OF 2(S)

VAR. / ID.	HMMI 29	HMMI 33	HMMI 35	HMMI 46	HMMI 55	HMMI 67	HMMI 68	HMMI 69	HMMI 78	HMMI 96	HMMI 97	HMMI 103	HMMI 107
Fe	0.998	1.017	0.993	1.001	1.008	0.991	0.999	1.015	1.000	1.008	1.011	1.004	1.011
Ni	0.000	0.000	0.000	0.000	0.000	0.000	0.000	0.000	0.000	0.000	0.000	0.000	0.000
Co	0.005	0.005	0.002	0.005	0.000	0.022	0.000	0.004	0.005	0.005	0.003	0.009	0.006
Ag	0.000	0.000	0.000	0.000	0.000	0.000	0.000	0.000	0.000	0.000	0.000	0.000	0.000
Cd	0.001	0.000	0.002	0.000	0.000	0.000	0.000	0.000	0.000	0.000	0.000	0.000	0.000
Sb	0.000	0.000	0.000	0.000	0.000	0.000	0.000	0.000	0.000	0.000	0.000	0.000	0.000
As	0.003	0.000	0.002	0.000	0.000	0.000	0.000	0.000	0.000	0.000	0.000	0.000	0.000
Cu	0.002	0.003	0.001	0.005	0.005	0.000	0.000	0.004	0.004	0.005	0.004	0.000	0.000
Zn	0.000	0.006	0.000	0.010	0.011	0.010	0.006	0.009	0.006	0.005	0.006	0.005	0.010
Total	1.009	1.032	1.000	1.021	1.024	1.023	1.005	1.032	1.015	1.023	1.024	1.019	1.027
S/(Fe+..Zn)	1.983	1.938	2.000	1.959	1.953	1.955	1.990	1.939	1.971	1.955	1.954	1.963	1.948

1943, Fleischer 1955, Loftus-Hills and Solomon 1967, Cambel and Jarkovsky 1969, Price 1972, Mercer 1976, Vaughan 1976, Weissburg et al. 1979 and Bralia et al. 1979). Sedimentary and diagenetic pyrites have a Co:Ni ratio less than unity and a S:Se ratio ⩽10,000:1, while igneous and hydrothermal pyrites have a Co:Ni ratio greater than unity and a S:Se ratio ⩾10,000:1 (Price 1972). Cobalt and nickel were considered to substitute for iron while selenium substitutes for sulphur in the pyrite structure (Vaughan 1976).

In this study, the selenium concentrations are less than the microprobe detection limit (i.e. < 0.005 at%), and accordingly the S:Se ratios are $> 10,000:1$. The cobalt concentrations are variable ranging between 0-1.07 wt% with an average of 0.25 wt%; nickel ranges between 0-0.29 wt% and averages 0.02 wt% and together they give an average Co:Ni ratio of around 12.5:1. However, as the levels of minor elements in the analysed pyrite grains are very low and the Se concentrations are below the detection limit there is less chance to rely on their application as was suggested above in the literature.

(b) Chalcopyrite

Fifteen microprobe analyses of chalcopyrite are presented in Table (5.13) together with their calculated stoichiometric formulae. Most of the analyses show nonstoichiometry with S/(Cu+.......Zn)<1.00. The chalcopyrites were analysed for major elements iron, copper, and sulphur and for trace and minor elements including cobalt, nickel, silver, cadmium, antimony, silver, arsenic, and zinc. The concentrations of most of the minor and trace elements are generally very low. Only cobalt and zinc are present in relatively considerable amounts. Cobalt concentrations range between 0-0.29 wt% and average 0.1 wt%, while nickel ranges between 0-0.29 wt%, and averages 0.02 wt%, giving an average Co:Ni ratio of 33.3:1. However, Farkas (1973) has pointed to the ability of chalcopyrite to incorporate nickel rather than cobalt in its

Table 5.13 : Electron microprobe analysis of chalcopyrite.

VAR. / ID.	Epidiorites											Metasediments			
	HMM 4	HMM 8	HMM 10	HMM 11	HMM 12	HMM 1	HMM 16	HMM 19	HMM 17	HMM 22	HMM 29	HMM 29	HMM 33	HMM 68	HMM 69
Cu	33.66	35.97	34.63	34.01	34.35	34.30	33.99	34.42	34.37	34.34	34.23	33.72	34.00	33.61	34.31
Fe	30.25	30.47	30.63	30.75	31.16	30.50	30.48	30.72	30.67	30.58	30.59	29.73	30.29	30.63	30.80
Ni	0.00	0.00	0.00	0.00	0.00	0.00	0.01	0.00	0.00	0.00	0.00	0.03	0.00	0.00	0.00
Co	0.29	0.12	0.00	0.07	0.00	0.05	0.05	0.00	0.22	0.19	0.28	0.09	0.12	0.00	0.00
Ag	0.00	0.00	0.00	0.00	0.00	0.00	0.01	0.00	0.00	0.00	0.00	0.01	0.00	0.00	0.00
Cd	0.00	0.00	0.00	0.00	0.00	0.00	0.05	0.00	0.00	0.00	0.00	0.33	0.00	0.00	0.00
Sb	0.00	0.00	0.00	0.00	0.00	0.00	0.01	0.00	0.00	0.00	0.00	0.07	0.00	0.00	0.00
As	0.00	0.00	0.00	0.00	0.00	0.00	0.04	0.00	0.00	0.13	0.10	0.41	0.00	0.00	0.00
Zn	0.21	0.04	0.13	0.48	0.00	0.06	0.07	0.22	0.13	0.16	0.00	0.12	0.00	0.27	0.00
S	34.18	34.91	34.42	34.48	34.88	34.54	33.96	34.71	34.72	34.72	34.53	34.51	34.48	34.42	34.67
TOTAL (WT%)	98.59	99.51	99.81	99.79	100.39	99.45	98.67	100.07	100.11	100.10	99.73	99.02	98.89	98.93	99.78
NUMBER OF ATOMS ON BASIS OF 2 (S)															
Cu	0.994	0.982	1.015	0.996	0.994	1.002	1.010	1.001	0.999	0.998	1.001	0.986	0.995	0.986	0.999
Fe	1.016	1.002	1.022	1.024	1.026	1.014	1.031	1.016	1.014	1.011	1.017	0.989	1.009	1.022	1.020
Ni	0.000	0.000	0.000	0.000	0.000	0.000	0.000	0.000	0.000	0.000	0.000	0.001	0.000	0.000	0.000
Co	0.009	0.004	0.000	0.002	0.000	0.002	0.002	0.000	0.007	0.005	0.009	0.003	0.004	0.000	0.000
Ag	0.000	0.000	0.000	0.000	0.000	0.000	0.000	0.000	0.000	0.000	0.000	0.000	0.000	0.000	0.000
Cd	0.000	0.000	0.000	0.000	0.000	0.000	0.001	0.000	0.000	0.000	0.000	0.006	0.000	0.000	0.000
Sb	0.000	0.000	0.000	0.000	0.000	0.000	0.000	0.000	0.000	0.000	0.000	0.001	0.000	0.000	0.000
As	0.000	0.000	0.000	0.000	0.000	0.000	0.001	0.000	0.000	0.003	0.003	0.010	0.000	0.000	0.000
Zn	0.006	0.001	0.004	0.014	0.000	0.002	0.002	0.006	0.004	0.006	0.000	0.003	0.000	0.008	0.000
Total	2.025	1.989	2.041	2.035	2.020	2.020	2.047	2.023	2.024	2.023	2.029	1.999	2.008	2.015	2.019
S/(Cu+..Zn)	0.988	1.005	0.980	0.983	0.990	0.990	0.977	0.989	0.988	0.989	0.986	1.000	0.996	0.993	0.991

153

structure and he related high Co:Ni ratios in chalcopyrite (greater than unity) to the high Co:Ni ratio of the ore fluid.

(c) Minor-Sulphide Phases

Sphalerite

Seven microprobe analyses of sphalerite and their calculated stoichiometry are presented in Table (5.14). Sphalerites were analysed for the major elements zinc and sulphur and also for iron, copper, and manganese. As for pyrite and chalcopyrite, S-vacancies due to low sulphur fugacity may have resulted in the observed nonstoichiometry. The analysed sphalerites show very low iron concentrations ranging between 0.008-0.166 wt% and averaging 0.1 wt%.

Pyrrhotite

Only one pyrrhotite analysis is presented in Table (5.14) containing trace amounts of nickel 0.42 wt%.

Covellite

Three microprobe analyses of covellite are presented in Table (5.14). They contain appreciable amounts of silver ranging between 0-4 wt%. Their low total values (<100) is probably due to the presence of certain minor and trace elements which are not determined.

Bornite

Only one bornite analysis is presented in Table (5.14). The analysis showed that minor concentrations of Ni, Co, Ag, Cd, Sb, and As are present.

Table 5.14 : Electron microprobe analysis of the minor sulphides.

A) Sphalerite

VAR. / ID.	HMM 4	HMM 8	HMM 10	HMM 11	HMM 12	HMM 17*	HMM 29*
Zn	61.23	57.98	57.40	58.06	59.36	60.20	66.87
Fe	5.44	7.39	9.60	4.76	8.09	4.61	0.44
Cu	0.28	0.57	0.65	4.77	0.36	2.25	0.34
Mn	0.14	0.00	0.00	0.00	0.00	0.00	0.06
S	32.89	33.09	33.31	32.82	33.13	32.90	32.86
TOTAL (WT%)	99.98	99.04	100.96	100.42	100.93	99.96	100.57
			NUMBER OF	ATOMS ON	BASIS OF	1 (S)	
Zn	0.913	0.860	0.845	0.868	0.879	0.898	0.998
Fe	0.095	0.128	0.166	0.083	0.140	0.080	0.008
Cu	0.004	0.009	0.010	0.074	0.005	0.035	0.005
Mn	0.003	0.000	0.000	0.000	0.000	0.000	0.001
Total	1.015	0.996	1.020	1.025	1.024	1.013	1.012
S Zn+..Mn	0.985	1.004	0.980	0.980	0.976	0.988	0.988

B) Pyrrhotite

VAR. ID.	HMM 57*
Fe	59.80
Ni	0.42
S	38.73
TOTAL WT%)	98.95

NUMBER OF ATOMS ON BASIS OF 1 (S)

Fe	0.887
Ni	0.006
Total	0.892
S/Fe+..Ni)	1.121

C) Covellite

VAR. ID.	HMM 11	HMM 11/	HMMI 69*
Fe	3.20	1.39	3.03
Ni	0.00	0.13	0.00
Ag	2.20	n.d	0.00
Cu	63.41	64.20	44.94
Zn	0.00	0.00	7.23
S	29.86	30.38	27.25
TOTAL WT%)	98.63	96.11	82.44

(D) Bornite

VAR. / ID.	HMMI 16
Fe	12.11
Ni	0.11
Co	0.11
Ag	0.04
Cd	0.15
Sb	0.03
As	0.22
Cu	61.34
S	12.11
TOTAL (WT%)	99.51

* Phases in metasediments.
/ contains 4% Ag

5.6 DISSCUSION AND SUMMARY ON THE TEXTURE OF THE OPAQUE MINERALS

Metamorphic textures are widespread in the studied opaque minerals on the microscopic scale, indicating that these minerals share with their host rocks a greenschist facies metamorphism and deformation. Metamorphism has resulted in the recrystallisation, deformation, and limited mobilisation of the opaque minerals. However, comparison between metamorphic and nonmetamorphic sulphides in several studies has pointed to the fact that sulphides are more chemically reactive and respond more readily to deformation and metamorphism than the associated silicates in a manner that masks their original features. This in turn makes it difficult to distinguish between premetamorphic and metamorphic sulphide textures. In the studied mineralisation, the stratiform fabric and possibly the fine compositional layering could be considered as original premetamorphic textures.

The observed metamorphic textures are similar to those described in metamorphosed sulphide deposits from greenschist and amphibolite facies terrains. These include the Scandinavian deposits in Norway (Waltham 1968, Vokes 1968, 1976), Sweden (Juve 1974 and Hutchinson and Scott 1980), and Greenland (Pedersen 1980); Appalachian Caledonides deposits in Virginia (Henry et al. 1979 and Pavlides et al. 1982), Carolina (Indrof 1981), and India (Deb 1980); the Archaean deposits in Canada (Rockingham and Hutchinson 1980 and Campbell and Etheir 1974), Spain (Cardellich 1982), east Carpathians (Kräutner 1984), Yugoslavia (Tufar and Strucl 1984) and Australia (Frater 1985 a&b).

Among the metamorphic textures observed in the studied area are those due to recrystalisation, deformation, and limited mobilisation and will be discussed in the following sections.

5.6.1 Recrystallisation Textures

All the opaque-mineral assemblages have recrystallised during metamorphism. Minerals of high form energy (i.e. pyrite and magnetite) occur in grains with proper crystallographic shape; normally as cubes in the case of pyrite (Plates 5.6, 5.12, and 5.13) and idiomorphic crystals in the case of magnetite. Minerals of low form energy (i.e. chalcopyrite, bornite, covellite, and sphalerite) occur in anhedral grains (Plate 5.18). Recrystallisation had also resulted in the formation of very large grains, usually as porphyroblasts in places full of other mineral inclusions, a process by which mineral grains grow at the expense of others (plates 5.11 and 5.13).

5.6.2 Deformed Textures

Some of the metamorphic textures observed in the studied mineral assemblages are textures demonstrating their response to deformation during metamorphism. A few pyrite grains deformed in a brittle manner by elongation parallel with the general trend of schistosity and in places are associated with rupturing perpendicular to the direction of elongation. Ductile minerals, examples are chalcopyrite and sphalerite, are deformed plastically by flowing and filling cracks and veins of other minerals. Another clear effect of deformation is the folding of the thin sulphide laminations and layers (Plate 5.3)

5.6.3 Mobilisation Textures

Mobilisation of minerals in sulphide ore bodies which have undergone deformation and metamorphism has been studied and reviewed by many authors (Kalliokoski 1965, McDonald 1967, Vokes 1969 and 1971, Mookherjee 1976 and Pedersen 1980) who concluded that sulphides can migrate over distances perhaps ranging between a few milimetres and a few metres during metamorphism. But the mechanism

of the process of such mobilisation is poorly understood.

However, limited mobilisation of the studied sulphides is noted. The mobilised minerals are generally coarse porphyroblasts up to 5cm across either disseminated through the rocks or present associated with quartz and/or calcite veins (Plates 5.2 and 5.4). On a microscopic scale the mobility of chalcopyrite is evident by its presence in fractures and veins of pyrite. The ore minerals and the silicates, quartz, and calcite are also found as veinlets following a variety of cooling or deformational cracks and fractures. Large mobilised and growing porphyroblasts are replacing other minerals (Plate 5.11). In rocks with folded schistosity relatively large pyrite crystals at the apex and hinge of the minor folds is noted (Plate 5.6).

5.7 DISCUSSION AND SUMMARY ON THE CHEMISTRY OF MINERALS

5.7.1 Non-Opaque Minerals

Petrographic study of the host rocks reveals the presence of localised development of metamorphic mineral assemblages; e.g. garnet, epidote, chlorite, quartz and calcite etc., which perhaps have a genetic relation with the ore formation. Microprobe analysis of these minerals reveals the presence of variable chemical compositions.

The amphiboles are actinolite in composition with $Mg/Mg+Fe^{2+}$ ratio between 0.5-0.9 (Fig. 5.3) controlled by the rock $Mg/Mg+Fe^{2+}$ (Fig. 5.5).

Garnets have variable spessartine, grossular, and almandine molecular proportions. The important feature demonstrated by the microprobe is the high manganese content of these garnets ranging between 6.86-18.41 MnO wt% with a mean of ($\bar{x}=12.52$) and a standard deviation of ($\sigma=3.31$), (Fig. 5.9). The manganese content is

158

preferentially enriched in garnets hosted by epidiorites compared to the metasediments (Figs. 5.6, 5.7 and 5.8). Similar manganese-bearing garnets have been described from other ore enviroments, for example, Cape Province, S. Africa (Stumpfl 1976 &1979); Broken Hill deposits, New South Wales (Stanton 1976a-d, 1979 and 1982, Plimer 1977, Stanton and Williams 1978 and Stanton and Vaughan 1979); Eastern Alps deposits (Tischler 1979) and Skorovas Norwegian Caledonides (Ferriday et al. 1981). This manganese enrichment is thought to accompany ore formation and it was transported by the same hydrothermal fluid. Later during metamorphism the Mn preferentially entered the garnet structure. Manganese is also present in other minerals (ilmenite, calcite, actinolite, and chlorite).

The composition of epidotes ranges between 23-32 Ps% (where pistacite % is the octahedral $Fe^{3+}/Fe^{3+}+Al^{6}$). The chlorites are ripidolites with Fe^{2+}/R^{2+} ratios between 0.25-0.75 (Fig. 5.12). The white micas are phengites in composition (with $Si:Al^{4}>3$). Feldspar are albite in composition.

5.7.2 Opaque Minerals

(a) Oxides

Of the oxide minerals, titanium-poor magnetite is the common mineral in the highly oxidised rocks especially the epidiorites. Compositionally they contain notable amounts of zinc (0-2.46 wt%). Rutile and ilmenite are preferentially developed within the metasedimentary rocks and compositionally, the ilmenite contains managanese (0-5.66 wt%).

(b) Sulphide minerals

Analyses of sulphide minerals reveal that they are nonstoichiometric. Their minor element contents are very low and in

good agreement with other analysed Dalradian sulphides (Willan and Hall 1980). The analysed pyrites have an average Co:Ni ratio = 12.5:1, suggestive of hydrothermal origin. However, Itoh and Kanehira (1967), Itoh (1971 a&b) and Loftus-Hills and Solomon (1967) have studied the Co:Ni ratios of pyrite from several cupriferous pyrite deposits and have pointed to the fact that their ratios are always greater than unity. The high S:Se ratio (>10,000:1) is not reliable as the Se content is not detected. Of the minor sulphide phases present, sphalerite contains very low iron values, and covellite contains up to 4 wt% silver. A trace of gold was noted as a veinlet in a porphyroblast pyrite.

5.8 EFFECT OF METAMORPHISM ON THE MINERALISATION

Metamorphism to greenschist facies at a pressure of 8-10 kb and temperature of 410-530°C (Graham 1983&1985), caused recrystallisation, deformation, and limited mobilisation of the opaque minerals.

Two types of veins are observed in the rocks; one type is mainly composed of quartz and/or calcite with oxide and sulphide minerals. In places they respond to deformation by thinning, flattening, and segmentation and they are believed to be associated with the premetamorphic ore formation process. The second type is comparatively thinner and criss-crosses the whole sample and in places displaces the older veins (Plate 5.8). The major minerals forming this type of vein and veinlets are in decreasing order of abundance : quartz, calcite, garnet, epidote, oxide, amphibole and chlorite with or without sulphide minerals. This latter type of vein and veinlet is thought to be perhaps of metamorphic origin probably resulting from late metamorphic fluids which circulate along fractures and cracks.

The presence of water during metamorphism, indicated by the formation of various hydrous minerals, helped to promote limited

160

replacement reactions during cooling. These include the alteration of pyrite and/or chalcopyrite porphyroblasts near the margin to a complex intergrowth of marcasite, magnetite, hematite, and sphalerite (Plate 5.9). Replacement of chalcopyrite by covellite and chalcocite along fractures and veinlets and perhaps replacement of chalcopyrite by pyrite and bornite (Plate 5.18). The rimming and replacement of magnetite by hematite (Plates 5.18 & 5.19).

This hydrous metamorphism is also believed to be responsible for the limited mobilisation of copper minerals and other sulphides, the mobilisation of quartz and calcite to form metamorphic veins and veinlets, and finally the mobilisation of some silicate minerals, e.g garnet, epidote and actinolite into large porphyroblasts associated with the ore and/or into thin veinlets

In specimens with accessory sphalerite content, although not so common, numerous chalcopyrite inclusions (chalcopyrite disease) sieving the sphalerite grains is noted (Plate 5.17). This texture has been observed in many ore deposits and different mechanisms have been suggested for its origin (Barton 1978, Henry et al. 1979, Craig et al. 1979, Wiggins and Craig 1980, Hutchinson and scott 1980 & 1981 and De Waad and Johnson 1981). However, the case present in Plate (5.17) is believed to be due recrystallisation of chalcopyrite and sphalerite intergrowth.

CHAPTER 6
GEOCHEMISTRY OF THE HOST ROCKS

6.1 INTRODUCTION

It was shown earlier in Chapter Five that the host rocks to the Abhainn Srathain copper mineralisation are characterised by the local development of certain metamorphic minerals such as epidote, garnet, micas, chlorite, quartz and carbonate indicating the possibility of premetamorphic alteration of the host rocks probably during the ore formation. One of the tasks of this chapter is therefore to investigate the chemistry of the host rocks in order to trace any premetamorphic chemical variations that had resulted from such alteration. However, the present chemistry of the metasedimentary rocks of the Upper Erins Quartzite is controlled by many factors: the nature of the original sediments and their sedimentary enviroments; the effect of volcanic activity; the effect of the proposed hydrothermal activity; the influence of the subsequent diagenetic processes and the effect of metamorphism. The present chemical composition of the epidiorites is the product of: the nature of the mother magma; changes which accompanied the intrusion; changes during the hydrothermal alteration and the process of mineralisation and the effect of metamorphism.

It is considered in this chapter that the study of the chemical composition of these rocks can help in distinguishing between these effects and deciding what was caused by the proposed hydrothermal alteration. Once the approximate premetamorphic chemical composition of these rocks is achieved, what was added and what was subtracted during this alteration can be assumed by visual comparison of these rocks with their unaltered equivalents and/or similar rocks.

162

Sixty-five selected samples were analysed for major, minor and trace elements and presented in Tables (6.1 a,b & 6.2). The results were obtained by X-ray fluorescence analysis performed at the Department of Geology, Glasgow University. The locations of the analysed samples are shown on Figs. (5.1 & 5.2B) and their mineralogical summary is presented in Appendix (A.5.2).

Brief summary on the methods of analysis, assesment of analysis and statistical treatment of the results will be given in the next sections before discussing the chemistry of the host rocks.

6.2 ANALYTICAL METHODS

The concentrations of the elements present in the analysed rocks were obtained by X-ray fluorescence using PW 1450 Instrument of the Geology Department, Glasgow University, except for ferrous iron, water and carbon dioxide which were determined by traditional methods in the wet chemistry laboratory of the above department. Loss on ignition was not determined but, ignoring the volatile components, the sum of water and carbon dioxide can be regarded as a close approximation to the loss on ignition.

6.2.1 Major Elements

(A) Preparation

The major elements are defined as SiO_2, TiO_2, Al_2O_3, total iron as Fe_2O_3, MnO, MgO, CaO, Na_2O, K_2O and P_2O_5. FeO was determined using a standard wet chemical analysis. Water and carbon dioxide were determined simultaneously.

Samples for analysis were prepared as glass discs according to the method of Harvey et al. (1973), in which 0.47 gm of sample was diluted by fusing with 2.5 gms of spectroflux 105. This flux contains high purity lithium tetraborate ($LiBO_4$), lithium carbonate

163

(LiCO$_3$) and the heavy absorber lanthanium oxide (LaO). The latter reduces the absorption and enhancement effects to give simple linear calibrations over a wide range of composition, with only a small correction required for interelement effects. The full procedure of fused beads (glass discs) preparation is given in Appendix (A.6.1).

Taking into consideration the variation of the copper content of the analysed samples which ranges between traces and a few weight percent, samples with high copper values might cause etching of the Pt/Ag crucible. To avoid this, fused discs of the samples with more than 1 wt% copper were prepared in a slightly modified procedure (Lawsie 1982, pers. comm.). Lawsie's modification involves dilution of 0.15 gm of the rock with 1.92 gms of the flux and then adding 0.3 gm of NaNO$_3$ to the mixture. The other important modified factor is the temperature of the hot plates. This varies with composition, a temperature of 160°C is used with basic and ultrabasic rocks and temperatures between 180-200°C with other compositions is used.

B) Analysis and instrumental conditions

All the major elements were analysed using the chromium tube. Appendix (A.6.2) gives details of the instrumental parameters during analysis.

The peak and background counting times have been calculated using the optimum-time split method of Jenkins and De Vries (1967) to give count rate errors of better than 1%, but with a maximum count time of 40 seconds (see Appendix A.6.3).

The calibration coefficients are established routinely using freshly made discs of the Glasgow standards supplemented by synthetic standards to increase the range of certain elements (Appendix A.6.4). Initially the composition of the Glasgow standards was determined by wet chemical analysis and on the XRF by calibrating against eleven International Standards (Appendix

A.6.4).

In brief, the analysis of a particular element involves construction of a calibration curve using the International Standards. This is done by plotting measured fluorescence intensities against concentration. Measured fluorescence intensities of samples are directly compared to this calibration to give their apparent concentrations. For the major elements a combination of matrix dilution and a mathematical correction is used. All calculations including corrections in the process are done by the computer.

(C) Accuracy

The International Standards were analysed as unknowns and the results are compared with the recommended values. These results therefore give a measure of the accuracy of the X-ray fluorescence analysis (Appendix A.6.4). The USGS III Standards were analysed with a more restricted calibration range than is now in operation. The results are for one run on one glass disc whereas the French Standards were analysed in duplicate on two glass discs.

(D) Precision

Appendix (A.6.5) gives details of replicate analyses of some of the Glasgow standards. All measurments were carried out on the same disc.

(E) Detection limits

The figures given in Appendix (A.6.3) are the average of values from each of the Glasgow standards.

(F) Ferrous iron determination

The determination of FeO in all the specimens analysed was performed at the Department of Geology, University of Glasgow using a wet chemical analysis by titration with standard potassium dichromate solution, see Appendix (A.6.6) for the complete procedure of the analysis.

Each sample was analysed in duplicate, and the average values being reported if the deviation of the average from the individual result is less than 3% relative. A third determination was made if the two determinations differed significantly. An average of two or three measurements is taken after considering the deviation. Normally duplicate analyses are sufficient.

The precision of the ferrous iron determination is high. A standard rock, schistose amphibolite (BL 3570) was analysed by a number of workers, on different days, in the laboratory of this department; the average of the eight replicate analyses is 7.55 + 0.17%. If this average is regarded as close to the true value (7.82%) as reported by Leake et al. (1969), this means that the analysis for this study are accurate to 0.4% relative.

(G) Water and carbon dioxide determination

Water and carbon dioxide are simultaneously determined in all the specimens analysed using apparatus of the Department of Geology, University of Glasgow. About 0.5 gm of dried powder is weighed into a previously ignited alumina boat. The boat with the sample is then inserted in a combustion tube. The water and carbon dioxide produced are removed with a current of nitrogen, absorbed and determined gravimetrically. A blank sample (empty alumina boat) is processed in a similar manner and the value is subtracted from the respective weights of water and carbon dioxide. For the complete procedure of this analysis see Appendix (A.6.7).

6.2.2 Trace Elements

(A) Preparation

The trace elements are analysed using pressed powder pellets prepared according to the method of Leake et al. (1969). A pellet consisting of six parts rock to one part binder enables elements to be determined down to levels of a few parts per million (ppm) which is not possible with a glass disc where the rock is diluted 1:5 with flux. The detail procedure of preparing pressed powder pellets is presented in Appendix (A.6.8).

(B) Analysis and instrumental conditions

All the trace elements are analysed or determined using the molybdenum tube, except for Nb and S which will be discussed later separately. Appendix (A.6.9) gives details of the instrumental parameters used for trace element determination.

The peak and background counting times have been calculated using the optimum-time split method of Jenkins and De Vries (1967), but with a maximum peak or background count time of 100 seconds.

Two International Standards were used in constructing the calibration curves; they are granite (G-GR 7500) and tholeiite (G-TH 7530). Appendix (A.6.10) explains the associated error e% with the upper limit of calibration in ppm.

(C) Accuracy

Appendix (A.6.10), column two gives an estimate of the accuracy of each calibration expressed as the standard error in the estimate of concentration. Column three gives the upper limit for which the calibration is marked by an asterisk and no confidence level on

accuracy can be placed on values which grossly exceed the upper limit.

(D) Precision

Two International Standards, granite (G-GR) and tholeiite (G-TH), were analysed nine times and the details of precision of these replicate analyses are given in Appendix (A.6.11).

(E) S and Nb determination

As mentioned before all trace elements were determined using the molybdenum tube, except Nb and S which were determined using the chromium tube and using uncorrected counts for the calibration graphs, as the Cr compton peak ratios do not correlate with the calculated absorption ratios. Good results are obtained for Nb over a wide range, however S is much less accurate. This is due to a lack of good standards and the problem of contamination from the vacuum pump oil which affects standards that are repeatedly analysed over a number of years. For best results a series of spiked rocks of appropriate composition should be made and used to calibrate specific groups of rocks. Appendix (A.6.11) gives the detailed instrumental conditions for determining Nb and S using the Cr-tube.

(F) Detection limit

The detection limits of the analysed trace elements are reported in Appendix (A.6.12). These values represent the average of the detection limits calculated from each of the Glasgow standards.

6.3 THE RESULTS

The results of the chemical analyses of the metasedimentary rocks (n=49) and the epidiorites (n=16) that host the Abhainn

Table 6.1a : Chemical analyses of the Upper Erins Quartzite pelites.

VAR. / ID.	HMM 24	HMM 25	HMMI 7	HMMI 9	HMMI 10	HMMI 13
SiO_2	68.60	42.57	41.18	66.01	52.82	63.31
TiO_2	0.29	0.68	0.57	0.61	0.62	0.61
Al_2O_3	8.47	19.01	17.06	15.31	15.95	14.45
Fe_2O_3	3.66	3.85	3.50	1.69	1.13	1.45
FeO	9.81	12.58	6.92	2.82	4.84	3.24
MnO	0.40	0.58	0.34	0.11	0.21	0.15
MgO	1.99	3.28	7.77	1.98	5.56	2.22
CaO	0.67	0.81	10.10	2.46	4.74	3.65
Na_2O	0.03	1.43	0.00	3.97	4.71	5.08
K_2O	1.35	7.10	1.29	1.81	0.66	1.09
P_2O_5	0.03	0.11	0.08	0.11	0.09	0.14
H_2O	2.94	3.58	3.37	1.71	3.75	1.28
CO_2	0.47	2.76	2.92	1.61	3.50	2.27
Total	99.66	98.96	95.29	100.76	98.71	99.07
Ba	550	4901	363	1072	336	631
Ce	38	77	66	96	84	90
Co	35	6	21	8	11	9
Cr	163	106	97	60	92	61
Cu	1372	37	13	10	3	16
Ga	12	28	23	16	14	14
La	26	55	44	55	48	49
Ni	16	35	47	15	30	16
Pb	4	5	14	8	3	5
Rb	34	159	27	52	16	32
S	6634	421	140	3807	71	258
Sr	18	94	721	159	198	165
Th	2	11	12	17	11	12
Y	28	27	28	38	27	36
Zn	358	93	157	42	184	52
Zr	161	131	157	213	153	203
si	329.3	115.8	98.0	283.1	160.8	250.6
ti	1.0	1.4	1.0	2.0	1.4	1.8
p	0.1	0.1	0.1	0.2	0.1	0.2
al	23.9	30.4	23.9	38.6	28.6	33.6
fm	68.4	51.1	48.4	28.6	40.8	28.7
c	3.4	2.4	25.8	11.3	15.5	15.5
alk	4.3	16.1	2.0	21.4	15.2	22.2
k	1.0	0.8	2.0	0.2	0.1	0.1
mg	0.2	0.3	0.6	0.4	0.6	0.5
w	25.1	21.6	31.3	35.0	17.4	28.7
al-alk	19.6	14.3	21.9	17.2	13.4	11.4
al-alf	23.8	26.6	23.9	22.2	14.7	14.2

Table 6.1a : Continued.

VAR. / ID.	HMMI 29	HMMI 30	HMMI 37	HMMI 38	HMMI 39	HMMI 41
SiO_2	65.11	52.14	58.08	47.46	49.60	65.57
TiO_2	0.51	0.68	0.94	1.23	1.15	0.49
Al_2O_3	11.66	13.44	13.51	17.71	14.56	11.85
Fe_2O_3	3.86	2.55	3.62	3.79	2.64	2.85
FeO	4.96	10.40	6.25	7.18	9.74	5.59
MnO	0.13	0.43	0.31	0.24	0.39	0.11
MgO	3.13	7.77	4.07	8.21	6.78	2.79
CaO	0.72	1.80	4.23	4.44	6.28	0.66
Na_2O	1.61	0.25	2.27	2.51	2.92	4.28
K_2O	0.45	1.66	0.35	0.30	0.65	0.33
P_2O_5	0.09	0.09	0.11	0.09	0.10	0.07
H_2O	2.58	3.66	2.34	0.99	0.11	2.17
CO_2	0.97	1.17	0.42	3.92	4.16	0.97
Total	98.02	96.31	97.37	99.72	99.49	99.65
Ba	91	873	428	275	1235	222
Ce	71	78	30	3	0	47
Co	22	16	11	27	46	18
Cr	46	184	250	368	339	189
Cu	916	8	138	85	103	95
Ga	11	25	15	19	16	19
La	34	49	23	9	9	30
Ni	11	28	57	129	98	13
Pb	0	5	1	4	5	4
Rb	10	55	10	8	29	10
S	19040	613	7023	7040	1757	29813
Sr	49	203	296	216	216	151
Th	10	13	4	0	1	4
Y	28	30	47	24	20	64
Zn	59	212	113	240	135	92
Zr	212	341	245	91	72	336
si	305.6	154.6	199.0	121.3	126.8	283.8
ti	1.8	1.5	2.4	2.4	2.2	1.6
p	0.2	0.1	0.2	0.1	0.1	0.1
al	32.2	23.4	27.2	26.6	21.9	30.2
fm	55.5	67.0	49.0	54.5	52.6	47.9
c	3.6	5.7	15.5	12.2	17.2	3.1
alk	8.7	3.9	8.3	6.7	8.3	18.8
k	0.2	0.8	0.1	0.1	0.1	0.0
mg	0.4	0.5	0.4	0.6	0.5	0.4
w	41.2	18.1	34.3	32.3	19.6	31.5
al-alk	23.5	19.6	18.9	19.9	13.6	11.3
al-alf	24.9	22.7	19.7	20.4	14.7	12.3

Table 6.1a : Continued.

VAR. / ID.	HMMI 42	HMMI 43	HMMI 45	HMMI 56	HMMI 65	HMMI 66	HMMI 69
SiO_2	59.37	53.90	62.55	46.95	64.63	39.98	37.76
TiO_2	1.33	1.03	1.05	2.51	0.43	1.23	0.79
Al_2O_3	13.53	12.38	12.50	14.04	12.43	22.74	16.28
Fe_2O_3	4.86	6.71	5.56	3.03	3.20	4.51	8.42
FeO	4.79	6.61	4.05	11.10	3.80	10.42	7.11
MnO	0.17	0.12	0.11	0.14	0.27	0.13	0.39
MgO	2.32	2.99	1.28	5.81	2.26	4.70	3.83
CaO	4.56	3.10	2.26	2.27	1.13	0.05	2.98
Na_2O	4.00	3.65	4.15	2.38	3.53	2.41	0.53
K_2O	0.47	0.76	1.56	2.22	3.45	9.35	6.94
P_2O_5	0.15	0.11	0.14	0.28	0.10	0.05	0.10
H_2O	0.43	2.27	1.13	3.08	0.95	3.47	2.89
CO_2	0.79	1.82	0.91	2.16	2.10	0.82	6.29
Total	98.25	100.18	100.27	96.16	99.11	100.90	99.05
Ba	251	575	2143	614	2552	7307	6916
Ce	54	56	74	36	52	174	83
Co	21	33	15	31	7	24	34
Cr	147	67	80	85	74	117	139
Cu	120	5932	122	56	66	51	7542
Ga	24	15	19	21	18	36	23
La	31	33	43	24	33	83	41
Ni	12	24	13	33	26	46	52
Pb	8	0	4	8	10	5	10
Rb	10	17	27	55	76	210	165
S	12181	37283	24748	355	4900	1645	29050
Sr	348	169	123	64	145	82	264
Th	5	5	4	0	6	29	12
Y	64	55	63	44	30	45	29
Zn	89	259	84	216	79	220	261
Zr	325	308	371	215	188	293	154
si	210.0	181.2	256.9	135.0	277.1	97.6	104.8
ti	3.5	2.6	3.2	5.4	1.4	2.3	1.6
p	0.2	0.2	0.2	3.0	0.2	0.1	0.1
al	28.1	24.5	30.2	23.8	31.3	32.7	26.6
fm	39.8	50.9	39.3	58.5	39.4	46.9	50.8
c	17.3	11.2	9.9	7.0	5.2	0.1	8.9
alk	14.8	13.5	20.6	10.7	24.1	20.3	13.7
k	0.1	0.1	0.2	0.4	0.4	0.7	0.9
mg	0.3	0.3	0.2	0.4	0.4	0.4	0.3
w	47.7	47.7	55.3	19.7	43.1	28.0	51.6
al-alk	13.4	11.0	9.6	13.1	7.3	12.4	12.9
al-alf	14.4	12.6	13.7	17.2	16.7	27.0	25.2

Table 6.1b : Chemical analyses of the Upper Erins Quartzite semipelitic and psammitic rocks.

VAR. / ID.	HMM 1	HMM 2	HMM 16	HMM 17	HMM 18	HMM 20
SiO_2	72.36	76.12	83.42	73.40	90.63	74.43
TiO_2	0.55	0.36	0.19	0.12	0.19	0.30
Al_2O_3	13.15	7.82	5.85	4.80	4.89	7.53
Fe_2O_3	1.48	0.01	2.63	5.79	1.87	3.57
FeO	2.57	2.48	0.55	1.64	0.34	1.15
MnO	0.06	0.10	0.08	0.05	0.01	0.02
MgO	1.48	1.82	0.35	0.00	0.29	0.20
CaO	0.11	3.17	4.21	0.39	0.05	3.90
Na_2O	0.65	1.41	0.00	1.31	0.00	0.14
K_2O	4.07	1.36	0.39	0.29	0.45	1.41
P_2O_5	0.07	0.04	0.02	0.00	0.02	0.00
H_2O	2.00	0.40	0.87	2.30	1.25	1.17
CO_2	0.52	4.32	0.49	1.30	0.06	0.95
Total	99.33	99.51	99.88	95.60	100.27	100.38
Ba	677	299	232	163	182	191
Ce	77	40	16	11	13	12
Co	4	3	3	26	0	26
Cr	68	45	49	268	126	42
Cu	14	0	3062	151	1120	176
Ga	17	8	10	8	6	9
La	45	24	11	0	7	7
Ni	15	0	3	20	0	26
Pb	7	12	5	3	2	0
Rb	143	41	14	10	12	11
S	1120	156	4800	41092	546	55165
Sr	44	46	377	14	16	151
Th	9	7	3	0	1	2
Y	20	18	9	7	6	9
Zn	67	26	26	151	17	176
Zr	244	278	217	138	189	136
si	435.8	503.5	743.2	702.7	1695.1	547.0
ti	2.5	1.8	1.3	0.9	2.7	1.7
p	0.2	0.1	0.1	0.0	0.2	0.0
al	46.6	30.4	30.7	27.0	53.8	32.6
fm	33.3	32.3	26.9	55.1	39.8	29.1
c	0.7	22.5	40.2	4.0	1.0	30.7
alk	19.4	14.8	2.2	13.9	5.4	7.6
k	0.8	0.4	1.0	0.1	1.0	0.9
mg	0.4	0.6	0.2	0.0	0.2	0.1
w	34.1	0.4	81.1	76.1	83.2	73.6
al-alk	27.2	15.7	28.4	13.1	48.4	25.0
al-alf	42.8	21.4	30.7	14.9	53.8	31.6

Table 6.1b : Continued.

VAR. / ID.	HMM 21	HMM 22	HMM 23	HMM 26	HMM 29	HMM 32
SiO_2	86.92	75.63	87.14	80.31	83.87	79.98
TiO_2	0.28	0.29	0.16	0.39	0.06	0.40
Al_2O_3	5.54	7.82	5.51	9.08	3.89	9.10
Fe_2O_3	1.93	4.43	1.99	1.11	0.27	0.84
FeO	0.54	0.44	1.06	2.17	3.41	1.80
MnO	0.08	0.08	0.06	0.05	0.01	0.06
MgO	0.19	0.18	0.65	0.83	0.06	1.15
CaO	0.38	3.97	0.42	0.10	0.20	0.57
Na_2O	0.28	0.94	0.41	0.98	1.75	1.81
K_2O	0.47	1.37	0.41	2.50	0.31	1.58
P_2O_5	0.02	0.00	0.02	0.05	0.00	0.05
H_2O	2.55	0.51	1.52	1.40	1.00	1.68
CO_2	0.82	1.87	0.42	0.66	1.02	1.70
Total	100.54	100.06	100.38	99.84	100.35	100.89
Ba	180	804	63	1320	174	402
Ce	22	44	19	39	15	38
Co	0	3	2	3	177	6
Cr	36	57	33	57	32	57
Cu	2560	7572	2660	38	12968	12
Ga	8	16	7	11	2	10
La	18	30	11	34	5	22
Ni	0	11	5	5	4	8
Pb	3	4	15	3	28	77
Rb	15	37	13	63	11	60
S	2018	16155	3060	175	28282	500
Sr	51	306	35	40	21	70
Th	2	1	3	6	1	8
Y	10	13	7	15	10	16
Zn	34	72	38	42	466	52
Zr	410	199	151	242	251	323
si	1339.9	515.7	1124.2	673.7	1112.8	633.3
ti	3.2	1.5	1.5	2.5	0.6	2.4
p	0.1	0.0	0.1	0.2	0.0	0.2
al	50.2	31.4	41.8	44.8	30.4	42.4
fm	34.7	27.5	43.9	33.0	41.7	30.9
c	6.3	29.0	5.8	0.9	2.8	4.8
alk	8.8	12.2	8.5	21.3	25.1	21.9
k	0.5	0.5	0.4	0.6	0.1	0.4
mg	0.1	0.1	0.3	0.3	0.0	0.4
w	76.3	90.1	62.8	31.5	6.7	29.6
al-alk	41.4	19.2	33.3	23.5	5.3	20.5
al-alf	46.0	25.2	36.7	36.9	7.9	28.5

Table 6.1b : Continued.

VAR. / ID.	HMMI 5	HMMI 6	HMMI 11	HMMI 14	HMMI 24	HMMI 51
SiO_2	83.40	88.84	83.22	72.18	76.71	89.16
TiO_2	0.27	0.19	0.24	0.45	0.47	0.22
Al_2O_3	5.40	3.90	6.47	9.86	10.39	5.22
Fe_2O_3	1.38	1.29	1.13	3.82	0.84	0.12
FeO	1.65	0.70	1.54	1.17	1.67	0.82
MnO	0.11	0.07	0.06	0.12	0.05	0.00
MgO	2.34	0.88	1.68	0.69	1.04	0.70
CaO	3.10	2.86	1.08	7.71	1.21	0.45
Na_2O	0.00	0.00	2.21	0.69	3.91	1.37
K_2O	0.25	0.22	0.71	0.34	1.27	0.81
P_2O_5	0.02	0.02	0.05	0.09	0.08	0.03
H_2O	1.96	0.64	1.30	0.64	1.33	0.42
CO_2	0.25	0.13	0.52	1.02	0.51	0.82
Total	100.16	99.85	100.50	99.01	99.61	100.24
Ba	13	14	501	108	645	391
Ce	22	15	21	56	56	21
Co	3	0	2	1	4	0
Cr	28	175	229	104	70	114
Cu	9	34	1	235	7	0
Ga	7	6	6	14	10	5
La	19	10	15	25	27	19
Ni	4	0	0	6	3	0
Pb	1	2	0	5	4	0
Rb	9	9	17	13	30	13
S	345	241	1735	746	93	147
Sr	278	273	71	678	55	31
Th	3	0	1	10	13	3
Y	13	9	12	26	28	10
Zn	47	27	35	29	24	28
Zr	423	278	274	259	255	213
si	658.2	1054.0	679.0	366.3	490.9	1235.1
ti	1.6	1.7	1.5	1.7	2.3	2.3
p	0.1	0.1	0.2	0.7	0.2	0.2
al	25.1	27.2	31.1	29.4	39.1	42.5
fm	47.5	34.8	38.4	25.3	23.2	25.3
c	26.2	36.4	9.4	41.9	8.3	6.7
alk	1.3	1.7	21.1	3.4	29.4	25.5
k	1.0	1.0	0.2	0.0	0.2	0.3
mg	0.6	0.5	0.5	0.2	0.4	0.6
w	42.9	62.4	39.8	74.6	31.2	11.6
al-alk	23.8	25.6	9.9	26.0	9.7	17.0
al-alf	25.1	27.2	13.7	26.8	14.9	24.2

Table 6.1b : Continued.

VAR. / ID.	HMMI 60	HMMI 62	HMMI 63	HMMI 64	HMMI 67	HMMI 73
SiO_2	86.57	69.53	88.40	88.70	74.58	82.27
TiO_2	0.26	0.47	0.23	0.24	0.29	0.31
Al_2O_3	5.54	12.57	5.36	5.16	9.34	6.61
Fe_2O_3	0.28	1.79	0.52	0.49	3.04	0.94
FeO	1.09	4.60	0.57	0.37	1.36	1.20
MnO	0.05	0.16	0.07	0.04	0.09	0.07
MgO	1.04	2.00	0.35	0.00	1.05	0.39
CaO	0.56	0.35	0.45	0.41	1.09	0.95
Na_2O	1.61	2.84	2.58	2.62	2.32	1.99
K_2O	0.63	2.85	0.56	0.51	2.28	2.05
P_2O_5	0.04	0.09	0.05	0.05	0.00	0.06
H_2O	0.10	1.46	0.18	0.21	1.15	1.94
CO_2	1.58	0.67	0.72	0.69	1.93	0.42
Total	99.45	100.00	100.26	99.63	99.78	99.60
Ba	230	2499	424	410	1351	749
Ce	22	72	26	22	32	22
Co	1	22	0	0	14	1
Cr	38	77	67	19	147	18
Cu	6	619	76	15	89	29
Ga	3	12	4	2	12	6
La	13	41	14	10	18	12
Ni	0	23	8	0	7	2
Pb	3	16	5	2	3	10
Rb	18	64	13	10	44	40
S	101	2394	1072	576	9617	2617
Sr	44	69	48	43	120	87
Th	3	9	4	4	2	4
Y	11	25	11	10	15	17
Zn	21	66	9	4	22	58
Zr	412	212	290	259	218	339
si	1013.7	336.7	1113.6	1259.0	483.4	786.3
ti	2.3	1.7	2.2	2.6	1.4	2.2
p	0.2	0.2	0.3	0.3	0.0	0.2
al	38.2	35.8	39.7	43.1	35.6	37.1
fm	31.9	40.3	18.3	10.1	32.8	22.4
c	7.0	1.8	6.1	6.2	7.6	9.7
alk	23.0	22.1	36.0	40.6	24.0	30.8
k	0.2	0.4	0.1	0.1	0.4	0.4
mg	0.6	0.4	0.4	0.0	0.3	0.2
w	18.8	25.9	45.1	54.4	66.8	41.3
al-alk	15.2	13.7	3.8	2.5	11.6	6.2
al-alf	19.9	22.5	8.2	7.1	21.0	18.7

Table 6.1b : Continued.

VAR. / ID.	HMMI 76	HMMI 77	HMMI 81	HMMI 83	HMMI 91	HMMI 93
SiO_2	84.21	68.82	76.61	76.37	78.22	73.84
TiO_2	0.27	0.17	0.20	0.22	0.30	0.33
Al_2O_3	5.90	3.99	9.05	6.09	6.56	7.46
Fe_2O_3	1.09	5.48	3.51	6.98	2.22	4.66
FeO	0.70	2.27	0.22	0.35	2.10	2.24
MnO	0.06	0.09	0.03	0.03	0.09	0.08
MgO	0.41	1.95	0.21	0.78	0.86	0.90
CaO	0.79	4.62	0.33	0.65	0.98	0.45
Na_2O	1.47	1.20	0.90	1.20	2.86	1.45
K_2O	1.74	1.06	1.59	1.59	1.60	1.82
P_2O_5	0.05	0.00	0.00	0.00	0.06	0.01
H_2O	1.44	0.72	0.55	0.45	2.63	1.30
CO_2	0.76	5.14	1.00	1.42	0.57	1.77
Total	99.35	99.72	100.69	100.33	99.61	100.22
Ba	941	1104	674	811	184	1297
Ce	27	53	16	35	30	38
Co	0	4	0	9	7	16
Cr	15	46	54	14	50	72
Cu	29	27	27	251	333	9756
Ga	5	2	4	6	10	10
La	14	14	8	17	14	21
Ni	0	11	9	3	6	17
Pb	20	695	39	12	205	8
Rb	45	29	26	37	30	43
S	3276	37367	61521	37921	4229	24984
Sr	297	355	47	61	69	43
Th	2	6	1	1	4	3
Y	13	11	10	23	10	20
Zn	21	25	5	59	128	319
Zr	378	210	274	303	267	278
si	944.4	379.4	714.7	579.6	580.3	519.5
ti	2.3	0.7	1.4	1.3	1.7	1.7
p	0.2	0.0	0.0	0.0	0.2	0.0
al	38.9	12.9	49.7	27.2	28.6	30.9
fm	23.2	49.6	29.4	51.0	35.5	47.7
c	9.5	27.3	3.3	5.3	7.8	3.4
alk	28.4	10.1	17.6	16.5	28.1	18.0
k	0.4	0.4	0.5	0.5	0.3	0.5
mg	0.3	0.3	0.1	0.2	0.3	0.2
w	58.4	68.5	93.5	94.7	48.8	65.2
al-alk	10.5	2.8	32.1	10.7	0.5	12.8
al-alf	23.0	6.5	41.6	18.4	8.1	21.1

Table 6.2 : Chemical analyses of the epidiorites associated with
Upper Erins Quartzite Formation.

VAR. / ID.	HMM 4	HMM 5	HMM 8	HMM 9	HMM 10	HMM 12
SiO_2	42.39	38.19	45.81	43.53	40.64	48.66
TiO_2	0.16	0.09	0.15	0.39	0.31	0.17
Al_2O_3	3.79	3.46	3.50	10.49	9.50	4.92
Fe_2O_3	5.37	8.01	4.07	7.00	8.62	4.55
FeO	7.89	7.28	6.45	4.26	5.51	4.21
MnO	1.87	1.52	1.04	1.70	1.65	0.52
MgO	5.51	4.90	7.90	3.08	3.78	3.38
CaO	18.90	20.20	16.92	20.86	20.98	18.86
Na_2O	0.00	0.35	0.90	0.00	0.31	0.40
K_2O	0.13	0.15	0.12	0.14	0.12	0.14
P_2O_5	0.07	0.00	0.01	0.05	0.07	0.00
H_2O	1.61	1.12	0.79	1.48	1.28	1.89
CO_2	11.96	11.74	5.85	6.52	3.02	9.17
Total	100.60	99.86	98.05	99.81	96.87	100.03
Ba	28	6	27	25	23	5
Ce	22	13	9	43	16	14
Co	20	31	7	7	15	17
Cr	30	28	51	71	78	54
Cu	2072	5166	19718	377	3220	12792
Ga	6	6	5	16	16	4
La	17	3	14	32	13	7
Ni	5	15	23	12	22	12
Pb	5	7	2	13	6	6
Rb	4	5	4	6	5	3
S	4854	19878	22710	1006	6068	16507
Sr	273	306	346	1129	964	330
Th	4	2	0	10	4	3
Y	9	6	8	18	12	8
Zn	2060	422	323	178	244	250
Zr	53	37	45	126	120	41
si	98.6	85.2	108.3	100.1	87.3	135.1
ti	0.3	0.2	0.3	0.7	0.5	0.4
p	0.1	0.0	0.0	0.0	0.1	0.0
al	5.2	4.5	4.9	14.2	12.0	8.0
fm	47.5	46.2	50.0	34.2	38.9	34.5
c	47.1	48.3	42.9	51.4	48.3	56.1
alk	0.2	1.0	2.2	0.2	0.8	1.3
k	1.0	0.2	0.1	1.0	0.2	0.2
mg	0.4	0.4	0.6	0.3	0.3	0.4
w	38.0	49.8	36.2	59.7	58.5	49.3
al-alk	5.0	3.6	2.6	14.0	11.2	6.7

Table 6.2 : Continued.

VAR. / ID.	HMM 13	HMM 30	HMMI 2	HMMI 12	HMMI 16	HMMI 18
SiO_2	42.62	49.92	49.23	43.95	43.30	48.46
TiO_2	0.08	1.84	0.48	0.11	0.10	0.15
Al_2O_3	1.82	13.49	13.75	2.60	3.32	4.00
Fe_2O_3	5.41	3.80	5.80	2.15	8.59	3.82
FeO	7.00	8.22	2.34	9.75	8.00	10.49
MnO	1.65	0.17	0.47	1.16	1.56	1.84
MgO	5.79	5.82	7.10	7.25	6.64	9.23
CaO	19.43	8.81	18.14	20.58	21.81	19.00
Na_2O	1.27	3.48	0.00	0.02	0.06	0.33
K_2O	0.10	0.26	0.10	0.12	0.13	0.11
P_2O_5	0.05	0.13	0.06	0.05	0.04	0.01
H_2O	1.37	3.19	2.69	1.62	1.22	0.98
CO_2	11.53	0.50	0.57	9.15	2.77	0.64
Total	99.15	99.74	100.94	98.80	97.91	100.29
Ba	7	51	23	8	27	34
Ce	14	18	61	6	9	16
Co	4	36	8	11	16	31
Cr	51	163	206	204	53	47
Cu	2684	52	59	658	1202	1515
Ga	11	20	22	5	6	5
La	11	14	37	16	20	13
Ni	7	42	37	0	16	24
Pb	8	2	8	0	4	11
Rb	7	6	4	4	5	3
S	6678	167	179	1573	1835	9232
Sr	567	183	1061	235	315	243
Th	3	0	9	1	3	4
Y	9	40	24	5	7	8
Zn	216	103	149	127	170	314
Zr	53	153	171	39	41	45
si	98.8	126.4	109.6	97.1	86.9	96.7
ti	0.1	3.5	0.8	0.2	0.2	0.2
p	0.0	0.1	0.1	0.0	0.0	0.0
al	2.5	20.1	18.0	3.4	3.9	4.7
fm	46.3	47.0	38.6	47.7	48.9	53.9
c	48.2	23.9	43.3	48.7	46.9	40.6
alk	3.0	9.0	0.1	0.2	0.3	0.8
k	0.0	0.0	1.0	0.8	0.6	0.2
mg	0.4	0.5	0.6	0.5	0.4	0.5
w	41.0	29.4	69.0	16.6	29.1	24.7
al-alk	0.5	11.1	17.9	3.2	3.6	3.9

Table 6.2 : Continued.

VAR. / ID.	HMMI 20	HMMI 21	HMMI 27	HMMI 49
SiO_2	43.11	43.88	49.18	48.93
TiO_2	0.35	0.23	3.26	1.08
Al_2O_3	9.44	5.59	12.12	14.39
Fe_2O_3	5.75	2.85	4.92	5.38
FeO	6.63	8.84	9.92	6.54
MnO	1.17	1.54	0.24	0.38
MgO	6.67	7.69	4.56	7.14
CaO	19.10	19.08	8.58	7.77
Na_2O	0.00	0.10	1.43	3.69
K_2O	0.19	0.13	0.70	0.68
P_2O_5	0.10	0.09	0.39	0.10
H_2O	4.22	1.12	2.24	1.97
CO_2	2.92	7.86	0.68	1.06
Total	100.01	99.45	98.47	99.48
Ba	69	27	355	316
Ce	49	29	50	17
Co	18	18	41	17
Cr	222	45	96	240
Cu	576	1424	273	42
Ga	13	9	19	17
La	30	19	27	5
Ni	27	21	48	93
Pb	10	1	6	8
Rb	6	5	25	11
S	1103	2072	753	2306
Sr	874	448	290	325
Th	6	3	4	0
Y	20	11	54	28
Zn	240	243	148	169
Zr	121	82	286	120
si	91.8	94.9	132.4	118.4
ti	0.6	0.4	6.6	2.0
p	0.1	0.1	0.4	0.1
al	11.8	7.1	19.2	20.5
fm	44.4	48.3	51.1	49.7
c	43.6	44.2	24.7	20.2
alk	0.3	0.4	4.9	9.7
k	1.0	0.5	0.2	0.1
mg	0.5	0.5	0.4	0.5
w	43.8	22.5	30.9	42.5
al-alk	11.6	6.7	14.3	10.8

Srathain copper mineralisation and the Knapdale Pyrite Horizon are presented in Tables (6.1 a,b & 6.2) respectively. They were analysed for thirteen major and minor oxides and sixteen trace and rare earth elements.

6.3.1 Total and the Estimation of the Quality of the Analysis

The reported totals in Tables (6.1 a,b & 6.2) represent the sum of all the analysed major, minor and trace elements. Analyses are generally accepted when the total lies between 99-101 wt%. Accordingly, of the sixty-five rock analyses; fifty-one analyses have a reasonable totals ranging between 99-101 wt% and are considered here as "good"; fourteen analyses are "fairly good" represent totals ranging from 98-99 wt% (n=7) and 95-98 wt% (n=7).

6.3.2 Statistical Analysis of the Results

When dealing with any geochemical data, the first step, is to establish the nature of their frequency distribution (i.e. normal, lognormal or non-normal) in order to apply the basic statistical parameters (mean, standard deviation, correlation coefficient etc.) in the interpretation. Data were checked for normality using kurtosis and skewness tests described by Jones (1969) and the coefficient of variation ($C=-\frac{\sigma}{x}-$) described by Shaw (1961), Koch and Link (1971) and Beus and Grigorian (1977).

The data were also transformed into logs to examine observation with lognormal distribution. The Statistical Package for the Social Sciences (SPPS) Studies on EMAS, was used to compute the statistical parameters for both arithmetic and log-transformed data. Pearson correlation coefficients of each analysed oxide/element against each of the other are also computed. This can help to score the correlative elements which might suggest detrital, hydrothermal or metamorphic origin.

180

A Frequency distribution

Metasedimentary rocks

For the metasedimentary rocks (n=49), the results of the tests are summarised in Tables (6.3 a&b) and the frequency distributions of their major oxides and trace elements are presented in Figure (6.1). Only a few elements are normally distributed, the majority are lognormally distributed and others are not normal. Among the major oxides; SiO_2,Al_2O_3, Fe_2O_3, Na_2O and H_2O have a normal but polymodal distributions; the remaining are lognormally distributed. Among the trace elements only Ga and Zr are normally distributed; Ce, La, Pb and Y show non-normal distribution; the remaining have non-normal to lognormal distribution.

The lack of regular distribution for some major oxides can be explained by the sporadic occurrence of certain minerals, for example, calcite (for CaO & CO_2), sphene and apatite (for CaO, TiO_2 and P_2O_5) etc. The irregularity in the distribution of some of the trace elements is in correspondance with the distribution of their geochemically coherent major oxides, example, CaO & Sr, K_2O & Rb, Ba etc.

Epidiorites

The epidiorites were also tested for normality and the results are tabulated in Tables (6.4 a&b) and plotted in Figure (6.2) as frequency distributions. The results are more or less similar to the observations noticed in the metasedimentary rocks that were described above.

(B) Pearson correlation

Metasedimentary rocks

Construction of a Pearson correlation matrix revealed a

Oxides	Min.	Max.	Mean	St.Dev.	Coeffic. Variat.	Normality[1] test	Arithmetic data Skew.	Arithmetic data Kurt.	Logarithmic data Skew.	Logarithmic data Kurt.	Normality[2] test
SiO_2	37.76	90.63	70.27	14.87	0.21	normal	-0.62	2.35	-0.79	-0.50	normal
TiO_2	0.06	2.51	0.51	0.43	0.84	lognormal	2.39	10.47	-0.38	0.52	lognormal
Al_2O_3	3.89	22.74	9.93	4.60	0.46	normal	0.62	2.62	-0.26	-0.76	normal
Fe_2O_3	0.01	8.42	2.78	1.95	0.70	lognormal	0.75	3.15	-2.25	7.60	normal
FeO	0.22	12.58	3.57	3.35	0.94	lognormal	1.13	3.21	-0.27	-0.88	lognormal
MnO	0.00	0.58	0.14	0.13	0.94	lognormal	1.66	5.19	-0.05	0.39	lognormal
MgO	0.00	8.21	2.11	2.18	1.04	lognormal	1.44	4.22	-0.46	-0.19	lognormal
CaO	0.05	10.10	2.09	2.19	1.05	lognormal	1.53	5.45	-0.28	-0.21	lognormal
Na_2O	0.00	5.08	1.85	1.40	0.75	lognormal	0.49	2.33	-1.96	5.03	normal
K_2O	0.22	9.35	1.60	1.83	1.15	lognormal	2.64	10.20	0.08	-0.12	lognormal
P_2O_5	0.00	0.28	0.06	0.05	0.86	lognormal	1.45	6.98	0.76	-0.23	lognormal
H_2O	0.10	3.75	1.59	1.04	0.66	lognormal	0.51	2.25	-1.11	0.97	normal
CO_2	0.06	6.29	1.51	1.36	0.90	lognormal	1.70	5.53	-0.26	1.06	lognormal

Table 6.3a : The results of the test for normal distribution for the major oxides of the metasedimentary rocks of the Upper Erins Quartzites (n=49). 1: using the coefficient of variation ($C = \dfrac{\sigma}{\bar{x}}$ Koch and Link 1971), 2: using limited values of skewness and kurtosis (Jones 1969).

Element	Min.	Max.	Mean	St.Dev.	Coeffic. Variat.	Normality[1] test	Arithmetic data Skew.	Arithmetic data Kurt.	Logarithmic data Skew.	Logarithmic data Kurt.	Normality[2] test
Ba	13	7307	987.10	1528.78	1.55	lognormal	3.05	12.02	-0.64	1.23	lognormal
Ce	0	174	43.69	31.37	0.72	lognormal	1.60	7.16	-1.43	3.72	not normal
Co	0	177	14.94	26.40	1.77	lognormal	4.88	30.31	-0.03	-0.88	lognormal
Cr	14	368	99.41	80.76	0.81	lognormal	1.62	5.32	-0.13	-0.30	lognormal
Cu	0	12968	1195.12	2778.34	2.32	lognormal	2.79	10.15	0.25	-0.43	lognormal
Ga	2	36	12.33	7.45	0.61	lognormal	0.88	3.63	-0.63	-0.03	normal
La	0	83	25.39	16.64	0.66	lognormal	1.06	4.25	-1.19	-3.35	not normal
Ni	0	129	18.31	24.79	1.35	lognormal	2.66	11.09	-0.24	-0.94	lognormal
Pb	0	695	26.37	102.22	3.88	lognormal	6.00	39.13	1.34	3.28	not normal
Rb	8	210	39.22	43.53	1.11	lognormal	2.41	8.52	0.37	-0.15	lognormal
S	71	61521	10792.45	15771.74	1.46	lognormal	1.61	4.66	0.01	-1.19	lognormal
Sr	14	721	153.49	153.70	1.00	lognormal	1.95	7.27	0.06	-0.59	lognormal
Th	0	29	5.59	5.47	0.98	lognormal	1.90	8.06	-0.01	-1.02	lognormal
Y	6	64	23.29	15.60	0.67	lognormal	1.22	3.76	-0.81	2.24	not normal
Zn	4	466	102.84	102.64	1.00	lognormal	1.56	5.13	-0.39	-0.03	lognormal
Zr	72	423	246.71	82.30	0.33	normal	0.17	2.63	-1.44	3.05	normal

Table 6.3b: The results of the test for normal distribution for the trace elements of the metasedimentary rocks of the Upper Erins Quartzite (n=49). 1: using the coefficient of variation (C = $\frac{\sigma}{\bar{x}}$; Koch and Link 1971), 2: using limited values of skewness and kurtosis (Jones 1969).

183
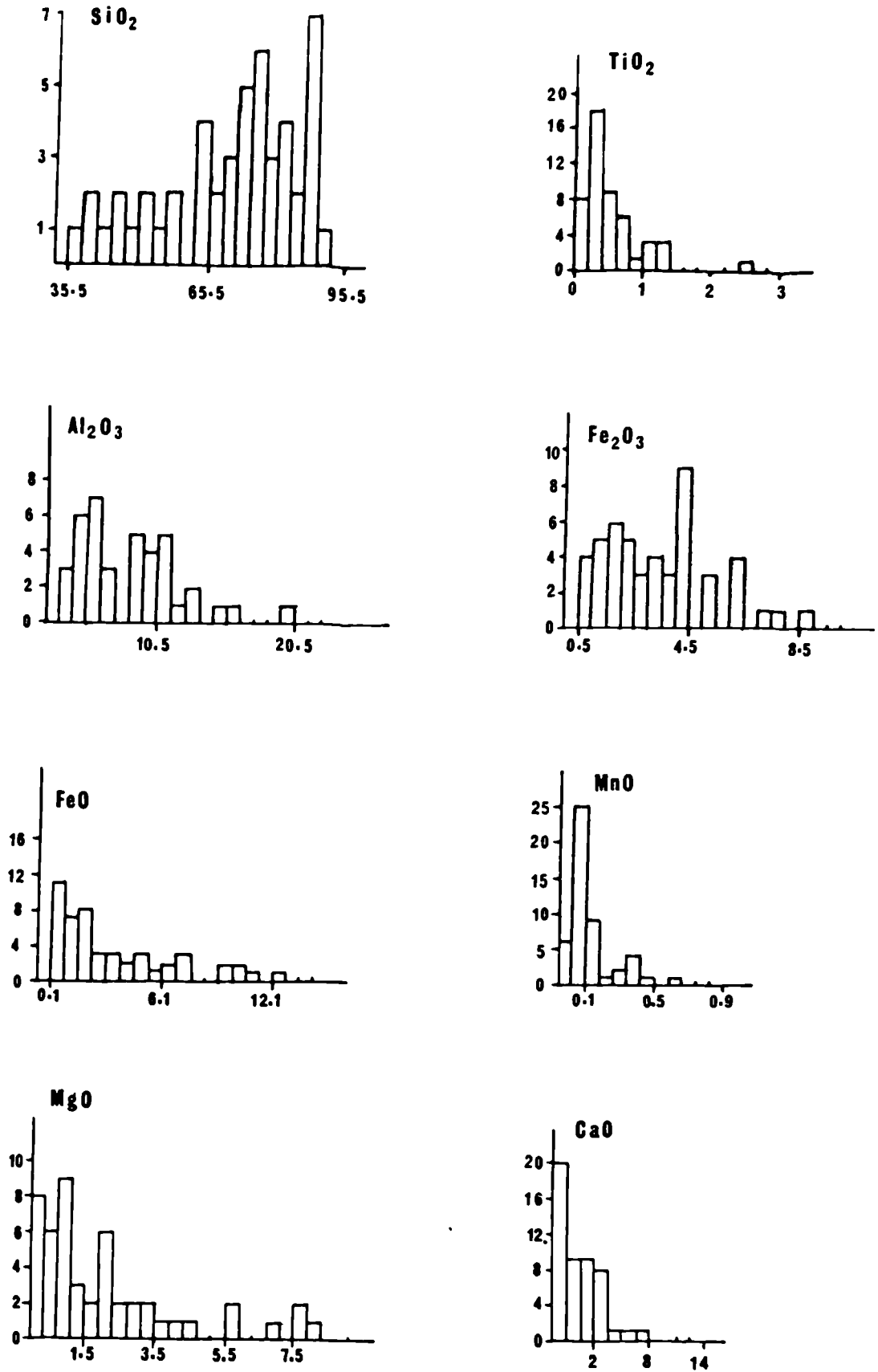
Fig. 6.1 : Major and trace element frequency histograms
for the metasedimentary rocks.
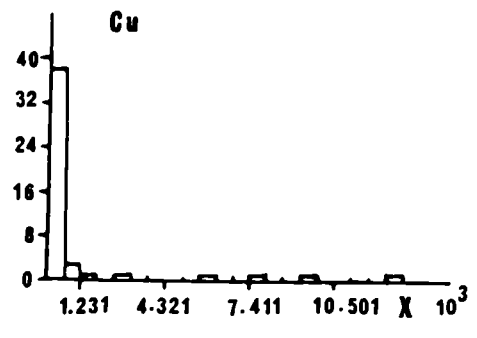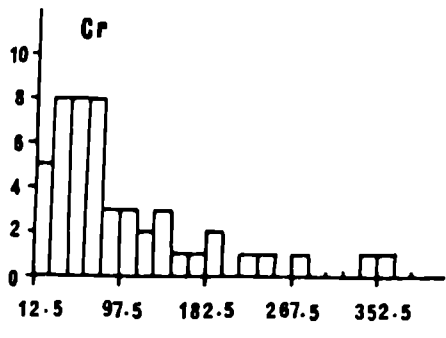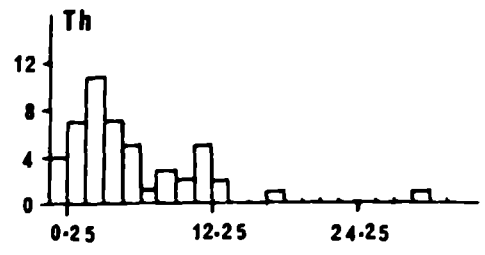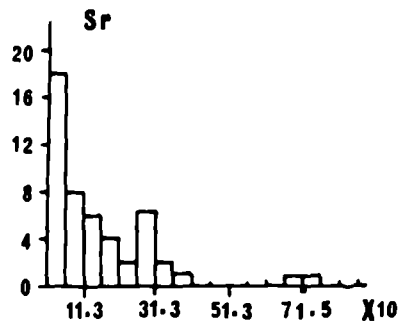
184

Fig. 6.1 : Continued.

Fig. 6.1 : Continued.

186

Fig. 6.1 : Continued.

Oxides	Min.	Max.	Mean	St.Dev	Coeffic. Variat.	Normality[1] test	Arithmetic data Skew.	Kurt.	Logarithmic data Skew.	Kurt.	Normality[2] test
SiO_2	38.19	49.92	45.11	3.56	0.08	normal	-0.14	1.99	-2.60	8.20	normal
TiO_2	0.08	3.26	0.56	0.85	1.53	lognormal	2.34	7.49	1.18	0.96	lognormal
Al_2O_3	1.82	14.39	7.26	4.49	0.62	lognormal	0.40	1.56	0.09	-0.81	normal
Fe_2O_3	2.15	8.62	5.38	1.92	0.36	normal	0.28	2.31	1.12	2.20	lognormal
FeO	2.34	10.49	7.08	2.23	0.32	normal	-0.42	2.59	-0.60	0.38	normal
MnO	0.17	1.87	1.16	0.61	0.52	lognormal	-0.47	1.66	-1.79	2.55	normal
MgO	3.08	9.23	6.03	1.75	0.29	normal	-0.15	2.19	-0.53	-0.48	normal
CaO	7.77	21.81	17.44	4.65	0.27	normal	-1.37	3.25	-1.66	1.51	normal
Na_2O	0.00	3.69	0.77	1.19	1.54	lognormal	1.72	4.60	-0.22	-0.10	normal
K_2O	0.10	0.70	0.21	0.19	0.93	lognormal	2.10	5.68	1.71	2.25	lognormal
P_2O_5	0.00	0.39	0.08	0.09	1.21	lognormal	2.61	9.76	0.39	-0.21	normal
H_2O	0.79	4.22	1.80	0.91	0.51	lognormal	1.38	4.26	1.06	1.13	lognormal
CO_2	0.50	11.96	5.12	4.33	0.85	lognormal	0.45	1.69	-0.80	-0.48	normal

Table 6.4a : The results of the test for normal distribution for the major oxides of the epidiorites of the Upper Erins Quartzites (n=16). 1: using the coefficient of variation (C = $\frac{\sigma}{\bar{x}}$ Koch and Link 1971), 2: using limited values of skewness and kurtosis (Jones 1969).

Element	Min.	Max.	Mean	St.Dev.	Coeffic. Variat.	Normality[1] test	Arithmetic data Skew.	Kurt.	Logarithmic data Skew.	Kurt.	Normality[2] test
Ba	5	355	64.44	107.33	1.67	lognormal	2.18	6.00	0.38	1.33	lognormal
Ce	6	61	24.13	17.06	0.71	lognormal	0.99	2.57	-0.22	0.91	normal
Co	4	41	18.56	10.93	0.59	lognormal	0.66	2.44	0.57	1.93	lognormal
Cr	28	240	102.44	76.07	0.74	lognormal	0.78	1.92	0.98	-0.04	normal
Cu	42	19718	3239.38	5415.09	1.67	lognormal	2.23	6.84	-0.67	0.04	normal
Ga	4	22	11.25	6.28	0.56	lognormal	0.34	1.58	0.12	-1.51	normal
La	3	37	17.38	9.77	0.56	lognormal	0.53	2.41	-0.57	-0.06	normal
Ni	0	93	25.25	22.34	0.88	lognormal	1.80	6.34	0.34	0.15	normal
Pb	0	13	6.06	3.66	0.60	lognormal	0.06	2.28	-0.92	0.33	normal
Rb	3	25	6.44	5.30	0.82	lognormal	2.93	10.75	0.90	1.11	lognormal
S	167	22710	6057.56	7324.71	1.21	lognormal	1.29	3.24	-0.07	0.52	lognormal
Sr	183	1129	493.06	322.43	0.65	lognormal	1.02	2.39	0.71	-0.56	normal
Th	0	10	3.50	2.90	0.83	lognormal	0.87	3.26	-0.04	-0.68	normal
Y	5	54	16.69	13.84	0.83	lognormal	1.55	4.49	1.08	0.20	normal
Zn	103	2060	334.75	467.41	1.40	lognormal	3.43	13.21	1.51	2.34	lognormal
Zr	37	286	95.81	68.08	0.71	lognormal	1.40	4.68	0.34	-1.73	normal

Table 6.4b : The results of the test for normal distribution for the trace elements of the epidiorites of the Upper Erins Quartzite (n=16). 1: using the coefficient of variation (C = $\frac{\sigma}{\bar{x}}$ Koch and Link 1971), 2: using limited values of skewness and kurtosis (Jones 1969).

189
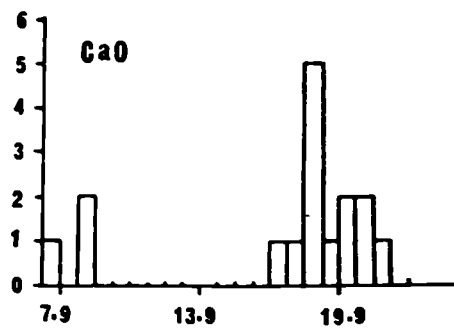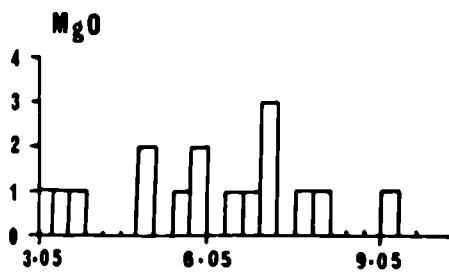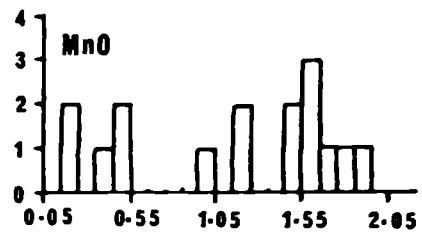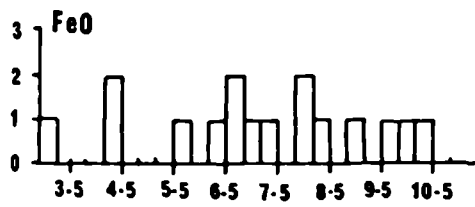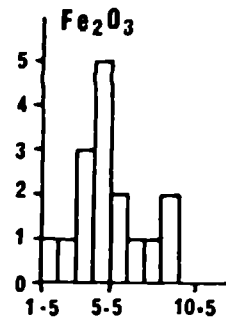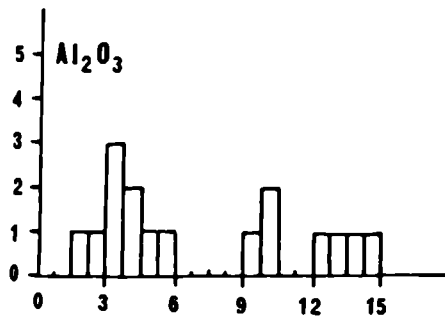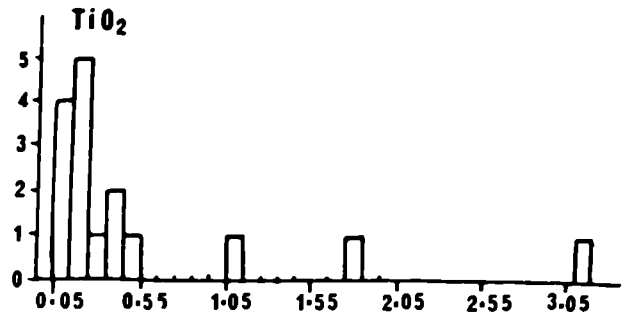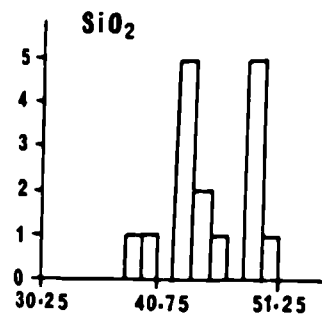
Fig. 6.2 : Major and trace element frequency histograms
for the epidiorites.

190

Fig. 6.2 : Continued.

191
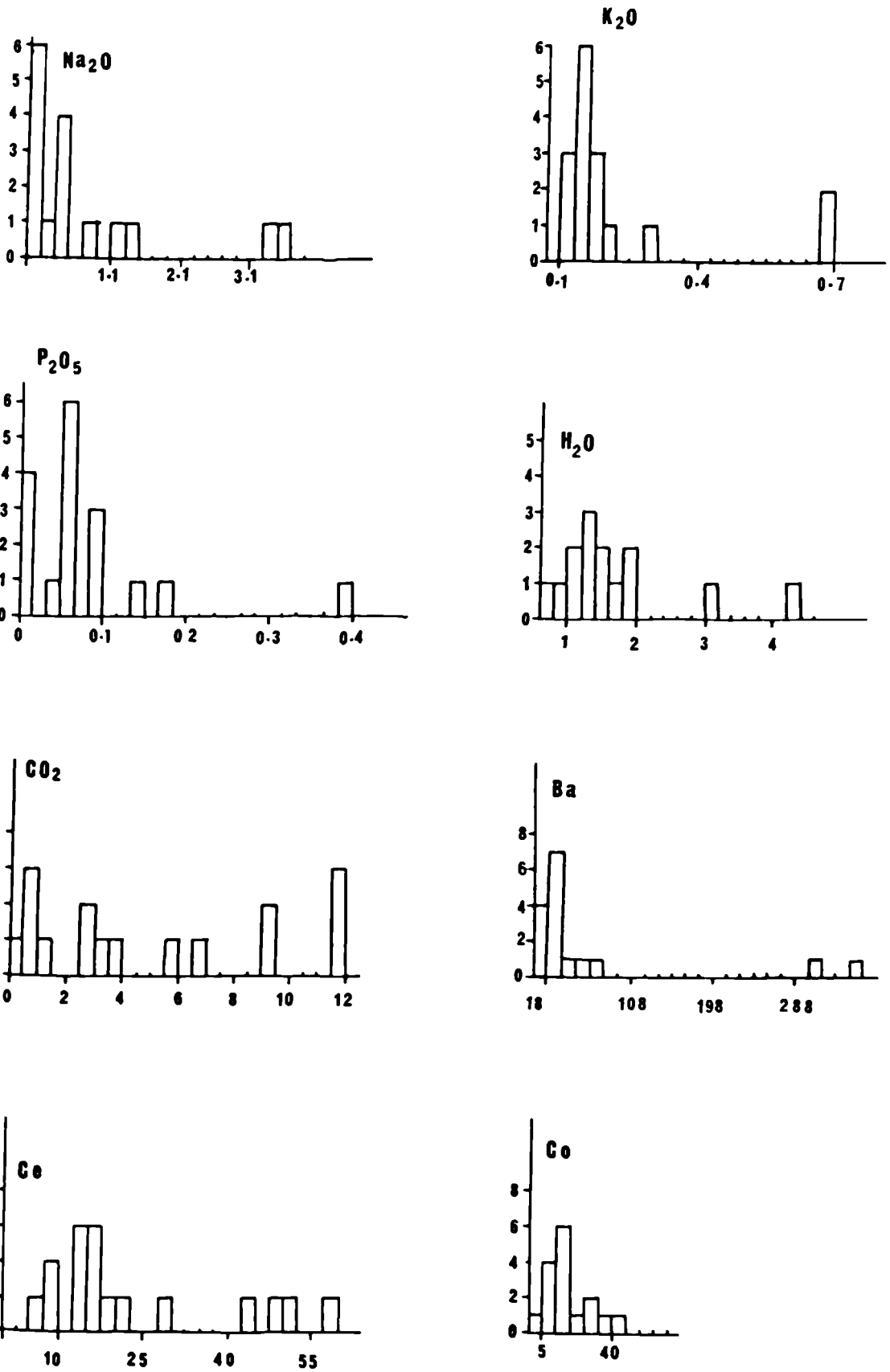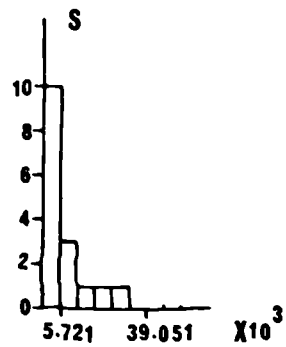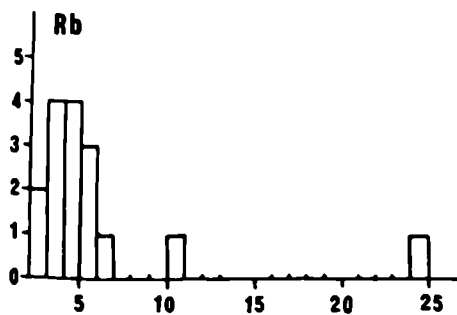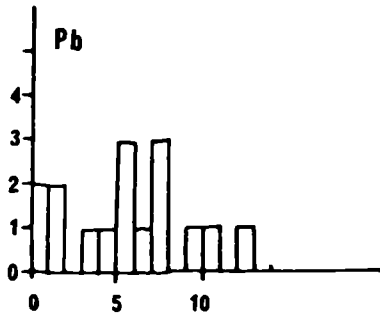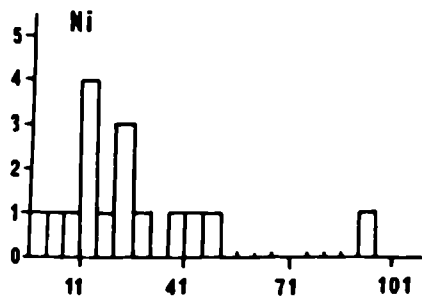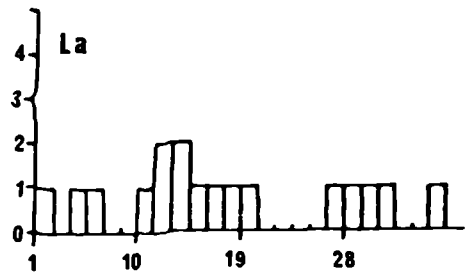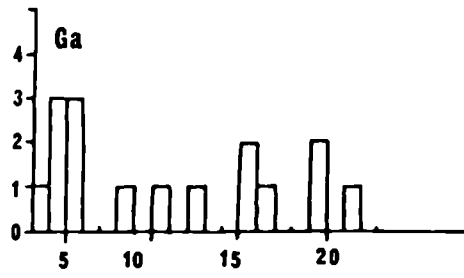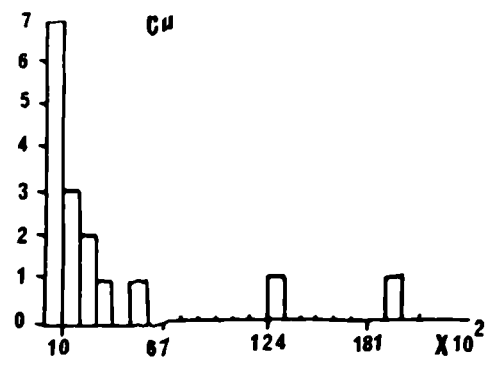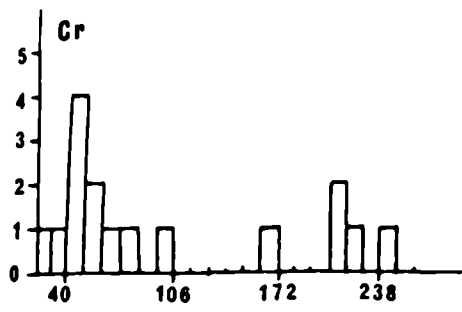
Fig. 6.2 : Continued.
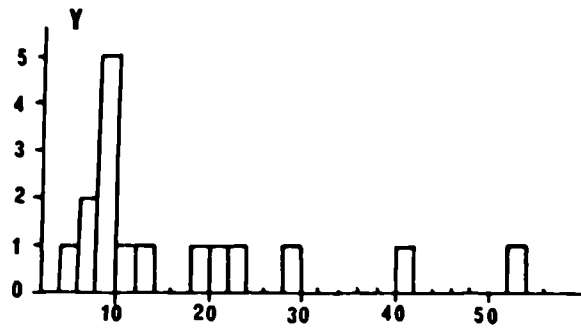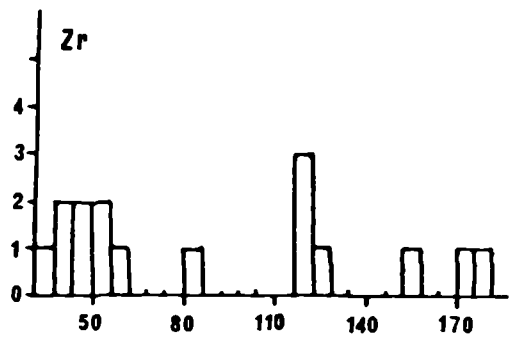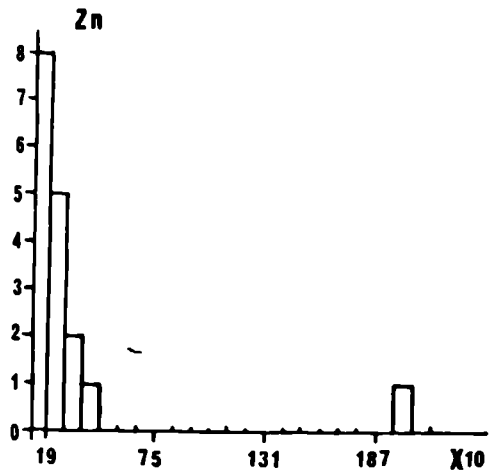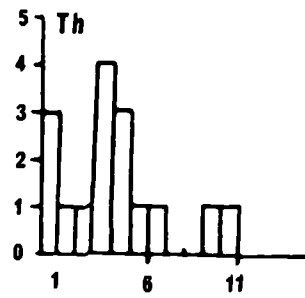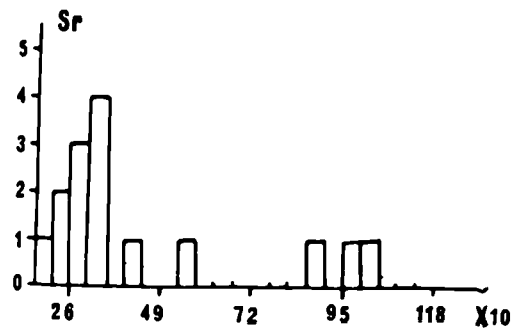
Fig. 6.2 : Continued.

considerable number of element pairs with positive or negative correlation coefficients greater than $\pm$ 0.5. Scatter plots of each element pair with a Pearson correlation coefficient greater than $\pm$ 0.5 are produced to avoid any induced apparent strong correlation resulting from the outlying few samples with values different from the usual values and a selection is shown in Figure (6.3).

Significant negative correlation between SiO_2 and Al_2O_3, FeO, MgO, MnO, and TiO_2 and to a lesser extent P_2O_5, CO_2, H_2O, Fe_2O_3 and K_2O is noticed among the major oxides (Table 6.5a). Also some of the Traces correlate negatively with SiO_2; significant negative correlation exists between SiO_2 and Ga and Ni and a weaker correlation between SiO_2 and La, Y, Ce, Ba and Th (Table 6.5c).

The strong positive correlation between Al_2O_3 and FeO, MgO and MnO accompanied by the strong positive correlation between FeO, MgO and MnO suggest that these components occur in garnet. Some of the FeO and MgO can form biotite and chlorite and this can explain the positive correlation between FeO, MgO and H_2O. The positive correlation between Al_2O_3, K_2O and H_2O can be explained by the presence of muscovite. Al_2O_3 correlates positively with P_2O_5 and TiO_2 which are low in concentration and both correlate positively with each other and with FeO and MgO and therefore probably occur as impurities in the biotite and chlorite. However, the strong correlation between TiO_2 and FeO (0.7) suggests that the large fraction of TiO_2 is present as accessory iron titanium oxides. It is surprising that no good correlation exists between Al_2O_3 and Na_2O (0.40), despite the presence of albite that was confirmed petrographically and analysed chemically. This might be due to the low concentrations of Na_2O (only a few albite-bearing specimens were analysed) and the fact that Al_2O_3 is distributed between a large number of Al-bearing silicates. The same sort of explanation can be applied to the absence of good correlations between CaO and Fe_2O_3; CaO and CO_2; CaO and P_2O_5; and CaO and TiO_2 despite the presence of epidote, calcite, apatite and sphene respectively in the analysed

194
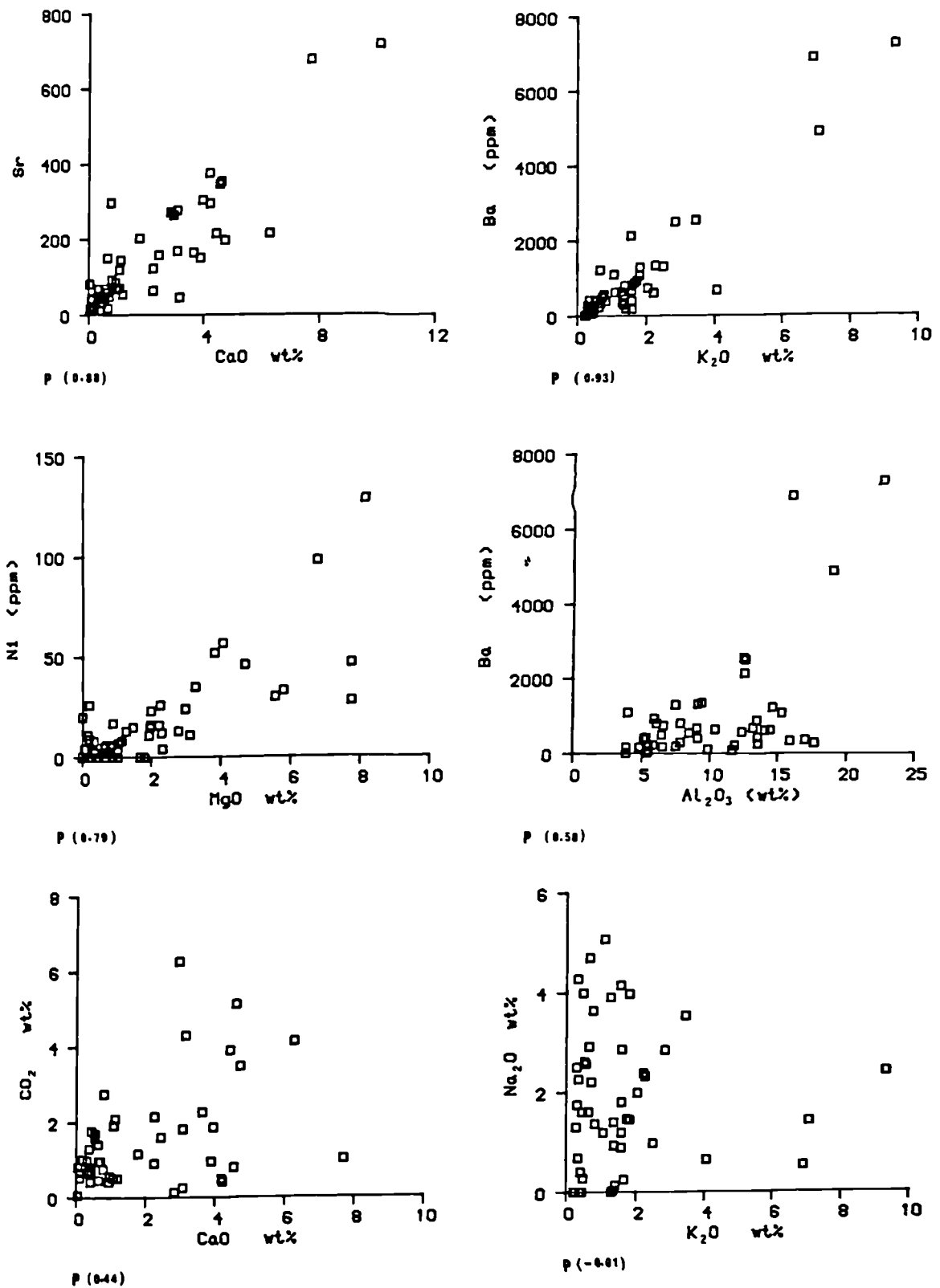
Fig. 6.3: Scatter plots of selective Pearson correlations between selected elements for the metasedimentary rocks.

	SiO_2	TiO_2	Al_2O_3	Fe_2O_3	FeO	MnO	MgO	CaO	Na_2O	K_2O	P_2O_5	H_2O	CO_2
SiO_2	1.00												
TiO_2	-0.72	1.00											
Al_2O_3	-0.90	0.69	1.00										
Fe_2O_3	-0.56	0.30	0.32	1.00									
FeO	-0.86	0.70	0.77	0.33	1.00								
MnO	-0.75	0.38	0.65	0.31	0.82	1.00							
MgO	-0.83	0.66	0.75	0.21	0.79	0.70	1.00						
CaO	-0.45	0.28	0.32	0.24	0.20	0.35	0.49	1.00					
Na_2O	-0.28	0.38	0.40	-0.04	0.16	0.01	0.16	0.00	1.00				
K_2O	-0.51	0.27	0.58	0.30	0.47	0.38	0.19	-0.22	-0.01	1.00			
P_2O_5	-0.61	0.85	0.64	0.11	0.60	0.42	0.54	0.26	0.53	0.17	1.00		
H_2O	-0.57	0.32	0.52	0.21	0.63	0.52	0.50	0.00	-0.04	0.43	0.32	1.00	
CO_2	-0.58	0.27	0.38	0.37	0.36	0.45	0.49	0.44	0.11	0.25	0.19	0.07	1.00

Table 6.5a : Pearson correlation coefficients for the major oxides of the metasedimentary rocks of the Upper Erins Quartzites.

	Ba	Ce	Co	Cr	Cu	Ga	La	Ni	Pb	Rb	S	Sr	Th	Y	Zn	Zr
Ba	1.00															
Ce	0.65	1.00														
Co	0.06	-0.04	1.00													
Cr	0.05	-0.14	0.12	1.00												
Cu	0.12	-0.07	0.62	-0.16	1.00											
Ga	0.61	0.69	0.05	0.34	-0.07	1.00										
La	0.61	0.95	-0.07	-0.07	-0.10	0.78	1.00									
Ni	0.30	0.09	0.22	0.70	-0.03	0.54	0.17	1.00								
Pb	-0.01	0.02	-0.05	-0.14	-0.06	-0.22	-0.13	-0.07	1.00							
Rb	0.88	0.68	-0.01	-0.05	0.03	0.62	0.67	0.21	-0.03	1.00						
S	0.02	-0.13	0.27	-0.05	0.30	-0.15	-0.25	0.00	0.23	-0.13	1.00					
Sr	-0.04	0.12	-0.09	0.13	-0.05	0.28	0.12	0.23	0.15	-0.11	-0.08	1.00				
Th	0.59	0.91	-0.07	-0.13	-0.15	0.60	0.86	0.12	0.00	0.64	-0.26	0.15	1.00			
Y	0.26	0.55	0.09	0.20	-0.08	0.68	0.59	0.28	-0.16	0.18	0.06	0.18	0.37	1.00		
Zn	0.22	0.13	0.76	0.25	0.61	0.33	0.14	0.42	-0.10	0.17	0.25	-0.05	0.05	0.24	1.00	
Zr	-0.15	0.02	-0.18	-0.42	-0.05	-0.20	0.00	-0.54	-0.04	-0.11	-0.07	-0.08	-0.02	0.14	-0.25	1.00
w	-0.12	-0.28	-0.31	-0.18	0.11	0.18	-0.38	-0.26	0.14	-0.21	0.49	0.16	-0.35	-0.28	-0.30	0.05
al-alk	-0.21	-0.18	-0.23	0.02	-0.04	-0.04	-0.10	-0.05	-0.27	-0.11	-0.06	0.07	-0.11	-0.24	-0.20	-0.06
al-alf	0.04	-0.05	-0.29	-0.12	-0.04	0.02	0.02	-0.11	-0.26	0.20	-0.07	-0.07	0.01	-0.30	-0.23	-0.03

Table 6.5b : Pearson correlation coefficients for the trace elements of the metasedimentary rocks of the Upper Erins Quartzites.

197

	SiO_2	TiO_2	Al_2O_3	Fe_2O_3	FeO	MnO	MgO	CaO	Na_2O	K_2O	P_2O_5	H_2O	CO_2
Ba	-0.55	0.27	0.58	0.42	0.48	0.43	0.22	-0.13	0.06	0.93	0.17	0.34	0.36
Ce	-0.59	0.33	0.71	0.26	0.45	0.30	0.33	0.05	0.32	0.67	0.37	0.51	0.17
Co	-0.19	0.12	0.06	0.08	0.31	0.09	0.14	0.00	0.07	-0.01	0.02	0.08	0.12
Cr	-0.41	0.33	0.34	0.21	0.45	0.45	0.54	0.26	0.10	-0.07	0.17	0.08	0.22
Cu	0.02	-0.13	-0.16	0.24	-0.03	-0.06	-0.17	-0.07	-0.15	0.03	-0.22	-0.02	0.13
Ga	-0.86	0.68	0.90	0.43	0.78	0.65	0.66	0.28	0.23	0.62	0.58	0.57	0.26
La	-0.64	0.40	0.79	0.19	0.55	0.44	0.43	0.09	0.32	0.66	0.45	0.56	0.15
Ni	-0.73	0.57	0.67	0.34	0.64	0.60	0.79	0.43	0.15	0.21	0.36	0.22	0.53
Pb	0.02	-0.14	-0.22	0.17	-0.09	-0.08	-0.05	0.12	-0.04	-0.03	-0.18	-0.08	0.35
Rb	-0.49	0.27	0.58	0.25	0.47	0.38	0.21	-0.21	-0.04	0.97	0.18	0.43	0.26
S	-0.06	-0.13	-0.15	0.60	-0.13	-0.20	-0.21	-0.05	-0.06	-0.05	-0.30	-0.12	0.14
Sr	-0.33	0.12	0.22	0.26	0.09	0.29	0.34	0.88	-0.14	-0.12	0.15	0.03	0.25
Th	-0.50	0.21	0.66	0.06	0.38	0.29	0.34	0.09	0.24	0.63	0.27	0.46	0.15
Y	-0.64	0.68	0.66	0.41	0.57	0.35	0.43	0.21	0.60	0.19	0.70	0.31	0.08
Zn	-0.47	0.31	0.29	0.34	0.57	0.36	0.39	0.06	0.00	0.18	0.12	0.43	0.23
Zr	0.39	-0.12	-0.31	-0.21	-0.31	-0.38	-0.32	-0.30	0.02	-0.12	-0.08	-0.09	-0.43
W	0.33	-0.34	-0.41	0.44	-0.54	-0.37	-0.49	0.00	-0.35	-0.16	-0.45	-0.29	-0.19
al-alk	0.19	-0.13	-0.09	-0.07	-0.16	-0.08	-0.06	0.04	-0.59	-0.15	-0.21	0.06	-0.25
al-alf	0.19	-0.17	-0.03	-0.07	-0.17	-0.09	-0.16	-0.16	-0.61	0.16	-0.26	0.10	-0.25

Table 6.5c : Pearson correlation coefficients for the majors against the traces of the metasedimentary rocks of the Upper Erins Quartzites.

rocks.

From the previous discussion it can be assumed that most of the Fe_2O_3 (total) is in biotite, chlorite, garnet; K_2O in muscovite and traces in feldspar; CaO in carbonate, epidote and garnet; MnO in garnet mainly and traces in calcite and chlorite; Na_2O in albite and Al_2O_3 distributed between these phases (excluding Fe-oxide, FeTi-oxides, and iron sulphides). Accordingly, correlations between traces, and between majors and traces, which are represented in Tables (6.5 b&c respectively) can be more easily studied.

The positive good correlation between Ba and Rb (0.88) and to a lesser extent between Ba and Ce (0.65) and Ba and Th (0.59) together with the positive correlations between Ba and Al_2O_3, K_2O; Ce and Al_2O_3, K_2O and H_2O; Rb and Al_2O_3 and K_2O; Th and Al_2O_3 and K_2O strengthen the connection between Al_2O_3, K_2O and H_2O which represent muscovite as discussed previously and suggest that these trace elements might be present in the muscovite. However, although of these elements, Ba and Rb are the most common elements to be hosted by muscovite, Th and Ce might also be present within the muscovite lattice (Atherton and Brotherton 1979). Also correlation between Th and Ce with the muscovite group of elements might probably result from the presence of carbon inclusions in muscovite (Willan 1983).

Applying this approach, the following conclusions can be added. Part of Ni and Ga is present in garnet; Cr and part of Ni and Ga in chlorite; Y, La and part of Ga in the micas; Sr in calcite only; and finally Co, Cu, Zn and part of iron in the sulphides.

Epidiorites

Correlations between majors, traces and between majors and traces for the epidiorites are documented in Tables (6.6a, b and c respectively) and a scatter plot of selective correlative element pairs is presented in Figure (6.4). Unlike the metasedimentary

rocks, the negative correlation between SiO_2 and the other major oxides is limited. SiO_2 correlates negatively with MnO, CaO, CO_2 and Fe_2O_3 only, and positively with TiO_2, Al_2O_3 and Na_2O. No significant negative correlation between SiO_2 and trace elements exist, except with Ni and with Y. This is not surprising because in the epidiorites the majority of the SiO_2 is present in the silicate minerals and only a minor quantity forms free quartz grains and quartz in veins.

By applying the same approach used previously for the metasedimentary rocks to relate correlative major oxides to mineralogy, good positive correlations between FeO, MgO and CaO; FeO, MnO, CaO and MgO; and Fe_2O_3 and CaO are expected because these are the groups that represent amphibole, garnet and epidote respectively which form the main constituents of the epidiorites (Sections 5.3.8 & 5.3.9). The results of the correlations between the major oxides (Table 6.6a) showed that this is not the case; the only significant correlations consistent with the mineralogy are the positive correlations between CaO and CO_2; Al_2O_3, K_2O and Na_2O Two groups of correlative major oxides can be distinguished from Table (6.6a); the first group includes SiO_2, Al_2O_3, MgO, Na_2O, K_2O, TiO_2 and P_2O_5 which correlate positively with each other and negatively with the second group. The second group includes CaO, MnO and CO_2 and Fe_2O_3.

Among the correlations between majors and traces (Table 6.6c) are highly significant positive correlations between Al_2O_3 and Ga, Zr, Y and Ni. Significant correlations between Al_2O_3 and Cr, Ce and Ba exist. Also Al_2O_3 correlates negatively with S. MgO and Fe_2O_3 do not show any significant correlations with trace elements. Nevertheless, Fe_2O_3 correlates weakly with Pb (0.43) and with Sr (0.45). MnO correlates negatively with the majority of the trace elements; highly significant negative correlation between MnO and Y and significant negative correlation between MnO and Ni, Zr, Cr, Ba and Ga exist. Also CaO correlates negatively with the majority of

200
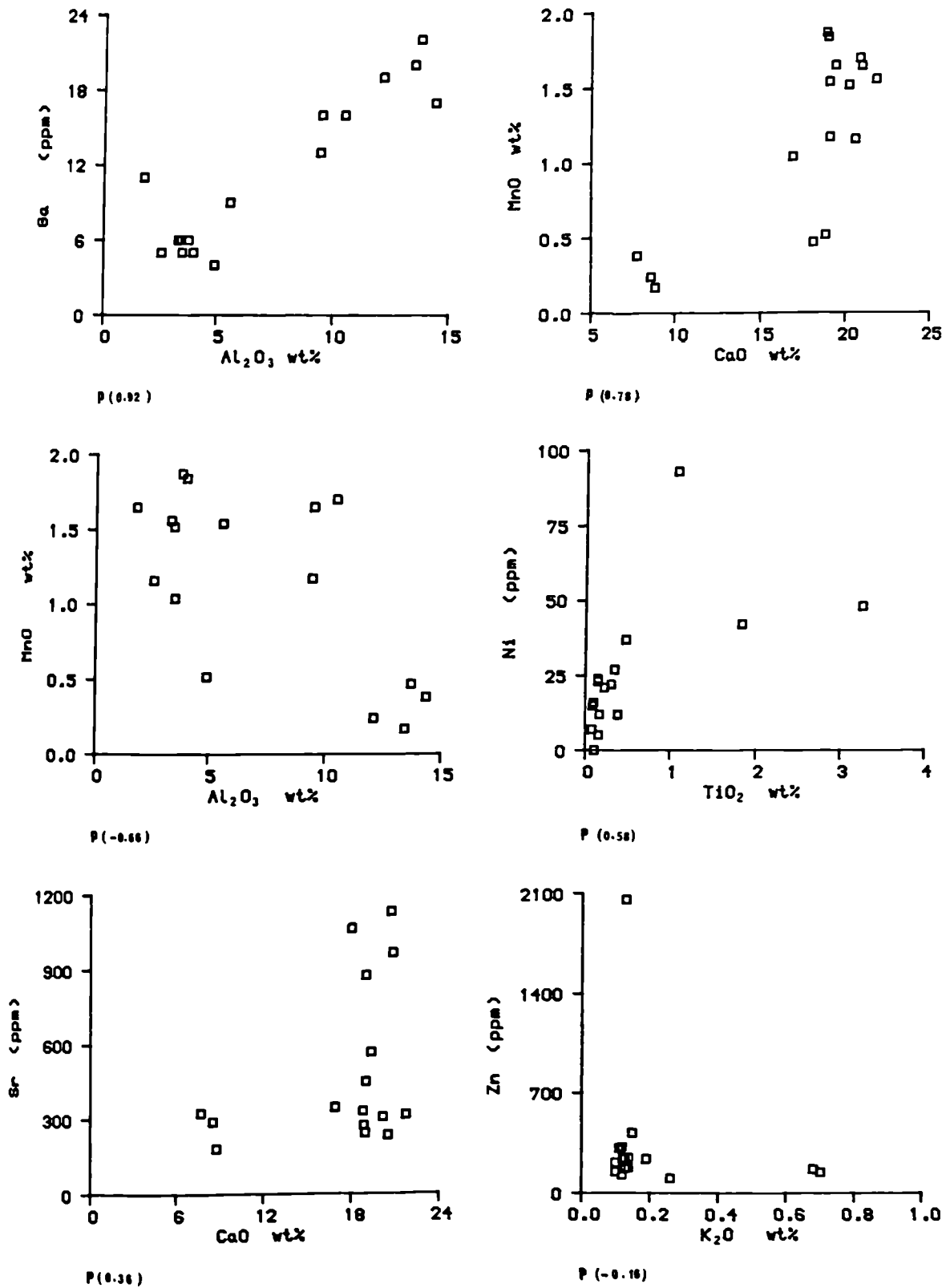
Fig. 6.4: Scatter plots of selective Pearson correlations between selected elements for the epidiorites.

	SiO_2	TiO_2	Al_2O_3	Fe_2O_3	FeO	MnO	MgO	CaO	Na_2O	K_2O	P_2O_5	H_2O	CO_2
SiO_2	1.00												
TiO_2	0.55	1.00											
Al_2O_3	0.53	0.64	1.00										
Fe_2O_3	-0.51	-0.14	0.10	1.00									
FeO	-0.01	0.26	-0.34	-0.42	1.00								
MnO	-0.75	-0.68	-0.66	0.29	0.17	1.00							
MgO	0.25	-0.20	-0.18	-0.49	0.43	0.06	1.00						
CaO	-0.68	-0.83	-0.66	0.30	-0.20	0.78	-0.06	1.00					
Na_2O	0.51	0.57	0.52	-0.19	0.13	-0.63	0.06	-0.88	1.00				
K_2O	0.46	0.81	0.59	-0.06	0.23	-0.62	-0.08	-0.85	0.67	1.00			
P_2O_5	0.35	0.92	0.52	-0.12	0.33	-0.49	-0.18	-0.66	0.33	0.76	1.00		
H_2O	0.33	0.39	0.60	-0.08	-0.19	-0.55	-0.07	-0.37	0.24	0.26	0.37	1.00	
CO_2	-0.62	-0.51	-0.69	0.04	-0.06	0.45	-0.33	0.49	-0.35	-0.42	-0.43	-0.37	1.00

Table 6.6a : Pearson correlation coefficients for the major oxides of the epidiorites of the Upper Erins Quartzites.

	Ba	Ce	Co	Cr	Cu	Ga	La	Ni	Pb	Rb	S	Sr	Th	Y	Zn	Zr
Ba	1.00															
Ce	0.30	1.00														
Co	0.44	0.06	1.00													
Cr	0.37	0.35	-0.07	1.00												
Cu	-0.26	-0.40	-0.25	-0.40	1.00											
Ga	0.47	0.67	0.13	0.54	-0.50	1.00										
La	0.04	0.85	-0.17	0.29	-0.37	0.49	1.00									
Ni	0.80	0.24	0.30	0.56	-0.22	0.60	-0.05	1.00								
Pb	0.11	0.45	-0.06	0.02	-0.25	0.26	0.26	0.14	1.00							
Rb	0.88	0.39	0.49	0.14	-0.26	0.48	0.19	0.50	0.07	1.00						
S	-0.30	-0.49	-0.04	-0.53	0.87	-0.60	-0.59	-0.25	-0.07	-0.30	1.00					
Sr	-0.20	0.62	-0.52	0.20	-0.19	0.50	0.63	-0.07	0.55	-0.13	-0.28	1.00				
Th	-0.16	0.77	-0.26	0.01	-0.34	0.36	0.78	-0.21	0.66	-0.03	-0.36	0.81	1.00			
Y	0.76	0.56	0.55	0.42	-0.37	0.79	0.35	0.66	0.08	0.80	-0.48	0.00	0.06	1.00		
Zn	-0.15	-0.08	0.05	-0.35	0.04	-0.32	-0.09	-0.29	-0.04	-0.18	0.10	-0.20	0.02	0.24	1.00	
Zr	0.69	0.74	0.40	0.39	-0.41	0.85	0.55	0.55	0.17	0.79	-0.53	0.29	0.32	0.93	-0.25	1.00

Table 6.6b : Pearson correlation coefficients for the trace elements of the epidiorites of the Upper Erins Quartzites.

203

	SiO$_2$	TiO$_2$	Al$_2$O$_3$	Fe$_2$O$_3$	FeO	MnO	MgO	CaO	Na$_2$O	K$_2$O	P$_2$O$_5$	H$_2$O	CO$_2$
Ba	0.46	0.79	0.58	-0.06	0.24	-0.56	-0.01	-0.81	0.59	0.99	0.78	0.24	-0.47
Ce	0.26	0.40	0.63	0.07	-0.35	-0.28	-0.14	-0.16	-0.17	0.23	0.50	0.58	-0.40
Co	0.26	0.65	0.23	-0.08	0.57	-0.30	-0.03	-0.52	0.33	0.48	0.52	0.21	-0.32
Cr	0.40	0.26	0.63	-0.22	-0.16	-0.59	0.24	-0.42	0.38	0.38	0.22	0.71	-0.45
Cu	-0.01	-0.28	-0.41	-0.10	-0.23	-0.04	-0.03	0.14	-0.10	-0.25	-0.38	-0.37	0.32
Ga	0.38	0.63	0.92	0.17	-0.34	-0.53	-0.23	-0.55	0.45	0.47	0.57	0.56	-0.59
La	0.16	0.21	0.40	0.05	-0.27	-0.07	-0.01	0.10	-0.38	-0.05	0.35	0.45	-0.38
Ni	0.57	0.58	0.76	-0.02	-0.04	-0.65	0.18	-0.83	0.76	0.82	0.44	0.33	-0.67
Pb	0.00	-0.05	0.27	0.43	-0.36	0.20	-0.23	0.13	-0.11	0.07	-0.05	0.16	-0.10
Rb	0.30	0.88	0.44	0.00	0.29	-0.46	-0.22	-0.66	0.39	0.86	0.93	0.20	-0.32
S	-0.22	-0.37	-0.53	0.05	-0.11	0.14	-0.03	0.22	-0.13	-0.28	-0.49	-0.49	0.46
Sr	-0.21	-0.19	0.38	0.45	-0.71	0.17	-0.32	0.36	-0.37	-0.26	-0.09	0.25	-0.14
Th	-0.07	-0.09	0.27	0.34	-0.51	0.23	-0.30	0.39	-0.56	-0.24	0.03	0.22	-0.10
Y	0.59	0.96	0.80	-0.10	0.08	-0.73	-0.17	-0.84	0.59	0.77	0.87	0.56	-0.60
Zn	-0.29	-0.21	-0.29	0.04	0.10	0.39	-0.06	0.15	-0.23	-0.16	-0.10	-0.13	0.48
Zr	0.46	0.87	0.82	0.04	-0.07	-0.59	-0.25	-0.63	0.33	0.66	0.87	0.52	-0.61

Table 6.6c : Pearson correlation coefficients for the majors against the traces of the epidiorites of the Upper Erins Quartzites.

the trace elements, except with Th (0.39) and with Sr (0.36) where a weak positive correlations exist. Highly significant negative correlations between CaO and Y, Ni and Ba and significant negative correlation between CaO and Rb, Zr, Ga and Co exist. Na_2O correlates positively with Ni, Y and Ba and negatively with Th. Highly significant positive correlations between K_2O and Ba, Rb, Ni and Y and significant positive correlation between K_2O and Zr exist. P_2O_5 and TiO_2 which represent minor oxides in the rock show highly significant positive correlations with Ba, Rb, Y and Zr on one hand and highly significant positive correlation with K_2O and to a lesser extent with Al_2O_3 on the other hand.

However, only a few of these correlations can be explained in terms of enrichment of certain traces in certain mineral phases while the majority represent unusual associations. An example is the good correlation between K_2O and Al_2O_3 on the one hand and between K_2O and Ba, Rb, Ni, Y, Zr, TiO_2 and P_2O_5 on the other hand. Of these traces, Ba, Rb and possibly Y, can substitute for K in the feldspar while the remainder does not and therefore their good positive correlations with K_2O and Al_2O_3 might be due to another reason as will be discussed below.

After careful examination of the above mentioned correlations between the majors and traces, the following picture emerges. The majority of the trace elements including Ba, Ce, Cr, Ga, Ni, Rb, Y and Zr correlate positively with Al_2O_3, K_2O, Na_2O, TiO_2 and P_2O_5 and with each other. The same trace element group shows negative correlation with CaO, MnO and CO_2. Trace elements that have weak negative correlations with Al_2O_3, K_2O, Na_2O, TiO_2 and P_2O_5 have weak positive correlations with CaO, MnO, Fe_2O_3 and CO_2. These include Cu, S, Sr, Th, Pb and Zn. This strengthens the connection between CaO, MnO, Fe_2O_3 and CO_2 as one group and between Al_2O_3, K_2O, Na_2O, TiO_2 and P_2O_5 as another group. Accordingly two general groups can be distinguished among the majors and traces. The first group includes SiO_2, Al_2O_3, K_2O, Na_2O, TiO_2, P_2O_5, Ba, Ce, Cr, Ga, Ni, Rb,

Y, and Zr. The second group includes CaO, MnO, Fe_2O_3, CO_2, Cu, S, Sr, Th, Pb, and Zn. FeO and MgO do not show any clear correlation and therefore it is tricky to decide to which group they must be added. It might be possible that these two oxides might represent another group.

As was mentioned earlier in Section (5.3.9), these rocks are highly altered and mineralised epidiorites and therefore the above correlations between the majors, traces and between the majors and traces might be explained in terms of the hydrothermal alteration that accompanied the mineralisation. The rocks with lowest Al_2O_3 values are the most altered and at the same time the most highly mineralised. This is reflected in the negative correlation between Al_2O_3 and S (-0.53) and the comparatively weaker negative correlations between Al_2O_3 and the base metals Cu and Zn (-0.41 and -0.29 respectively). During this hydrothermal alteration, probably SiO_2, Al_2O_3, K_2O, Na_2O, P_2O_5, TiO_2, Ba, Ce, Cr, Ga, Ni, Rb, Y and Zr were removed or diluted and CaO, MnO, Fe_2O_3, CO_2, Cu, S, Zn, Pb, Sr and Th were added. This will be discussed later in more detail in Section (6.7.2) when considering the average composition of the epidiorites.

6.4 THE CHEMICAL COMPOSITION OF THE METASEDIMENTARY ROCKS

The present chemistry of the metasedimentary rocks was controlled by many factors. These include, the original sediment composition which is controlled in turn by the environment of deposition, the subsequent diagenetic processes, the effect of the assumed hydrothermal activity, the effect of metamorphism and finally their weathering history.

Great chemical variations between the analysed metasedimentary rocks exist reflecting various lithologies. Gradation from orthoquartzite with up to 90.63 wt% SiO_2 to highly chloritic schist with 37.76 wt% SiO_2 exist. These host rocks are assumed to

206

represent metamorphosed argillaceous and arenaceous sediments which are referred to as, pelites and psammites respectively. Therefore a distinction between the two groups seems necessary to simplify their chemical study in order to find their premetamorphic precursors.

Pelites are very variable in composition and some authors consider a quartz content of 50 percent is roughly the upper limit of pelites (see Winkler 1976); others consider the SiO_2 content of pelites to range from 56.9 to 66.2 wt% and average 61.54 wt% (Shaw 1956). Psammites contain a higher amount of quartz (generally over 70 percent). Semi-pelites are intermediate in composition between pelites and psammites. Mohamad (1980) used Niggli si and al-alk as useful indicies to separate pelites from psammites of Glen Esk metasedimentary rocks. Before applying any of the above criteria on the studied rocks, a brief summary on the Niggli Numbers will be given in the next section.

6.4.1 Niggli Numbers

In many studies, Niggli values were used as useful criteria to study the nature of the sedimentary precursor of metasedimentary rocks, to examine the effect of metamorphism on the bulk chemistry of the rocks, to distinguish between pelites and psammites and to distinguish metamorphosed basic magmatic rocks from the metasedimentary rocks (see Wilson and Leake 1972 for the last usage).

For the purposes mentioned above, for each analysis Niggli Numbers were calculated (Tables 6.1 a&b and 6.2), following procedures described by Niggli (1954), Barth (1962) and Cox et al. (1979) and summarised in Appendix (A.6.13) together with the explanation of the terms used. Tests for normality were also performed on Niggli Numbers using the same criteria described earlier in Section (6.3.2). The results of tests are summarised in Tables (6.7 a&b). The results show that they are either normally or

log-normally distributed.

6.4.2 Pelitic and Psammitic Rocks

For the studied metasedimentary rocks and as a preliminary separation, distinction between pelitic and psammitic rocks is held using the SiO_2 wt% and the Niggli si values as limitations (pelite with < 70 wt% SiO_2 and si < 300). However, petrographic study of these rocks had showed that these rocks contain quartz veins and this ruled out the possibility of relying on the SiO_2 wt% and si alone as a criteria to distinguish between pelitic and psammitic lithologies. This can be overcome by using another supplement Niggli Number calculated irrespective of the silica content of the rocks.

The parameter si versus al-alk (Fig. 6.6) which was used successfully to distinguish pelite from psammite in Glen Esk (Mohamad 1980) is not applicable in the studied area. This might be due to allocating all the K_2O as K-feldspar, while petrographic study had showed that very rare K-feldspar is present but sericite $\pm$ muscovite are abundant in some of the pelitic and psammitic rocks. Accordingly the clay mineral fraction cannot be defined by the parameter al-alk. Instead the molecular number $Al_2O_3 - Na_2O$ rather than $Al_2O_3 - (Na_2O + K_2O)$ is a better index of the Al-bearing metamorphic minerals excluding feldspars. By doing so, no clear separation between pelitic and psammitic rocks is obtained (Fig. 6.6) probably because of the presence of various Al-bearing metamorphic minerals. An attempt was made to find another suitable Niggli Number or parameter to distinguish between the two groups. Among the calculated Niggli Numbers, Niggli fm together with si seems the most reliable criterion for this purpose. The plot of si versus fm (Fig. 6.6) separates the analysed metasedimentary rocks into two groups through two imaginary lines of si=300 and fm=40. The first group is characterised by low si (<300) and high fm (>40) values and represents pelites. The second group is characterised by

Niggli Numbers	Min.	Max.	Mean	St.Dev.	Coeffi. Variat.	Normality[1] test	Arithmetic data Skew.	Kurt.	Logarithmic data Skew.	Kurt.	Normality[2] test
si	97.60	1695.10	549.23	391.03	0.71	lognormal	0.90	3.12	-0.18	-1.13	normal
ti	0.60	5.40	1.95	0.81	0.41	normal	1.65	8.22	-1.10	4.80	not normal
p	0.00	0.70	0.15	0.12	0.80	lognormal	1.98	11.14	-----	-----	not normal
al	12.90	53.80	32.90	8.23	0.25	normal	0.49	3.14	-3.05	15.12	normal
fm	10.10	68.40	39.45	12.57	0.32	normal	0.13	2.63	-1.10	2.43	normal
c	0.10	41.90	11.50	10.66	0.93	lognormal	1.37	4.00	-1.08	2.52	normal
alk	1.30	40.60	16.17	9.36	0.58	lognormal	0.32	2.62	-2.10	5.33	normal
k	0.00	1.00	0.43	0.32	0.75	lognormal	0.60	2.12	-----	-----	normal
mg	0.00	0.60	0.34	0.17	0.51	lognormal	-0.15	2.30	-----	-----	normal
w	0.40	94.70	45.28	23.80	0.53	lognormal	0.37	2.28	-3.03	14.41	normal
al-alk	0.50	48.40	16.73	9.62	0.58	lognormal	1.02	4.45	-1.79	5.30	normal
al-alf	6.50	53.80	22.15	10.23	0.46	normal	0.95	3.97	-0.15	-1.10	normal

Table 6.7a : The results of the test for the normal distribution for the Niggli Numbers of the metasedimentary rocks of the Upper Erins Quartzites. 1: using the coefficient of variation ($C = \frac{\sigma}{\bar{x}}$ Koch and Link 1971), 2: using limited values of skewness and kurtosis (Jones 1969).

Niggli Numbers	Min.	Max.	Mean	St.Dev.	Coeffic. Variat.	Normality test [1]	Arithmetic data Skew.	Arithmetic data Kurt.	Logarithmic data Skew.	Logarithmic data Kurt.	Normality test [2]
si	85.20	135.10	104.23	16.04	0.15	normal	0.75	2.32	-1.25	3.67	normal
ti	0.10	6.60	1.06	1.72	1.61	lognormal	2.45	8.05	1.03	1.03	lognormal
p	0.00	0.40	0.07	0.10	1.48	lognormal	2.24	8.21	---	---	normal
al	2.50	20.50	10.00	6.55	0.65	lognormal	0.50	1.69	0.20	-0.83	normal
fm	34.20	53.90	45.45	5.85	0.13	normal	-0.79	2.54	-0.25	0.88	normal
c	20.20	56.10	42.40	10.36	0.24	normal	-1.14	3.12	-1.45	0.99	normal
alk	0.10	9.70	2.15	3.09	1.44	lognormal	1.67	4.36	0.53	-0.53	lognormal
k	0.00	1.00	0.44	0.39	0.89	lognormal	0.46	1.55	---	---	normal
mg	0.30	0.60	0.45	0.09	0.20	normal	0.00	2.33	---	---	normal
w	16.60	69.00	40.06	14.60	0.36	normal	0.32	2.30	-0.43	-0.21	normal
al-alk	0.50	17.90	7.92	5.10	0.64	lognormal	0.36	1.97	-0.10	-1.42	normal

Table 6.7b : The results of the test for the normal distribution for the Niggli Numbers of the epidiorites of the Upper Erins Quartzites. 1: using the coefficient of variation (C = $\frac{\sigma}{\bar{x}}$ -- Koch and Link 1971), 2: using limited values of skewness and kurtosis (Jones 1969).

high si (>300) and low fm (<40) values and represents psammites. Only Samples Number HMMI 9 and HMMI 13 are pelites with low fm (28.6 and 28.7 respectively) values possibly as a result of their high Na_2O content. Among the psammites, Samples Number HMM 17, HMMI 5, HMMI 77, HMMI 83 and HMMI 93, have high fm values and plotted outside the psammite field. The reason for this is probably because these rocks are either epidotised and/or calcareous.

6.4.3 The Average Chemical Composition of the Pelites

The average chemical composition of nineteen pelites from the studied area is presented in Table (6.8a) in comparison with similar rock averages. In Table (6.8b) the unmetamorphosed equivalent of these averages were recalculated in a volatile-free basis to remove the effect of dehydration and redox reactions caused by metamorphism in order to enable direct comparison of the element concentrations between the averages. The Meall Mòr pelites have slightly lower SiO_2, Al_2O, and K_2O values and higher Fe_2O, (total), MgO, CaO and Na_2O values than the world average pelite. The standard deviations of most of the oxides of Meall Mòr pelites are high reflecting their wide range of compositional variation.

Meall Mòr average pelite is close in its major oxide chemistry to shale analysis (Tables 6.8 a&b) but with higher Fe_2O, (total), MgO and Na_2O values and comparatively lower Al_2O, and K_2O values.

In comparison with other Dalradian pelites, Meall Mòr average pelite is poorer in Al_2O, and K_2O and richer in Fe_2O, (total), MgO, CaO and Na_2O.

The average trace element contents of the analysed pelites is presented in Table (6.8c) together with the average trace element abundances of similar rocks. It is clear that Meall Mòr average pelite is highly enriched in Cu, S and Ba and to a lesser extent in Cr, Zn and Zr and comparatively depleted in Ni, Rb, Pb, and Sr

Oxides	Meall Mór			1 average Shale	2 average Greywacke	3 World average Pelite	L.Dalradian 4 average Appin Group Slate	M.Dalradian 5 average Ben Eagach Schist		U.Dalradian 6 average Glen Esk Pelite	7 average S.Highland Group Slate
	Min.	Max.	Mean					a (background)	b (anomalous)		
SiO$_2$	37.76	68.60	54.61	58.10	66.70	61.54	59.64	60.33	60.08	57.58	58.91
TiO$_2$	0.29	2.51	0.88	n.g.	n.g.	0.82	0.72	0.79	0.81	1.24	1.14
Al$_2$O$_3$	8.47	22.74	14.57	15.40	13.50	16.95	21.26	18.69	19.95	18.97	17.07
Fe$_2$O$_3$	---	---	11.74	6.74	5.50	6.89	6.23	5.08	4.58	9.25	8.42
MnO	0.11	0.58	0.25	n.g.	n.g.	n.g.	0.01	0.09	0.06	0.12	0.12
MgO	1.28	8.21	4.14	2.44	2.10	2.52	3.15	3.21	2.44	2.49	2.71
CaO	0.05	10.10	3.00	3.11	2.50	1.76	1.00	1.74	0.72	1.04	0.91
Na$_2$O	0.00	5.08	2.62	1.30	2.90	1.84	1.22	1.46	1.13	1.90	2.22
K$_2$O	0.30	9.35	2.20	3.24	2.00	3.45	3.50	3.93	4.58	3.91	3.14
P$_2$O$_5$	0.03	0.28	0.11	n.g.	n.g.	n.g.	0.09	0.15	0.14	0.17	0.17
H$_2$O	0.11	3.75	2.25	2.63	1.20	3.47	n.g.	n.g.	n.g.	3.68	3.21
CO$_2$	0.42	6.29	2.11	5.00	3.00	1.67	n.g.	n.g.	n.g.	---	0.26

Table 6.8a : The average composition of the Upper Erins Quartzite pelites of Meall Mór in comparison with some analyses of similar rocks.

1 & 2 : after Pettijohn (1975); 3 : after Shaw (1956); 4 : average of 95 analyses (Hickman 1975); 5a : average of 67 analyses (Willan 1983); 5b : average of 39 analyses (Willan 1983); 6 : average of 44 analyses (Mohamad 1980); 7 : average of 6 analyses (Mather 1970).

Oxides	average Meall Mor Pelite	1	2	3	4	5a	5b	6	7
SiO_2	57.69	64.32	70.06	64.26	59.64	60.33	60.08	59.78	62.13
TiO_2	0.94	n.g.	n.g.	0.86	0.72	0.79	0.81	1.28	1.20
Al_2O_3	15.38	17.05	14.18	17.70	21.26	18.69	19.95	19.71	18.00
Fe_2O_3	12.19	7.46	5.78	7.19	6.23	5.08	4.58	9.61	8.88
MnO	0.67	n.g.	n.g.	n.g.	0.01	0.09	0.06	0.12	0.13
MgO	4.44	2.70	2.21	2.63	3.15	3.21	2.44	2.58	2.86
CaO	3.21	3.44	2.62	1.84	1.00	1.74	0.72	1.07	0.96
Na_2O	2.75	1.44	3.05	1.92	1.22	1.46	1.13	1.97	2.34
K_2O	2.35	3.59	2.10	3.60	3.50	3.93	4.58	4.06	3.31
P_2O_5	0.11	n.g.	n.g.	n.g.	0.09	0.15	0.14	0.18	0.18

* For names and references of analyses 1-7, see Table 6.8a.

Table 6.8b : Comparison of the average Meall Mor pelites with some analyses of similar rocks. All analyses are recalculated on volatile-free basis.

compared to the trace element contents of shale. Ce, Co and Ga are about comparable. Although a distinctly high Ba concentration hosted by muscovite had been observed among some of the analysed samples with high values reaching up to 7307 ppm, the absolute quantities of barium are still insufficient to form Ba-bearing silicates like in Aberfeldy for example.

6.4.4 The Average Chemical Composition of the Psammites

The average analysis of thirty psammitic rocks from the studied area is presented in Table (6.9a) and is compared with average analyses of unmetamorphosed sandstones and with some Dalradian quartzites and greywackes. The analyses are recalculated on a volatile-free basis (Table 6.9b). The results showed that Meall Mór average is comparable in chemical composition with arkose analysis more than with orthoquartzite. Nevertheless, individual analyses showed that similarity to both rock types, orthoquartzite and arkose exist. Specimens Number HMM 2, HMM 26, HMM 32 HMMI 73, HMMI 81 and HMMI 93, for example have chemical compositions approaching arkose. Specimens Number HMM 16, HMM 18, HMM 20, HMM 22, HMM 23 etc., although having lower SiO_2 wt% values for orthoquartzite, are comparable with orthoquartzite chemistry but with higher Al_2O_3, Fe_2O_3 (total) and CaO values reflecting their epidote content. Others are intermediate in composition between orthoquartzite and arkose. This suggests that the premetamorphic precursor to the Meall Mór psammitic rocks could be a mixture of quartz arenites, arkose and subarkose.

Comparison of the average analysis of Meall Mór psammites with other similar Dalradian rocks is presented in Table (6.9b). The information provided by this table can be summarised as follows:

(1) Comparison with the Middle Dalradian Carn Mairg Quartzite of Aberfeldy showed that Meall Mór is richer in Al_2O_3, Fe_2O_3 (total), MgO and CaO and slightly poorer in SiO_2. TiO_2, MnO, Na_2O, K_2O and

| | Meall Mór | | | | | | | | |
Elements	Min.	Max.	Mean	1	4	5a	5b	6	7
Ba	91	7307	1649	580	577	947	9254	834	1025
Ce	0	174	64	59	77	n.g	n.g	94	42
Co	6	46	21	19	n.g	52	48	30	45
Cr	46	368	140	90	126	127	138	101	162
Cu	3	7542	878	45	29	27	31	29	21
Ga	11	36	19	19	25	n.g	n.g	29	30
La	9	83	38	n.g	44	n.g	n.g	n.g	19
Ni	11	129	37	68	20	22	24	54	71
Pb	0	14	5	20	18	23	178	17	*300*
Rb	8	210	53	140	140	144	162	139	157
S	71	37283	9830	2400	1340	n.g	n.g	745	503
Sr	18	721	194	300	137	117	108	177	154
Th	0	29	8	n.g	15	14	18	n.g	10
Y	20	64	38	n.g	22	n.g	n.g	n.g	23
Zn	42	358	155	95	83	96	548	118	108
Zr	72	371	219	160	204	186	182	271	183

* 1; after Turekian and Wedepohl (1961); 7 : average of 8 analyses (Wilson and Leake 1972);
For analyses 4-6, see Table 6.8a.

Table 6.8c : The average trace element contents of Meall Mór pelites in comparison with average trace element abundances in similar rocks.

Table 6.9a : The average composition of the Upper Erins Quartzite psammite of Meall Mór in comparison with some analyses of similar rocks.

Oxides	Meall Mór Min.	Max.	Mean	1 average Ortho-Qzite	2 average Arkose	L. Dalradian 3 average Eilde Qzite	4 average Binnein Qzite	5 Appin Qzite	6 average Islay Qzite	M. Dalradian 7 average Carn Mairg Qzite	U. Dalradian 8 average Glen Esk psammite	9 average Tayvalich psammite	10 average SW-Highland greywacke
SiO_2	68.82	90.63	80.19	95.40	77.10	90.00	96.64	93.69	95.19	89.51	74.67	76.39	75.77
TiO_2	0.06	0.55	0.28	0.20	0.30	0.24	0.09	0.08	0.07	0.20	0.71	0.19	0.66
Al_2O_3	3.89	13.15	7.00	1.10	8.70	5.29	1.86	2.07	1.76	5.74	11.37	8.02	10.88
Fe_2O_3	---	---	3.77	0.60	2.30	0.67	0.36	0.87	0.46	0.87	4.30	2.73	3.92
MnO	0.00	0.16	0.06	n.g.	0.20	0.01	0.00	0.04	0.04	0.01	0.07	0.06	0.05
MgO	0.00	2.34	0.82	0.10	0.50	0.23	0.11	0.09	0.26	0.15	1.50	1.12	1.29
CaO	0.05	7.71	1.52	1.60	2.70	0.50	0.06	1.26	1.30	0.22	1.18	4.65	0.78
Na_2O	0.00	3.91	1.36	0.10	1.50	1.06	0.16	0.45	0.29	1.15	2.84	1.77	2.63
K_2O	0.22	4.07	1.22	0.20	2.80	1.96	0.71	1.38	0.59	1.54	2.11	1.25	2.44
P_2O_5	0.00	0.09	0.03	n.g.	0.00	0.04	0.01	n.g.	0.02	0.05	0.08	0.21	0.07
H_2O	0.10	2.63	1.17	n.g.	n.g.	n.g.	n.g.	0.16	0.31	n.g.	1.45	0.68	1.37
CO_2	0.06	5.14	1.14	n.g.	n.g.	n.g.	n.g.	0.08	0.05	n.g.	n.g.	3.00	n.g.

1 : average of 26 analyses (Pettijohn 1975); 2 :average of 32 analyses (Pettijohn 1975); 3 : average of 52 analyses (Hickman 1975); 4 : average of 54 analyses (Hickman 1975); 5 : one analysis (Sabine et al. 1969); 6 : average of two analyses (Sabine et al. 1969); 7 : average of 25 analyses (Willan 1983); 8 : average of 31 analyses (Mohamad 1980); 9 : average of 9 analyses (Wilson and Leake 1972); 10 : average of 8 analyses (Mather 1970).

Oxides	average Meall Mór psammite	1 average ortho-Qzite	2 average Arkose	L. Dalradian				M.Dalradian	U. Dalradian		
				3 average Eilde Qzite	4 average Binnein Qzite	5 Appin Qzite	6 average Islay Qzite	7 average Carn Mairg Qzite	8 average Glen Esk psammite	9 average Tayvallich psammite	10 average SW-Highland greywacke
SiO_2	83.31	96.07	80.23	90.00	96.64	93.76	95.21	89.51	75.55	79.25	77.16
TiO_2	0.29	0.02	0.31	0.24	0.09	0.08	0.07	0.20	0.72	0.20	0.67
Al_2O_3	7.27	1.11	9.05	5.29	1.86	2.07	1.76	5.74	11.51	8.32	11.08
Fe_2O_3	3.92	0.60	2.39	0.67	0.36	0.87	0.46	0.87	4.35	2.83	3.70
MnO	0.06	n.g.	0.21	0.01	0.00	0.04	0.04	0.03	0.07	0.06	0.05
MgO	0.85	0.10	0.52	0.23	0.11	0.09	0.26	0.15	1.52	1.16	1.31
CaO	1.58	1.61	2.81	0.50	0.06	1.26	1.30	0.22	1.19	4.82	0.79
Na_2O	1.41	0.10	1.56	1.06	0.16	0.45	0.29	1.15	2.87	1.84	2.68
K_2O	1.27	0.20	2.91	1.96	0.71	1.38	0.59	1.54	2.14	1.30	2.48
P_2O_5	0.03	n.g.	0.00	0.04	0.01	n.g.	0.02	0.05	0.08	0.22	0.07

For references of analyses 1-10, see Table 6.9a.

Table 6.9b : Comparison of the average Meall Mór psammite with some similar rocks. All the analyses are recalculated on volatile-free basis.

P_2O_5 are about comparable.

(2) The same observations are noticed when comparing with the Lower Dalradian quartzites, except that Meall Mór is richer in Na_2O.

(3) Comparison with the Upper Dalradian quartzites and greywackes showed that Meall Mór average is poorer in TiO_2, Al_2O_3, MgO, Na_2O and K_2O and richer in CaO compared to the SW-Highland greywackes. The Fe_2O_3 (total), MnO and P_2O_5 averages are comparable. Compared with Glen Esk psammite, Meall Mór is richer in SiO_2 only and poorer in Al_2O_3, Na_2O, K_2O, MgO and TiO_2. Total Fe_2O_3, MnO, CaO and P_2O_5 averages are comparable.

The variations in Fe_2O_3 (total), MgO, Na_2O and K_2O of the Upper Erins Quartzite psammites of Meall Mór is represented in a compositional triangle with the above mentioned rocks (Fig. 6.5). Meall Mór psammites span the fields of both the ferromagnesian potassic and the sodic sandstones. However, the average Meall Mór analysis together with the mean of the Southern Highlands Group psammites plot within the field of the ferromagnesian potassic sandstone illustrating their Fe and Mg rich nature in comparison with the potassic Carn Mairg Quartzite and Appin Group Quartzite which fall within the potassic sandstone field.

The average trace element contents of Meall Mór psammites is presented in Table (6.9c). With Cu, Pb, S and Zr as exceptions, trace element concentrations are lower in the psammites than in pelites. Meall Mór average psammite is highly enriched in Cu and S compared to all other Dalradian quartzites and psammites with higher Zn, Pb, Cr, Ce, Sr and Zr compared to the Lower Dalradian quartzites and higher Ba, Pb, Sr, Zn and Zr compared to the Middle Dalradian Carn Mairg Quartzite and higher Pb but lower Ni compared with similar Upper Dalradian rocks.

Fe$_2$O$_3$+MgO

Ferromagnesian
Potassic
Sandstone

Sodic
Sandstone

Potassic
Sandstone

Na$_2$O   **K$_2$O**

x Mean for Meall Mór psammites
□ Mean for Southern Highland Group grits
△ Mean for Carn Mairg Quartzite
▲ Mean for Appin Group Quartzite
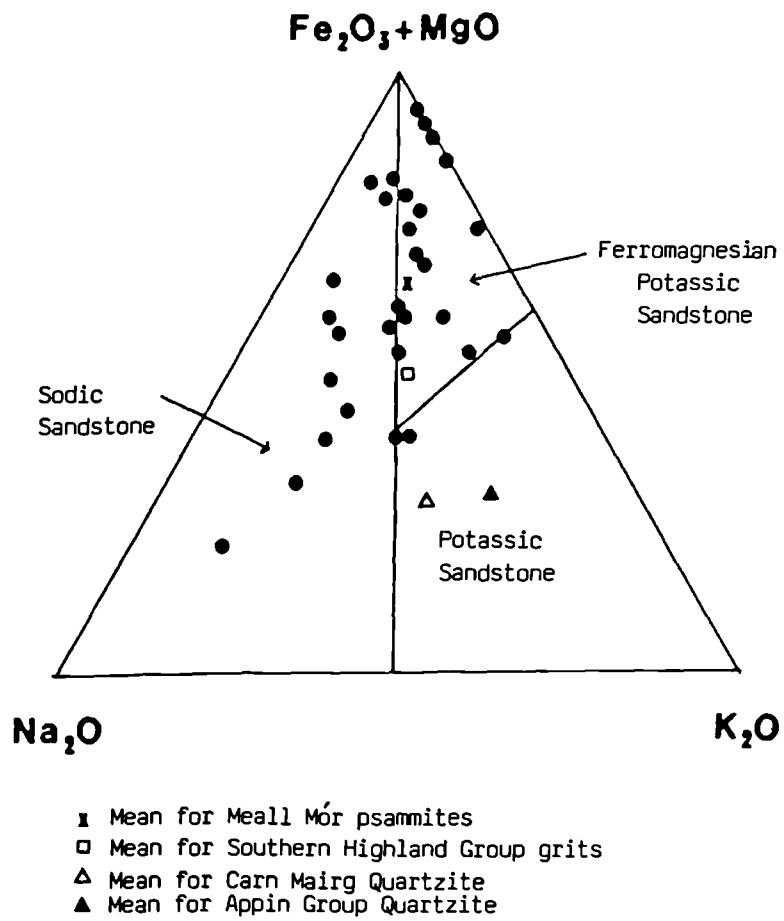
Fig. 6.5 : The compositional diagram for the Meall Mór
psammites illustrating their ferromagnesian
potassic nature.

219

Element	Meall Mór psammites			L. Dalradian				M.Dalradian	U.Dalradian	
				3	4	5	6	7	8	9
	Min	Max.	Mean	average Eilde Qzite	average Binnein Qzite	Appin Qzite	average Islay Qzite	average Carn Mairg Qzite	average Glen Esk psammite	average Tayvallich psammite
Ba	13	2499	568	477	194	1500	10	361	619	262
Ce	11	77	31	26	15	n.g	n.g	n.g	43	25
Co	0	177	11	n.g	n.g	10	10	115	n.g	14
Cr	14	268	74	n.g	n.g	10	10	n.g	59	78
Cu	0	12968	1396	n.g	n.g	180	10	4	12	13
Ga	2	17	8	n.g	n.g	10	10	n.g	15	7
La	0	45	18	10	7	n.g	n.g	n.g	n.g	9
Ni	0	26	7	n.g	n.g	10	10	n.g	26	21
Pb	0	695	40	n.g	n.g	n.g	n.g	7	13	20
Rb	9	143	31	50	25	n.g	n.g	n.g	68	29
S	93	61521	11402	n.g	n.g	n.g	n.g	n.g	n.g	231
Sr	14	678	128	46	11	90	10	19	174	97
Th	0	13	4	n.g	n.g	n.g	n.g	n.g	n.g	5
Y	6	28	14	11	6	n.g	n.g	n.g	n.g	7
Zn	4	466	70	9	6	n.g	n.g	10	59	25
Zr	136	423	264	339	184	179	20	190	266	190

* See Table 6.9a for references for analyses 3-9.

Table 6.9c : The average trace element contents of Meall Mór psammites in comparison with average trace element abundances in similar rocks.

220

6.4.5 Mineralogical Variations of the Metasedimentary Rocks in Relation to Increasing Quartz Content

It has been shown in Sections (6.4.3 & 6.4.4) that the studied metasedimentary rocks represent two groups, pelites and psammites, with some semipelitic rocks whose chemical compositions are compared to shale, arkose and orthoquartzite. In most studied metamorphosed arenaceous and argillaceous sedimentary rocks, increasing Niggli si value is accompanied by a systematic mineralogical variation indicating that metamorphism does not alter their chemical sedimentary trends. Of these variations are the main negative correlation between quartz and clay minerals; a positive correlation between quartz and feldspars; and a negative correlation between quartz and the clay mineral to feldspar ratio. Construction of a Pearson correlation matrix between the Niggli Numbers is presented in Table (6.10) and scatter plots of Niggli si against other Niggli Numbers are presented in Figure (6.6). The correlation results show that there is a positive correlation between si and al (0.64); a negative correlation between si and fm (-0.51); Niggli ti, p, c, k and alk do not correlate with si; Niggli w, al-alk and al-alf have a very weak positive correlation (<0.3); Niggli mg has a weak negative correlation (-0.32).

In summary, assuming that metamorphism of the studied rocks was isochemical, there are no systematic mineralogical variations nor any sedimentary compositional trends with increasing quartz content of the rocks. The unexpected mineralogical variations, especially the variation of the clay mineral contents, which instead of decreasing with increasing quartz content show either independent distribution with (si>400) or weak positive correlation with (si< 400). This together with the absence of any correlation between trace element concentrations and clay mineral contents (Section 6.4.6 and Fig. 6.7) suggest that bulk chemistry of these rocks and their present trace element distributions are not controlled by their sedimentary environment only and that any enrichment or

	si	ti	p	al	fm	c	alk	k	mg	w	al-alk	al-alf
si	1.00											
ti	0.02	1.00										
p	0.02	0.43	1.00									
al	0.64	0.25	0.17	1.00								
fm	-0.51	-0.11	-0.33	-0.61	1.00							
c	-0.10	-0.18	0.12	-0.41	-0.20	1.00						
alk	0.24	0.12	0.17	0.41	-0.58	-0.51	1.00					
k	0.08	-0.18	-0.33	0.03	0.19	0.16	-0.47	1.00				
mg	-0.32	0.09	0.13	-0.22	0.16	0.10	-0.13	-0.01	1.00			
w	0.31	-0.14	-0.15	0.17	-0.20	0.27	-0.19	0.19	-0.62	1.00		
al-alk	0.32	0.10	-0.01	0.46	0.05	0.14	-0.62	0.48	-0.05	0.33	1.00	
al-alf	0.33	0.11	-0.05	0.60	-0.04	-0.05	-0.41	0.60	-0.12	0.33	0.91	1.00

Table 6.10 : Pearson correlation coefficients between Niggli Numbers for the the metasedimentary rocks.

222
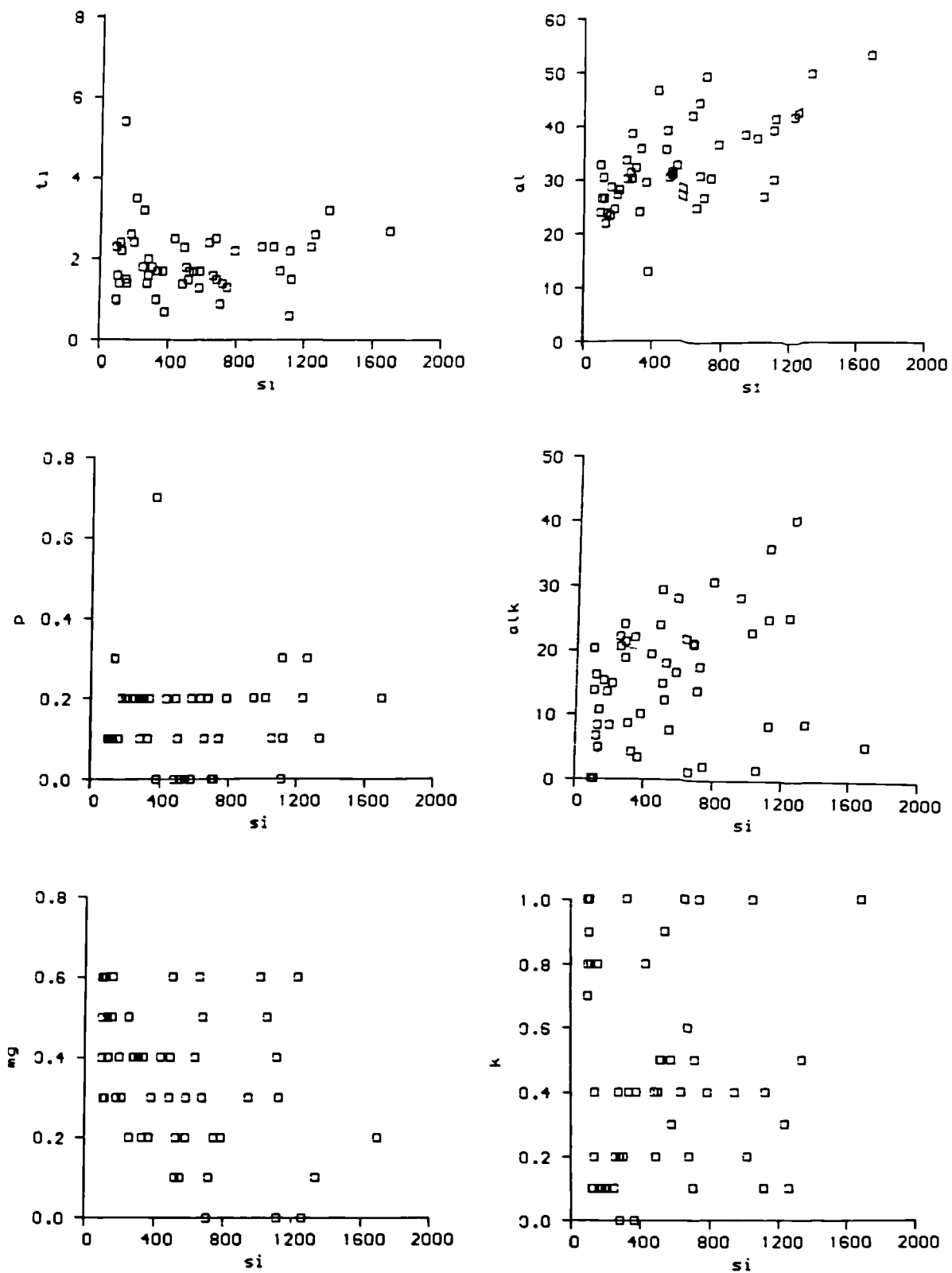
Fig. 6.6 : Plot of Niggli si against other Niggli Numbers.

Fig. 6.6 : Continued.

224
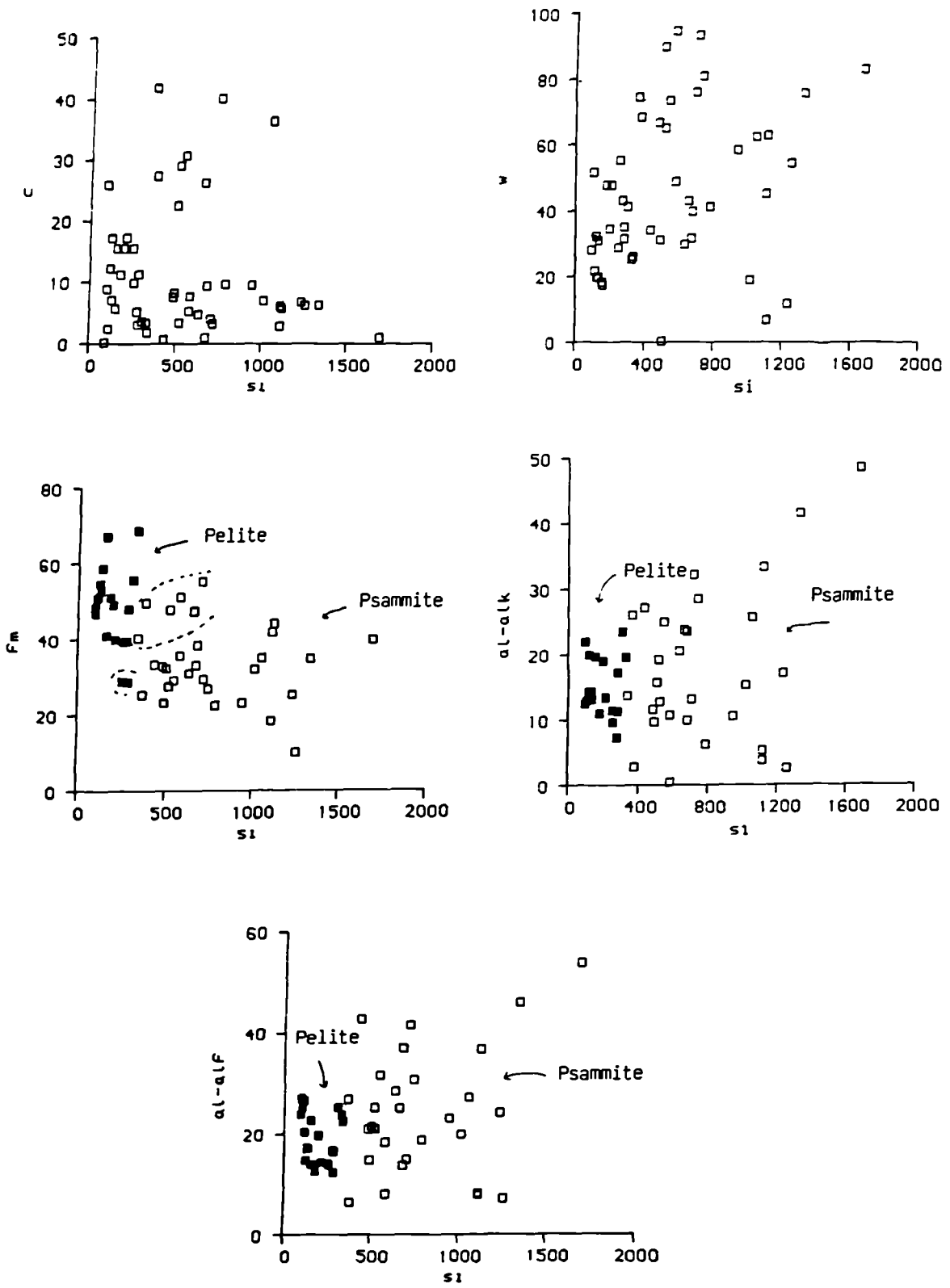
depletion in the concentrations might be explained, with other evidence by a premetamorphic alteration probably during the ore formation (Section 6.8).

6.4.6 Trace Element Variations in Relation to Clay Minerals

Assuming that Niggli al-alk is an approximate index to the clay mineral content, the distribution of the trace and minor elements in relation to increasing clay mineral content is presented in Figure (6.7) and Pearson correlation coefficients between al-alk and the trace elements are presented in Table (6.5 b) respectively. None of the trace elements show a clear correlation with increasing clay mineral contents. Instead, they all have the same pattern of distribution showing a gradual increase with increasing Niggli al-alk values with the maximum values corresponding to (10<al-alk<25) above which the element concentrations decrease with increasing clay mineral contents.

Before reaching any conclusion from the above observations, it is worth checking the validity of using Niggli al-alk as a clay mineral index for the studied rocks. Al_2O_3 is shared by clay minerals, micas, chlorite and feldspars; alkalis (Na_2O and K_2O) are largely contained in the feldspars. So the actual Al_2O_3 confined to the sheet minerals is the alumina left after allocation to feldspars (i.e. Niggli al-alk). However, in the studied rocks the so derived Niggli al-alk could give an underestimated value for the clay mineral contents. This is due to the fact that petrographic study in the previous chapter had revealed that potassium is contained in muscovitic micas and that only trace K-feldspar is recognised. To overcome this problem, only sodium is allocated to feldspars and accordingly the alumina present in the Al-bearing minerals except feldspar will be represented by Al-(Na) instead of Al-(Na+K). The new derived parameter is termed al-alf and corresponds to all Al-bearing minerals excluding feldspars.

225
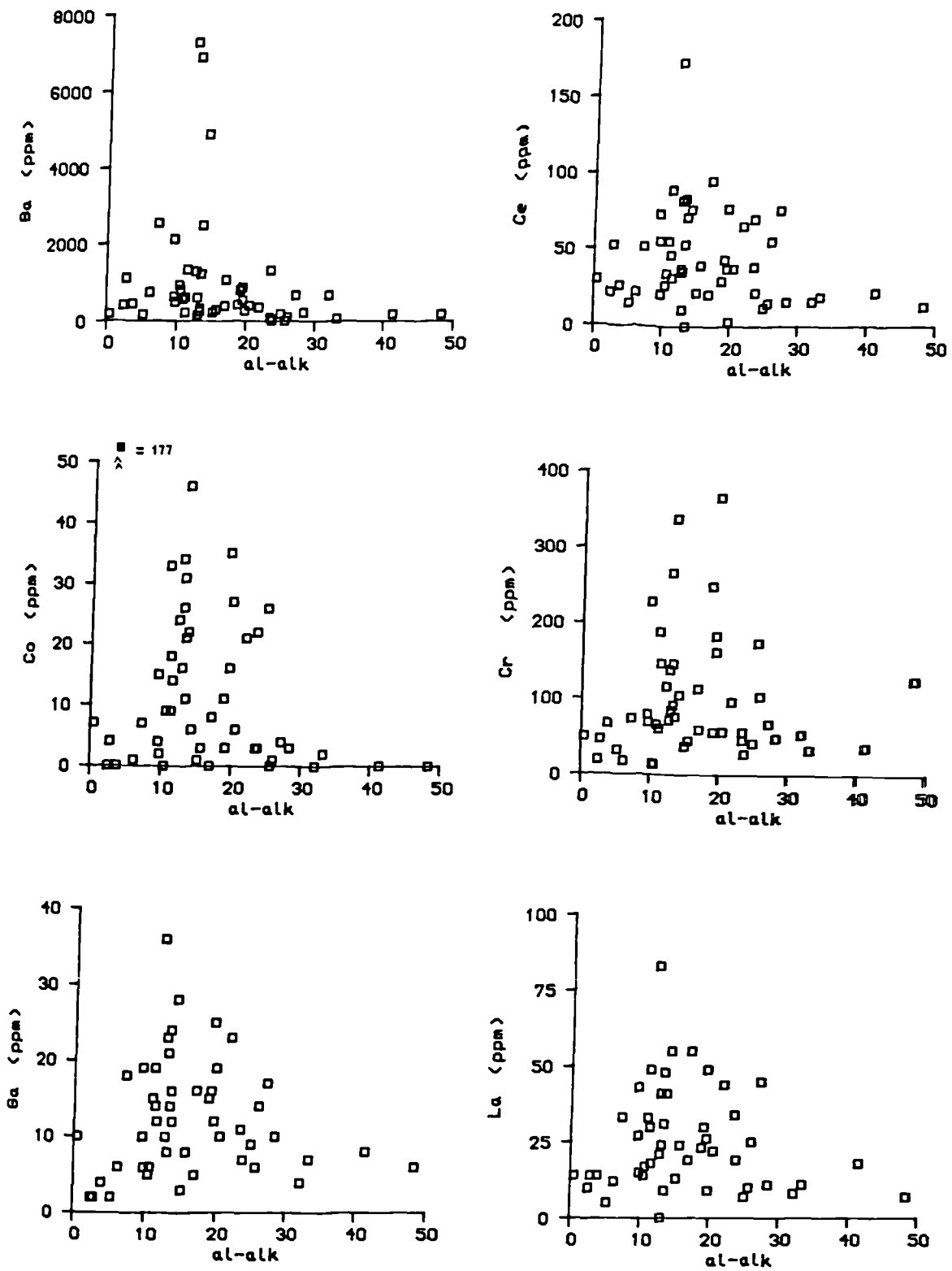
Fig. 6.7 : The distribution of trace elements and some minor
elements with increasing al-alk.

226
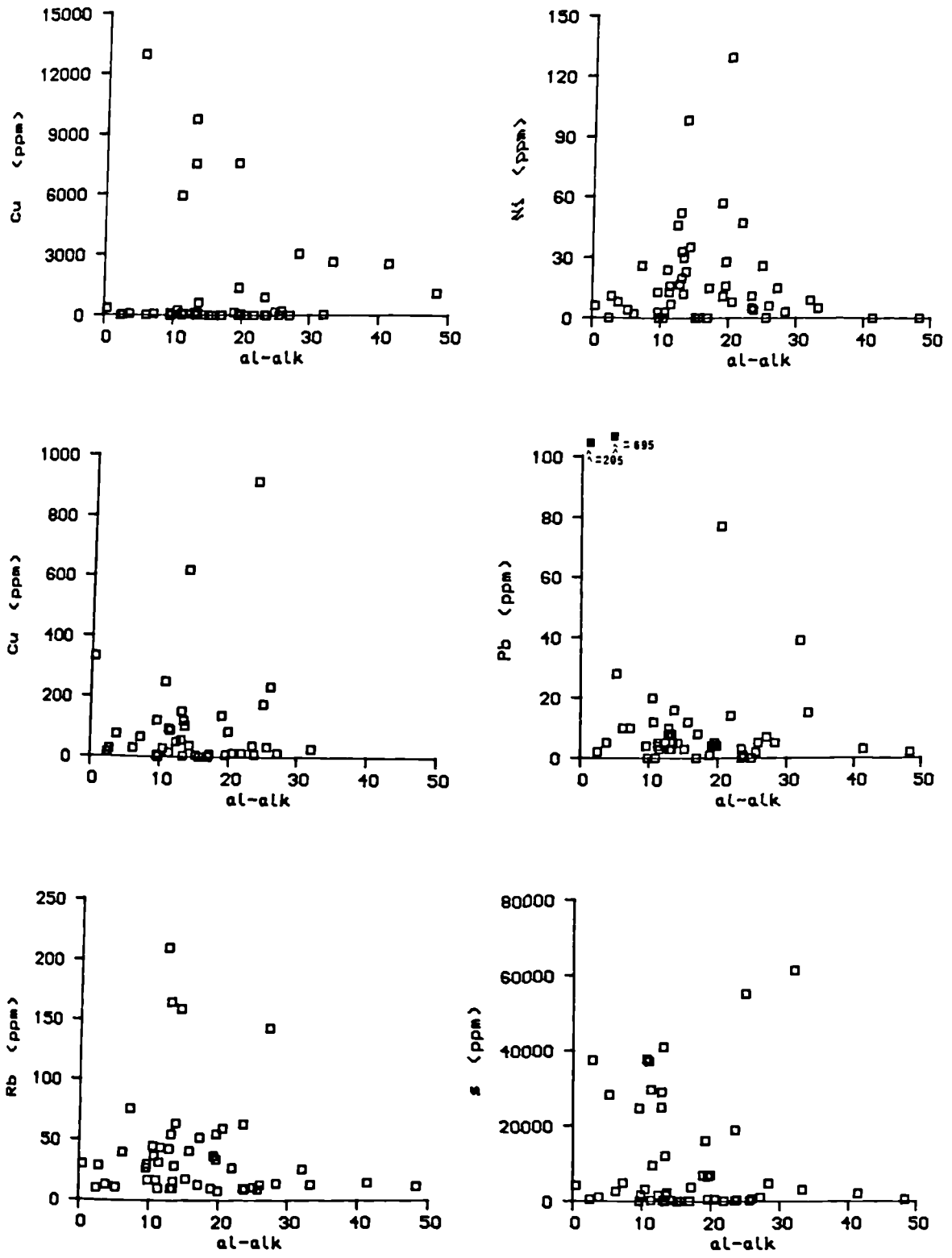
Fig. 6.7 : Continued.

Fig. 6.7 : Continued.

228
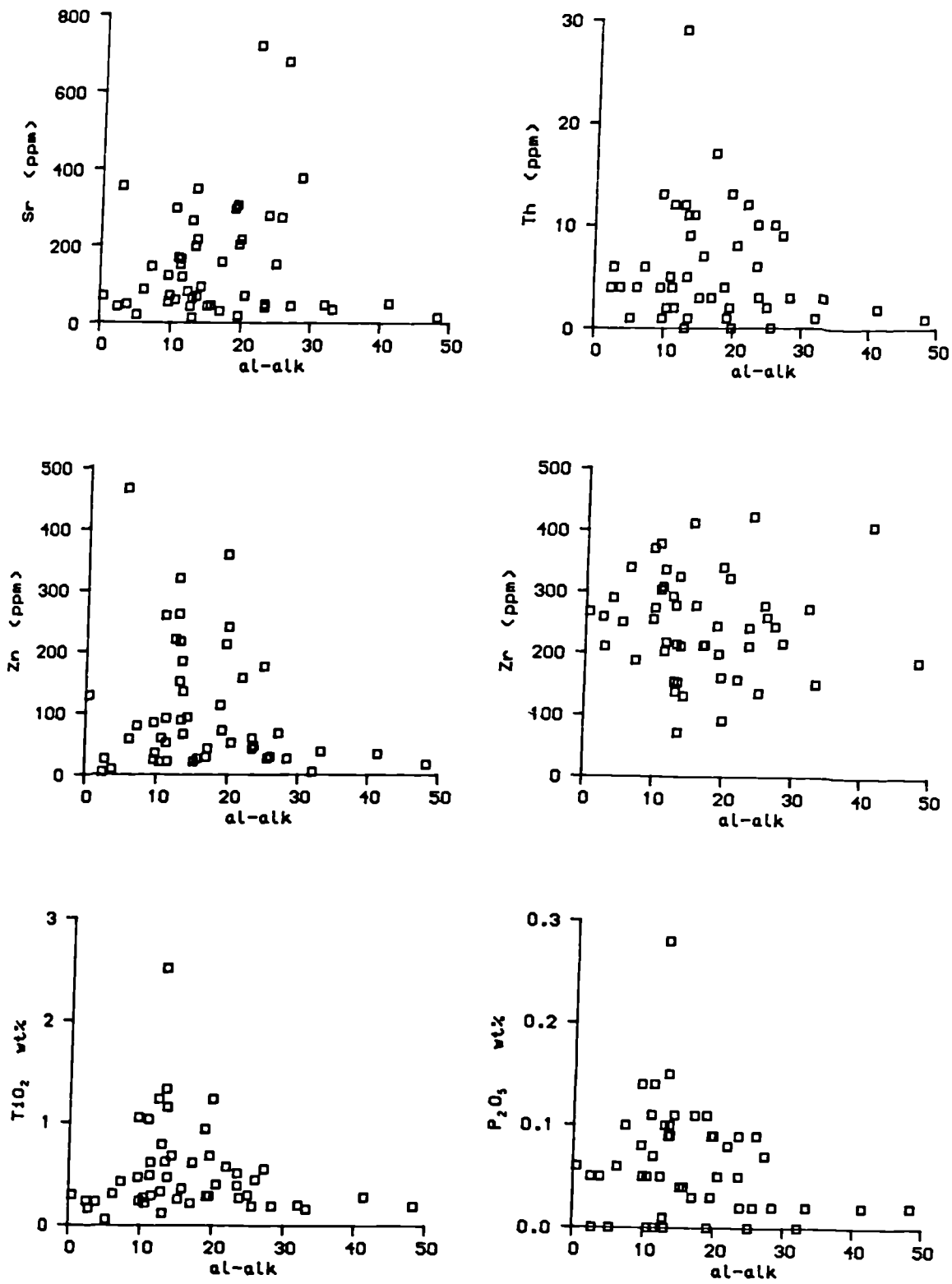
The relationships between the element concentrations and the derived al-alf parameter are presented in Figure (6.8). The information provided by the figure are: no clear correlation is present among all the examined elements; and they all show the same pattern of distribution similar to their distributions in Figure (6.7). This suggests that the underestimation of the clay mineral contents that resulted from applying Niggli al-alk as an index of clay mineral content is not the factor that influenced the distribution of the trace elements neither does it cause the absence of good correlations of trace elements with clay mineral content.

To summarise, no simple correlation between trace element variations with increasing al-alk nor with increasing al-alf exist. All the examined elements in Figures (6.7 & 6.8) have the same pattern of distribution and that is increase with increasing clay minerals up to (10<al-alk<25) and (10<al-alf<30). Above this the element concentrations decrease with increasing clay mineral contents. However, many studies have shown that the bulk chemical composition of the rock does not change when subjected to progressive regional metamorphism, except the decrease in H_2O, CO_2, Fe_2O, FeO ratio and probably some volatiles (Shaw 1956, Miyashiro and Seki 1958, Engel and Engel 1958 & 1962, Vallance 1960, Ronov et al. 1977 and Winkler 1976). There are also indications of a limited mobility of trace elements during regional metamorphism (Youth and Tan 1975, Ronov et al. 1977 and Senior and Leake 1978). Bearing this in mind, the information obtained from Figures (6.7 & 6.8) suggest that the observed trace element variations in the studied rocks must represent their premetamorphic trace element chemistry and that these variations cannot be related to increasing clay mineral content. Therefore such variations might be the result of the assumed hydrothermal alteration that accompained the ore formation. However, in case of Zr, TiO_2 and P_2O_5, the presence of detrital phases such as zircon, rutile,ilmenite and apatite might cause absence of correlation between these traces and the clay mineral content.
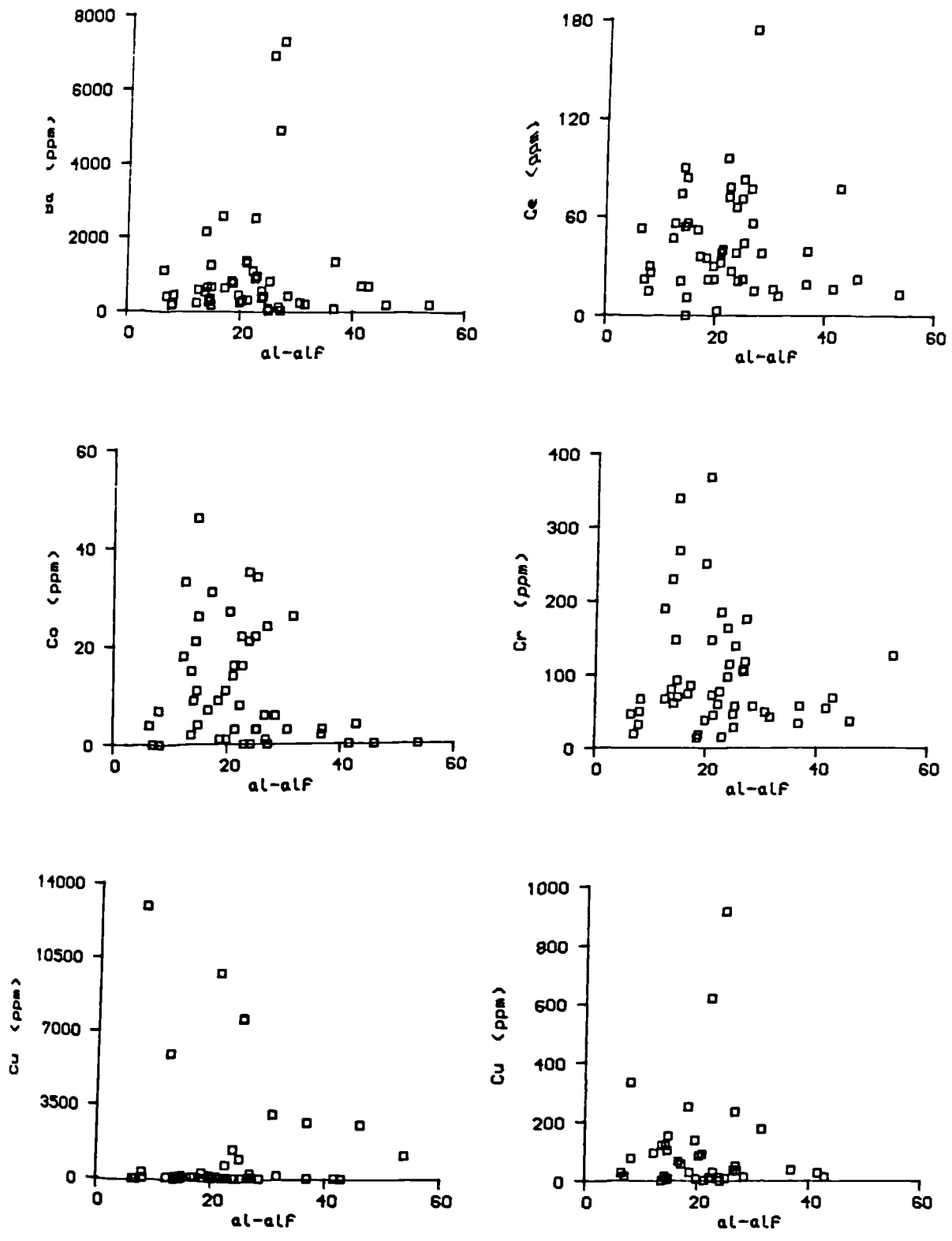
Fig. 6.8 : The distribution of trace and some minor elements with
increasing al-alf.

Fig. 6.8 : Continued.

231
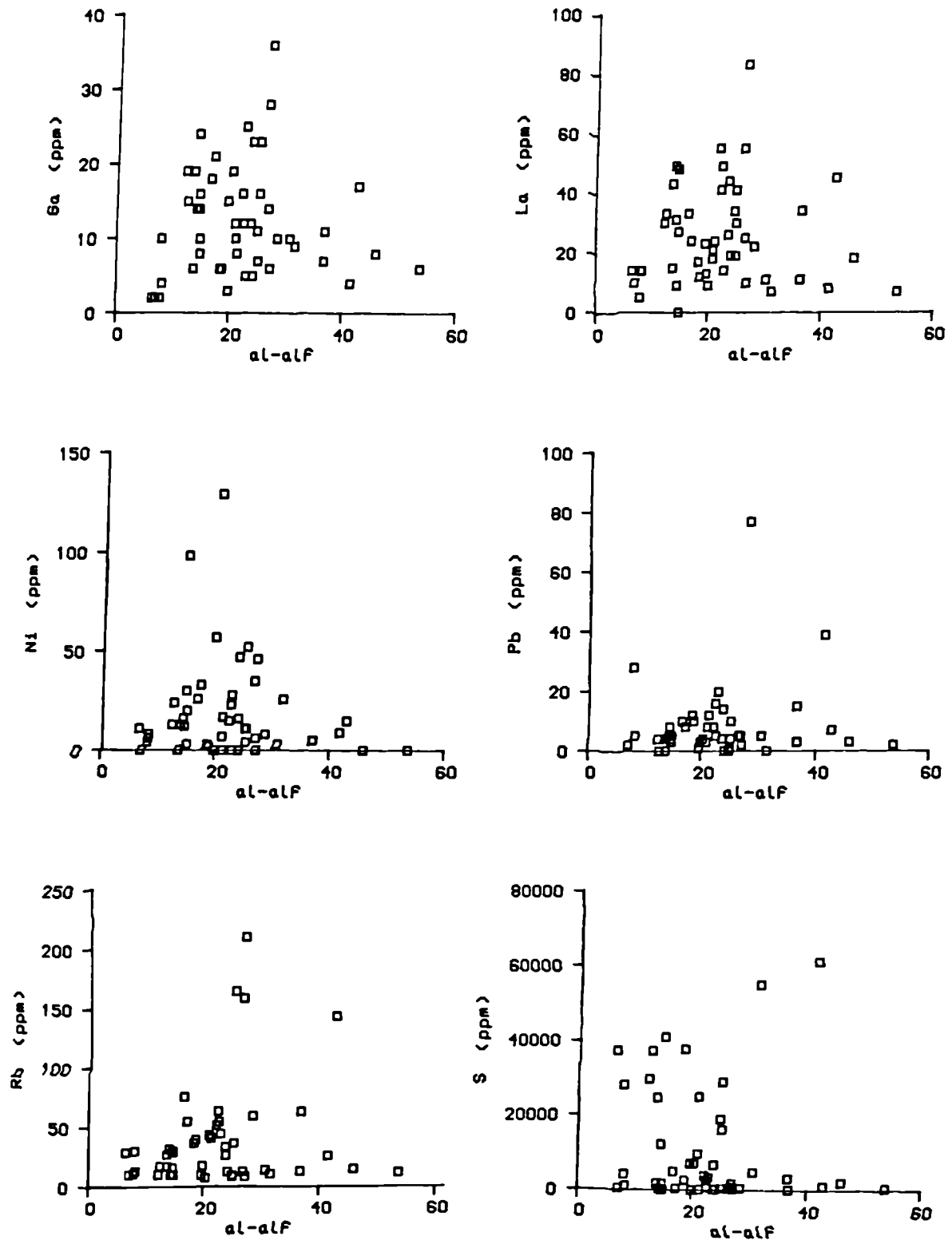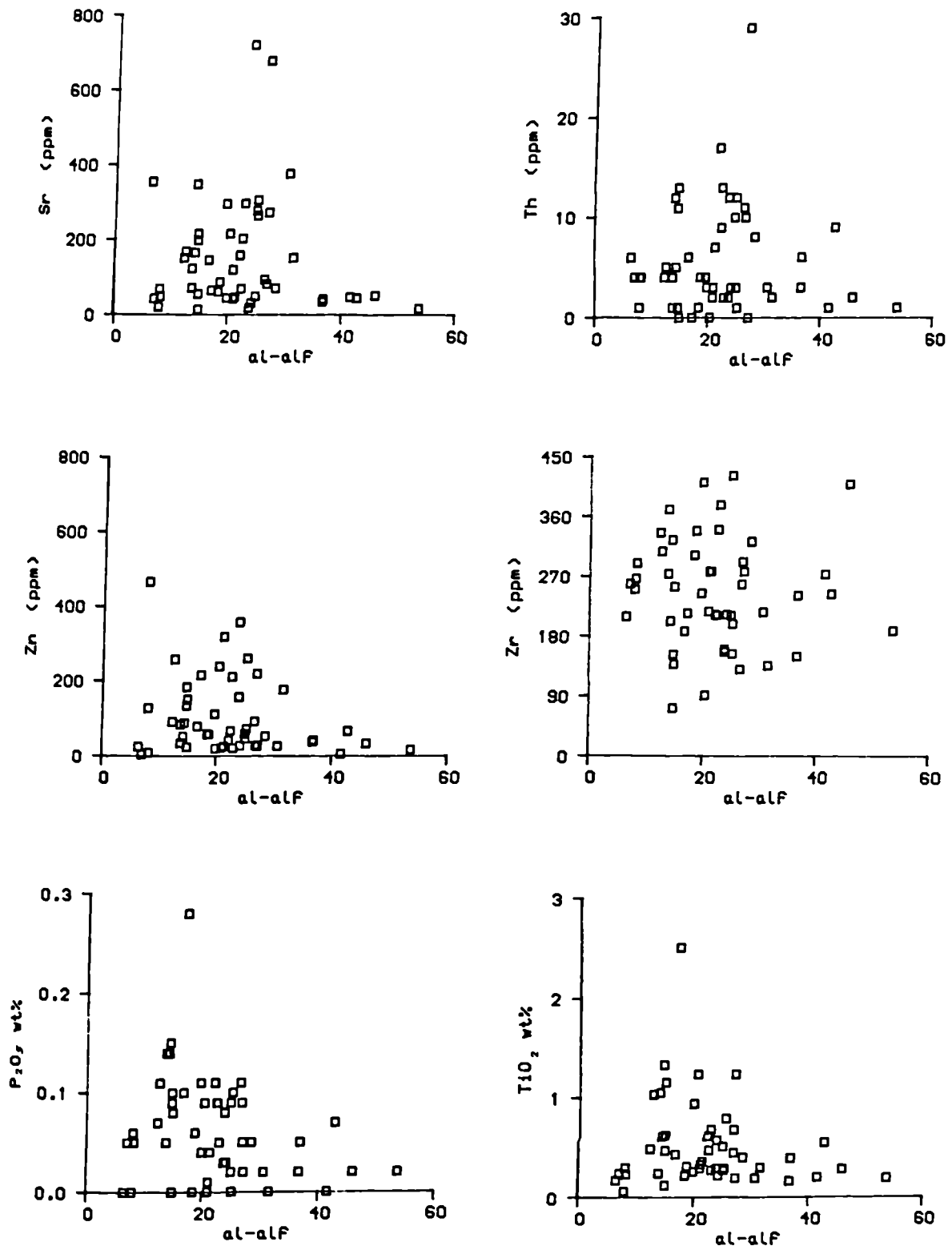
Fig. 6.8 : Continued.

6.5 THE DISTINCTION BETWEEN EPIDIORITES AND METASEDIMENTARY ROCKS USING NIGGLI NUMBERS

The host rocks to the copper mineralisation consist of epidiorites and metasedimentary rocks. Distinction between the two groups was very easy and clear for the majority of the specimens from the rock description and from their mineral assemblages under the microscope. However in the mine area the sampled boreholes contain several epidiorites interlayered with metasedimentary rocks and accordingly specimens taken at the contact between the two rock types are problematic. Bearing in mind that both rock types had undergone premetamorphic alteration, it was difficult for a few specimens, especially the highly chloritised and/or epidotised ones with few amphibole grains per slide, to decide to which rock type they belonged by using microscopic description only.

Detailed examination of the chemical characteristics of the metasedimentary rocks was discussed earlier in Section (6.4) and that of the epidiorites will be discussed in the next section. In this section an attempt is made to identify the rock type of the "problematic" rocks using distinctive chemical criteria and distinctive Niggli Numbers. Niggli Numbers are used here as criteria for this examination because these numbers were calculated independently of the rock SiO_2 wt% contents (except si) which eliminates the effect of SiO_2 mobilisation during metamorphism. Besides, Niggli Numbers were used successfully to distinguish Dalradian metamorphosed basic magmatic rocks from the Dalradian metasedimentary rocks in the Tayvallich Peninsula (Wilson and Leake 1972).

All the examined epidiorites give lower Niggli si (<150), al (<20), alk (<5) values and higher Niggli c (>40) values compared to the metasedimentary rocks with Niggli si usually (>150), al (>20), alk usually (>5) and c (<40) values. Also, the metasedimentary

on the whole have lower MnO values ranging between 0-0.58 and averaging 0.14 wt% and higher Ba content ranging between 13-7307 and averaging 987 compared to the epidiorites with MnO ranging between 0.17-1.87 and averaging 1.28 wt% and Ba ranging between 5-60 and averaging 26 ppm excluding Specimen Numbers HMMI 7, HMMI 27, HMMI 42 and HMMI 49.

On the plot of Niggli si against al (Fig. 6.9a), the epidiorites cluster in a narrow field occupying the lower left corner of the figure while the majority of the metasedimentary rocks fall in a separate field spanning the upper half of the figure. Also the al against c plot (Fig. 6.9b) separates the two rock types. However in both figures complete separation is not achieved. The pelitic rocks which represent chlorite and/or mica schist have low si values placing them at the edge of the metasedimentary field within a third distinct field on the si against al plot and these are clearly plotted within the metasedimentary field on the al against c plot (Fig. 6.9b). The same holds for the calcareous and epidotised metasedimentary rocks which are plotted higher on the al against c plot approaching the epidiorite field but these are clearly separated within the metasedimentary field on the si against al plot.

Having established that Niggli si, al and c together with the MnO and Ba contents of the rocks can give fairly good separation of the epidiorites from the metasedimentary rocks, it is now appropriate to look at the four petrographically indistinguishable (problematic) rocks after discussing the positions of the chloritic, epidotised and calcareous rocks on the two plots. The problematic rocks include Specimen Numbers HMMI 7, HMMI 27, HMMI 42 and HMMI 49.

On the plot of Niggli si against al the two fields, epidiorites and metasedimentary rocks, are separated by two lines; si~150 and al ~ 20. A third field is distinct in the figure including sixteen
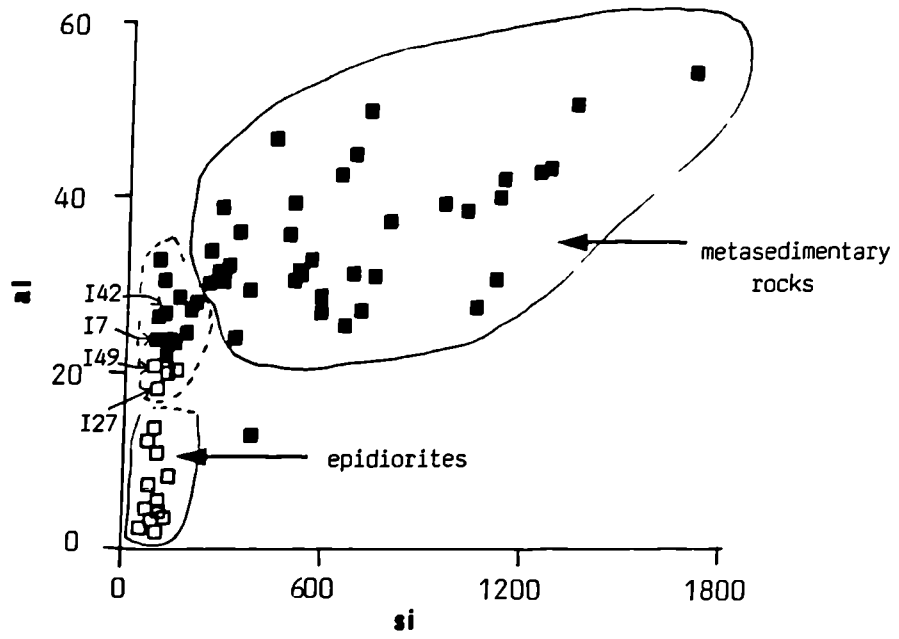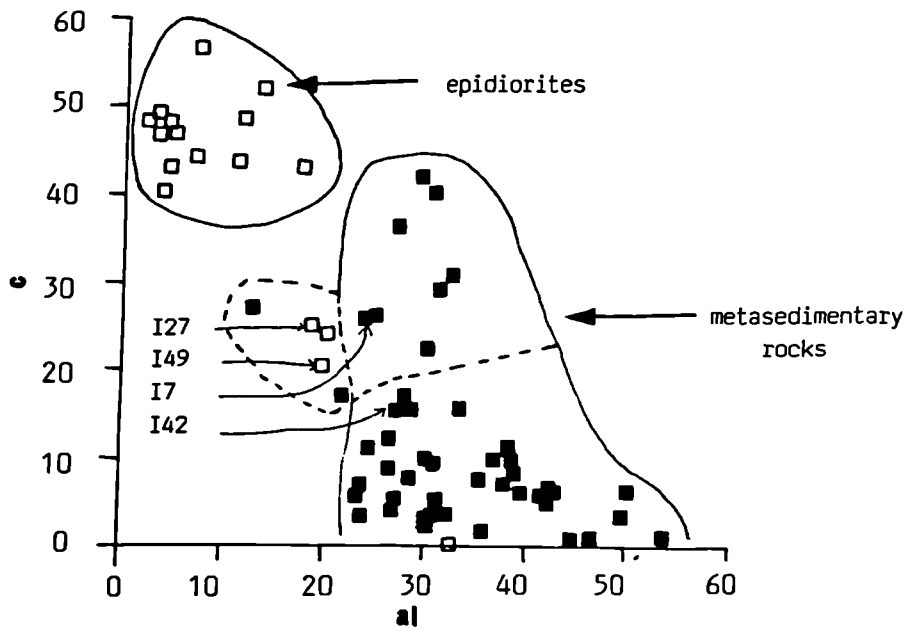
Fig. 6.9 : Plots of Niggli si against al (a) and Niggli al against c (b).

235

samples and the four problematic rocks are among them. However, Sample Numbers HMM 25, HMMI 10, HMMI 30, HMMI 38, HMMI 39, HMMI 43, HMMI 56, HMMI 66 and HMMI 69 are petrographically pelites but have relatively low si values for metasedimentary rocks and therefore plotted at the edge of the metasedimentary field. They have low MnO below 0.58 and high Ba greater than 300 ppm (Table 6.1a); features most compatible with the metasedimentary rocks. They also have high al>20 and low c<40 and therefore plotted clearly within the field of the metasedimentary rocks on the plot of al against c (Fig. 6.9b). Sample Number HMMI 77 is the only one with al<20 and is plotted outside the field of the metasedimentary rocks on the si against al plot. This is because it represents an epidotised psammitic rock and is plotted within the Ca-bearing metasedimentary rocks on the al against c plot. Sample Number HMMI 2, although plotted at the edge of the epidiorite field within the third field as a result of its relatively high al value is petrographically epidiorite. Also, it has high c (>40) and low Ba (23) content (Table 6.2) and is plotted clearly within the epidiorite field on the al against c plot. Also, Sample Number HMM 30 is petrographically epidiorite with low SiO_2 <50 wt%, low Niggli si <150 and low Ba values (51 ppm), features shared with the epidiorites. However, like Specimen HMMI 2, its Niggli al value (20.1) places it at the upper edge of the epidiorite field but unlike Specimen HMMI 2, its Niggli c value is not high enough to place it within the epidiorite field on the al against c plot and instead it plots within the metasedimentary field. This is because Specimen HMM 30 is weakly-altered epidiorite rock with very little epidote and carbonate and accordingly has a low c value for an epidiorite, the majority of which are altered rocks. The same approach can be used for the problematic petrographically indistinguishable Specimens, HMMI 27 and HMMI 49, that were plotted at the upper edge of the epidiorite field on the si against al plot and within the metasedimentary field on the al against c plot. Both Specimens have few characteristics shared with epidiorites; they have SiO_2<50 wt% and Niggli si less than 150. On the other hand they contain 0.24 & 0.38 wt% MnO and 355 & 316 ppm Ba values

respectively and give Niggli c values below 40, all characteristics shared with metasedimentary rocks. Again like Specimen HMM 30, these might be considered as unaltered epidiorite with relatively high Niggli al and low c. Their low MnO content probably resulted from their low- or free-garnet nature and their comparatively high Ba content is accompanied by their relatively high K_2O.

Specimen HMMI 42, which was petrographically indistinguishable has high silica for an epidiorite (59.37 wt% SiO_2) and high Niggli si value of 210; it has also al>20, c<40, MnO=0.17 wt% and Ba=251 ppm, all features that classify it as a pelitic rock. Its position near the edge of the metasedimentary rock field on the si against al plot results from its Niggli si value of 210 but its relatively low c groups it with the metasedimentary rock field on the al against c plot.

Specimen HMMI 7, which is petrographically indistinguishable, is also chemically inseparable. It falls within the intermediate field shared by both the epidiorites and metasedimentary rocks on the si against al plot and within the calcareous group of the metasedimentary rocks on the al against c plot. It might represent therefore either Ca-bearing metasedimentary rock or an unaltered epidiorite. However its low MnO content of 0.34 wt% and high Ba of 363 ppm together with its high Al_2O_3 (17.06 wt%) and H_2O (3.37) rule out the possibility of it being epidiorite and it is therefore classified as pelite (Table 6.1a).

6.6 THE SIGNIFICANCE OF THE PRESENCE OF AMPHIBOLE, ALBITE AND CHLORITE RICH METASEDIMENTARY ROCKS

In the previous section it was suggested that the highly chloritic schists represent metamorphosed pelitic rocks of Mg-rich origin. However, shale with high MgO content may be formed as a result of biotitic and chloritic detrital input. Also, Mg-rich shale might result from the presence of igneous material either as a

detrital or as coeval tuffaceous material within the sedimentary pile.

Both pelitic and psammitic units of the Upper Erins Quartzite in the studied area contain considerable amounts of albite. Texturally, the majority of the albite grains are untwinned and difficult to distinguished from quartz grains. Some of the albite grains are porphyroblasts, twinned and contain various inclusions (Section 5.4.2). This suggests that it can be either detrital or metamorphic in origin. However, Na-rich shales might result also from either precipitation in highly saline seawater or as the result of coeval tuffaceous material input during sedimentation.

Anyway, the presence of many epidiorite bodies that represent metamorphosed basic igneous rocks within the Upper Erins Quartzite Formation as a whole and their maximum development within the copper mineralisation zone in particular support the possibility of the Mg and Na enrichment being a result of coeval igneous activity. This does not rule out the possibility of the existence of some detrital chlorite, biotite and albite.

The mean TiO_2 content in the studied pelitic unit of the Upper Erins Quartzite is about 0.88 wt% reaching a maximum of 2.5 wt% and the mean Co:Ni ratio of the analysed pyrite is 12.5:1. These figures and the presence of amphibole-bearing metasedimentary rocks are further evidence to support the possibility of the existence of coeval tuffaceous material. In support of this is also the good correlation between MgO and Ni in the chloritic schists (Fig. 6.3).

6.7 THE CHEMICAL COMPOSITION OF THE EPIDIORITES

The results of the chemical analyses of sixteen epidiorite samples are presented in Table (6.2). The epidiorites are both chemically and mineralogically variable. The data presented in Table (6.4a) demonstrate the great variation in their major oxides

content. The analysed epidiorites have values ranging between; 38.19-49.92 wt% SiO_2; 1.82-14.39 wt% Al_2O_3; 3.08-9.23 wt% MgO; 2.15-8.62 wt% Fe_2O_3; 2.34-10.49 wt% FeO; 7.77-21.81 wt% CaO; 0-3.69 wt% Na_2O; 0.08-3.26 wt% TiO_2; 0.17-1.87 wt% MnO; 0.1-0.7 wt% K_2O; 0.79-4.22 wt% H_2O and 0.5-11.96 wt% CO_2. In addition great variations in their trace element contents also exist. Such variations cannot be related to variations in magmatic compositions nor to metamorphic redistribution. This together with the mineralogical evidence described earlier in Sections (5.3.8 & 5.3.9) suggests that some of the analysed epidiorite samples, especially the epidotised ones from the mine area, have been subjected to premetamorphic hydrothermal alteration either during their intrusion within the sediments or during the sulphide mineralisation.

Having established the possibility of the existence of hydrothermal alteration, it is necessary therefore to investigate the nature of such alteration in an attempt to relate it to the mineralisation. The first step is to find the composition of the premetamorphic igneous equivalent of the unaltered rocks and secondly to estimate the average composition of the altered ones in order to compare prealteration and altered compositions.

6.7.1 The Average Composition of the Unaltered to Weakly Altered Epidiorites

Representative analyses of the three unaltered (or very weakly altered) epidiorite specimens (HMM 30, HMMI 27 and HMMI 49) are presented in Table (6.2) and their average is reported in Table (6.11a). On the initial assumption that metamorphism has been isochemical except for the introduction of H_2O, CO_2 and some volatiles, the average composition of these unaltered rocks is recalculated on a volatile-free basis in order that likely premetamorphic composition of these rocks may be examined and compared with averages of some common similar igneous rocks from the literature. Meall Mór average shows a close similarity with

VAR. / ID.	Min.	Max.	Mean	St. Dev.
SiO_2	48.93	49.92	49.34	0.51
TiO_2	1.08	3.26	2.06	1.11
Al_2O_3	12.12	14.39	13.33	1.14
Fe_2O_3	3.80	5.38	4.70	0.81
FeO	6.54	9.92	8.23	1.69
MnO	0.17	0.38	0.26	0.11
MgO	4.56	7.14	5.84	1.29
CaO	7.77	8.81	8.39	0.55
Na_2O	1.43	3.69	2.87	1.25
K_2O	0.26	0.70	0.55	0.25
P_2O_5	0.10	0.39	0.21	0.16
H_2O	1.97	3.19	2.47	0.64
CO_2	0.50	1.06	0.75	0.29
Ba	51	355	240	165
Ce	17	50	28	19
Co	17	41	31	13
Cr	96	240	166	72
Cu	42	273	122	131
Ga	17	20	19	2
La	5	27	15	11
Ni	42	93	61	18
Pb	2	8	5	3
Rb	6	25	14	10
S	167	2306	1075	1105
Sr	183	325	266	74
Th	0	4	1	2
Y	28	54	41	13
Zn	103	169	140	34
Zr	120	286	186	88

Table 6.11a : The average chemical composition of the three unaltered to very weakly altered epidiorites of Meall Mór.

240

VAR. / ID.	Meall Mór (unaltered) Volatile-free	1	2	3	4	5	6
SiO_2	51.51	50.18	49.12	49.90	51.25	49.85	50.86
TiO_2	2.15	1.14	2.18	2.98	3.50	2.32	3.09
Al_2O_3	13.92	15.26	14.48	14.12	13.57	16.90	12.16
Fe_2O_3	4.91	2.86	1.94	2.92	1.75	1.74	1.91
FeO	8.59	8.05	11.13	11.55	13.72	11.16	13.34
MnO	0.27	0.19	0.23	0.27	0.35	0.30	0.22
MgO	6.10	6.78	6.47	5.74	3.11	3.93	4.91
CaO	8.76	9.24	10.82	8.69	8.10	8.72	8.97
Na_2O	3.00	2.56	2.54	2.69	1.94	3.45	2.75
K_2O	0.57	1.04	0.41	0.62	1.20	0.31	0.68
P_2O_5	0.22	0.27	0.28	0.52	0.63	0.27	0.41
H_2O	0.00	2.50	0.00	0.00	0.80	1.00	0.00
CO_2	0.00	0.18	0.00	0.00	0.00	0.00	0.00
QZ	0.16	1.40	0.81	2.88	8.52	----	2.99
ORC	2.90	6.12	2.46	3.67	8.34	1.67	4.04
AB	31.70	21.63	20.74	22.73	16.24	28.82	23.28
ZR	0.02	-----	----	-----	----	-----	-----
AN	21.47	27.12	24.42	24.59	23.91	30.02	18.86
DIOP	6.36	12.89	20.86	12.52	10.90	10.27	19.37
WO	6.49	-----	----	----	----	-----	----
HY	18.27	20.93	14.77	22.35	20.72	21.13	21.07
OL	5.93	----	6.36	----	----	----	1.54
MT	3.52	4.15	1.72	4.23	2.32	2.55	2.00
ILM	0.89	2.67	4.16	5.66	6.69	4.41	5.86
AP	0.28	0.63	0.66	1.23	1.34	0.34	0.97

1: typical dolerite composition (Cox et al. 1979), 2: average of seven Dalradian metadolerites, Perthshire recalculted on volatile-free basis (Graham and Bradbury 1981 , 3: average of 32 Scottish epidiorites (Van de kamp 1970), 4: garnet-biotite-clinozoisite-albite amphibolite (Wiseman 1934), 5: biotite-epidote-albite amphibolite (Wiseman 1934), 6: average of three ferrodolerites from the garnet isograd in South Knapadale (Graham 1976).

Table 6.11b : Comparison of the average chemical analysis of the unaltered to weakly altered epidiorites of Meall Mór with some averages of similar rocks.

241

dolerite except for somewhat lower SiO_2, Al_2O_3, MgO, CaO and K_2O and higher Fe_2O_3, MnO, TiO_2, and P_2O_5 (Table 6.11b).

The bulk chemical analyses allow calculation of the normative mineralogical composition "CIPW" of the analysed epidiorites. This was done using a computer program and following the procedure given by (Cox et al. 1979). The analysed epidiorites contain significant CO_2 which is normally allocated as calcite in calculating CIPW norms and accordingly removing some CaO that would otherwise form normative diopside or anorthite. This is because $CaCO_3$ is assumed to be additional to the original igneous composition. For the same reason the iron in pyrite, chalcopyrite and sphalerite has been subtracted. Also the ratio FeO/Fe_2O_3 has been arbitrarily adjusted to 10:1, a figure appropriate to dolerite and basalt composition (Cann 1971 and Graham and Bradbury 1981). The remaining oxides have been recalculated to 100 wt% total.

The results presented in Table (6.13) give unusual CIPW norms for the altered epidiorites which will be discussed later in the next section. However, the CIPW norms results for two of the three unaltered epidiorites suggest that they were originally close to pyroxene- hypersthene normative dolerite.

6.7.2 The Average Composition of the Altered Epidiorite

The second distinguished epidiorite group is characterised by low Al_2O_3 ranging between 1.82-5.59 wt% and averaging 3.67 wt% compared to normal dolerite with up to 15 wt% Al_2O_3 Only nine specimens that contain less than 6 wt% Al_2O_3 are grouped here as highly altered epidiorites and as mentioned earlier only three samples with Al_2O_3 >12 wt% were considered unaltered in the previous section. The remaining samples contain Al_2O_3 values ranging between 9-11 wt% and are considered to be moderately altered.

| VAR. / ID. | ------Meall Mór altered epidiorites---------- | | | | | | |
	Min.	Max.	Mean (a)	St.Dev.	Mean (b)	1	2
SiO_2	38.19	48.66	44.14	3.23	49.84	41.38	49.00
TiO_2	0.08	0.23	0.14	0.05	0.16	1.79	1.50
Al_2O_3	1.82	5.59	3.67	1.13	4.14	18.46	15.40
Fe_2O_3	2.15	8.59	4.98	2.16	5.62	7.83	4.10
FeO	4.21	10.49	7.77	1.86	8.77	5.92	6.10
MnO	0.52	1.87	1.41	0.43	1.59	0.19	0.18
MgO	3.38	9.23	6.48	1.77	7.32	5.15	5.30
CaO	16.92	21.81	19.42	1.36	21.92	18.03	7.60
Na_2O	0.00	1.27	0.38	0.44	0.43	0.57	4.10
K_2O	0.10	0.15	0.13	0.02	0.15	0.23	1.10
P_2O	0.00	0.09	0.04	0.03	0.05	0.00	0.30
H_2O	0.79	1.89	1.30	0.35	0.00	0.00	3.20
CO_2	0.64	11.96	7.85	4.26	0.00	0.45	2.40
Ba	5.00	34.00	19.00	12.00			
Ce	6.00	29.00	15.00	7.00			
Co	4.00	31.00	17.00	9.00			
Cr	28.00	204.00	63.00	54.00			
Cu	658.00	19718.00	5248.00	6605.00			
Ga	4.00	11.00	6.00	2.00			
La	3.00	20.00	13.00	6.00			
Ni	0.00	24.00	14.00	8.00			
Pb	0.00	11.00	5.00	4.00			
Rb	3.00	7.00	4.00	1.00			
S	1573.00	22710.00	9482.00	8198.00			
Sr	235.00	567.00	340.00	106.00			
Th	0.00	4.00	3.00	1.00			
Y	5.00	11.00	8.00	2.00			
Zn	127.00	2060.00	458.00	607.00			
Zr	0.00	0.00	0.00	0.00			

(a) mean for nine altered epidiorites of Meall Mór.

(b) the above mean recalculated on a volatile-free basis.

1 average of five SW-Highland epidotites (Graham 1976).

2 average of 225 rocks described as spilites (Vallance 1969).

Table 6.12 : Comparison and the average chemical composition of the studied altered epidiorites.

243

Table 6.13 : Results of the calculated CIPW norms for the analysed epidiorites.

VAR. / ID.	Altered Epidiorites											unaltered epidiorites	
	HMM 4	HMM 5	HMM 8	HMM 12	HMM 13	HMMI 16	HMMI 18	HMMI 21	HMM 9	HMM 10	HMMI 20	HMM 30	HMMI 49
SiO_2	42.39	38.19	45.81	48.66	42.62	43.30	48.46	43.88	43.53	40.64	43.11	49.92	48.93
TiO_2	0.16	0.09	0.15	0.17	0.08	0.10	0.15	0.23	0.39	0.31	0.35	1.84	1.08
Al_2O_3	3.79	3.46	3.50	4.92	1.82	3.32	4.00	5.59	10.49	9.50	9.44	13.49	14.39
Fe_2O_3	5.37	8.01	4.07	4.55	5.41	8.59	3.82	2.85	7.00	8.62	5.75	3.80	5.38
FeO	7.89	7.28	6.45	4.21	7.00	8.00	10.49	8.84	4.26	5.51	6.63	8.22	6.54
MnO	1.87	1.52	1.04	0.52	1.65	1.56	1.84	1.54	1.70	1.65	1.17	0.17	0.38
MgO	5.51	4.90	7.90	3.38	5.79	6.64	9.23	7.69	3.08	3.78	6.67	5.82	7.14
CaO	18.90	20.20	16.92	18.86	19.43	21.81	19.00	19.08	20.86	20.98	19.10	8.81	7.77
Na_2O	0.00	0.35	0.90	0.40	1.27	0.06	0.33	0.10	0.00	0.31	0.00	3.48	3.69
K_2O	0.13	0.15	0.12	0.14	0.10	0.13	0.11	0.13	0.14	0.12	0.19	0.26	0.68
P_2O_5	0.07	0.00	0.01	0.00	0.05	0.04	0.01	0.09	0.05	0.07	0.10	0.13	0.10
H_2O	1.61	1.12	0.79	1.89	1.37	1.22	0.98	1.12	1.48	1.28	4.22	3.19	1.97
CO_2	11.96	11.74	5.85	9.17	11.53	2.77	0.64	7.86	6.52	3.02	2.92	0.50	1.06
Total	100.60	99.86	98.05	100.03	99.15	97.91	100.29	99.45	99.81	96.87	100.01	99.74	99.48
QZ	25.00	18.66	16.25	36.01	17.97	0.00	0.67	5.99	12.72	0.00	2.19	0.32	0.00
ORC	1.08	1.33	0.93	1.14	0.84	0.85	0.67	0.91	0.99	0.81	1.26	1.60	4.22
AB	0.00	4.44	9.95	4.64	12.49	0.56	2.88	1.00	0.00	3.00	0.00	30.61	32.79
ZR	0.01	0.01	0.01	0.01	0.01	0.01	0.01	0.01	0.02	0.02	0.02	0.02	0.02
AN	13.95	11.12	6.74	15.38	2.24	9.27	9.38	17.00	33.74	27.65	28.17	21.22	21.73
DIOP	4.73	11.90	21.50	13.94	13.91	38.25	34.19	26.60	17.58	29.86	23.37	8.23	4.49
WO	4.68	11.77	22.84	14.08	13.88	37.80	34.87	27.24	16.92	28.86	23.59	8.37	4.61
HYP	44.64	34.50	17.52	10.73	34.40	5.98	12.74	16.89	13.32	3.53	16.54	22.15	14.39
OLV	0.00	0.00	0.00	0.00	0.00	1.91	0.00	0.00	0.00	0.99	0.00	0.00	11.85
MT	5.28	6.04	3.87	3.64	3.72	5.08	4.30	3.63	3.70	4.45	3.87	3.54	3.50
ILM	0.43	0.26	0.37	0.44	0.20	0.21	0.29	0.52	0.89	0.67	0.74	3.63	2.15
AP	0.23	0.00	0.03	0.00	0.16	0.10	0.02	0.25	0.14	0.19	0.26	0.31	0.24

Representative individual analyses of these rocks are given in Table (6.2) and their average major oxide composition is presented in Table (6.12) while their calculated CIPW norms are summarised in Table (6.13). It is clear from Tables (6.11 a&b and 6.12) that the major oxide compositions of these rocks are far too different to be considered as normal metamorphosed dolerite equivalents. Comparison of major and trace element compositions of these rocks with their metamorphosed unaltered equivalent (Section 6.7.1) reveal that these rocks had much lower values of Al_2O_3, SiO_2, MgO, TiO_2, Na_2O and K_2O and higher MnO, CaO, Fe_2O_3 and CO_2 values.

The results of the calculated CIPW norms for these rocks are quite different from the common normative dolerite (Table 6.13) and again suggest that these rocks have suffered alteration before they were subjected to metamorphism. During this alteration their composition is modified as a result of loss, gain, dilution and redistribution of their components. The normative anorthite is remarkably low being between 0-17 compared to the doleritic normative anorthite of 23-30. This is so despite the high CaO content of these rocks with a minimum value of 16.92 wt% CaO which is in itself twice the average CaO content found in typical dolerite (9.24 wt% CaO, Table 6.11b). This indicates that the normative anorthite is limited by the available alumina which was diluted during this alteration and not by the available lime. Likewise the normative albite is also very low as a result of low alumina and alkali values. Excess free silica or up to 36 CIPW norm is probably produced from this hydrothermal alteration and was redeposited into quartz veins.

6.7.3 Relationship with Spilites

Spilite is a term used for a group of igneous rocks both extrusive and intrusive that are characterised chemically by high soda concentration coupled with variable depletion in CaO. Despite the controversy between the various studies that have discussed the

245

basis of recognition and of genesis of spilites (e.g. Amstutz 1968, Smith 1968, Cann 1969, Vallance 1969 and Hughes 1972), they all emphasise the redistribution of chemical components during reaction with hydrous fluid probably under hydrothermal or burial metamorphism. This reaction involves the replacement of calcic plagioclase by albite and the fixation of the librated CaO as epidote and/or calcite such that the modal plagioclase remains essentially constant. Also, Smith (1968) has demonstrated a chemical, mineralogical and genetic relationship between sodic spilite and associated epidotites (epidote-rich rocks). Graham (1976) concluded a spilitic affinity for some of the SW-Highland metabasites and epidotites of both extrusive and intrusive type.

Chemical analyses of the studied epidiorites show that nonepidotised epidiorites have CaO and Na_2O wt%, normative albite and normative anorthite which are comparable with doleritic composition with neither CaO loss nor Na_2O gain. On the other hand, the epidotised rocks are enriched with CaO and other oxides and elements and depleted in Al_2O_3, Na_2O, K_2O and other oxides (Section 6.7.2) and associated wih a large loss in the amount of the normative plagioclase (Table 6.13). This together with the high copper enrichment within these epidiorites and chloritisation, epidotisation and sericitisation of the associated metasedimentary rocks suggests that epidotisation of some of the studied epidiorites might not be the result of spilitic alteration but it might be the result of the interaction between these rocks (both epidiorites and metasedimentary) and a hydrothermal fluid generated from a local hydrothermal cell driven by the intruded sills (see Chapter Eight).

6.8 HYDROTHERMAL ALTERATION

Local epidotisation, carbonation, chloritisation, sericitisation and to a lesser extent spessartisation that characterise the host rocks of the Abhainn Srathain copper mineralisation is used here as mineralogical evidence of the

presence of a premetamorphic hydrothermal alteration. This is supported by the observed chemical evidence that will be discussed below.

In case of the epidiorite rocks, the presence of a few metamorphosed unaltered or very weakly altered rocks in the area, permits the determination of their original doleritic composition on one hand and strengthens the possiblity of the presence of the postulated premetamorphic hydrothermal alteration on the other hand. In order to give a measure and hence an idea of the behaviour of the major oxides, trace and base elements during this alteration, the ratio Al_2O_3/SiO_2 is considered here as a measure of the degree of alteration and against this all the elements are plotted (Fig. 6.10) in comparison with the typical dolerite composition. The information provided from the figure suggests that a clear decrease in MgO, TiO_2, Na_2O, K_2O, Cr, Ga, Ni, Rb, Y, and Zr with increasing degree of alteration exist. CaO, MnO, CO_2, Fe_2O_3, S, Cu and Zn increase with increasing degree of alteration. Ba, Co, La, Sr, and Th have no clear trend but they all show a slight decrease towards the altered rocks. These obeservations are supported by the visual comparison of the premetamorphic equivalents of the averages of both the altered and the unaltered rocks (Table 6.11b and 6.12).

Unlike the epidiorite rocks, separation between altered and unaltered metasediments is very difficult due to variations in the original sediments that resulted in various lithologies. Nevertheless, it was shown earlier in Sections (6.4.5 and 6.4.6) through Niggli Numbers that the great chemical and mineralogical variations of the metasedimentary rocks within the mineralised area cannot be related to regular changes in the clastic components as they lack any sedimentary trends nor can they be the result of metamorphic redistribution because mineralogical and petrographic study of these rocks in Chapter Five had shown that there has been no major mobilisation during metamorphism apart from local grain growth and some silica and carbonate segregation. Besides, many
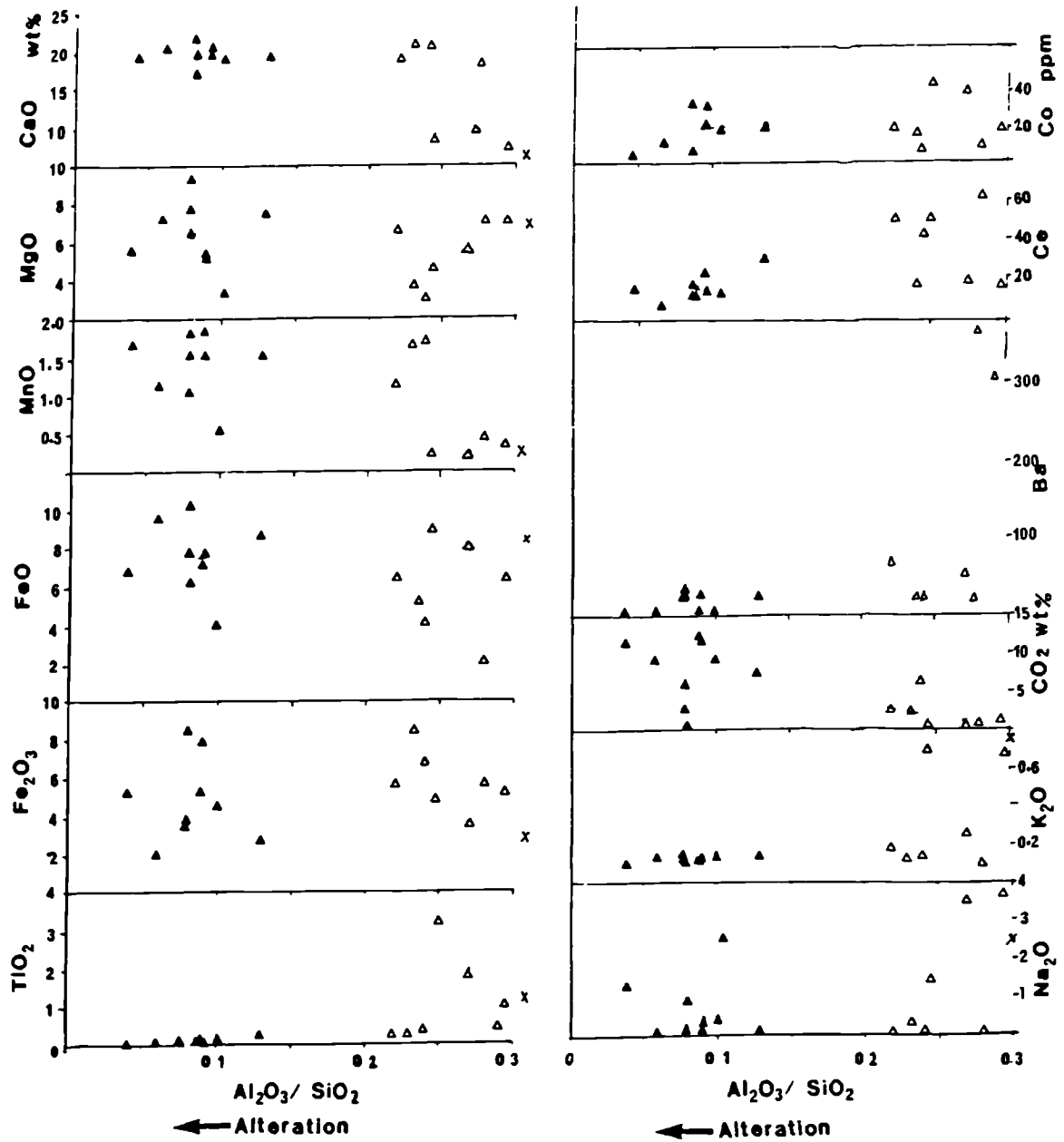
Fig 6.10 : Variation diagrams for the major and trace elements of the
epidiorites in relation with increasing degree of alteration.
▲ :highly altered,△:weakly altered,x: normal epidiorite
(Cox et al. 1979).

248
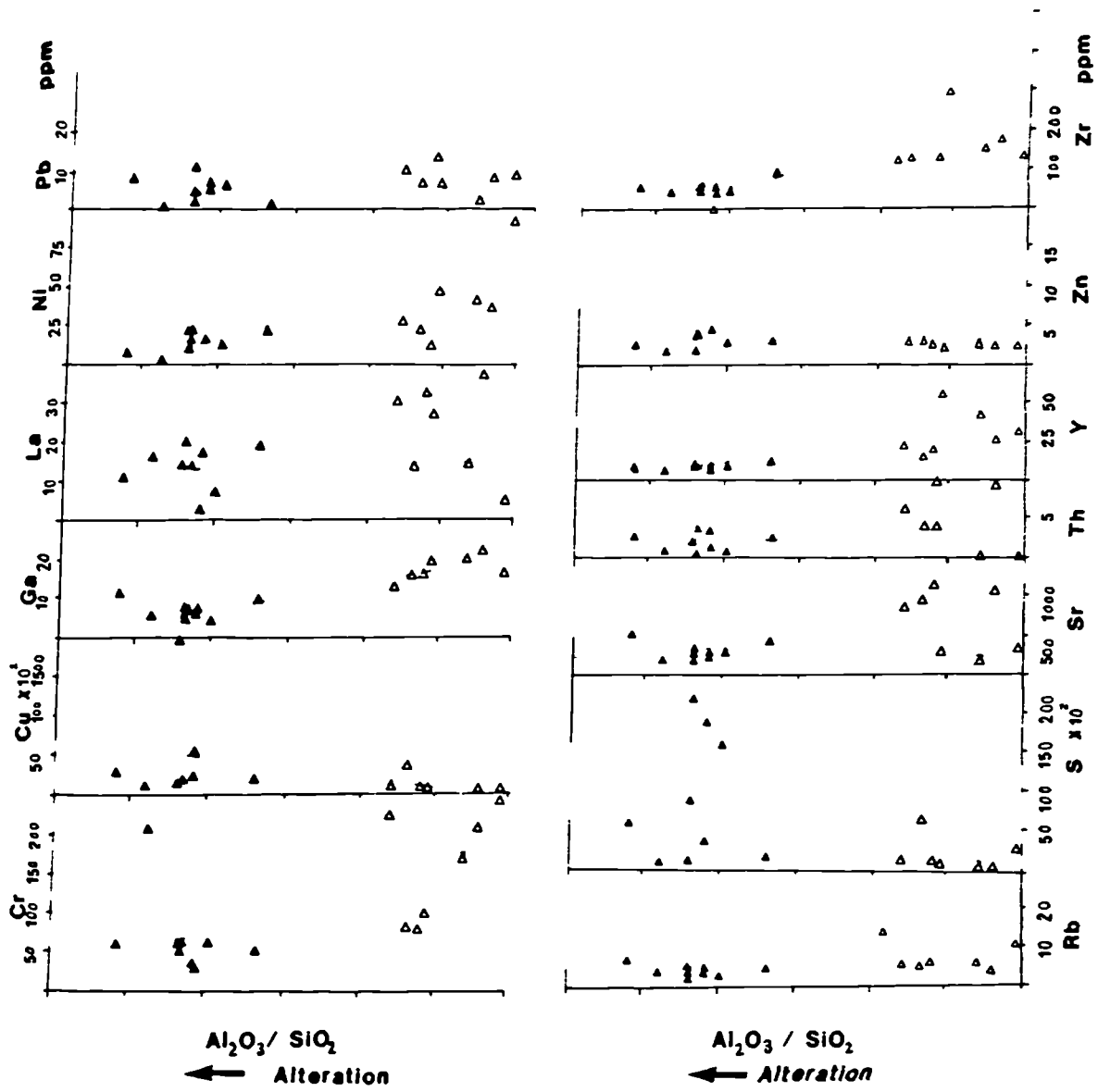
Fig. 6.10 : Continued.

studies have shown that metamorphism up to the amphibolite facies is isochemical apart from H_2O, CO_2, oxidation ratio and some volatiles. Therefore, it is suggested that these variations are premetamorphic and might be the result of local hydrothermal alteration that produced epidotisation, chloritisation, sericitisation, carbonation and silicification of these rocks. In addition to all these is the clear premetamorphic alteration of the associated epidiorites.

Although the B.G.S had reported that epidotisation is restricted to a zone 250m wide which extends along strike 400m north-northeast and 1300m south-southwest of the Abhainn Srathain mine (Section 4.6.3), the size and the shape of the altered zone is very difficult to ascertain because of the lack of outcrops, the restricted borehole sites and the structural complexity of the mine area. But it is quite clear that the highly altered rocks occur in the immediate vicinity of the copper mineralisation centred on the epidiorite bodies.

Such hydrothermal alteration could have happened either during the intrusion of the doleritic sills if intrusion had postdated the mineralisation or during the mineralisation that might either postdate the doleritic intrusions or be associated with it. The latter possibility is more likely as will be discussed later in Chapter Eight.

6.8.1 Element Variations of the Host Rocks in Relation to
      Increasing Oxidation Ratio of the Rocks (w)

An attempt is made to study the variations of the major and trace element concentrations in relation to the oxidation ratio of the rocks (w), expressed as $(2Fe_2O_3 \times 100/2Fe_2O_3 + FeO)$ in moles. However, assuming that metamorphism is isochemical a decrease in the Fe_2O_3 / FeO ratio during regional metamorphism was reported in many studies as was mentioned earlier in Section (6.4.6). However, even

if this is the case, the present variations in the values of the oxidation ratios of these rocks can still be assumed to be inherited from their premetamorphic variations. The average oxidation ratio for the analysed epidiorites is 40.06. This value is close to the normal oxidation ratio of dolerite (Table 6.11b) and therefore it is assumed that this oxidation state is inherited and not modified by metamorphism. The highest MnO, Cu and Co values that might be expected to be associated with the highly oxidised rocks are present in the reduced rock as well (Fig. 6.11). Al_2O_3 and MgO are as expected highly concentrated in the more reduced rocks. This suggests that MnO, Co and Cu with other elements were added to these rocks and therefore support the possibility of the presence of a premetamorphic hydrothermal alteration.

6.8.2 Chemical Variation of the Host Rock in Relation to Increasing Sulphur Content

It is now necessary to relate this postulated premetamorphic hydrothermal alteration to the presence of the sulphide minerals. Of course the best way to get such information is by examining certain chemical trends in cross-sections through the host rocks and across the mineralised zone as was demonstrated at Broken Hill for example (Plimer 1979) and elsewhere. Unfortunately this cannot be achieved in the Abhainn Srathain area because of the limited number of exposures and boreholes on the one hand and because of the structural complexity of the area on the other hand. Instead element variations against increasing sulphur content are examined. The data obtained by constructing Pearson correlation coefficients of sulphur with each of the major oxides for the metasedimentary rocks (Table 6.5c) showed that only one value greater than 0.5 exists between S and Fe_2O_3 (0.6); all the other oxides have very weak correlations of <0.3. Also S has a very weak correlation with other trace elements (Table 6.5b). No correlation coefficients greater than ±0.5 exist. The highest positive correlation values are between S and Cu (0.3); S and Co (0.27); S and Zn (0.26) and S
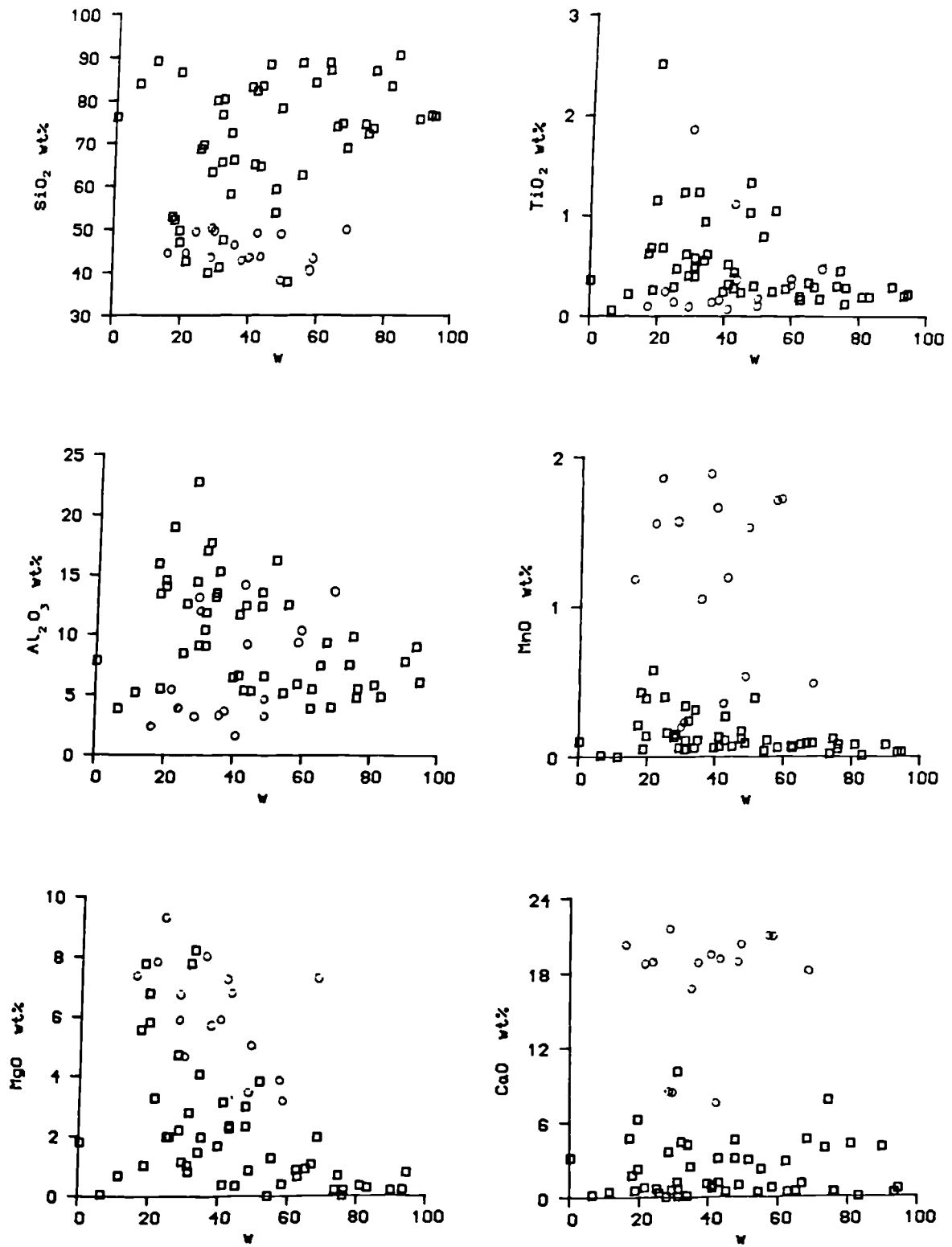
Fig. 6.11 : Element variations in relation with increasing oxidation
ratio of the rocks (w). □: metasedimentary rocks,
○: epidiorites.

Fig. 6.11 : Continued.

Fig. 6.11 : Continued.

254
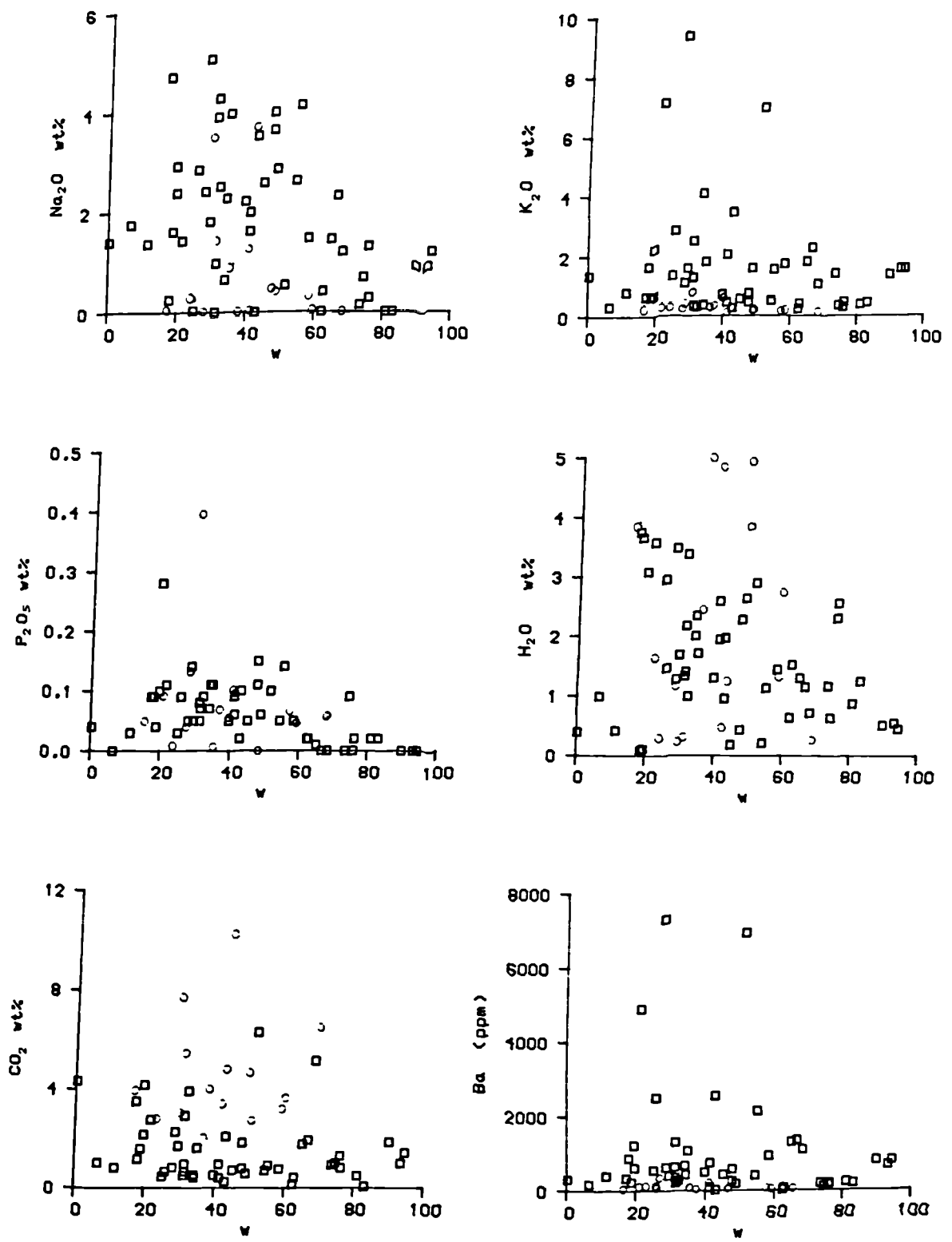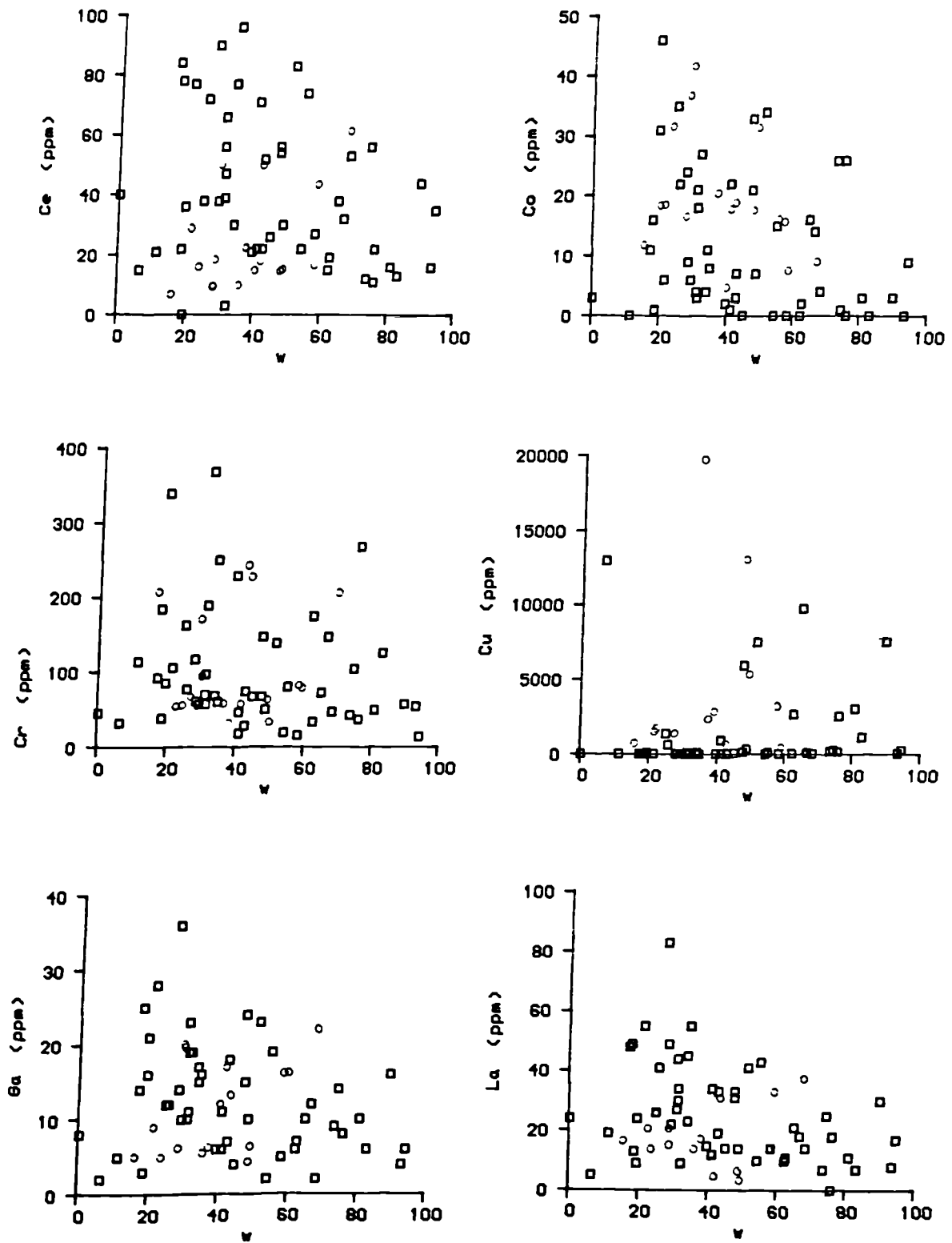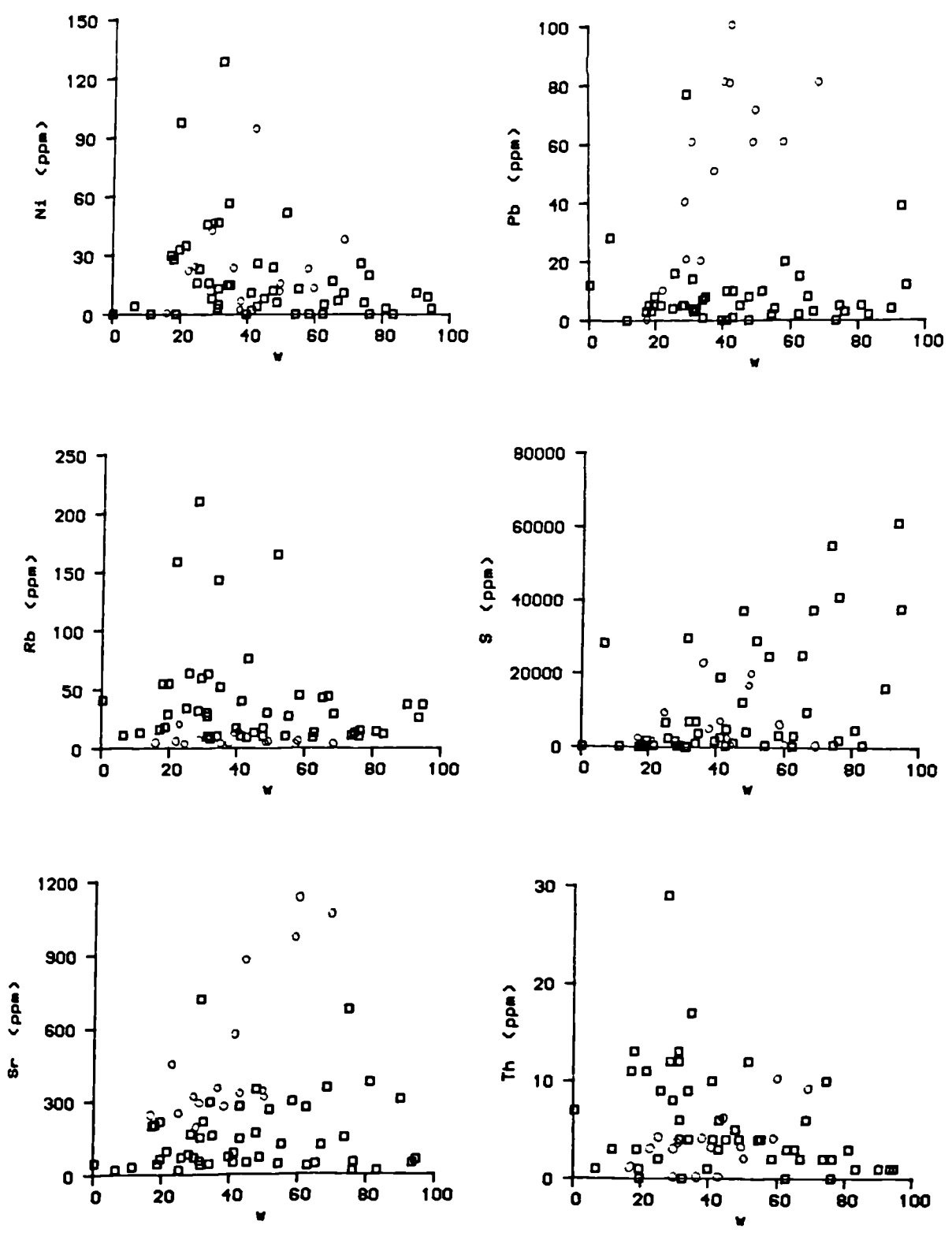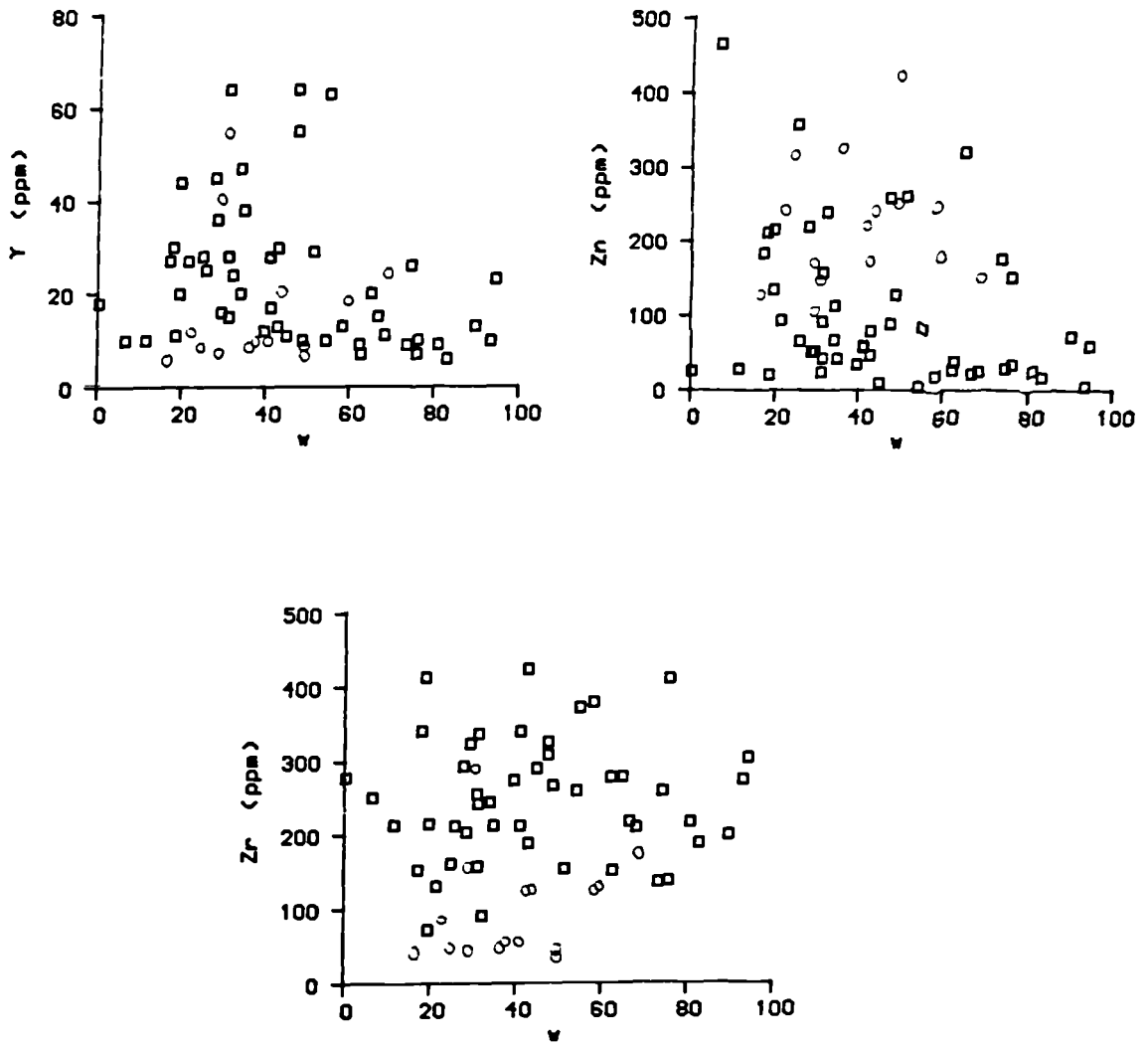
Fig. 6.11 : Continued.

Fig. 6.11 : Continued.

and Pb (0.23). Th correlates very weakly and negatively with S (-0.25) and so does La (-0.23). Similar observations are noticed among Pearson correlation coefficients of sulphur with other major and trace elements (Tables 6.6 b&c) and was discussed earlier in Section (6.3.2). Also, Figure (6.12) shows that there is no simple distinct trends with increasing sulphur content. This is due to the sporadic occurrence of sulphides, garnet, chlorite, epidotes, calcite and quartz. All the elements show a slight increase with increasing sulphur up to 0.1 wt% S, above which the highly mineralised rocks show variable concentrations.

6.9 SUMMARY AND CONCLUSIONS

Chemical analyses of the studied Upper Erins Quartzite Formation that hosts the mineralisation show that it is mainly composed of pelitic and psammitic units. The pelites represent the metamorphosed equivalent of shale but with higher Fe_2O_3 (total), MgO and Na_2O and lower Al_2O_3 and K_2O values compared to the world average pelite and with other Dalradian pelites. The high MgO, TiO_2 and Na_2O values together with the presence of amphibole-bearing pelite, the good correlation between the high MgO values and Ni and the mean Co:Ni ratio of 12.5:1 for the analysed pyrite indicate the presence of coeval tuffaceous material within the sedimentary pile. On the basis of trace elements, these pelites are highly enriched in Cu, S and to a lesser extent Ba. The premetamorphic precursor to the analysed Meall Mór Psammitic rocks is a mixture of quartz arenite, arkose and subarkose of ferromagnesian potassic nature.

The analyses of the epidotised and nonepidotised epidiorites suggest a premetamorphic dolerite composition for the nonepidotised epidiorites and infer a premetamorphic alteration for the epidotised ones. During this alteration these rocks lost MgO, FeO, SiO_2, TiO_2, Na_2O, K_2O and other elements and gained CaO, MnO, Fe_2O_3, CO_2, S, Cu and Zn. Their Al_2O_3-content is diluted as a result of the additive elements.

257
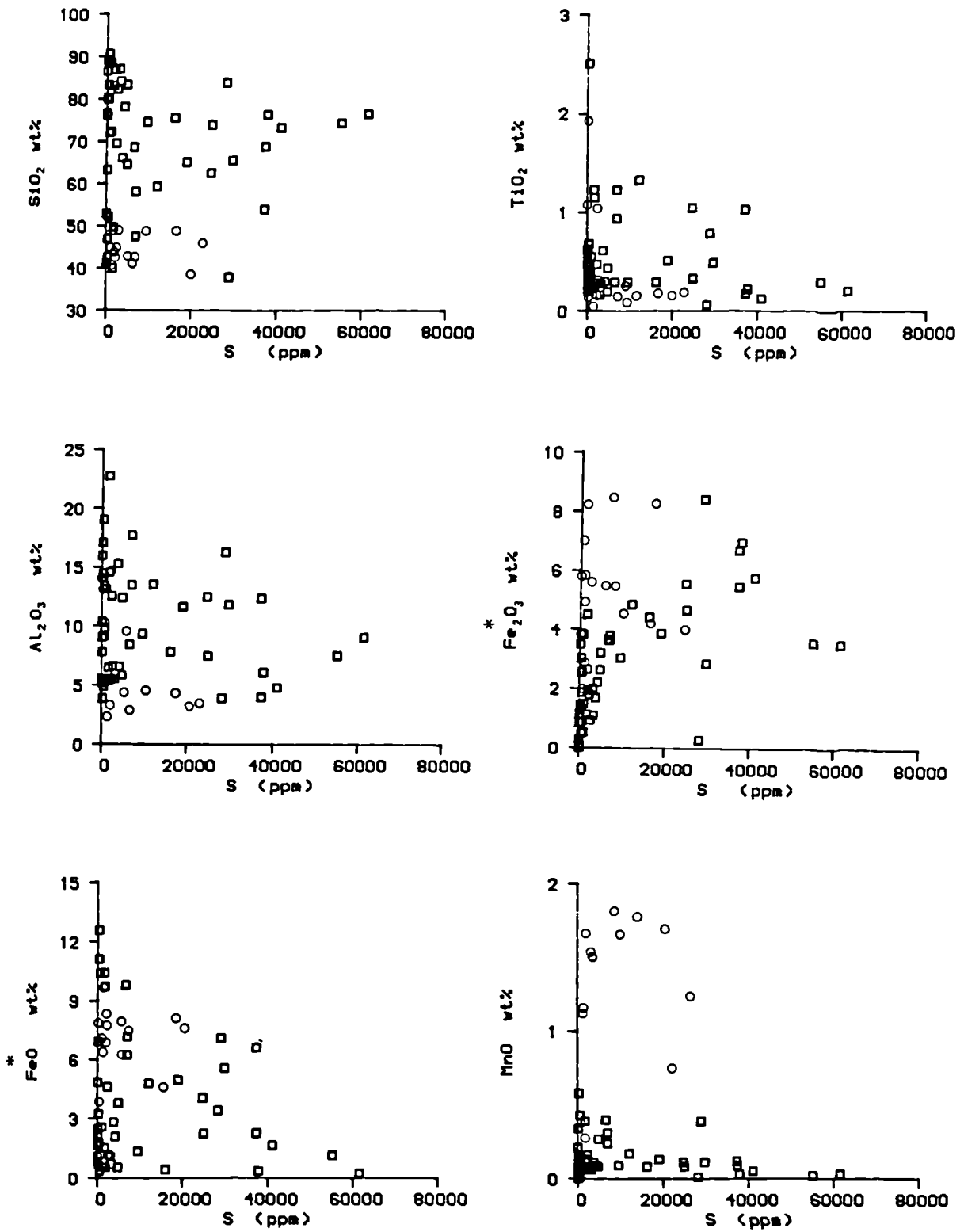
* FeO and Fe₂O₃ values for samples with high S-content are uncertain.

Fig. 6.12 : Element variations in relation with increasing sulphur content.
□:metasedimentary rocks. o:epidiorites.

258

Fig. 6.12 : Continued.

259

Fig. 6.12 : Continued.

260
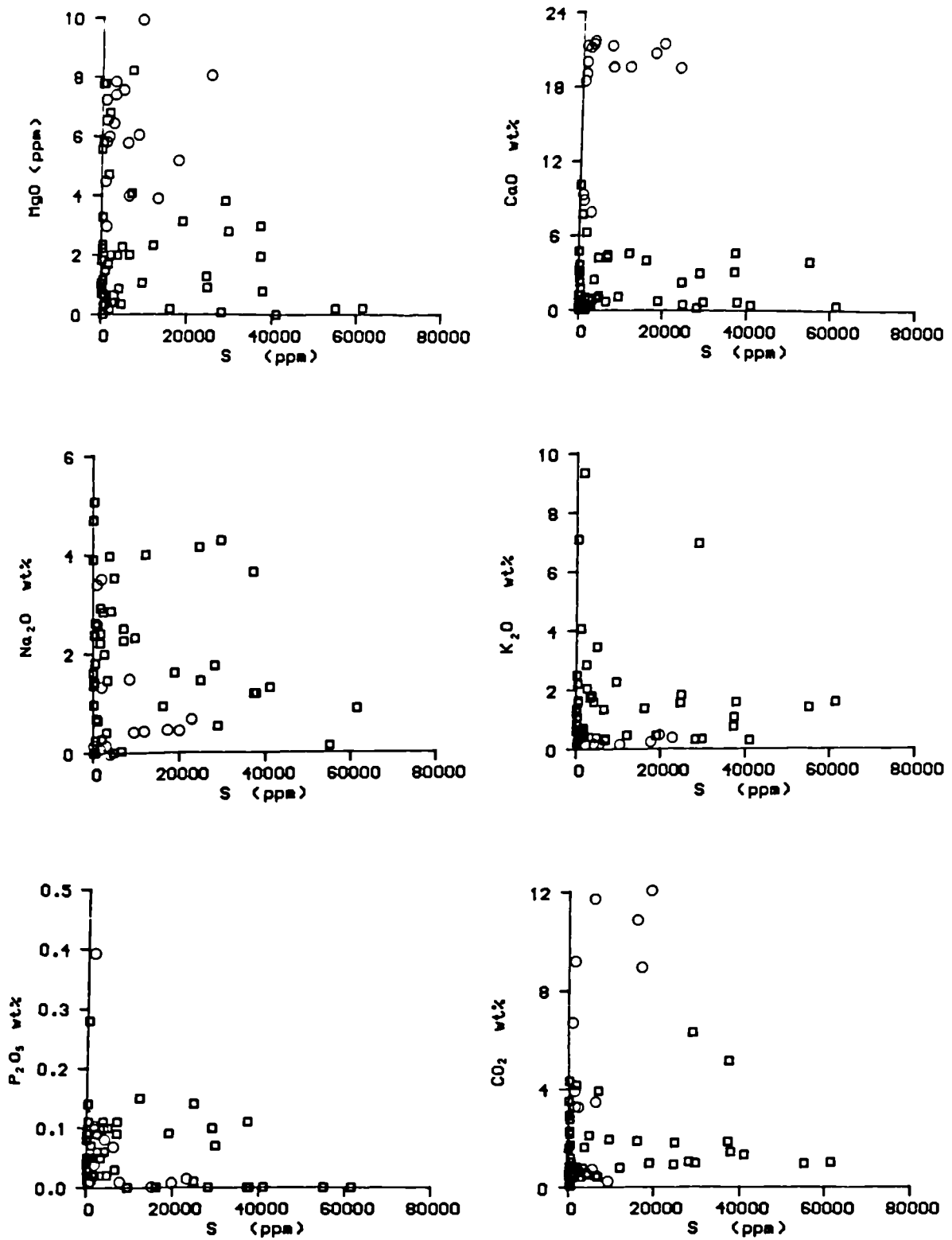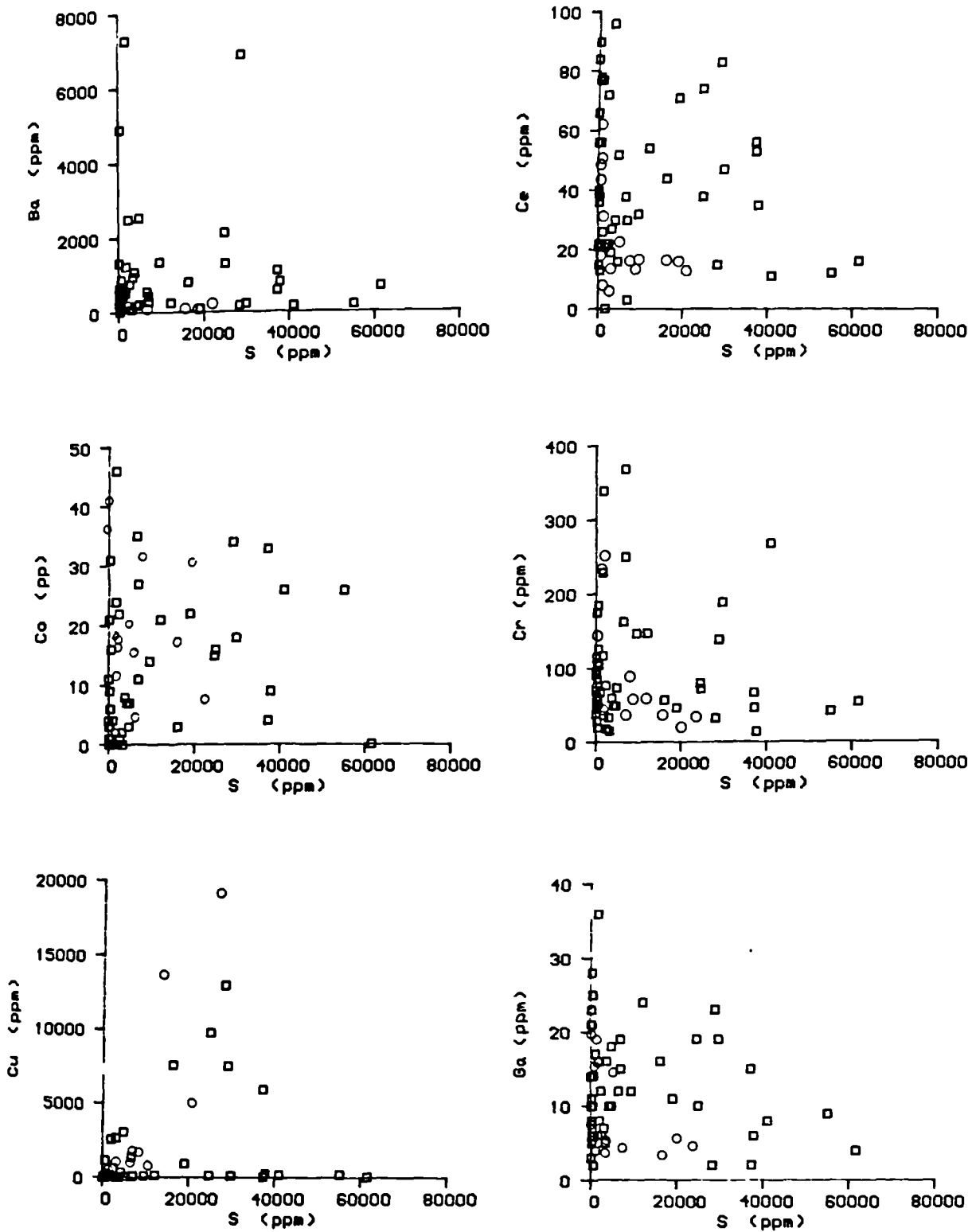
Fig. 6.12 : Continued.

Fig. 6.12 : Continued.

262
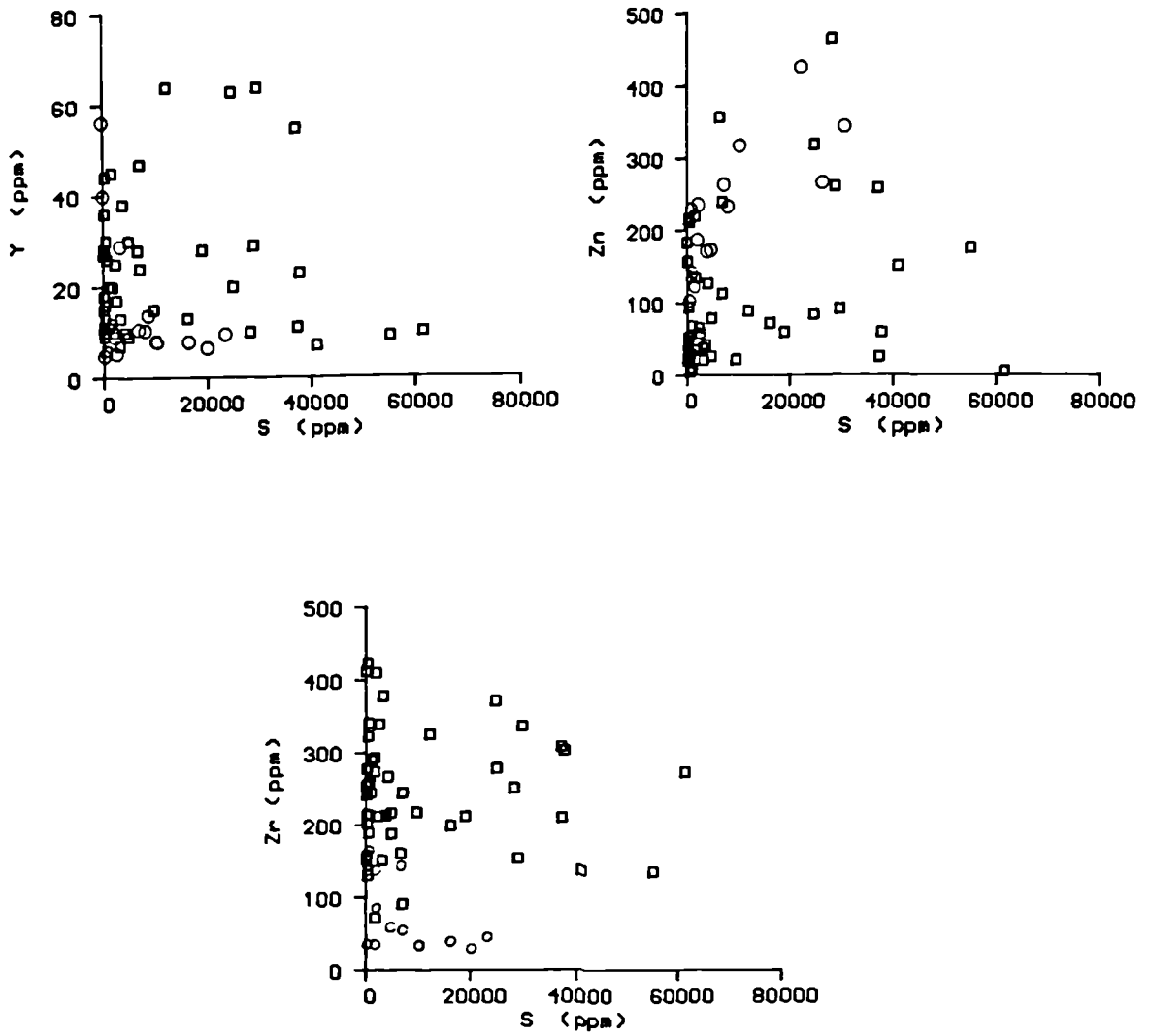
Using Niggli Numbers and some chemical trends it is possible to distinguish between the studied metamorphosed basic igneous rocks and the studied metasedimentary rocks. Such criteria might be invaluable for identifying similar rocks.

There is no systematic mineralogical variation with increasing quartz content nor any correlation between element distribution and increasing clay minerals content for the metasedimentary rocks. This with the absence of correlation between MnO, Cu and Co and the oxidation ratio of these rocks suggest that the bulk chemistry of these rocks was not controlled by their sedimentary environment only and therefore enrichment and depletion in their chemistry might have accompanied the sulphide mineralisation.

It is concluded therefore, that the metasedimentary rocks and the epidiorites that host the mineralisation have undergone local premetamorphic alteration during the process of mineralisation. During this alteration CaO, Fe_2O_3, CO_2, MnO, Cu, S and to less extent Ba and other elements were added. Al_2O_3 was diluted and MgO, FeO and some of the alkalis and trace elements are subtracted. The epidiorites are more altered and epidotised than the associated metasedimentary rocks with the highest MnO, CaO, Fe_2O_3 and CO_2 being contained within the epidiorites due to their more reactive nature.

CHAPTER 7
SULPHUR ISOTOPE STUDY

7.1 INTRODUCTION

Thirty-nine sulphide samples (pyrite and chalcopyrite) from both the Knapdale Pyrite Horizon in the area and from the Abhainn Srathain copper mineralisation were analysed for sulphur isotope composition. The analyses were carried out on a 602C mass spectrometer at the Isotope Geology Unit of the British Geological Survey in London.

In this chapter I have tried to obtain all of the possible information on the sulphur isotopic composition of the hydrothermal fluid, which together with previously discussed geological, mineralogical and geochemical information, can contribute to the understanding of the source of sulphur and metals and of the genesis of the Meall Mór sulphide mineralisation. Where possible closely coexisting pyrite and chalcopyrite were sampled to provide evidence for isotopic equilibrium or disequilibrium. Also, this chapter discusses the behaviour of sulphides on metamorphism.

A brief summary on the significance of sulphur isotope determination and on the sampling techniques used will be given in the next sections before discussing the results.

7.2 THE SIGNIFICANCE OF SULPHUR ISOTOPE DETERMINATION

The principle and the applications of sulphur isotope study has been reviewed by Jensen (1967), Rye and Ohmoto (1974), Sangster (1976), Faure (1977), Coleman (1977), Nielsen (1978 & 1979), Ohmoto and Rye (1979), Hoefs (1980) and Valley et al. (1986). Sulphur isotopes and fluid inclusions studies have been very extensively

used in most recent studies of ore deposits. This is because these techniques can provide us with all the information that are required for constructing genetical model for any deposit. This information includes the source of metals and sulphur, the nature and origin of the transporting fluid and the physiochemical conditions of ore deposition. Fluid inclusion studies in ore and gangue minerals of some ancient unmetamorphosed deposits, such as Cyprus, Kuroko and the Irish deposits (Ohmoto and Rye 1974, Spooner and Bray 1977 and Samson 1983), were used successfully to obtain much of the information about the ore formation. However, for deposits that are metamorphosed such as the Dalradian mineralisations, application of fluid inclusion study might be difficult because no feeder system or stockwork has yet been discovered. Therefore, the sulphur isotope ratios and variations in the isotopic composition of sulphide and sulphate minerals can provide us with much of the information concerning the ore formation.

Sulphur isotope analyses of baryte have the power to discriminate between certain hypotheses of ore genesis and in this may be important in mineral exploration. Baryte has been successfully used in sulphur isotopic studies of the Irish base-metal deposits and gives sulphur isotopic values the same as Lower Carboniferous seawater supporting a synsedimentary origin for these deposits and reveals seawater sulphur as the sulphide source. Also, more recently Willan and Coleman (1983) in studying the sulphur isotopic composition of the Dalradian Mineralisation confirm the derivation of the Aberfeldy baryte sulphate from contemporaneous Vendian seawater and support a synsedimentary hydrothermal nature for the ore deposits.

In the present sulphur isotope study no baryte is associated with the mineralisation and therefore sulphur isotopic determination was carried out on sulphide mineral species only. However, the source of the sulphide sulphur is more difficult to establish. Many studies showed that the source of sulphur may be either from

265

bacterial reduction of seawater sulphate, from reduced sulphur carried in hydrothermal solution or mixture of both (Ohmoto and Rye 1979).

7.3 SAMPLING AND ANALYTICAL TECHNIQUES

Thirty-nine sulphide mineral samples representing the three styles of mineralisation (stratiform, disseminated and porphyroblasts in cross-cutting veins) were taken from different lithologies at the Abhainn Srathain copper mineralisation and from the Knapdale Pyrite Horizon. Most samples were taken from B.G.S. boreholes 1, 2 and 3 (Figs. 7.3 to 7.5). Nine samples were collected in the field along a track across the strike of the Knapdale Pyrite Horizon and from the spoil heaps of the old Abhainn Srathain mine (Fig. 7.2).

For all samples polished sections and /or polished thin sections were made for petrographic descriptions and their summaries are presented in Table (7.1) and were also included in Appendix (A.5.2). The sulphide minerals were separated by crushing followed by hand-picking. Only two samples (HMM 7 & 12) were obtained using a dental drill on polished sections. Each sulphide phase was then confirmed by powder X-ray diffraction (smear mounts) and an estimation of the purity was obtained by comparing XRD peaks. Samples were found to be mostly monomineralic (Table 7.3).

All the isotopic analyses were carried out on a modified Micromass 602C mass spectrometer at the Isotope Geology Unit of the Institute of Geological Sciences, London. Sulphur dioxide from sulphides was extracted for analysis by oxidation with cuprous oxide at $1070^{\circ}C$, using the method described by Robinson and Kusakabe (1975). The SO_2 yields were run on a VG Micromass double collector spectrometer, using SO_2 extracted from a chalcopyrite standard as a reference gas.

266

The results were corrected for isobaric interference and instrumental crosstalk following the procedure by Coleman (1980). Analytical precision was estimated from duplicate analyses to be about ± 0.2 per mil. The methods of SO_2 extraction, $\delta^{34}S$ measurment and the raw data corrections are summarised in Appendix (A.7.1).

All data are reported in del per mil difference relative to the Canon Diablo troilite (C.D.T.) standard.

$$\delta^{34}S_{sample} = \left[\frac{^{34}S/^{32}S_{sample}}{^{34}S/^{32}S_{standard}} - 1 \right] \times 1000$$

Where the $^{34}S/^{32}S_{standard} = 0.0450045$ (Jensen and Nakai 1963).

The difference in $\delta^{34}S$ between two coexisting phases (pyrite and chalcopyrite) is approximated and expressed as :

$$\Delta^{34}S_{chp-py} = {}^{34}S_{chp} - {}^{34}S_{py} \ ‰$$

7.4 RESULTS

All isotopic compositions of the thirty-nine mineral separates, both pyrite (n=31) and chalcopyrite (n=8) together with the description of the analysed samples are presented in Table (7.1) and plotted in Figure (7.1). They show a range of + 4.4 to + 12.8 per mil with a mean of +7.4 per mil. The distribution of these results is unimodal ($\sigma = +1.67$), with a slight skew to heavier values. Most samples are falling in the range + 6 to +9 per mil (n = 29). Excluding four isotopically light values (4 - 6 ‰) and six heavy values (9- 13 ‰), the mean $\delta^{34}S$ (n = 29) value is 7.2 ($\sigma = 0.77$).

The mean isotopic value for pyrite (n=31) is +7.6 ‰ ($\sigma=1.71$) and for chalcopyrite (n=8) is +6.4 ‰ ($\sigma=1.05$). Excluding eight samples falling out of the range +6 to +9‰, the mean (n=23) is +7.2

Sample Number	Locality N.G.R (Square NR)	Rock-Type	Mineralogical Composition	Style of Mineralisation	$\delta^{34}S$ ‰ Chp.	$\delta^{34}S$ ‰ Pyr.
HMM 7	836 737	epidiorite	Am. 35%, gar. 35%, qz&alb. 10%, cal. 5%, se. 2%, pyr. 7%, chp. 1.5%, mag. rimmed with hem. 1.5%, with traces of epd., chl., sph. and bor.	sulphide and oxide porphyroblasts in qz/cal. cross-cutting veins	4.4	7.0
HMM 12	836 737	epidotised epidiorite	Am. 20%, epd. 25%, qz.&alb. 20%, cal. 18%, gar. 5%, chp. 7%, pyr. 3% mag. rimmed with hem. 2%, with traces of chl., se., and sph.	disseminated pyrite cubes in thin refolded layers	7.6	6.8
HMM 56	8404 7425 Meall Mòr track	quartzite	Qz. 85%, chl. 5%, pyr. 5%,with traces of alb.,bit.,mus.,cal.,and zr.	disseminated	---	9.2
HMM 58	8398 7435 Meall Mòr track	quartzite	Qz. 75%, chl. 10%, se 3%, pyr. 6%, chp. 3%, with traces of bit., mus gar., and ilm.	disseminated	---	9.6
HMM 59	8474 7717 Artilligan Burn	feldspathic quartzite	Qz. 73%, alb. 10%, mus. 7%, pyr. 7%, with traces of zr., and ilm.	disseminated	---	10.8
HMM 60	8374 7482 Meall Mòr track	feldspar-mica quartzite	Qz. 65%, alb. 10%, mus. 15%, bit. 3%, pyr. 5%, with traces of se., cal., and rut.	disseminated coarse porphyroblasts	6.7	7.0
HMM 61	8445 7688 Artilligan Burn	feldspar-mica quartzite	Qz. 80%, alb. 15%, pyr. 2%, with traces of mus., bit., epd., sph., and rut.	disseminated	---	12.8
HMM 62	8442 7685 Artilligan Burn	quartzite	Quartzite with disseminated pyrite cubes.	disseminated	----	4.5

Table 7.1 : Sulphur isotope data from both the Knapdale Pyrite Horizon and the Abhainn Srathain copper mineralisation , Meall Mòr.

	8438 7697 Artilligan Burn	quartzite	Quartzite with refolded sulphide laminations.	fine alternating sulphide layers		
HMM 63					5.2	10.2
HMMI 1	BH.3, 17.95m	epidotised epidiorite	Am. 20%, epd. 20%, qz.&alb. 20%, cal. 20%, gar. 10%, chp. 7%, pyr. 3%, with traces of mag., hem., and sph.	disseminated grains in quartz vein	7.7	7.9
HMMI 3	BH.3, 24.1m	epidotised epidiorite	Am. 10%, epd. 70%, qz. 5%, se. 5%, pyr. 10%, with traces of gar., cal., and chp.	disseminated	---	8.0
HMMI 9	BH.3, 33.3m	mica-chlorite schist	Qz. 55%, chl. 15%, mus. 20%, cal. 10%, with traces of epd. and pyr.	porphyroblasts in veins	---	8.0
HMMI 16	BH.3, 10.2m	epidiorite	Am. 35%, epd. 15%, gar. 15%, qz.&alb. 10%, cal. 10%, mag. rimmed with hem. 8%, pyr. 7%, with traces of se., chp., and bor.	porphyroblasts in veins	---	7.6
HMMI 18	BH.3, 11.45m	epidiorite	Am. 60%, epd. 15%, gar. 15%, cal. 5%, qz.&alb. 3%.	vein-type mineralisation	---	6.1
HMMI 20	BH.3, 14.3m	epidotised epidiorite	Yellowish green (pistachite) rock mainly of epidote with small quantities of gar., am., and quartz filling very fine veins.	very fine disseminated	---	7.9
HMMI 21	BH.3, 14.95m	epidiorite	Am. 55%, cal. 25%, gar. 13%, epd. 5%, qz.&alb. 2%.	fine disseminated grains in vein	---	6.0
HMMI 34	BH.1, 9.8m	mica-chlorite schist	Qz. 30%, mus. 30%, chl. 15%, cal. 10%, se. 5%, pyr. 10%, with traces of alb., ilm., mag., and rut.	disseminated	---	8.0
HMMI 35	BH.1, 10.2m	epidotised quartz-mica-feldspar schist	Qz. 35%, alb. 10%, chl. 15%, bit. 10%, epd. 10%, mus. 3%, gar. 3%, pyr. 7%, chp. 3%, ilm., rut., and mag. 3%.	stratiform fine layers	---	7.3

Table 7.1 : Continued.

Sample	Borehole, depth	Rock type	Mineralogy	Texture		
HMI 37	BH.1, 12.0m	micaceous quartzite	Qz., bit., chl. and pyr.	disseminated	---	6.0
HMI 38	BH.1, 13.4m	schist	Dark greenish grey rock mainly of qz., chl., bit. and pyr.	disseminated	---	7.0
HMI 39	BH.1, 14.65m	schist	Mainly of qz.,chl.and bit. with little pyr. and chp.	disseminated	6.5	6.6
HMI 41	BH.1, 18.5m	micaceous quartzite	Qz., chl. bit. and pyr.	disseminated	---	6.8
HMI 42	BH.1, 19.7m	epidotised epidiorite	Qz. 23%, epd. 20%, alb. 10%, chl. 10%, bit. 7%, am. 5%, ger. 5%, cal 2%, pyr. 10%, ilm. 5%, with traces of chp. and bor.	stratiform layers	---	7.1
HMI 43	BH.1, 20.6m	micaceous quartzite	Mainly of qz., bit. and chl. and is very rich in pyr.	coarse disseminated	---	6.6
HMI 69	BH.2, 10.0m	calcareous schist	Qz. 20%, ser. 33%, cal. 20%, alb. 5%, bit. 5%, pyr.&chp. 10%, mag.& hem. 5%, with traces of chl., cov., and bor.	disseminated in vein type	6.8	8.5
HMI 76	BH.2, 19.5m	quartz-mica schist	Qz. 65%, mus. 20%, bit. 5% and pyrite 5%.	coarse disseminated porphyroblasts	---	9.0
HMI 78	BH. 2, 20.5m	mica-schist	Qz. 60%, mus.&bit. 35%, pyr. 3.5%, rut. 1.5%, with traces of alb., cal., apt., and ilm.	disseminated	---	9.8
HMI 87	BH.2, 27.67m	feldspathic quartzite	Qz. 45%, alb. 10%, cal. 10%, mus. 3%, pyr. 25%, with traces of se., chp., sph., and bor.	disseminated in very fine layers	---	6.2
HMI 92	BH.2, 31.0m	quartzite	Qz. 80%, bit. 10%, cal. 3%, chp. & pyr. 3%, with traces of sph.&mag.	disseminated in quartz vein	6.3	6.1

Table 7.1 : Continued.

270

HMMI 101	BH.2, 37.75m	mica-schist	Qz. 55%, mus. 15%, alb. 5%, bit. 4%, cal. 4%, se. 2%, pyr. 15%, with traces of chp., bor., rut., and ilm.	disseminated	--	7.2
HMMI 107	BH.2, 40.65m	quartz-mica schist	Qz. 25%, bit. 40%, mus. 15%, alb. 5%, cal. 5%, pyr. 7%, rut. 3%, with traces of se., chp., bor., and mag.	disseminated in very fine highly deformed veins	--	5.3
1	Srondoire, NR 8700 7870	quartzite	Quartzite with less than 5% pyrite		6.8	--
2	Cruachan Gille Bheagain NR 8280 7260	quartzite	Quartzite with disseminated pyrite		1.3	--
3	Meall Mór NR 8375 7461	quartzite	Quartzite cut by veinlets of chalcopyrite and pyrite		--	4.2
4	Abhainn Srathain NR 8340 7360	epidotised epidiorite	Epidotised epidiorite with pyrite and chalcopyrite		6.3	9.2

Abbreviations for minerals:-

alb.	: albite	am.	: amphibole	apt.	: apatite	bit.	: biotite	bor.	: bornite	cal.	: calcite
chl.	: chlorite	chp.	: chalcopyrite	cov.	: covellite	epd.	: epidote	feld.	: feldspar	gar.	: garnet
hem.	: hematite	ilm.	: ilmenite	mag.	: magnetite	mar.	: marcasite	mus.	: muscovite	pyr.	: pyrite
pyrh.	: pyrrhotite	qz.	: quartz	rut.	: rutile	se.	: sphene	ser.	: sericite	sph.	: sphalerite
zr.	: zircon										

Table 7.1 : Continued.

271
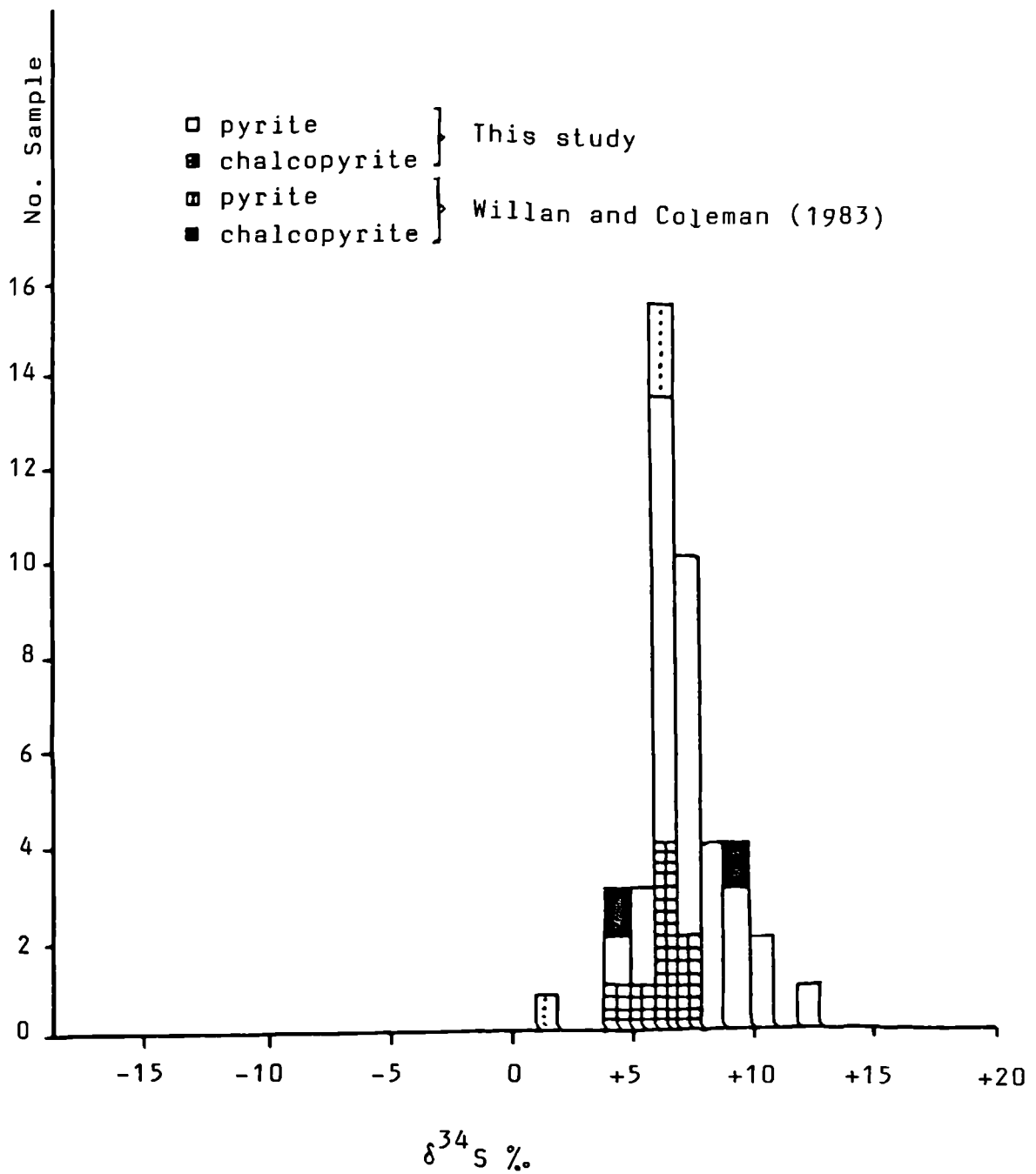
Fig. 7.1 : The distribution of the sulphur isotope data of the
sulphides from both the Abhainn Srathain copper min-
eralisation, Meall Mòr and from the Knapdale Pyrite
Horizon.

272

per mil, $\sigma = 0.81$.

Five sulphide mineral samples taken from the Abhainn Srathain copper mineralisation and through the Knapdale Pyrite Horizon including both pyrite (n=3) and chalcopyrite (n=2) were analysed by Willan and Coleman (1983) and give similar isotopic results. Four of the five analyses have $\delta^{34}S$ values ranges between 4.2-9.2 ‰, falling within the observed values in this study. Only one analysis of pyrite has a very low value of 1.3 ‰. Description and results of these five analyses are also included in Table (7.1) and plotted in Figure (7.1).

7.4.1 Variation of $\delta^{34}S$ along the Knapdale Pyrite Horizon

Figure (7.2) shows the distribution and the variation of $\delta^{34}S$ sulphide within the Knapdale Pyrite Horizon presented by samples taken from the few outcrops through the horizon. It appears from the data that the variations in the $\delta^{34}S_{pyrite}$ values along the mineralised horizon are similar to the variation of $\delta^{34}S_{pyrite}$ at the Abhainn Strathain copper mineralisation and that $\delta^{34}S_{pyrite}$ becomes heavier to the north of the Abhainn Srathain site.

7.4.2 Variation of $\delta^{34}S$ with Depth

It is extremely difficult to determine which is the way up in the sampled B.G.S. boreholes. This will need detailed surface mapping and more drilling to unravel the structure. As a tentative guess to the structure, Willan (1983) suggested that the sequence is inverted in places and that each borehole is younging downward (see Figs. 5.2 A&B). However, it is still worth checking the variation in the sulphur isotopic ratio in these boreholes vertically no matter which way up they are.

Figure (7.3) shows the variation of $\delta^{34}S_{pyrite}$ in borehole 1 in which only the upper part of the section was available for
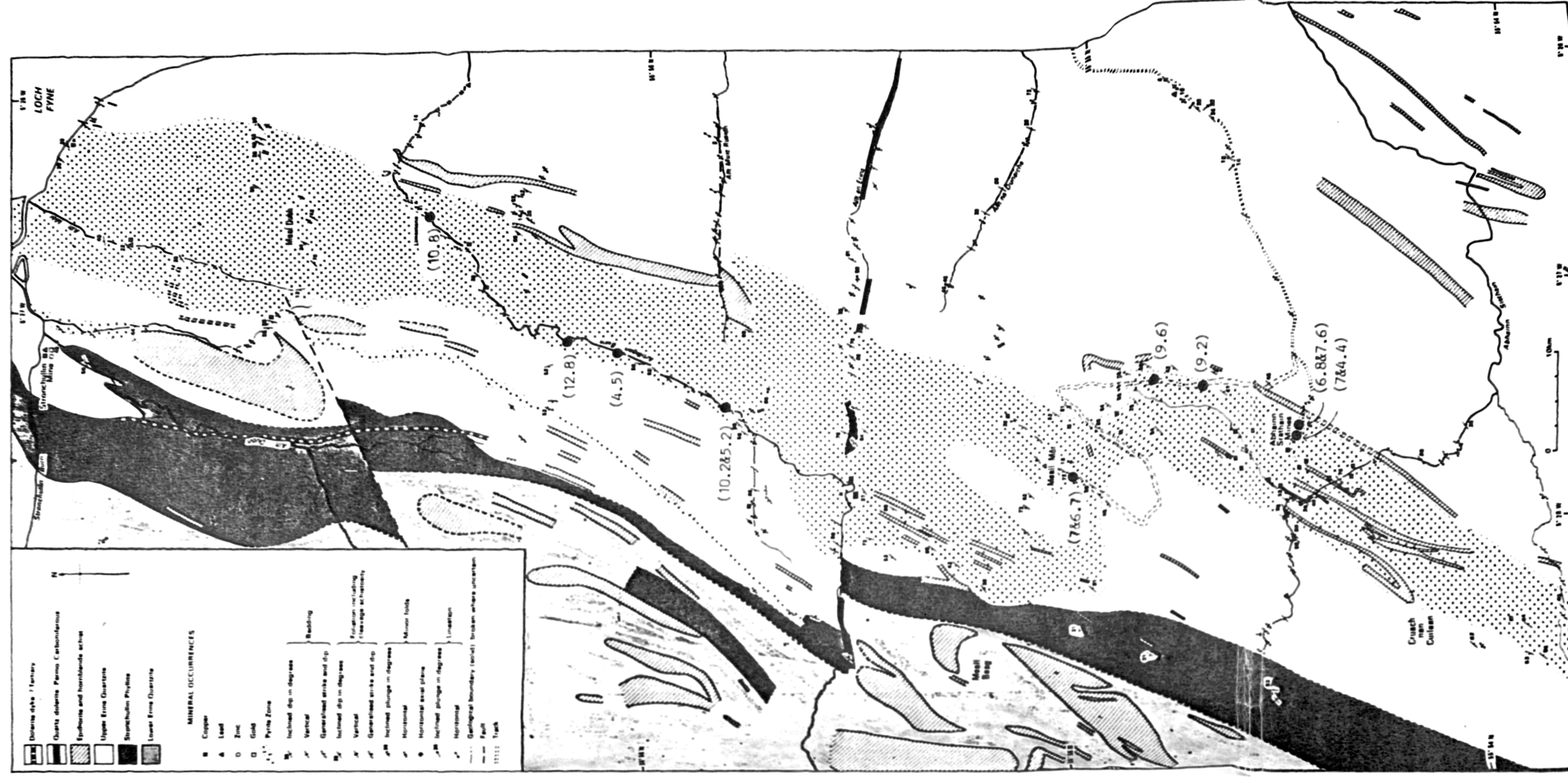
Fig. 7.2 : Location of the analysed surface samples and their isotopic values in brackets.

274

sampling. An increase in $\delta^{34}S$ pyrite upwards is evident. The same relation is obtained for borehole 2 (Fig. 7.4) while in borehole 3 (Fig. 7.5) the lower part of the section shows a nearly constant $\delta^{34}S$ pyrite value with variable values in the upper part. Also, information from these figures (Figs. 7.3 to 7.5) shows that no clear relationship of $\delta^{34}S$ pyrite to copper content is present, but it is worth pointing out that in some parts of the sections, the $\delta^{34}S$ pyrite becomes heavier with increase in copper content.

7.4.3 Variation of $\delta^{34}S$ with Lithology

The variation of $\delta^{34}S$ pyrite with lithology is tested using both surface samples and samples taken from B.G.S. boreholes 1, 2 and 3. No consistent variation in $\delta^{34}S$ pyrite was observed in different lithologies (Fig. 7.6). The distribution of $\delta^{34}S$ pyrite in both epidiorites and metasediments (quartzites, micaceous-quartzites and schists) is unimodal with nearly the same mean. The same pattern is also noticed for the $\delta^{34}S$ chalcopyrite (Fig. 7.7).

No significant variation in $\delta^{34}S$ sulphide can be seen between disseminated, stratiform or vein mineralisation.

7.5 DISCUSSION

7.5.1 The $\delta^{34}S$ Variations in Metamorphosed Deposits and Isotopic Geothermometry

Detailed studies on metamorphosed stratiform deposits (Lusk 1972, Mauger 1972, Rye and Ohmoto 1974 and Willan and Coleman 1981 & 1983) led to the conclusion that during metamorphism up to amphibolite facies large scale premetamorphic $\delta^{34}S$ variations are generally preserved while small scale sulphur isotopic changes are in many cases superimposed upon the original distributions. Lusk and Crocket (1969) pointed out that isotopic reequilibration usually

Fig. 7.4 : Variation of $\delta^{34}S_{sulphide}$ with depth in BH.2.
Geological summary Log and Cu-content are taken
from Smith et al. 1978.

Overburden

Epidotised rock

Epidiorite
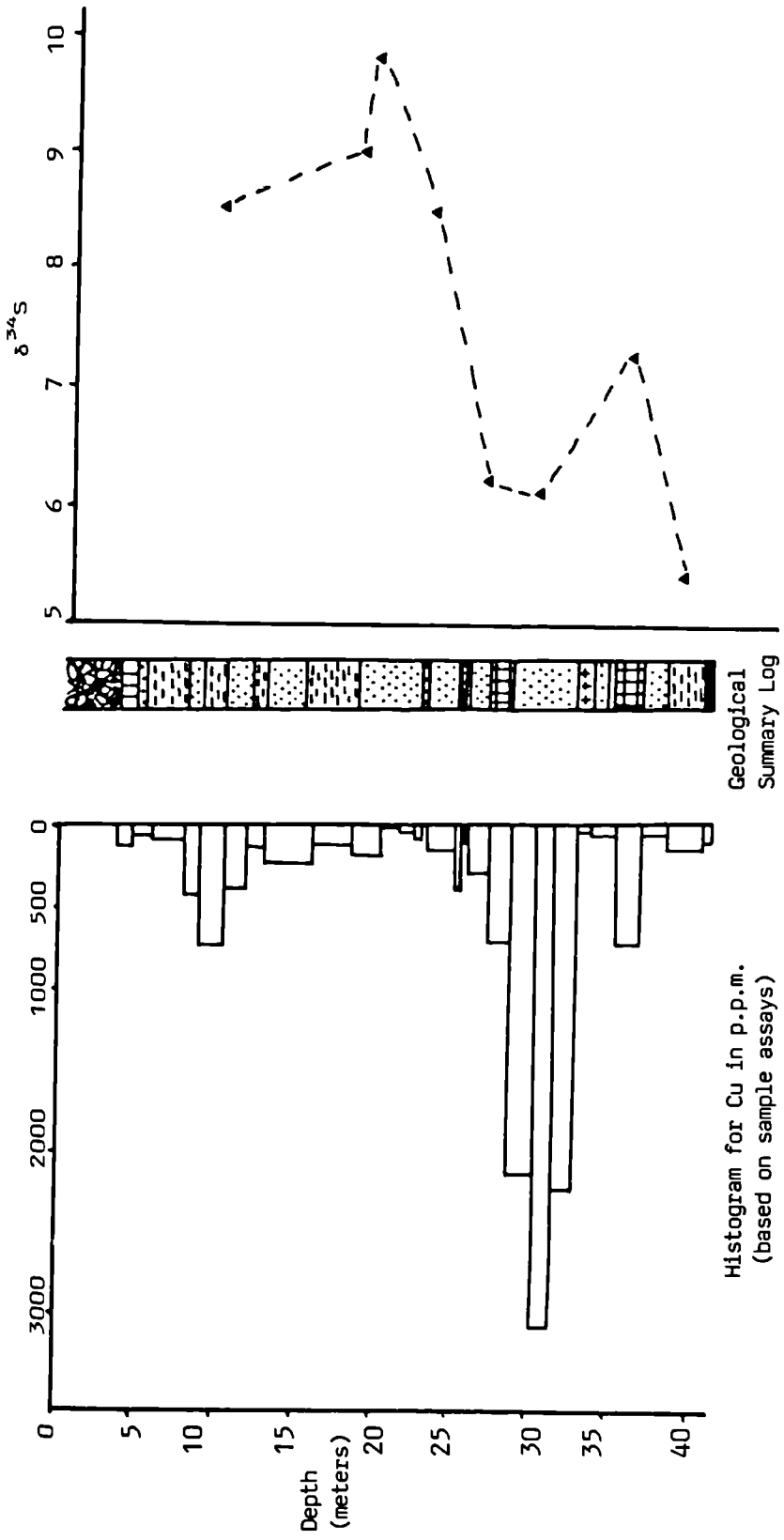
Sparsely micaceous and micaceous quartzite

Chlorite(+biotite+sericite)-quartz-schist

Chlorite(+sericite+biotite)-schist

$\delta^{34}S$

Geological Summary Log

Histogram for Cu in weight%
(Based on sample assays)

Depth (meters)
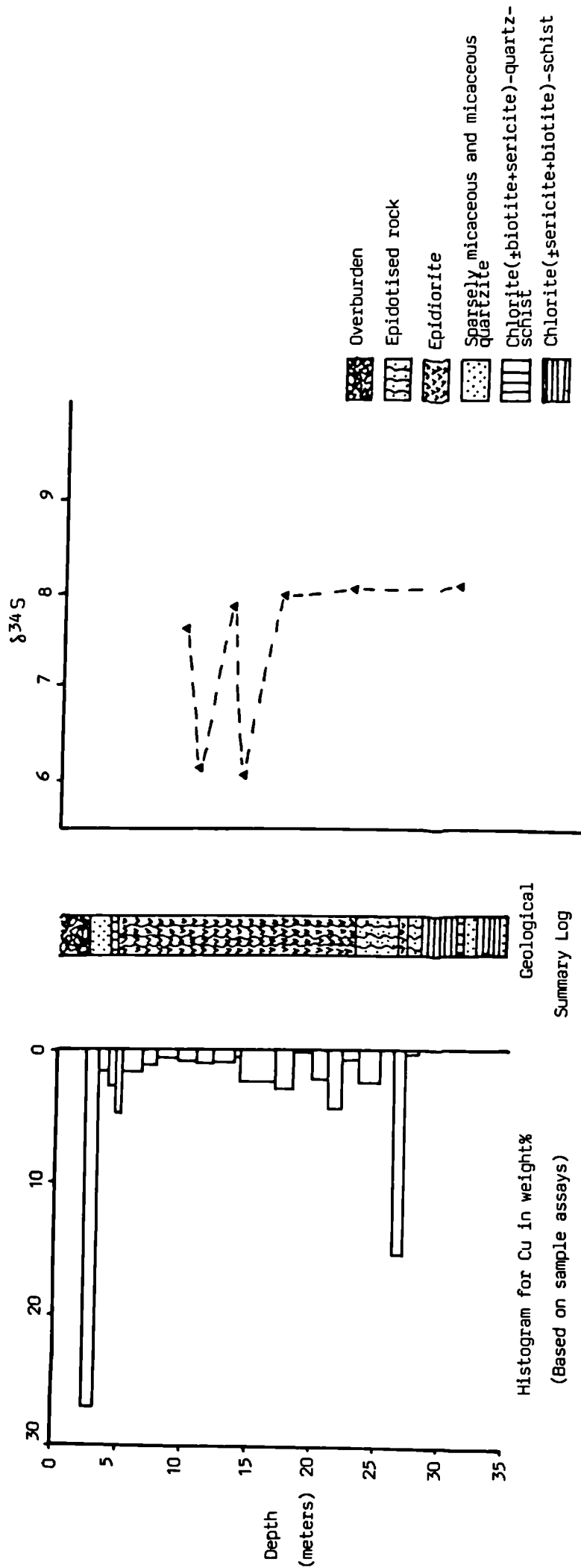
Fig. 7.5 : Variation of $\delta^{34}S$ sulphide with depth in BH.3. Geological summary and Cu-content are taken from Smith et al. 1978.

A : Quartzite, Micaceous Quartzite and Schist

n = 24

σ = 1.86

B : Epidiorite

n = 7

σ = 0.74

δ ^{34}S ‰
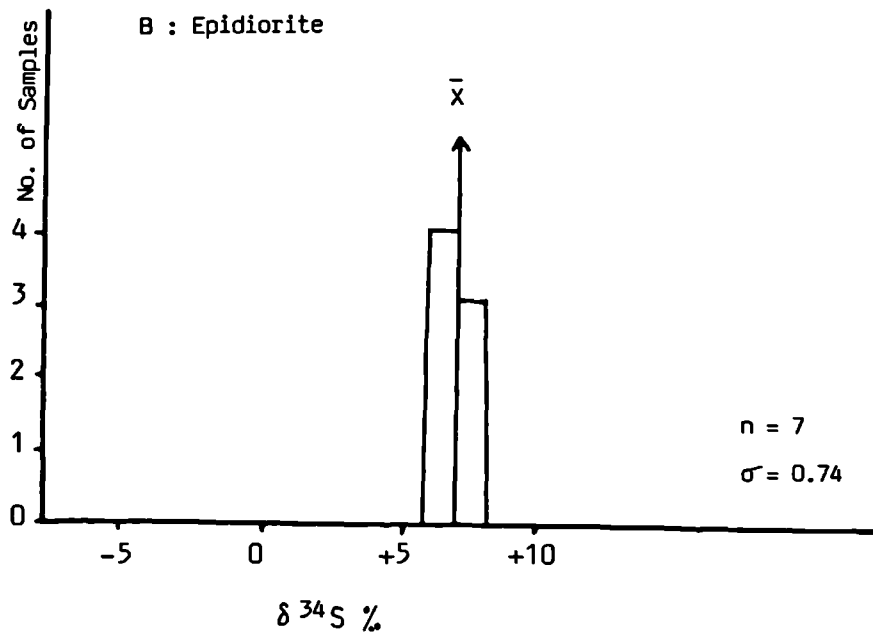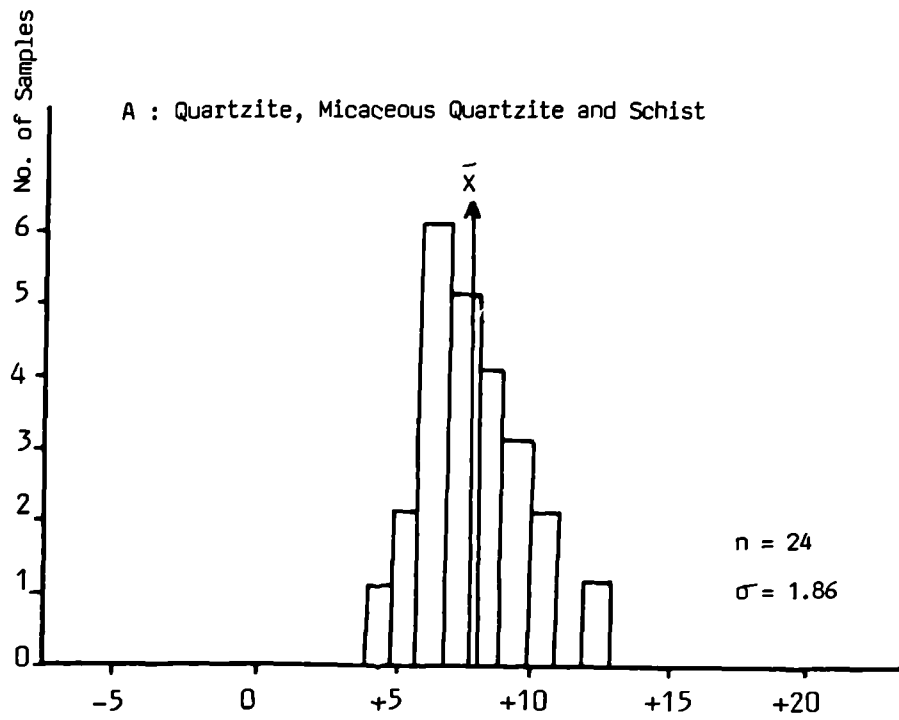
Fig. 7.6 : Summary of the variation of δ ^{34}S$_{pyrite}$ and its mean in different lithologies.
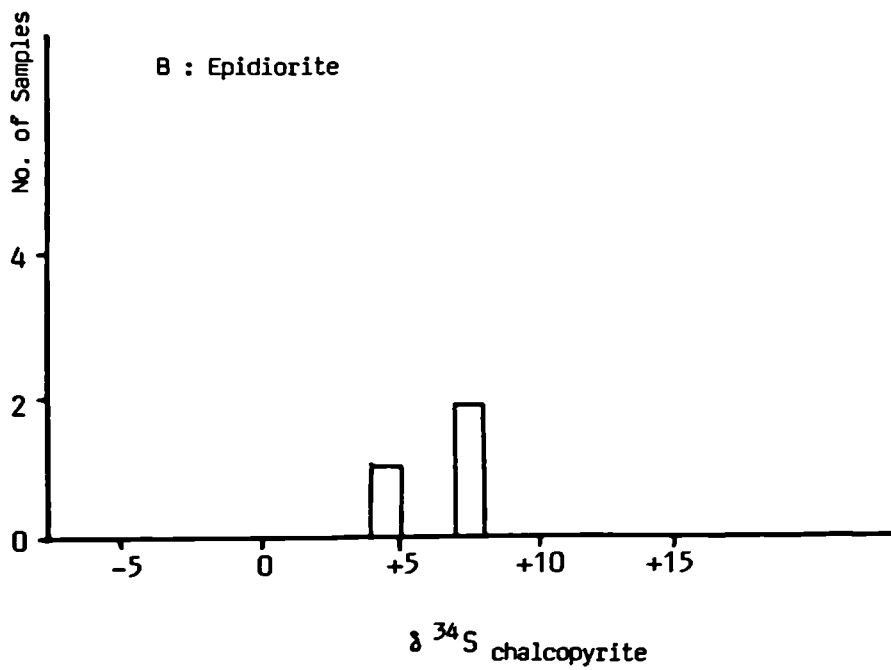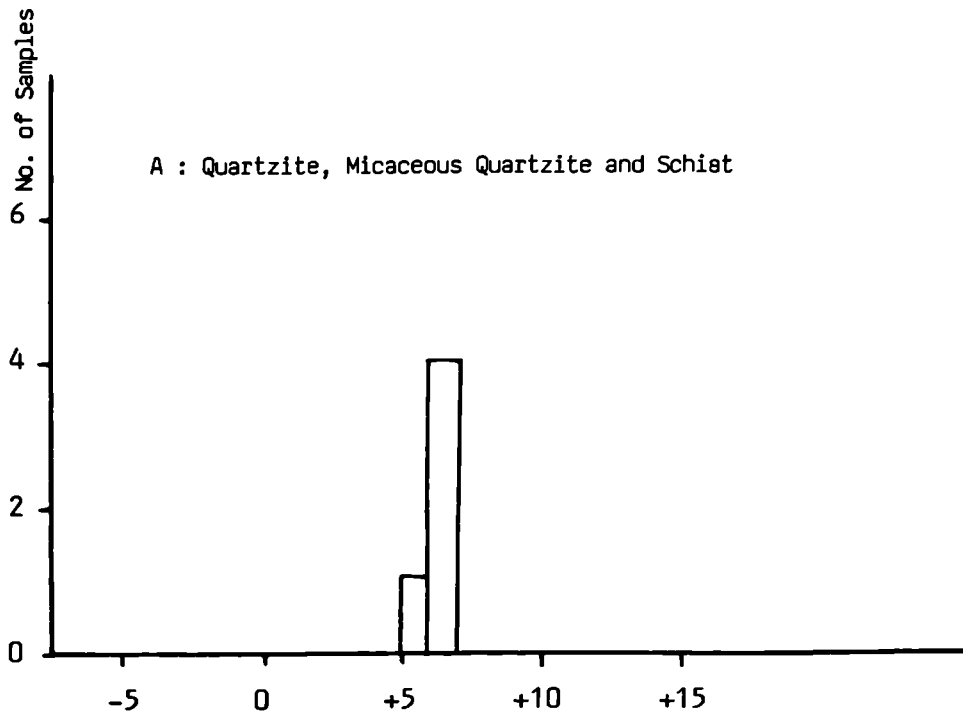
Fig. 7.7 : Summary of the variation of $\delta^{34}S$ of chalcopyrite in different lithologies.

was not complete at metamorphic conditions below upper amphibolite facies unless there was a change in mineralogy. Recently Willan and Coleman (1981 & 1983) presented the first sulphur isotopic data from the Dalradian mineralization, and they concluded that sulphur-bearing minerals have not reequilibrated over a distance of ~1cm during greenschist to lower amphibolite facies metamorphism and therefore, variations in the $\delta^{34}S$ must be due to variation at source and/or variation of the kinetic and equilibrium processes operating during ore formation.

Sakai (1968), Gavelin et al. (1960), Friedlich et al. (1964) and Yamamoto (1967) reported that in many polymetallic deposits a regular trend of isotopic fractionation exists among coexisting sulphide minerals and the order of enrichment in $\delta^{34}S$ is :

Pyrite > Sphalerite > Chalcopyrite > Galena

Fractionation factors, $\delta^{34}S$ for different mineral pairs have been calibrated as geothermometers (Smith et al. 1978, Friedman and O'Neil 1977). Figure (7.8) and Table (7.2) are taken from Ohmoto and Rye (1979), showing the best experimental fractionation factors and the theoretical equations between sulphur compounds relative to H_2S.

The measured isotopic fractionation data of eight pairs of coexisiting pyrite and chalcopyrite from the mineralised area are given in Table (7.3) together with the corresponding temperatures calculated using experimentally derived equations (Table 7.2) given by Ohmoto and Rye (1979). These authors show that the sensitivity of the pyrite-chalcopyrite pair, caused from a typical analytical uncertainty of ± 0.2 for the $\Delta^{34}S$ value is $40°C$ (Table 7.2). It is imperative to examine mineral pairs for impurities since apparent disequilibrium relationships may be due to impure separates, for example a sphalerite-galena pair formed in equilibrium at $145°C$ ($\Delta^{34}S=4.0$ ‰) would show an apparent $\Delta^{34}S$ value of 2.9 and hence an

Mineral Pair	Equation $(T$ in Kelvin; $\Delta = \delta^{34}S_A - \delta^{34}S_B)$	Uncertainties[a]	
		1	2
Sulfates-chalcopyrite	$T = \dfrac{2.85 \times 10^3}{(\Delta \pm 1)^{1/2}}$ $(T > 400°C)$	$\pm 25^3$	$\pm 5^3$
	$T = \dfrac{2.30 \times 10^3}{(\Delta - 6 \pm 0.5)^{1/2}}$ $(T < 350°C)$	± 10	± 5
Sulfates-pyrite	$T = \dfrac{2.76 \times 10^3}{(\Delta \pm 1)^{1/2}}$ $(T > 400°C)$	$\pm 25^3$	$\pm 5^3$
	$T = \dfrac{2.16 \times 10^3}{(\Delta - 6 \pm 0.5)^{1/2}}$ $(T < 350°C)$	± 10	± 5
Pyrite-galena	$T = \dfrac{(1.01 \pm 0.04) \times 10^3}{\Delta^{1/2}}$	± 25	± 20
Sphalerite(pyrrhotite) -galena	$T = \dfrac{(0.85 \pm 0.03) \times 10^3}{\Delta^{1/2}}$	± 20	± 25
Pyrite-chalcopyrite	$T = \dfrac{(0.67 \pm 0.04) \times 10^3}{\Delta^{1/2}}$	± 35	± 40
Pyrite-pyrrhotite (sphalerite)	$T = \dfrac{(0.55 \pm 0.04) \times 10^3}{\Delta^{1/2}}$	± 40	± 55

[a] 1 = uncertainty in the calculated temperature due to the uncertainty in the equation (at $T = 300°C$); 2 = uncertainty in the calculated temperature due to the analytical uncertainty of $\pm .2°_{oo}$ for Δ values (at $T = 300°C$); 3 = uncertainties in the calculated temperature at $T = 450°C$.

Table 7.2 : A summary of the best equations relating $\delta^{34}S$ and temperature for sulphur-bearing mineral pairs (from Ohmoto and Rye 1979).
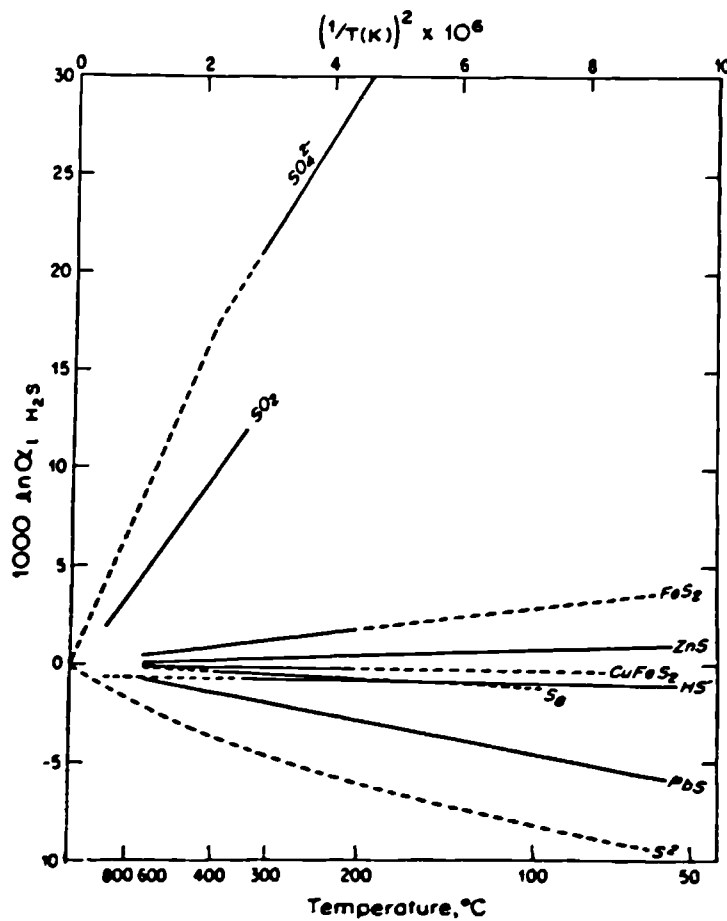
Fig. 7.8 : Equilibrium isotopic fractionation factors among
sulphur compounds relative to H₂S. Solid lines—
experimentally determined. Dashed lines--extra-
polated or theoretically calculated. The figure
is taken from Ohmoto and Rye 1979.

sample No.	contaminants	δ³⁴S ‰	δ³⁴S ‰	Δ³⁴S	T°C	Uncertainty T°C
HMM 7	less than 1% calcite	+7.0	+4.4	+2.6	146°C	40°C
HMM 12	pyrite with traces of marcasite, chalcopyrite is pure.	+6.8	+7.6	-0.8	disequilibrium	---
HMM 60	pure	+7.0	+6.7	+0.3	114°C	40°C
HMM 63	pure	+10.2	+5.2	+5.0	25°C	40°C
HMMI 39	pyrite with less than 0.1% covellite, chalcopyrite with less than 1% pyrite.	+6.6	+6.5	+0.1	1580°C	40°C
HMMI 69	less than 1% calcite	+8.5	+6.8	+1.7	240°C	40°C
HMMI 92	pure	+6.1	+6.3	-0.2	disequilibrium	---
HMMI 1	pyrite is pure while chalcopyrite contains less than 1% pyrite.	+7.9	+7.7	+0.2	1025°C	40°C

Table 7.3 : Sulphur isotope fractionation data for pyrite-chalcopyrite pairs from the Meall Mòr area.

apparent temperature of 215 °C, if each of the mineral separates contained 10 vol % of the other mineral phase (Ohmoto and Rye 1979). On the other hand Coomer and Robinson (1976) reported that the presence of calcite in the mineral separates gave no significant variation in $\delta^{34}S$ value. For example 100 % pyrite gives a $\delta^{34}S$ value of -33.8 ± 0.9 per mil, while a mixture of 50 % pyrite and 50% of calcite by volume gives a $\delta^{34}S$ value of -33.5 ± 0.8 per mil. The above two examples indicate that the $\Delta^{34}S$ of the eight mineral pairs of this study which may contain up to 1% sulphide impurities and 2% calcite impurity are not affected to the extent of being incorrect because of impurities.

The $\Delta^{34}S_{py-chp}$ for eight mineral pairs show considerable variation from -0.8 to +5.1 ‰ . This variation may be due to differences in temperature of formation or may reflect disequilibrium conditions. Most of the isotopic fractionation data for the analysed pyrite-chalcopyrite pairs indicate either fractionation factors deviating from isotopic equilibrium (negative $\Delta^{34}S$) (e.g. Samples HMM 12 & HMMI 92 or isotopic temperatures which seem to have no geological meaning. Very high temperatures are calculated for Samples HMM 60, HMMI 39 and HMMI 1 (1114 °C, 580 °C and 1025 °C respectively) while very low temperature is calculated for Sample HMM 63 (25 °C). Samples HMM 7 & HMMI 69 give apparent temperatures 146 & 240 °C respectively which are very low for the estimated (410° - 530 °C) temperatures of garnet amphibolite facies metamorphism in the SW-Highlands (Graham 1985). However, although the pyrite-chalcopyrite pairs are the less reliable pair among the sulphides (Ohmoto and Rye 1979), studies on the sulphur isotopic fractionation between coexisting pyrite and chalcopyrite minerals for Kuroko deposits in Japan by Kajiwara and Date (1971) gave a uniform distribution with $\Delta^{34}S$ values ranging from + 1.3 to + 1.6 per mil and this in turn gave reasonable isotope temperatures ranging between 250 to 300 °C implying the possibility of using the coexisting pyrite-chalcopyrite pair as a good reliable geothermometer. Nevertheless, sulphur isotopic fractionation

studies between pyrite and chalcopyrite in regionally metamorphosed deposits (e.g. Runnells 1969, Lusk and Crocket 1969, Bachinski 1977, Ripley and Ohmoto 1977 and Yamamoto et al. 1983) showed that there is no normal fractionation between most mineral pairs in such deposits.

Therefore, the isotopic fractionation data between the eight pyrite- chalcopyrite pairs of Meall Mór (-0.8 to +5.1‰) and the accordingly calculated apparent temperatures (25 to 1,114°C) suggest that they were not deposited in isotopic equilibrium nor were they reequilibrated during greenschist to lower amphibolite facies metamorphism. The latter suggestion is in keeping with other isotopic evidence on the lack of reequilibration for other Dalradian mineralisations at Aberfeldy (Willan and Coleman 1983 and Fisk 1986) and at Auchtertyre Fisk 1986 and Scott 1987). Although Moles (1983 & 1985 argued for equilibration during metamorphism of the Aberfeldy deposit on the basis of both isotopic and silicate equilibrium evidence.

Abnormal sulphur isotopic temperatures can be obtained if chal opyrite and pyrite are not contemporaneous (Ohmoto and Rye 1979 . This is because pyrite tends to precipitate over a much longer period of the paragenesis than chalcopyrite allowing less chance for the minerals to precipitate under identical conditions. On the other hand, the sulphur isotopic composition of the fluid and the temperature may not be uniform enough to give useful temperatures.

Accordingly, the present isotopic fractionation data of the Meall Mór pyrite-chalcopyrite pairs is regarded as the original depositional values. These original variations imply a disequilibrium condition during sulphide precipitation. Pyrite and chalcopyrite do not necessarily reach isotopic equilibrium under normal hydrothermal conditions Ohmoto and Rye 1979 because formation of pyrite and chalcopyrite from iron and copper complexes

in the solution involve redox reaction that requires both H_2S and SO_4^{2-} according to the following reactions (taken from Ohmoto and Rye 1979):

$$4Fe^{2+} + 7H_2S + SO_4^{2-} \longrightarrow 4FeS_2 + 4H_2O + 6H^+$$

$$8Cu^+ + 8Fe^{2+} + 15H_2S + SO_4^{2-} \longrightarrow 8CuFeS_2 + 4H_2O + 22H^+$$
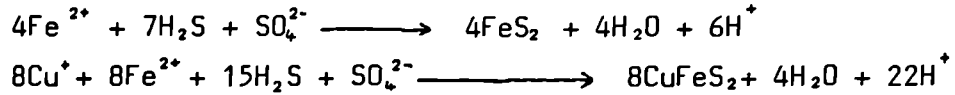
Pyrite and chalcopyrite formed in such a disequilibrium system may inherit the $\delta^{34}S$ values of H_2S and SO_4^2 in such manner as:

$$\delta^{34}S_{py} = 7\,8\ \delta^{34}S_{H_2S} + 1/8\ \delta^{34}S_{SO_4^{2-}}$$

$$\delta^{34}S_{chp} = 15/16\ \delta^{34}S_{H_2S} + 1/16\,\delta^{34}S_{SO_4^{2-}}$$

7.5.2 Variation of $\delta^{34}S_{sulphide}$ and the Source of Sulphur

It is impossible to elucidate the source of the sulphur from the isotopic data alone since sulphides of the same genesis may exhibit different $\delta^{34}S$ distribution and those of different genesis may have similar $\delta^{34}S$ values and show similar $\delta^{34}S$ distributions. The sulphide sulphur in many base metal deposits is thought to have a dual origin, being carried as reduced sulphur in the mineralising solutions and mixed sulphide formed by reduction of seawater sulphate Ohmoto and Rye 1979 and Brock 1980). Reduced sulphur could originate by bacterial sulphate reduction at low temperature with large fractionation; or from sulphide contained in the sedimentary pile; and or sulphate reduced to H_2S by abiological reaction with organic matter equation (1), Dhannoun and Fyfe 1972, Toland 1960 and Kiyosu 1980) or ferrous iron (equation (2), Hajash 1975, M ttl et al. 1979 and Seyfried and Dibble 1980) at temperatures greater than 250°C.

$$2CH_2O + SO_4^{2-} \longrightarrow 2CO_2 + 2H_2O + S^{2-} \qquad (1)$$

$$8Fe^{2+} + 8H^+ + SO_4^{2-} \longrightarrow 8Fe^{3+} + 4H_2O + S^{2-} \qquad (2)$$
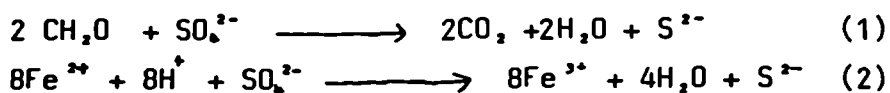
This latter process would lead to H_2S with an isotopic c mposition of up to 25 % lower than the original $\delta^{34}S$ of the

sulphate depending on temperature (Ohmoto et al. 1976 and Ohmoto and Rye 1979).

The present study shows that sulphur isotope compositions of pyrite and chalcopyrite from the studied area is in the range +4.43 to +12.76 per mil (Fig. 7.1). Isotopic composition of Late Precambrian-Lower Cambrian seawater sulphate (Fig. 7.9) measured from evaporitic sequences in Siberia, Australia and North America ranges from +24 to +35 per mil with a mean of +30 per mil (Claypool et al. 1980). An isotopic composition of +35‰ has been suggested for the Dalradian seawater in restricted basins such as in Aberfeldy by Willan and Coleman (1983). Assuming the same value of 35‰ for Meall Mor, this leads to a $\Delta^{34}S_{sw\ -ss}$ from 22.2 to 30.6 for the present samples Fig. 7.10).

Similar isotopic compositions were reported by Willan and Coleman 1981 & 1983 for sulphides from some Dalradian stratiform mineralisations and from Auchtertyre mineralisation with average of +6.3 and +7.2 per mil resulting in average $\Delta^{34}S_{sw\ -ss}$ values of 28.7 and 27.8 per mil respectively. The source of sulphur in these deposits was considered to be a bacteriogenically reduced seawater sulphate. Accordingly, the isotopic composition of the Meall Mor sulphides might suggest a bacterial reduction of seawater sulphate as a source for the sulphur in the sulphides. However Rye and Ohmoto 1974 pointed out that a deposit cannot be proven to be bacteriogenic in origin on the basis of the range or statistical distribution of $\delta^{34}S$ values alone. Caution is required because some deposits previously considered bacteriogenic on this basis have been shown, on reexamination with careful attention to geological and geochemical details to have resulted from inorganic processes. Bearing this in mind, the consistent $\delta^{34}S$ of the present analysed sulphides, their narrow range of variation with the majority (n=29) having $\delta^{34}S$ ranging from 6 to 9 per mil and the lack of isotopic equilibrium between the pyrite and chalcopyrite suggest that the sulphur in the sulphides was not produced by bacterial reduction of

288
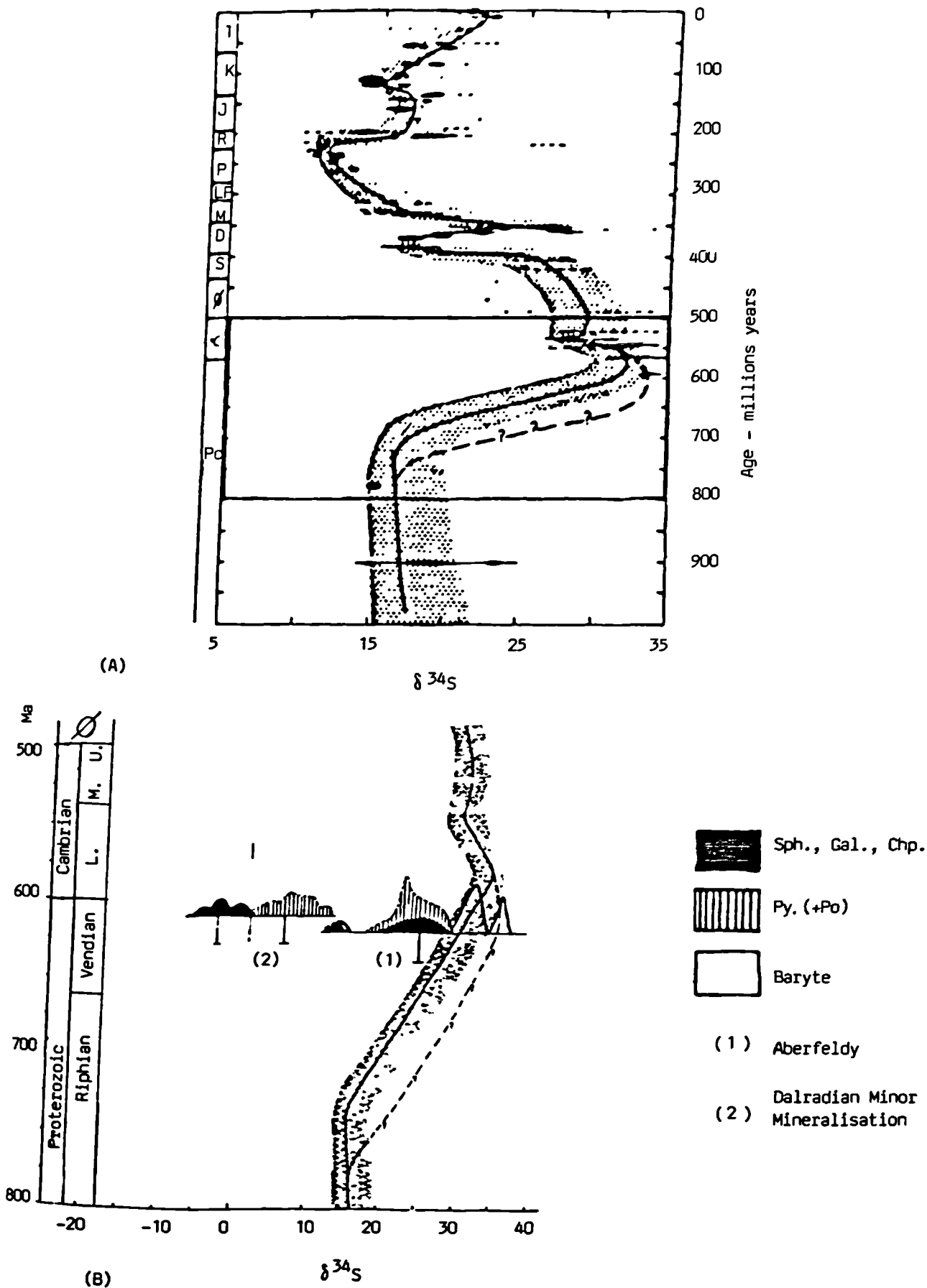
Fig. 7.9 : (A) : Summary sulphur isotope age curve for marine sulphate (Claypool
et al. 1980). (B) : The distribution of sulphur isotope ratios
in the Dalradian compared with Late Precambrian and Cambrian age
curve (Willan 1983). The vertical line indicates the age uncer-
tainty for each deposit.
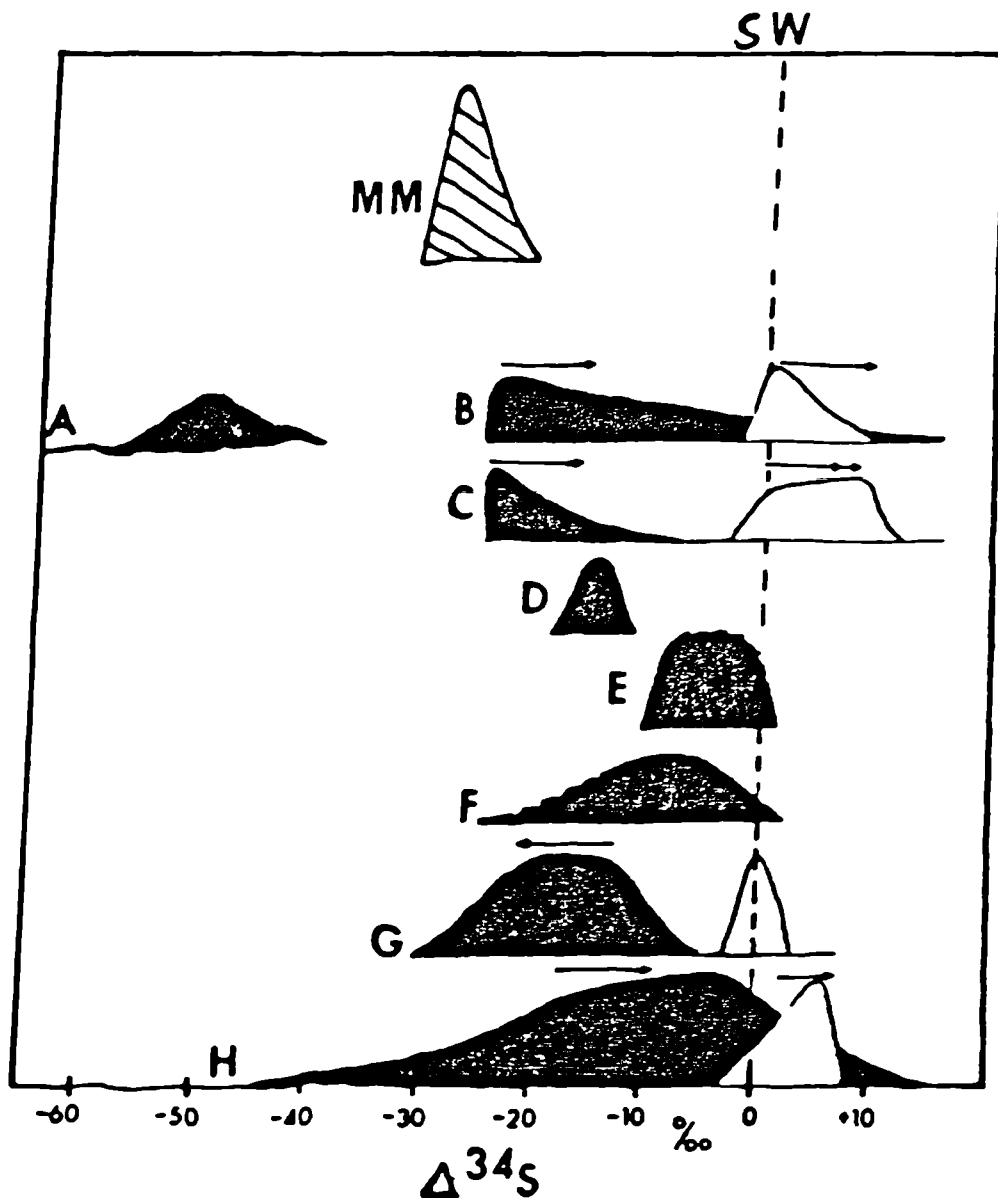
(A) : Bacteriogenic sulphide precipitated in an environment open to influxes of sulphate
and removal of sulphide, in which the rate of reduction of sulphate is slow, e.g.
deep water euxinic enviroments and some shallow water enviroments.

B) : Bacteriogenic sulphide and residual seawater sulphate in an enviroment closed to
influxes of fresh sulphate, e.g. enclosed marine basins and lagoons and beneath
basal brine layers or the sediment/water interface.

(C) : As for (B), except closed to the removal of sulphide.

(D) : H_2S derived from the thermal decomposition of organic compounds above 50 C.

(E) : H_2S derived from seawater sulphate reduced by reaction with carbonaceous material
above 250 C (Kiyosu 1980).

(F) : H_2S derived from seawater sulphate by reaction with ferrous minerals above 250 C.

(G) : The isotopic spread in volcanic-hosted deposits.

(H) : The isotopic spread in sediment-hosted deposits (Sasaki and Kajiwara 1971).

Fig. 7.10 : The $\delta^{34}S$ distribution of Meall Mor sulphide (MM) in the
Dalradian plotted as $\Delta^{34}S$ between seawater and sulphide,
compared with $\Delta^{34}S$ values of sulphide and sulphate when
sulphate is reduced by various mechanisms to sulphide
from Ohmoto and Rye 1979). Baryte (hollow distribution)
and sulphide (solid distribution). SW=parental-.sea-water
sulphate. The arrows indicate the trends with time.

the seawater sulphate. Therefore, in this section an attempt is made to elucidate carefully the possible source for the sulphide sulphur after considering the previously discussed geological, textural, mineralogical and geochemical evidence.

The presence of local premetamorphic hydrothermal alteration expressed by the local development of epidote, spessartine garnet and cross-cutting quartz and/or calcite veins bearing sulphide porphyroblasts, together with the unimodal distribution of Meall Mór $\delta^{34}S$ sulphides (Fig. 7.1), the similarity of the distribution and mean values of both pyrite and chalcopyrite, the very low variance $\sigma=1.67$, the lack of isotopic equilibrium between pyrite and chalcopyrite and the similarity of disseminated, vein and stratiform sulphides suggest that sulphur carried in hydrothermal fluid together with Cu, Mn, Fe, CO_2, Ca, Au and Ag is the main source for the Meall Mór sulphides. Oxygen isotope analyses of two quartzitic samples from Meall Mor yielded values of around 8%. suggesting a mixture of detrital and hydrothermal components (Fisk 1986).

Sulphur carried in hydrothermal fluid could originate from sulphur leached from sulphides contained within the sedimentary pile, ulphur leached from the epidiorite rocks, inorganic reduction of seawater sulphate or a combination of these. The obtained isot pic comp siti ns of Meall Mór sulphides with $\delta^{34}S$ values ranging from +4.4 to 12.8 per mil suggest that sulphur leached from epidi rites is not the only source and that sulphur from seawater sulphate is also in orporated into the formation of the sulphides. But the la k of 1 ot pic equilibrium between the analysed pyrite and chalcopyrite could possibly reflect a disequilibrium condition between H_2S and SO_4 carried by the hydrothermal fluid (see Sakai et al. 1980 . Accordingly it is very difficult to quantify the relative contribution of sulphur from the basalt and that from seawater sulphate. The evidence for the presence of sulphur as SO_4 or H_2S in the hydrothermal fluid is difficult to resolve. It was concluded earlier on the basis of mineralogical and geochemical

evidence that the hydrothermal fluid is capable of carrying sulphur together with Cu, Mn, Ca, SiO_2, CO_2, Fe, Co, Ni, Ag and Au.

The geochemical conditions of the hydrothermal fluid responsible for this hydrothermal alteration and ore mineralisation is not well understood at this stage due to the lack of sufficient isotopic data. Information concerning the chemistry of the trapped fluid might be obtained later from the results of fluid inclusion work on calcite and quartz bearing sulphide veins from the Abhainn Srathain copper mineralisation. Therefore delineation of the chemical parameters of the hydrothermal fluid at this stage is considerably difficult. However it still possible to suggest approximate limits on some of the chemical parameters, such as temperature, oxygen fugacity, sulphur fugacity and pH for the mineralising fluid, based on published equilibrium thermodynamic data and on mineral assemblages present in the area.

Styrt et al. 1981) have shown that deposits with copper are associated with solutions existing at temperatures close to $350°C$ on the East Pacific Rise. This association is in keeping with the experimental data of Crerar and Barnes (1976) who found a rapid decrease in the solubility of chalcopyrite in NaCl solutions between 350 and $250°C$. Assuming a temperature between $250°C$ and $350°C$ for the Meall Mòr fluid and applying the calculated equilibrium thermodynamic data presented by Hayba et al. (1985, Figs. 7.18 & 7.19 for the Summitville ores, the pH of the hydrothermal fluid might be between 4.5 & 6 based on the occurrence of muscovite rather than K-feldspar. Also the presence of pyrite as the major iron-bearing species with chalcopyrite, magnetite and hematite set the limits of Log aS_2 and Log aO_2 at between -10 to -11 and -33 to -35 respectively. Under these conditions, sulphur carried in the hydrothermal fluid is in the form of H_2S and SO_4 .

From the above discussion it can be assumed that inorganically reduced Dalradian seawater sulphate together with some sulphur from the enclosed basaltic rocks is the source of sulphur for the sulphides. This is in contrast with the stratiform nature of the mineralisation in which part of the reduced sulphur is expected to be bacteriogenically reduced Dalradian seawater sulphate. However the $\delta^{34}S$ for the analysed pyrite sampled through the Knapdale Pyrite Horizon has values close to $\delta^{34}S$ of the analysed sulphides at the site of the Abhainn Srathain copper mineralisation suggesting that the local sulphur values for the sulphides by bacteriogenic reduction has an average of +7‰ on one hand and making it difficult to differentiate between bacteriogenic and hydrothermal sulphides on the other hand.

7.6 SUMMARY AND CONCLUSION

The $\delta^{34}S$ values of the analysed sulphides are very consistent ranging between +4.4 and 12.8 per mil and averaging around +7.4 per mil $\sigma=1.67$. The majority of the analyses (n=29) have $\delta^{34}S$ ranging between +6 and +9 and averaging +7.2 per mil ($\sigma=0.77$). The mean 1 t pic value for pyrite is +7.6 per mil ($\sigma = 1.71$) and for chalc pyrite is +6.4 per mil $\sigma=1.05$.

The unimodal distribution of the sulphur isotope ratios, their narr w range of variation, their consistent values regardless of p siti n, depth, lithology and style of mineralisation, the lack of equilibrium between pyrite and chalcopyrite are all evidence indi ating that sulphides originating by bacterial reduction is a le s likely mechanism and suggesting that a single source of sulphur was a tive in the formation of the different styles of mineralisation. Sulphur carried in hydrothermal solution with Cu, Mn, Fe, CO_2, Ca, Ag and Au is the source of sulphur for the sulphide. This is supported by the presence of local premetamorphic hydr thermal alteration of the host rocks. The sulphur carried in the hydrothermal fluid is a mixture of inorganically reduced

Dalradian seawater sulphate and sulphur leached from the enclosed basaltic rocks.

Testing the applicability of the isotopic geothermometry of the pyrite-chalcopyrite pair, indicate disequilibrium situations in this deposit which underwent upper greenschist to lower amphibolite facies metamorphism. This supports the view that no equilibration has occurred during metamorphism and that original values are preserved through metamorphism. This lack of equilibrium also means that no major remobilisation of the disseminated sulphides by late metamorphic fluids and redeposition in cross-cutting veins as proposed by Smith et al. (1978) has taken place.

CHAPTER 8
A MODEL FOR THE MEALL MÓR COPPER MINERALISATION

8.1 INTRODUCTION

In this concluding chapter, an attempt is made to construct a possible geometrical model for the Abhainn Srathain copper mineralisation based on evidence from the published information on the geologic setting summarised in Chapter 3, characteristics of the mineralisation in relation to the other stratiform Dalradian mineralisation summarised in Chapters 2 and 4 and on the present mineralogical, geochemical and isotopic studies of this thesis discussed in Chapters 5, 6 and 7 respectively. The evidence form Sections 8.2 to 8.6, while Section 8.7 describes a geometrical model of the events that led to the formation of the Abhainn Srathain copper mineralisation. Some suggestions for more research in the area constitute Section 8.8 of this chapter.

8.2 CONCLUSIONS REGARDING THE EVOLUTION OF THE DALRADIAN BASIN PARTICULARLY IN THE STUDIED AREA

The Dalradian Supergroup was deposited in a basin undergoing subsidence as a result of lithosphere stretching. During the late Riphean, gentle subsidence to the south resulted in the deposition of the Grampian and Appin Groups consisting of thin sands, muds and stromatolitic limestones and dolomites which accumulated in shallow water tidal flats and intra-cratonic shelves. This was followed during early Vendian time by an increase in instability resulting in the formation of major syndepositional faulting characterising the time of deposition of the Argyll Group. By mid-Vendian time (during the deposition of the Easdale and Crinan Grits Subgroups), the Dalradian terrain underwent major rifting and was broken into a series of fault-bounded marginal shelves depositing shallow water

295

evaporitic sediments and deep second-order basins depositing thick sedimentary sequences of arenites and subarkoses. This was also accompanied by pretectonic igneous activity, especially in the Islay-Loch Awe area, expressed by progressive sill intrusions from bottom to top. Each sill was injected at a shallower depth into soft sediments, a process similar to the present day Gulf of California. Further increase in the crustal tension led by the end of the Precambrian or early in the Cambrian ($\sim$600 Ma) to the extrusion of the tholeiitic Tayvallich Volcanics.

During the Argyll Group depositional time, several subsidence episodes took place as a result of increasing extension and thinning of the basement marked by several sedimentary turning points. This was highly extensive during the Easdale and Crinan Grits Subgroups, and in places was accompanied by hydrothermal activity as a result of high geothermal gradient caused by increasing extension and thinning of the basement permitting percolation of Dalradian seawater down into the hot sedimentary pile.

8.3 CONCLUSIONS REGARDING THE FIELD CHARACTERISTICS OF THE MINERALISATION AND ITS AGE IN RELATION TO OTHER STRATIFORM DALRADIAN MINERALISATIONS

The Meall Mór copper mineralisation forms one of several mineralised localities within the Dalradian Supergroup of the Grampian Highlands of Scotland. It is contained within a zone of weak pyritic enrichment consisting mainly of orthoquartzites and quartz-mica schists of the Upper Erins Quartzite. A zone of weak stratiform pyrite enrichment, traceable for about 190km from Knapdale to Glenshee through the Ben Lawers and the equivalent formation (Ardrishaig phyllite and the ?Upper Erins Quartzite) was delineated by B.G.S. workers and implies that the Perthshire Pyrite Horizon and the Knapdale Pyrite horizon are of the same age. However, lithostratigraphic correlations described earlier in Section (3.3.1) correlate the Lower Erins Quartzite to the

296

Ardrishaig Phyllite; the Stronchullin Phyllite to the St. Catherine's Graphitic Schist and the Upper Erins Quartzite to the Crinan Grits, suggesting that the Knapdale Pyrite Horizon is a younger development of pyritic enrichment rather than an along-strike extension of the Perthshire Pyrite Horizon. Whatever the stratigraphic position is, the weak pyritic enrichment of the Knapdale Pyrite Horizon is the result of weak exhalative activity accompanying the deposition of the Upper Erins Quartzite Formation probably at about the time of the major sedimentary turning point from the calcareous muds of the Ardrishaig Phyllite and its equivalent Lower Erins Quartzite to the pebbly feldspathic sands of the Crinan Grits and the laterally equivalent the Upper Erins Quartzite.

Throughout the Knapdale Pyrite Horizon, pyrite occurs in fine disseminated grains and in trails parallel to the bedding and early schistosity with small quantities of chalcopyrite and sphalerite distributed sporadically. It also occurs in stratiform laminations and in stratiform blebs and trails. In places the quartzitic rocks contain alternating thin pyrite and sphalerite laminations indicating the stratiform exhalative nature of this horizon.

In the area between Meall Mór summit and the Abhainn Srathain region and still within the Knapdale Pyrite Horizon, the amount of chalcopyrite together with pyrite increases towards the south with the maximum development being around the area where several epidioritic bodies exist near the site of the old mine workings and where the host rocks, both epidiorites and metasediments, are being epidotised and carbonated. The sulphides, both pyrite and chalcopyrite, show contrasting styles of mineralisation. They occur as fine disseminations, stratiform layers and laminations and as large porphyroblasts up to 5cm across in quartz and/or calcite veins that are either parallel to the compositional layering or cross-cutting it.

8.4 CONCLUSIONS REGARDING THE TEXTURES, MINERAL ASSEMBLAGES AND MINERAL CHEMISTRY OF BOTH THE ORE MINERALS AND THE HOST ROCKS

The occurrence of weak disseminated pyrite enrichment with small amounts of chalcopyrite and sphalerite in the quartzitic rocks of the Upper Erins Quartzite with local stratiform sulphides in alternating laminations classify, with no doubt, the Knapdale Pyrite Horizon as of syngenetic exhalative nature. On the other hand, the Abhainn Srathain copper mineralisation displays complex microscopic textures implying a bimodality in their interpretation which at the outset, make the mineralisation look epigenetic but also provide evidence of originally syngenetic deposition.

The Abhain Srathain copper mineralisation has some textural characteristics considered to be syngenetic implying that the mineralisation and the Knapdale Pyrite Horizon formed as a result of the same hydrothermal activity. The most important of these, is the stratiform thin layers or laminations that are parallel to the compositional layering in both the epidiorites and the metasediments quartzites and schists). Although in the schistose host rocks it is difficult to ascertain whether such textures are primary sedimentary features, the presence of deformed (folded) sulphide laminations in quartzitic rocks demonstrates their premetamorphic nature. On the other hand, the presence of large sulphide porphyroblasts in cross-cutting veins together with the epidotisation and carbonation of the host rock were considered by some workers as evidence for epigenetic origin of the cross-cutting copper mineralisation and were interpreted to be formed as a result of mobilisation either during regional metamorphism (Smith et al. 1978) or during sill intrusions (Willan 1983). However, the presence of discontinuous stratiform chalcopyrite layers and laminations within the epidiorites themselves, together with the alternating banded nature of the epidotised and nonepidotised epidiorites, which locally show very fine alternating contrast laminations, suggest that sill intrusion very shortly predated the

cross-cutting copper mineralisation. Also, the strongly developed metamorphic fabrics expressed by recrystallisation, deformation and local mobilisation of the ore minerals and the host assemblages together with the presence of a few deformed quartz and/or calcite veins indicate with a greater degree of confidence that the cross-cutting copper mineralisation predated the metamorphism.

Variable chemical compositions of the analysed minerals within one microscopic section exist, suggesting that equilibrium during metamorphism was not attained on the scale of microscopic section and therefore there is less chance that major mobilisation had occurred.

The presence of Mn-rich garnets preferentially within the site of cross-cutting mineralisation and to a lesser extent Mn-bearing ilmenite and chlorite, gold-bearing pyrite and silver-bearing covellite indicate that Mn, Au, and Ag were present in the hydrothermal solution. The sporadic occurrence of garnet is related to the presence or absence of sedimentary Mn-enrichment. The lack of baryte or any celsian rocks within the mineralisation could probably be interpreted as indicating the primary absence of barium in the hydrothermal solution.

8.5 CONCLUSIONS REGARDING THE PREMETAMORPHIC HYDROTHERMAL ALTERATION OF THE HOST ROCKS

Chemical analysis of the host rocks revealed the presence of coeval tuffaceous material during the time of the deposition of the Upper Erins Quartzite and indicated the local premetamorphic hydrothermal alteration of the host rocks during ore formation. During this process, the argillaceous and arenaceous sediments together with the sill bodies were partially altered either to epidote, quartz, calcite, chlorite, K-mica, spessartine-rich garnet, sulphides and minor oxides or to their premetamorphic precursors. Similar hydrothermal mineral assemblages have been recognised in

several present active geothermal systems and may also occur in
regional low-grade metamorphic rocks. But the strong association
between these locally diverse metamorphic minerals and the
cross-cutting copper mineralisation in the area suggests that they
are not the product of regional low-grade metamorphism of normal
sediments.

Hydrothermal alteration in active geothermal fields has been
reviewed and described recently by Browne (1978) who concluded that
temperature, pressure, rock type and permeability are the main
factors controlling the formation of hydrothermal minerals which
vary in relative importance from field to field. McKibben (1979)
focussed on the genesis of hydrothermal ores including pyrite,
hematite, sphalerite, chalcopyrite, pyrrhotite, marcasite and
galena. These sulphides occur as (1) synsedimentary/diagenetic
below $250^\circ C$, (2) metamorphic sulphides above $250^\circ C$ or (3) as
sulphide-dominated vein mineral assemblages below 750m depth.

There are similarities, in terms of petrological, mineralogical
and textural characteristics between the proposed hydrothermal
alteration associated with the cross-cutting copper mineralisation
and the active geothermal system, East Mesa in the Salton Trough of
California Elders 1981 where original Plio-Pleistocene deltaic
sediments are altered to quartz + epidote + chlorite + albite +
phengite + calcite + actinolite + sphene assemblages at above $300^\circ C$
(McDowell and Elders 1980).

However, in the studied area, as the rocks were later
regionally metamorphosed to greenschist facies it is very difficult
to assume what were the originally-formed hydrothermal minerals.
Anyway, if the present mineral assemblages are the recrystallised
equivalents of the original hydrothermal minerals or the metamorphic
equivalents of their precursors it is evident from their
mineralogical and textural characteristics that ascending
metalliferous hot water at $>250^\circ C$ and at a shallow depth had reacted

with the wet, unlithified sands, shales and arkoses and the epidiorite body and caused silicification of the porous sandy lithology and the epidiorite body. Also, at this stage of alteration, the phyllosilicates and other detritals were altered to epidote, quartz, chlorite, K-mica, Mn-rich garnet, actinolite, sphene, pyrite and chalcopyrite. This was followed by a second stage where descending cold seawater reacted with the hot rocks and dissolved silica and precipitated calcite with minor oxides in hydrothermal cycles similar to what was suggested for the Salton Trough geothermal systems (Elders 1981, Muffler and White 1969 and McDowell and Elders 1979).

8.6 CONCLUSIONS REGARDING THE SOURCE OF SULPHUR

Disseminated and stratiform pyrites of the Knapdale Pyrite Horizon give isotopic values ranging between +4.5 to 12.8 per mil and averaging 8.7 per mil, representing local sulphur values for sulphides formed as a result of bacteriogenically reduced Dalradian seawater sulphate in the area. Similar isotopic values are obtained for sulphides from the Abhainn Srathain copper mineralisation ranging between +4.4 to 12.8 per mil and averaging around +7.4 per mil and were interpreted with the textural, mineralogical and geochemical data to be inherited from sulphur values within the hydrothermal solution formed by a mixture of inorganically reduced d wnward percolating Dalradian seawater sulphate and sulphur leached from the igneous rocks within the sedimentary pile.

Unfortunately, from the obtained sulphur isotope compositions it is very difficult to differentiate between bacteriogenic and hydrothermal sulphides in terms of their sulphur isotopic values.

Isotopic geothermometry of the pyrite-chalcopyrite pairs indicates disequilibrium conditions during the regional metamorphism and therefore precludes the possibility that the cross-cutting Abhainn Srathain copper mineralisation was formed by remobilisation

301

of copper from the Knapdale Pyrite Horizon during metamorphism.

8.7 MODEL FOR THE FORMATION OF THE ABHAINN SRATHAIN COPPER MINERALISATION

On the basis of the preceding discussion it is possible to construct a geometrical model summarising the event that led to the formation of the Abhainn Srathain copper mineralisation (Fig. 8.1). The nature, source and chemistry of the hydrothermal solution is not considered here because such parameters are very difficult to examine in a metamorphic terrain. Instead it is assumed therefore that a hydrothermal solution capable of carrying the metals and sulphur and depositing them when possible is the required hydrothermal solution. An outline of the proposed geometrical model will be summarised below and although it might not be the only one, I believe it is a suitable model that explains the data.

1. Arenaceous and argillaceous sediments of the Upper Erins Quartzite have been deposited in an evolving unstable Dalradian basin broken into a series of blocks and basins bounded by synsedimentary faulting. Deposition of the Upper Erins Quartzite and the underlying formation, the Lower Erins Quartzite, was associated with pretectonic igneous activity as a result of increasing thinning and stretching expressed by the coeval tuffaceous materials and by the shallow intrusion of sill bodies.

2. Intrusion of the sill bodies at shallow depth into the wet and unlithified porous sediments of the Lower Erins Quartzite and part of the Upper Erins Quartzite together with increasing thinning of the crust resulted in the shallow convection of the seawater.

3. The descending seawater is then heated through its percolation down the high geothermal gradient and changes its chemistry by losing Mg, Na and SO_4 and gaining Si, Fe, Ca, Al, K, Ti, Mn, S, CO_2, Cu, Ag, Au, Zn and other elements leached from the sedimentary pile

302
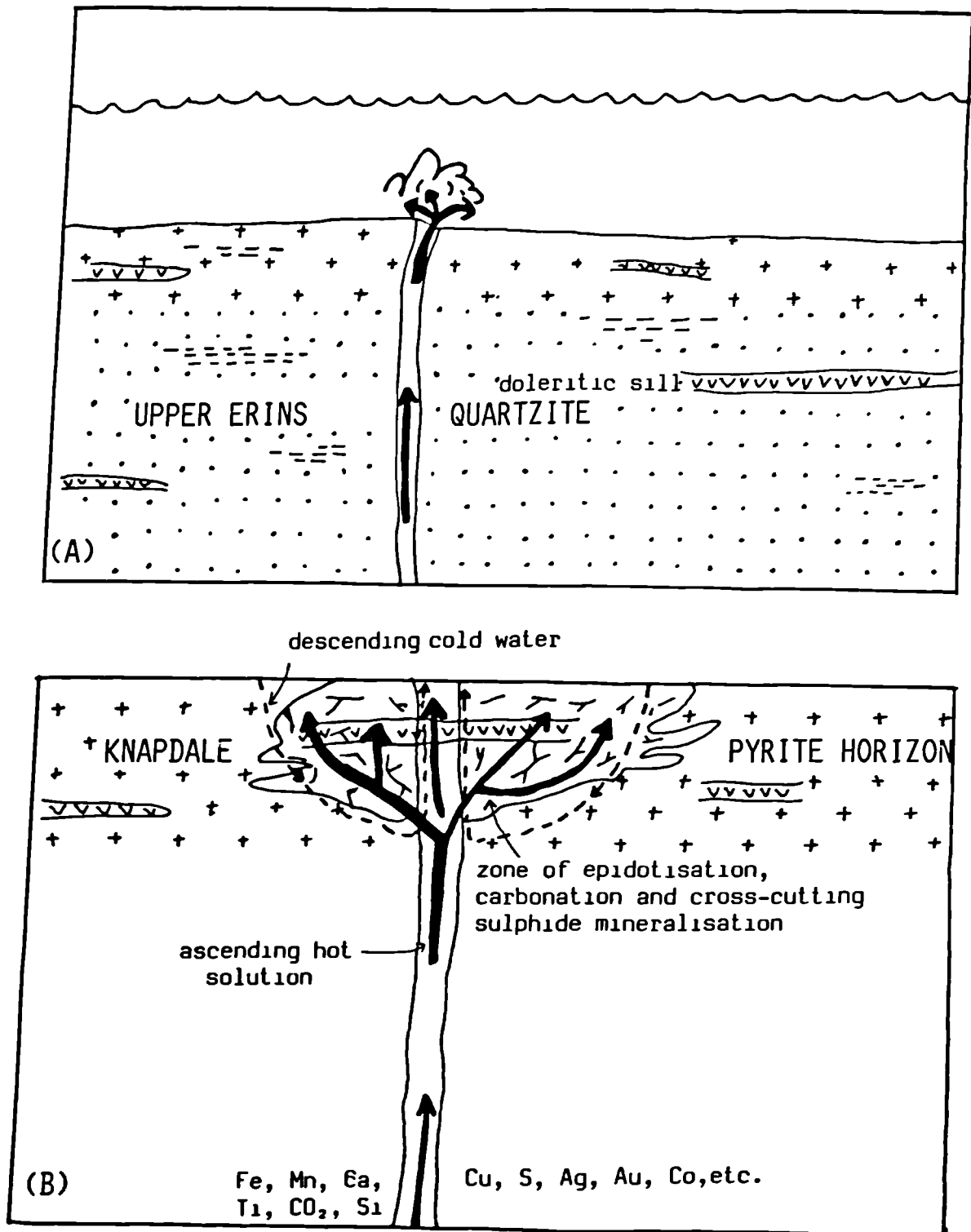
Fig. 8.1 : Schematic diagram for the formation of the Abhainn
Srathain, Meall Mór, copper mineralisation and the
Knapdale Pyrite Horizon. (A) early stage, (B) late
stage.

303

(Seyfried and Mottl 1982).

4. This modified seawater is then carried upwards and the initial stage is expressed by weak exhalation during mid-time deposition of the Upper Erins Quartzite to form the Knapdale Pyrite Horizon.

5. Increasing intensity of this exhalative activity resulted in the creation of geothermal systems. It is believed that one of these geothermal systems was centred at the site of the present Abhainn Srathain copper mineralisation and possibly shortly after the intrusion of the epidiorite sills in the area.

6. The ascending hot modified seawater ($>250^{\circ}C$) reacted with the arenaceous and argillaceous sediments and the epidiorite rocks at shallow depth and precipitated pyrite and chalcopyrite as disseminations, thin layers parallel to the lithological layering and as coarser grains in cross-cutting quartz veins. Also, at this stage silicification of the porous sandy lithologies, transformation of the sediments into quartz, phengite, epidote, chlorite, K-mica, albite, Mn-rich garnet and the epidiorites into epidote, actinolite, quartz and Mn-rich garnet assemblages took place.

7. At the same time, descending cold water into these hot rocks resulting from the shallow intrusion of the sills in the area caused another stage of alteration by dissolving silica and precipitating calcite and minor oxides both as free calcite grains and cross-cutting veins.

8. The hydrothermal system then started to die and this was marked by very weak exhalation and deposition of pyrite with traces of chalcopyrite and sphalerite at distal places.

9. Later all the rocks and the ore minerals underwent polyphase deformation and regional metamorphism during Lower Ordovician time. Some of the stratiform textures are preserved but the majority of

the original textures were destroyed and replaced by metamorphic fabrics.

8.8 SUGGESTIONS FOR MORE RESEARCH IN THE AREA

This study shows that in the Meall Mór area there are some problems that are still needed to be solved in order to understand the mineralisation in more detail. Stratigraphic work is needed to ascertain correlations between formations outcroping in this area and their lateral equivalents in the Central Highlands in order to understand the age relationship between the Knapdale Pyrite Horizon and the Perthshire Pyrite Horizon. Detailed surface mapping and more drilling are needed to unravel the complex structure at the mine area in order to know which way up the rocks are. Also, more structural investigations are needed in the area 200-300m to the NW of Meall Mór where another zone 39-70m wide with pyritic enrichment exists Fig. 3.8 in an attempt to examine the possibility of this being a tectonic repetition of the main zone.

No Sb-bearing mineral was identified in this study but the strong anomalous distribution of Sb shown by the B.G.S. geochemical drainage survey and the similarity in the distribution of Sb and Cu is worth investigation. Also, the presence of thin alternating pyrite and sphalerite laminations in quartzitic rocks could be a promising target for sphalerite mineralisation in the area.

Much work needs to be concentrated on the quartz and/or calcite veins especially a fluid inclusion study in order to get some information about the solution from which these minerals crystallised and the temperature at which crystallisation took place.

The presence of highly localised metamorphic minerals, Mn-rich garnets and epidiorite bodies are all clues that can be used in exploring for similar mineralisation within the Knapdale Pyrite Horizon and within the Dalradian as a whole.

305

<u>Appendix (A.5.1)</u>: Preparation of petrographic sections.

In the Department of Applied Geology where this work is undertaken, different types of sections can be prepared using conventional techniques by the technical staff. These include thin section, polished block, polished-thin section, and polished wafers. The polished wafers are used to study fluid inclusions trapped in minerals during their growth. Only three types of sections were used in this study, for petrographic and microprobe analysis purposes, and the procedure for their preparation will be outlined briefly.

(A) Thin Section

Thin sections are prepared by cementing thin slice of rock to glass, followed by hand grinding to 30 micron, using 400 to 600 mesh carborundum and water on glass. Finally a cover slip is cemented on top of the layer of rock using Canada *Balsam*.

(B) Polished Blocks

Polished blocks are used to study opaque minerals under the reflected light microscope and for microprobe analysis also. It represents a rock fragment set in resin and polished. There are many different procedures for the preparation of a flat polished surface free of relief and scratches, depending on the nature of the rock, polishing materials, and equipment available (e.g. Lister 1978).

(1) Cutting

Rocks were cut into pieces measuring 2cm x 2cm x 0.5cm with a diamond saw and were cleaned ultrasonically for three minutes, dried and labelled.

(2) Mounting

The cleaned sample was placed in a mould, back upwards, containing 35g of Fazaplas 105 resin, premixed with 2 drops accelerator and 6 drops catalyst. Vacuum

306

pumping were used to avoid air bubbles. The sample with the resin is left over about 12-24 hours to harden. It was then trimmed to a thickness of 14mm to produce parallel sides and a hole is drilled in the back surface.

(3) Grinding

Each block was ground by Logitech machine using 400 mesh carborundum and water as lubricant. This was followed by three stages of hand-grinding using 600, 800, and 1000 mesh carborundum and water. Each grinding stage lasted approximately ten minutes. The block should be cleaned ultrasonically inbetween stages.

(4) Polishing

Prior to polishing, each block was examined under reflected light binocular microscope (x 100 magnification) to make sure that the specimen is free from pits and scratches. Specimen was polished on Engis Kent Mark 2A machine, on P.S.U Pellon cloth laps, and using 6, 3, 1, and 1/4 mesh diamond paste as abrasive and Hyprez lubricant. Slow polishing speeds (100 rev/min, and polishing load of 0.5-1.5kg) were used. The time required for each polishing stage ranges between 10-45 minutes depending on the nature of the rock.

(5) Buffing

The specimen is then polished briefly (2 min) using gamma alumina on relatively soft cloth laps as abrasive and water as lubricant. The finished block has a diameter of 3.5 cm and is 1.4 cm thick.

(C) Polished-Thin Section

They are thin sections with polished surface required for special purpose such as electron microprobe analysis. Preparation of polished-thin section involves combination of the two procedures used for thin section and polished block.

307

(1) <u>Cutting</u>

Rock slices measuring 44mm x 25mm were cut with a diamond saw and cleaned ultrasonically in detegent, carbon tetrachloride, and water. The time required in each cleaning stage is three minutes and the sample is then dried.

(2) <u>Mounting</u>

The mounting is the same as in the ordinary thin sections. The sample is mounted on a glass slide, using Petroxy 154 resin and hardener (10:1). The sample is then trimmed to 200 micron on a Logitech machine.

(3) <u>Grinding</u>

The specimen is hand ground on a glass plate using 600, 800, and 1000 mesh carborundum and water, a procedure similar to that of the polished blocks. the pre-polishing thickness, however, depends on the rock type. Soft rocks such as carbonates and phyllites were ground down to 45 micron and the hard rocks such as quartzites were ground down to 30 micron.

(4) <u>Poli hing</u>

The section is polished up to 1/4 micron diamond paste for oxides and silicates, and gamma alumina for sulphide species.

Appendix (A.5.2): Summary on the mineralogical compositions of the examined rocks.

Sample Number	Locality N.G.R (Square NR)	Rock-Type	Mineralogical Composition
HMM 1	8530 7420	quartz-mica schist	Qz. 45%, ser. 30%, bit. 15%, pyr. 3%, ilm. 2%, with traces of cal., gar., chl., alb., se., and sph.
HMM 2	8527 7435	quartz-carbonate-mi a schist	Qz 60%, alb. (5%, mus. 15%, cal. 20%, with traces of se. and pyr.
HMM 4	836 737 Abhainn Srathain	epidotised epidiorite	Am. 35%, epd. 20%, gar. 15%, cal. 12%, qz. 5%, pyr.& chp. 8%, mag. rimmed with hem. 5%, with traces of sph. and bor.
HMM 5	836 737	epidiorite	Am. 30%, gar. 20%, qz.&alb. 15%, cal. 15%, epd. 5%, mag. rimmed with hem. 8%, chp. 4%, pyr. 3%, with traces of chl., se. and sph.
HMM 7	836 737	epidiorite	Am. 35%, gar. 35%, qz. 10%, cal. 5%, se. 2%, pyr. 7%, chp. 1.5%, mag. rimmed with hem. 1.5%, with traces of epd., chl., sph., bor.
HMM 8	836 737	epidotised epidiorite	Am. 25%, epd. 20%, gar. 15%, qz.&alb. 10%, cal. 10%, chp. 15%, pyr. 3%, hem. 2%, with traces of chl., se., mag., sph., mar., bor., cov.
HMM 9	836 737	epidiorite	Am. 35%, gar. 30%, qz.&alb. 5%, cal. 15%, epd. 5%, mag. rimmed with hem. 7%, chp. 3%, with traces of pyr.
HMM 10	836 737	epidotised epidiorite	Am. 25%, epd. 23%, gar. 20%, qz&alb. 10%, cal. 10%, chp.10%, pyr. 5% mag. rimmed with hem. 3%, with traces of se., sph., and mar.
HMM 11	836 737	epidiorite	Am. 30, epd. 15%, qz.&alb. 20%, cal. 15%, gar. 10%, chp. 7%, pyr. 3%, with traces of chl., sph., mag., hem., and mar.

309

Appendix (A.5.2): Continued.

HMM 12	836 737	epidotised epidiorite	Am. 20%, epd. 25%, qz.&alb. 20%, cal. 18%, gar. 5%, chp. 7%, pyr. 3%, mag. rimmed with hem. 2%, with traces of chl., se., and sph.
HMM 14	836 737	epidiorite (pyrite porphyroblast in a vein)	Am. 5%, epd. 5%, gar. 5%, qz.&alb. 1%, cal. 4%, pyr. 80%, with traces of chp., bor., mag., and hem.
HMM 15	836 737	epidiorite	Am. 25%, cal. 25%, qz.&alb. 20%, epd. 15%, chp. 7%, pyr. 7%, with traces of chl., and sph.
HMM 16	8355 7350	epidotised quartzite	Qz. 55%, epd. 30%, mus. 4%, bit. 2%, chp. 7%, pyr. 2%, with traces of cal., sph., ilm., and secondary bor. and cov.
HMM 17	8355 7350	epidotised quartzite	Qz. 78%, epd. 10%, alb. 2%, chp. & pyr. 8%, with traces of chl., cal., mus., sph., mag., and hem.
HMM 18	8355 7350	micaceous quartzite	Qz. 80%, mus. 15%, epd. 2%, with traces of pyr., chp. and secondary bor. and cov. 3%.
HMM 19	8355 7350	micaceous quartzite	Qz. 65%, mus. 20%, epd. 3%, cal. 2%, bor. and cov. 7%, pyr. 3%, with traces of chp.
HMM 20	8357 7365	epidotised quartzite	Qz. 50%, epd. 35%, cal. 12%, chp. 3%, with traces of mus. and sph.
HMM 21	8357 7365	epidotised quartzite	Qz. 75%, epd. 10%, mus. 10%, chp. 4%, with traces of alb., bit., chl., pyr., and ilm.
HMM 22	8357 7365	epidote-mica schist	Qz. 50%, mus. 20%, epd. 20%, chp. 6%, pyr. 3%, with traces of ilm., bor., and rut.

Appendix (A.5.2): Continued.

HMM 23	8357 7365	epidotised quartzite	Qz. 65%, chl. 7%, epd. 5%, cal. 5%, chp. 10%, pyr. 4%, ilm. 4%, with traces of mag., bor., and cov.
HMM 24	837 745	quartz-mica schist	Qz. 20%, bit. 25%, chl. 23%, gar. 16%, chp. 12%, pyr. 4%, with traces of ser. and sph.
HMM 25	837 745	chlorite-mica-schist	Mus. 40%, bit. 25%, qz. 15%, chl. 15%, cal. 5%, with traces of alb.
HMM 26	837 745	quartzite	Qz. 90%, mus. 7%, bit. 1%, with traces of chl. and alb.
HMM 26	837 745	mica-schist	Mus. 50%, bit. 35%, qz. 10%, cal. 5%, with traces of alb. and secondary chl.
HMM 29	837 745	quartzite	massive quartzite with chalcopyrite filling fractures, with traces of pyr., sph., and rut.
HMM 30	839 738 Meall Mór track	epidiorite	Am. 55%, epd. 10%, alb. 5%, mus. 5%, qz. 5%, cal. 5%, se. 10%, pyr. 5%.
HMM 32	853 743	micaceous quartzite	Qz. 70%, alb. 10%, mus. and bit. 15%, cal. 5%.
HMM 44	unlocated	epidotised schist	Qz. 40%, bit. 20%, epd. 15%, chl. 15%, alb. 5%, pyr.6%, with traces of gar., chp., ilm., and rut.
HMM 52	836 737 Abhainn Srathain	micaceous quartzite	Qz 80%, bit. 10%, chl. 5%, pyr. 5%, with traces of alb., cal.,and se
HMM 53	8400 7442 Meall Mór track	limestone	Cal. 60%, qz. 30%, alb. 5%, mus. 5%, with traces of pyr.

311

Appendix (A.5.2): Continued.

	Grid ref.	Locality	Rock type	Composition
HMM 54	839 738	Meall Mór track	epidiorite	Am. 60%, qz. 20%, epd. 5%, gar. 5%, chp. 10%, with traces of alb., pyr., mag., and hem.
HMM 55	8420 7455	Meall Mor track	feldspar-chlorite schist	Qz. 45%, chl.30%, alb. 20%, with traces of mus., epd., cal., pyr., rut., ilm., and mag.
HMM 56	8404 7425	Meall Mór track	quartzite	Qz. 85%, chl. 5%, pyr. 5%, with traces of alb.,bit.,mus.,cal.,and zr.
HMM 57	8390 7415	Meall Mór track	micaceous quartzite	Qz. 70%, chl. 10%, mus. and bit. 5%, se 5%, pyr. 9%, rut. 1%, with traces of alb.
HMM 58	8398 7435	Meall Mór track	quartzite	Qz. 75%, chl. 10%, se 3%, pyr. 6%, chp. 3%, with traces of bit., mus gar., and ilm.
HMM 59	8474 7717	Artilligan Burn	feldspathic quartzite	Qz. 73%, alb. 10%, mus. 7%, pyr. 7%, with traces of zr., and ilm.
HMM 60	8374 7482	Meall Mór track	feldspar-mica quartzite	Qz. 65%, alb. 10%, mus. 15%, bit. 3%, pyr. 5%, with traces of se., cal., and rut.
HMM 61	8445 7688	Artilligan Burn	feldspar-mica quartzite	Qz. 80%, alb. 15%, pyr. 2%, with traces of *mus.*, *bit.*, *epd.*, *sph.*, and rut.
HMM 62	8442 7685	Artilligan Burn	quartzite	Quartzite with disseminated pyrite cubes.
HMM 63	8438 7697	Artilligan Burn	quartzite	Quartzite with alternating sulphide bands.

Appendix (A.5.2): Continued.

HMMI 1	BH.3, 17.95m	epidotised epidiorite	Am. 20%, epd. 20%, qz.&alb. 20%, cal. 20%, gar. 10%, chp. 7%, pyr. 3%, with traces of mag., hem., and sph.
HMMI 2	BH.3, 23.8m	epidotised epidiorite	Am. 35%, epd. 65%, with traces of qz. and gar.
HMMI 3	BH.3, 24.1m	epidotised epidiorite	Am. 10%, epd. 70%, qz.&alb. 5%, se. 5%, pyr. 10%, with traces of gar., cal., and chp.
HMMI 4	BH.3, 25.03m	epidotised epidiorite	Am. 10%, epd. 65%, qz.&alb. 10%, se 5%, with traces of chp. and pyr.
HMMI 5	BH.3, 32.2m	epidotised quartzite	Qz. 67%, epd. 15%, chl. 15%, with traces of cal. and mus.
HMMI 6	BH.3, 32.35m	epidotised quartzite	Qz. 80%, epd. 15%, chl. 5%.
HMMI 7	BH.3, 32.53m	epidotised schist	Chl. 50%, mus. 15%, cal. 10%, qz. 10% and epd. 20% with traces of am
HMMI 8	BH.3, 32.9m	chlorite-mica schist	Qz. 60%, chl. 20%, mus. 10%, cal. 10%, pyr. 3%, with traces of epd.
HMMI 9	BH.3, 33.3m	mica-chlorite schist	Qz. 45%, alb. 10%, chl. 15%, mus. 20%, cal. 10%, pyr. 5%.
HMMI 10	BH.3, 34.1m	chlorite-mica schist	Qz. 50%, alb. 10%, chl. 25%, mus. 10%, and cal. 5%.
HMMI 11	BH.3, 34.4m	epidotised quartzite	Qz. 60%, chl. 10%, bit and mus. 10%, epd. 5%, alb. 10% and cal. 5%.
HMMI 12	BH.3, 2.7m	epidiorite	Am. 55%, cal. 15%, epd. 10%, gar. 10%, qz.&alb. 10% with traces pyr.
HMMI 13	BH.3, 1.3m	feldspar-mica schist	Qz. 60%, mus. 15%, chl. 10%, alb. 10%, pyr. 3%, ilm. 2%, with traces of bit., cal., and epd.

Appendix (A.5.2): Continued.

HMMI 14	BH.3, 1.8m	epidotised schist	Qz. 40%, epd. 35%, bit. 10%, alb. 5%, cal. 5%, chl. 3%, and mus. 2%
HMMI 15	BH.3, 7.6m	epidotised epidiorite	Am. 15%, epd. 40%, qz.&alb. 15%, gar. 13%, cal. 10%, chp. 7%, with traces of mag. and hem.
HMMI 16	BH.3, 10.2m	epidiorite	Am. 35%, epd. 15%, gar. 15%, qz.&alb. 10%, cal. 10%, mag. rimmed with hem. 8%, pyr. & chp, 7%, with traces of se. and bor.
HMMI 17	BH.3, 10.3m	epidiorite	Am. 35%, cal. 20%, qz.&alb. 18%, epd. 10%, gar. 10%, chp. 5%, mag. rimmed with hem. 1%, with traces of se., pyr., and born.
HMMI 18	BH.3, 11.45m	epidiorite	Am. 60%, epd. 15%, gar. 15%, cal. 5%, qz.&alb. 3%, pyr. & chp. 2%.
HMMI 19	BH.3, 12.25m	epidotised epidiorite	Am. 12%, epd. 35%, gar. 12%, cal. 10%, qz.&alb. 10%, chl. 5%, se 3%, pyr. 8%, chp. 3%, mag. rimmed with hem. 2%, with traces of ilm., sph and bor.
HMMI 20	BH.3, 14.3m	epidotised epidiorite	Yellowish green (pistachite) rock mainly of epidote with small quantities of gar., am. and quartz filling very fine veins.
HMMI 21	BH.3, 14.95m	epidiorite	Am. 55%, cal. 25%, gar. 13%, epd. 5%, qz.&alb. 2%, pyr. & chp 5%.
HMMI 22	BH.3, 15.3m	epidotised epidiorite	Am. 15%, epd. 75%, gar. 5%, cal. 5%.
HMMI 23	BH.1, 1.6m	quartz-mica-chlorite schist	Qz. 65%, bit. 15%, chl. 10%, gar. 3%, ilm. 5%, with traces of epd., mus., alb., and rut.
HMMI 25	BH.1, 2.0m	feldspathic schist	Qz. 50%, alb. 10%, chl. 15%, bit. 10%, se. 5%, rut. and ilm. 5%, pyr. 2%, with traces of mus., gar., cal., and epd.

314

Appendix (A.5.2): Continued.

HMMI 26	BH.1, 3.1m	mica-schist	Qz. 45%, mus. 15%, bit. 10%, se. 10%, cal. 5%, pyr. 15%, with traces of alb. and chl.
HMMI 27	BH.1, 3.43m	epidiorite	Qz. 50%, chl. 15%, bit. 15%, am. 5%, epd. 7%, alb. 5%, chp. and pyr. 3%, with traces of gar., cal., and ilm.
HMMI 28	BH.1, 4.5m	feldspathic quartzite	Qz. 60%, alb. 15%, chl. 15%, bit. 5%, mus. 3%, with traces of cal., gar., and ser.
HMMI 29	BH.1, 5.05m	epidotised schist	Qz. 25%, chl. 15%, epd. 10%, bit. 10%, alb. 85, cal. 5%, gar. 2%, pyr. 15%, chp. 5%, ilm. 5%, with traces of alb. and rut.
HMMI 31	BH.1, 7.85m	epidiorite	Am. 20%, bit. 20%, epd. 15%, chl. 10%, cal. 5%, qz.&alb. 15%, ilm. 15%, with traces of chp., pyr., mag., and hem.
HMMI 32	BH.1, 8.8m	epidotised schist	Qz. 25%, epd. 25%, chl. 15%, bit. 10%, alb. 5%, cal. 5%, ilm. 10%, pyr. 5%, with traces of se., chp., sph., and bor.
HMMI 33	BH.1 9.2m	feldspathic schist	Qz. 40%, alb. 15%, chl. 15%, bit 10%, gar. 5%, epd. 5%, ilm. 7%, pyr. 3%, with traces of apt., and chp.
HMMI 34	BH.1, 9.8m	mica-chlorite schist	Qz. 30%, mus. 30%, chl. 15%, cal. 10%, se. 5%, pyr. 10%, with traces of alb., ilm., mag., and rut.
HMMI 35	BH.1, 10.2m	epidotised quartz-mica-feldspar schist	Qz. 35%, alb. 10%, chl. 15%, bit. 10%, epd. 10%, mus. 3%, gar. 3%, pyr. 7%, chp. 3%, ilm., rut., and mag. 3%.
HMMI 42	BH.1, 19.7m	epidotised schist	Qz. 23%, epd. 20%, alb. 10%, chl. 10%, bit. 7%, am. 5%, gar. 5%, cal 2%, pyr. 10%, ilm. 5%, with traces of chp. and bor.

315

Appendix (A.5.2): Continued.

HMMI 44	BH.1, 20.8m	quartz-mica-feldspar schist	Qz. 35%, bit. 25%, alb. 15%, epd. 10%, pyr. 7%, ilm. 7%, with traces of mus., gar., and chl.
HMMI 46	BH.1, 21.14m	epidotised schist	Qz. 45%, epd. 20%, chl. 10%, bit. 5%, gar. 5%, pyr. 8%, ilm. 7%, with traces of alb., apt., chp., and rut.
HMMI 47	BH.1, 23.2m	epidotised schist	Qz. 40%, epd. 20%, chl. 15%, bit. 10%, se 10%, pyr. 5%, with traces of alb., car., gar., chp., and bor.
HMMI 48	BH.1, 24.3m	epidotised schist	Qz. 35%, epd. 25%, chl. 10%, bit 5%, cal. 3%, se. 2%, pyr. 17%, chp. 3%, with traces of gar., alb., and bor.
HMMI 49	BH.1, 25.8m	epidiorite	Am. 40%, qz.&alb. 25%, chl. 15%, bit. 8%, epd. 5%, pyr. 7%, with traces of se., and chp.
HMMI 50	BH.1, 35.65m	quartz-mica-feldspar schist	Qz. 45%, alb. 10%, ser. 20%, cal. 10%, bit. 5%, chl. 5%, pyr. 3%, with traces of se.
HMMI 52	BH. 1, 31.4m	quartz-mica-feldspar schist	Qz. 45%, alb. 15%, bit. 20%, cal. 8%, mus. 7%, pyr. 5%, with traces of epd., and se.
HMMI 53	BH.1, 32.6m	calcareous quartzite	Qz. 60%, mus. 10%, cal. 15%, bit. 5%, pyr. 5%, with traces of alb., and rut.
HMMI 54	BH.1, 29.0m	quartz-mica schist	Qz. 50%, bit. 20%, mus. 10%, alb. 5%, cal. 5%, pyr. 5%, ilm. 5%, with traces of chl., and zr.,
HMMI 55	BH.1, 27.0m	epidotised schist	Qz. 40%, epd. 20%, bit 10%, chl. 10%, cal. 10%, pyr. 10%, with traces of se., chp. and rut.
HMMI 57	BH.1, 38.3m	micaceous quartzite	Qz. 37%, alb. 5%, mus. 12%, cal. 7%, bit. 5%, pyr. 30%, with traces of se., zr., chp., sph., mag., hem., and bor.

316

Appendix (A.5.2): Continued.

HMI 59	BH.2, 42.8m	feldspar-mica schist	Qz. 40%, bit. 20%, alb. 10%, cal. 10%, mus. 8%, pyr. 10%, mag. rimmed with hem. 2%, with traces of rut., and ilm.
HMI 61	BH.1, 25.5m	quartz-mica-chlorite schist	Qz. 40%, mus. 20%, chl. 15%, cal. 12%, pyr. 10%, rut. 3%, with trace of chp.
HMI 62	BH.2, 4.4m	feldspar-mica quartzite	Qz. 60%, alb. 15%, bit. & mus. 15%, cal. 5%, gar. 5%.
HMI 63	BH.2, 4.7m	quartzite	Qz. 90%, bit. 5%, alb. 3%, with traces of gar., and zr.
HMI 64	BH.2, 5.3m	quartzite	Qz. 90%, cal. 5%, mus. 2%, alb. 3%.
HMI 65	BH.2, 7.0m	quartz-mica-chlorite schist	Qz. 60%, chl. 15%, ser. 10%, alb. 5%, cal. 5%, pyr.&chp. 3%, mag.& hem 2%.
HMI 66	BH.2, 7.6m	mica-schist	Ser. 50%, qz. & alb. 5%, 1bit. 25%, chl. 15%, with traces of gar.
HMI 67	BH.2, 9.0m	mica-schist	Qz. 50%, ser. 30%, cal. 5%, epd. 5%, pyr. 3%, with traces of bit., chl. and chp.
HMI 68	BH.2, 9.67m	quartzite	Qz. 60%, musc. 10%, feld. 2%, se 5%, pyr. 20%, with traces of bit., chl., cal., apt., chp., sph., and mag.
HMI 69	BH.2, 10.0m	calcareous schist	Qz. 20%, ser. 33%, cal. 15%, chl. 5%, bit. 5%, pyr.&chp. 10%, mag.& hem. 5%, with traces of chl., cov., and bor.
HMI 70	BH.2, 13.35m	quartzite	Qz. 75%, mic. 5%, alb. 5%, cal. 5%, pyr. 10%, with traces of zr., chp., and mag.

317

Appendix (A.5.2): Continued.

HMMI 71	BH.2, 16.49m	feldspathic quartzite	Qz. 70%, alb. 10%, mus., and bit. 10%, chl. 2%, cal. 3%, pyr. 5%, with traces of zr., chp., rut., and mag.
HMMI 72	BH.2, 16.6m	feldspathic quartzite	Qz. 60%, alb. 10%, mus., and bit. 10%, chl. 3%, cal. 10%, pyr. 5%, with traces of chp., sph., and mag.
HMMI 73	BH.2, 17.28m	calcareous quartzite	Qz. 80%, alb. 5%, cal. 5%, mus. 5%, pyr. 5%.
HMMI 76	BH.2, 19.5m	mica-schist	Qz. 65%, alb. 5%. mus. 20%, mic. 5%, pyr. 5%.
HMMI 77	BH.2, 19.96m	calcareous quartzite	Qz. 50%, cal. 10%, alb. 10%, epd. 10%, mus. & chl. 3%, pyr. 10%, with traces of se., rut., and ilm.
HMMI 78	BH. 2, 20.5m	mica-schist	Qz. 60%, mus.&bit. 35%, pyr. 3.5%, rut. 1.5%, with traces of alb., cal., apt., and ilm.
HMMI 79	BH.2, 20.86m	mica-schist	Qz. 65%, mus.&bit. 30%, pyr. 5%, with traces of alb. and cal.
HMMI 80	BH.2, 21.14m	calcareous quartzite	Qz. 65%, mus. 10%, cal. 15%, alb. 5%, pyr. 5%, with accessory zr.
HMMI 81	BH.2, 22.3m	quartzite	Qz. 70%, mus. 7%, epd. 5%, cal. 3%, pyr. 12%, rut. 3%.
HMMI 82	BH.2, 22.86m	quartz-mica schist	Qz. 62%, mus. 30%, cal. 3%, pyr. 5%, with traces of zr.
HMMI 83	BH.2, 25.05m	mica-schist	Qz. 50%, mus. 15%, epd. 10%, alb. 8%, cal. 2%, pyr. 15%.
HMMI 84	BH.2, 25.8m	mica-schist	Qz. 60%, mus. 30%, pyr. 10%, with traces of alb., and chp.
HMMI 85	BH.2, 27.03m	micaceous quartzite	Qz. 68%, mus. 15%, cal. 2%, pyr. 15%, with traces of rut.

Appendix (A.5.2): Continued.

HMMI 87	BH.2, 27.67m	feldspathic quartzite	Qz. 45%, alb. 10%, cal. 10%, mus. 3%, pyr. 25%, with traces of se., chp., sph., and bor.
HMMI 88	BH.2, 27.73m	calcareous quatzite	Qz. 55%, cal. 20%, mus. 5%, pyr. 20%, with traces of se., rut., and ilm.
HMMI 90	BH.2, 29.75m	micaceous quartzite	Qz. 73%, bit. 20%, mus. 5%, cal. 2%, with traces of chl.
HMMI 92	BH.2, 31.0m	quartzite	Qz. 80%, bit. 10%, cal. 3%, chp. & pyr. 3%, with traces of sph.&mag.
HMMI 93	BH.2, 32.84m	micaceous quartzite	Qz. 60%, mus. 12%, bit. 5%, chl. 2%, cal. 2%, alb. 3%, pyr. 6%, chp. 6%, mag. rimmed with hem. 2%, with traces of sph.
HMMI 94	BH.2, 34.18m	calcareous quartzite	Qz. 65%, cal. 20%, alb. 5%, mus. 5%, bit. 3%, with traces of pyr.
HMMI 95	BH.2, 34.38m	quartz-mica schist	Qz. 45%, mus. 20%, cal. 10%, bit. 5%, chl. 5%, pyr. 10%, chp. 2%, with traces of alb., rut., and bor.
HMMI 96	BH.2, 34.93m	feldspathic quartzite	Qz. 68%, alb. 15%, mus. 3%, pyr. 10%, rut. 2%, with traces of cal., bit., chl., zr., and apt.
HMMI 97	BH.2, 35.64m	feldspathic schist	Qz. 57%, alb. 5%, mus. 15%, cal. 10%, bit. & chl. 5%, pyr. 5%, rut. 3%, with traces of apt., ilm., and mag.
HMMI 98	BH.2, 35.75m	feldspathic schist	Qz. 45%, alb. 15%, mus. 10%, cal. 10%, bit. 5%, pyr. 10%, rut. 5%, with traces of chl., chp., sph., and bor.
HMMI 99	BH.2, 35.95m	calcareous schist	Qz. 25%, cal. 20%, alb. 15%, bit. 20%, chl. 5%, pyr. 7%, rut. 5%, with traces of chp. & mag.

319

Appendix (A.5.2): Continued.

HMI 100	BH.2, 36.97m	feldspathic schist	Qz. 40%, chl. 25%, alb. 10%, bit. & mus. 15%, cal. 10%.
HMI 101	BH.2, 37.75m	mica-schist	Qz. 55%, mus. 15%, alb. 5%, bit. 4%, cal. 4%, se. 2%, pyr. 15%, with traces of chp., bor., rut., and ilm.
HMI 102	BH.2, 38.25m	feldspathic quartz-mica chlorite schist	Qz. 30%, mus. 20%, bit. & chl. 15%, alb. 15%, cal. 10%, pyr. 7%, rut. 3%.
HMI 103	BH.2, 38.7m	micaceous quartzite	Qz. 68%, mus. 10%, alb. 5%, chl. 3%, cal. 3%, pyr. 7%, rut. 2%, with traces of bit., zr., and ilm.
HMI 104	BH.2, 38.93m	quartz-biotite schist	Qz. 65%, bit. 20%, chl. 3%, cal. 3%, mus. 2%, pyr. 5%, with traces of alb., zr., rut., and ilm.
HMI 106	BH.2, 40.07m	quartz-biotite schist	Qz. 50%, bit. 25%, cal. 10%, chl. 5%, pyr. 9%, with traces of alb., se., zr., and rut.
HMI 107	BH.2, 40.65m	quartz-mica schist	Qz. 25%, bit. 40%, mus. 15%, alb. 5%, cal. 5%, pyr. 7%, rut. 3%, with traces of se., chp., bor., and mag.

Abbreviations for minerals:-

alb.	: albite	am.	: amphibole	apt.	: apatite
chl.	: chlorite	chp.	: chalcopyrite	cov.	: covellite
hem.	: hematite	ilm.	: ilmenite	mag.	: magnetite
pyrh.	: pyrrhotite	qz.	: quartz	rut.	: rutile
zr.	: zircon				

bit.	: biotite	bor.	: bornite	cal.	: calcite
epd.	: epidote	feld.	: feldspar	gar.	: garnet
mar.	: marcasite	mus.	: muscovite	pyr.	: pyrite
se.	: sphene	ser.	: sericite	sph.	: sphalerite

320

Appendix A.5.3 : Electron microprobe analysis of amphibole. Calculation is made by
assuming the total iron as FeO.

VAR. / ID.	HMM 5	HMM 8	HMM 9	HMM 10	HMM 11	HMM 12	HMM 14	HMM 15	HMM 1	HMM 3	HMM 16	HMM 19	HMM 31	HMM 23*
SiO_2	51.69	54.10	53.61	52.56	54.36	55.05	53.63	54.49	53.77	56.10	52.88	53.01	49.09	43.77
Al_2O_3	2.74	0.87	1.04	1.56	1.75	0.46	0.70	1.92	0.99	1.57	0.47	4.38	5.36	11.05
TiO_2	0.04	0.00	0.00	0.00	0.00	0.00	0.00	0.00	0.01	0.00	0.01	0.00	0.00	0.30
Cr_2O_3	0.04	0.00	0.00	0.00	0.12	0.00	0.00	0.00	0.00	0.00	0.00	0.00	0.00	0.00
FeO	17.24	14.29	17.76	17.65	13.25	11.96	17.36	11.11	15.21	8.03	17.74	17.38	18.03	20.27
MnO	0.97	0.90	1.36	1.34	0.65	0.86	1.23	0.75	1.07	0.86	1.50	1.05	0.30	0.20
MgO	12.55	14.90	12.68	12.38	15.00	16.50	12.47	16.82	13.53	18.82	12.09	11.10	11.83	8.34
CaO	11.40	12.09	11.82	11.84	11.97	12.57	11.83	12.40	11.82	12.38	11.82	11.23	11.57	11.06
Na_2O	0.56	0.00	0.00	0.33	0.00	0.00	0.00	0.00	0.25	0.00	0.15	0.63	0.89	1.87
K_2O	0.03	0.00	0.00	0.00	0.00	0.00	0.00	0.00	0.05	0.00	0.03	0.21	0.22	0.41
TOTAL (wt%)	97.25	97.16	98.07	97.69	97.10	97.40	97.22	97.49	96.76	97.76	96.88	98.99	97.29	97.28
NUMBER OF IONS ON BASIS OF 23(O)														
Si	7.67	7.89	7.86	7.79	7.88	7.93	7.94	7.80	7.93	7.88	7.92	7.69	7.33	6.67
Al^{iv}	0.33	0.11	0.14	0.21	0.12	0.07	0.06	0.20	0.07	0.12	0.08	0.31	0.67	1.33
Total	8.00	8.00	8.00	8.00	8.00	8.00	8.00	8.00	8.00	8.00	8.00	8.00	8.00	8.00
Al^{vi}	0.15	0.04	0.04	0.06	0.17	0.01	0.06	0.12	0.00	0.14	0.00	0.44	0.27	0.03
Ti	0.00	0.00	0.00	0.00	0.00	0.00	0.00	0.00	0.00	0.00	0.00	0.00	0.00	0.00
Cr	0.00	0.00	0.00	0.00	0.01	0.00	0.00	0.00	0.00	0.00	0.00	0.00	0.00	0.00
Fe^{2+}	2.14	1.74	2.19	2.19	1.61	1.44	2.15	1.33	1.88	0.94	2.25	2.11	2.25	2.58
Mn	0.12	0.11	0.17	0.17	0.08	0.10	0.15	0.09	0.13	0.10	0.19	0.13	0.04	0.03
Mg	2.78	3.24	2.78	2.73	3.24	3.54	2.75	3.59	2.97	3.94	2.70	2.40	2.63	1.89
Total	5.19	5.13	5.18	5.15	5.11	5.09	5.05	5.13	5.08	5.13	5.14	5.08	5.20	5.19
Ca	1.81	1.89	1.87	1.88	1.86	1.94	1.88	1.90	1.87	1.86	1.90	1.75	1.85	1.81
Na	0.16	0.00	0.00	0.09	0.00	0.00	0.00	0.00	0.07	0.00	0.04	0.18	0.26	0.55
K	0.01	0.00	0.00	0.00	0.00	0.00	0.00	0.00	0.00	0.00	0.01	0.04	0.04	0.08
Fe^{2+}	0.00	0.00	0.00	0.00	0.00	0.00	0.00	0.00	0.00	0.00	0.00	0.00	0.00	0.00
Total	1.98	1.89	1.87	1.97	1.86	1.94	1.88	1.90	1.94	1.86	1.95	1.96	2.15	2.44

* Amphibole in micaceous quartzite.

321

Appendix A.5.4 : Electron microprobe analysis of garnet. Calculation is made by assuming all the iron as FeO.

VAR. / ID.	Epidiorites									Metasediments					
	HMM 4	HMM 5	HMM 8	HMM 9	HMM 11	HMM 14	HMM 1	HMM 16	HMM 19	HMM 1	HMM 44	HMM 25	HMM 29	HMM 33	HMM 46
SiO_2	37.41	37.41	37.66	37.20	37.39	37.51	37.28	36.75	36.48	37.76	37.99	37.61	36.95	46.79	37.55
Al_2O_3	18.19	18.00	20.07	18.43	19.70	18.52	18.69	17.42	18.04	21.10	21.47	20.47	20.58	17.63	20.83
TiO_2	0.34	0.17	0.17	0.19	0.16	0.26	0.19	0.15	3.94	0.00	0.14	0.17	0.13	0.17	0.00
Cr_2O_3	0.00	0.00	0.00	0.09	0.00	0.06	0.01	0.00	0.00	0.00	0.00	0.01	0.02	0.00	0.00
FeO	17.25	18.29	13.26	13.79	15.16	16.89	13.74	16.66	11.10	24.67	26.27	24.56	21.03	16.91	25.55
MnO	12.56	11.62	15.51	18.41	12.71	14.40	16.00	15.43	14.00	8.26	6.86	9.31	13.48	12.11	6.91
MgO	0.00	0.00	0.13	0.23	0.43	0.08	0.20	0.21	0.00	0.53	0.89	0.71	0.60	0.41	0.76
CaO	14.14	14.73	14.08	12.12	14.45	13.56	13.75	13.24	15.85	8.71	8.11	7.99	7.39	7.71	8.87
TOTAL (wt%)	99.88	100.23	100.88	100.45	100.00	101.26	99.86	99.88	99.41	101.02	101.73	100.81	100.17	101.73	100.47

NUMBER OF IONS ON BASIS OF 24 (O)

	HMM 4	HMM 5	HMM 8	HMM 9	HMM 11	HMM 14	HMM 1	HMM 16	HMM 19	HMM 1	HMM 44	HMM 25	HMM 29	HMM 33	HMM 46
Si	6.08	6.07	6.00	6.04	6.01	6.03	6.05	6.04	5.88	6.02	6.00	6.03	5.98	7.10	6.01
Al^{IV}	0.00	0.00	0.00	0.00	0.00	0.00	0.00	0.00	0.12	0.00	0.00	0.00	0.02	0.00	0.00
Total	6.08	6.07	6.00	6.04	6.01	6.03	6.05	6.04	6.00	6.02	6.00	6.03	6.00	7.10	6.01
Al^{VI}	3.48	3.45	3.77	3.53	3.73	3.51	3.57	3.38	3.31	3.97	4.00	3.87	3.91	3.15	3.94
Ti	0.00	0.00	0.02	0.02	0.02	0.03	0.02	0.02	0.48	0.00	0.02	0.02	0.02	0.02	0.00
Cr	0.00	0.00	0.00	0.01	0.00	0.01	0.00	0.00	0.00	0.00	0.00	0.00	0.00	0.00	0.00
Total	3.48	3.45	3.79	3.56	3.75	3.55	3.59	3.40	3.79	3.97	4.02	3.89	3.93	3.17	3.94
Fe^{2+}	2.34	2.48	1.77	1.87	2.04	2.27	1.86	2.29	1.50	3.29	3.47	3.29	2.85	2.14	3.42
Mn	1.73	1.60	2.09	2.53	1.73	1.96	2.20	2.15	1.91	1.11	0.92	1.26	1.85	1.56	0.94
Mg	0.00	0.00	0.03	0.06	0.10	0.02	0.05	0.05	0.00	0.13	0.21	0.17	0.14	0.09	0.18
Ca	2.46	2.56	2.41	2.11	2.49	2.34	2.39	2.33	2.74	1.49	1.37	1.37	1.28	1.25	1.52
Total	6.53	6.64	6.30	6.57	6.36	6.59	6.50	6.82	6.15	6.02	5.97	6.10	6.10	5.05	6.07

END-MEMBER COMPOSITION (MOL%)

	HMM 4	HMM 5	HMM 8	HMM 9	HMM 11	HMM 14	HMM 1	HMM 16	HMM 19	HMM 1	HMM 44	HMM 25	HMM 29	HMM 33	HMM 46
Pyrope	0.00	0.00	0.00	0.00	1.87	0.00	0.00	0.00	0.00	2.10	3.51	2.91	2.45	1.97	3.08
Spessartine	33.09	30.94	37.01	47.88	30.90	37.25	41.01	42.43	37.18	18.80	15.29	21.78	31.38	32.91	15.90
Grossular	47.12	49.61	42.51	39.86	44.44	44.36	44.59	46.06	53.22	25.00	22.89	23.65	211.77	26.49	25.78
Almandine	19.79	19.46	20.48	12.26	22.79	18.40	14.40	11.51	9.61	54.20	58.31	51.65	44.40	38.64	55.24
Total	100.00	100.01	100.00	100.00	100.00	100.00	100.00	100.00	100.01	100.10	100.00	99.99	100.00	100.00	100.00

322

Appendix A.5.5 : Electron microprobe analysis of chlorite. Calculation is made by assuming all the iron as FeO

VAR. / ID.	HMM I	HMM 44	HMM 57	HMMI 25	HMMI 26	HMMI 29	HMMI 33	HMMI 35	HMMI 42	HMMI 46
					Metasediments					
SiO_2	35.53	25.21	25.22	27.00	27.91	24.18	24.57	24.67	24.42	24.30
Al_2O_3	21.31	21.15	21.59	16.35	20.78	20.74	20.91	20.80	20.02	20.13
TiO_2	0.00	0.00	0.00	0.05	0.05	0.08	0.00	0.06	0.09	0.00
FeO	20.82	25.07	24.22	29.77	21.48	26.26	23.03	23.27	27.26	31.56
MnO	0.00	0.54	0.38	0.22	0.35	0.44	0.56	0.49	0.44	0.60
MgO	7.37	15.10	15.89	13.45	18.12	14.50	16.89	16.38	13.69	11.19
CaO	0.00	0.00	0.00	0.09	0.01	0.00	0.00	0.01	0.02	0.00
Na_2O	0.00	0.00	0.00	0.02	0.01	0.01	0.00	0.02	0.02	0.00
K_2O	0.00	0.00	0.00	0.02	0.00	0.00	0.00	0.00	0.00	0.00
TOTAL (wt%)	85.03	87.07	87.30	86.96	85.78	86.20	85.96	85.70	85.96	87.78
				NUMBER OF IONS ON BASIS OF 28 (O)						
Si	7.25	5.36	5.31	5.89	5.67	5.24	5.25	5.29	5.34	5.32
Al^{iv}	0.75	2.64	2.69	2.11	2.33	2.76	2.75	2.71	2.66	2.68
Total	8.00	8.00	8.00	8.00	8.00	8.00	8.00	8.00	8.00	8.00
Al^{vi}	4.40	2.66	2.68	2.10	2.64	2.55	2.52	2.55	2.50	2.53
Ti	0.00	0.00	0.00	0.01	0.01	0.01	0.00	0.01	0.02	0.00
Fe^{2+}	3.55	4.46	4.27	5.44	3.65	4.76	4.12	4.18	4.99	5.78
Mn	0.03	0.10	0.07	0.04	0.06	0.08	0.10	0.09	0.08	0.11
Mg	2.24	4.78	4.99	4.38	5.48	4.69	5.38	5.24	4.46	3.65
Ca	0.00	0.00	0.00	0.02	0.00	0.00	0.00	0.03	0.01	0.00
Na	0.00	0.00	0.00	0.01	0.01	0.01	0.00	0.00	0.02	0.00
K	0.00	0.00	0.00	0.01	0.00	0.00	0.00	0.00	0.00	0.00
Total	10.22	11.99	12.00	12.00	11.85	12.10	12.12	12.10	12.08	12.08

Appendix A.5.5 : Continued

VAR. / ID.	Metasediments						Epidiorites			
	HMMI 50	HMMI 55	HMMI 61	HMMI 67	HMMI 69	HMMI 96	HMM 11	HMMI 19	HMMI 31	HMMI 31A
SiO_2	25.26	26.20	25.58	36.71	36.15	29.11	25.63	26.78	24.05	41.94
Al_2O_3	20.35	20.28	20.59	15.98	15.50	16.41	19.84	19.07	20.16	13.12
TiO_2	0.06	0.00	0.04	0.00	0.00	0.00	0.00	0.00	0.06	0.00
FeO	21.67	20.75	18.41	23.68	21.23	12.86	25.25	0.00	29.42	20.19
MnO	0.44	0.48	0.25	0.13	0.16	0.26	1.13	1.51	0.43	0.26
MgO	17.30	19.02	19.44	7.31	9.26	25.83	15.22	11.16	12.27	7.37
CaO	0.00	0.00	0.00	0.00	0.00	0.00	0.00	0.00	0.01	0.00
Na_2O	0.01	0.00	0.02	0.00	0.00	0.00	0.00	0.00	0.02	0.00
K_2O	0.02	0.00	0.00	0.00	0.00	0.00	0.00	0.00	0.00	0.00
TOTAL (wt%)	85.46	86.73	84.32	83.81	82.30	84.47	87.07	90.11	86.42	82.87

NUMBER OF IONS ON BASIS OF 28 (O)

Si^4	5.45	5.46	5.42	7.76	7.70	5.96	5.47	5.70	5.30	8.69
Al^4	2.55	2.54	2.58	0.24	0.00	2.04	2.53	2.30	2.70	0.00
Total	8.00	8.00	8.00	8.00	7.70	8.00	8.00	8.00	8.00	8.69
Al^6	2.55	2.44	2.56	3.74	3.60	1.93	2.47	2.48	2.54	3.20
Ti	0.01	0.00	0.01	0.00	0.00	0.00	0.00	0.00	0.01	0.00
Fe^{2+}	3.86	3.62	3.26	4.19	3.78	2.20	4.51	5.62	5.42	3.50
Mn	0.08	0.09	0.05	0.02	0.03	0.05	0.20	0.27	0.08	0.05
Mg	5.49	5.91	6.13	2.30	2.94	7.88	4.85	3.54	4.03	2.28
Ca	0.00	0.00	0.00	0.00	0.00	0.00	0.00	0.00	0.00	0.00
Na	0.00	0.00	0.01	0.00	0.00	0.00	0.00	0.00	0.00	0.00
K	0.00	0.00	0.00	0.00	0.00	0.00	0.00	0.00	0.01	0.00
Total	11.99	12.05	12.02	10.25	10.35	12.06	12.03	11.91	12.09	9.03

Appendix A.5.6 : Electron microprobe analysis of white mica. Calculation is made by assuming all the iron as FeO.

VAR. / ID.	HMM 1	HMM 57	HMMI 26	HMMI 50	HMMI 69	HMMI 78	HMMI 96	HMMI 97	HMMI 103
SiO_2	47.69	48.13	47.57	48.16	46.98	48.44	46.85	45.35	47.25
Al_2O_3	30.82	29.62	28.12	27.17	27.14	23.12	30.51	29.83	28.41
TiO_2	0.40	0.75	0.38	0.42	0.87	1.55	0.60	0.76	0.60
FeO	3.13	3.51	3.77	3.39	5.81	5.70	2.34	4.06	3.80
MnO	0.00	0.11	0.01	0.02	0.00	0.00	0.00	0.14	0.00
MgO	1.65	2.15	2.68	2.94	2.03	2.76	2.00	1.68	2.10
CaO	0.09	0.00	0.00	0.00	0.00	0.09	0.00	0.12	0.00
Na_2O	0.59	0.53	0.50	0.30	0.00	0.00	0.67	0.00	0.36
K_2O	10.05	10.44	9.84	9.31	10.62	10.58	9.88	9.87	10.35
TOTAL (wt%)	94.42	95.24	92.88	91.71	93.45	92.24	92.85	92.15	92.87

NUMBER OF IONS ON BASIS OF 22 (O)

VAR. / ID.	HMM 1	HMM 57	HMMI 26	HMMI 50	HMMI 69	HMMI 78	HMMI 96	HMMI 97	HMMI 103
Si	6.45	6.49	6.57	6.69	6.55	6.84	6.43	6.34	6.54
Al^{4}	1.55	1.51	1.43	1.31	1.45	1.16	1.57	1.66	1.46
Total	8.00	8.00	8.00	8.00	8.00	8.00	8.00	8.00	8.00
Al^{6}	3.37	3.20	3.15	3.14	3.01	2.69	3.36	3.26	3.18
Ti	0.04	0.08	0.04	0.04	0.09	0.17	0.06	0.08	0.06
Fe^{2}	0.36	0.40	0.44	0.39	0.68	0.67	0.27	0.48	0.44
Mn	0.33	0.01	0.00	0.00	0.00	0.00	0.00	0.02	0.00
Mg	0.01	0.43	0.55	0.61	0.42	0.58	0.41	0.35	0.43
Total	4.10	4.12	4.18	4.18	4.20	4.11	4.10	4.18	4.12
Ca	0.01	0.00	0.00	0.00	0.00	0.01	0.00	0.02	0.00
Na	0.16	0.14	0.13	0.08	0.00	0.00	0.18	0.09	0.10
K	1.72	1.79	1.72	1.64	1.88	1.89	1.72	1.75	1.82
Total	1.89	1.93	1.85	1.72	1.88	1.90	1.90	1.86	1.92

Appendix (A.6.1) : Preparation of fused beads.

The procedure for fused peads preparation that was used and practised at the Department of Geology, Glasgow University will be outlined below.

Equipment

1. Furnace - 1000°C.

2. Hotplate I with plunger assembly - 225°C ± 10.

3. Hotplate II with hard asbestos rings and blocks - 200°C ± 10.

4. Meka or blast burners, tripods with vitrosil triangles.

5. Crucibles and lids - Pt/5%Ag.

6. Platinum tipped tongs.

7. Nickel shovel.

8. Flux - SPECTROFLUX 105 containing lithium carbonate, lithium tetraborate and lanthanum oxide.

Method

1. Samples should be crushed to at least 100 mesh and dried for 24 hours.

2. Switch on furnace at 1000°C, hotplate I at 225°C and hotplate II at 200°C and let them stabilise for approximately one day before use.

3. Make sure that all the equipment needed is clean.

4. Weigh 0.46875 gm of rock powder and 2.5 gm of flux into a crucible and mix. Record the total weight, crucible number and sample number.

5. Place the crucible in the furnace with a lid for 15 minutes, then remove and allow to cool on aluminium surface, (keep lid on).

6. Reweigh and record.

326

7. Every 5-10 samples a 'blank' should be run to determine the weight loss on the flux.

8. After reweighing, the rock-flux mixture is remelted over a blast burner, slowly at first or other wise the glass will crack and jump out. Any undissolved powder or droplets of melt on the sides of the crucible should be incorporated into the melt and the whole mixed by swirling the melt around in the crucible. An attempt should be made to remove any bubbles that are precent. The melt should be at a dull red heat prior to pressing, not bright orange.

9. Form bead by raising plunger and quickly pouring the melt into the centre of the platten. Then lower the plunger firmly, raise again and transfer the platten and bead (if successful) onto the second hotplate using the nickel shovel. Any melt that clings to the lip of the crucible can be removed by touching the melt on the platten with the lip of the crucible.

10. The platten and bead are placed in the centre of the asbestos ring between two asbestos blocks. Mark the top of the block with sample number and crucible number in pencil. Old numbers will rub off with a tissue.

11. Leave bead on the second hotplate for 30 minutes, then remove still enclosed within asbestos blocks and allow to cool on the bench.

12. When cool remove the bead. Do not use any metal implement as this will damage the platten. If difficulty is experienced in removing the bead warm the bead and the platten on the hotplate for a short time.

13. Trim off any burrs from the bead and label the undersurface (bevelled) using a self adhesive label. Record the sample number, flux batch and weight loss correction factor.

14. When the crucible is cool tap it gently on a steel plate to remove any glass left in it. Soak in warm 50/50 HCl for 10-15 minutes to remove any remaining traces of glass, rinse in distilled water and dry.

327

Cleaning the platinum crucibles

Any pieces of fused rock remaining in a crucible after use must removed by the finger nail only. Never use a scalpel or any metal implement which will scratch the surface of the crucible. Scratches cause fused rock to adhere to the crucibles. Therefore the crucibles should be cleaned as follows:

1. Heat some sodium carbonate (Na_2CO_3) in the crucible on a tripod above a bunsen until molten.

2. Swirl the liquid around the sides of the crucible to dissolve any remaining fused rock.

3. Allow to cool and then drop gently into a 10% HNO_3 solution.

4. After the reaction has ceased, boil until the Na_2CO_3 and fused rock has been dissolved.

5. Wash thoroughly in warm water, followed by distilled water and dry in the oven at 100^oC.

Care of the platinum tipped tongs

1. Never allow Na_2CO_3 to come into contact with the platinum tips, as it will attack the platinum.

2. Always place the tongs with tips uppermost on the bench, to avoid contamination.

3. Never use the tongs for inserting crucibles into any liquid, or heat the tips in a bunsen flame.

Bead failure-some answers

1. Bubbles in the bead, especially near the edges:

328

plunger hotplate too hot, burner too hot.

2. Bead sticks to plunger when raised: burner too hot prior to forming of bead., attempt to raise plunger too quickly after forming the bead.

3. Bead cracks: plunger hotplate too cool, melt too cool.

<u>Appendix (A.6.2)</u> : Instrumental parameters for the major elements analysis using Glasgow
PW 1450 X-ray Fluorescence Spectrometer.

Sample holder 32 mm	X-ray tube target Cr
Diaphragm 28 mm	Generator manual setting: kV = 40, mA = 20
Monitor 3570/02	
Beam path VAC	

Crystal	
Pos.	Type
1	LIF 200
2	GE
3	PE
4	TLAP
5	LIF 220

PHS					
Pos.	L.L.	W	Pos.	L.L.	W
M			5	400	300
1	50	1000	6	300	400
2	150	600	7	400	400
3	200	500	8	350	400
4	200	600	9	300	500

Spectrometer Settings

Element		Line	X-tal	Angle	Det.	Coll.	Filter	PHS	kV	mA
Ca	11	Kα	1	113.11	F	f	NO	1	40	10
	12		1	124.31	F	f	NO	1	40	10
Ti	9	Kα	1	86.12	F	f	NO	6	60	20
	10		1	84.00	F	f	NO	6	60	20
Fe	1	Kα	1	57.53	F	f	NO	1	60	20
	2		1	55.30	F	f	NO	1	60	20
Mn	3	Kα	5	95.35	F	c	YE	2	60	45
	4		5	98.90	F	c	YE	2	60	45
Na	25	Kα	4	55.18	F	c	NO	8	50	60
	26		4	61.00	F	c	NO	8	50	60
Mg	23	Kα	4	45.11	F	f	NO	5	50	60
	24		4	48.00	F	f	NO	5	50	60
Al	21	Kα	3	144.90	F	c	NO	9	50	45
	22		3	139.00	F	c	NO	9	50	45
Si	19	Kα	3	109.02	F	c	NO	8	50	45
	20		3	112.00	F	c	NO	8	50	45
P	17	Kα	2	141.00	F	c	NO	8	50	45
	18		2	143.00	F	c	NO	8	50	45
K	13	Kα	1	136.69	F	f	NO	1	60	20
	14		1	140.00	F	f	NO	1	60	20

Abbreviations :
X-tal = crystal
Det. = detector
Coll. = collimator
F = flow detector
C = coarse primary collimator
f = fine primary collimator

Appendix (A.6.3) : Count rate and calibration statistics for major elements.

Oxide	count rate error %	st. error of $\hat{Y}$ in regression wt%	calibration range lower limit	calibration range upper limit	detection limits wt%
SiO_2	0.60	0.54	8.00	80.00	0.09
TiO_2	0.80	0.03	0.00	3.20	0.02
Al_2O_3	1.00	0.52	0.00	23.00	0.09
Fe_2O_3	1.00	0.15	0.00	14.80	0.05
MnO	3.00	0.01	0.00	0.20	0.01
MgO	1.50	0.30	0.00	50.00	0.17
CaO	0.60	0.09	0.00	32.50	0.01
Na_2O	0.70	0.20	0.00	5.40	0.16
K_2O	0.60	0.07	0.00	5.00	0.00
P_2O_5	1.60	0.01	0.00	0.60	0.01

331

Appendix (A.6.4) : The accuracy of the major elements of XRF analyses on recent International standards and the comparison of their observed (XRF) and recomended (rec) values. Recommended values are from Govindaraju (1980) for AN-G, BE-N and MA-N, and from Abbey (1982) for the USGS III standard (BV-1 to QLO-1).

	Oxides	Anorth-osite AN-G 8400	Basalt BE-N 8410	Granite MA-N 8420	Hawaiian Basalt BHVO-1 8500	Marine Mud MAG-1 8510	Rhyolite RGM-1 8520	Cody Shale SDO-1 8530	Mica Schist SDO-1 8540	Shale shale SGR-1 8550	Nepheline Syenite STM-1 8560	Qz-Latite QLO-1 8570
rec.	SiO_2	46.40	38.47	66.93	49.90	51.19	73.47	63.39	66.15	28.30	59.66	65.93
	TiO_2	0.22	2.56	0.03	2.69	0.75	0.27	0.62	1.00	0.24	0.13	0.62
	Al_2O_3	29.03	9.77	17.67	13.35	16.46	13.80	13.70	15.75	6.49	18.44	16.37
	Fetot	3.20	13.00	0.41	12.23	6.98	1.89	5.22	6.85	2.98	5.20	4.29
	MnO	0.05	0.19	0.05	0.17	0.10	0.04	0.05	0.12	0.03	0.22	0.09
	MgO	1.73	13.25	0.00	7.31	3.13	0.28	2.76	1.70	4.57	0.10	0.09
	CaO	15.83	13.77	0.61	11.38	1.38	1.15	2.64	1.39	8.32	1.09	1.04
	Na_2O	1.54	3.18	5.72	2.29	3.91	4.12	0.95	2.10	3.02	8.95	3.24
	K_2O	0.20	1.41	3.09	0.54	0.72	4.35	2.82	3.24	1.68	4.29	4.23
	P_2O_5	0.01	1.01	1.37	0.28	0.18	0.05	0.22	0.18	0.29	4.29	3.63
												0.26
XRF	SiO_2	46.30	38.20	66.60	49.28	51.29	74.55	63.80	66.36	29.80	58.97	65.13
	TiO_2	0.22	2.61	0.01	3.61	0.70	0.22	0.59	0.92	0.24	0.11	0.58
	Al_2O_3	29.80	10.07	17.62	13.34	15.76	13.13	13.73	15.29	6.87	17.27	15.92
	Fetot	3.38	12.88	0.47	12.51	7.07	1.90	5.35	6.82	2.98	5.22	4.18
	MnO	0.04	0.20	0.04	0.17	0.10	0.03	0.05	0.13	0.03	0.20	0.08
	MgO	1.60	13.15	0.04	7.38	2.99	0.40	3.02	1.70	5.01	0.29	1.09
	CaO	15.90	13.87	0.59	11.15	1.50	1.24	2.74	1.51	9.15	1.23	3.13
	Na_2O	1.63	3.18	5.84	2.49	3.72	4.28	1.35	2.79	3.35	8.27	4.19
	K_2O	0.13	1.39	3.18	0.51	3.60	4.51	2.89	3.18	1.76	4.08	3.60
	P_2O_5	0.01	1.05	1.39	0.26	0.16	0.05	0.20	0.14	0.30	0.16	0.25

Appendix (A.6.5) : Precision, mean ($\bar{x}$), standard deviation (s) and coefficient of precision (c) for replicate analyses of Glasgow standards.

Oxides	7510 G-GN			7570 G-SL			7520 G-TR		
	$\bar{x}$	s	c	$\bar{x}$	s	c	$\bar{x}$	s	c
SiO_2	70.14	0.46	0.66	55.07	0.42	0.76	65.78	0.54	0.82
TiO_2	0.23	0.01	4.30	1.29	0.02	1.55	0.39	0.01	2.56
Al_2O_3	14.77	0.12	0.81	18.62	0.14	0.75	15.71	0.18	1.15
Fe_2O	2.87	0.07	2.44	10.37	0.15	1.45	3.27	0.07	2.14
MnO	0.06	0.02	33.30	0.18	0.02	11.10	0.11	0.02	11.20
MgO	1.69	0.17	10.10	2.32	0.15	6.47	0.52	0.04	7.69
CaO	2.17	0.05	2.30	1.49	0.02	1.34	1.55	0.03	1.94
Na_2O	5.38	0.17	3.16	2.76	0.12	4.35	5.35	0.12	2.24
K_2O	1.17	0.02	1.71	2.90	0.03	1.03	4.93	0.08	1.62
P_2O_5	0.06	0.01	16.70	0.23	0.01	4.35	0.06	0.00	0.00

<u>Appendix (A.6.6)</u> : Determination of the ferrous oxide.

This procedure was also carried out at the Geology Department, University of Glasgow. Ferrous iron is determined by titration with standard dichromate solution after the rock has been attacked by sulphuric and hydrofluoric acids.

<u>Reagents</u>

1. Hydrofluoric acid.

2. Sulphuric acid, 50% (vol./vol.).

3. Phosphoric acid, 85% (wt/vol.).

4. Boric acid.

5. Standard potassium dichromate. Weigh out accurately 2.73 gms of potassium dichromate A.R. (dried at 130°C) and dissolve in water. Dilute to 2 litres. This solution contains 2 mgs per ml. equivalent ferrous iron.

6. Diphenylamine-sulphate indicator. Prepare a 0.2% solution of sodium diphenylamine sulphonate in distilled water.

<u>Procedure</u>

Weigh out accurately about 0.5 gm of sample into a platinum crucible with a tight lid. Moisten with water and add 10 ml. 50% sulphuric acid from a tilt measure. Place on the hot plate for about five minutes (dial at 3.5) until almost boiling. Add 5 ml of hydrofluoric acid and heat for ten minutes (till puffing starts). The lid should be kept on the crucible during heating to prevent oxidation by the air. Whilst the sample is being attacked, prepare the following solutions:

Half fill a 600 ml. beaker with fresh distilled water and add:

10ml 50% sulphuric acid

1oml syrupy phosphoric acid

10g boric acid (approximately)

10 drops indicator solution

334

When the sample has been decomposed, transfer to the beaker with the lid on until the crucible is completely below the surfaace and stir and titrate rapidly with standard dichromate to apurple end point lasting for at least thirty seconds. The solution will turn green before the end point.

Calculation

$$\%FeO = \frac{\text{volume of standard dichromate} \times 0.2}{\text{weight of sample}}$$

<u>Appendix (A.6.7)</u> : Determination of water and carbon dioxide.

Using the method practised at the Geology Department , University of Glasgow, water and carbon dioxide are simultaneously determined in the rocks. The water and carbon dioxide produced are removed with a current of nitrogen, absorbed and determined gravimetrically.

<u>Apparatus</u>

A simplified schematic diagram of the apparatus used is presented in Fig. (A.6.7.1). The nitrogen gas from a cylinder is passed via a multistage regulator and needle valve, through a bubble counter containing concentrated sulphuric acid. It is purified by passage through tubes containing fused calcium chloride soda asbestos and finally anhydrous magnesium perchlorate. The gas enters the combustion tube in which is placed the rock sample. The combustion tube is supported inside the high temperature furnace and is made of mullite. The gas plus water and carbon dioxide enter the "copper" tube so that sulphur compounds and oxides of nitrogen can be removed. This tube is also supported in a furnace and is packed with alternate layers of copper wire and silver pumice. The gases enter the water absorption tube, where water is removed, which is filled with anhydrous magnesium perchlorate and then a bubbler containing saturated chromium trioxide in phosphoric acid. This bubbler removes sulphur dioxide in any rocks with a high sulphur content. The gases enter another tube with magnesium perchlorate and finally the carbon dioxide absorption tube, where carbon dioxide is removed, which is packed with soda asbestos with a small amount of anhydrous magnesium perchlorate at the end.

<u>Procedure</u>

For the majority of rock samples, the main furnace should be run at 100°C. The flow of nitrogen should be regulated to about three litres per hour. Each day before use, allow nitrogen to pass through the apparatus and absorption tubes for about 20 minutes. The absorption tubes, which are cleared and refilled each day, are wiped carefully and weighed to five decimal places. About o.5 gm. of dried powder is
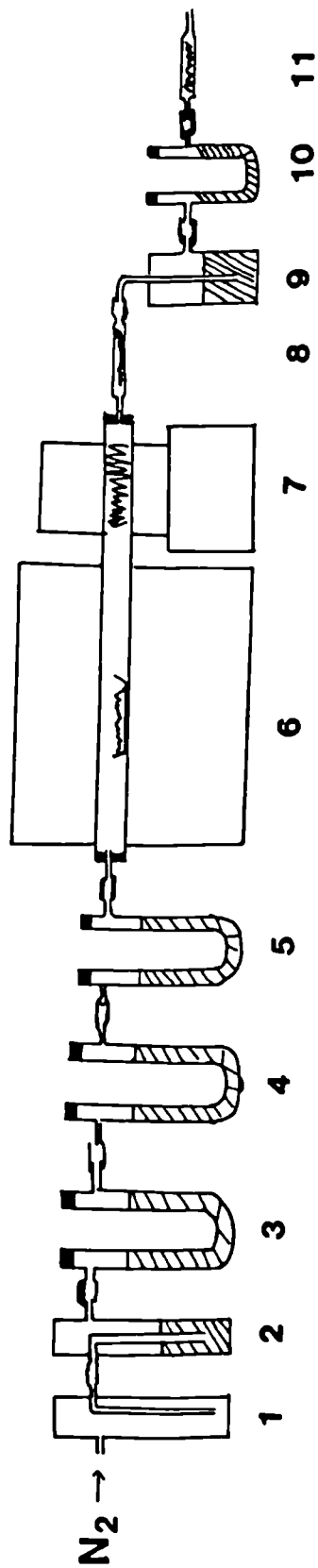
1. Empty bubbler for suck-back safety.
2. Sulphuric acid bubble counter.
3. Calcium chloride in U-tube.
4. Soda asbestos in U-tube.
5. Magnesium perchlorate in U-tube.
6. High temperature furnace with combustion tube at 1100°C containing alumina boat with sample.
7. Small furnace at 725° C with copper wire and silver gauze.
8. Water absorption tube containing magnesium perchlorate.
9. Saturated chromium trioxide in bubbler.
10. U-tube containing magnesium perchlorate.
11. Carbon dioxide absorption tube containing soda asbestos.

Fig. A.6.7.1 : Simplified schematic diagram of the apparatus used for water and carbon dioxide determinations.

337

weighed into a previously ignited alumina boat. The boat is inserted into the end of the combustion tube and nitrogen is allowed to flush air out of the apparatus for about one minute. The weighed absorption tubes are then connected and the boat is pushed into the middle of the furnace by means of a stainless steel rod. After heating for 30 minutes, the absorption tubes are removed, wiped and reweighed to 5 decimal places. A blank sample (empty alumina boat) is carried out in a similar manner. After each determination the spent boat is removed ready for the next sample and the same absorption tubes are used all day. The blank is subtracted from the respective weights of water and carbon dioxide.

Calculations

$$\% H_2O = \frac{Wt \text{ of } H_2O \text{ obtained} \times 100}{Wt \text{ of sample taken}}$$

$$\% CO_2 = \frac{Wt \text{ of } CO_2 \text{ obtained} \times 100}{Wt \text{ of samole taken}}$$

Appendix (A.6.8): Preparation of pressed powder pellets.

Equipment

1. 30 ton press.
2. Stainless steel plattens.
3. Spexmixer.
4. Polishing lap with paper laps and diamond paste.
5. Nickel spatula
6. Polythene vials and lids.
7. Glass balls.
8. RO 214.1 resin-phenol formaldehyde
9. Oven at 110°C.

Method

1. Weigh out 6 gms. of rock (3 decimal places) and 1 gm. of resin into a clean vial, (use the tare facility if possible). Add one glass bead and replace the cap. Label with sample number using a chinagraph pencil (vials can then be reused).

2. Mix powder using the spexmixer for 30 minutes-3 or 4 can be mixed at the same time

3. After mixing pour out the contents onto glossy paper and use the spatula to retrieve the glass ball. Great care must be taken not to leave the ball in the powder or it will damage the plattens, resulting in many hours work repolishing.

4. Assemble the plattens and former casing. Ensure that all the surfaces are clean- use acetone if powder is difficult to remove.

(a) Place base plate of former in position and drop bottom platten into position (Fig. A.6.8.1a,b).

(b) Pour in the powder and tap the former casing to level the surface of the powder (Fig. A.6.8.1c).

(c) Put the upper platten into the former followed by plunger, Fig. (A.6.8.1d).

339

(d) Place the complete former assembly centrally on the press platform and align the top of the plunger with the press plunger (Fig. A.6.8.1e).

5. Raise the pressure to 30 tons and leave for about one minute, then slowly release the pressure. Turn the valve handle anticlockwise to release.

6. To remove the pellet:

   (a) Remove the base plate of the former.
   (b) Stand the remainder of the former on the plastic cylinder in the press. Take care to ensure that the plastic cylinder does not obstruct the free fall of the pellet.
   (c) Pump the press until the pellet falls out of the former casing. If the lower platten comes out before this last step it should be placed face up on the foam in the plastic cylinder.

7. Label the pellet on the side with a fine felt tip pen - keep your fingers clear of the surfaces.

8. Place the pellet on a clean glass plate and when half a dozen or so have been made put the plate onto an asbestos block in the oven for 20-25 minutes to cure the resin.

9. Allow to cool and store in tissue in a labelled pill box.

10. Clean vials in ultrasonic cleaner.

<u>Na_2O contamination</u>

Remember that Na_2O is determined on the pellets, therefore keep fingers away from the inside of the former casing, the surfaces of the plattens and the surfaces of the finished pellets.

<u>Repolishing the plattens</u>

After 10-12 pellets have been made from a pair of plattens, they must be
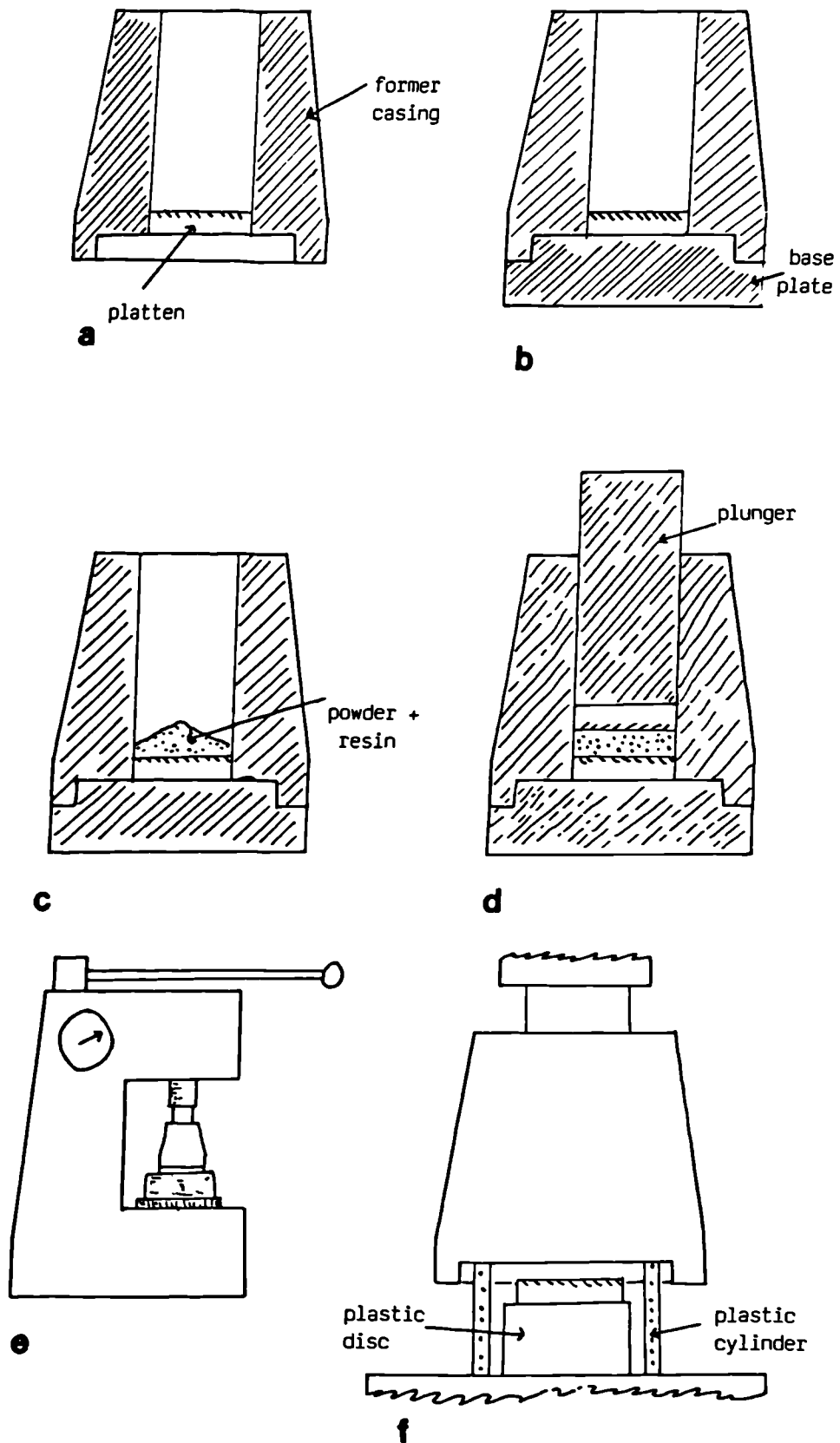
Fig. A.6.8.1 : Simplified schematic diagram illustrating
the stages for the pellet press.

341

repolished. Remember that repolishing will not remove scratches of indentations caused by leaving the glass ball in the powder; these have to be removed by grinding on 600 grade carborundum.

Appendix (A.6.9) : Instrumental parameters for the trace elements analysis using Glasgow PW 1450 X-ray Fluorescence Spectrometer.

Sample holder 32 mm	X-ray tube target Mo	Crystal		PHS					
Diaphragm 28 mm	Generator manual setting: kV = 40, mA = 20	Pos.	Type	Pos.	L.L.	W	Pos.	L.L.	W
		1	LIF 200	M	150	1000	5	400	300
Monitor G-SL 7570		2	GE	1	50	1000	6	300	400
		3	PE	2	150	600	7	400	400
Beam path VAC		4	TLAP	3	200	500	8	350	400
		5	LIF 220	4	200	600	9	300	500

Spectrometer Settings

Element	Line	X-tal	Angle	Det.	Coll.	Filter	PHS	kV	mA
M1	Mo Kβ	5	26.80	S	F	NO	9	70	30
Y1		5	Kα-1.0	S	F	NO	4	70	30
Y	Kα	5	33.83	S	F	NO	4	70	30
Y2		5	Kα+0.9	S	F	NO	4	70	30
Sr	Kα	5	35.83	S	F	NO	4	70	30
S2		5	Kα+0.8	S	F	NO	4	70	30
U	Lα	5	37.30	S	F	NO	4	70	35
Rb	Kα	5	37.93	S	F	NO	4	70	35
R2		5	Kα+0.67	S	F	NO	4	70	30
Th	Lα	5	39.22	S	F	NO	4	70	30
Pb	Lβ	5	40.40	S	F	NO	4	70	30
P2		5	Lβ+0.52	S	F	NO	4	70	30
G1		5	Kα-0.75	Fs	F	NO	4	70	30
Ga	Kα	5	56.15	Fs	F	NO	4	70	30
G2		5	Kα+0.7	Fs	F	NO	4	70	30
Zn	Kα	5	60.50	Fs	F	NO	9	70	30
Z2		5	Kα+1.0	Fs	F	NO	9	70	30
C1		5	Kα-0.5	Fs	F	NO	4	70	30
Cu	Kα	5	65.53	Fs	F	NO	4	70	30
C2		5	Kα+0.6	Fs	F	NO	4	70	30
N1		5	Kα-1.0	Fs	F	NO	3	70	30
Ni	Kα	5	71.24	Fs	F	NO	3	70	30
Z3		5	Kα-0.45	S	F	NO	4	70	30

Zr	K	5	32.05	S	F	NO	4	70	30
Fe	K	1	57.49	F	F	NO	1	40	10
F1		1	Kα-2.23	F	F	NO	1	40	10
C3		5	K -0.6	Fs	F	NO	5	70	30
Co	K	5	77.90	Fs	F	NO	5	70	30
C4		5	Kα+0.6	Fs	F	NO	5	70	30
C5		1		Fs	F	NO	8	60	45
Cr	K	1	69.30	Fs	F	NO	8	60	45
C6		1		Fs	F	NO	8	60	45
C7		1	Lβ-1.0	Fs	C	NO	8	60	45
Ce	Lβ	1	71.55	Fs	C	NO	8	60	45
C8		1	Lβ+3.0	Fs	C	NO	8	60	45
Ti	K	1	86.08	F	F	NO	6	60	20
T1		1	Kα+2.0	F	F	NO	6	60	20
B3	Lβ	5	128.92	F	C	NO	8	70	30
B1		5	43.30	F	C	NO	8	70	30
L1		5	Lβ-2.0	F	C	NO	6	70	30
La	L	5	138.94	F	C	NO	6	70	30
M2	Mo Kβ	5	26.80	S	F	NO	9	70	30

Abbreviations :

X-tal = crystal
Det. = detector
Coll. = collimator
F   = flow detector
C   = coarse primary collimator
f   = fine primary collimator
S   = scintillation detector
Fs   = flow-scintillation detector

Appendix (A.6.10) : Errors, precisions and accuracy for trace elements.

	Count rate error E%	Std. error of y in regression ppm	Upper limit of calibration ppm	Replicate analyses of G-GR 7500			Replicate analyses of G-TH 7550		
				$\bar{x}$	s	c%	$\bar{x}$	s	c%
Zr	0.70	10	300	138	15.90	11.54	269	4.60	1.71
Y	0.90	4	150	9	0.50	5.77	45	1.10	2.37
Sr	0.90	14	800	866	8.80	1.03	534	4.50	0.85
U	4.00	1	100	3	0.30	10.72	2	0.90	55.95
Rb	0.90	9	600	79	1.60	2.00	23	1.00	4.32
Th	3.00	4	400	12	0.90	7.42	7	1.40	20.60
Pb	6.00	9	100	34	0.80	2.63	9	1.10	12.06
Ga	3.00	3	100	20	0.40	2.13	25	1.00	4.07
Zn	2.00	12	1400	40	1.30	3.37	142	2.30	1.60
Cu	1.50	8	400	3	1.80	54.14	21	2.30	10.85
Ni	1.50	12	2500	6	2.30	40.38	23	3.30	14.50
Co	0.50	3	250	4	1.20	31.81	40	2.00	4.98
Cr	1.20	22	3200	12	1.30	10.91	17	1.00	5.88
Ce	2.20	8	500	34	1.60	4.74	120	2.40	2.03
Ba	0.90	10	2500	1265	22.70	1.79	769	20.80	2.71
La	2.50	6	250	21	1.90	8.91	50	3.00	6.06
Nb	2.50	4	980						
S ppm	2.50	75	5000						
S %			42%						

Appendix (A.6.11) : Operating conditions for the Nb and S (Cr-tube).

Sample holder 32 mm	X-ray tube target Cr	Crystal		PHS					
		Pos.	Type	Pos.	L.L.	W	Pos.	L.L.	W
Diaphragm 28 mm	Generator manual setting:	1	LIF 200	M			5	400	300
	kV = 40, mA = 20								
Monitor G-SL 7570		2	GE	1	50	1000	6	300	400
		3	PE	2	150	600	7	400	400
Beam path VAC		4	TLAP	3	200	500	8	350	400
		5	LIF 220	4	200	600	9	300	500

Spectrometer Settings

Element	Line	X-tal	Angle	Det.	Coll.	Filter	PHS	kV	mA
S 15	Kα	3	75.80	F	C	NO	4	50	60
S1 16	-2.9	3	72.90	F	C	NO	4	50	60
N2 32	1.0	5	29.35	S	f	NO	4	70	30
N3 33	Kα	5	30.35	S	f	NO	4	70	30
N3 34	+2.6	5	32.95	S	f	NO	4	70	30

Abbreviations:

X-tal = crystal

Det. = detector

Coll. = collimator

F = flow detector

C = coarse primary collimator

f = fine primary collimator

S = scintillation detector

346

Appendix (A.6.12) : Detection limits for trace elements.

Element	Detection Limit ppm
Zr	2.7
Y	1.4
Sr	1.5
U	9.4
Rb	1.7
Th	11.5
Pb	11.6
Ga	2.4
Zn	1.8
Cu	4.4
Ni	4.8
Co	3.2
Cr	1.9
Ce	3.2
Ba	12.3
La	3.9
S	7.1
Nb	7.3

Niggli Numbers are a series of molecular proportions of the major and minor oxides in a rock. The grouping of the oxides is such that each number represents a relative proportion among a mineral or a group of minerals. The calculation of the Niggli Numbers, except si, is independent of the SiO_2 wt% of the rocks and that eliminates the effect of SiO_2 mobilisation during metamorphism.

The following Niggli Numbers are used with their representative minerals or groups of minerals:

si	= quartz (and minor feldspars)
al	= clay minerals, feldspars, micas and chlorite
fm	= chlorite, iron oxides, clay minerals and (sulphides)
alk	= feldspars (and micas)
c	= carbonate (and possibly minor ca-plagioclase)
ti	= rutile and clay mineral
p	= phosphorous oxides
al-alk	= clay minerals (and possibly minor ca-plagioclase)

Niggli Numbers are calculated from the chemical analysis of the rocks. The chemical analysis of the rocks usually expresses the oxides in weight percentages. The procedure of calculating these numbers is as follow:

(1) Calculate the molecular proportions of the several oxides of the rock by dividing the weight percentage of each oxide by its corresponding molecular weight.

(2) Multiply each of the above molecular proportion values by 1000 to get the corresponding molecular numbers.

(3) Convert the molecular number of Fe_2O_3 to the equivalent FeO by multiplying by 2 and then add it to FeO.

(4) In order to use the Niggli terms mentioned above, the molecular numbers of the oxides should be grouped as follow:

GP1 = Na_2O + K_2O (including rare alkali earths)

GP2 = CaO + Sr + Ba

GP3 = FeO + MnO + MgO + CaO + Ni

GP4 = Al_2O_3 + Cr + rare earths
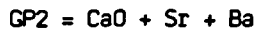
(5) Calculate the sum of the four groups and let it be (T).

(6) Recalculate the above total (T) to 100 and assign these groups to the corresponding Niggli Numbers:

$$al = \frac{Gp4 \times 100}{T}$$

$$fm = \frac{GP3 \times 100}{T}$$

$$c = \frac{GP2 \times 100}{T}$$

$$alk = \frac{GP1 \times 100}{T}$$

Thus al + fm + c + alk = 100.

(7) To obtain Niggli si, ti and P, divide their corresponding molecular numbers by the total (T) of step (5), i.e :

$$si = \frac{\text{Molecular Number of } SiO_2 \times 100}{T}$$

$$ti = \frac{\text{Molecular Number of } TiO_2 \times 100}{T}$$

$$p = \frac{\text{Molecular number of } P_2O_5 \times 100}{T}$$

(8) The Niggli values obtained in step (7) represent the most important chemical constituents of the rock. However, it is desirable to indicate the ratio of the equivalent value of K_2O to that of the sum of the alkalis and also to establish what proportion of the femic oxides is MgO. This can be achieved by calculating the two parameters k and mg, respectively.

$$k = \frac{\text{Molecular Number of } K_2O}{GP1 \text{ (in step 4)}}$$

$$mg = \frac{\text{Molecular Number of } MgO}{GP3 \text{ (in step 4)}}$$

The oxidation ratio of the rock can be also calculated using this formula:

$$w \text{ (mol. prop.)} = \frac{Fe_2O_3 \times 100}{(2Fe_2O_3 + FeO)}$$

Appendix (A.7.1): Sulphur isotope analysis of sulphides.

The methods of converting sulphide minerals to SO_2 gas and the isotopic determination of the $\delta^{34}S$ values that will be outlined below were practised in the Isotope Geology Unit of the Institute of Geological Sciences, London.

Extraction of SO_2 gas

For any isotopic analysis, care must be taken to ensure a complete yield at this stage in order to avoid possibility of kinetic fractionation during extraction. Therefore the method of Robinson and Kusakabe (1975) is being used in the extraction of SO_2 gas in this institute. This method minimises the production of sulphur trioxide, the sulphate and the other contaminant gases, particularly CO_2. The full procedure used in the extraction is as follow:

(1) Weigh accurately 10mg of pyrite or chalcopyrite concentrate (enough to produce ~3ml SO_2 gas sufficient to run on the mass spectrometer) using a Cahn 26 microbalance.

(2) Add to it ~200mg of freshly prepared cuprous oxide (Cu_2O) as an oxidant and mix in micromill for three minutes to homogenise the mixture.

(3) Carefully transfer the homogenised mixture to a silica tube two centimeters long and put silica wool plugs on both ends. The sample now is ready for extraction.

(4) Put the sample in the unheated part of the furnace tube. Evacuate the system and then heat the furnace to 1070°C.

(5) Isolate the section of the extraction line (Fig. A.7.1.1, below) from the main furnace to valve (1) from the vacuum system. Push the sample into the hot part of the furnace using the external magnet.
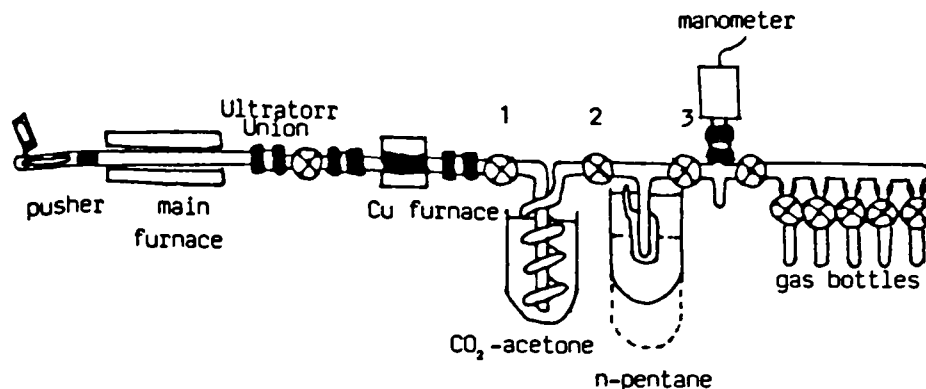
Fig.A.7.1.1 : Extraction line. Each section of the line has independent

access to roughing and high vacuum via valves which, for

simplicity, are not shown (the main furnace has rough pumping

only); and similarly each section except the manometer has a

thermocouple vacuum gauge. Taken from Coleman and Moore (1978).

(6) Apply the solid CO_2/acetone to the coil trap and the liquid nitrogen to the n-pentane trap.

(7) After 15 minutes heating, isolate the section as far as valve (3) from the vacuum and then open valve (1).

(8) Wait till all the evolved gas is frozen into the nitrogen cooled trap and all water vapour trapped in the coil. This usually takes 10-15 minutes and is indicated by the recovery of the vacuum to about 10. Torr on the thermocouple gauges.

(9) Close valve (2) and pump out the furnace and the coil section. Switch off the main furnace in preparation for running the next sample.

(10) Lower the liquid nitrogen so that the collected gas sublimes and recondenses in the part of the trap surrounded by n-pentane.

(11) Pump out the noncondensable gases and separate CO_2 gas by fractional sublimation

352

at -131°C (Oana and Ishikawa 1966).

(12) Collect the remaining pure SO_2 gas by deposition under vacuum in a gas bottles.

(13) Prepare using the same method SO_2 gas extracted from the laboratory standard.

(14) Prepare a batch of SO_2 samples sufficient for one day work on the mass spectrometer with at least two of the laboratory standard.

It is very important to measure the SO_2 yield for each run as incomplete combustion or insufficient separation of CO_2 from SO_2 can cause fractionation of ^{32}S and ^{34}S.

$$\% SO_2 \text{ yield} = \frac{\text{number (ml) of } SO_2 \text{ extracted}}{\text{mg of concentrate} \times \text{theoretical } SO_2 \text{ yield}} \times 100$$

$\delta^{34}S$ measurement

The four natural isotopes of sulphur have atomic masses 32, 33, 34 and 36. Their approximate abundances are 94.9, 0.75, 4.3 and 0.02 % respectively (MacNamara and Thode 1950). In sulphur isotopic studies, the ratio of the most abundant trace isotope (^{34}S) against the major isotope (^{32}S) is measured as follow:

$$\frac{^{34}S\ ^{16}O_2}{^{32}S\ ^{16}O_2} = \frac{^{66}SO_2}{^{66}SO_2}$$

The analysis is made with a double-collector mass spectrometer where signals from the ion beams of $^{34}SO_2$ and $^{32}SO_2$ are measured at the same time and produce a ratio. The mass spectrometer measurement is repeatedly standarised against gas of known isotopic ratio (reference gas), using the method introduced by Murphey (1947). The reference gas is calibrated against the internal laboratory standard at the begining and at the end of each day so that instrumental drift is monitored. The parameter measured from the mass spectrometer is in the form of the ratio (R^{34} sample/R^{34}

353

reference) where R^{34} is the ratio $^{34}S/^{32}S$.

The obtained R ^{34}sample/R^{34} reference ratios from the mass spectrometer is then corrected for inlet valve and crosstalk and isobaric interference following the procedure of Deines (1970) and then converted to $\delta^{34}S$ values with respect to the international Canon Diablo Triolite.

$$\delta^{34}S \, / \, \text{sample} \quad = \quad \frac{^{34}S/^{32}S \quad \text{sample}}{^{34}S/^{32}S \quad \text{standard}} \quad -1 \quad \times 1000$$

where $^{34}S/^{32}S$ of sandard = 0.0450045 (Jensen and Nakai 1963).

The calculations are performed by a programmable calculator at the Isotope Geology Unit of the Institute of Geological Sciences, London and is described in Coleman (1980).

REFERENCES

Abbey S. 1982. An evaluation of USGS III. Geostandards Newsletter, 6, 47-76.

Amstutz G.C. 1968. Spilites and spilitic rocks. In: Hess H.H. and Poldervaart A. (eds.). The poldervaart treatise on rocks of basaltic composition. Intrscience, New York, 689-736.

Anderton R. 1974. Middle Dalradian sedimentation in Argyll, with particular reference to the Jura Quartzite, Scarba Conglomerate and Craignish Phyllite. Unpubl. PhD Thesis, University of Reading.

Anderton R. 1975. Tidal flat and shallow marine sediments from the Craignish Phyllites, Middle Dalradian, Argyll, Scotland. Geol. Mag., 112, 337-348.

Anderton R. 1976. Tidal-shelf sedimentation: an example from the Scottish Dalradian. Sedimentology, 23, 429-458.

Anderton R. 1977. The Dalradian rocks of Jura. Scott. Jl. Geol., 13, 135-142.

Anderton R. 1979. Slopes, submarine fans and syndeposional faults : sedimentology of parts of the Middle and Upper Dalradian in the SW-Highlands of Scotland. In: Harris A.L., Holland C.H. and Leake B.E. (eds.). The Caledonides of the British Isles-reviewed. Spec. Publ. Geol. Soc. Lond., No.8, Scottish Academic Press, Edinburgh, 483-488.

Anderton R. 1980a. Did Iapetus start to open during the Cambrian ? Nature, 286, 706-708.

Anderton R. 1980b. Distinctive pebbles as indicators of Dalradian Provenance. Scott. Jl. Geol., 16, 143-152.

Anderton R. 1982. Dalradian deposition and the late Precambrian-Cambrian history of

the N. Atlantic region: a review of the early evolution of the Iapetus Ocean. Jl. Geol. Soc. Lond., 139, 421-431.

Anderton R. 1985. Sedimentation and tectonics in the Scottish Dalradian. Scott. Jl. Geol., 21, 407-436.

Anderton R., Bridges P.H., Leeder M.R. and Sellwood B.W. 1979. A dynamic stratigraphy of the British Isles. George, Allen and Unwin, London.

Arthurs J.W. 1976. The geology and metalliferous mineral potential of the Sperrin Mountains area. Unpubl. Rep. Geol. Survey Northern Ireland, Belfast.

Arthurs J.W. 1977. The geology and metalliferous mineral potential of northeast Antrim. Unpubl. Rep. Geol. Survey Northern Ireland, Belfast.

Atherton M.P. 1964. The garnet isograd in pelitic rocks and its relation to metamorphic facies. Am. Min., 49, 1331-1349.

Atherton M.P. 1965. The chemical significance of isograd. In: Pitcher W.S. and Flinn W. (eds.). Controls of metamorphism. Oliver and Boyd, Edinburgh, 169-202.

Atherton M.P. 1968. The variation in garnet, biotite and chlorite compositions in medium grade pelitic rocks from the Dalradian of Scotland, with particular reference to the zonation in garnet. Contr. Min. Petr., 18, 347-371.

Atherton M.P. 1977. The metamorphism of the Dalradian rocks of Scotland. Scott. Jl. Geol., 13, 331-370.

Atherton M.P. and Brotherton M.S. 1979. Thorium and Uranium in some pelitic rocks from the Dalradian, Scotland. Chem. Geol., 27, 329-342.

Bachinski D.J. 1977. Sulphur isotopic composition of ophiolitic cupriferous iron sulphide deposits, Norte Dame Bay, Newfoundland. Econ. Geol., 72, 243-257.

Bailey E.B. 1983. Eddies in mountain structure. Q. Jl. Geol. Soc. Lond., 94, 607-625.

356

Bailey S.W. 1984. Micas. Min. Soc. Am. Mineralogical Reviews in Mineralogy, 13.

Baldwin C.T. and Johnson H.D. 1977. The Dalradian rocks of Lunga, Luing and Shuna. Scott. Jl. Geol., 13, 143-154.

Baraclough A.K. 1981. Sedimentology of the Crinan Grits and associated Dalradian sediments in Argyll and Donegal. Unpubl. PhD Thesis, University of Strathclyde.

Barnes H.L. 1967. Geochemistry of hydrothermal ore deposits. 1st Edn., New York, Holt Reinhart and Winston.

Barnes H.L. 1979. Geochemistry of hydrothermal ore deposits. 2nd Edn., Wiley-Interscience.

Barrow G. 1893. On an intrusion of muscovite-biotite gneiss in the Southeast Highlands of Scotland and its accompanying metamorphism. Q. Jl. Geol. Soc. Lond., 49, 330-358.

Barrow G. 1912. On the geology of lower Deeside and the Southern Highland Border. Proc. Geol Assoc., 23, 268-284.

Barth T.F.W. 1962. Theoritical petrology. Wiley and Son, New York (2nd edt.).

Barton P.B. 1978. Some ore textures involving sphalerite from the Furatobe mine, Akita Prefecture, Japan. Mining Geol., 28, 293-300.

Berger B.R. and Bethke P.M. 1985. Geology and geochemistry of epithermal systems. Rev. Econ. Geol., 2.

Beus A.A. and Grigorian S.V. 1977. Geochemical exploration methods for mineral ueposits. Applied Publishing, Illionois.

Borradaile G.J. 1973. Dalradian structure and stratigraphy of the northern Loch Awe district, Argyllshire. Trans. R. Soc. Edinb., 69, 1-21.

Borradaile G.J. and Johnson H.D. 1973. Finite strain estimates from the Dalradian Dolomitic Formation, Islay, Argyll, Scotland. Tectonophysics, 18, 249-259.

Bowes D.R. and Leake B.E. 1978. Crustal evolution in northwestern Britain and adjacent regions. Geol. Jl. Spec. Issue No. 10, Seel House Press, Liverpool.

Bowie S.H.V., Kualheim A. and Haslam H.W. 1978. Mineral deposits of Europe, Vol. 1, northwest Europe. Instn. Min. Metall.

Bradbury H.J., Harris A.L. and Smith R.A. 1979. Geometry and emplacement of nappes in he Central Scottish Highlands. In : Harris A.L., Holland C.H. and Leake B.E. (eds.). The Caledonides of the British Isles-reviewed. Spec. Publ. Geol. Soc. No. 8, Scottish Academic Press, Edinburgh, 213-220.

Bradbury H.J., Smith R.A. and Harris A.L. 1976. "Older" granites as time-markers in Dalradian evolution. Jl. Geol. Soc. Lond., 132, 677-684.

Bralia A., Sabatini G. and Troja F. 1979. A reevaluation of the Co:Ni ratio in pyrite as a geochemical tool in ore genesis problems. Mineral. Deposita, 14, 353-374.

Brewer M.S., Brook M. and Powell D. 1979. Dating of the tectono-metamorphic history of the southwestern Moine, Scotland. In: Harris A.L., Holland C.H. and Leake B.E. (eds.). The Caledonides of the British Isles-reviewed. Spec. Publ. Geol. Soc. Lond., Scottish Academic Press, Edinburgh, 129-137.

Brock T.D. 1980. Precambrian evolution. Nature, 288, 214-215.

Brook M., Powell D. and Brewer M.S. 1977. Grenville events in Moine rocks of the Northern Highlands, Scotland. Jl. Geol. Soc. Lond., 133, 489-496.

Brown E.H. 1967. The greenschist facies in part of Eastern Otago, Newzealand. Contr. Mineral. Petr., 14, 259-292.

Brown G. and Norrish K. 1952. Hydrous micas. Min. Mag., 29, 929-932.

Browne P.R.L. 1978. Hydrothermal alteration in active Geothermal fields. Ann. Rev. Earth Planet Sci., 6, 279-350.

Buddington A.F. and Lindsley D.H. 1964. Iron-titanium oxide minerals and synthetic equivalents. Jl. Petr., 5, 310-357.

Cambel B. and Jarkovsky J. 1966. Rare elements in pyrites deposits of the western Carpathians in connection with genetic problems of mineralisation in: Khitarov H.I. (ed.). Problems of geochemistry. Vol. 1, 266-282.

Campbell A. 1980. Water-rock interaction. Int. Assoc. Geochem. and Cosmochem. /Alberta Res. Council 3rd International Symposium.

Campbell F.A. and Ethier V.G. 1974. Sulphur isotopes, iron content of sphalerites and ore textures in Anvil orebody, Canada. Econ. Geol., 69, 482-493.

Cann J.R. 1969. Spilites from the Carlsberg Ridge, Indian Ocean. Jl. Petr., 10, 1-19.

Cann J.R. 1971. Major element variation in ocean floor basaltic rocks. Earth Planet Sci. Lett., 10, 7-11.

Cardellach E., Phillips R. and Ayora C. 1982. Metamorphosed stratiform sulphides of the Liat area, central Pyrenees, Spain. Trans. Instn. Min. Metall., 91, B90-B94.

Chinner G.A. 1960. Pelitic gneisses with varying ferrous ferric ratios from Glen Clova, Angus, Scotland. Jl. Petr., 1, 178-217.

Chinner G.A. 1966. The distribution of pressure and temperature during Dalradian .etamorphism. Q. Jl. Geol. Soc. Lond., 122, 159-186.

Chinner G.A. 1980. Kyanite isograd of Grampian metamorphism. Jl. Geol. Soc. Lond., 137, 35-39.

Chinner G.A. and Heseltine F.J. 1979. The Grampide andalusite-kyanite isograd. Scott. Jl. Geol., 15, 117-127.

359

Claypool G.E., Holser W.T., Kaplan I.R., Sakai H. and Zak I. 1980. The age curves of sulphur and oxygen isotopes in marine sulphate and their mutual interpretation. Chem. Geol., 28, 199-260.

Clough C.T. 1913. The copper lodes of Inveryne and Kilfinan, Argyllshire. Summary of Progr. Geol. Survey for 1912, H.M.S.O., London, 92-95.

Clough C.T., Hinxman L.W., Wilson J.S.G., Grampton C.B., Wright W.B., Bailey E.B., Anderson E.M. and Carruthers R.G. 1911. Geology of the Glasgow district. Mem. Geol. Survey. Scotland.

Coats J.S., Forty N.J., Gallagher M.J. and Grout A. 1984. Stratiform barium enrichment in the Dalradian of Scotland. Econ. Geol., 79, 1585-1595.

Coats J.S., Smith C.G., Fortey N.J., Gallagher M.J., May F. and McCourt W.J. 1980. Stratabound barium-zinc mineralisation in Dalradian schist near Aberfeldy, Scotland. Trans. Instn. Min. Metall., 89, B110-B122.

Coats J.S., Smith C.G. and others. 1981. Stratabound barium-zinc mineralisation in Dalradian schist near Aberfeldy, Scotland. Min. Recc. Progr. Rep. Inst. Geol. Sci. No. 40.

Cochran Patrick 1878. Early records relating to mining in Scotland.

Coleman M.L. 1977. Sulphur isotopes in petrology. Jl. Geol. Soc. Lond., 133, 593-608.

Coleman M.L. 1980. Corrections for mass spectrometer analysis of SO . Inst. Geol. Sci. Isotope Geology Unit, Stable Isotope Rep., No. 45.

Coleman M.L. and Moore M.P. 1978. Direct reduction of sulphates to sulphur dioxide for isotopic analysis. Anal. Chem., 50, 1594-1595.

Coomer P.G. and Robinson B.W. 1976. Sulphur and sulphate-oxygen isotopes and the origins of the Silvermines deposits, Ireland. Mineral. Deposita, 11, 155-169.

Cowie J.H., Rushton A.W.A. and Subblefield C.J. 1972. A correlation of Cambrian rocks in the British Isles. Geol. Soc. Lond. Spec. Rep. No. 2.

Cox K.G., Bell J.D. and Pankhurst R.J. 1979. The interpretation of igneous rocks. George Allen and Unwin, Lond. (Ist edn.).

Craig G.Y. 1965. The geology of Scotland. 1st Edn., Edinburgh, Oliver and Boyd.

Craig G.Y. 1983. Geology of Scotland. 2nd Edn., Scott. Academ. Press, Edinburgh.

Craig J.R., Vaughan D.J. and Higgins J.B. 1979. Phase relations in the Cu-Co-S system and mineral associations of the Carrollite (CuCo S)-linnaeite (Co S) series. Econ. Geol., 74, 657-671.

Crerar D.A. and Barnes H.L. 1976. Ore solution chemistry v. solubilities of chalcopyrite and chalcocite assemblages in hydrothermal solution at 200 C to 500 C. Econ. Geol., 71, 772-794.

Cummins W.A. and Shackleton R.M. 1955. The Ben Lui recumbent syncline (SW-Highlands). Geol. Mag., 92, 353-363.

Deb M. 1980. Genesis and metamorphism of two stratiform massive sulphide deposits at Ambaji and Deri in the Precambrian of western India. Econ. Geol., 75, 572-591.

Deer W.A., Howie R.A. and Zussman J. 1963. Rock-forming minerals : ortho and ring silicates, Vol. 1, Longman.

Deer W.A., Howie R.A. and Zussman J. 1963. Rock-forming minerals: chain silicates, Vol. 2, Longman.

Deer W.A., Howie R.A. and Zussman J. 1963. Rock-forming minerals: sheet silicates, Vol. 3, Longman.

Deer W.A., Howie R.A. and Zussman J. 1966. An introduction to the rock forming minerals. Longman.

361

Deines P. 1970. Mass spectrometer correction factors for determination of small isotopic variations of carbon and oxygen. Int. Jl. Mass. Spectrom. Ion. Phys., 4, 283-295.

De Waal S.A. and Johnson J.A. 1981. Chemical hetrogeneity of sphalerite in a base metal sulphide deposit. Econ. Geol., 76, 694-705.

Dewey J.F. 1969. Evolution of the Appalachian -Caledonian orogeny. Nature, 222, 124-129.

Dewey J.F. 1971. A model for the Lower Phanerozoic evolution of the southern margin of the Caledonides of Scotland and Ireland. Scott. Jl. Geol., 7, 219-240.

Dewey J.F. 1982. Plate tectonics and the evolution of the British Isles. Jl. Geol. Soc. Lond., 139, 371-412.

Dewey J.F. and Pankhurst R.J. 1970. Evolution of the Scottish Caledonides in relation to their isotopic age pattern. Trans. R. Soc. Edinburgh, 68, 361-389.

Dewey J.F. and Shackelton R.M. 1984. A model for the evolution of the Grampian tract in the early Caledonides and Appalachians. Nature, 312, 115-120.

Dhannoun H.Y. and Fyfe W.S. 1972. Reaction rates of hydrocarbons with anhydrite. Progr. Experim. Petr., 2, 69-71.

Downie C., Lister T.R., Harris A.L. and Fettes D.J. 1971. A palynological investigation of the Dalradian rocks of Scotland. Rep. No. 71/9 Inst. Geol. Sci., 30 pp.

Dunham K.C. 1952. Age relations of the epigenetic mineral deposits of Britain. Trans. Geol. Soc. Glasgow, 21, 395-429.

Dunham K., Beer K.E., Ellis R.A., Gallagher M.J., Nutt M.J.C. and Webb B.C. 1978. United Kingdom. In: Bowie S.H.V., Kualheim A. and Haslan H.W. (eds.). Mineral deposits of Europe, Vol. 1, Northwest Europe, 263-317.

Dunning F.W. 1972. Dating events in the metamorphic Caledonides : impressions of the
Symposium held in Edinburgh, Sept., 1971. Scott. Jl. Geol., 8, 179-192.

Elders W.A. 1979. Guidebook: geology and geothermics of the Salton Trough. Geol. Soc.
Am., 92nd Annual Meeting, San Diego, 70-76.

Elders W.A. 1981. Application of petrology and geochemistry of the study of active
geothermal systems in the Salton Trough of California and Baja California. In:
Hausen D.M. and Park W.C. (eds.). Process mineralogy, extractive metallurgy, mineral
exploration, energy resources. The Metallurgical Socity of AIME, Report No. 81/6,
591-606.

Elles G.L. 1931. Notes on the Portrsoy coastal district. Geol. Mag., 68, 24-34.

Elles G.L. and Tilley C.E. 1930. Metamorphism in relation to structure in the Scottish
Highlands. Trans. R. Soc. Edinb., 56, 621-646.

Ellis R.A. and others, 978. Disseminated sulphide mineralisation at Garbh Achadh,
Argyllshire, Scotland. Miner. Reconn. Progr. Rep. Inst. Geol. Sci. No. 23.

Engel A.E.J. and Engel C.G. 1958. Progressive metamorphism and granitisation of the
major paragneiss, northwest Adirondack Mountains, New York. Jl. Geol. Soc. Am.
Bull., 69, 1369-1414.

Engel A.E.J. and Engel C.E. 1962. Hornblend formed during progressive metamorphism of
amphibolites, NW Adirondack Mountain, New York. Geol. Soc. Am. Bull., 73, 1499-1515.

Ernst W.G. 1963. Significance of phengitic micas from low-grade schists. Am. Min.,
48, 1357-1373.

Eugster H.P. and Bones D.R. 1962. Stability relations of the ferruginous biotite,
annite. Jl. Petr., 3, 82-125.

Eyles C.H. and Eyles N. 1983. Glaciomarine model for upper Precambrian diamictites of
the Port Askaig Formation, Scotland. Geology, 11, 692-696.

Fairchild I.J. 1980a. Sedimentation and origin of a late Precambrian "dolomite" from Scotland. Jl. Sed. Petr., 50, 423-446.

Fairchild I.J. 1980b. Stages in a Precambrian dolomitisation, Scotland: cementing versus replacements : preservation of diagenetic textures. Jl. Geol. Soc. Lond., 142, 167-185.

Farkas A. 1973. A trace-element study of the Texas Gulf orebody. Timmins, Ontario. Unpubl. Thesis, University of Albert, quoted in Wolf 1976.

Faure G. 1977. Principles of isotope geology. John Wiley and Sons, New York.

Ferriday I.L., Halls C. and Hembre O.S. 1981. Stratigraphic and mineralogical identity of exhalative sediments with relationship to the stratiform volcanogenic orebody at Skorvas, Norwegian Caledonides. In Hall A.J. and Gallagher M.J. (eds.). Caledonian-Appalachians stratabound sulphides. Correlation of Caledonian stratabound sulphides, Glasgow Abstract Volume, 34-41.

Fettes D.J. 1979. A metamorphic map of the British and Irish Caledonides. In: Harris A.L., Holland C.H. and Leake B.E. (eds.). The Caledonides of the British Isles-reviewed. Spec. Publ. Geol. Soc. Lond., No. 8, Scottish Academic Press, Edinburgh, 306-321.

Fettes D.J. 1983. Metamorphism in the British Caledonides. In: Schenk P.E. (ed.). Regional trends in the geology of the Appalachian-Caledonian-Hercynian-Mauritanide orogen, Reidel Publishing Company, 205-219.

Fettes D.J., Graham C.M., Sassi F.P. and Scolari A. 1976. The basal potassic white micas and facies series variations across the Caledonides. Scott. Jl. Geol., 12, 227-236.

Fisk S. 1986. An oxygen isotope study of siliceous rocks associated with stratabound mineralisation in Scoland and Ireland. Unpubl. PhD. Thesis, University of Strathclyde.

Fleischer M. 1955. Minor elements in some sulphides. Econ. Geol. 50th anniversary volume, 970-1024.

Forty N.J. and Beddoes-Stephens B. 1982. Barium silicates in stratabound Ba-Zn mineralisation in the Scottish Dalradian. Min. Mag., 46, 63-72.

Foster M.D. 1956. Correlation of dioctahedral potassium micas on the basis of their charge relations. Bull. U.S. Geol. Surv., 1036D, 57-67.

Foster M.D. 1960. Interpretation of the composition of trioctahedral micas. U.S. Geol. Surv. Prof. Paper 354B, 11-46.

Foster M.D. 1962. Interpretation of the composition and classification of the chlorites. U.S. Geol. Surv. Prof. Paper, 414A, 1-33.

Frater K.M. 1985a. Mineralisation at the Golden Grove Cu-Zn deposit, western Australia, I: premetamorphic textures of the opaque minerals. Can. Jl. Earth Sci., 22, 1-14.

Frater K.M. 1985b. Mineralisation at the Golden Grove Cu-Zn deposit, western Australia, II: deformation textures of the opaque minerals. Can. Jl. Earth Sci., 22, 15-26.

Friedman I. and O'Neil J.R. 1977. Compilation of stable isotope fractionation factors of geochemical interest. In: Data Geoch, 6th Edn. Geol. Surv. Prof. Paper, 440KK.

Friedrich G., Schachner D. and Nielsen H. 1964. S-Isotopenuntersuchungen and sulfiden aus dem Erzvorkommen der sierra de Cartagena in Spanien. Geochim. Cosmochim. Acta, 28, 683.

Gallagher M.J. and Coats J.S. 1984. Prospecting in areas of glaciated terrain. Trans. Instn. Min. Metall.

Garson M.S. and May F. 1976a. Copper mineralisation at Vidlin, Shetland. Trans. Instn. Min. Metall., 85, B153-B157.

Garson M.S. and May F. 1976b. Investigations of copper mineraliosation at Vidlin,

Shetland. Miner. Reconn. Progr. Rep. Inst. Geol. Sci., No.4.

Garson M.S. and Plant J. 1973. Alpine type ultramafic rocks and episodic mountain building in the Scottish Highlands. Nature, 242, 34-38.

Gavelin S., Parwel A. and Ryhage R. 1960. Sulphur isotope fractionation in sulphide mineralisation. Econ. Geol., 55, 510-530.

Govindaraju K. 1980. Report (1980) on three GII-TWG rock reference samples: Anorthosite from Greenland, AN-G; Basalte d'Esseyla-Cote, BE-N; Granite de Beauvoir, MA-N. Geostandards News letter, 4, 49-138.

Gower P.G. 1973. The Middle-Upper Dalradian boundary with special reference to the Loch Tay Limestone. Unpubl. Thesis, University of Liverpool (quoted in Anderton R. 1985).

Graham Callander 1904. A stone mould for casting flat bronze axes, etc. Proc. Antig. Soc., xxxviii, P. 487,

Graham C.M. 1973. Chemical Petrology of metamorphosed basic rocks of the Dalradian series, with particular reference to the Knapdale area of Argyll. Unpubl. PhD Thesis, Edinburgh University.

Graham C.M. 1974. Metabasite amphiboles of the Scottish Dalradian. Contr. Mineral. Petr., 47, 165-185.

Graham C.M. 1976. Petrochemistry and tectonic significance of the Dalradian metabasaltic rocks of the SW Scottish Highlands, Jl. Geol. Soc. Lond., 132, 61-84.

Graham C.M. 1983. High-pressure greenschist to epidote-amphibolite facies metamorphism of Dalradian rocks of the SW Scottish Highlands: isograd and P-T conditions (abst). Newsl. Geol. Soc. Lond., 12, 23.

Graham C.M. 1985. High-pressure greenschist to epidote-amphibolite facies metamorphism of Dalradian rocks of the S-W Scottish Highlands: isograd and P-T conditions. In:

Graham C.M. and Harte B. (eds.). Conditions of the Dalradain metamorphism. Jl. Geol. Soc. Lond., 142, 3-4.

Graham C.M. and Bradbury H.J. 1981. Cambrian and Late Precambrian basaltic igneous activity in the Scottish Dalradian: a review. Geol. Mag., 118, 271-237.

Graham C.M. and Harte B. 1985. Conditions of Dalradian metamorphism. Jl. Geol. Soc. Lond., 142, 1-5.

Grant Wilson and Cadell 1884. Breadalbane Mines, Proc. R. Phys. Soc. Edinburgh, viii, P.197.

Gribble C.D. and Hall A.J. 1985. A practical introduction to optical mineralogy. George Allen and Unwin.

Grout A. and Gallagher M.J. 1980. Barium determination in rock and overburden by portable X.R.F. spectrometer. Trans. Instn. Min. Metall., 89, B130-B133.

Guidotti C.V. 1984. Micas in metamorphic rocks. In: Bailey S.W.(ed.). Micas. Min. Soc. Am. Rev. in Mineralogy, 13, 357-467.

Gumbel C.W. Von 1874. "Die palaolithischen E ruptivgesteine des Fichtelgebirges: Munich (quoted in Wiseman J.D.H. 1934).

Gunn W., Clough C.T. and Hill J.B. 1897. The geology of cowal. Mem. Geol. Survey Scotland, H.M.S.O., Edinburgh.

Hackman B.D. and Knill J.L. 1962. Calcareous algae from the Dalradian of Islay. Palaeontology, 5, 268-271.

Hajash A. 1975. Hydrothermal processes along mid-ocean ridges : an experimental investigation. Contr. Min. Petr., 53, 205-226.

Hall A.J. 1982. Gypsum as a precursor to pyrrhotite in metamorphic rocks: evidence from Ballachulish, Scotland. Mineral. Deposita, 17, 401-409.

Hall A.J. and Gallagher M.J. 1981. Caledonian-Appalachian stratabound sulphides. Correlation of Caledonian stratabound sulphides, Glasgow, Abstract Volume.

Harland W.D. and Gayer R.A. 1972. The Arctic Caledonides and earlier oceans. Geol. Mag., 109, 289-314.

Harper C.T. 1967. The geological interpretation of potassium-argon ages of metamorphic rocks from the Scottish Caledonides. Scott. Jl. Geol., 3, 46-66.

Harris A.L., Baldwin C.T., Bradbury H.J., Johnson H.D. and Smith R.A. 1978. Ensialic basin sedimentation: the Dalradian Supergroup. In: Bowes D.R. and Leake B.E. (eds.). Crustal evolution in northwestern Britain and adjacent regions. Geol. Jl. Spec. Issue No. 10, 115-138.

Harris A.L., Bradbury H.J. and McGongal M.H. 1976. The evolution and transport of the Tay Nappe. Scott. Jl. Geol., 12, 103-113.

Harris A.L., Holland C.H. and Leake B.E. 1979. The caledonides of the British Isles-reviewed. Spec. Publ. Geol.Soc. Lond., No.8, Scottish Academic Press, Edinburgh, 483-488.

Harris A.L. and Pitcher W.S. 1975. The Dalradian Supergroup. In : Harris A.L., Shackelton R.M., Watson J., Downie C., Harland W.B. and Moorbath S. (eds.). A correlation of Precambrian rocks in the British Isles. Spec. Publ. Geol. Soc. Lond., No. 6, 52-75.

Harris A.L., Shackleton R.M., Watson J., Downie C., Harland W.B. and Moorbath S. 1975. A correlation of Precambrian rocks in the British Isles. Spec. Publ. Geol. Soc. Lond., No. 6.

Harvey P.K., Taylor D.M., Hendry R.D. and Bancroft R.D. 1973. An accurate fusion method to the analysis of rocks of chemically related materials by X-ray fluorescence spectrometry. X-ray Spectrometry, 2, 33-44.

Haselock P.J., Winchester J.A. and Whittles K.H. 1982. The stratigraphy and structure of the southern Monadhliath Mountains between Loch Killin and Glen Roy. Scott. Jl. Geol., 18, 275-290.

Hawthorne F.C. 1976. The crystal chemistry of the amphiboles : the structure and chemistry of Arfivedsonite. Canad. Mineral., 14, 346-356.

Hayba D.O., Bethke P.M., Healde P. and Foley N.K. 1985. Geologic, Mineralogic and geochemical characteristics of volcanic-hosted epithermal precious-metal deposits. In: Berger B.R. and Bethke P.M. (eds.). Geology and geochemistry of epithermal systems. Rev. Econ. Geol., 2, 129-169.

Hegemann F. 1943. Die geochemische Bedentung von kobalt und nickel im pyrite. Z. Angew. Mineral, 4, 122-239 (quoted in Wolf 1976).

Henry D.K., Craig J.R. and Gilbert M.C. 1979. Ore mineralogy of the Great Gossan Lead, Virginia. Econ. Geol., 74, 645-656.

Hess H.H. and Poldervaart A. 1968. Basalt : the Poldervaart treatise on rocks of basaltic composition. Interscience, New York.

Hey M.H. 1954. A new review of the chlorites. Min. mag., 30, 277-292.

Hickman A.H. 1975. The stratigraphy of late Precambrian metasediments between Glen Roy and Lismore. Scott. Jl. Geol., 11, 117-142.

Hill J.B., Peach B.N., Clough C.T. and Kynaston J.B. 1905. The geology of Mid-Argyll. Explanation of sheet No. 37. Mem. Geol. Survey, Scotland, H.M.S.O., Glasgow.

Hillebrand W.F. and Lundell G.E.F. 1929. Applied inorganic analysis, New York (Wiley).

Hinxman L.W. 1896. Explanation of sheet 75 (west Aberdeenshire), Banffshire, parts of Elgin and Inverness. Mem. Geol. Survey, Scotland.

Hoefs J. 1980. Stable isotope geochemistry. Springer-Verlag, 2nd edition.

Hoffer E. 1978. On the "late" formation of paragonite and its breakdown in pelitic rocks of the southern Damara orogen (Nambia). Contr. Min. Petr., 67, 209-219.

Hopkinson E.G. 1970. Mineralisation of the area around Kilfinan and Inveraray, Loch Fyne, Argyllshire, Scotland. Unpupl. MSc. Thesis, University of Strathclyde.

Howarth R.J. 1971. The Port Askaig Tillite succession (Dalradian) of Con Donegal. Proc. R. Ir. Acad., 71B, 1-35.

Hsu L.C. 1968. Selected phase relationships in the system Al-Mn-Fe-Si-O-H: a model for garnet equilibria. Jl. Petr., 9, 40-83.

Hughes C.J. 1972. Spilites, keratophyres and the igneous spectrum. Geol. Mag., 109, 513-527.

Hunter J.R. S. 1884. The Silurian districts of Leadhills and Wanlockhead. Trans. Geol. Soc. Glasgow, vii, P.376.

Hutchinson M.N. and Scott S.D. 1980. Sphalerite geobarometry applied to metamorphosed sulphide ores at the Swedish Caledonides and U.S. Appalachians. Norges Geol. Unders., 360, 59-71.

Hutchinson M.N. and Scott S.D. 1981. Sphalerite geobarometry in the copper-iron-zinc system. Econ. Geol., 76, 143-153.

Indrof C.P. 1981. The Silver Hill zinc deposit and associated deposits, central .orth Carolina. Econ. Geol., 76, 1170-1185.

Itoch S. 1977a. Chemical compositions of the country rocks and minor elements in sulphide minerals from bedded cupriferous pyrite deposits of Tenryn River basin. Bull. Geol. Survey, Japan, 22, 117-132.

Itoch S. 1977b. Minor elements in sulphide minerals from Shirataki mine, Kochi Prefecture, Japan. Bull. Geol. Survey, Japan, 22, 367-384.

Itoch S. and Kanehira I. 1967. Trace elements in sulphide minerals from the Tsuchikura. Shiga Prefecture with special reference to the contents of cobalt and nickel. Min. Geol. Japan, 17, 251-260 (in Japanese with English abstract).

Jager E. and Hunziker J.C. 1979. Lectures in isotope geology. Springer, Berlin - Heidelberg-New York.

Jenkins R. and De Vries J.L. 1967. Practical X-ray spectrometry. Macmillan, London (1st edn.).

Jensen M.L. 1967. Sulphur isotopes and mineral genesis. In : Barnes H.L. (ed.). Geochemistry of hydrothermal ore deposits. Holt, Rinehart and Winston, New York, 143-165.

Jensen M.L. and Nakai N. 1963. Sulphur isotope meteorite standards : results and recommendations. In: Biochemistry of sulphur isotopes. Proceedings National Science Foundation, Yale University, 30-35.

Johnson M.R.W. 1963. Some time relations of movement and metamorphism in the Scottish Highlands. Geol. en Mijnb., 5, 121-142.

Johnson M.R.W. 1983. Dalradian. In: Craig G.Y. (ed.). Geology of Scotland (2nd edn.), 77-104. Scottish Academic Press, Edinburgh.

Johnson M.R.W., Sanderson D.J. and Soper N.J. 1979. Deformation in the Caledonides of England, Ireland and Scotland. In: Harris A.L., Holland C.H. and Leake B.E. (eds.). The Caledonides of the British Isles-reviewed. Spec. Publ. Geol. Soc. Lond., No.8, Scottish Academic Press, Edinburgh, 165-186.

Johnson M.R.W. and Stewart F.H. 1963. The British Caledonides. Oliver and Boyd, Edinburgh.

Johnstone G.S. 1966. British regional geology, the Grampian Highlands. H.M.S.O., Edinburgh (2nd edn.).

371

Johnstone G.S. 1975. The Moine succession. In: Harris A.L., Shackleton R.M., Watson J., Downie C., Harland W.B. and Moorbath S. (eds.). A correlation of Precambrian rocks in the British Isles. Spec. Publ. Geol. Soc. Lond., No. 6, 30-42.

Johnstone G.S. and Gallagher M.J. 1980a. Caledonian stratabound sulphides in the United Kingdom. In: Vokes F.M. and Zachrisson E. (ed.). Review of Caledonian-Appalachian stratabound sulphides. Geol. Surv. Ireland. Spec. Paper No. 5, 63-66.

Johnstone G.S. and Gallagher M.J. 1980b. Compilation of stratabound mineralisation in the Scottish Caledonides. Miner. Reconn. Progr. Rep. Inst. Geol. Sci., No. 37.

Johnstone G.S. and Smith D.I. 1965. Geological observations concerning the Breadalbane hydro-electric project, Perthshire. Bull. Geol. Surv. G.B., 22, 27.

Johnstone G.S., Smith D.I. and Harris A.L. 1969. Moinian assemblage of Scotland. In: Kay M. (ed.). North Atlantic- geology and continental drift, a Symposium Mem. Am. Assoc. Petrol. Geol., 12, 159-180.

Jones T.A. 1969. Skewness and kurtosis as criteria of normality in observed frequency distribution. Jl. Sed. Petr., 39, 1622-1627.

Juve G. 1974. Ore microscopy and ore types of the Stekenjokk ore deposit, central Scandinavian Caledonides, Sweden. Sver. Geol. Unders., C706.

Juve G. 1977. Metal distribution at Stekenjokk : primary and metamorphic patterns. Geol. For. Stockh. Forh., 99, 149-158.

Kajiwara Y. 1971. Sulphur isotope study of the Kuroko-ores of the Shakanai No.1 deposits, Akita Prefecture, Japan. Geochem. Jl. 4, 157-181.

Kajiwara Y. and Date J. 1971. Sulphur isotope study of Kuroko-type and Kueslager-type stratabound massive sulphide deposits in Japan. Geochem. Jl., 5, 133-150.

Kalliokoski J. 1965. Metamorphic features in north American massive sulphide deposits. Econ. Geol., 60, 485-505.

Kay M. 1969. North-Atlantic-geology and continental drift. A Symposium Mem. Am. Assoc. Petrol. Geol., 12.

Kennedy W.Q. 1958. The tectonic evolution of the Midland Valley of Scotland. Trans. Geol. Soc. Glasgow, 23, 106-133.

Kerrich R., Beckinsale R.D. and Durham J.J. 1977. The transition between deformation regimes dominated by intercrystalline diffusion and intercrystalline creep evaluated by oxygen isotope thermometry. Tectonophysics, 38, 241-258.

Kilburn C., Pitcher W.S. and Shackleton R.M. 1965. The stratigraphy and origin of the Port Askaig Boulder Bed Series (Dalradian). Geol. Jl., 4, 343-360.

Kiyosu Y. 1980. Chemical reduction and sulphur isotope effects of sulphate by organic matter under hydrothermal conditions. Chem. Geol., 30, 47-56.

Knill J.L. 1963. A sedimentary history of the Dalradian series. In: Johnson M.R.W. and Stewart F.H. (eds.). The British Caledonides. Oliver Boyd, Edinburgh, 99-121.

Koch G.S. and Link R.F. 1971. The coefficient of variation- a guide to the sampling of ore deposits. Econ. Geol., 66, 293-301.

Krautner H.G. 1984. Syngenetic models for the pyrite and polymetallic sulphide ores of the east Carpathians. In: Wauschkuhn A., Kluth C. and Zimmermann R.A. (eds.). Syngenesis and epigenesis in the formation of mineral deposits. Springer-Verlag Berlin Heidelberg, 537-552.

Laird J.O. and Albee A.L. 1981. High pressure metamorphism in mafic schists from northern Vermont. Am. Jl. Sci., 281, 97-126.

Lambert R.S.J. 1959. The mineralogy of metamorphism of the Moine schists of the Morar and Knoydart districts of Inverness-shire. Trans. R. Soc. Edinburgh, 63, 553-588.

Lambert R.S.J., Holland J.G. and Winchester J.A. 1982. A geochemical comparison of the

Dalradian Leven Schists and the Grampian Division Monadhliath Schists of Scotland. Jl. Geol. Soc. Lond., 139, 71-84.

Lambert R.S.J. and McKerrow W.S. 1976. The Grampian Orogeny. Scott. Jl. Geol., 12, 271-292.

Leake B.E. 1978. Nomenclature of amphiboles. Can. Min., 16, 501-520.

Leake B.E., Hendry G.L., Kemp A., Plant A.G., Harvey P.K., Wilson J.R., Coats J.S., Aucott J.W., Lunel T. and Howarth R.J. 1969. The chemical analysis of rock powder by automatic X-ray fluorenscence. Chem. Geol., 5, 7-86.

Lister B. 1978. The preparation of polished thin sections. Inst. Geol. Sci. Rep. No. 78/27.

Litherland M. 1970. Stratigraphy and structure of the Dalradian rocks around Loch Creran, Argyll. Unpubl. PhD. Thesis, University of Liverpool.

Litherland M. 1980. The stratigraphy of the Dalradian rocks around Loch Creran, Argyll. Scott. Jl. Geol., 16, 105-123.

Litherland M. 1982. The structure of Loch Creran Dalradian and a new model for the SW.Highlands. Scott. Jl. Geol., 18, 205-225.

Loftus-Hills G. and Solomon M. 1967. Cobalt, nickel and selenium in sulphides as indicators of ore genesis. Mineral. Deposita, 2, 228-242.

Long J.V. 1977. Electron microanalysis. In: Zussman J. (ed.). Methods in determinative mineralogy. Academic Press, 2nd Edn., 273-341.

Lowell J.D. and Guilbert J.M. 1970. Lateral and vertical alteration -mineralisation zoning in porphyry ore deposits. Econ. Geol., 65, 373-408.

Lusk J. 1972. Examination of volcanic-exhalative and biogenic origins for sulphur in the stratiform massive sulphide deposits of New Brunswick. Econ. Geol., 67, 169-183.

374

Lusk J. and Crocket J.H. 1969. Sulphur isotope fractionation in coexisiting sulphides from the Heath Steele B-1 orebody, New Brunwick, Canada. Econ. Geol., 64, 147-155.

MacGregor S.M.A. and Roberts J.L. 1963. Dalradian pillow lavas, Ardwell Bridge, Banffshire. Geol. Mag., 100, 17-23.

MacNamara J. and Thode H.G. 1950. Comparison of the isotopic constitution of terrestrial meteoritic sulphur. Phys. Rev., 78, 307.

Mather J.D. 1970. The biotite isograd and lower greenschist facies in the Dalradian r cks of Scotland. Jl. Petr., 11, 253-275.

Matkovskiy O.I. 1971. Manganese garnets in the Ukrainian Carpathians. Doklady Acad. Sci. U.S.S.R. Earth Science Section, 196, 141-143.

Mauger R.L. 1972. A sulphur isotope study of the Ducktown Tennessee district, U.S.A. Econ. Geol., 67, 497-510.

McDonald J.A. 1967. Metamorphism and its effects on sulphide assemblages. Mineral. Deposita, 2, 200-220.

McDowell S.D. and Elders W.A. 1979. Geothermal metamorphism of sandstone in the Salton Sea geothermal system. In: Elders W.A. (ed.). Guidebook: geology and geothermics of the Salton Trough. Geol. Soc. Am. Bull., 92nd Annual Meeting, San Diego. P. 70-76.

McDowell S.D. and Elders W.A. 1980. Authigenic layer silicate minerals in Salton Sea geothermal field. Contr. Min. Petr., 74, 293-310.

McKenzie D. 1978. Some remarks on the development of sedimentary basins. Earth Plan. Sci. Letters, 40, 25-32.

McKibben M.A. 1979. Ore minerals in the Salton Sea geothermal system, Imperial Valley, California, U.S.A. Msc. Thesis, University of California Riverside. UCR/IGPP Report 79/17.

375

Mercer W. 1976. Minor elements in metal deposits in sedimentary rocks- a review of the recent literature. In: Wolf K.H. (ed.). Handbook of stratabound and stratiform ore deposits. Elsevier, 1, 1-24.

Mercy E.L.P. 1965. Caledonian igneous activity. In: Craig G.Y. (ed.). The geology of Scotland. Edinburgh, Oliver and Boyd, 1st Edn., 229-267.

Mi hel R. 1953. Les schistes cristallins des massifs du grand paradis et de Sezialanzo (Alpes Franco-Italiennes): Sci. de la Terre.,V.1, quoted in Veide 1965.

Mitchell A.H.G. 1978. The Grampian orogeny in Scotland : arc-continent collision and polarity reversals. Jl. Geol., 86, 643-646.

Miyashiro A. 1953. Calcium-poor garnets in relation to metamorphism. Geochim. Cosmochem. Acta, 4, 179-208.

Miyashiro A. 1961. Evolut on of metamorphic belts. Jl. Petr., 2, 277-311.

Miyashiro A. 1973. Metamorphism and metamorphic belts. George Allen and Unwin.

Miyashiro A. and Seki Y. 1958. Enlargement of composition field of epidote and piemontite with rising temperature. Am. Jl. Sci., 256, 423-430.

Mohamad H.B. 1980. Geochemistry and petrology of the Southern Highlands (Upper) Dalradian pelitic-psammitic schists at Glen Esk, Angus, Scotland. Unpubl. PhD. Thesis, University of Strathclyde.

Moles N.R. 1983. Sphalerite composition in relation to deposition and metamorphism of the Foss stratiform Ba-Zn-Pb deposit, Aberfeldy, Scotland. Min. Mag., 47, 487-500.

Moles N.R. 1985. Metamorphic conditions and uplift history in central Perthshire: evidence from mineral equilibria in the Foss celsian-barite-sulphide deposit, Aberfeldy. Jl. Geol. Soc. Lond., 142, 39-52.

Mookherjee A. 1976. Ores and metamorphism : temporal and genetic relationships. In: Wolf K.H. (ed.). Handbook of stratabound and stratiform ore deposits. Elsevier, 4, 203-251.

Moorbath S. 1962. Lead isotope abundance studies on mineral occurrences in the British Isles and their geological significance. Phil. Trans. R. Soc. Lond., A254, 295-360.

Moore D.G. 1973. Plate edge deformation and crustal growth, Gulf of California structural province. Geol. Soc. Am. Bull., 84, 1883-1906.

Moseley F. 1977. Caledonian plate tectonics and the place of the English Lake district. Geol. Soc. Am. Bull., 88, 764-768.

Mottl M.J, Holland H.D. and Corr R.F. 1979. Chemical exchange during hydrothermal alteration of basalt by seawater. II- Experimental results for Fe, Mn and sulphur species. Geochim. Cosmochim. Acta., 43, 869-884.

Muffler L.J.P. and White D.W, 1969. Active metamorphism of upper Cenozoic sediments in the Salton Sea geothermal field and the Salton Trough, southeastern California, Geol. Soc. Am. Bull., 80, 157-182.

Muller G. and Schneider A. 1971. Chemistry and genesis of garnets in metamorphic rocks. Contr. Min. Petr., 31, 178-200.

Murphey B.F. 1947. The temperature variation of the thermal diffusion factors for binary mixtures of H, D and He. Phys. Rev., 72, 834-837.

Nicholson K. 1983. Manganese mineralisation in Scotland. Unpubl. PhD Thesis, University of Strathclyde.

Nielson H. 1978. Sulphur isotopes. In: Wedepohl K.H. (ed.). Handbook of geochemistry. Springer, Berlin Heidelberg, New York.

Nielson H. 1979. Sulphur isotopes. In: Jager E. and Hunziker J.C. (eds.). Lectures in isotope geology. Springer, Berlin Heidelberg, New York. 283-312.

Niggli P. 1954. Rocks and mineral deposits. Freeman San Francisco.

Oana S. and Ishikawa H. 1966. Sulphur isotopic fractionation between sulphur and sulphuric acid in the hydrothermal solution of sulphur dioxide. Geochem. Jl., 1, 45-50.

Odeh T. 1970. Reconnaissance geochemistry of the host rocks to the Craignure copper-nickel deposit, Argyllshire, Scotland. Unpubl. Msc. Thesis, University of strathclyde.

Ohmoto H. 1972. Systematics of sulphur and carbon isotopes in hydrothermal ore deposits. Econ. Geol., 67, 551-578.

Ohmoto H., Cole D.R. and Mottl M.J. 1976. Experimental basalt-seawater interaction: sulphur and oxygen isotope studies. Trans. Am. Geophys. Union Eos., 57, 342.

Ohmoto H. and Rye R.O. 1979. Isotopes of sulphur and carbon. In: Barnes H.L. (ed.). Geochemistry of hydrothermal ore deposits, 2nd edn., Wiley Interscience, 509-567.

Pankhurst R.J. 1970. The geochronology of the basic igneous complexes. Scott. Jl. Geol., 6, 83-107.

Pankhurst R.J. and Pidgeon R.T. 1976. Inherited isotope systems and the source region prehistory of early Caledonian granites in the Dalradian series of Scotland. Earth Plan. Sci. Letters, 31, 55-68.

Pantin H.M. 1956. The petrology of the Ben Vrackie epidiorites and their contact rocks. Trans. Geol. Soc. Glasgow, 22, 48-79.

Papike J.J., Cameron K.L. and Baldwin K. 1974. Amphiboles and pyroxenes : characterisation of other than quadrilateral components and estimates of ferric iron from microprobe data. (abstr.) Geol. Soc. Am. Abstr. with Prog., 6, 1053-1055.

Pavlides L., Gair J.E. and Crawford L.S. 1982. Central Virginia volcanic-plutonic belt

378

as a host for massive sulphide deposits. Econ. Geol., 77, 233-272.

Peach B.N. 1930. Chapters in the Geology of Scotland. Oxford University Press.

Peach B.N., Kynaston H. and Muff H.B. 1909. Geology of the seaboard of mid-Argyll. Explanation of sheet 36. Geol. Survey Scotland, H.M.S.O., Glasgow.

Peach B.N., Wilson J.S.G., Hill J.B., Bailey E.B. and Graham G.W. 1911. The geology of Knapdale, Jura and North Kintyre. Explanation of sheet 28, with parts of 27 and 29. Mem. Geol. Survey Scotland, H.M.S.O., Edinburgh.

Pederson F.D. 1980. Remobilisation of the massive sulphides of the Black Angel mine, central west Greenland. Econ. Geol., 75, 1022-1041.

Pettijohn F.J. 1975. Sedimentary rocks. Harper and Row, 2nd edn.

Phillips F.C. 1930. Some mineralogical and chemical changes induced by progressive metamorphism in the Green Bed group of the Scottish Dalradian. Min. Mag., 22, 239-256.

Phillips W.E.A., Stillman C.J. and Murphy T. 1976. A Caledonian plate tectonic model. Jl. Geol. Soc. Lond., 132, 579-609.

Phillips W.E., Taylor W.E. and Sanders I.S. 1975. An analysis of the geological history of the Ox-mountain inlier. Sci. Proc. R. Publ. Soc., 5A, 311-329.

Piasecki M.A.J. 1980. New light on the Moine rocks of the Central Highlands of Scotland. Jl. Geol. Soc. Lond., 137, 41-59.

Pichon Le. X. and Sibuet J.C.J. 1981. Passive margins- a model of formation. Jl. Geophys. Res., 86B, 3708-3720.

Piper J.D.A. 1982. Proterozoic palaeomagnetism and single continent plate tectonics. Geophys. Jl. R. Astron. Soc., 74, 163-197.

Pitcher W.S. and Flinn W. 1965. Controls of metamorphism. Oliver and Boyd, Edinburgh.

Plimer I.R. 1977. The mineralogy of the high grade metamorphic rocks enclosing the Broken Hill orebodies, Australia. N. Jb. Miner. Abh., 131, 115-139.

Plimer I.R. 1979. Sulphide rock zonation and hydrothermal alteration at Broken Hill, Australia. Trans. Instn. Min. Metall., 88, B161-B176.

Porteous W.G. 1973. Metamorphic index minerals in the eastern Dalradian. Scott. Jl. Geol., 9, 29-43.

Powell D. 1974. Stratigraphy and structure of the western Moine and the problem of Moine orogenesis. Jl. Geol. Soc. Lond., 130, 575-593.

Price B.G. 1972. Minor elements in pyrites from the Smithers map area, B.C. and exploration applications of minor elements studies. Unpubl. PhD. Thesis, University of British Columbia, quoted in Bralia et al. (1979).

Pringle I.R. 1972. Rb-Sr age determinations on shales associated with the Varanger Ice age, Geol. Mag., 109, 465-472.

Rast N. 1963. Structure and metamorphism of the Dalradian rocks of Scotland. In: Johnson M.R.W. and Stewart F.H. (eds.). The British Caledonides. Oliver and Boyd, Edinburgh, 123-142.

Rast N. and Crimes T.P. 1969. Caledonian orogenic episodes in the British Isles and Northwest France and their tectonic and geochronological interpretation. Tectonophysics, 7, 277-307.

Read H.H. 1923. The geology of Banff Huntly, Turriff. Mem. Geol. Surv. Scotland.

Read H.H. 1925. Metamorphism and migmatisation in the Xthan Valley, Aberdeenshire. Trans. Geol. Soc. Edinburgh, 15, 265-279.

Read H.H. 1961. Aspects of Caledonian magmatism in Britain. Liverpool Manchester Geol. Jl., 2, 653-683.

Reed S.J.B. 1975. The electron micrprobe. Cambridge University Press, Cambridge.

Ribbe P.H. 1974. Sulphide mineralogy. Mineral. Soc. Am. Rev. in Mineralogy (formerly: Short Course Notes), V. 1.

Rice C.M. 1970. Mineralogical examination of Phyllites from Loch Fyne, Scotland. Inst. Geol. Sci. Min. Eval. Unit. Rep. No. 82.

Richardson S.W. and Powell R. 1976. Thermal causes of the Dalradian metamorphism in the Central Highlands of Scotland. Scott. Jl. Geol., 12, 237-268.

Rickwood P.C. 1968. On recasting analyses of garnet into end-member molecules. Contr. Mineral. Petr., 18, 175-198.

Ringrose C.R. 1978. Geology of the area SW of Newton Hill in Glen Fyne, Argyllshire and an investigation of the minor mineralisation associated with the Loch Tay Limestones. Unpubl. Bsc. Thesis, University of Strathclyde.

Ripley E.M. and Ohmoto H. 1977. Mineralogic, sulphur isotope and inclusion studies of the stratabound copper deposit at the Paul mine, Peru. Econ. Geol., 72, 1017-1041.

Roberts J.L. 1966. Sedimentary affilations and stratigraphic correlation of the Dalradian rocks in the SW-Highlands of Scotland. Scott. Jl. Geol., 2, 200-223.

Roberts J.L. 1974. The structures of the Dalradian rocks in the southwest Highlands of Scotland. Jl. Geol. Soc. Lond., 130, 93-134.

Roberts J.L. 1977. The Dalradian rocks of Knapdale and North Kintyre. Scott. Jl. Geol., 13, 113-124.

Roberts J.L. and Treagus J.E. 1964. A reinvestigation of the Ben Lui fold. Geol. Mag., 101, 512-516.

Roberts J.L. and Treagus J.E. 1977. The Dalradian rocks of the Southwest Highlands-

introduction. Collection of 7 excursion guides, Scott. Jl. Geol., 13, 85-184.

Roberts J.L. and Treagus J.E. 1979. Stratigraphical and structural correlations between
the Dalradian rocks of the SW and Central Highlands of Scotland. In: Harris A.L.,
Holland C.H. and Leake B.E. (eds.). The Caledonides of the British Isles-reviewed.
Spec. Publ. Geol. Soc. Lond., No. 8, 199-204.

Robinson B.W. and Kusakabe M. 1975. Quantitative preparation of SO for S/ S
analyses from sulphides by combustion with cuprous oxide. Anal. Chem., 47, 1179-
1181.

Robinson P. and Jaffe H. 1969. Chemographic explanation of amphibole assemblages from
the central Maschusetts and southwestern New Hampshire. Spec. Pap. Miner. Soc. Am.,
2, 251-274.

Rockingham C.J. and Hutchinson R.W. 1980. Metamorphic textures in Archean Cu-Zn massive
sulphide deposits. Can. Inst. Min. Bull., 73, 104-112.

Ronov A.B., Migdisov A.A. and Lobach-Zhuchenko S. B. 1977. Regional metamorphism and
sediment composition evolution. Geochem. Intern., 14, 90-112.

Rui I.J. and Bakke I. 1975. Stratabound sulphide mineralisation in the Kjoli area,
Roros district, Norwegian Caledonide. Norsk Geol. Tidsskr., 55, 51-75.

Runnells D.D. 1969. The mineralogy and sulphur isotopes of the Ruby Creek copper
prospect, Bornite, Alaska. Econ. Geol., 64, 75-90.

Russell M.J. 1968. Structural controls of base metal mineralisation in Ireland in
relation to continental drift. Trans. Instn. Min. Metall., 77, B117-B128.

Russell M.J. 1978. Downward-excavating hydrothermal cells and Irish-type ore deposits:
importance of an underlying thick Caledonian prism. Trans Instn. Min. Metall., 87,
B168-B171.

Russell M.J. 1983. Major sediment-hosted exhalative zinc+lead deposits: formation from

hydrothermal convection cells that deepen during crustal extension. In: Sangester D.F. (ed.). Sediment-hosted stratiform lead-zinc deposits. Min. Assoc. Can. Short Course Handbook, 9, 251-282.

Russell M.J., Hall A.J., Willan R.C.R., Allison I., Anderton R. and Bowes G.E. 1984. On the origin of the Aberfeldy celsian+baryte+base metal deposits, Scotland. In: Gallagher M.J. and Coats J.S. (eds.). Prospecting in areas of glaciated terrain, 159-170.

Russell M.J., Solomon M. and Walshe J.L. 1981a. The genesis of sediment-hosted, exhalative zinc+lead deposits. Mineral. Deposita, 16, 113-127.

Russell M.J., Willan R.C.R., Anderton R., Hall A.J., Nicholson K. and Smythe D.K. 1981b. Genetic model and tectonic setting for Dalradian stratiform mineral deposits, Grampian Highlands, Scotland. Trans. Instn. Min. Metall., 90, B58.

Rye R.O. and Ohmoto H. 1974. Sulphur and carbon isotopes and ore genesis: a review. Econ. Geol., 69, 826-842.

Sabine P.A., Guppy E.M. and Seargeant G.A. 1969. Geochemistry of sedimentary rocks: petrography and chemistry of arenaceous rocks. Instn. Geol. Sci. Rep. 69/1.

Sakai H. 1968. Isotopic properties of sulphur compounds in hydrothermal processes. Geochem. Jl., 2, 29-49.

Sakai H., Takenaka T. and Kishima N. 1980. Experimental study of the rate and isotope effect in sulphate reduction by ferrous iron oxides and silicates under hydrothermal conditions. In: Campbell A. (ed.). Water-rock interaction. Int. Assoc. Geochem. and Cosmochem. /Alberta Res. Council 3rd International Symposium, 75-76.

Samson I.M. 1983. Fluid inclusion and stable isotope studies of the Silvermines orebodies, vein deposits. Unpubl. PhD. Thesis, University of Strathclyde.

Sangester D.F. 1976. Sulphur and lead isotopes in stratabound deposits. In: Wolf K.H. (ed.). Handbook of stratabound and stratiform ore deposits. Elsevier, 2, 219-266.

Sangester D.F. 1983. Sediment-hosted stratiform lead-zinc deposits. Min. Assoc. Can. Short Course Handbook, 9.

Sasakai A. and Kajiwara Y. 1971. Evidence of isotopic exchange between seawater sulphate and some syngenetic sulphide ores. Soc. Min. Geol. Japan Special Issue, 3, 289-294.

Schaller W.T. 1950. An interpretation of the composition of high-silica sericite. Min. Mag., 29, 406-415.

Schenk P.E. 1983. Regional trends in the geology of the Appalachian-Caledonian-Hercynian-Mauritanide orogen, Reidel Publishing Company, 205-219.

Scott R.A. 1987. Lithostratigraphy, structure and mineralisation of the Argyll Group Dalradian near Tyndrum, Scotland. Unpubl. PhD. Thesis, University of Strathclyde.

Senior A. and Leake B.E. 978. Regional metasomatism and geochemistry of the Dalradian metasediments of Connemara. Jl. Petr., 19, 584-625.

Seyfried W. and Dibble W.E. 1980. Seawater-peridotite interaction at 300 C and 500 bars. Implication for the origin of oceanic serpentinites. Geochim. Cosmochem. Acta, 44, 309-321.

Seyfried W.E. and Mottl M.J. 1982. Hydrothermal alteration of basalt by seawater under seawater-dominated conditions. Geochim et Cosmochim. Acta, 46, 985-1002.

Shaw D.M. 1956. Geochemistry of pelitic rocks. III: major elements and geochemistry. Geol. Soc. Am. Bull., 67, 919-934.

Shaw D.M. 1961. Element distribution laws in geochemistry. Geochim. et Cosmochim. Acta, 23, 116-134.

Shackleton R.M. 1958. Downward-facing structures of the Highland Border. Q. Jl. Geol. Soc. Lond., 113, 361-392.

Shackleton R.M. 1979. The British Caledonides: comments and summary. In: Harris A.L., Holland C.H. and Leake B.E. (eds.). The Caledonides of the British Isles-reviewed. Spec. Publ. Geol. Soc. Lond., No.8, Scottish Academic Press, Edinburgh, 299-304.

Sissons J.B. 1976. Scotland. Methuen

Sivaprakash C. 1981. Chemographic analysis of metabasite assemblages from Central Scottish Highlands. Lithos, 14, 29-33.

Smith C.G. 1977. Investigation of stratiform mineralisation in parts of the Dalradian of central Perthchire, Scotland. Trans. Instn. Min. Metall., 86, B50-B51.

Smith C.G. 1981. Excursion guide to Dalradian of the Scottish Highlands stratabound mineralisation and geology. Correlation of Caledonian Stratabound Sulphides, Glasgow, 25-32.

Smith C.G., Gallagher M.J., Coats J.S. and Parker M.E. 1981. Detection and general characteristics of stratabound mineralisation in the Dalradian of Scotland. In: Hall A.J. and Gallagher M.J. (eds.). Caledonian-Appalachian stratabound sulphide, Glasgow, Abstract volume presented at the meeting held at the University of Strathclyde, 16-19.

Smith C.G., Gallagher M.J. and others 1981. Stratabound base metal mineralisation in Dalradian rocks near Tyndrum, Scotland. Miner. Reconn. Progr. Inst. Geol. Sci., Prelim. Rep.

Smith C.G., Gallagher M.J. and others. 1984. Detection and general characteristics of stratabound mineralisation in the Dalradian of Scotland. Trans. Instn. Min. Metall., 93, B125-B133.

Smith C.G. and others. 1977a. Investigation of stratiform mineralisation in parts of central Perthshire. Miner. Reconn. Prog. Rep. Inst. Geol. Sci., No.8.

Smith C.G. and others 1977b. Investigation of stratiform sulphide mineralisation at

McPhun's Cairn, Argyllshire. Miner. Reconn. Prog. Rep. Inst. Geol. Sci., No. 13.

Smith C.G. and others 1978. Investigation of stratiform sulphide mineralisation at Meall Mor, South Knapdale, Argyll. Miner. Reconn. Prog. Rep. Inst. Geol. Sci. No. 15.

Smith D.G.W. 1976. Micrbeam techniques. Min. Assoc. Canada, Short Course Handbook, 1.

Smith J.W., Burns M.S. and Croxford N.J.W. 1978. Stable isotope studies of mineralisation at Mount Isa. Mineral. Deposita, 13, 369-381.

Smith R.A. and Harris A.L. 1976. The Ballachulish rocks of the Blair Atholl district. Scott. Jl. Geol., 12, 153-157.

Smith R.E. 1968. Redistribution of major elements in the alteration of some basic lavas during burial metamorphism. Jl. Petr., 9, 191-219.

Soper N.J. and Anderton R. 1984. Did the Dalradian slides originate as extentional faults? Nature, 307, 357-360.

Spencer A.M. 1969. Late Precambrian glaciation in Scotland. Proc. Geol. Soc. Lond., 1657, 1777-178.

Spencer A.M. 1971. Late Precambrian glaciation in Scotland. Mem. Geol. Soc. Lond., No.6.

Spencer A.M. 1975. Late Precambrian glaciation in the North Atlantic region. In: Wright A.E. and Moseley F. (eds.). Ices ages: ancient and modern. Geol. Jl. Spec. Issue No. 6, Seel House Press, Liverpool, 217-240.

Spencer A.M. and Spencer M.O. 1972. The late Precambrian/ lower Cambrian Bonahaven Dolomite of Islay and its stromatolites. Scott. Jl. Geol., 8, 269-282.

Spooner E.T.C. and Bray C.J. 1977. Hydrothermal fluids of seawater salinity in ophiolitic sulphide ore deposits in Cyprus. Nature, 266, 808-812.

Stanton R.L. 1976a. Petrochemical studies of the ore environment at Broken Hill, New South Wales. 1: constitution of "banded iron formation". Trans. Instn. Min. Metall., 85, B33-B46.

Stanton R.L. 1976b. Petrochemical studies of the ore environment at Broken Hill, New South Wales. 2: regional metamorphism of the banded iron formations and their immediate associates. Trans Instn. Min. Metall., 85, B118-B131.

Stanton R.L. 1976c. Petrochemical studies of the ore environment at Broken Hill, New South Wales. 3: banded iron formations and sulphide orebodies, constitutional and genetic ties. Trans. Instn. Min. Metall., 85, B132-B141.

Stanton R.L. 1976d. Petrochemical studies of the ore environment at Broken Hill, New South Wales. 4: environmental synthesis. Trans. Instn. Min. Metall., 85, B221-B223.

Stanton R.L. 1979. An alternative to the Barrovian interpretation: evidence from stratiform ores. Text of the Charles F.Davidson Memorial lecture, University of St Andrews, Nov.

Stanton R.L. 1982. An alternative to the Barrovian interpretation? Evidence from stratiform ores. Proc, Austral. Inst. Min. Metall., 282, 11-32.

Stanton R.L. and Vaughan J.P. 1979. Facies of ore formation: a preliminary account of the Pegmont deposit as an example of potential relations between small "iron formations" and stratiform sulphide ores. Proc. Austral. Instn. Min. Metall., 270, 25-38.

Stanton R.L. and Williams K.L. 1978. Garnet compositions at Broken Hill, New South Wales as indicators of metamorphic processes. Jl. Petr., 19, 514-529.

Statham P.J. 1975. Quantitative X-ray energy spectrometry : the application of a Si (Li) detector to electron microprobe analysis. Unpubl. PhD Thesis, University of Cambridge (quoted in Mohamad 1980).

Stout J.H. 1972. Phase petrology and mineral chemistry of coexisting amphiboles from

Telemark, Norway. Jl. Petr., 13, 99-145.

stumpfl E.F. 1976. Stratabound ore deposits and metamorphism: new aspects. 25th Inter. Geol. Cong., Sidney, Abstr. 1, 194-195.

Stumpfl E.F. 1979. Mn haloes surrounding metamorphosed stratabound base metal deposits. Mineral. Deposita, 14, 207-217.

Sturt B.A. 1961. The geological structure of the area south of Loch Tummel. Q. Jl. Geol. Soc. Lond., 117, 131-156.

Sturt B.A. 1962. The composition of garnets from pelitic schists in relation to the grade of regional metamorphism. Jl. Petr., 3, 181-191.

Styrt M.M., Brackmann A.J. and others 1981. The mineralogy and the isotopic composition of sulphur in hydrothermal sulphide / sulphate deposits on the East Pacific Rise 21 N latitude. Earth Plant Sci. Letters, 53, 382-390.

Sweatman T.R. and Long J.V.P. 1969. Quantitative electron-probe microanalysis of rock froming minerals. Jl. Petr., 10, 332-379.

Swenson D.H., Laux S.J., Burns A.R., Perley P.C. and Boats A.M. 1981. The Foss baryte deposit, Aberfeldy: deposition and structural history of a Dalradian stratabound orebody. (Abstr.), Correlation Caledonian stratabound sulphides meeting, university of Strathclyde, Glasgow.

Templeman-Kluit D.J. 1972. The geology and origin of the Faro, Vangorda and Swin concordant lead-zinc deposits, central Yukon Territory. Geol. Surv. Canada Bull., 208,

Thomas P.R. 1979. New evidence for a Central Highland root zone. In: Harris A.L., Holland C.H. and Leake B.E. (eds.). The Caledonides of the British Isles-reviewed. Spec. Pupbl. Geol. Soc. Lond., No. 8, Scottish Academic Press, Edinburgh, 205-211.

Thomas P.R. 1980. The stratigraphy and structure of the Moine rocks of the Schiellalion

complex, Scotland. Jl. Geol. Soc. Lond., 137, 469-482.

Tilley C.E. 1925. A preliminary survey of metamorphic zones in the Southern Highlands of Scotland. Q. Jl. Geol. Soc., Lond., 81, 100-112.

Tischler S.E. 1979. Ophiolite related mineralisation in the Tauern Window, eastern Alps (Austria). Proceed. IAVCE1-Ophiolite Sympo. Nicosia, Cyprus.

Toland W.G. 1960. Oxidation of organic compounds with aqueous sulphate. Jl. Am. Chem. Soc., 82, 1911-1916.

Tufar W. and Strucl I. 1984. The Sasa lead-zinc deposits (Macedonian/ Yugoslavia) and its position in the Serbian-Macedonian ore province.

Turekian K.K. and Wedopohl K.H. 1961. Distribution of the elements in some major units of the earth's crust. Geol. Soc. Am. Bull., 72, 175-192.

Tyler I.M. and Ashworth J.R. 1981. Garnet zoning and re-equilibration in the Strontian area, Scotland. Min. Mag., 44, 293-300.

Vallance T.G. 1960. Note on metamorphic and plutonic rocks and their biotites from the Wantabadgery-Adelong-Tumbarumba district, N.S.W., Proc. Linn. Soc., N.S.W., 85, 94-104.

Vallance T.G. 1969. Spilites again: some consequences of degradation of basalts. Proc. Linn. Soc., N.S.W., 94, 8-53.

Valley J.W., Taylor H.P. and O'Neil J.R. 1986. Stable isotopes. Min. Soc. Am. Review in Mineralogy, 16.

Van Breeman O., Pidgeon R.T. and Johnson M.R.W. 1974. Precambrian and palaeozoic pegmatites in the Moines of northern Scotland. Jl. Geol. Soc. Lond., 130, 493-509.

Van De Kamp P.C. 1970. The green beds of the Scottish Dalradian series : geochemistry, origin and metamorphism of mafic sediments. Jl. Geol., 78, 281-303.

Vaughan D.J. 1976. Sedimentary geochemistry and mineralogy of the sulphides of lead, zinc, copper and iron and their occurrences. In : Wolf K.H. (ed.). Handbook of stratabound and stratiform ore deposits. Elsevier, 2, 317-358.

Vaughan D.J. and Craig J.R. 1978. Mineral chemistry of metal sulphides. Cambridge University Press.

vieten K. and Hamm H.M. 1971. Zur Berechnung der kistallchemischem klinopyroxenen aus Elektronen strahl- microanalysen. Neus Jahrb. Mineral. Mh., 310-314 (qouted in Hawthorne F.C. 1976).

Vine J.D. and Tourtelot E.B. 1970. Geochemistry of black shale deposits- a summary report. Econ. Geol., 65, 253-272.

Vokes F.M. 1969. A review of the metamorphism of sulphide deposits. Earth Sci. Rev., 5, 99-143.

Vokes F.M. 1971. Some aspects of the regional metamorphic mobilisation of preexisting sulphide deposits. Mineral. Deposita, 6, 122-129.

Vokes F.M. 1976. Caledonian massive sulphides deposits in Scandinavian : a comparitive review. In Wolf K.H. (ed.). Handbook of stratabound and stratiform ore deposits. Elsevier, 6, 79-127.

Vokes F.M. and Zachrisson E. (eds.). Review of Caledonian-Appalachain stratabound sulphides. Geol. Survey Ireland Special Paper No. 5, 63-66.

Waltham A.C. 1968. Classification and genesis of some massive sulphide deposits in Norway. Trans. Instn. Min. Metall., 77, B153-B161.

Washington H.S. 1910. Manual of the chemical analysis of rocks, 2nd Edn., New York (Wiley).

Watson J. 1984. The dating of the Caledonian orogeny in Scotland. Jl. Geol. Soc. Lond.,

141, 193-214.

Wauschkuhn A., Kluth C. and Zimmermann R.A. 1984. Syngenesis and epigenesis in the formation of mineral deposits. Springer-Verlag Berlin Heidelberg.

Wedepoh K.H. 1978. Handbook of geochemistry. Springer, Berlin, Heidelberg, New York.

Weissberg B.G., Brown P.R.L. and Seward M. 1979. Ore metals in active geothermal system. In: Barnes H. L. (ed.). Geochemistry of hydrothermal ore deposits. 2nd Edn., 738-780.

Wells P.R.A. and Richardson S.W. 1979. Thermal evolution of metamorphic rocks in the Central Highlands of Scotland. In: Harris A.L., Holland C.H. and Leake B.E. (eds.). The Caledonides of the British Isles-rviewed. Spec. Publ. Geol. Soc. Lond., No. 8, Scottish Academic Press, Edinburgh, 339-344.

White D.E. 1981. Active geothermal systems and hydrothermal ore deposits. Econ. Geol., 75th Anniv. Vol., 392-423.

White J.L. and Burns A.F. 1963. Infra-red spectra of hydronium ion in micaceous minerals. Science, 141, 800-801.

Wiggins L.B. and Craig J.R. 1980. Reconnaissance of the Cu-Fe-Zn-S system : sphalerite phase relationchips. Econ. Geol., 75, 7742-751.

Willan R.C.R. 1980. Stratabound sulphide mineralisation in the Dalradian Supergroup of the Grampian Highlands, Scotland. Norges Geol. Unders., 360, 241-256.

Willann R.C.R. 1981. Discussion of trace elements results. In : Smith C.G. (ed.). Excursion guide to Dalradian of the Scottish Highlands stratabound mineralisation and geology. Correlation of Caledonian Stratabound Sulphides, Glasgow, 25-32.

Willan R.C.R. 1983. Stratiform baryte and sulphide in Dalradian metasediments of the Grampian Highlands, Scotland: geological setting, mineralogy, sulphur isotopes and geochemistry. Unpubl. PhD. Thesis, University of Strathclyde.

Willan R.C.R. 1nd Coleman M.L. 1981. Sulphur isotope study on stratabound baryte and sulphide from the Dalradian metamorphic terrain, Scotland. Instn. Geol. Sci. Isotope Geology Unit, Stable Isotope Report No. 60.

Willan R.C.R. and Coleman M.L. 1983. Sulphur isotope study of the Aberfeldy barite, zinc, lead deposit and minor sulphide mineralisation in the Dalradian metamorphic terrain, Scotland. Econ. Geol., 78, 1619-1656.

Willan R.C.R. and Hall A.J. 1980. Sphalerite geobarometry and trace element studies on stratiform sulphide from McPhun's Cairn, Argyll, Scotland. Trans. Instn. Min. Metall., 89, B31-B40.

Williams C.E. and McArdle P. 1978. Ireland. In : Bowie S.H.U., Kualheim A. and Haslam H.W. (eds.). Mineral deposits of Europe. Instn. Min. Metall./ Min. Soc. Lond., 319-145.

Wilson G.V. 1921. The le d, zinc, copper and nickel ores of Scotland. Mem. Geol. Surv. Spec. Rep. Min. res., G.B., 17.

Wilson J.R. and Leake B.E. 1972. The petrochemistry of the epidiorites of the Tayvallich Peninsula. North Knapdale, Argyllshire. Scott. Jl. Geol., 8, 215-252.

Winchester J.A. 1974. The zonal pattern of regional metamorphism in the Scottish Caledonides. Jl. Geol. Soc. Lond., 130, 509-524.

Winkler H.G.F. 1976. Petrogenesis of metamorphic rocks, 4th Edn., Springer-Verlag, Heidelberg.

Wiseman J.D.H. 1934. The Central and SW Highlands epidiorite : a study in progrssive metamorphism. Q. Jl. Geol. Soc. Lond., 90, 354-417.

Wolf K.H. 1976. Handbook of stratabound and stratiform ore deposits. Elsevier, Volume One.

Wolf K.H. 1976. Handbook of stratabound and stratiform ore deposits. Elsevier, Volume Two.

Wolf K.H. 1976. Handbook of stratabound and stratiform ore deposits. Elsevier, Volume Four.

Wolf K.H. 1976. Handbook of stratabound and stratiform ore deposits. Elsevier, Volume Six.

Wood S. 1964. Some structures in the Dalradian pillow lavas of the Tayvallich Peninsula Argyll. Geol. Mag., 101, 481-487.

Wright A.E. 1969. The Precambrian rocks of England, Wales and southeast Ireland. Am. Assoc. Petrol. Geol. Mem., 12, 93-109.

Wright A. 1974. Summary, Loch Fyne Project. Unpubl. Rep. Consolidated Gold Field.

Yamamato M. 1967. S/ S and Se/S and Co/Fe in Iwami mine, Shimane-prefecture. Presented at the annual meeting of the Geochem. Soc. Japan, held at Nagoyo University.

Yamamato M., Kase K. and Ueda A. 1983. Fractionation of sulphur isotopes and selenium between coexisting pyrite and chalcopyrite from the Hitachi deposit, Ibaraki Prefecture, Japan. Geochem. Jl. 17, 29-39.

Yardley B.W.D., Vine F.J. and Baldwin C.T. 1982. The plate tectonic setting of N.W. Britain and Ireland in late Cambrian and early Ordovician times. Jl. Geol. Soc. Lond., 139, 455-463.

Youth C.C. and Tan L.P. 1975. Element distribution in the black shale and their metamorphic products along the south cross- island highway, Taiwan. Proc. Geol. Soc. China, 18, 17-28.

Zachrison E. 1971. The structural setting of the Stekenjokk ore bodies, central Swedish Caledonides. Econ. Geol., 66, 641-652.

Zen E. 1981. Metamorphic mineral assemblages of slightly calcic pelitic rocks in and
around the Tactonic Allochthon, southwestern Massachusetts and adjacent Connecticut,
New York. U.S. Geol. Surv. Prof. Paper, 1113, 1-128.

Zussman J. 1977. Physical methods in determinative mineralogy. Academic Press, 2nd Edn.